UNIVERSITY OF SOUTHERN CALIFORNIA

Department of Civil Engineering

FROM SEISMIC SOURCE TO STRUCTURAL RESPONSE: CONTRIBUTIONS OF PROFESSOR MIHAILO D. TRIFUNAC

Edited by:

Vinay K. Gupta
IIT Kanpur, India

Report CE 04-04

December, 2004

Los Angeles, California

www.usc.edu/dept/civil_eng/Earthquake_eng/

Professor Mihailo D. Trifunac

BIOGRAPHICAL SKETCH
OF
PROFESSOR MIHAILO D. TRIFUNAC

Professor Mihailo Dimitrije Trifunac was born in Kikinda, Yugoslavia, on November 7, 1942. He received his Dipl. Ing. degree in Civil Engineering from the University of Belgrade in 1965, M.S. degree in Civil Engineering from Princeton University in 1966, and Ph.D. degree in Civil Engineering and Geophysics from the California Institute of Technology (Caltech) in 1969. After graduation, he spent one more year at Caltech as Research Fellow in Applied Mechanics, and the following two years at the Lamont-Doherty Geological Observatory of Columbia University, first as a Research Scientist and then as a Research Associate and Lecturer. In 1972, he returned to Caltech as Assistant Professor of Applied Science. In 1975, he moved with his research group to University of Southern California (USC) as Associate Professor of Civil Engineering, and has been working as Professor there since 1980. His other appointments include: J.S.P.S. Research Professor, School of Civil Engineering, Kyoto University (1988-89); Consultant to the Advisory Committees on Reactor Safeguards (1971-1994) and Nuclear Waste (1989-1994), of the Nuclear Regulatory Commission; and Consultant of United Nations Development Program in India, Yugoslavia and Soviet Union.

Professor Trifunac is a member of the American Geophysical Union, the American Society of Civil Engineers, the Seismological Society of America, Sigma Xi, Earthquake Engineering Research Institute, European Association for Earthquake Engineering, and the New York Academy of Sciences. He is a member of the editorial boards of: Soil Dynamics and Earthquake Engineering; ISET Journal of Earthquake Technology; and Journal of Seismology and Earthquake Engineering. He is also an Honorary Fellow of Indian Society of Earthquake Technology, a Foreign Member of the Yugoslav Academy of Engineering, and Foreign Member of the Russian Academy of Natural Sciences. He has been the recipient of the ISET Award for the *Overall Best Paper in 1987*, the ISET Hanumantacharaya Joshi Award for the *Best Paper in Structural Dynamics in 1985-88*, the Lockheed Martin Senior Research Award of USC School of Engineering in 2000, and P.L. Kapitsa Gold Medal *To the Author of Scientific Discovery* of the Russian Academy of Natural Sciences in 2002.

Professor Trifunac is one of the leading international experts in Earthquake Engineering and Engineering Seismology. His success as a researcher is due to the rare combination of sound theoretical knowledge, physical intuition, an ability to recognize practical problems and find simple analytical solutions, vision, energy and persistence. With formal education both in Geophysics and Civil Engineering, he was one of the first to successfully introduce the knowledge of Geology and Geophysics into Earthquake Engineering applications. His work is marked by originality, and has always been well ahead of the current state of the art. His work

includes many milestones, both in Earthquake Engineering and in Seismology, where he has created several lines of research and a large following.

Professor Trifunac's work has been both theoretical and experimental, on a variety of topics including: earthquake source mechanism, empirical scaling of strong ground motion, strong motion instrumentation and arrays deployment, seismic wave propagation and site effects on strong ground motion, seismic hazard assessment, structural dynamics and soil-structure interaction, full-scale testing of structures, strong motion data processing, statistics of earthquake response, and tsunami. He is an author or co-author of more than 360 technical publications, and his work is frequently cited by others. With about 3,500 citations in the Thomson ISI database, he is one of the few most-cited researchers in the history of Earthquake Engineering. His most cited papers include: (i) his pioneering work in the early 1970s on wave propagation through sedimentary basins and scattering of waves from near-surface topographies, which is a line of research pursued today by many seismologists and earthquake engineers; and (ii) his pioneering work on three dimensional, finite source inversion of the 1971 San Fernando earthquake using strong motion records, which is now a standard procedure performed following a major earthquake.

Professor Trifunac is one of the pioneers in deployment of modern strong motion arrays in the U.S. The arrays he has deployed are the Bear Valley Array in 1972-73, the San Jacinto Array in 1973-74, and finally, the Los Angeles and Vicinity Strong Motion Network in 1979-80, which with 80 stations has the distinction of being the first urban strong motion network in the world. He is also the author of the first modern data processing software for strong motion accelerograms (in the early 1970s), which is still the core of the standard software packages for accelerogram data processing used by government agencies and laboratories worldwide.

TABLE OF CONTENTS

INTRODUCTION

This collection of eleven papers has been brought out to recognize the scientific contributions of Professor Mihailo D. Trifunac, fondly called as Misha by his friends and colleagues, on the occasion of his 60th birthday. Professor Trifunac is singularly credited for emphasizing the relevance of strong motion seismology in earthquake engineering, thus enabling it to become more realistic in ground motion characterization. He is also credited for his vision in emphasizing several issues in earthquake engineering, which were seriously considered by the professional community much later. The papers in this collection are the review papers on those topics that have formed the core of his vast research contributions to earthquake engineering and engineering seismology during a period of about 35 years. These papers have been written by his past students (I.D. Gupta, Ljupco Jordanovski, Vinay Gupta, Tzong-Ying Hao), and by his colleagues and friends (Francisco Sánchez-Sesma, Ivanka Paskaleva, Vincent Lee, and Maria Todorovska), and were published in the 2002 volume of the ISET Journal of Earthquake Technology.

The first paper, by Professor Vincent Lee, describes the major contributions of Professor Trifunac to digitization and processing of analogue earthquake records since the days of semi-automatic hand digitization in 1960s when it took four days to digitize and process a single record, and very few properly digitized records were available. After making a determined beginning at Caltech, Professor Trifunac led the efforts at USC to reduce this time to few minutes and at a much reduced cost, while making use of the overall developments in the commercially available scanning and computer hardware. The improved techniques also focussed on increasing the useful frequency bandwidth of accelerograms, synchronizing the origins of the time coordinate in all three components, settling issues related to non-uniform film speed, low-pass filtering to eliminate the high-frequency digitization errors, developing instrument correction algorithms, and on base-line correcting the raw accelerograms to remove the long-period recording and processing noise. The paper by Lee also mentions the contributions of Professor Trifunac to advanced data processing issues such as misalignment and cross-axis sensitivity, corrections for tilt and angular accelerations, and to electronic data dissemination by access to the EQINFOS database, via modem in the 1980s and through internet in the present times.

One of the key reasons behind the efforts of Professor Trifunac in obtaining accurate signatures of strong ground motions has been the finite fault modelling of the earthquake sources from the near-field strong motion records. The second paper, by Professors Ljupco Jordanovski and Maria Todorovska, is a review paper on the studies based on solving this inverse problem. Though the problem is complex and ill-posed, and the solutions are very approximate, such studies are important for understanding of the earthquake source mechanism, and for prediction

of the strong ground motions. The work of Professor Trifunac on the inversion of the source mechanism of the 1966 Parkfield and 1971 San Fernando earthquakes marks the pioneering first step in this direction. In fact, source inversion has now become one of the central topics in studying a well-recorded earthquake. The paper by Jordanovski and Todorovska talks about the strong motion arrays installed by Professor Trifunac for obtaining data for such studies. The paper also discusses his recent work on using maregrams for source inversion of submarine earthquakes, slides and slumps.

The third paper, by Professor Francisco Sánchez-Sesma, discusses the local site effects of geology, soil deposits, and topography on strong ground motion during earthquakes, and the significant role of the empirical and theoretical models proposed by Professor Trifunac. Notable is his analytical solution for the response of semi-circular and elliptical alluvial valleys and canyons to incident SH waves, which has helped in understanding the basic phenomena of interference, scattering and diffraction, and in verifying numerical solutions.

Professor Trifunac led the efforts at USC to provide useful interpretations of strong ground motion through elementary analyses. The fourth paper, by Professor Ivanka Paskaleva, presents a review of such studies, particularly on spatial attenuation of strong motion, interpretation of its frequency content, the strong motion magnitude scale, and the principles of empirical scaling of strong motion. These analyses have been very valuable for the development of more refined regression models for prediction of strong ground motion from a particular earthquake, and for use in probabilistic seismic hazard analyses. For example, contour maps of the spatial distribution of peaks and spectral amplitudes of strong ground motion have helped in refining the frequency-dependent attenuation laws to include dependency on the geology along the propagation path and thus in reducing scatter in the regression models. Similarly, studies of the propagation of wave energy in areas close to faults have led to a methodology for synthesis of realistic artificial accelerograms with a sound physical basis. The observation that for frequencies up to 7 Hz, the largest peaks of strong motion can propagate deterministically over large distances, and that beyond that frequency the strong motion consists of randomly scattered waves, could lead to a fresh treatment of scaling laws and attenuation models. The observation on non-linear soil response during strong earthquake shaking has highlighted the limitations of the site amplification studies based on microtremors and aftershocks. Professor Trifunac also emphasized the utility of the local magnitude scale for the engineering scaling of strong motion, and proposed an alternative ‘strong motion’ local magnitude scale based on the computed response of a Wood-Anderson torsional seismometer to recorded accelerograms. He used this magnitude scale to facilitate extrapolation of empirical scaling models for strong motion from one tectonic region to another. The paper by Paskaleva also highlights the attempts of Professor Trifunac to look beyond the use of peak ground acceleration as a scaling parameter for seismic

hazard studies, and his introduction of the concept of uniform hazard spectrum (UHS) as an alternative scaling functional.

The fifth, sixth and seventh papers, by Professor Vincent Lee, discuss the pioneering and extensive contributions of Professor Trifunac to the development of empirical scaling equations for various functionals of strong ground motion in terms of simple, readily available parameters like earthquake magnitude (or modified Mercalli intensity), epicentral distance, site conditions (site geology/depth of sediments and/or local site classification). Whereas in case of absolute acceleration response functional, the development of scaling equations fundamentally changed the way response spectra were hitherto characterized (from being determined from peak ground acceleration and site-dependent shape to being directly characterized), the scaling of other functionals got started with this. Part I (the fifth paper) describes how the scaling models for pseudo spectral velocity spectra (and other functionals like Fourier spectrum, pseudo spectral acceleration) gradually developed in three stages, as more and more uniformly processed strong motion data became available. Initially those were based on the attenuation law of Richter. In the second generation, this law was replaced by a frequency-dependent attenuation function, which was further refined in the third generation models. The third generation of scaling models also made a leap forward through a much more comprehensive treatment of the local site conditions, and by inclusion of propagation path type. Part I also describes Professor Trifunac's contribution to the extension of the frequency range of the scaling models beyond that permitted by the recorded data.

Professor Trifunac's contributions to the analysis and scaling of strong motion duration are described in Part II (the sixth paper). He proposed definitions of strong motion duration suitable to describe the energy input to structures. The definition initially proposed by him considered the interval of strong motion in an accelerogram to be continuous. The second definition he proposed was frequency-dependent, and considered the duration of strong motion as a collection of disjointed intervals corresponding to strong pulses in the accelerogram. Part II also describes his work on development of scaling models for prediction of strong motion duration, as it depends on the duration of rupture, wave dispersion, regional geology, and on the effects of the local soil.

Part III (the seventh paper) describes Professor Trifunac's work on synthesizing translational accelerograms such that those are compatible with a specified set of Fourier spectra and strong motion duration (of a recorded motion, or as predicted by a scaling model), and with the regional geology (modelled by parallel layers). These (translational) accelerograms were then used to synthesize complementary torsional and rocking accelerograms, and surface strains and curvature time histories, by using the theory of linear wave propagation. Implemented in several stages in the well-known SYNACC software package, this work was pioneering in simulating ensembles of translational motions with realistic temporal variations in frequency content. This

work also heralded the synthesis of rocking and torsional strong motion accelerograms, well before such motions could be recorded.

The eighth paper, by Dr. I.D. Gupta, compares the deterministic and probabilistic approaches to seismic hazard assessment, and shows the important role of the scaling relations developed by Professor Trifunac in both approaches. Professor Trifunac also proposed how to combine the effects of deterministic earthquake occurrences, based for example on expert opinion predictions, with those of Poissonian earthquakes, which occur statistically, within the framework of probabilistic seismic hazard analysis, and introduced the concept of Uniform Hazard Spectrum. He is also credited for generalizing the concept of seismic zoning maps to include other functionals like peak strain or liquefaction potential.

Professor Trifunac made important contributions to the manner in which the engineering profession looks at the response of structural systems to a given characterization of ground motion. For impulsive excitations and for problems involving soil-structure interaction, he advocated the use of wave propagation analysis. Further, to integrate the structural response into the general framework of seismic hazard characterization, he proposed to obtain the structural response in probabilistic terms (for uncertainty regarding the time-description of the anticipated ground motion) through the use of response spectra. The ninth paper, by Professor Vinay Gupta, discusses these contributions of Professor Trifunac, and highlights various response techniques based on his idea of using response spectrum to account for non-stationarity in a seismic response process. Professor Trifunac also led beyond the conventional ideas of predicting the largest response peak and showed how all other orders of response peaks could be estimated. His papers in the early 1970s also gave the starting point for a series of techniques proposed later for obtaining 'equivalent stationary' power spectral density functions of excitation processes from the response spectra.

The tenth paper, by Professor Maria Todorovska, highlights the efforts of Professor Trifunac to emphasize the need of full-scale testing for experimental investigation of structural response and of soil-structure interaction. Professor Trifunac has been one of the most persistent advocates of the full-scale experimental investigation of soil-structure interaction as the only approach that captures the complete physics of the problem, and can reveal new phenomena in response, and as the only true test of model-based simulations. His work on ambient and forced vibration tests of buildings and on analyses of recorded earthquake response has helped in formulating soil-structure interaction models based on more realistic assumptions. For example, it was shown that (i) the rigid slab assumption for building foundations is not always appropriate, (ii) foundation impedances for rigid surface foundations are not always adequate and there is a need to include the effects of embedment, (iii) simple foundation models fail to account for the large radiation damping in horizontal vibrations, and (iv) time-dependent lengthening of system period during strong ground shaking may be due to the non-linear response of soil-foundation system, and

more extensive levels of instrumentation (e.g., those for measuring the rotation of the building foundation) need to be employed to develop further the appropriate soil-foundation models. The paper also highlights the work of Professor Trifunac on using soil-structure interaction to reduce the structural response.

The eleventh paper, by Dr. Tzong-Ying Hao, gives an insight into the work of Professor Trifunac to include the non-linear behaviour of soil-foundation systems in the analysis of response of structures. It describes an energy-based formulation to estimate the total energy dissipation in structures (including that due to the non-linear response of the soil and radiation damping) at any instant during the excitation. This formulation is important in estimating the damage potential of a given earthquake ground motion and in designing suitable energy dissipation devices to limit damage in a system of known energy dissipation capacity. The paper shows how the recorded data may be used to estimate the total input energy in terms of the energy manifested by the free-field velocity time-history at the site of the structure. Through the examples of five buildings, it also shows that the energy dissipation is underestimated when the soil-structure interaction is ignored or when the soil-foundation is assumed to behave linearly.

Though the eleven papers included in this volume give a broad idea of Professor Trifunac's contributions to strong motion seismology and earthquake engineering in a span of about 35 years, those are by no means exhaustive. There are several other topics and areas he contributed to and wrote about, like historical review on the origins of the Response Spectrum Method, his work to preserve and interpret poorly recorded accelerograms, and recently, the studies he initiated on scientific citations with aim to improve the visibility and reputation of the Earthquake Engineering profession. Those have not been adequately covered by this collection of papers, but those undoubtedly have received a serious attention of Professor Trifunac and the profession has gained from his penchant to think ahead of time.

In December of 2002, Professor Trifunac delivered the 23rd ISET Annual Lecture at Roorkee, India, in which he described the origins of the Response Spectrum Method in 1932, and how this method influenced the thinking and direction of research during the following 70 years[1].

Professor Trifunac helped in preserving old and difficult-to-decipher recordings of strong motion. The old accelerograms recorded on light sensitive paper, during March 10, 1933, Long Beach earthquake, and May 19, 1940, Imperial Valley earthquake, at El Centro, both in California, were exposed by stray light and became difficult to interpret and digitize. Rinaldi strong motion, recorded during Northridge 1994, California, earthquake, which produced so far the largest peak velocity of 1.7 m/s, had numerous stalls, caused by irregular progression of 70

[1] ISET Journal of Earthquake Technology, Vol. 40, No. 1, 2003, pp. 19-50

mm film record[2]. These and many other difficult or important accelerograms (e.g., Pacoima Dam accelerogram[3]) were all digitized, corrected and preserved by Professor Trifunac. All modern digital data collections with strong motion accelerograms include his digitized versions of these records.

In 2002, Professor Trifunac initiated the first studies of publication and citation rates in Earthquake Engineering. He showed that in terms of their publication rates, the earthquake engineers are as productive as the other scientists and engineers, and how detailed analyses of citations can be invaluable for self-improvement and direction[4].

I wish to thank Professor Maria Todorovska for suggesting the idea of this volume to celebrate the 60th birthday of Professor Trifunac, and to Secretary, Indian Society of Earthquake Technology (ISET) for permitting the papers published in the ISET Journal of Earthquake Technology to be reproduced for this volume. Thanks are also due to my Ph.D. student, Mr. Sandip Das, who helped with substitution of some of the figures in the published papers by the scanned images of better quality.

Vinay K. Gupta
IIT Kanpur, India

December 2004

[2] Earthquake Spectra, Vol. 14, No. 1, 1998, pp. 225-239
[3] Bulletin of the Seismological Society of America, Vol. 61, No. 5, 1971, pp. 1393-1411
[4] Report CE 04-03, Department of Civil Engineering, University of Southern California, Los Angeles, 2004

ISET Journal of Earthquake Technology, Paper No. 417, Vol. 39, No. 1-2, March-June 2002, pp. 55-72

DIGITIZATION, DATA PROCESSING AND DISSEMINATION OF STRONG MOTION EARTHQUAKE ACCELEROGRAMS

V.W. Lee
Department of Civil Engineering
University of Southern California
Los Angeles, CA 90089-2531, U.S.A.

ABSTRACT

The modern techniques for digitization of strong-motion accelerograms and subsequent data processing were first developed in the late 1960s and early 1970s, at which time the only available digitization technology was semi-automatic hand digitization. Following the development of image processing technologies in the early 1970s, an automatic digitization and data processing system, driven by a mini-computer, was developed by Trifunac and Lee. The currently used digitization technology is based on personal computers and flat bed digital scanners, which appeared respectively in the early and late 1980s. The data processing part has been continuously evolving, thus improving the performance of the entire system. This paper presents a review of the developments in hardware and software for digitization of strong-motion accelerograms, data processing and data dissemination. In the 1980s, digital strong motion accelerographs became commercially available, and currently all new deployments are digital. However, it takes time to record a large number of strong motion accelerograms, and as of now, by far, most of the strong motion data has been recorded in analog form.

KEYWORDS: Digitization, Data Processing, Earthquake Accelerograms

INTRODUCTION

The first strong motion accelerographs were analog, and were built and installed at free-field sites and in buildings in the early 1930s. Soon after, strong motion was first recorded, on March 10, 1933, during the Long Beach, California earthquake. In the 1980s, digital strong motion accelerographs became commercially available (Trifunac and Todorovska, 2001a), and at present, essentially all new installations are digital. Yet, so far the largest number of strong motion records have been recorded in analog form, on light sensitive paper or on film. For analysis, analog strong motion records must be digitized and processed in a form suitable for subsequent analyses. This paper reviews the developments in digitization, processing (Trifunac et al., 1999a,1999b), and dissemination of strong motion accelerograms (Lee and Trifunac, 1982).

The concept of response spectrum as a tool in earthquake-resistant design was formulated in 1932, one year before the first recording of strong ground motion (Biot, 1932, 1933, 1934). Before the 1960s, spectra had to be computed with the aid of analog mechanical devices (e.g., torsional pendulum; see Biot, 1941, 1942) or electrical analog computers (Caughey et al., 1960). The modern era of digitization and processing of strong motion accelerograms started in the 1960s (Figure 1), with the availability of digital computers and semi-automatic digitizing machines (Hudson, 1979).

In the late 1960s and early 1970s, the only available technology for digitization of strong motion accelerograms was a semi-automatic, hand digitization system (Hudson, 1979; Trifunac and Lee, 1973). This system worked as follows. First, the film record (or its enlargement) was placed on the digitizing table, lining up by eye the horizontal axis to an estimated zero axis. The traces were digitized by placing manually the crosshair on successive points on the trace. The digitizer converted the coordinates to numbers, directly punched on cards or recorded on paper tape. A set of computer programs was then used to read and to plot the data on same scale as that of the original digitized record. This plot was checked against the original analog traces. Any errors found were corrected manually. This cycle was iterated until the final plot agreed well with the record. The raw data was then ready for routine computer processing (Trifunac and Lee, 1973).

The semi-automatic digitization system was operating from 1967 to about 1975. It was slow (it took about four days to digitize, check and load data onto magnetic tapes), accurate, and its noise characteristics were analyzed and documented (Trifunac et al., 1971, 1973a, 1973b). It was used to generate all the data published in the so-called Caltech "blue book data reports" (Hudson et al., 1969, 1971, 1972a, 1972b), which became the "standard" source for strong motion data all over the world. The digitized data of many famous older accelerograms in the blue book reports, such as March 10, 1933 Long Beach (Heck et al., 1936), May 18, 1940, El Centro (Trifunac and Brune, 1970), July 21, 1952, Taft (Hudson et al., 1969), and February 9, 1971, Pacoima Dam (Trifunac and Hudson, 1971), were all redigitized by Trifunac using this semi-automatic digitization system, because the previously digitized versions had inadequate sampling rate and occasionally missed or misinterpreted peaks in the strong motion part of the records.

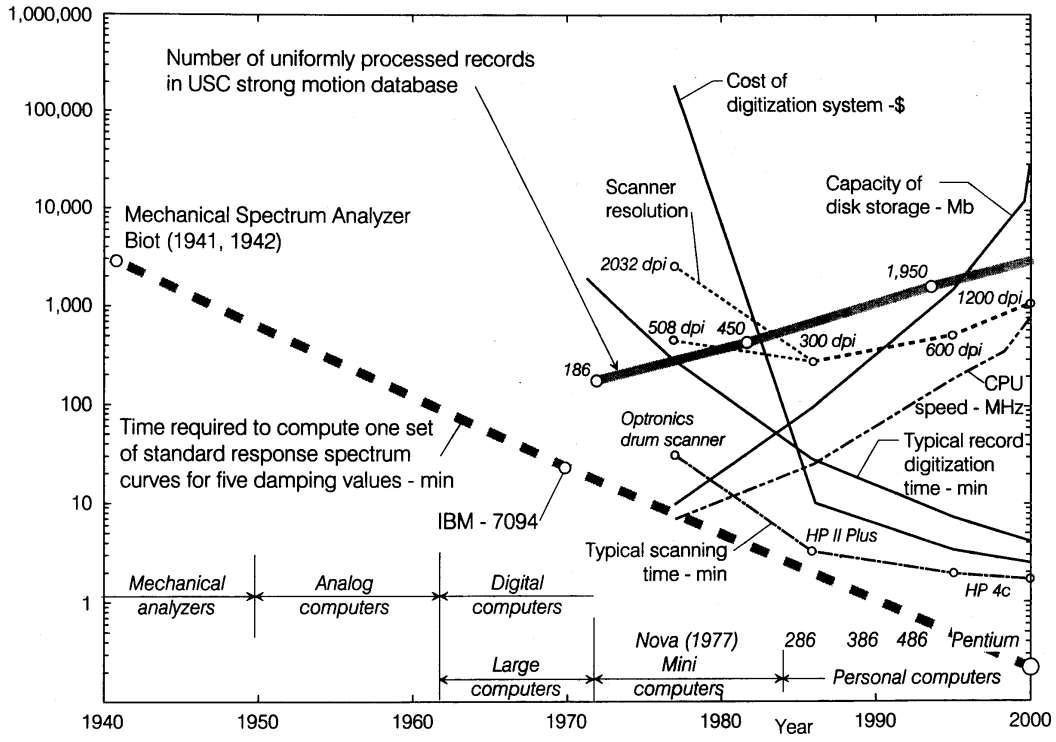

Fig. 1 Trends in capabilities and cost of accelerogram digitization and data processing systems

DIGITIZATION

1. The First Automatic Digitization System

The first automatic system for digitization of strong-motion accelerograms was developed by Trifunac and Lee (1979), using the commercially available hardware for image processing (Photoscan P-1000 photodensitometer by Optronics) and a Data General NOVA-3 minicomputer. With this system, up to four 10-inch sections of the accelerogram could be reproduced on a 10 × 10 in (254 × 254 mm) negative film (Figure 2), which was then placed onto the drum of the photodensitometar for scanning. It took only two to three hours to digitize a typical record using the new system, in contrast to several days on using the previous manual and semi-automatic systems. Another important difference was in the average sampling rate of the digitized record, which was 30 to 50 points per second for the old manual system, compared to greater than 200 points per second for the automatic system.

2. The New Automatic Digitization System

The first automatic digitization system (Trifunac and Lee, 1979; Trifunac, 1980) was modernized through the mid- and late 1980s, following the developments in personal computer hardware. The first digitization system in 1979 employed a photodensitometer table with a rotating drum (with cost over $30,000 at that time), and it had to be interfaced with a minicomputer, which was costly to acquire

($150,000) and expensive to maintain ($15,000 per year in 1976 and $7,000 per year in 1988). It used a Tektronix terminal ($12,000 in 1975), one of the best and the only high-resolution graphics terminal during the late 1970s.

In the 1980s, inexpensive high-speed personal computers (PCs) and desktop digital scanners appeared in the market and reduced the cost of the system to several thousand dollars (Figure 1). Our new software package "LeAuto," consisting of LeFilm, LeTrace, LeTV and LeScribe computer programs, now runs on a Pentiuum PC with 128 MB or more of RAM, running Windows98 or higher operating system, and with a fast Super VGA graphics monitor. The software has been continuously updated and improved to be compatible with the new scanners that have appeared in the market. By 2000, the cost of the hardware dropped to less than US $2,000 (Figure 1). The current resolution of digitization is > 200 points/s (assuming film speed of 1 cm/s), with gray levels resolved by 8, 10 or 12 bits (256, 1024 or 4098 gray levels) (Lee and Trifunac, 1990; Trifunac et al., 1999a, 1999b).

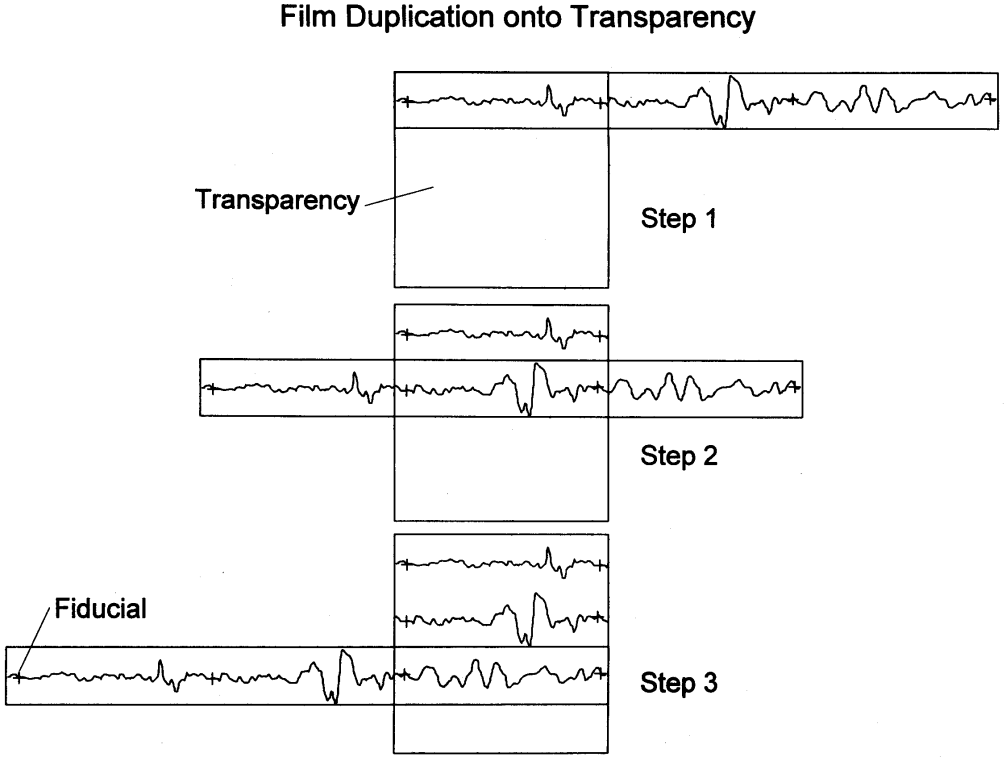

Fig. 2 Schematic diagram of duplication of original 70 mm film with recorded accelerogram, onto a 10 × 10 in (25.4 × 25.4 cm) negative, which is subsequently mounted on Optronics drum for scanning (Trifunac and Lee, 1979)

3. Hardware Components

The elements of the new automatic digitization system are shown schematically in Figure 3. The reading of an 8.5×11 inch film positive is performed by a Hewlett-Packard desktop digital scanner ("ScanJet"), interfaced with the PC. The PC needs to have a large hard disk drive and a minimum of 2 MB random access memory (RAM), while most modern PCs have 64, 128, 256 MB or larger RAM. In the early 1990s, the automatic digitization system ran on operating system DOS version 5.00 or higher (preferably DOS 6.2), and currently (early 2000s), it runs on Microsoft Windows 98 or higher operating system. The PC is interfaced with a Super VGA graphics display monitor, and a LaserJet printer, while other Windows-supported (e.g., DeskJet and InkJet) printers can also be used.

A typical strong-motion accelerogram is usually several tens of seconds long, but may be one minute or longer, if the complete length of useful recording is considered. Then, considering a typical SMA-1 70 mm wide film record, one would have to digitize a rectangular area 70 mm (2.75 in) wide and up to say 80 s (80 cm, 31.5 in) long. ScanJets are designed to scan a rectangular area up to 8.5×11 inches or 8.5×14 inches. Figure 2 shows a solution for handling long records, which was developed in the late 1970s for use with an Optronics rotating drum densitometer. A transparency film with fiducial marks was used,

with the original accelerograph record copied in 10-inch long segments onto a rectangular negative (10 × 10 in), with up to four segments for simultaneous digitization.

At present, each 11-inch long segment ("page") is scanned by LeFilm and written onto consecutive disk files. Program LeTrace then processes (reads the scanned data and identifies the traces) each "page" sequentially. Using the program LeTV, the operator can edit each "page" one by one. The program LeScribe then reads the trace segments for each "page" and assembles them. This procedure thus enables one to digitize very long records. At present, LeFilm can also scan a 12-inch wide film records used by central recording system (CR-1), with 13 or more acceleration traces.

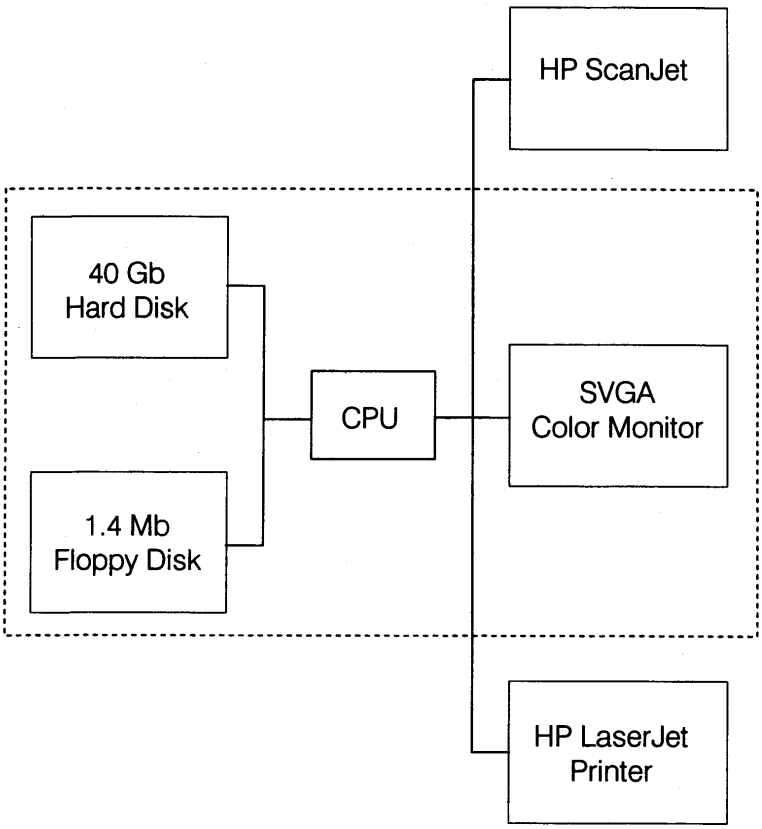

Fig. 3 Hardware components of the automatic digitization and data processing system

4. Noise Characteristics of the New System

The response and Fourier amplitude spectra of the digitization noise for the overall automatic digitization process are evaluated when the system is first assembled, and when it is upgraded. These spectra are used to determine the frequency range in which the signal-to-noise ratio for a digitized accelerogram trace is greater than unity, and which represents accurately the recorded motions. In general, the amplitudes of this noise depend on the scanner resolution, but also and mostly on the thickness of the trace and on the record length. Comparing records from acceleration and displacement transducers, Trifunac and Lee (1974) found that, for the old semi-automatic digitization, the typical digitization noise, after integration, might result in displacements up to several centimeters.

While for the old semi-automatic hand digitization system (Trifunac and Lee, 1973), the horizontal resolution (number of digitized points per unit length of the record) was a major factor determining the noise characteristics of the system, for the automatic digitization systems it is not, as the physical resolution (in pixels per mm) can be chosen sufficiently small not to affect the noise amplitudes. For the automatic system using Optronics photodensitometer (Trifunac and Lee, 1979), a resolution of 200 points/cm was sufficient (pixels 50 μ × 50 μ) for the noise amplitudes to depend mainly on the thickness of the traces. For the automatic system with a flat bed scanner used today, the typical resolution is 300, 600 or 1200 points/inch (dpi). Then, for 1 cm/s film speed and 600-dpi scan, the resolution is 236 points/s implying Nyquist frequency of 118 Hz which is more than sufficient for most recorded accelerograms.

The "noise acceleration traces" were created as follows. For several SMA-1 accelerograms, the pair of baselines was digitized and processed (scaled, instrument and baseline-corrected, and band-pass filtered between 0.07 and 25 Hz) considering one of them as a "zero" acceleration trace and the other one as a zero baseline, and response and Fourier amplitude spectra were finally calculated. Figure 4 (Lee and Trifunac, 1990) shows smoothed average spectral amplitudes for five damping values (0, 2, 5, 10 and 20 percent of critical) for 45 and 90 s long records. The overall spectrum amplitudes are similar to those for the automatic digitization system with an Optronics scanner (Trifunac and Lee, 1979).

A comparison of spectral amplitudes of noise of various recorders with those typical of recorded strong earthquake ground motion for magnitudes $4 < M < 7$ and for frequencies $0.1 < f < 20$ Hz is shown in Figure 5. It also shows nominal noise amplitudes for SMA-1, QDR and PDR accelerographs (Trifunac and Todorovska, 2001b).

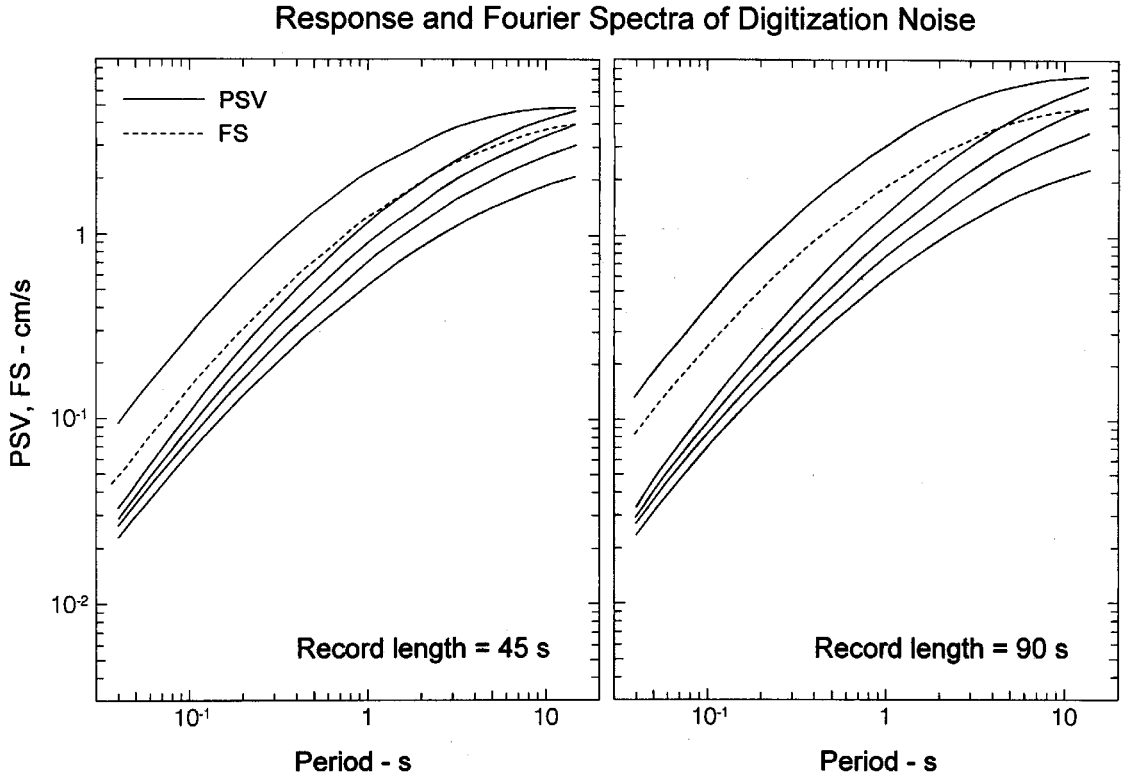

Fig. 4 Fourier spectra (dashed lines) and response spectra (solid lines) for damping ζ_0 = 0, 0.02, 0.05, 0.10 and 0.20 (top to bottom), for records 45 seconds long (left) and 90 seconds long (right)

5. Capabilities of the Most Recent Automatic Digitization System

The current capabilities of the automatic digitization system, last upgraded in 2000/2001, have the following new features and capabilities:

(1) digitization with selectable 600-1200 (up to 2000) dpi resolution and up to 4096 levels of gray (upgraded from 256 levels of gray),

(2) possibility to scan up to 9 (8.5x11 inches) "pages" of a record sequentially, equivalent to 250 s (= 4.167 min) record length, for typical 1 cm/s film speed,

(3) possibility to scan wide (11 inches = 28 cm) records from central recording system with 13 or more acceleration traces.

The above increase in resolution of scanning equipment does not necessarily indicate an improvement in the quality of digitized accelerogram (Trifunac et al., 1999b), but may help identify high frequency content of a record.

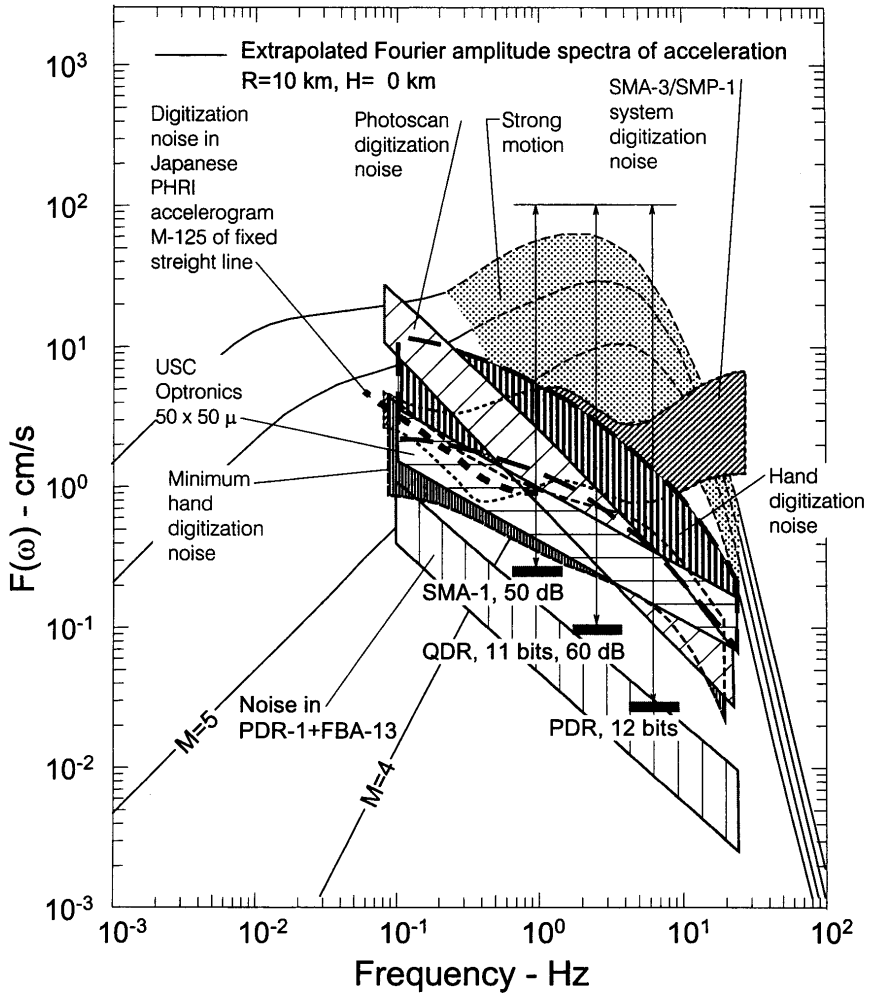

Fig. 5 Comparison of different noise spectra associated with different recording instruments and different methods of digitization (modified from Trifunac and Todorovska, 2001b)

6. Advanced Digitization and Raw Data Pre-processing

6.1 Accurate Selection of the Trace Onset

The position of the first digitized point of an acceleration trace determines the origin of its time coordinate. Because of the common trigger mechanism, all the three traces (*L*, *V* and *T*) start to be recorded simultaneously, but if the first point is not digitized properly, there will be a time delay in the digitized time series. Synchronization of the origin time and of the running time scales for all the components on a film record is crucial for many applications, for example in inverse analyses of the earthquake source mechanism ("random" time delays in the digitized data affect the numerical stability of the inversion), applications that require linear combination of the recorded components of motion, such as computation of the radial and transverse components of motion (affect the accuracy of peak amplitudes in the rotated directions; Todorovska and Trifunac, 1997), in analyses of building response from wave propagation viewpoint, or in correction of accelerograms for cross-axis sensitivity and transducer misalignment (these corrections are meaningless unless the three components are synchronized; Todorovska, 1998; Todorovska et al., 1995, 1998; Wong and Trifunac, 1977).

One way to reduce these errors is intervention by the operator who can choose manually the first point, but this is time consuming and is subjective. To increase the efficiency of this step and to eliminate subjectivity, in 1994 we introduced an algorithm that determines automatically the "best" starting point for each acceleration trace. This algorithm was tested on hundreds of accelerograms, and was found to be successful (error less than one pixel) in about 95% of cases). Difficult cases would still require operator intervention (Trifunac et al., 1999b). An example of a circumstance that can complicate this task is when

the gap between the end of the previous record and the onset of the current record is too short or the traces overlap, so that they appear as continuous on the scanned image. When such traces are displaced (i.e. the trace starts with a large amplitude), this problem is eliminated (Trifunac et al., 1999b).

6.2 Non-uniform Film Speed

The nominal film speed for typical strong motion accelerographs is 1 cm/s (SMA-1, CR-1). For the M02 accelerograph used in New Zealand, which records on a 35 mm film, the actual film speed is 1.5 cm/s, which is equivalent to 3 cm/s for a 70 mm film (SMA-1). Increasing the film speed improves the resolution and accuracy of digitization of the high frequency accelerations not only in time, but also in amplitude. The old AR-240 accelerograph (which recorded the Pacoima Dam accelerogram during the 1971 San Fernando, California, earthquake) had a recording speed of 2 cm/s (equivalent to 0.5 cm/s on a 70 mm film; Hudson, 1970).

Most instruments have one or two relays which produce two-pulses-per-second (2PPS) signals recorded along the top and bottom edges of the film or paper. About 20 years ago, one of these relays was converted to work with a local clock which produced a binary code of the Julian day, hour, minute and second, every 10 s. At first, it was believed that absolute trigger time was not necessary for recorded strong ground motions (Hudson, 1970), but since it was first introduced in the early 1970s (Dielman et al., 1975), it opened many new possibilities for advanced wave propagation studies in strong motion seismology.

The 2PPS signal accuracy is believed to be within ~ l% of nominal, but it is rarely calibrated. Since the early 1970s, we have assumed that the time coordinate of analog records is scaled more accurately using 2PPS pulses (generated electronically) rather than by the nominal speed of the film (driven mechanically), and have used it to correct for minor variations in the film speed (Lee and Trifunac, 1990; Trifunac and Lee, 1973, 1979). Exceptions are records for which the 2PPS and absolute clock relays malfunctioned simultaneously (e.g. see Trifunac et al., 1999a).

Occasionally, the film speed may experience abrupt changes and stalls. This is caused by friction in the film driving mechanism, friction in the film cassette or by faulty motors, and in general cannot be corrected uniquely. The duration of short stalls can be estimated by measuring the shortening of the distance between consecutive pulses of the 2PPS signal. The digitized data then can be corrected approximately, by inserting “gaps” into the scanned bitmap image, and by recreating manually the missing portion of the traces (Lee and Trifunac, 1984). A description of processing an accelerogram with many stalls can be found in Trifunac et al. (1999a).

DATA PROCESSING

1. Previous Work

The data processing of strong-motion accelerograms evolved alongside with digitization of analog records, after the first earthquake accelerogram was recorded on March 10, 1933, during the Long Beach earthquake in California. This remarkable event, which triggered numerous pioneering accomplishments in strong motion instrumentation, was commemorated during the 50th anniversary of strong-motion seismology at the University of Southern California in Los Angeles (Hudson, 1984). Through the 1930s, 1940s and 1950s, there were only a dozen or so recorded “significant” strong motion accelerograms (Biot 1941, 1942; Hudson, 1976, 1979). The accelerograph data processing then required lengthy manual calculations, or the use of analog computers (Biot, 1941). The 1960s marked the beginning of the rapid growth in the number of recordings and of the development and use of digital computers. With these, new methods associated with digital data processing slowly gained in speed, accuracy, access and popularity. In the early 1970s, after the 1971 San Fernando earthquake in California, the large number of recorded accelerograms, and the need of many investigators to compare their results on a common basis, finally resulted in the need for a systematic development of routine data processing of strong-motion accelerograms (Hudson et al., 1969, 1971, 1972a, 1972b).

The first systematic development of routine computer programs for processing strong-motion earthquake accelerograms was completed in the early 1970s (Trifunac and Lee, 1973). Almost all of the records then were in analog form and were digitized manually (on Benson-Lehner 099D digitizer), which is the case for the records from the 1971 San Fernando earthquake (Hudson, 1976). The routine data

processing software was then developed for the manual digitization scheme. The computer programs (Trifunac and Lee, 1973) were first written for the IBM 7094 and IBM 360 computers. These programs involved the following steps:

(i) Volume I Processing (scaled data; Hudson et al., 1969): The half-second timing marks are first checked for "evenness" of spacing, and then smoothed by a (1/4, 1/2, 1/4) running average filter. The x-coordinates of each trace are next scaled to units of time in seconds. Each fixed trace (baseline) is smoothed and subtracted from the corresponding acceleration trace, with the y-coordinates subsequently scaled to units $g/10$ ($g = 9.81$ m/s^2).

(ii) Volume II Processing (corrected data; Hudson et al., 1971): The scaled uncorrected Volume I acceleration data is next corrected for instrument response (Trifunac, 1972) and baseline adjustment (Trifunac, 1970, 1971). The data is first low-pass filtered with an Ormsby filter having a cutoff frequency $f_c = 25$ Hz and a roll-off termination frequency $f_t = 27$ Hz. Instrument correction is next performed using the instrument constants. These constants are the natural frequency and ratio of critical damping of the instrument, which is considered as a single-degree-of-freedom system (Trifunac and Hudson, 1970; Todorovska, 1998). These are determined from calibration tests for each accelerograph transducer. The data is then baseline-corrected by a high-pass Ormsby filter. The cutoff and roll-off frequencies of the filter are usually determined from the signal-to-noise ratio of each component (Trifunac and Lee, 1978). The acceleration data is then integrated twice to get velocity and displacement. To avoid long period errors resulting from uncertainties in estimating the initial values of velocity and displacement, the computed velocities and displacements are high-pass filtered at each stage of integration, using the Ormsby filter with the same cutoff and roll-off frequencies as for the corrected accelerogram (Hudson et al., 1971).

(iii) Volume III Processing (response spectra; Hudson et al., 1972a): Using an approach based on an exact analytical solution of the Duhamel integral for successive linear segments of excitation, the Fourier and response spectra for up to 91 periods and 5 damping ratios are calculated. The times of maximum response for all periods and damping ratios are also recorded (Lee and Trifunac, 1979, 1986).

Following the development of the automatic digitization system (Trifunac and Lee, 1979), the above computer programs, originally developed in 1969/70 (Trifunac and Lee, 1973), were modified in 1978/79 (Trifunac and Lee, 1979) to run on a Data General mini computer. The new approach, which took advantage of image processing techniques, increased the speed of the overall data processing by one order of magnitude (Figure 1).

(iv) Volume IV Processing (Fourier amplitude spectra; Hudson et al., 1972b): Using the Fast Fourier Transform (FFT) algorithms (Cooley and Tukey, 1965; Udwadia and Trifunac, 1977) for applications that require equally spaced data on Fourier amplitude spectra, Volume IV data were computed and presented in the series of "Blue Book Data Reports" since 1972. This data was used in numerous empirical studies of Fourier spectrum amplitudes. It offered an opportunity to routinely identify significant frequencies in the records using Fisher (1929) test of significance in harmonic analyses. At present, Volume IV data processing is not performed routinely because of the high speed with which FFT can be calculated with modern computers, as required for each particular application.

2. The Current System

In general, the principles and the requirements governing the routine data processing of strong-motion records have changed little, if any, since the early 1970s. However, since then, we have witnessed a remarkable progress in digital signal processing techniques, in their accuracy, efficiency, speed of execution and in the major hardware cost reduction. These improvements have been incorporated into the routine data processing of strong-motion accelerograms (Lee and Trifunac, 1984, 1990). The currently used system, along with the automatic digitization system, runs on a Windows PC.

3. Volume II Low-Pass Filtering

Low-pass filtering is performed to eliminate the high-frequency digitization errors. The design of low-pass filters is well documented in digital signal processing textbooks (Gold and Rader, 1975; Rabiner and Gold, 1975; Hamming, 1977). These filters are divided into two main groups according to their

design: Finite Impulse Reponses (FIR) and Infinite Impulse Response (IIR) filters. The Ormsby filter, first introduced in strong-motion accelerograms processing by Trifunac (1970, 1971), is a FIR filter. The elliptic (Sunder, 1980) and Butterworth (Converse, 1984) filters, also proposed and used in accelerogram data processing, are IIR filters.

Strong motion consists of transient body and of dispersed surface waves, and therefore to preserve its physical nature and enable analyses of its phases, all data processing operations on recorded accelerograms must not alter the original phase. The FIR filters can be designed to have zero phase shift, so as not to introduce a phase shift between the recorded and processed signal. The IIR filters, on the other hand, do introduce phase shift. To "cancel" this phase shift, a time reversal technique has been used (Rabiner and Gold, 1975). However, at the beginning of time series, it takes time for an elliptic filter to "settle" down after a sudden change in the input. The non-recursive Ormesby filter, on the other hand, has much smaller transient response. Because of such problems, and because of instabilities and phase shifts, the recursive filters tend to be used only for very long signals, which are more or less stationary in character. The non-recursive filters are simpler to understand, design, and use, and are more suitable for signals that are more transient in nature, as strong motion accelerograms, for example.

The transfer function of an elliptic IIR filter also has ripples in both the pass-band and stop-band. Ripples are tolerated in the design for optimality in the order of the filter. Processing of strong motion accelerograms involves consecutive application of many filters. Besides the low- and high-pass filtering, the instrument correction also involves application of a differentiation filter twice (to compute the first and second order derivatives of the signal), and the integration performed to compute velocity and displacement involves double application of an integration and a high-pass filter. If the signal passes through M such filters, each with ripple amplitudes $(1 + \varepsilon)$ in the passband, the resulting ripple peaks will have amplitude $(1 + \varepsilon)^M$, and may be confused with real ripples in the data. Ripples in the passband are thus not desirable in signal processing involving many consecutive filters (Lee and Trifunac, 1989). Ripples in the stopband are not desirable for the same reason. This problem can and should be avoided by using filters that vary smoothly throughout their pass-band. A set of design criteria for low-pass filters for processing accelerograms can be found in Lee and Trifunac (1990). A good general discussion of guidelines and a comparison of the performance of FIR and IIR filters can be found in Hamming (1977).

4. Volume II-Instrument Correction

A seismometer or an accelerometer usually records the relative displacement or velocity response of its transducer mass. Instrument correction is then applied to remove the effect of the transducer transfer-function on the recorded signal $y(t)$ and to compute the input ground motion $x(t)$. For most strong-motion accelerographs, the dynamic equation of motion of the transducer as a single-degree-of-freedom system is

$$\ddot{y} + 2\zeta_0\omega_0\dot{y} + \omega_0^2 y = -\ddot{x} \tag{1}$$

where $x(t)$ is the input displacement, $y(t)$ is the relative displacement of the transducer mass, ω_0 is the natural frequency of the transducer, and ζ_0 is the fraction of critical damping. Hence, the instrument correction involves numerical differentiation.

Many differentiation filters are available, including the central difference scheme and other higher-order formulae. The filter used should have zero phase-shift and result in no phase-distortions. The transfer function of the filter should be purely imaginary, as the ideal differentiation filter has transfer-function $H(\omega) = i\omega$. Design criteria for a differentiation filter for instrument correction can be found in Lee and Trifunac (1990).

There are other accelerometers and seismometers with transducers that do not behave as a mechanical single-degree-of-freedom system (Novikova and Trifunac, 1991), and will thus require specialized instrument correction algorithms. Lee and Wang (1983) developed an instrument correction algorithm for the RDZ1-12-66 strong-motion pendulum galvanometer produced in China, and Novikova and Trifunac (1991) developed an algorithm for coupled transducer-galvanometer systems, which have produced a large number of records, for example, in former Soviet Union. Novikova and Trifunac (1992) also developed instrument correction algorithms for a force-balance accelerometer (FBA) (Amini and Trifunac, 1983, 1985; Amini et al., 1991).

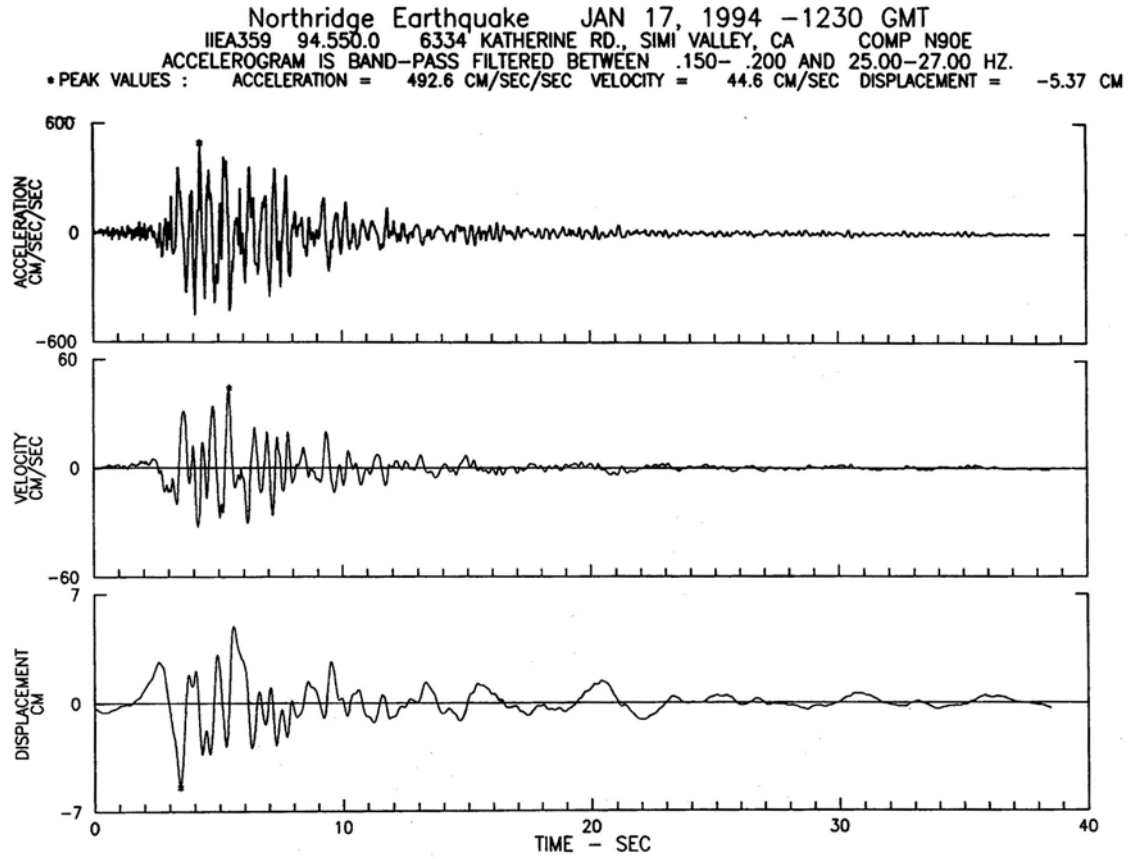

Fig. 6 Typical output from Volume II processing: corrected accelerogram and integrated velocity and displacement versus time

5. Baseline Correction and Noise-Free Frequency Band

Accelerograms low-pass filtered and corrected for the instrument transfer-function are next baseline-corrected by high-pass filtering, to remove the long period recording and processing noise. The record is initially high-pass filtered with cutoff frequency of 0.07 Hz, corresponding to cutoff period of ~14 s which is sufficiently long for most strong-motion accelerograms (Trifunac et al., 1973a, 1973b). The final cutoff frequency is later determined separately for each acceleration trace from the signal-to-noise ratio (Trifunac and Lee, 1979).

For a trace digitized at 200 points/s sampling rate, the Nyquist frequency is 100 Hz. Then, high-pass cutoff frequency of 0.1 Hz implies ratio between the highest and the lowest frequency of 1/1000 and a very small fraction of the whole frequency band of the data. This constitutes a narrow band filtering or a narrow band rejection.

An IIR elliptic/Butterworth filter (Converse, 1984) has been proposed to replace the FIR Ormsby filter (Trifunac and Lee, 1979), but, as discussed earlier, it distorts the phase of the output signal, unless a time reversal technique is used. Lee and Trifunac (1984, 1990) proposed an efficient implementation of narrow-band filtering using the algorithm of Rabiner and Crochiere (1975), which involves decimation followed by interpolation, using FIR filters, and this was implemented in their accelerogram processing software.

The next step is to determine the appropriate high-pass cutoff frequency for each trace, based on the signal-to-noise ratio. When the routine data processing software was first developed, all records were band-pass filtered between 0.07 and 25 Hz (Trifunac, 1971). These cutoff frequencies were based on a detailed study of the digitization error of the system available in the early 1970s (Trifunac et al., 1973a, 1973b), and do not apply to records digitized with different systems. Also, smaller amplitude accelerograms may require a more restrictive lower cutoff frequency, depending on its signal-to-noise ratio (Amini et al., 1987; Lee et al., 1982; Trifunac, 1977; Trifunac and Lee, 1978).

In the early stages of the development of routine accelerogram processing software, it became clear that the optimum cutoff frequencies had to vary from one record to another, if one were to eliminate all the significant noise from the digitized data. Trifunac and Lee (1978) considered a batch of 186 records of uniformly processed earthquake ground acceleration recorded in the western United States of America for the period 1933-1971. These were again band-pass filtered with frequencies predetermined by visual inspection to maximize the signal-to-noise ratio within the band. Of the 186 records or 558 components considered, 69% were originally processed with the standard 15 s (0.07 Hz) long period cutoff, and the remaining 31% with 8 s (0.125 Hz) long period cutoff. Following the requirement for uniform signal-to-noise ratio, as much as 50% of the records routinely filtered at 15 s were refiltered with a shorter long period cutoff ranging from 1 to 15 s. Similarly, about 12% of the records, routinely filtered at 8 s were refiltered with cutoff periods ranging from 1 to 8 s.

In the late 1970s and early 1980s, in the routine data processing software, a subroutine was included that determined automatically the cut-off frequencies for each individual acceleration trace based on the signal-to-noise ratio, and the record was then refiltered. This resulted in processed data with a variable, higher than 0.07 Hz, cutoff frequencies, depending on the amplitudes of the record, which in turn depend on the magnitude of the earthquake, local geology and distance from the source (Lee et al., 1982).

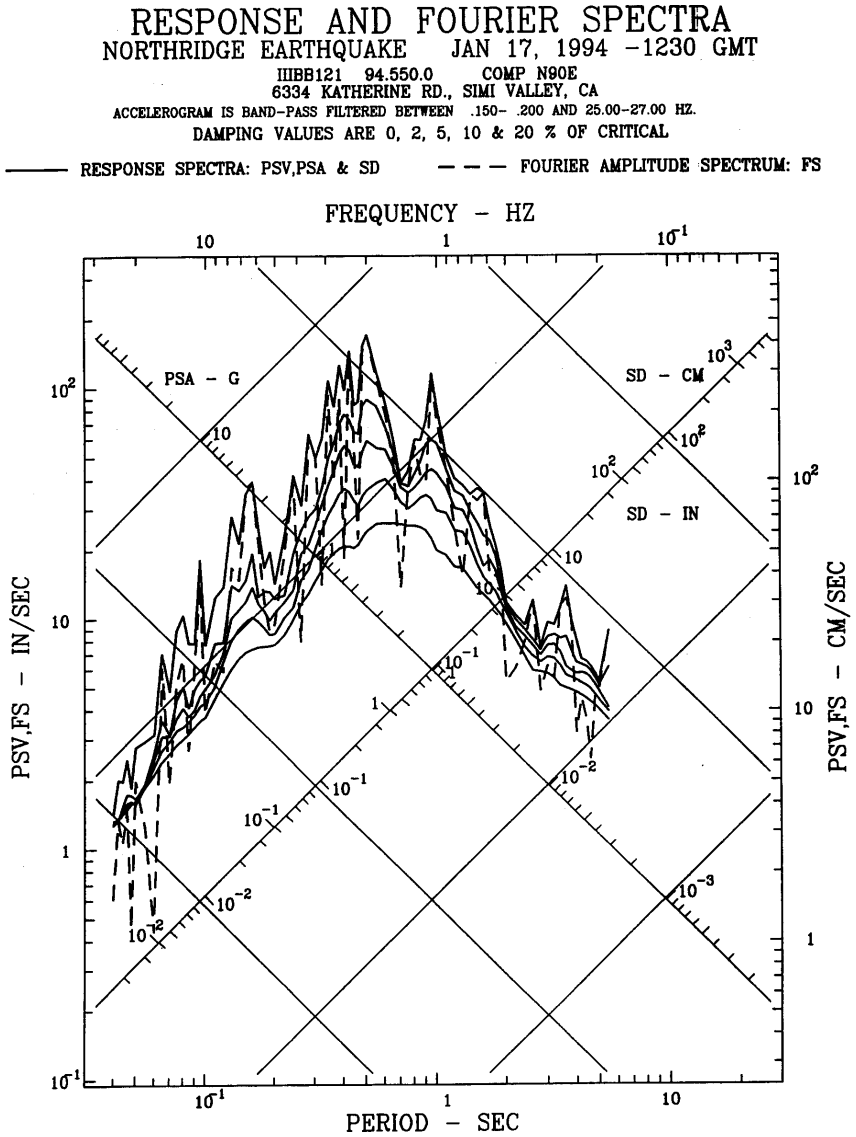

Fig. 7 Typical output from Volume III processing: Fourier (dashed) and pseudo relative velocity spectra for five damping values ζ_0 = 0, 0.02, 0.05, 0.1 and 0.20 (top to bottom)

6. Integration and Response Calculations

The next step is integration of the instrument-corrected and band-pass filtered acceleration twice to get velocity and displacement. Many integration filters are available, including the trapezoidal rule and other higher order formulae. The filter used should have phase $-\pi/2$ as the ideal integrator $H(\omega) = 1/(i\omega)$, so that there is no phase distortion. Sunder (1980) proposed a 7-term integration formulae (Schussler-Iber) which does not have phase $-\pi/2$, thus resulting in phase-distorted output. A set of design criteria for integration of a digital signal, to obtain velocities and displacements from acceleration, can be found in Lee and Trifunac (1990).

There exist efficient algorithms for the calculation of velocity and displacement from acceleration (Lee, 1984, 1990), but we prefer to use the original algorithm (Nigam and Jennings, 1969; Hudson et al., 1971; Trifunac and Udwadia, 1979) based on exact integration of piecewise straight line representation of an accelerogram with equally spaced points. Figure 6 shows a plot of the corrected acceleration, velocity and displacement for one typical component of an earthquake record.

The next step consists of the computation of response spectra at discrete periods and for five damping values (Hudson et al., 1972a). Figure 7 shows a plot of the pseudo relative velocity (PSV), relative displacement (SD), and pseudo acceleration (PSA) response spectra on a tripartite logarithmic plot. Such a tripartite plot is possible because of the relationship between PSV, SD and PSA (Hudson et al., 1972a).

HIGHER-ORDER CORRECTIONS

So far in this paper, the standard data processing algorithms were described, which are suitable for routine, large scale processing of analog strong motion records. For specialized studies requiring higher accuracy, further corrections may be required. In the following, we describe two such corrections.

1. Misalignment and Cross-axis Sensitivity

In routine data processing of three-component acceleration records, it is assumed that the three sensitive axes (longitudinal, transverse and vertical) are mutually perpendicular. Careful tilt table measurements show however that this is not so and that each sensitivity vector can be misaligned by small (few degree) angles (Todorovska, 1998; Todorovska et al., 1995, 1998; Wong and Trifunac, 1977). For accelerometers, which are sensitive to static tilt, the misalignment angles can be measured by simple tilt tests followed by data processing (Todorovska et al., 1995, 1998). These angles then can be used to perform exact corrections of cross-axis sensitivity and misalignment, resulting in corrected accelerations along three mutually orthogonal coordinate axes.

Measurements of the misalignment angles and corrections for misalignment and cross-axis sensitivity have been performed for all instruments of the Los Angeles strong motion network (Todorovska et al., 1998) and for the stations of the Los Angeles Department of Water and Power (Todorovska et al., 1999) for strong motion data recorded during and following Northridge, California earthquake of 17 January, 1994.

2. Corrections for Tilt and Angular Accelerations

Let X_1, X_2 and X_3 be the mutually perpendicular coordinate axes of displacement in longitudinal (L) Transverse (T) and Vertical (V) directions, and let ϕ_1, ϕ_2 and ϕ_3 represent the rotations about X_1, X_2 and X_3 directions. For small transducer deflections $y_i = r_i\alpha_i$ where α_i is the angle of deflection of the *i*-th pendulum from its equilibrium position, and r_i is its corresponding lever arm, the equations of motion of the three penduli of an accelerometer (e.g. SMA-1) are (Todorovska, 1998):

$$\mathrm{L}: \ddot{y}_1 + 2\omega_1\varsigma_1\dot{y}_1 + \omega_1^2 = \ddot{X}_1 + \phi_2 g - \ddot{\phi}_3 r_1 + \ddot{X}_2\alpha_1 \tag{2a}$$

$$\mathrm{T}: \ddot{y}_2 + 2\omega_2\varsigma_2\dot{y}_2 + \omega_2^2 y_2 = -\ddot{X}_2 + \phi_1 g - \ddot{\phi}_3 r_2 + \ddot{X}_1\alpha_2 \tag{2b}$$

$$\mathrm{V}: \ddot{y}_3 + 2\omega_3\varsigma_3\dot{y}_3 + \omega_3^2 y_3 = -\ddot{X}_3 - \ddot{\phi}_1 r_3 - \ddot{X}_2\alpha_3 \tag{2c}$$

where ω_i and ζ_i are respectively the natural frequency and fraction of critical damping of the *i*-th transducer. The second and third terms on the right hand side of Equations (2a) and (2b) represent

contributions from tilting (ϕ_1 and ϕ_2) and angular acceleration ($\ddot{\phi}_3$) to the recorded responses y_1 and y_2. The tilting of an instrument does not contribute to the linearized equation for y_3 (Equation (2c)), but the angular acceleration ($\ddot{\phi}_1$) does. The last terms on the right hand side in all three equations are contributions to the response from cross-axis sensitivity.

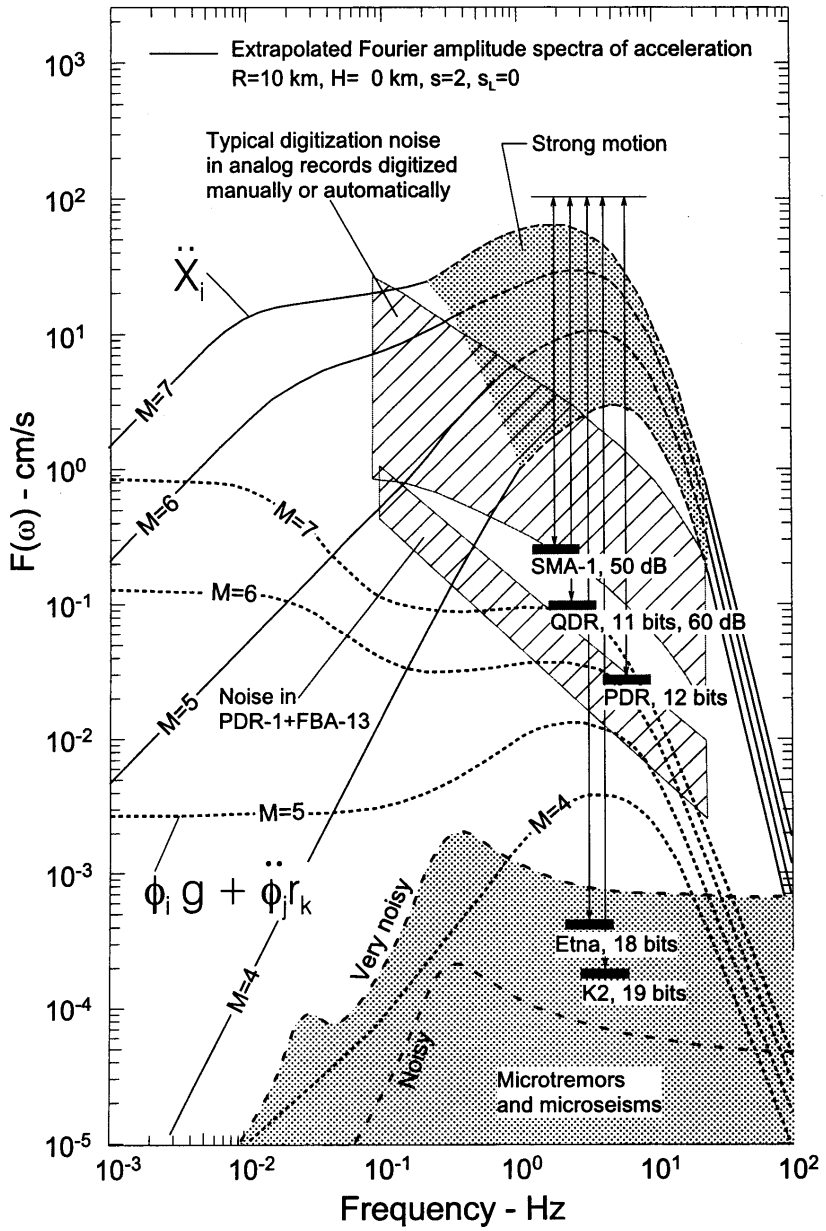

Fig. 8 Comparison of Fourier amplitude spectra of translation, $\ddot{X}_i$ with spectra of contribution from $\phi_i g + \ddot{\phi}_j r_k$, analog digitization noise, digital digitization noise (PDR), and microtremor and microseism noise (redrawn from Trifunac and Todorovska, 2001b)

Figure 8 shows a comparison of Fourier amplitudes of $\ddot{X}_i$ and of $\phi_i g + \ddot{\phi}_j r_k$, at epicentral distance R = 10 km, for magnitudes $4 \le M \le 7$, and for frequencies $10^{-3} \le f \le 10^2$ Hz. It shows that for analog records from SMA-1 accelerographs, for example, the contributions of $\phi_i g + \ddot{\phi}_j r_k$ are smaller than the digitization noise and can be neglected. For recorders with resolution higher than about 12 bits (e.g., PDR-12 bits; Etna-18 bits; K2-19 bits; see Trifunac and Todorovska, 2001b), the contribution of $\phi_i g + \ddot{\phi}_j r_k$ terms cannot be neglected. This means that for the instrument and baseline correction of digital accelerographs, the recorded data on ϕ_1 and $\ddot{\phi}_i$ must be provided simultaneously with the records

of y_i, so that correct $\ddot{X}_i$ can be calculated. Without ϕ_1 and $\ddot{\phi}_i$, accurate estimation of $\ddot{X}_i$ is not possible. In other words, the data from high-resolution digital accelerographs will be represented by the entire right hand side of Equation (2), not just $\ddot{X}_i$. This means that recording with high-resolution (higher than about 12 bits) accelerographs will be meaningful only if all three translations X_i and three rotations ϕ_i are recorded simultaneously (Trifunac and Todorovska, 2001b). Assuming that such recordings are available in future, it will be possible to formulate the required instrument and baseline correction procedures.

DATA DISSEMINATION - EQINFOS SYSTEM

The first computerized dissemination system for strong motion data was the EQINFOS system (Strong Motion Earthquake Data Information System), developed by Lee and Trifunac (1982) in the early 1980s, years before the Internet and modern electronic communication capabilities. It operated on Data General, Eclipse S/130 mini computer. It (1) provided data to the users via ordinary telephone lines and acoustic modems, (2) allowed outside users to use the data processing software at USC laboratory and (3) provided means for remote data digitization and processing. Software was provided for off-line plotting, printing and data storage. The system also maintained a searchable uniformly processed strong motion database on disk (Trifunac and Lee, 1978; Trifunac, 1977). This database could be searched by selecting geographic coordinates, time of occurrence, geologic and soil site conditions at the recording site, peak amplitudes, magnitude range, or Intensity range, for example.

We also initiated the development of EQINFOS-compatible strong motion databases for different parts of the world. In the first set, we included all strong motion data recorded at free-field stations in the western U.S. between 1933 and 1984 (Lee and Trifunac, 1987). This was followed by a database recorded in former Yugoslavia, between 1975 and 1983 (Jordanovski et al., 1987), in Bulgaria, between 1981 and 1987 (Nenov et al., 1990), in India between 1967 and 1991 (Gupta et al., 1993; Chandrasekaran et al., 1993), and the Northridge 1994 earthquake and its major aftershocks, in California (Todorovska et al., 1999).

By extensive empirical studies based on these databases during the past 20 years, we found that the EQINFOS data formats and the accompanying cross-referencing tables are suitable and complete for most of the modern earthquake engineering research. With rapid developments of the Internet and wide-spread use of the World Wide Web, at present we are expanding and generalizing the use of EQINFOS concept to the modern web applications. Our web site at http://www.usc.edu/dept/civil_eng/Earthquake_Earthquake_eng/ is now used to store and distribute the strong motion data, we recorded with Los Angeles strong motion array (Trifunac and Todorovska, 2001a), or gathered from other sources.

CONCLUSIONS

In this paper, we summarized the historical developments that led to the present capabilities for digitization of analog film or paper records, data processing and dissemination. In future with further developments in digital recording, the need for image processing of analog records will diminish, but considering the volume of analog recordings so far, it may take many years before all this data is available in digital form.

REFERENCES

1. Amini, A. and Trifunac, M.D. (1983). “Analysis of a Feedback Transducer”, Report 83-03, Department of Civil Engineering, University of Southern Calif., Los Angeles, California, U.S.A.
2. Amini, A. and Trifunac, M.D. (1985). “Analysis of a Force Balance Accelerometer”, Int. J. Soil Dynamics and Earthquake Eng., Vol. 4, No. 2, pp. 82-90.
3. Amini, A., Trifunac, M.D. and Nigbor, R.L. (1987). “A Note on the Noise Amplitudes in Some Strong Motion Accelerographs”, Int. J. Soil Dynamics and Earthquake Eng., Vol. 6, No. 3, pp. 180-185.

4. Amini, A., Hata, O. and Trifunac, M.D. (1991). "Experimental Analysis of RJL-1, Chinese Force Balance Accelerometer", Earthquake Engineering and Engineering Vibration, Vol. 11, No. 1, pp. 77-88.
5. Biot, M.A. (1932). "Vibrations of Building during Earthquake", Chapter II in Ph.D. Thesis No. 259 entitled "Transient Oscillations in Elastic Systems", Aeronautics Department, Calif. Inst. of Tech., Pasadena, California, U.S.A.
6. Biot, M.A. (1933). "Theory of Elastic Systems Vibrating under Transient Impulse with an Application to Earthquake-Proof Buildings", Proc. National Academy of Sciences, Vol. 19, No. 2, pp. 262-268.
7. Biot, M.A. (1934). "Theory of Vibration of Buildings during Earthquake Stresses", Bull. Seism. Soc. Am., Vol. 31, No. 2, pp. 151-171.
8. Biot, M.A. (1941). "A Mechanical Analyzer for the Prediction of Earthquake Stresses", Bull. Seism. Soc. Am., Vol. 31, No. 2, pp. 151-171.
9. Biot, M.A. (1942). "Analytical and Experimental Methods in Engineering Seismology", ASCE Transactions, Vol. 108, pp. 365-408.
10. Caughey, T.K., Hudson, D.E. and Powell, R.V. (1960). "The C.I.T. Mask II Response spectrum Analyzer for Earthquake Engineering Studies", Proc. Second World Conf. on Earthquake Eng., Vol. II, pp. 1137-1148.
11. Chandrasekaran, A.R., Das, J.D., Trifunac, M.D., Todorovska, M.I., Lee, V.W. (1993). "Strong Earthquake Ground Motion Data in EQINFOS for India: Part 1B", Report CE 93-04, Dept. of Civil Eng., Univ. of Southern California, Los Angeles, California, U.S.A.
12. Converse, A. (1984). "AGRAM: A Series of Computer Programs for Processing Digitized Strong-Motion Accelerograms", Open-File Report 84-525, U.S. Geological Survey.
13. Cooley, J.W. and Tukey, J.W. (1965). "An Algorithm for the Machine Calculation of Complex Fourier Series", Math. Comput, Vol. 19, pp. 297-301.
14. Dielman, R.J., Hanks, T.C. and Trifunac, M.D. (1975). "An Array of Strong Motion Accelerographs in Bear Valley, California", Bull. Seism. Soc. Am., Vol. 65, pp. 1-12.
15. Fisher, R.A. (1929). "Test of Significance in Harmonic Analysis", Proc. Royal Soc. A, Vol. 125, pp. 54-59.
16. Gold, B. and Rader, C.M. (1975). "Digital Processes of Signals", McGraw Hill, New York, U.S.A.
17. Gupta, I.D., Rambabu, V., Joshi, R.G., Trifunac, M.D., Todorovska, M.I. and Lee, V.W. (1993). "Strong Earthquake Ground Motion Data in EQINFOS for India : Part 1A", Report CE 93-03, Dept. Civil Eng., Univ. of Southern Calif., Los Angeles, California, U.S.A.
18. Hamming, R.W. (1977). "Digital Filters", Prentice Hall, New Jersey, U.S.A.
19. Heck, N.H., McComb, H.E. and Ulrich, F.P. (1936). "Strong Motion Program and Tiltmeters", Chapter 2 in "Earthquake Investigations in California 1934-1935", U.S. Department of Commerce, Coast and Geodetic Survey, Washington, D.C., U.S.A., pp. 4-30.
20. Hudson, D.E. (1970). "Ground Motion Measurements in Earthquake Engineering", in Earthquake Engineering (ed. by R.L. Wiegel), Prentice Hall Inc., Englewood Cliffs, New Jersey, U.S.A.
21. Hudson, D.E. (1976). "Strong Motion Earthquake Accelerograms - Index Volume", Earthquake Eng. Research Laboratory, Report EERL 76-02, Calif. Inst. of Tech., Pasadena, California, U.S.A.
22. Hudson, D.E. (1979). "Reading and Interpreting Strong Motion Accelerograms", Monograph Series, Earthquake Eng. Res. Institute, 262 Telegraph Ave., Berkeley, California, U.S.A.
23. Hudson, D.E. (1984). "Golden Anniversary Workshop on Strong Motion Seismology, March 30-31, 1983", Dept. of Civil Eng., Univ. of Southern California, U.S.A.
24. Hudson, D.E., Brady, A.G. and Trifunac, M.D. (1969). "Strong-Motion Earthquake Accelerograms, Digitized and Plotted Data", Report EERL 70-20, Earthquake Engineering Research Laboratory, California Institute of Technology, Pasadena, California, U.S.A., Vol. 1.

25. Hudson, D.E., Trifunac, M.D., Brady, A.G. and Vijayaraghavan, A. (1971). "Strong-Motion Earthquake Accelerograms, II : Corrected Accelerograms and Integrated Velocity and Displacement Curves", Report EERL 71-51, Earthquake Engineering Research Laboratory, , California Institute of Technology, Pasadena, California, U.S.A.
26. Hudson, D.E., Trifunac, M.D. and Brady, A.G. (1972a). "Strong-Motion Accelerograms, III : Response Spectra", Report EERL 72-80, Earthquake Engineering Research Laboratory, California Institute of Technology, Pasadena, California, U.S.A.
27. Hudson, D.E., Trifunac, M.D., Udwadia, F.E., Vijayaraghavan, A. and Brady, A.G. (1972b). "Strong Motion Earthquake Accelerograms, IV : Fourier Spectra", Report EERL 71-100, Earthquake Engineering Research Laboratory, California Institute of Technology, Pasadena, California, U.S.A.
28. Jordanovski, L., Lee, V.W., Manić, M.I., Olumčeva, T., Sinadinovski, C., Todorovska, M.I. and Trifunac, M.D. (1987). "Strong Earthquake Ground Motion Data in EQINFOS: Yugoslavia, Part I", Report 87-05, Department of Civil Engineering, University of Southern Calif., Los Angeles, California, U.S.A.
29. Lee, V.W. (1984). "A New Fast Algorithm for the Calculation of Response of a Single-Degree-of-Freedom System to Arbitrary Load in Time", Int. J. Soil Dynamics and Earthquake Eng., Vol. 3, No. 4, pp. 191-199.
30. Lee, V.W. (1990). "Efficient Algorithm for Computing Displacement, Velocity, and Acceleration Responses of an Oscillator for Arbitrary Ground Motion", Int. J. Soil Dynamics and Earthquake Eng., Vol. 9, No. 6, pp. 288-300.
31. Lee, V.W. and Trifunac, M.D. (1979). "Time of Maximum Response of Single-Degree-of-Freedom Oscillator for Earthquake Excitation", Report 79-14, Department of Civil Engineering, University of Southern Calif., Los Angeles, California, U.S.A.
32. Lee, V.W. and Trifunac, M.D. (1982). "EQINFOS (The Strong-Motion Earthquake Data Information System)", Report 82-01, Department of Civil Engineering, University of Southern Calif., Los Angeles, California, U.S.A.
33. Lee, V.W. and M.D. Trifunac (1984). "Current Developments in Data Processing of Strong Motion Accelerograms", Report CE 84-01, Dept. of Civil Eng., Univ. Southern California, Los Angeles California, U.S.A.
34. Lee, V.W. and Trifunac, M.D. (1986). "A Note on Time of Maximum Response of Single Degree of Freedom Oscillator to Earthquake Excitation", Int. J. Soil Dynamics and Earthquake Eng., Vol. 5, No. 2, pp. 119-129.
35. Lee, V.W. and Trifunac, M.D. (1987). "Strong Motion Ground Motion Data in EQINFOS: Part I", Report 87-01, Department of Civil Engineering, University of Southern California, Los Angeles, California, U.S.A.
36. Lee, V.W. and Trifunac, M.D. (1989). "A Note on Filtering Strong Motion Accelerograms to Produce Response Spectra of Specified Shape and Amplitude", European Earthquake Eng., Vol. III, No. 2, pp. 38-45.
37. Lee, V.W. and Trifunac, M.D. (1990). "Automatic Digitization and Processing of Accelerograms Using PC", Rep. CE 90-03, Dept. of Civil Eng., Univ. Southern California, Los Angeles, California, U.S.A.
38. Lee, V.W. and Wang, Y.Y. (1983). "On the Instrument Correction of the RDZ-I Strong-Motion Pendulum Galvanometer in China", Earthquake Eng. and Eng. Vibration, Vol. 3, Part 4.
39. Lee, V.W., Trifunac, M.D. and Amini, A. (1982). "Noise in Earthquake Accelerograms", Proc. ASCE, Eng. Mech. Div., Vol. 108, pp. 1121-1129.
40. Nenov, D., Georgiev, G., Paskaleva, I., Lee, V.W. and Trifunac, M.D. (1990). "Strong Earthquake Ground Motion Data in EQINFOS: Accelerograms Recorded in Bulgaria between 1981 and 1987", Bulg. Academy of Sciences, CLSMEE, Sofia, Bulgaria, also Report 90-02, Dept. of Civil Eng., Univ. Southern California, Los Angeles, California, U.S.A.
41. Nigam, N.C. and Jennings, P.C. (1969). "Calculation of Response Spectra from Strong-Motion Earthquake Records", Bull. Seism. Soc. Am., Vol. 59, pp. 909-922.

42. Novikova, E.I. and Trifunac, M.D., (1991). "Instrument Correction for a Coupled Transducer-Galvanometer System", Report CE 91-02, Dept. of Civil Eng., Univ. Southern California, Los Angeles, California, U.S.A.
43. Novikova, E.I. and Trifunac, M.D. (1992). "Digital Instrument Response Correction for the Force-Balance Accelerometer", Earthquake Spectra, Vol. 8, No. 3, pp. 429-442.
44. Rabiner, L.R. and Chochiere, R.E. (1975). "A Novel Implementation for Narrow-Band FIR Digital Filters", IEEE Trans. on Acoustics, Speech and Signal Processing, Vol. ASSP 23, No. 5, pp. 457-464.
45. Rabiner, L.R. and Gold, B. (1975). "Theory and Application of Digital Signal Processing", Prentice Hall, New Jersey, U.S.A.
46. Sunder, S. (1980). "On the Standard Processing of Strong-Motion Earthquake Signals", Research Report R80-38, School of Engineering, Mass. Inst. of Tech., Cambridge, Mass., U.S.A.
47. Todorovska, M.I. (1998). "Cross-Axis Sensitivity of Accelerographs with Pendulum like Transducers: Mathematical Model and the Inverse Problem", Earthquake Eng. and Structural Dynamics, Vol. 27, No. 10, pp. 1031-1051.
48. Todorovska, M.I. and Trifunac, M.D. (1997). "Amplitudes, Polarity and Time of Peaks of Strong Ground Motion during the Northridge, California Earthquake", Soil Dynamics and Earthquake Engineering, Vol. 16, No. 4, pp. 235-258.
49. Todorovska, M.I., Trifunac, M.D., Novikova, E.I. and Ivanovic, S.S. (1995). "Correction for Misalignment and Cross Axis Sensitivity of Strong Earthquake Motion Recorded by SMA-1 Accelerographs", Report 95-06, Dept. of Civil Eng., Univ. Southern California, Los Angeles, California, U.S.A.
50. Todorovska, M.I., Trifunac, M.D., Novikova, E.I. and Ivanovic, S.S. (1998). "Advanced Accelerograph Calibration of the Los Angeles Strong Motion Array", Earthquake Eng. and Struct. Dynamics, Vol. 27, No. 10, pp. 1053-1068.
51. Todorovska, M.I., Trifunac, M.D., Lee, V.W., Stephens, C.D., Fogelman, K.D., Davis, C. and Tognazzini, R. (1999). "The M_L = 6.4 Northridge, California, Earthquake and Five M > 5 Aftershocks between 17 January and 20 March 1994 - Summary of Processed Strong Motion", Report CE 99-01, Dept. of Civil Engrg, Univ. of Southern California, Los Angeles, California, U.S.A.
52. Trifunac, M.D. (1970). "Low Frequency Digitization Errors and a New Method for Zero Baseline Correction of Strong Motion Accelerograms", Report EERL 70-07, Earthquake Engineering Research Laboratory, California Institute of Technology, Pasadena, California, U.S.A.
53. Trifunac, M.D. (1971). "Zero Baseline Correction of Strong-Motion Accelerograms", Bull. Seism. Soc. Am., Vol. 61, pp. 1201-1211.
54. Trifunac, M.D. (1972). "A Note on Correction of Strong-Motion Accelerograms for Instrument Response", Bull. Seism. Soc. Am., Vol. 62, pp. 401-409.
55. Trifunac, M.D. (1977). "Uniformly Processed Strong Earthquake Ground Accelerations in the Western United States of America for the Period from 1933 to 1971: Pseudo Relative Velocity Spectra and Processing Noise", Report CE 77-04, Department of Civil Engineering, University of Southern Calif., Los Angeles, California, U.S.A.
56. Trifunac, M.D. (1980). "Recent Developments in Automatic Digitization of Analog Film Records", Proc. 7th World Conference on Earthquake Engineering, Istanbul, Turkey, Vol. 2, pp. 545-552.
57. Trifunac, M.D. and Brune, J.N. (1970). "Complexity of Energy Release during Imperial Valley, California, Earthquake of 1940", Bull. Seism. Soc. Am., Vol. 60, pp. 137-160.
58. Trifunac, M.D. and Hudson, D.E. (1970). "Laboratory Evaluation and Instrument Corrections of Strong Motion Accelerographs", Report EERL 70-04, Earthquake Engineering Research Laboratory, California Institute of Technology, Pasadena, California, U.S.A.
59. Trifunac, M.D. and Hudson, D.E. (1971). "Analysis of the Pacoima Dam Accelerogram - San Fernando, California, Earthquake of 1971", Bull. Seism. Soc. Am., Vol. 61, No. 5, pp. 1393-1411.
60. Trifunac, M.D and Lee, V.W. (1973). "Routine Computer Processing of Strong Motion Accelerograms", Report EERL 73-03, Earthquake Eng. Res. Lab., Calif. Inst. of Tech., Pasadena, California, U.S.A.

61. Trifunac, M.D. and Lee, V.W. (1974). "A Note on the Accuracy of Computed Ground Displacements from Strong-Motion Accelerogram", Bull. Seism. Soc. Am., Vol. 64, pp. 1209-1219.
62. Trifunac, M.D. and Lee, V.W. (1978). "Uniformly Processed Strong Earthquake Ground Accelerations in the Western United States of America for the Period from 1933 to 1971: Corrected Acceleration, Velocity and Displacement Curves", Report CE 78-01, Dept. of Civil Engr., Univ. of Southern California, Los Angeles, California, U.S.A.
63. Trifunac, M.D. and Lee, V.W. (1979). "Automatic Digitization and Processing of Strong Motion Accelerograms : II and I", Report 79-15, Dept. of Civil Eng., Univ. of Southern California, Los Angeles, California, U.S.A.
64. Trifunac, M.D. and Todorovska, M.I. (2001a). "Evolution of Accelerographs, Data Processing, Strong Motion Arrays and Amplitude and Spatial Resolution in Recording Strong Earthquake Motion", Soil Dynamics and Earthquake Eng., Vol. 21, No. 6, pp. 537-555.
65. Trifunac, M.D. and Todorovska, M.I. (2001b). "A Note on Useable Dynamic Range in Accelerographs Recording Translation", Soil Dynamics and Earthquake Eng., Vol. 21, No. 4, pp. 275-286.
66. Trifunac, M.D. and Udwadia, F.E. (1979). "Effect of Initial Base Motion on Response Spectra", Proc. ASCE, Eng. Mech. Div., Vol. 105, pp. 204-206.
67. Trifunac, M.D., Udwadia, F.E. and Brady, A.G. (1971). "High Frequency Errors and Instrument Corrections of Strong-Motion Accelerograms", Report EERL 71-05, Earthquake Engineering Research Laboratory, California Institute of Technology, Pasadena, California, U.S.A.
68. Trifunac, M.D., Udwadia, F.E. and Brady, A.G. (1973a). "Analysis of Errors in Digitized Strong-Motion Accelerograms", Bull. Seism. Soc. Am., Vol. 63, pp. 157-187.
69. Trifunac, M.D., Udwadia, F.E. and Brady, A.G. (1973b). "Recent Developments in Data Processing and Accuracy Evaluations of Strong Motion Acceleration Measurements", Proc. 5th World Conf. Earthquake Engineering, Rome, Italy, Vol. I, pp. 1214-1233.
70. Trifunac, M.D., Todorovska, M.I. and Lee, V.W. (1999a). "The Rinaldi Strong Motion Accelerogram of the Northridge California Earthquake of 7 January, 1994", Earthquake Spectra, Vol. 14, No. 1, pp. 225-239.
71. Trifunac, M.D., Todorovska, M.I. and Lee, V.W. (1999b). "Common Problems in Automatic Digitization of Strong Motion Accelerograms", Soil Dynamics and Earthquake Eng., Vol. 18, No. 7, pp. 519-530.
72. Udwadia, F.E. and Trifunac, M.D. (1977). "A Note on the Estimation of the Fourier Amplitude Transforms", Report 77-01, Department of Civil Engineering, University of Southern Calif., Los Angeles, California, U.S.A.
73. Wong, H.L. and Trifunac, M.D. (1977). "Effects of Cross-Axis Sensitivity and Misalignment on Response of Mechanical-Optical Accelerographs", Bull. Seism. Soc. Am., Vol. 67, pp. 929-956.

ISET Journal of Earthquake Technology, Paper No. 418, Vol. 39, No. 1-2, March-June 2002, pp. 73-91

INVERSE STUDIES OF THE EARTHQUAKE SOURCE MECHANISM FROM NEAR-FIELD STRONG MOTION RECORDS

L. Jordanovski* and M.I. Todorovska**

* Seismological Observatory, Faculty of Natural Sciences and Mathematics
St. Cyril and Methodius University, P.O. Box 422, Skopje 91 000, Republic of Macedonia

** Department of Civil Engineering
University of Southern California, Los Angeles, California 90089-2531, U.S.A.

ABSTRACT

This paper presents a review of finite fault modeling, i.e. inversion of the earthquake source mechanism using near-source strong motion records as input. The first earthquakes for which there was adequate strong motion data for such studies were the 1966 Parkfield and 1971 San Fernando, California earthquakes. Since then, the finite fault modeling has become an integral part of the modern earthquake studies. Knowledge of the features of the earthquake source mechanism, as retrieved from near-field strong motion records, is valuable for understanding the physical processes related to brittle release of tectonic strain during earthquakes, and for prediction of strong ground motion from future earthquakes in seismic design of structures. The paper includes a review of (1) the published literature on this topic, (2) the methodology (theoretical source models and solution of the inverse problem) with emphasis on the difficulties and limitations, and (3) the strong motion data that has been used as input in these studies. The paper also comments on the source mechanism of submarine earthquakes, slides and slumps, and discusses the possibility of using maregrams for inversion of their source mechanism.

KEYWORDS: Earthquake Source Mechanism, Inverse Problem, Near-Field Strong Motion Data, Tsunami Sources

INTRODUCTION

There are many scientific reasons why detailed knowledge of the earthquake source is valuable, but the destructive effects of earthquakes are a sufficient driving force to learn as much as possible about their nature and effects. Because direct measurement of the source activity is not feasible, one can learn about the source only from distant (weak motion) and near (strong-motion) records. The inversion can be associated with different source parameters, depending on the mathematical model, but ultimately the goal is to learn as much as possible about the nature of the source. In earthquake engineering, understanding of the earthquake source is important for prediction of ground motion from future possible earthquakes, which is needed for seismic design of structures.

In the last several decades, much research has been done in strong motion seismology, which has led to better understanding of the nature of earthquake source. The early studies focused on determining the orientation of fault plane. An important factor in the further development of source mechanism research was the deployment of strong-motion accelerographs. Developed mainly for engineering purposes, to measure the seismic forces in structures, the accelerographs are now the main source of near-field data used to study the earthquake source (Trifunac and Todorovska, 2001), and have contributed significantly to the earthquake source investigations.

The problem of characterizing the earthquake source from recorded data is an inverse type of problem, i.e. one in which the input of a system has to be determined from the output. The system function here describes the modification of the motion radiated from the source by the propagation path. A major difficulty in finding a unique solution to this problem is detailed specification of the system function. Even though the associated wave propagation phenomena are well understood at this time, too detailed modeling of the system function would (1) make the inverse problem too complex to solve numerically, and (2) even be useless for practical applications, because the three-dimensional geologic structure along the propagation path is usually known only on a rough scale. One remedy for this problem is to use records (system output) from stations very close to the fault, which are least influenced by the

propagation path. The likelihood of recording many such records for every damaging earthquake, however, is not very high because the exact time and place of occurrence of such earthquakes is not known, and it is still prohibitively expensive to saturate the earth with sufficiently dense strong motion arrays. Hence, the propagation path effects have to be included in the model. Because of these constraints, the system function implemented in the model is only an approximation of the real world, and cannot predict all the features contained in the recorded motions (system output). This problem is treated as "noise" in the data. Another type of noise results from approximations due to the finite arithmetics of the digital computers. All of this leads to the inverse problem being "ill-posed". The finite source modeling, hence, reduces mathematically to a solution of an inherently ill-posed inverse problem, which does not have a unique solution. Solving this problem means finding an acceptable solution, using some regularization techniques and imposing physical constraints.

This paper presents a review of the developments in seismic source inversion using near-source records, typically recorded by the strong motion accelerograph networks. This problem is also known as finite source modeling (the source has a finite size), in contrast to point source modeling in the studies that use distant records, typically recorded by the seismological networks. The paper first reviews published literature on this topic, which is followed by a review of the methodology, including theoretical source models and formulation and solution of the inverse problem (which, for a number of reasons mentioned in the preceding paragraphs, is ill-posed). Finally, as the progress in finite source inversion has been strongly conditioned on the quantity and quality of strong motion records available for such studies, this paper also reviews the developments in recording strong motion data that has been used in such studies. The consideration of other types of data, such as teleseismic body waves, surface waves, and static fault offset and geodetic data, and their use in source inversion is beyond the scope of this paper. This paper also comments on the possibility of source inversion for submarine earthquakes, slides and slumps using maregrams.

HISTORICAL REVIEW

The first useful recordings for inverse analyses, resulting from the systematic deployment of accelerographs in California, were those of the 1966 Parkfield earthquake (Housner and Trifunac, 1967), and of the 1971 San Fernando earthquake (Trifunac and Hudson, 1971). The proximity of the accelerographs to the source (< 50 km) and their ability to record high frequencies (f < 25 Hz) produced records at distances comparable to the wave lengths of the energy radiated by the source, and of the same order as the source dimensions, thus reducing the complications caused by the propagation path. The 1966 Parkfield earthquake was recorded by a linear strong motion array, perpendicular to and near the southeastern end of the surface rupture (Trifunac and Udwadia, 1974). The 1971 San Fernando earthquake was recorded by more than 90 accelerographs, in the free-field or in building basements. Five of these stations (four surrounding the fault, with fault-to-station distances less than 50 km, and one, the Pacoima Dam site, centered above the fault) could be used for inversion of the fault slip (Trifunac, 1974).

Figure 1 illustrates the accumulation of strong motion data for the period between 1933 and 1994. It shows the total number of "free field" strong motion accelerograms recorded during main events (solid points), and the cumulative number of strong motion accelerographs in U.S. and in Japan up to 1980. The times of selected California earthquakes contributing to the strong motion database for southern California are also shown on the same time scale.

The trial and error, forward simulations of recorded strong ground motion near a source first appeared following the Parkfield, California, earthquake of 1966 (Aki, 1968, 1979; Haskell, 1969; Boore et al., 1971; Tsai and Patton, 1973; Niazy, 1973; Boore and Zoback, 1974a; Anderson, 1974, 1976; Kawasaki, 1975; Levy and Mall, 1975; Hartzell et al, 1978; Bouchon, 1979, 1982; Murray, 1967; Luco and Anderson, 1985; Anderson, 1976; Liu and Helmberger, 1983), Borego Mountain earthquake of 1968 (Heaton and Helmberger, 1977) and San Fernando, California earthquake of 1971 (Mikumo, 1973; Boore and Zoback, 1974b; Niazy, 1975; Bouchon and Aki, 1977; Bouchon, 1978; Heaton and Helmberger, 1979). The number of forward studies of more recent well-recorded earthquakes is too large to enumerate here.

The first inverse studies were performed by Trifunac (1974) and by Trifunac and Udwadia (1974). In this pioneering work, the fault surface was divided into subfault segments, and the slip in each segment was chosen to give the best fit, in the least square sense, to the observed displacements integrated from

the recorded accelerograms. The fault geometry, the dislocation velocity, the dislocation rise time and the sense of the dislocation propagation were chosen using other independent information, or by a trial and error procedure. Ten years later, following the Imperial Valley California earthquake of 1979 (Hartzell and Helmberger, 1982; Hartzell and Heaton, 1983), the inverse method for selecting the dislocation amplitudes was revived and further improved (Olson and Apsel, 1982; Jordanovski et al., 1986; Jordanovski and Trifunac, 1990a, 1990b). The reason for this delay was that up to that time, there were very few good quality near-field records that could be used for source inversion, and that the theoretical model of the source required too many *a priori* prescribed parameters, which led to non-uniqueness of the solution.

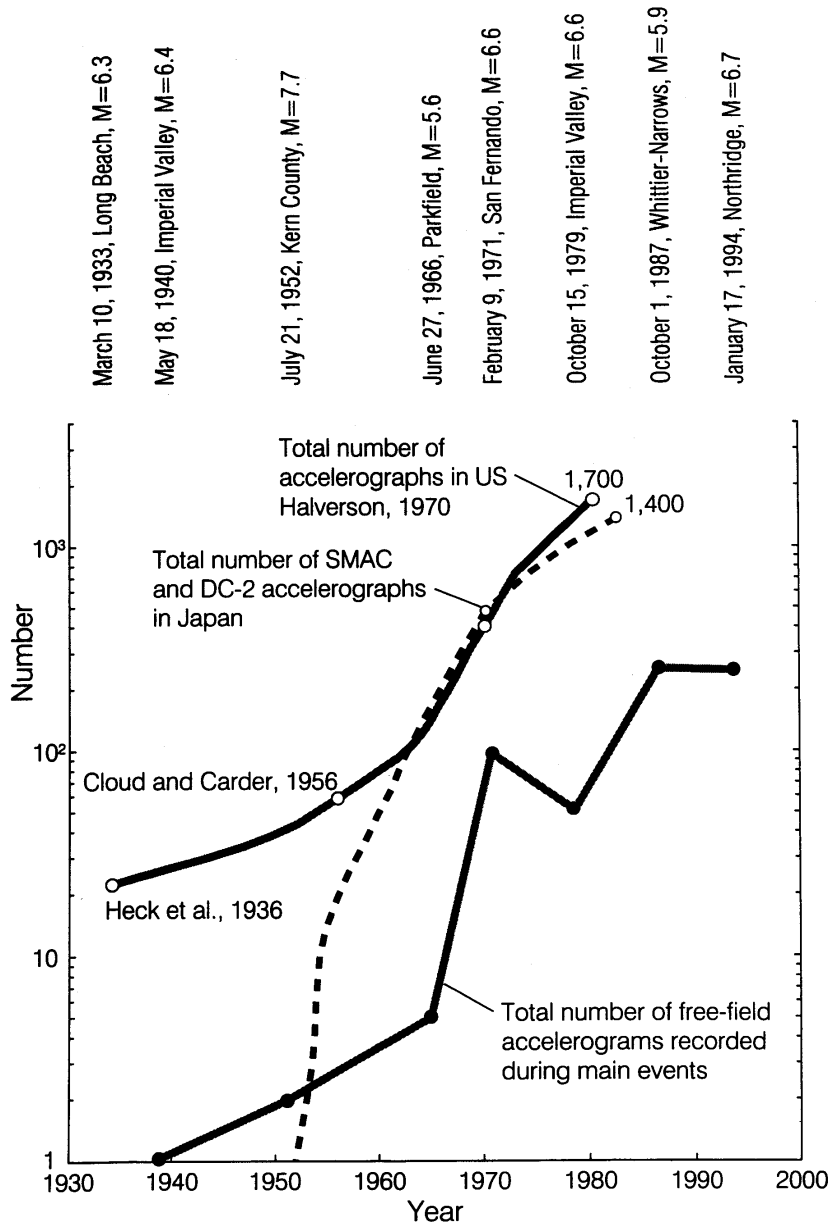

Fig. 1 Total number of "free field" strong motion records recorded during main events (solid points), and the cumulative number of strong motion accelerographs in U.S. and in Japan up to 1980 (selected California earthquakes contributing to the strong motion database for southern California are also shown on the same time scale)

The next well-recorded earthquake which provided data for source inversion was the October 1, 1987, Whittier-Narrows earthquake. This was also the first significant event to be recorded by the Los Angeles strong motion array (Trifunac, 1988; Trifunac and Todorovska, 2001). Together with the stations operated by the United States Geological Survey (USGS) and California Division of Mines and Geology

(SDMG), with many strong motion stations surrounding the source, it provided unprecedented new possibilities for advanced source inversion studies (Hartzell, 1990). Since 1987 and through 1990s, it has became common to have hundreds of accelerograms from major earthquakes (Figure 1), and since the Loma Prieta, 1989, California earthquake, the inversion of the fault slip based on strong motion records has became one of the central topics in the study of all well-recorded major earthquakes.

Other earthquakes, for which inverse studies of the fault slip could be carried out, are: Parkfield, 1966, California (Trifunac and Udwadia, 1974); San Fernando, 1971, California (Trifunac, 1974); Tabas, 1978, Iran (Hartzell and Mendoza, 1991); Imperial Valley, 1989, California (Jordanovski and Trifunac, 1990a,1990b; Hartzell and Heaton, 1983; Olson and Apsel, 1982); Izu-Hanto-Toho-Oki, 1980, Japan (Takeo, 1988); Naganoken-Seibu, 1984, Japan (Takeo, 1987; Takeo and Mikami, 1987); Morgan Hill, 1984, California (Beroza and Spudich, 1988; Hartzell and Heaton, 1986; Mikumo and Miyatake, 1995); Central Chile, 1985, Chile (Mendoza et al., 1994); Michoacan, 1985, Mexico (Mendoza and Hartzell, 1989); North Palm Springs, 1986, California (Hartzell, 1989); Superstition Hills, 1987, California (Wald et al., 1990); Whittier-Narrows, 1987, California (Hartzell, 1990; Hartzell and Iida, 1990; Iida and Hartzell, 1991; Zeng et al., 1993); Loma Prieta, 1989, California (Beroza, 1991; Steidl et al., 1991; Wald et al., 1991); Sierra Madre, 1991, California (Wald, 1992); Landers, 1992, California (Wald and Heaton, 1994a; Hartzell and Liu, 1995); Northridge, 1994, California (Wald and Heaton, 1994b; Wald et al., 1996; Hartzell et al., 1996); and Chi-Chi, 1999, Taiwan (Chi et al., 2001; Ma et al., 2001; Zeng and Chen, 2001; Oglesby and Day, 2001; Wu et al., 2001; Wang et al., 2001).

The source mechanism and near-field studies on land have benefited from the steady accumulation of recorded strong motion data (see Figure 1), and from the relative simplicity of the physical problem (linear wave propagation through a solid, from the source to the receiver). In contrast, the source mechanism studies of submarine earthquakes, slides and slumps, and analyses of near-field wave motion in an ocean (tsunami) caused by the movement of the ocean bottom are, at present, only in the early stages of development. First, the source mechanism studies using tsunami wave recordings are complicated, because the wave propagation through both the solid and fluid must be considered, and second, there are no near-field, open ocean recordings surrounding a tsunami source, so far. Traditional source studies, which used tsunami recordings, at teleseismic distances, were based on a point-source representation of the earthquakes (Ben-Menahem and Rosenman, 1972; Kanamori, 1972; Comer, 1982; Ward, 1980, 1981, 1982; Okal, 1988). More recent studies of localized tsunami run-up (e.g., Heinrich et al., 2000) and of unusually large tsunami run-ups (e.g., Pelayo and Wiens, 1992), suggest that slow earthquakes and submarine slides and slumps can be powerful, but spatially complicated sources of tsunami in the near-field (Todorovska and Trifunac, 2001; Todorovska et al., 2002; Trifunac et al., 2001a, 2001b, 2002a, 2002b; Trifunac and Todorovska, 2002). For "fast" earthquake dislocations, which spread with velocities between 1.5 and 3 km/s, wave propagation in the fluid layer often can be neglected, and the tsunami amplitudes above the source can be assumed to be the same as on the ocean bottom (Geist, 1999; Satake, 1987, 1989). Under those conditions, the presence of the fluid layer may be neglected. For "slow" source processes, when the uplift of the ocean bottom spreads with velocities comparable to the long period tsunami velocity $c_T = \sqrt{gh}$ (g is acceleration due to gravity, and h is the depth of the ocean), the near-field waves in the fluid cannot be ignored and the process of searching for the earthquake source mechanism or for the time-dependent evolution of slides and slumps becomes difficult (Trifunac et al., 2001a, 2001b, 2002a, 2002b, 2002c). Assuming that the records of water wave motion versus time in the near-field become available, it will be possible, in principle, to invert for the time-dependent vertical displacements of the ocean bottom (Trifunac et al., 2002c). After time and space-dependent movement of the ocean bottom has been deciphered, it will then be possible, in the second stage, to perform inverse studies of the causative fault slip, or of slide or slump motions.

REVIEW OF METHODOLOGY

1. Seismic Source Models

Solving an inverse or identification problem consists of matching theoretical results with observations. Hence, the first step is to define a theoretical model of the source process (de Hoop, 1958). This model has to represent the physical process with satisfactory accuracy, or at least to represent its overall characteristics (Luco, 1987).

During the 1950s, for the first time, the problem of seismic source radiation was examined from the viewpoint of dislocation theory, which assumes the source to be a displacement discontinuity across the fault surface. Veedenskaya (1956) defined a system of forces equivalent to a rupture, and a few years later, Knopoff and Gilbert (1959, 1960) presented a detailed analysis of the dislocation problems for modeling a seismic source. They showed that an earthquake could be modeled as a combination of several fundamental problems.

In the 1960s, Maruyama (1963) presented a rigorous formulation of the force-equivalent representation for a general dynamic dislocation, and a year later, Burridge and Knopoff (1964) reformulated the body force equivalents using the theory of distributions. These two approaches showed that the double couple representation is the appropriate way to model the source radiation. The third important paper was that by Haskell (1969) on elastic displacements in the near-field of a propagating fault, using body force equivalents for a full elastic space, a rectangular fault, and a dislocation with a ramp time function, moving with constant velocity along the fault length. Haskell's model has been used with slight modification in almost all source inversion analyses, and will be reviewed in more detail later in this paper.

After 1964, when the foundations of the mathematical models of the source were well established, many analyses have been carried out that use a source model in practical applications. Explicit solutions have been derived for a homogeneous and a layered half-space (Sato, 1975; Apsel, 1979). The solutions then have been used to synthesize near-field and far-field ground motions, and to explain the radiation properties of earthquakes by solving the forward (Aki, 1968), or inverse (Trifunac, 1974) problem. Two basic types of source models were developed, kinematic and dynamic models, as discussed in the following.

1.1 Kinematic Models

The kinematic models assume that the entire dislocation time history is known at each point on the fault. It enables one to calculate the magnitude of the double couple in the body force equivalent representation of the source, and then the response of the surrounding medium, by using an integral representation or the equilibrium equations. Historically, this was the first source model. Due to the relatively simple numerical computations, it has been applied extensively to source inversion problems.

The weakness of the kinematic model is its requirement for *a priori* knowledge of the dislocation time history. The dislocation time history is determined by the interaction of forces in the source region, and physically meaningful functions are selected from the closed form solution for the propagation of a simple shear crack (Kostrov, 1964), or from numerical solutions for dynamic source models (Madariaga, 1976; Das and Aki, 1977; Day, 1982; Archuleta and Frazier, 1978). The basic characteristics of the dislocation time function are: (1) the square root singularity of its derivative with respect to time at the tip of the dislocation (this implies a significant change in slope at the initial time of its growth), and (2) that it reaches the final offset value with no additional jumps or sudden changes in slope.

Aki (1968) used a Heaviside step function as a dislocation time function, and compared synthetic seismograms from a moving dislocation model with those observed (i.e., computed from recorded accelerograms) during the Parkfield earthquake of June 28. In spite of the simplicity of the dislocation time function, his model matched successfully the spike shape of the displacement component perpendicular to the fault trace.

The most common dislocation time function used in kinematic models is the ramp function, first considered by Haskell (1964, 1969), and referred to as “Haskell's source model”. It is described by

$$a(\tau) = \begin{cases} \dfrac{D_0 \tau}{T_R} & 0 < \tau < T_R \\ D_0 & T_R < \tau \end{cases} \tag{1}$$

where D_0 is final dislocation amplitude (offset) and T_R is the rise time. Its main characteristics are: rectangular fault shape, one-dimensional rupture propagation along the fault length with constant velocity, instantaneous rupture propagation along the fault width, ramp time history, and a constant dislocation final offset. This model has been used by many researchers, e.g., by Trifunac (1974) and Trifunac and Udwadia (1974), to estimate the final dislocation offset for the 1971 San Fernando and the 1966 Parkfield

earthquakes, and by a number of Japanese researchers to compute theoretical seismograms (Sato, 1975; Kawasaki et al., 1975; Sudo, 1972).

The other kinematic models are more or less smoother versions of the ramp function, with continuous time derivatives, converging continuously to zero at time t = 0, as opposed to the ramp function which has a discontinuous (rectangular shaped) time derivative at t = 0. For example, Ohnaka (1973) used the combination of a linear and exponential time functions, while Hartzell (1978) used a quadratic dislocation during the rise time.

A qualitatively different dislocation function used by the kinematic models is the one obtained from Kostrov's self-similar solution for shear-crack propagation. However, Anderson and Richards (1975) have shown that the differences in the near-field displacements between the ramp dislocation and the Kostrov's function are small.

1.2 Dynamic Models

The dynamic models describe the fault behavior by prescribing the force and stress distribution over the fault surface. Archambeau (1968) was the first one who formulated the source process as a stress relaxation problem. Under the influence of a pre-stress system, failure occurs within a given region where the material properties suddenly change (plastic flow), and strain energy is released. A part of that energy generates motion of the fault walls, and another part is radiated into the surrounding medium. Obviously, the dynamic approach is a more general and natural one, and the displacement history on the fault is obtained by solving the dynamic problem. Unfortunately, the physical processes that take place in the source region during an earthquake are still mathematically too difficult to model, making it impossible to solve the problem without a great simplification.

The first solution of the stress relaxation problem was presented by Kostrov (1964). He considered motion produced by a uniformly expanding circular shear crack in an infinite homogeneous medium pre-stressed by a constant stress. This problem is self-similar and, although it represents a very simplified earthquake model, it is of great importance for understanding the dislocation behavior. Kostrov presented a closed form solution for the dislocation $a(\xi,t)$

$$a(\xi,t)=\begin{cases} D_0\sqrt{v^2t^2-|\xi|^2} & |\xi|<vt \\ 0 & |\xi|<vt \end{cases} \tag{2}$$

where t is time, ξ is the coordinate of a point on the fault, v is the rupture velocity, and D_0 is a constant depending on the material properties and stress drop. In space, the dislocation is an ellipse, growing hyperbolically with time. Burridge and Willis (1969) extended Kostrov's solution by considering an elliptical fault expanding with different velocities in the prestressed and in the perpendicular direction. Their solution is analogous to Kostrov's self-similar solution.

Richards (1973, 1976) examined the properties of an elliptical crack in detail. His results showed that, in order to have a finite value of the stress in the front of the rupture tip, in the prestressed direction the rupture velocity has to be equal to the Rayleigh velocity, and in the perpendicular direction it must approach the shear wave velocity. However, for other directions, the stresses are still singular. Richards' analysis also showed that the breaking phase causes sudden changes in the particle accelerations, but these changes are almost impossible to notice in the displacement time histories.

Brune (1970) proposed a very simple dynamic model, in which the stress drop occurs instantaneously over the entire fault surface. By solving the equation of motion, he obtained a linear rise of the dislocation amplitudes with time. To account for the effects of the finite dimensions of the fault, Brune introduced an exponential decay factor such that

$$\frac{d}{dt}a(\xi,t)=\frac{\Delta\tau\beta}{\mu}e^{-t/T} \tag{3}$$

and

$$a(\xi,t)=\frac{\Delta\tau\beta T}{\mu}\left(1-e^{-t/T}\right) \tag{4}$$

where, $\Delta\tau$ is the shear stress drop, β is the shear wave velocity of the medium, and μ is Lame constant (shear modulus). Although his model is intuitive, it has proven to be very useful to obtain the global source parameters like seismic moment, stress drop or corner frequency (Trifunac, 1972a, 1972b; Hanks, 1972).

The models reviewed so far did not consider quantitatively the effects due to the finite fault dimensions. By introducing a stopping phase and finiteness of the fault, the dynamic model becomes very complicated to analyze analytically. However, several authors have investigated these effects by using numerical analysis. Madariaga (1976) examined the sudden stopping of a circular rupture, and showed that Kostrov's solution is good up to the time when the effects of the boundaries reach the observation point.

Day (1982) considered a rectangular fault, and his results are similar to those for a circular finite fault except for the point near the edge where he observed a very strong stopping phase in the stress time history. Das and Aki (1977) investigated two-dimensional spontaneous rupture propagation for an in-plane and an anti-plane shear crack.

In general, the dynamic models, so far, have been used mostly to investigate the nature of the dislocation, and have not yet found wide application in source inversion, with the exception of Brune's model. However, they have been very important for the kinematic models by setting realistic criteria for selection of their dislocation time functions.

2. Formulation of the Inverse Problem

Let $\sum$ and V be three-dimensional vector spaces representing the fault surface and the surrounding medium. Then, a mathematical model of the earthquake source radiation can be used either to solve for the displacement at a point $\mathbf{x} \in \mathrm{V}$, given a dislocation $a(\xi,t),\ \xi \in \sum$ (the forward problem), or to solve for the dislocation $a(\xi,t),\ \xi \in \sum,$ given the displacements at points $\mathbf{x} \in \mathrm{V}$ (the inverse problem).

Based on the body force equivalent representation, the displacement at any point $\mathbf{x} \in \mathrm{V}$ due to a displacement discontinuity $a(\xi,t)$ across the fault plane $\sum$, for $t \in (-\infty, T)$, where T is the duration of the source process, is given by

$$u_n(\mathbf{x},t) = -\int_{-\infty}^{t}\int_{\sum} a_i(\xi,\tau) K_{in}(\mathbf{x},\xi,t-\tau)\, d\sum d\tau \tag{5}$$

where

$$K_{in}(\mathbf{x},\xi,t-\tau) = C_{ijpq} n_j(\xi) \frac{\partial}{\partial \xi_q} G^P_{n,q}(x,\xi,t-\tau) \tag{6}$$

is the kernel of the integral Equation (5), which depends on the tensor C_{ijnq} of the material properties of the geological medium; $n_j(\xi)$ is the normal to the fault surface; and $G^P_n(\mathbf{x},\xi,t-\tau)$ is the fundamental solution of a wave created by double couple forces. If one could find the inverse operator $K^{-1}_{in}(\mathbf{x},\xi,t-\tau)$, the dislocation $a(\xi,t)$ would be obtained easily. However, this is not an easy task. The usual approach consists of the following steps:

1 Choosing a kernel (6) consistent with the boundary conditions for integral Equation (5): The kernel $K_{in}(\mathbf{x},\xi,t-\tau)$ given by Equation (6) is the fundamental solution of a wave created by double couple forces, propagating through inhomogeneous media, and can be very complicated and difficult to use in practical applications. Consequently, many researchers have used simpler models of the propagation path, assuming a homogeneous, isotropic, and elastic full-space, and accounting for the free surface effect by doubling the value of the displacement (Trifunac, 1974; Trifunac and Udwadia, 1974; Jordanovski et al., 1986). Some authors have considered layered viscous half-space (Olson and Apsel, 1982; Hartzell and Heaton, 1983), but their results show that in some cases, simple full or half-space solutions are justified considering a trade-off between the complexity of the model and the accuracy of the final results. On the other side, the propagation path effects can be reduced if the recording stations are close to the fault.

The use of empirical Green's functions has attracted much attention. This method consists of representing the ground motion from a large earthquake, by using motions from small and medium earthquakes as kernels, and by convolution of these motions with the dislocation time history. In principle, because the empirical Green's functions intrinsically include propagation path effects and site characteristics, this method has an advantage that strong ground motion from a large earthquake can be predicted with satisfactory accuracy in a wider frequency range. The weakness of this method is the lack of records of small earthquakes in the fault region of a large earthquake, and the lack of small earthquakes with similar source characteristics (such as radiation pattern and dislocation time history, for example) to the ones for the main event.

2. Defining a dislocation function $a(\xi,t)$ *in which the parameters to be assessed are unknown:* In general, there are several basic characteristics of the dislocation which must be specified *a priori*: its temporal behavior, the rupture velocity or more generally the time when it reaches a given point on the fault, the rise time (time it takes to reach the final dislocation value), and the rake (direction) of the dislocation vector $a(\xi,t)$, $\xi \in \sum$. Another set of parameters that have to be specified *a priori* are those that define the geometry and position of the fault. In almost all source studies, the fault is considered as a plane (Olson and Apsel, 1982; Hartzell and Heaton, 1983; Jordanovski et al., 1986), or as a combination of planes to fit a more complex fault geometry (Trifunac, 1974). The only unknown parameters remaining to be estimated by inversion are the final amplitudes of the dislocation. Obviously, many of the parameters of the dislocation and of the fault must be defined *a priori*, or otherwise the inverse problem would be highly non-linear. Consequently, the current inversions of the earthquake source mechanism rely heavily on independent information about the earthquake that can help narrow down the set of admissible solutions.

According to the available theoretical and numerical solutions of dynamic earthquake source models, the dislocation function has the following properties: (a) its time derivative, $\dot{\mathbf{a}}(\xi,t)$, has a finite jump at time t = 0; (b) its time derivative, $\dot{\mathbf{a}}(\xi,t)$, does not change sign, so that the dislocation is monotonic function of time (nondecreasing or nonincreasing), and (c) the final offset value is reached during a specified time, called rise time, T_R, and $\dot{\mathbf{a}}(\xi,t)$ is allowed to have a finite discontinuity at time $t = T_R$. Physically, this means that a sudden stop in the further dislocation growth is allowed. Condition (b) also assumes the possibility that the dislocation velocity is zero at some instant $t < T_R$, which implies that the dislocation can stop and later on continue to grow. The dislocation behavior at time $t < T_R$ is not uniquely defined by condition (b). Hence, there remains a certain amount of ambiguity. Anderson and Richards (1975) showed that quite different fault motions can produce very similar near-field displacements.

3. Solving the forward problem by solving eqns (5): The entire fault is divided into subfaults and, for each subfault, the theoretical displacement at a given point is calculated by convolving the kernel with a dislocation time history of unit amplitude. Many authors have used Haskell or Haskell-like dislocation for this purpose. The main feature of Haskell's model is that the ramp time function for the dislocation allows closed form solution. Further, he assumed that the dislocation occurs instantaneously along the entire fault width W, and propagates with constant velocity v along the fault length. Considering the entire fault as one rectangular plane is obviously a very crude approximation. Consequently, one has to divide the fault into a number of smaller rectangular subfault elements. On each such subfault, the dislocation will be a ramp function in time but with different amplitudes of the final offset. The size of the elements will depend on the desired resolution.

4. Scaling the theoretical displacements to fit the observed displacements: The final theoretical displacement is a superposition of the displacements due to the individual subfaults, and the final dislocation amplitudes of the subfaults are the unknowns. The solution is required to be such that the agreement between the observed and theoretical displacements is "best" in some sense. The method of trial and error was often used to solve the problem, until 1974 when Trifunac (1974) showed that direct inversion is possible. In almost all inversion works, the "best" solution is the least squares (LSQ) solution, i.e. the one that minimizes the sum of the squares of the difference between the recorded and theoretical

data. The LSQ approach can be thought of as a minimization of energy type criterion. If only the final dislocation amplitudes are unknown, the LSQ model becomes linear.

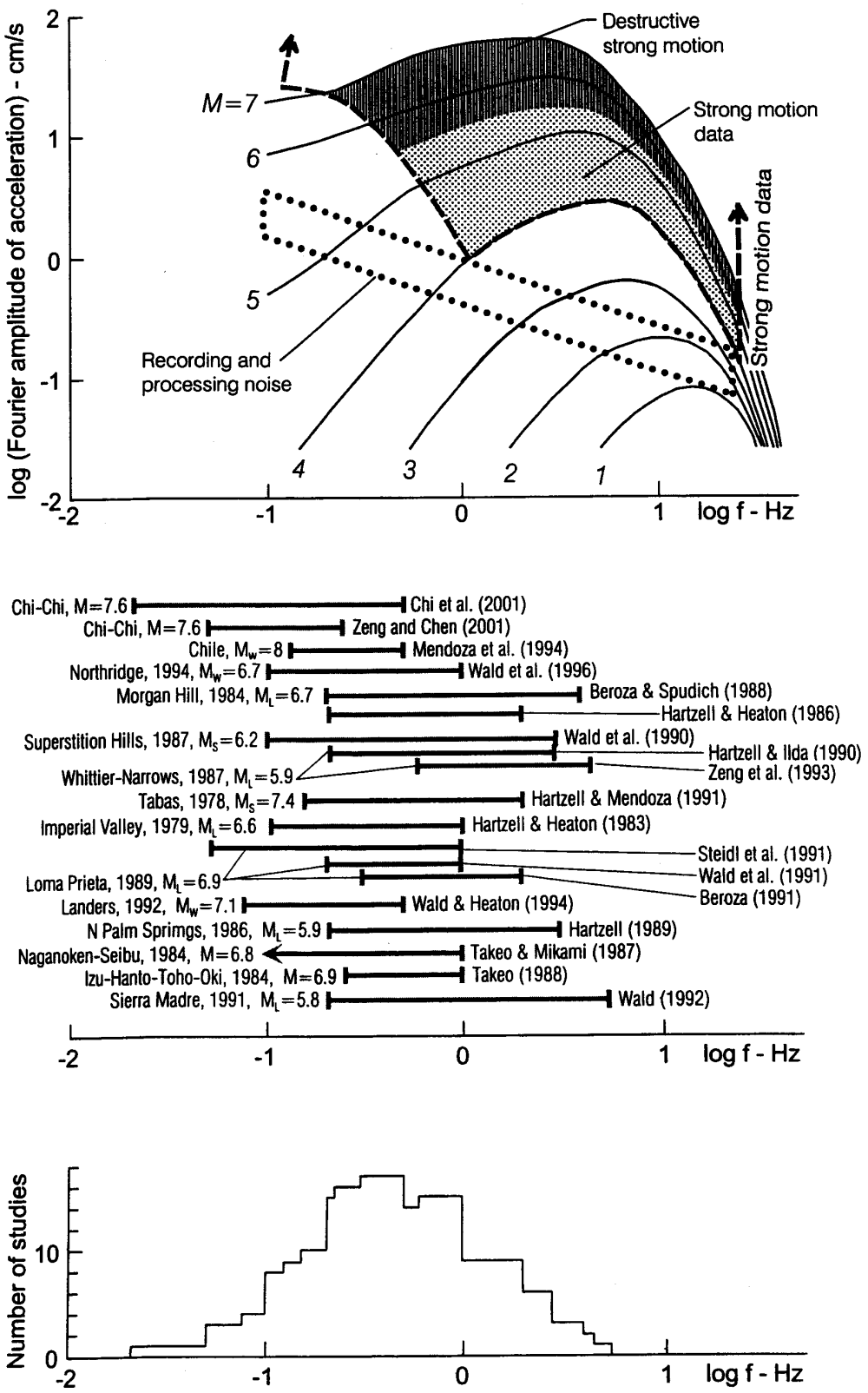

Fig. 2 Top: amplitude-frequency domain of recorded strong motion accelerograph data (also shown is the typical digitization noise for analog records (parallelogram shaped zone with dotted borders)). center: the frequency bands of strong motion data selected for nineteen inverse source mechanism studies (shown by horizontal gray bars); bottom: histogram of the number of studies cited above that use particular frequency bands of strong motion data

Most inverse source mechanism studies are able to resolve only the frequencies of strong motion smaller than 1 to 2 Hz. Furthermore, at small frequencies, the signal-to-noise ratio of most strong motion accelerographs becomes small (Lee et al., 1982; Trifunac and Lee, 1973), so that the useful frequency band that can be used in inverse studies is limited to the range from about 0.1 to 2 Hz. This is illustrated in Figure 2. The top part illustrates the spectral content and amplitudes for the bulk of the strong motion data that has been used so far for source inversion studies (except for the recent 1999 Hector Mine, California, and the 2001 Chi-Chi, Taiwan, earthquakes, most of the strong motion records used for source inversion studies have been recorded by analog accelerographs). The amplitude levels for each magnitude correspond to the average levels predicted by regression models. The dotted parallelogram illustrates the amplitudes of typical digitization and processing noise for analog accelerograms. The central part shows the frequency bands (shown by horizontal gray bars) of strong motion data used in nineteen inverse source mechanism studies. The bottom part shows a histogram of the number of studies cited in the central part that use particular frequency bands of strong motion data. It is seen that approximately 90 percent of all studies used at least the interval between 0.2 and 1 Hz, while only ~ 50 percent of the studies used at least the interval from 0.1 to 2 Hz.

3. Least Square Solution of the Inverse Problem

The displacement vector on the fault surface, $\mathbf{a}$, is in general a function of two spatial variables (ξ_1, ξ_2) and of time, and can be represented as

$$\mathbf{a}(\xi_1, \xi_2, t) = D(\xi_1, \xi_2)d(t) \tag{7}$$

where vector $\mathbf{d} = [D_1, D_2, ...D_J]$ represents the dislocation offset amplitudes on different subfaults, and function $d(t)$ describes the time dependence that is common for all the subfaults. The unknown to be determined is vector $\mathbf{D}$. In most studies, satisfactory spatial resolution has been achieved by dividing the fault into rectangular subfaults. For each subfault, the displacement at an observation point, due to unit dislocations in the ξ_1 and ξ_2 directions, are calculated using the model. The total theoretical response is represented as a linear combination of the contributions from all subfaults. The number of unknowns is equal to twice the number of subfaults, and depends on: a) the desired resolution of the fault elements, b) the stability of the numerical model, and c) the available computer storage.

The error function to be minimized is given by

$$E(\mathbf{D}) = \sum_{i=1}^{I} \int_0^T [f_i(t) - \sum_{j=1}^{J} \phi_{ij} D_j]^2 dt \tag{8}$$

where $f_i(t)$, $i = 1, 2, ...I$ are the observed displacements, $\phi_{ij}(t)$, $i = 1, 2, ...I$; $j = 1, 2, ...J$ is the theoretical prediction of the displacement at the i-th observation channel due to the j-th unit dislocation, I is the total number of observation channels to be matched (based on three components per site), J is the total number of displacements on the subfaults (based on two displacements per subfault), and $\sum_{j=1}^{J} D_j \phi_{ij}(t)$, $i = 1, 2, ...I$ is the total theoretical displacement at the i-th observation channel.

Minimization of the error function $E(\mathbf{D})$ then leads to the following normal equations

$$\mathbf{A}^T \mathbf{A}\mathbf{d} = \mathbf{A}^T \mathbf{f} \tag{9}$$

where matrix **A** and vector **f** are given by

$$[\mathbf{A}^T \mathbf{A}]_{jk} = \int_0^T \phi_{ij}(t)\phi_{ik}(t)dt \tag{10}$$

and

$$[\mathbf{f}]_j = \int_0^T \phi_{ij}(t) f_i(t) dt \tag{11}$$

The normal Equation (9) can be derived also from the condition that, at each discrete time, the theoretical displacement must be equal to the recorded time function. This leads to the equation

$$\mathbf{Ad} = \mathbf{f} \tag{12}$$

For a large number of unknowns, the system of the normal equations can be singular. To deal with this problem, some kind of regularization has to be utilized. Olson and Apsel (1982) used dumped least squares to overcome this difficulty, and Jordanovski et al. (1986) applied Tihonov regularization which reduced the problem to minimization of the functional

$$M_\alpha(\mathbf{d},\mathbf{f}) = \|\mathbf{Ad}-\mathbf{f}\|^2 + \alpha^2 \|\mathbf{Ld}\|^2 \tag{13}$$

where α is the regularization parameter or dumping factor, and **L** is a matrix satisfying some physical requirements. Minimization of $M_\alpha(\mathbf{d},\mathbf{f})$ leads to the system of the equations

$$\begin{bmatrix} \mathbf{A} \\ \alpha\mathbf{L} \end{bmatrix} \mathbf{d} = \begin{Bmatrix} \mathbf{f} \\ 0 \end{Bmatrix} \tag{14}$$

In practical applications, for example, if **L** is a discrete version of the $p-$th differentiation operator, then the regularization given by (14) attempts to minimize the $p-$th derivative of **d,** and this has a smoothing overall effect on the solution **d**. A further improvement in obtaining a physically meaningful solution was achieved by imposing appropriate constraints on the dislocation amplitudes (Olson and Apsel, 1982; Jordanovski et al., 1986). Constraints such as the requirement that the dislocations at neighboring subfaults point in the same general direction, has led to satisfactory and physically acceptable solutions.

Jordanovski et al. (1986), and Jordanovski and Trifunac (1990a) also analyzed what they called "time shifting error". This error is due to the fact that the majority of strong motion records used for source inversion so far do not have absolute time, and that the strong-motion instruments do not record the very first strong-ground motion because of the relatively high trigger levels. On the other hand, for the theoretical displacements, the exact time of all arrivals at a station are known exactly. As a consequence, if the theoretical first motions are used as reference time in the LSQ fit, an error is introduced, which is difficult to estimate. The numerical method proposed by Jordanovski and Trifunac (1990a) to reduce this error improved noticeably the solution. It consists of expanding the theoretical displacements into Fourier series, and shifting the displacements in time, which is equivalent to multiplication of the coefficient of the Fourier expansion by a shifting rotation matrix. The optimization then consists of calculating these rotation matrices. This proposed approach and numerical method are effective if the timing error is not too large. It should be noted here that, with the use of digital accelerographs, that are very sensitive and have absolute time and pre-event memory, the "time shift error" can be reduced but not eliminated, because of the errors in the model predictions of the arrival times, based on a simplified model of the geology and of the wave phenomena along the propagation path.

The spatial resolution of the inverted dislocation amplitudes along the fault depends on the number of subfaults used in the inversion. However, while increasing the number of subfaults increases the resolution, it also increases the number of unknowns, and the LSQ system of equations eventually becomes ill-conditioned. Jordanovski and Trifunac (1990a) noted that, for a typical case, the sampling rate of the time histories is not a significant factor affecting the choice of the number of subfaults. The decision on the number of subfaults to be used is mostly influenced by the disk storage and by the numerical stability of the inversion. In typical applications, the dimension of the subfaults is of the order of several kilometers. This does not yield good spatial resolution, which limits the reliability of the estimates of the high frequencies by the model. Jordanovski and Trifunac (1990b) approached this problem by expanding the final offset over the fault in a series of appropriate spatial functions in the ξ_1 and ξ_2 directions, which reduced the LSQ problem to determining the unknown coefficients of the expansion. This approach is known as Galerkin method and it offers several benefits. Firstly, with appropriate selection of the expansion functions, the boundary condition can be satisfied exactly. For example, the dislocation is zero at the boundary of the ruptured fault, and if the boundary reaches the free surface, then the zero-dislocation condition can be relaxed. Secondly, when the coefficients of the expansion are evaluated, the final offset is known at each point on the fault. Thirdly, the high frequencies generated as artifacts of the discretization (the dislocation offset across the boundaries between adjacent

subfault is discontinuous) are avoided. Finally, the number of unknowns is greatly reduced leading to a more stable LSQ system.

4. Source Mechanism of Submarine Earthquakes, Slides and Slumps

For inverse studies of the source mechanism of shallow submarine earthquakes, the procedures outlined above remain the same, provided (1) the speed of the spreading dislocation is an order of magnitude greater than the long period speed of tsunami, $\sqrt{gh}$ (Geist, 1999; Satake, 1987, 1989), and (2) the inversion is feasible in terms of only the vertical components of motion of the ocean bottom.

When the speed of spreading of the uplift of the ocean bottom is of the same order as the long wavelength speed of tsunami, $\sqrt{gh}$, the above procedure, again only in terms of the vertical components of motion, can be broken down into two consecutive inversion schemes. In the first stage, maregrams in the near-field surrounding the source can be inverted to determine the time-space evolution of the history of the ocean bottom uplifts. Unfortunately, near-field, open-sea maregrams of tsunami do not exist at present, and in this paper, we only comment that such inversions would be possible. It can be formulated in terms of a Monte Carlo simulation, where the movement of the ocean bottom is represented as a superposition of elementary "uplifts" spreading in one or two directions. Examples of such elementary tsunami sources can be found in Todorovska and Trifunac (2001), Trifunac et al. (2001a, 2001b), and Trifunac et al. (2002a, 2002b, 2002c). Once the vertical motion of the ocean floor is determined in time and space, the second stage of inversion can be initiated, again using only the vertical displacement components, to determine the temporal and spatial evolution of the slip on the causative fault.

STRONG MOTION DATA FOR SOURCE INVERSION STUDIES

The first multi-station recordings of strong earthquake motion that could be used for inverse studies occurred as a fortunate by-product of the ongoing overall deployment of strong motion accelerographs in Southern California, rather than from a carefully planned observation program (Housner and Trifunac, 1967; Trifunac and Todorovska, 2001). The first "arrays" of strong motion accelerographs were installed along lines perpendicular to faults, to measure the attenuation of peak accelerations perpendicular to the fault. Although intuition, as well as analysis (Miyatake et al., 1986; Iida et al., 1988), and practical experience in solving inverse problems suggest that such a configuration is one of the least convenient for strong motion studies, many accelerographs in United States and abroad have been arranged in such linear arrays (Hudson, 1983). If there were prior knowledge available about the mechanism of an earthquake to be recorded near a particular fault, it would be possible to search systematically for an optimum array configuration (Miyatake et al., 1986; Iida et al., 1988). However, at present, limitations associated with: (1) the lack of sufficiently detailed knowledge of the source mechanism and of the foci of future earthquakes, (2) the highly irregular geology between the source and the station, and (3) the lack of adequate funding for the required number and capability of the recording instruments have limited the number and quality of the strong motion records that have become available periodically for inversion studies. The early studies of the Parkfield, California, earthquake of 1966 discuss and illustrate these limitations. Such findings could have been used more systematically to improve the quality of the ongoing strong motion observation programs. However, because of the multiple objectives in deployment of strong motion arrays, the large number of organizations involved in strong motion observation, and the high costs involved, the overall quality of the observation programs has not improved dramatically following the 1966 Parkfield and the 1971 San Fernando earthquakes (Trifunac and Todorovska, 2001). The area covered and overall number of instruments has increased, and this has resulted in more of the earthquakes, that have occurred, to be recorded by multiple stations in the near-field, but the inter-station distance is still of the order of 10 km to several kilometers. This has contributed to increased understanding of the source mechanism, so far, more through the number of studies of different earthquakes than through an in-depth investigation of each recorded event.

Other earthquakes for which inverse studies of the fault slip could be carried out are: Parkfield, 1966, California; San Fernando, 1971, California; Tabas, 1978, Iran; Imperial Valley, 1989, California; Izu-Hanto-Toho-Oki, 1980, Japan; Naganoken-Seibu, 1984, Japan; Morgan Hill, 1984, California; Central Chile, 1985, Chile; Michoacan, 1985, Mexico; North Palm Springs, 1986, California; Superstition Hills, 1987, California; Whittier-Narrows, 1987, California; Loma Prieta, 1989, California; Sierra Madre, 1991,

California; Landers, 1992, California; Northridge, 1994, California; and Chi-Chi, 1999, Taiwan. The numerous studies of these earthquakes are cited earlier in this paper.

A recent example of well-recorded strong motion is that of the M_w = 7.6, Chi-Chi, Taiwan, earthquake of 20 September 1999. The main shock triggered over 700 strong motion stations across the island, and yielded 65 near-field records (< 20 km from the epicenter). Many detailed inverse source mechanism studies of this event have already been published (Chi et al., 2001; Ma et al., 2001; Zeng and Chen, 2001; Oglesby and Day, 2001; Wu et al., 2001; Wang et al., 2001), and can be used to illustrate the relative differences in the final results. These studies use 15 to 47 strong motion stations surrounding the source, quote seismic moment estimates M_o = (2 to 4) $\times 10^{27}$ dyne-cm, and consider source duration of 28 to 40 s. The estimate(s) of the maximum dislocation amplitudes are from 15 to 20 m, of rise times are 6 to 8 s, of average slip velocity is 2.5 m/s, of peak slip rate is 4.5 m/s, and of the average dislocation spreading velocity are 2.5 to 2.6 km/s. The calculated distributions of slip vectors across the fault show some similarity, but those are very different when compared in detail. Clearly, the resolving power of the state-of-the-art inversion methods is still restricted to long periods of strong motion, longer than 2 s in these examples.

The first strong motion array, with absolute timing and designed specifically for the inverse analyses of source mechanism, was installed by Trifunac in Bear Valley, California, in 1972 (Trifunac and Todorovska, 2001). Few weeks later, it recorded excellent data, which served to compare near, intermediate and far-field inverse analyses of the source mechanism (Dielman et al., 1975). To enable recordings and analyses of the propagating dislocations during moderate and large earthquakes, Trifunac and Hanks installed the 59 station San Jacinto array in 1973-74, along the active portion of the San Jacinto and San Andreas faults in Southern California (Trifunac and Todorovska, 2001). In 1979, this array contributed excellent data for inverse studies of the Imperial Valley, California earthquake. During subsequent years, this array recorded numerous earthquakes in this highly active area (e.g., Superstition Hills, 1987; Whittier-Narrows, 1987; Landers, 1992; Big Bear, 1992; Northridge, 1994; Hector Mine, 1999). In 1979-80, Trifunac and co-workers installed the two-dimensional strong motion array with absolute time in the Greater Los Angeles Metropolitan area (Trifunac and Todorovska, 2001) to study the source mechanism of the earthquakes in this area and the three-dimensional wave propagation through the sediments in the Los Angeles basin. The data this array recorded during the 1987 Whittier-Narrows and 1994 Northridge earthquakes is unprecedented.

Many of the deficiencies of the current strong motion programs in the U.S. (e.g., absolute time, high sensitivity and dynamic range, real-time telemetry and coverage of larger areas) will be addressed by the Advanced National Seismic System (ANSS) program, launched by the U.S. Geological Survey and partner seismological institutions. The deployment of the southern California element of ANSS (TriNet) has almost been completed, and will probably be one of the elements with the highest density of stations. TriNet is a high-tech and somewhat denser version of the San Jacinto Array and the Los Angeles and Vicinity Strong Motion networks combined, but with inter-station distance still of the same order of magnitude as for the Los Angeles and Vicinity Strong Motion network. So far, and while still in the process of implementation, TriNet has recorded only one significant event, the 1999 Hector Mine earthquake, for which finite source modeling studies have not yet been published.

CONCLUSIONS

The review of the above-discussed source mechanism studies suggests the following general conclusions:

1. At present, only the gross features of the distribution of dislocations over the fault area can be determined from strong motion data for shallow faults (source depth less than about 20 km) and for periods longer than about 1 s.
2. To improve the resolution of the motion on the fault, either many more strong motion records must be available around the causative fault, or a very detailed description of the three-dimensional geology between the source and the recording stations must be used in the inverse analyses.
3. All the strong motion records used in the inversion must have absolute time to determine the wave arrival times with accuracy better than 0.01 s (Jordanovski and Trifunac, 1990a).
4. More general dislocation models are being developed, which allow variable speed of spreading dislocations, repeated slips, smoother representation of the dislocation amplitudes, and more

complicated fault geometries. Many of these improvements can now be implemented because of the larger memory and speed of the digital computers.

5. Analogous inverse studies of the distribution of slip on submarine faults are possible, but will require recording of tsunami in open-sea and surrounding the causative fault (or slump or a slide).

REFERENCES

1. Aki, K. (1968). "Seismic Displacement near a Fault", J. Geophys. Res., Vol. 73, pp. 5359-5376.
2. Aki, K. (1979). "Characterization of Barriers on an Earthquake Fault", J. Geophys. Res., Vol. 84, pp. 6140-6148.
3. Anderson, J.G. (1974). "A Dislocation Model for the Parkfield Earthquake", Bull. Seism. Soc. Am., Vol. 64, pp. 671-686.
4. Anderson, J.G. (1976). "Motions near a Shallow Rupturing Fault: Evaluation of the Effects due to the Free Surface", J. Geophys. Res., Vol. 16, pp. 575-593.
5. Anderson, J.G. and Richards, P.G. (1975). "Comparison of Strong Ground Motion from Several Dislocation Models", Geophys. J.Royal Astr. Soc., Vol. 42, pp. 347-373.
6. Apsel, J.J. (1979). "Dynamic Green's Function for Layered Media and Applications to Boundary-Value Problem", Ph.D. Dissertation, University of San Diego, U.S.A.
7. Archambeau, C.B. (1968). "General Theory of Elastodynamic Source Fields", Rev. of Geophys., Vol. 6, p. 241.
8. Archuleta, R.J. and Fraizer, G.A. (1978). "Three Dimensional Numerical Simulations of Dynamic Faulting in a Half-Space", Bull. Seism. Soc. Am., Vol. 58, No. 3, pp. 541-572.
9. Ben-Menahem, A. and Rosenman, M. (1972). "Amplitude Patterns of Tsunami Waves from Submarine Earthquakes", J. Geoph. Res., Vol. 77, No. 17, pp. 3097-3128.
10. Beroza, G.C. (1991). "Near-Source Modeling of the Loma Prieta Earthquake: Evidence for Heterogeneous Slip and Implications for Earthquake Hazard", Bull. Seism. Soc. Amer., Vol. 81, No. 5, pp. 1573-1602.
11. Beroza, G.C. and Spudich, P. (1988). "Linearized Inversion for Fault Rupture Behavior: Application for the 1984 Morgan Hill, California, Earthquake", J. Geophys. Res., Vol. 93, pp. 6275-6296.
12. Boore, D.M., Aki, K. and Todd, T. (1971). "A Two-Dimensional Moving Dislocation Model for a Strike Slip Fault", Bull. Seism. Soc. Am., Vol. 61, pp. 177-194.
13. Boore, D.M. and Zoback, M.D. (1974a). "Near-Field Motions from Kinematic Models of Propagating Faults", Bull. Seism. Soc. Am., Vol. 64, pp. 321-342.
14. Boore, D.M. and Zoback, M.D. (1974b). "Two-Dimensional Kinematic Fault Modeling of the Pacoima Dam Strong-Motion Recordings of the February 9, 1971, San Fernando Earthquake", Bull. Seism. Soc. Am., Vol. 64, pp. 555-570.
15. Bouchon, M. (1978). "A Dynamic Crack Model for the San Fernando Earthquake", Bull. Seism. Soc. Am., Vol. 68, pp. 1555-1576.
16. Bouchon, M. (1979). "Predictability of Ground Displacement and Velocity near an Earthquake Fault: An Example, the Parkfield Earthquake of 1966", J. Geophys. Res., Vol. 84, pp. 6149-6156.
17. Bouchon, M. (1982). "The Rupture Mechanism of the Coyote Lake Earthquake of August 6, 1979 Inferred from Near Field Data", Bull. Seism. Soc. Am., Vol. 72, pp. 745-759.
18. Bouchon, M. and Aki, K. (1977). "Discrete Wave-Number Representation of Seismic-Source Wave Fields", Bull. Seism. Soc. Am., Vol. 67, pp. 259-277.
19. Brune, J.N. (1970). "Tectonic Stress and Spectra of Seismic Shear Waves from Earthquakes", J. Geophys. Res., Vol. 75, pp. 4997-5009.
20. Burridge, R. and Knopoff, L. (1964). "Body Force Equivalent for Seismic Dislocation", Bull. Seism. Soc. Am., Vol. 54, No. 6, pp. 1875-1888.
21. Burridge, R. and Willis, J. (1969). "The Self-Similar Problem of the Expanding Elliptical Crack in an Anisotropic Solid", Proc. Cambridge Phil. Soc., Vol. 66, pp. 443-468.

22. Chi, W.-C., Dreger, D. and Kaverina, A. (2001). "Finite Source Modeling of the 1999 Taiwan (Chi-Chi) Earthquake Derived from a Dense Strong-Motion Network", Bull. Seism. Soc. Am., Vol. 91, No. 5, pp.1144-1157.
23. Comer, R.P. (1982). "Tsunami Generation by Earthquakes", Ph.D. Thesis, Earth and Planetary Sciences, Mass. Inst. of Tech., Cambridge, Mass, U.S.A.
24. Das, S. and Aki, K. (1977). "A Numerical Study of Two-Dimensional Spontaneous Rupture Propagation", Geophys. J. Royal Astr. Soc., Vol. 50, pp. 643-668.
25. Day, S.M. (1982). "Three-Dimensional Finite Difference Simulation of Fault Dynamics: Rectangular Faults with Fixed Rupture Velocity", Bull. Seism. Soc. Am., Vol. 72, No. 3, pp. 705-728.
26. de Hoop, A.T. (1958). "Representation Theorems for the Displacement in an Elastic Solid and Their Application to Elastodynamic Diffraction Theory", Thesis, Techniche Hogeschool, Delft.
27. Dielman, R.J., Hanks, T.C. and Trifunac, M.D. (1975). "An Array of Strong Motion Accelerographs in Bear Valley, California", Bull. Seism. Soc. Am., Vol. 65, pp. 1-12.
28. Geist, E.L. (1999). "Local Tsunamis and Earthquake Source Parameters", Advances in Geophysics, Vol. 39, pp. 117-209.
29. Hanks, T.C. (1972). "A Contribution to the Determination and Interpretation of Seismic Source Parameters", Ph.D. Dissertation, California Institute of Technology, Pasadena, California, U.S.A.
30. Hartzell, S.H. (1978). "Interpretation of Earthquake Strong Ground Motion and Implications for Earthquake Mechanism", Ph.D. Dissertation, University of California at San Diego, La Jolla, California, U.S.A.
31. Hartzell, S.H. (1989). "Comparison of Seismic Waveform Inversion Results for the Rupture History of a Finite Fault: Application to the 1986 North Palm Springs, California, Earthquake", J. Geophys. Res., Vol. 94, pp. 7515-7534.
32. Hartzell, S.H., Frazier, G.A. and Brune, J.N. (1978). "Earthquake Modeling in a Homogeneous Half-Space", Bull. Seism. Soc. Am., Vol. 68, pp. 301-316.
33. Hartzell, S.H. and Helmberger, D.V. (1982). "Strong-Motion Modeling of the Imperial Valley Earthquake of 1979", Bull. Seism. Soc. Am., Vol. 72, pp. 571-596.
34. Hartzell, S.H. and Heaton, T.H. (1983). "Inversion of Strong Ground Motion and Teleseismic Waveform Data for the Fault Rupture History of the 1979 Imperial Valley, California, Earthquake", Bull. Seism. Soc. Am., Vol. 73, pp. 1553-1583.
35. Hartzell, S.H. and Heaton, T.H. (1986). "Rupture History of the 1984 Morgan Hill, California, Earthquake, from the Inversion of Strong Motion Records", Bull. Seism. Soc. Am., Vol. 76, pp. 649-674.
36. Hartzell, S.H. and Iida, M. (1990). "Source Complexity of the 1987 Whittier Narrows, California, Earthquake from the Inversion of Strong Motion Records", J. Geophys. Res., Vol. 95, pp. 12475-12485.
37. Hartzell, S. and Liu, P. (1995). "Determination of Earthquake Source Parameters Using a Hybrid Global Search Algorithm", Bull. Seism. Soc. Am., Vol. 85, No. 2, pp. 516-524.
38. Hartzell, S. and Mendosa, C. (1991). "Application of an Iterative Least-Squares Waveform Inversion of Strong Motion and Teleseismic Records to the 1978 Tabas, Iran, Earthquake", Bull. Seism. Soc. Am., Vol. 81, No. 2, pp. 305-331.
39. Hartzell, S., Liu, P. and Mendoza, C. (1996). "The 1994 Northridge, California, Earthquake: Investigation of Rupture Velocity, Rise Time and High Frequency Radiation", J. Geophys. Res., Vol. 101, No. B9, pp. 20091-20108,
40. Haskell, N.A. (1964). "Total Energy and Energy Spectral Density of Elastic Wave Radiation from Propagating Faults", Bull. Seism. Soc. Am., Vol. 54, pp. 1811-1841.
41. Haskell, N.A. (1969). "Elastic Displacements in the Near Field of a Propagating Fault", Bull. Seism. Soc. Am., Vol. 59, pp. 865-908.
42. Heaton, T.H. and Helmberger, D.V. (1977). "A Study of the Strong Ground Motion of the Borrego Mountain, California, Earthquake", Bull. Seism. Soc. Am., Vol. 67, pp. 315-330.

43. Heaton, T.H. and Helmberger, D.V. (1979). "Generalized Ray Models of the San Fernando Earthquake", Bull. Seism. Soc. Am., Vol. 69, pp. 1311-1341.
44. Heinrich, P., Piatanesi, A., Okal, E. and Hebert, H. (2000). "Near-Field Modeling of the July 17, 1998 Tsunami in Papua New Guinea", Geophys. Res. Letters, Vol. 27, No. 19, pp. 3037-3040.
45. Housner, G.W. and Trifunac, M.D. (1967). "Analysis of Accelerograms – Parkfield Earthquake", Bull. Seism. Soc. Am., Vol. 57, pp. 1193-1220.
46. Hudson, D.E. (1983). "Proceedings of the Golden Anniversary Workshop on Strong Motion Seismometry", Dept. of Civil Eng., Univ. Southern California, Los Angeles, California, U.S.A.
47. Iida, M. and Hartzell, S. (1991). "Source Effects on Strong Motion Records", Proc. First International Conf. on Seismology and Earthquake Eng., Teheran, I.R. Iran, Vol. I, pp. 407-415.
48. Iida, M., Miyatake, T. and Shimazaki, K. (1988). "Optimum Strong Motion Array Geometry for Source Inversion", Earthquake Eng. and Structural Dyn., Vol. 16, pp. 1213-1225.
49. Jordanovski, L.R., Trifunac, M.D. and Lee, V.W. (1986). "Investigation of Numerical Methods in Inversion of Earthquake Source", Report 86-01, Dept. of Civil Eng., Univ. Southern California, Los Angeles, California, U.S.A.
50. Jordanovski, L.R. and Trifunac, M.D. (1990a). "Least Square Inversion with Time Shift Optimization and an Application to Earthquake Source Mechanism", Soil Dyn. and Earthquake Eng., Vol. 9, No. 5, pp. 243-254.
51. Jordanovski, L.R. and Trifunac, M.D. (1990b). "Least Square Model with Spatial Expansion: Application to the Inversion of Earthquake Source Mechanism", Soil Dyn. and Earthquake Eng., Vol. 9, No. 6, pp. 279-283.
52. Kanamori, H. (1972). "Mechanism of Tsunami Earthquakes", Phys. Earth Planet. Inter., Vol. 6, pp. 346-359.
53. Kawasaki, I. (1975). "On the Dynamical Process of the Parkfield Earthquake of June 28, 1966", J. Phys. Earth, Vol. 23, pp. 127-144.
54. Kawasaki, I., Suzuki, Y. and Sato, R. (1975). "Seismic Waves due to a Shear Fault in a Semi-Infinite Medium, Part II: Moving Source", J. Phys. Earth, Vol. 23, pp. 43-61.
55. Knopoff, L. and Gilbert, F. (1959). "Radiation from a Strike Slip Fault", Bull. Seism. Soc. Am., Vol. 49, pp. 163-178.
56. Knopoff, L. and Gilbert, F. (1960). "First Motion from Seismic Source", Bull. Seism. Soc. Am., Vol. 50, pp. 117-134.
57. Kostrov, B. V. (1964). "Self-Similar Problems of Propagation of Shear Cracks", PMM, Vol. 28, No. 5, pp. 889-898.
58. Lee, V.W., Trifunac, M.D. and Amini, A. (1982). "Noise in Earthquake Accelerograms", Proc. ASCE, J. Eng. Mech. Div., Vol. 108, pp. 1121-1129.
59. Levy, N.A. and Mal, A.K. (1976). "Calculation of Ground Motion in a Three-Dimensional Model of the 1966 Parkfield Earthquake", Bull. Seism. Soc. Am., Vol. 66, pp. 405-423.
60. Liu, H.L. and Helmberger, D.V. (1983). "The Near-Source Ground Motion of the 6 August 1979 Coyote Lake, California, Earthquake", Bull. Seism. Soc. Am., Vol. 73, pp. 201-218.
61. Luco, J.E. (1987). "Dislocation Models of Near Source Earthquake Ground Motion: A Review, Vol. 3", in "Selection of Earthquake Resistant Design Criteria for Nuclear Power Plants - Methodology and Technical Cases", NUREG/CR-4903, U.S. Nuclear Regulatory Commission, Washington, D.C., U.S.A.
62. Luco, J.E. and Anderson, J.G. (1985). "Near Source Earthquake Ground Motion from Kinematic Fault Models, in "Strong Ground Motion Simulation and Earthquake Engineering Applications (eds. R.E. Scholl and J.L. King), Publication 85-02, Earthquake Engineering Research Institute, pp. 18-1/18-20.
63. Ma, K.-F., Mori, J., Lee, S.-J. and Yu, S.B. (2001). "Spatial and Temporal Distribution of Slip for the 1999 Chi-Chi, Taiwan, Earthquake", Bull. Seism. Soc. Am., Vol. 95, No. 5, pp. 1069-1987.
64. Madariaga, R. (1976). "Dynamics of an Expanding Circular Fault", Bull. Seism. Soc. Am., Vol. 66, No. 3, pp. 639-666.

65. Maruyama, T. (1963). "On the Force Equivalent of Dynamic Elastic Dislocation with Reference to the Earthquake Mechanism", Bull. of Earthq. Res. Inst., Vol. 41, pp. 467-468.
66. Mendoza, C. and Hartzell, S. (1989). "Slip Distribution of the 19 September 1985 Michoacan, Mexico, Earthquake: Near-Source and Teleseismic Constraints", Bull. Seism. Soc. Am., Vol. 79, pp. 655-669.
67. Mendoza, C., Hartzell, S. and Monfret, T. (1994). "Wide-Band Analysis of the 3 March 1985 Central Chile Earthquake: Overall Source Process and Rupture History", Bull. Seism. Soc. Am., Vol. 84, No. 2, pp. 269-283.
68. Mikumo, T. (1973). "Faulting Process of the San Fernando Earthquake of February 9, 1979 Inferred from Static and Dynamic Near-Field Displacements", Bull. Seism. Soc. Am., Vol. 63, pp. 249-269.
69. Mikumo, T. and Miyatake, T. (1995). "Heterogeneous Distribution of Dynamic Stress Drop and Relative Fault Strength Recovered from the Results of Waveform Inversion: The 1984 Morgan Hill, California, Earthquake", Bull. Seism. Soc. Am., Vol. 85, No. 1, pp. 178-193.
70. Miyatake, T., Iida, M. and Shimazaki, K. (1986). "The Effect of Strong Motion Array Configuration on Source Inversion", Bull. Seism. Soc. Am., Vol. 76, No. 5, pp. 1173-1185.
71. Murray, G.I. (1967). "Note on Strong Motion Records from the June 1966 Parkfield Earthquake Sequences", Bull. Seism. Soc. Am., Vol. 57, pp. 1259-1266.
72. Niazy, A. (1973). "Elastic Displacements Caused by Propagating Crack in an Infinite Medium: An Exact Solution", Bull. Seism. Soc. Am., Vol. 63, pp. 357-379.
73. Niazy, A. (1975). "An Exact Solution for a Finite, Two-Dimensional Moving Dislocation in an Elastic Half-Space with Application to the San Fernando Earthquake of 1971", Bull. Seism. Soc. Am., Vol. 65, pp. 1797-1826.
74. Oglesby, D.D. and Day, S.M. (2001). "Fault Geometry and the Dynamics of the 1999 Chi-Chi (Taiwan) Earthquake", Bull. Seism. Soc. Am., Vol. 91, No. 5, pp. 1099-1111.
75. Ohnaka, M. (1973). "A Physical Understanding of the Earthquake Source Mechanism", J. Phys. Earth, Vol. 21, pp. 39-59,
76. Okal, E.A. (1988). "Seismic Parameters Controlling Far-Field Tsunami Amplitudes: Review", Natural Hazards, Vol. 1, pp. 67-96.
77. Olson, A.H. and Apsel, R.J. (1982). "Finite Faults and Inverse Theory with Applications to the 1979 Imperial Valley Earthquake", Bull. Seism. Soc. Am., Vol. 72, pp. 1969-2001.
78. Pelayo, A.M. and Wiens, D.A. (1992). "Tsunami Earthquakes: Slow Thrust-Faulting Events in the Accretionary Wedge", J. Geoph. Res., Vol. 97, No. BII, pp.15, 321-15,337.
79. Richards, P.G. (1973). "The Dynamic Field of a Growing Plane Elliptical Shear Crack", Int. J. Solids Struct., Vol. 9, pp. 843-861.
80. Richards, P.G. (1976). "Dynamic Motion near an Earthquake Fault: A Three-Dimensional Solution", Bull. Seism. Soc. Am., Vol. 66, pp. 1-32.
81. Satake, K. (1987). "Inversion of Tsunami Waveforms for the Estimation of a Fault Heterogeneity: Method and Numerical Experiments", J. Phys. Earth, Vol. 35, pp. 241-254.
82. Satake, K. (1989). "Inversion of Tsunami Waveforms for the Estimation of Heterogeneous Fault Motion of Large Submarine Earthquakes: The 1968 Tokachi-Oki and 1983 Japan Sea Earthquakes", J. Geophys. Res., Vol. 94, pp. 5627-5636.
83. Sato, R. (1975). "Fast Computation of Theoretical Seismogram for an Infinite Medium, Part I: Rectangular Fault", J. Phys. Earth, Vol. 23, pp. 323-331.
84. Steidl, J.H., Archuleta, R.J. and Hartzell, S.H. (1991). "Rupture History of the 1989 Loma Prieta, California, Earthquake", Bull. Seism. Soc. Am., Vol. 81, No. 5, pp. 1573-1602.
85. Sudo, K. (1972). "Radiation of Seismic Waves from a Propagating Source near the Free Surface, Part I: Formulation and an Example", J. Phys. Earth, Vol. 20, pp. 127-145.
86. Takeo, M. (1987). "An Inversion Method to Analyze the Rupture Process of Earthquakes Using Near-Field Seismograms", Bull. Seism. Soc. Am., Vol. 77, pp. 490-513.
87. Takeo, M. (1988). "Rupture Process of the 1980 lzu-Hanto-Oki Earthquake Deduced from Strong Motion Seismograms", Bull. Seism. Soc. Am., Vol. 78, pp. 1074-1091.

88. Takeo, M. and Mikami, N. (1987). "Inversion of Strong Motion Seismograms for the Source Process of the Naganoken-Seibu Earthquake of 1984", Tectonophysics, Vol. 144, pp. 271-285.

89. Todorovska, M.I. and Trifunac, M.D. (2001). "Generation of Tsunamis by Slowly Spreading Uplift of the Sea Floor", Soil Dyn. and Earthq. Eng., Vol. 21, No. 2, pp. 151-167.

90. Todorovska, M.I., Hayir, A. and Trifunac, M.D. (2002). "A Note on Tsunami Amplitudes above Submarine Slides and Slumps", Soil Dyn. and Earthquake Eng., Vol. 22, No. 2, pp. 129-141.

91. Trifunac, M.D. (1972a). "Stress Estimates for San Fernando, California Earthquake of February 9, 1971: Main Event and Thirteen Aftershocks", Bull. Seism. Soc. Am., Vol. 62, pp. 721-750.

92. Trifunac, M.D. (1972b). "Tectonic Stress and Source Mechanism of the Imperial Valley, California, Earthquake of 1940", Bull. Seism. Soc. Am., Vol. 2, pp. 1283-1302.

93. Trifunac, M.D. (1974). "A Three-Dimensional Dislocation Model for the San Fernando, California, Earthquake of February 9, 1971", Bull. Seism. Soc. Am., Vol. 64, pp. 149-172.

94. Trifunac, M.D. (1988). "A Note on Peak Accelerations during 1 and 4 October 1987 Earthquakes in Los Angeles, California", Earthquake Spectra, Vol. 4, No. 1, pp. 101-113.

95. Trifunac, M.D. and Hudson, D.E. (1971). "Analysis of the Pacoima Dam Accelerogram, San Fernando, California Earthquake of 1971", Bull. Seism. Soc. Am., Vol. 61, pp. 1392-1411.

96. Trifuanc, M.D. and Lee, V.W. (1973). "Routine Computer Processing of Strong Motion Accelerograms", Earthquake Eng. Res. Lab., Report EERL 73-03, Calif. Inst. of Tech., Pasadena, California, U.S.A.

97. Trifunac, M.D. and Todorovska, M.I. (2001). "Evolution of Accelerographs, Data Processing, Strong Motion Arrays and Amplitude and Spatial Resolution in Recording Strong Earthquake Motion", Soil Dyn. and Earthq. Eng., Vol. 21, No. 6, pp. 537-555.

98. Trifunac, M.D. and Todorovska, M.I. (2002). "A Note on Differences in Tsunami Source Parameters for Submarine Slides and Earthquakes", Soil Dyn. and Earthq. Eng., Vol. 22, No. 2, pp. 143-155.

99. Trifunac, M.D. and Udwadia, F.E. (1974). "Parkfield, California Earthquake of June 27, 1966: A Three-Dimensional Moving Dislocation", Bull. Seism. Soc. Am., Vol. 64, pp. 511-533.

100. Trifunac, M.D., Hayir, A. and Todorovska, M.I. (2001a). "Near-Field Tsunami Waveforms from Submarine Slumps and Slides", Report CE 01-01, Dept. of Civil Eng., Univ. of Southern California, Los Angeles, California, U.S.A.

101. Trifunac, M.D., Hayir, A. and Todorovska, M.I. (2001b). "Tsunami Waveforms from Submarine Slides and Slumps Spreading in Two-Dimensions", Report CE 01-06, Dept. of Civil Eng., Univ. of Southern California, Los Angeles, California, U.S.A.

102. Trifunac, M.D., Hayir, A. and Todorovska, M.I. (2002a). "Was Grand Banks Event of 1929 a Slump Spreading in Two Directions?", Soil Dynamics and Earthquake Eng. (in press).

103. Trifunac, M.D., Hayir, A. and Todorovska, M.I. (2002b). "A Note on the Effects of Nonuniform Spreading Velocity of Submarine Slides and Slumps on the Near-Field Tsunami Amplitudes", Soil Dynamics and Earthquake Eng. (in press).

104. Trifunac, M.D., Hayir, A. and Todorovska, M.I. (2002c). "A Note on the Effects of Nonuniform Displacement Amplitudes of Submarine Slides and Slumps on the Near-Field Tsunami Amplitudes" (submitted for publication).

105. Tsai, Y.B. and Patton, H.J. (1973). "Near Field Small Earthquakes-Dislocation Motion", Semi-Annual Report I, Texas Instruments Inc., Prepared for Air Force Office of Scientific Research Contract F44620-72-C-0073.

106. Veedenskaya, A.V. (1956). "The Determination of Displacement Fields by Means of Dislocation Theory", Akad. Nauk. SSSR, Izv. Ser. Geofiz., Vol. 3, p. 227.

107. Wald, D.J. (1992). "Strong Motion and Broadband Teleseismic Analysis of the 1991 Sierra Madre, California Earthquake", J. Geophys. Res., Vol. 97, No. B7, pp. 11033-11046.

108. Wald, D.J. and Heaton, T.H. (1994a). "Spatial and Temporal Distribution of Slip for the 1992 Landers, California, Earthquake", Bull. Seism. Soc. Am., Vol. 84, pp. 668-691.

109. Wald, D.J. and Heaton, T.H. (1994b). "A Dislocation Model of the 1994 Northridge, California, Earthquake Determined from Strong Ground Motions", Open-File Report 94-278, U.S. Geol. Surv.

110. Wald, D.J., Heaton, T.H. and Hudnut, K.W. (1996). "The Slip History of the 1994 Northridge, California, Earthquake Determined from Strong-Motion, Teleseismic, GPS, and Leveling Data", Bull. Seism. Soc. Am., Vol. 86, No. 1B, pp. S49-S70.

111. Wald, D.J., Helmberger, D.V. and Hartzell, S.H. (1990). "Rupture Process of the 1987 Superstitions Hills Earthquake from the Inversion of Strong Motion Data", Bull. Seism. Soc. Am., Vol. 80, pp. 1079-1098.

112. Wald, D.J., Helmberger, D.V. and Heaton, T.H. (1991). "Rupture Model of the 1989 Loma Prieta Earthquake from the Inversion of Strong Motion and Broadband Teleseismic data", Bull. Seism. Soc. Am., Vol. 81, pp. 1540-1572.

113. Wang, W.-H., Chang, S.-H. and Chen, C.-H. (2001). "Fault Slip Inverted from Surface Displacements during the 1999 Chi-Chi, Taiwan, Earthquake", Bull. Seism. Soc. Am., Vol. 91, No. 5, pp. 1144-1157.

114. Ward, S.N. (1980). "Relationships of Tsunami Generation and an Earthquake Source", J. Phys. Earth, Vol. 28, pp. 441-474.

115. Ward, S.N. (1981). "On Tsunami Nucleation: I, A Point Source", J. Geoph. Res., Vol. 86, pp. 7895-7900.

116. Ward, S.N. (1982). "On Tsunami Nucleation: II, An Instantaneous Modulated Line Source", Phys. Earth and Planet. Interiors, Vol. 27, pp. 273-285.

117. Wu, C., Takeo, M. and Ide, S. (2001). "Source Process of the Chi-Chi Earthquake: a Joint Inversion of Strong Motion Data and Global Positioning System Data with Multifault Model", Bull. Seism. Soc. Am., Vol. 91, No. 5, pp. 1128-1143.

118. Zeng, Y. and Chen, C.-H. (2001). "Fault Rupture Process of the 20 September 1999 Chi-Chi, Taiwan, Earthquake", Bull. Seism. Soc. Am., Vol. 91, No. 5, pp. 1088-1098.

119. Zeng, Y., Aki, K. and Teng, T.L. (1993). "Source Inversion of the 1987 Whittier Narrows Earthquake, California, Using the Isochron Method", Bull. Seism. Soc. Am., Vol. 83, No. 2, pp. 358-377.

ISET Journal of Earthquake Technology, Paper No. 423, Vol. 39, No. 3, September 2002, pp. 167-193

ESTIMATION OF LOCAL SITE EFFECTS DURING EARTHQUAKES: AN OVERVIEW

Francisco J. Sánchez-Sesma*, Víctor J. Palencia** and Francisco Luzón***

* Instituto de Ingeniería, UNAM; Cd. Universitaria, Apdo. 70-472, Coyoacán; 04510, México D.F.; MEXICO

** División de Matemáticas e Ingeniería, UNAM – Campus Acatlán

Alcanfores y San Juan Totoltepec s/n, Naucalpan; 53150, Edo. de México; MEXICO

*** Departamento de Física Aplicada, Universidad de Almería; Cañada de San Urbano s/n; 04120, Almería; SPAIN

ABSTRACT

A summary of methodologies to estimate local site effects of geology and topography on strong ground motion during earthquakes is presented. Some canonical solutions obtained by analytical methods for simple geometries are reviewed. Most common numerical methods used for complex geometries are briefly discussed. Experimental and hybrid methods are also described. A wide set of references is provided for the interested reader.

KEYWORDS: Site-Effects, Ground Motion, Analytical Solutions, Numerical Methods

INTRODUCTION

When observed with long scales, our planet has a relatively simple structure. In a first approximation, it is formed by spherical shells that surround the inner core up to the crust. A closer look (with scales of hundreds of kilometers) reveals that Earth has significant heterogeneities, both vertically and laterally. In fact, plate tectonics gives rise to most of the seismic activity. For smaller scales, the Earth is very heterogeneous, and its varying surface geology (topography, faults, alluvial basins, etc.) is at the origin of significant spatial variations of seismic ground motion.

It is now well known that local site characteristics may produce large ground motion amplifications during earthquakes. This issue can be investigated by means of the analysis of actual seismic records and the study of synthetic seismograms as well. In fact, our knowledge on local site effects has been historically improved, thanks to parallel advances in research of both branches. On one hand, seismic records give us a picture of "reality", on which theoretical and empirical speculations can be posed. On the other hand, by simplifying "reality", and representing it by models, we can split different contributions to a single effect; theory allows us to explain observations.

Early work by Reid (1910) pointing out the subject, when reporting on the San Francisco, California, earthquake of April 18, 1906, was followed by some pioneering investigations, including those by Sezawa (1927) on the scattering and diffraction of elastic waves by rigid cylinders embedded in an elastic space. By last century's middle years, effects of local soil and geological conditions were studied mainly in terms of peak accelerations or peak velocities (see, e.g., Kanai, 1949, 1951; Medvedev, 1955; Gutenberg, 1957; Duke, 1958). A decade later, Zhou (1965) introduced the idea of interpreting local site effects in terms of the changes of the shape of response spectra. During the 70's, a significant number of empirical studies, among others those conducted by Prof. M.D. Trifunac (e.g., Trifunac, 1971a, 1976a, 1976b, 1976c, 1978, 1979, 1980, 1987; Trifunac and Udwadia, 1974; Trifunac and Anderson, 1977; Trifunac and Brady, 1975a, 1975b, 1975c; Trifunac and Lee, 1978; Trifunac and Westermo, 1977; Wong and Trifunac, 1977), and theoretical ones (e.g., Trifunac, 1971b, 1973; Wong and Trifunac, 1974a) contributed to the overall understanding of local site effects. They also provided models and solutions which, even today, are used for validation of new methods to take into account this phenomenon.

The effects of topography on surface ground motion have been observed and studied from field experiments. Trifunac and Hudson (1971), Davis and West (1973), Wong et al. (1977), Griffiths and Bollinger (1979), and Tucker et al. (1984) among others, recorded significant amplifications. However, as remarked by Bard and Tucker (1985) and later by Geli et al. (1988), the amplifications observed in the field are systematically larger than the values predicted using theoretical models. They suggested that the models should incorporate layering, variations in wave velocities, and even irregular

two- and three-dimensional configurations in order to better explain the observations. Bard and Tucker (1985) tested several such models and improved the predictions, but still showed amplifications smaller than the observed ones. Sánchez-Sesma and Campillo (1991) studied a set of relatively simple but extreme topographical profiles under various types of seismic waves, and proposed that the maximum amplification due to topographical effects is generally lower than about four. In a more recent study, Pedersen et al. (1994) found good agreement between experiments and models. They found that diffracted waves recorded at the reference station might explain the large amplitudes in the spectral ratios.

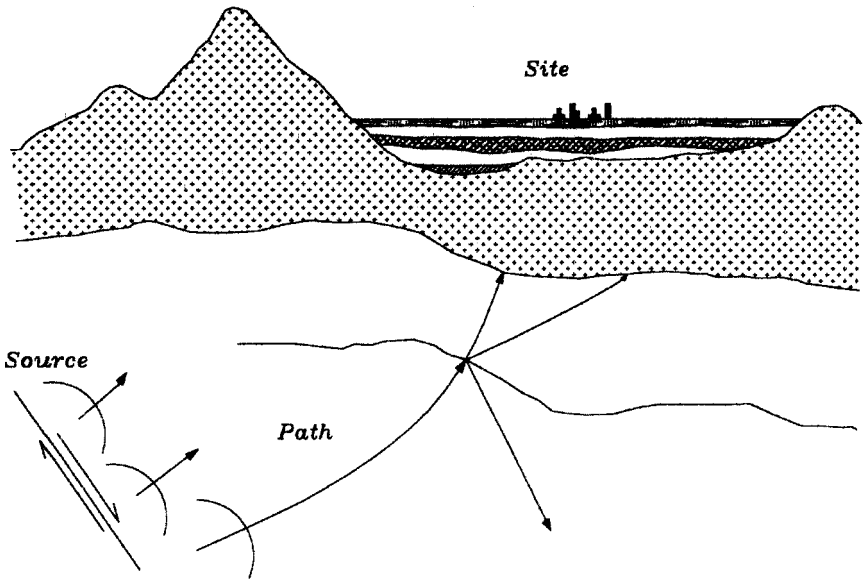

Fig. 1 Main factors in earthquake ground motion: source, path and site characteristics

Almost fifteen years ago, Aki (1988) considered that site effects could be adequately inferred if the input motions and the distributions of velocities, densities and attenuation of the materials are known. In fact, he presented several successful examples in which such conditions are met. He was foreseeing the spectacular advances in the computational power and the available numerical methods. Nowadays, the speed and processing capacity of computers is impressive. However, the majority of the procedures are expensive in terms of the required input. The most common situation is the poor knowledge of the geometry and the mechanical properties of the geological materials. Uncertainties are often large. The same is true when we talk about size and location of earthquake sources. For several applications, Aki pointed out that significant correlations exist between amplifications and geotechnical and geological characteristics. He also suggested that these relationships could be represented by meaningful microzonation maps. Now, thanks to modern Geographical Information Systems (GIS) technology, microzonation maps are a reality.

Trifunac (1989) and Trifunac and Lee (1989) have proposed a statistical approach that uses extensively recorded strong motion data, and some theoretical results to assess amplifications and response spectra ordinates at regional scale. Later, Trifunac (1990) proposed a simple equation to describe the frequency-dependent amplification of strong ground motion, which is based both on physical basis and on various regression analyses. Such an equation provides reasonable average estimates. Essentially, this is in agreement with Aki's proposal.

The quantitative prediction of strong ground motion at a given site involves dealing with the source of seismic waves, their paths to the site, and the effects of site conditions (see Figure 1). Moreover, uncertainty has to be explicitly taken into account. The great difficulty of the problem is well known. However, for many practical circumstances, the use of random vibration theory results (e.g., Udwadia and Trifunac, 1974; Vanmarcke, 1976) allows approximate descriptions of both ground motions and the corresponding response spectra, when simplified seismological models of source and path are explicitly considered (e.g., Boore, 1983; Rovelli et al., 1988). This simplified approach, which is essentially inspired by Trifunac's ideas, produces practical and reliable estimates of ground motion at a given location, when reasonable values of ground motion duration (e.g., Trifunac and Brady, 1975b) are available. Site effects can be taken into account if appropriate transfer functions are used (e.g., Reinoso et al., 1990). Of course, care is needed in selecting the characteristics of the incoming wave field.

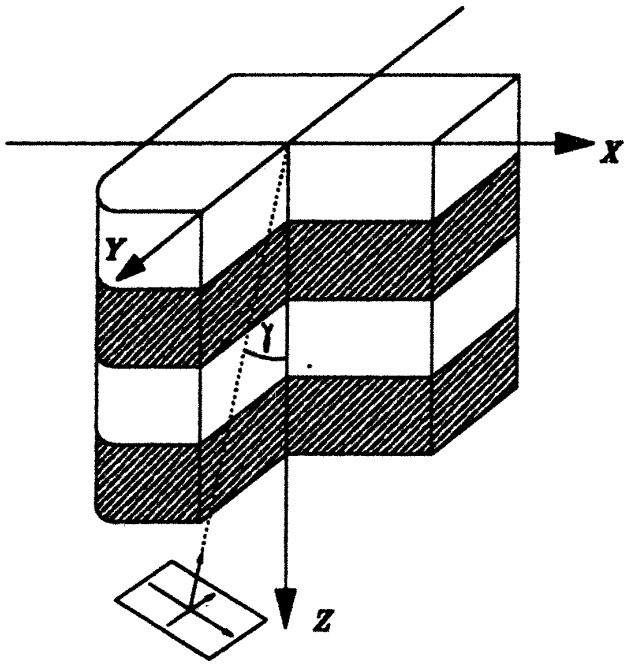

(a)

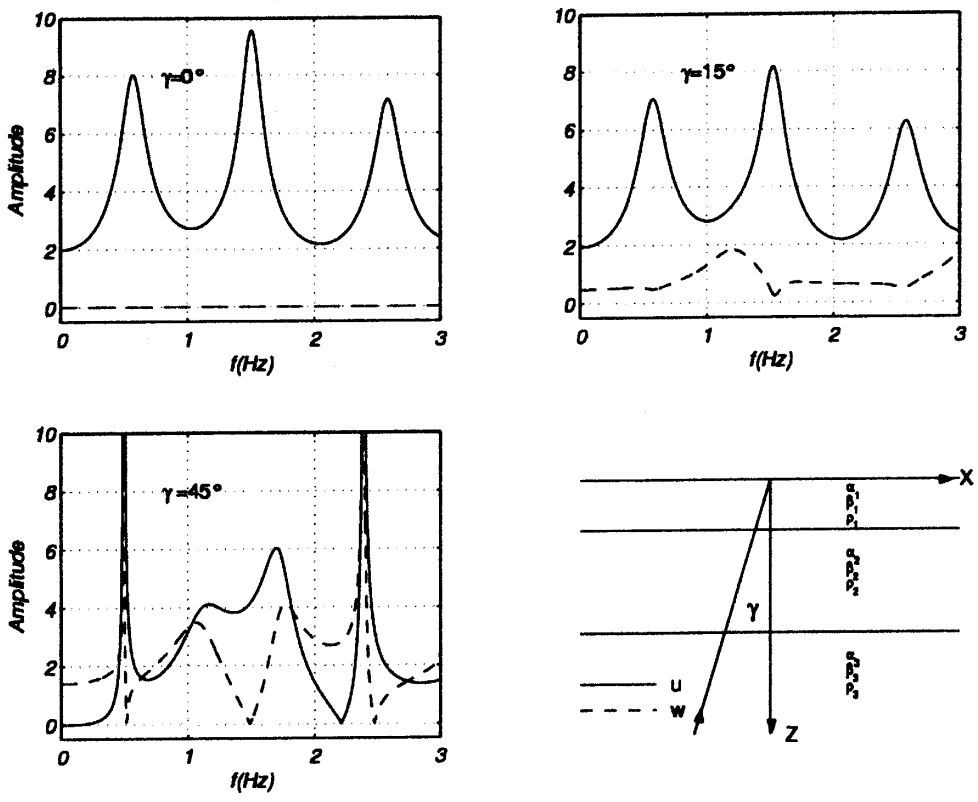

(b)

Fig. 2 (a) Plane layers model with incident plane waves, (b) Surface response versus frequency of horizontal (continuous) and vertical (dashed) displacements of a system of two layers over a half-space; material properties, with arbitrary but compatible units, are: 1.0, 1.5, 5.0 for P-wave velocities and 0.5, 0.7, 2.5 for shear velocity in layers 1, 2 and the half-space, respectively; density is 1.0 for all media; depth of layers are $h_1 = 1$ and $h_2 = 2$

A popular approach that accounts for source, path and site effects is the use of small earthquakes as empirical Green's functions (Hartzell, 1978; Irikura, 1983; Somerville et al., 1991; Hutchings, 1994; Ordaz et al., 1995). This method requires some records at the site from small earthquakes at the potential source area. Usually, the mechanism of the target event should be the same as the one for empirical Green's functions. The adoption of a few constraints to account for the source characteristics is necessary, but the technique offers the possibility of exploring the effects due to various source scenarios. However, the trouble is that having a complete set of records that can be used as empirical Green's functions at a given site is still a rare fact. For this reason, in most cases, the assessment for site effects should rely on mathematical models. Yet, significant difficulties and uncertainties may arise in the selection of input motion.

The last two decades witnessed significant progress in the evaluation of site effects and dramatic examples of its reality as well (e.g., Campillo et al., 1988; Sánchez-Sesma et al., 1988a; Borcherdt and Glassmoyer, 1992; Trifunac and Todorovska, 1998). In this work, some common methodologies to estimate local site effects are reviewed. These can be classified in several ways. We think of them as analytical, numerical, experimental and hybrid methods. In the next paragraphs, some relevant analytical and numerical methods are presented, and their main characteristics are discussed. The use of experimental and hybrid methods is also described. Some previous reviews on this subject are those of Sánchez-Sesma (1987, 1996), Aki (1988), Luco and De Barros (1990) and Faccioli (1991).

This paper attempts to give a broad coverage of a rapidly growing field, namely the estimation of the effects of local geology and topography on ground motion due to earthquakes. Most of the issues touched here may be changing. A review like this one also reflects the experience and preferences of the writers. The idea is to provide a basic starting point to someone interested in the assessment of site effects in strong ground motion.

ANALYTICAL METHODS

Various analytical solutions have been proposed to predict site effects in simplified configurations, such as horizontal layers, semicircular, triangular or rectangular valleys, wedges, and so on. In what follows, the simplest solutions are reviewed.

The incidence of elastic plane waves upon a system of overlapping layers with different elastic properties is a well-known matter (e.g., Ewing et al., 1957; Aki and Richards, 1980). In particular, the propagator-matrix formalism proposed by Thomson (1950) and corrected and applied by Haskell (1953, 1960, 1962) provides a systematic solution of the governing equations of elastodynamics in stratified media. In this method, the conditions of continuity of the tractions and displacements in each interface among strata, and the condition of null tractions at the free surface are satisfied. The Thomson-Haskell method allows for 3D wave fields despite the 1D description of the layered media. In practice, it is frequent to assume vertical incidence of shear waves, and this gives a scalar description of the problem. This assumption provides a first order account of amplification in a stack of layers, and in many cases, it is enough for useful applications. Sometimes, however, the vector interaction of various fields may lead to complexity in the surface recorded ground motions. The Thomson-Haskell method can present numerical difficulties in some cases of oblique incidence of SV waves and in computations of dispersion curves for surface waves. Several measures aimed to remedy this problem have been proposed (e.g., Dunkin, 1965), and even the method has been reformulated in terms of transmission-reflection coefficients (Kennett, 1983), stiffness matrices (Kausel and Roesset, 1981) and global generalized reflection/transmission matrices (Chen, 1990, 1995, 1996, 1999).

Figure 2a shows a stack of parallel layers with an incident plane wave coming from the underlying half-space. In order to illustrate, with a simple two-layers model over half-space, the effects of varying the incidence angle for in-plane SV waves, Figure 2b depicts the amplitudes of both horizontal and vertical displacements at the free surface. Three values of the incidence angle are considered (γ = 0, 15 and 45 degrees, respectively). Material properties are given in the figure caption. Horizontal amplitudes for 0 and 15 degrees are similar, but the latter incidence shows vertical components, suggesting the presence of converted P waves within the layers. For 45 degrees, when horizontal and vertical components of the incidence are equal, the pattern is notoriously different and very large peaks appear at certain frequencies in both horizontal and vertical components. In fact, the existence of such sharp peaks at certain frequencies for incoming plane SV waves at the critical incidence and larger angles

in layered media has been pointed out by several authors (e.g., Burridge et al., 1980; Shearer and Orcutt, 1987; Kawase et al., 1987; Mateos et al., 1993; Papageorgiou and Kim, 1993), but it is still not widely known. Mateos et al. (1993) studied the 1D response of a stack of layers under incident SV waves. In their computations, the narrow-band amplifications reached thousands. However, none of the above mentioned papers discussed the basic mechanism involved. Nowadays, it has been generally accepted that amplifications were produced at certain frequencies and incidence angles, due to the very efficient generation of diffracted P waves inside the layer and the underlying half-space. Sánchez-Sesma and Luzón (1996) dealt with the subject, and the relative contributions of P and S waves to the surface motion of a simple layered model were obtained. They showed that the huge amplifications in soft layers are due to the trapping of S waves.

When the boundaries are curved and/or wave fronts are not plane, a phenomenon called diffraction arises in almost all cases. This may be viewed as a kind of natural smoothing effect to avoid discontinuities in wave fields. It appears when the incident wave propagates at obstacles or openings with dimensions comparable to its wavelength. In accordance with Huygens' Principle, the boundaries of the obstacle act as sources of secondary waves spreading in all directions. Many problems of diffraction of elastic waves have been solved using suitable wave functions, when geometry allows the use of the technique of separation of variables (e.g., Lee and Trifunac, 1979, 1982; Moeen-Vaziri and Trifunac, 1981, 1985, 1986). The excellent monograph of Mow and Pao (1971) on the subject presents many such solutions for infinite domains. Using this technique, Trifunac (1971b, 1973) found analytical solutions for the response of semi-circular alluvial valleys and canyons under incident SH waves. Figures 3 and 4 reproduce some of the classical Trifunac's results on these issues. These canonical examples exhibit the spectacular effects in both a topographical profile and a soft alluvial inclusion. While the former simulation reveals clear interferences with energy focusing, the model for a soft sedimentary deposit shows conspicuous amplifications due to the energy trapping by the inclusion and also the influence of the angle of incidence. Since a good deal of the phenomena involved is related with the geometry, differences in the mechanical properties between the half-space and the valley, as well as the direction of the incoming wave, may play a significant role in the surface response. Later, Wong and Trifunac (1974a, 1974b) extended the study to elliptical shapes. These solutions have been most useful, both to understand basic aspects of the phenomena involved and to validate numerical solutions.

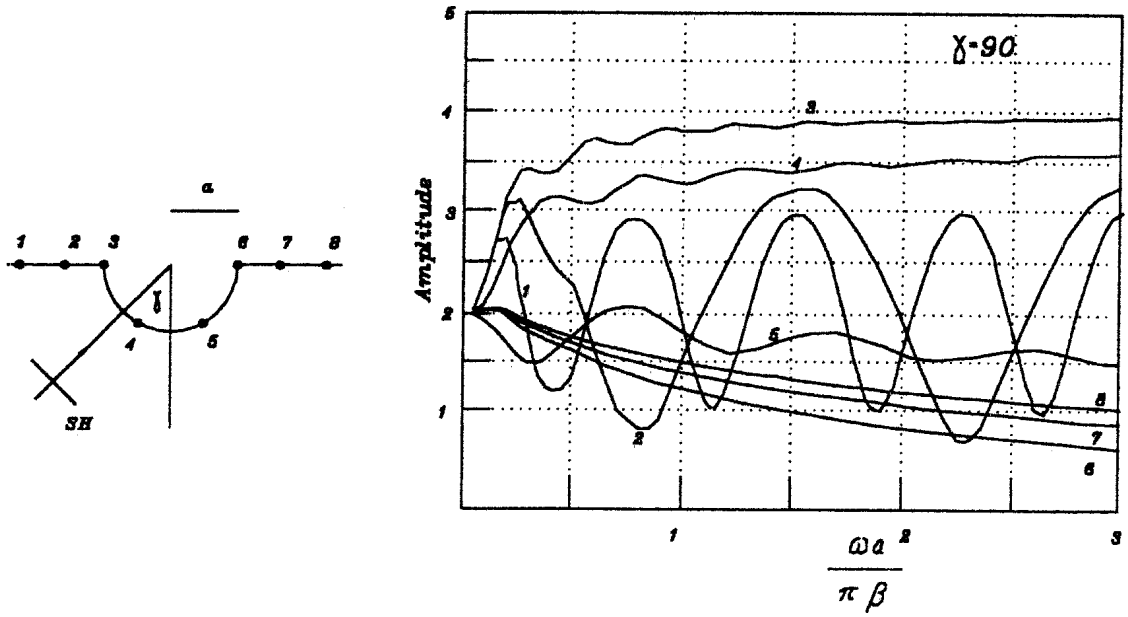

Fig. 3 Transfer functions for eight receptors located on the surface of a semi-circular topography for a 90 degrees incidence angle; here a = radius of the canyon, ω = circular frequency and β = shear wave velocity; largest amplifications occur at receptor No. 3 where the incident wave meets the canyon; note that receptors No. 5 to 8 are in the shadow zone, still motion is recorded (after Trifunac, 1973)

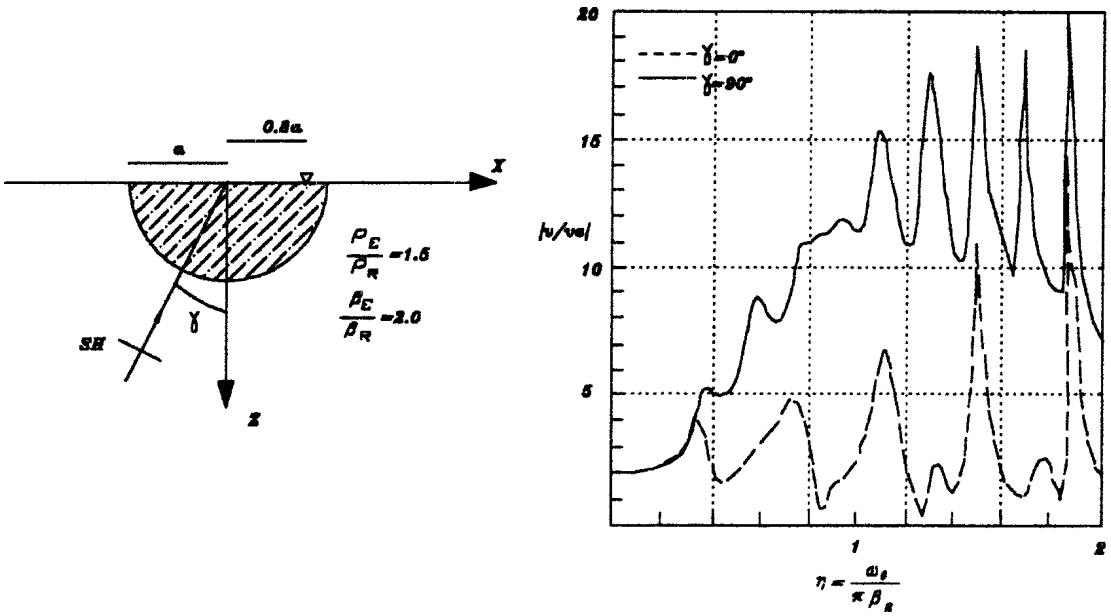

Fig. 4 Transfer function for a station located at $0.8a$ on the surface of a semi-circular alluvial valley under two different incidence angles of incoming SH waves; here a = radius of the valley, η = dimensionless frequency, ω = circular frequency, ρ = mass density and β = shear wave velocity; subscripts E and R stand for the half-space and the inclusion, respectively; $|v/v_0|$ is the absolute value of the ratio between the amplitude of the displacement at the station and that of the free-space solution (after Trifunac, 1971b)

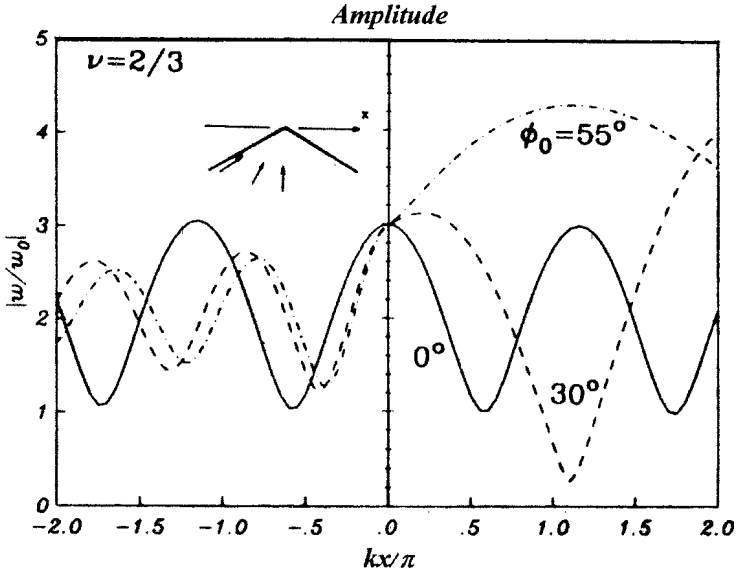

Fig. 5 Amplification in a wedge-like configuration under incidence of SH waves; here $|w/w_0|$ is the absolute value of the ratio between the amplitudes of the displacements along the wedge and those of the free-space solution; kx/π is the normalized coordinate in the horizontal direction with origin at the vertex; the amplification at the vertex remains the same for all incidences (after Sánchez-Sesma, 1985)

The exact solution for a wedge-like configuration under incidence of SH waves is due to Sánchez-Sesma (1985) who adapted MacDonald's (1902) solution in terms of series expansions of Bessel functions of fractional order and discovered a simple rule to predict the amplification at the vertex. He found that, for any incident angle, the amplitudes at the vertex of the wedge are 2/ν times those at the free space, where νπ is the internal angle of the wedge (with $0 < \nu < 2$). Figure 5 illustrates this fact for a

wedge where ν = 2/3 under wave incidences of 0, 30 and 55 degrees, respectively. Although the amplification along the *x*-axis is different for the various incident angles displayed, and differences are notorious in the shadow zone, the amplification at the vertex remains constant with a value of 2/ν = 3 for all incidences. Faccioli (1991) pointed out that this solution can be used to assess amplifications in varying profiles.

In almost all analytical solutions, use should be made of the computer to evaluate the solution, i.e. the spectra and synthetics. There are some approaches that require some more computations, but still are named analytical. That is the case in the study of a 3D alluvial valley of hemispherical shape under incidence of elastic waves. Lee (1984) succeeded in obtaining power series expansions of the eigenfunction coefficients and the corresponding boundary conditions. He wrote down an infinite system of equations which, once truncated, can be solved. This approach is limited to the studied hemispherical shape and to low frequencies as well. For shallow circular geometries, several analytical solutions of this type have been obtained (e.g., Todorovska and Lee, 1990, 1991a, 1991b) for incident P and SV and Rayleigh waves.

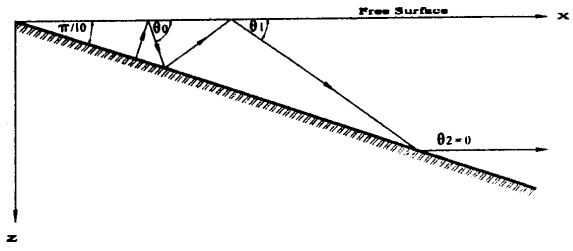

(a)

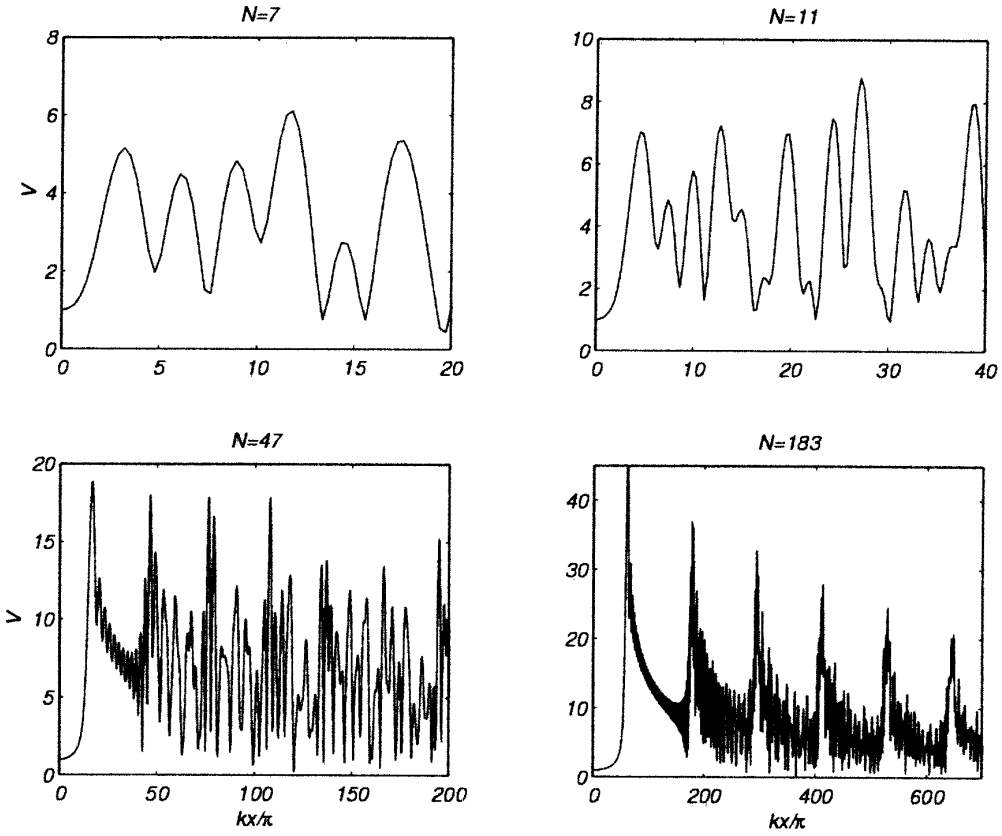

(b)

Fig. 6 (a) Dipping layer model and geometrical construction of the path of a wave inside the layer for N = 5, (b) Transfer functions for different dipping angles (N = 7, 11, 47 and 183)

The exact solution for the antiplane SH motion of a dipping layer overlaying a moving rigid base was found by only geometrical means (Sánchez-Sesma and Velázquez, 1987). For a family of dipping angles of the form $\pi / 2N$, where N is an odd integer, it came out that there is no diffraction, and the whole solution is attained by a very simple combination of plane waves. In Figure 6, reflected wave propagation is illustrated by ray tracing for $N = 5$. It can be seen that the last ray is horizontal and, therefore, satisfies by itself the free-surface boundary condition. Figure 6 displays the transfer functions for $N = 7$, 11, 47 and 183, respectively. The model has no attenuation and reveals complicated interferences of geometrical nature. For large values of N, results approach asymptotically to the 1D case. Notice that this solution is self-similar, as there is no scale involved. This model allowed a simple approximation, valid in high frequencies, for the response of a class of alluvial valleys of triangular shape (Sánchez-Sesma et al., 1988b). The same approach leads to the exact solution for the incidence of plane SH and SV waves upon some infinite mountain-like wedges, in which the complete field has been obtained again by only geometrical means (Sánchez-Sesma, 1990). Thus, only plane waves are needed to fulfill boundary conditions. Faccioli (1991) presents examples of the use of these simple solutions. A large simplified wedge model has been proposed recently to explain a relatively large broad-band amplification of southern locations in the Valley of Mexico, relative to northern ones (Montalvo-Arrieta et al., 2002).

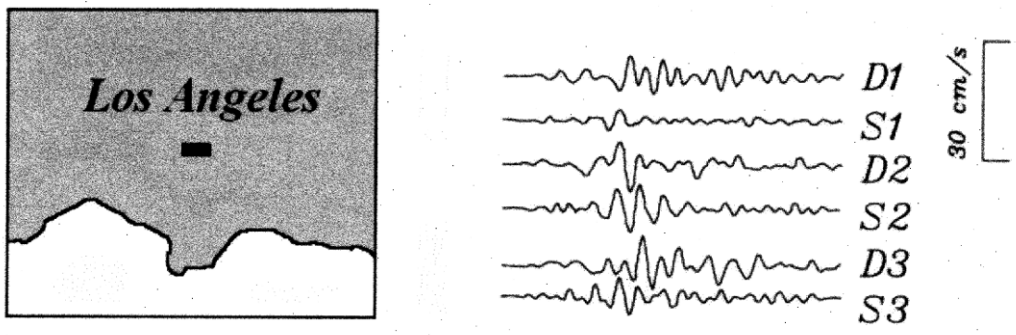

Fig. 7 Comparison between data and synthetic seismograms calculated by Olsen (2000) for a receiver located in the Los Angeles basin (shaded area delimited by the coast line); recorded data (D) and synthetic (S) in three orthogonal directions: 1, 2 and 3 are compared (redrawn from Olsen, 2000)

NUMERICAL METHODS

For arbitrary geometries and/or general heterogeneous media, analytical solutions are no longer valid. Therefore, numerical techniques had to be developed. They all are based on the wave equation, and many different models have been proposed to take account of several of the various aspects of site effects. We can classify such techniques into domain methods, boundary methods and asymptotic methods. In the first two approaches, discretization is required for the media and the boundaries, respectively. In a general sense, domain methods are more useful for complex structures, but are also more computationally demanding than boundary methods. On the other hand, asymptotic methods make use of Ray Theory and geometrical techniques.

1. Domain Methods

Examples of domain methods used to study elastic wave propagation are the finite-difference (e.g., Boore, 1972; Virieux, 1984, 1986; Hill and Levander, 1984; Fäh, 1992; Yamanaka et al., 1989; Olsen and Schuster, 1991; Frankel and Vidale, 1992; Yomogida and Etgen, 1993; Frankel, 1993; Moczo et al., 1996; Schenková and Zahradnik, 1996; Graves, 1998; Wang et al., 2001; Hayashi et al., 2001) and finite-element methods (e.g., Lysmer and Drake, 1972; Smith, 1975; Toshinawa and Ohmachi, 1992; Li et al., 1992; Rial et al., 1992).

The most realistic simulations to date are those of finite differences. Use of this technique implies that the differential equations governing the movement are replaced by a group of recursive equations, expressed in form of finite differences that discretely approximate the partial derivatives. The medium is usually divided by means of a regular or structured grid, and the solution in each node of the grid is

obtained in successive intervals of time. This method was first used in order to study wave propagation in elastic media by Alterman and Karal (1968). Since then, finite difference algorithms, models and meshing schemes have been growing in complexity, mainly due to the notorious improvement in available computational resources. Among the many good recent results obtained, we can mention the paper by Frankel (1993) on the response of the San Bernardino Valley or those of Olsen et al. (1995, 1997) for the Los Angeles basin to nearby earthquakes. In Figure 7, a comparison between data and synthetic seismograms, obtained by Olsen (2000), for a receptor located in the Los Angeles basin is provided. Notice the agreement in the second component between both, data and synthetic, as well as the good approximation in the other two components. Irregular grids have been explored recently, and they offer interesting possibilities (e.g., Wang et al., 2001; Hayashi et al., 2001).

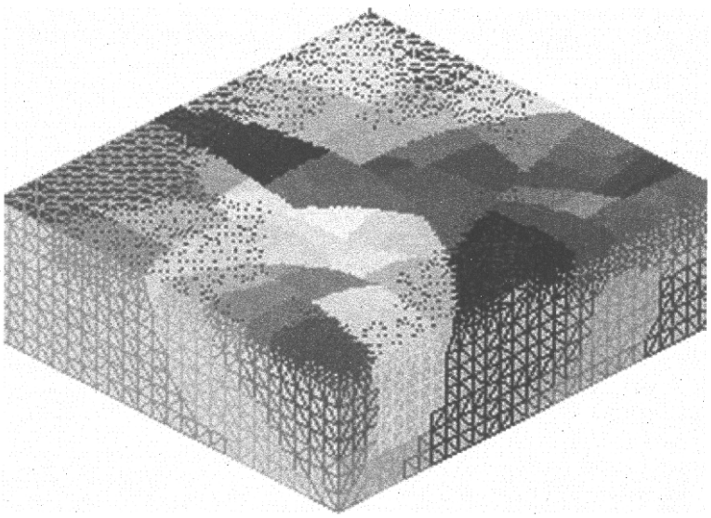

(a)

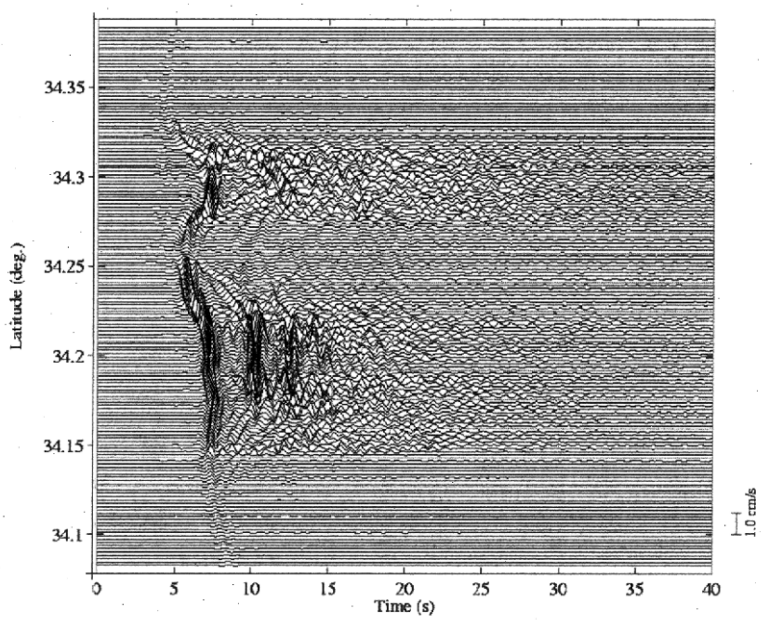

(b)

Fig. 8 (a) Mesh for the San Fernando Basin simulation using finite elements; the 77 million elements mesh is partitioned into 256 subdomains; the coarser mesh is shown for 64 subdomains, (b) E-W surface velocity component along a N-S axis (redrawn from Bao et al., 1998)

On the other hand, in finite-element techniques, the medium is divided into 2D or 3D elements that do not have to be of equal size or of equal form. The displacement field anywhere inside the medium is related to that at certain points, called nodes, by means of shape functions. Nodal values are then obtained

from a discrete system of equations that results from appropriate integrations of the field equations (see, e.g., Zienkiewicz and Taylor, 1989). The finite element technique provides a natural great meshing flexibility, and can deal with non-linear behavior of soils (e.g., Joyner and Chen, 1975; Joyner, 1975).

These methods (finite differences and finite elements methods) are inherently more computationally demanding than other domain methods. However, they are quite general and accurate, and fit handily into large-memory supercomputers and systems for parallel computation. This fit accounts for their current popularity. Figure 8a depicts the model for a rectangular parallelopiped, 54 km long by 33 km wide by 15 km deep, in the San Fernando Basin in Southern California, as used by Bao et al. (1996, 1998). The mesh consists of 77 million tetrahedra, is generated in 13 hours on one processor of a DEC 8400, and requires 7.7 Gb of memory. Figure 8b shows the E-W surface velocity component along N-S axis. Longer durations are associated with the deeper parts of the valley. It seems that the constructive interference of surface and trapped body waves in the shallower regions of the valley is responsible for the stronger motion amplification observed on the surface overlying those regions. It is also noteworthy that no spurious wave reflections seem to be generated at the artificial boundaries.

A natural extension of the finite elements method, the spectral elements method, has been recently applied by Komatitsch and Vilotte (1998) to simulate the seismic response of 2D and 3D geological structures. This is a high-order variational method for the spatial approximation of elastic-wave equations, which is highly efficient in terms of computer resources. Paolucci et al. (1999) have used this method to perform the 3D numerical simulation of the seismic response of a 250 m high hill, by using a last-generation PC in about 15 hours of computer time.

A different approach within domain methods, the so-called pseudo-spectral or Fourier method (Kosloff and Baysal, 1982), makes use of transforms (usually of Fourier type) to compute the spatial derivatives, and a finite difference scheme for the time derivatives, in order to solve various wave propagation problems. The method has allowed the analysis of two-dimensional (Ávila et al., 1993), 2.5-D (Furumura and Takenaka, 1996), and three-dimensional problems (Faccioli et al., 1997). A clear and comprehensive review of this technique is the one by Faccioli et al. (1996).

A compilation of works on the numerical modeling of seismic waves propagation (Kelly and Marfurt, 1990) gives a good account of the so-called domain methods.

2. Boundary Methods

In the last two decades, boundary methods have gained increasing popularity. With such algorithms, only the conditions at the boundaries and their discretization are used to solve the wave equation. This kind of techniques avoids the introduction of the fictitious boundaries for the problem that domain methods usually require. There are two main approaches: (1) boundary methods specifically based on the expansion of wave fields in terms of a complete family of functions, each one of them satisfying the differential equations that governs the problem, and (2) methods based on representation theorems that make use of Green's functions, where the wave field is expressed as an overlapping of plane waves, including the inhomogeneous ones, spreading in all the directions from the boundaries of the elastic space.

In a pioneering work, Aki and Larner (1970) introduced a numerical method, the so-called Discrete Wavenumber method, based on a discrete superposition of plane waves. Bouchon (1973) and, later, Bard (1982) and Geli et al. (1988), used the Aki-Larner technique to study the response of irregular topographies. With the same approach, Bard and Bouchon (1980a, 1980b) studied 2D alluvial valleys. Three-dimensional problems have been also dealt with the Aki-Larner method (e.g., Horike et al., 1990; Ohori et al., 1990; Jiang et al., 1993). The Discrete Wavenumber method, however, cannot deal with large slope features because of numerical difficulties to accurately simulate locally upgoing waves. Sánchez-Sesma et al. (1989a) showed that the Rayleigh *ansatz* (trial solution) is exact, but the problems are of numerical nature; they are associated to a very slow convergence of the representation.

Another type of boundary method has been used to deal with topographies, valleys and layered media. In its many variants, including in some cases three-dimensional problems and layered media, the technique is based upon the superposition of solutions for sources, with their singularities placed outside the region of interest. The singularities may be distributed close to the boundaries or may be of multipolar type, i.e. by using expansions of complete families of solutions. Boundary conditions are satisfied in a least-squares sense, and a system of linear equations for the sources' strengths is obtained.

In fact, Wong (1982) considered the problem as that of generalized inversion. In some applications, however, the location of sources requires particular care, and the trial and error process needed is difficult to apply. This is particularly true when many frequencies are to be computed (see, e.g., Sánchez-Sesma, 1978; Sánchez-Sesma and Rosenblueth, 1979; Sánchez-Sesma and Esquivel, 1979; Wong, 1979, 1982; Dravinski, 1982; Sánchez-Sesma, 1983; Sánchez-Sesma et al., 1984; Dravinski and Mossessian, 1987; Sánchez-Sesma et al., 1985, 1989b; Jiang and Kuribayashi, 1988; Moeen-Vaziri and Trifunac, 1988a, 1988b; Bravo et al., 1988; Eshraghi and Dravinski, 1989; Khair et al., 1989; Bouden et al., 1990; Mossessian and Dravinski, 1990).

Algorithms based on boundary integral equations approaches and their discretizations are known as Boundary Elements Methods (BEM). They have produced many successful solutions to various problems in dynamic elasticity. Recognized advantages over domain approaches are the dimensionality reduction, the relatively easy fulfillment of radiation conditions at infinity, and the high accuracy of results. Excellent surveys of the available literature on these methods in elastodynamics are those of Kobayashi (1987) and Manolis and Beskos (1988).

The most popular approaches are the so-called direct methods, because in their formulation, the unknowns are the sought values of displacements and tractions. These methods arise from the discretization of integral representation theorems. On the other hand, the Indirect Boundary Elements Method (IBEM) formulates the problem in terms of force or moment boundary densities, which can give a deep physical insight on the nature of diffracted waves. In fact, the indirect method has a longer history than the direct one, and is closely related to classical work on integral equations (see, e.g., Manolis and Beskos, 1988).

The combination of discrete wavenumber expansions for Green's functions (Bouchon and Aki, 1977; Bouchon, 1979) with boundary integral representations has been successful in various studies of elastic wave propagation. Bouchon (1985), Campillo and Bouchon (1985), Campillo (1987), Gaffet and Bouchon (1989), Bouchon et al. (1989), and Campillo et al. (1990) used source distributions on the boundaries, whereas Kawase (1988), Kawase and Aki (1989), and Kim and Papageorgiou (1993) used Somigliana representation theorem. These are discrete wavenumber versions of BEM, indirect and direct, respectively. Such combination is particularly attractive: the singularities of Green's functions are not present in each one of the terms of the discrete wavenumber expansion. The integration along the boundary effectively makes the singularities to vanish and improves convergence as well. However, such procedures require a considerable amount of computer resources. As the singularities of Green's functions are integrable (see, e.g., Brebbia, 1978; Banerjee and Butterfield, 1981; Kobayashi, 1987; Manolis and Beskos, 1988; Brebbia and Domínguez, 1992), the sources can be put at the boundary and their effects properly considered. In this way, the uncertainty about the location of sources is eliminated, and the linear system of equations that arises from the discretization can be directly solved. Therefore, the IBEM approach retains the physical insight of the sources method, with all the benefits of analytical integration of exact Green's functions. In the various applications reported here, diffracted fields are represented with the superposition of the radiation from boundary sources, using exact expressions of the 2D Green's functions in an unbounded elastic space. This method can be regarded as a numerical realization of Huygens' principle. The single layer integral representation of elastic wave fields allows computing tractions, once the boundary singularity is appropriately interpreted. Boundary conditions lead to a system of integral equations for boundary sources.

Nearly thirty years ago, Wong and Jennings (1975) used a direct formulation to study arbitrary canyon geometries. More recently, Zhang and Chopra (1991) studied the scattering of elastic waves by topographical irregularities. The response of 2D alluvial settings has been dealt with by Reinoso et al. (1994), whereas 3D problems have been studied by Shinozaki and Yoshida (1992), and Kawano et al. (1994).

The IBEM has been applied by Sánchez-Sesma and Campillo (1991, 1993) to study the diffraction of P, SV and Rayleigh waves by topographical irregularities on the surface of a half-space. The seismic response of 2D alluvial valleys was dealt with by Sánchez-Sesma et al. (1993a), whereas 3D site effects cases were studied by Sánchez-Sesma and Luzón (1995), Ortiz-Alemán et al. (1998), and Gil-Zepeda et al. (2001). The 3D response of 2D topographies, the so-called 2.5D problem, has also been considered by Luco et al. (1990) and Pedersen et al. (1994) by using the IBEM. This method has also been applied to study irregular layering under the incidence of elastic waves (Vai et al., 1999).

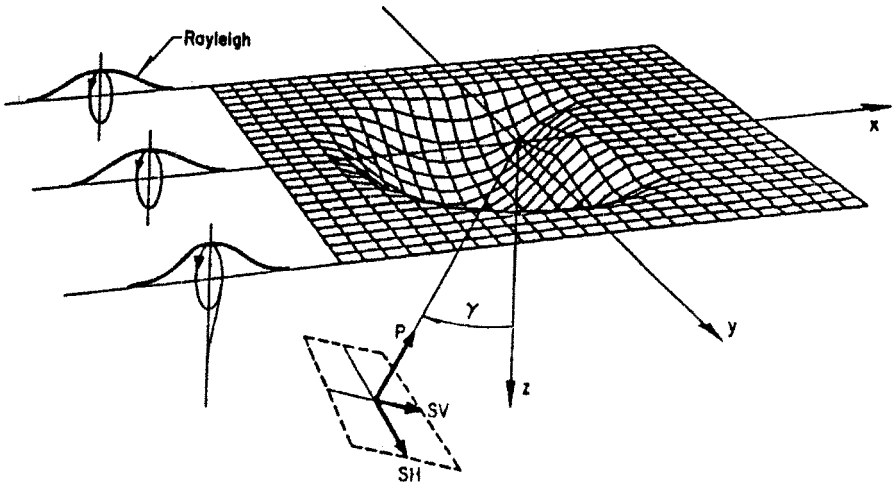

(a)

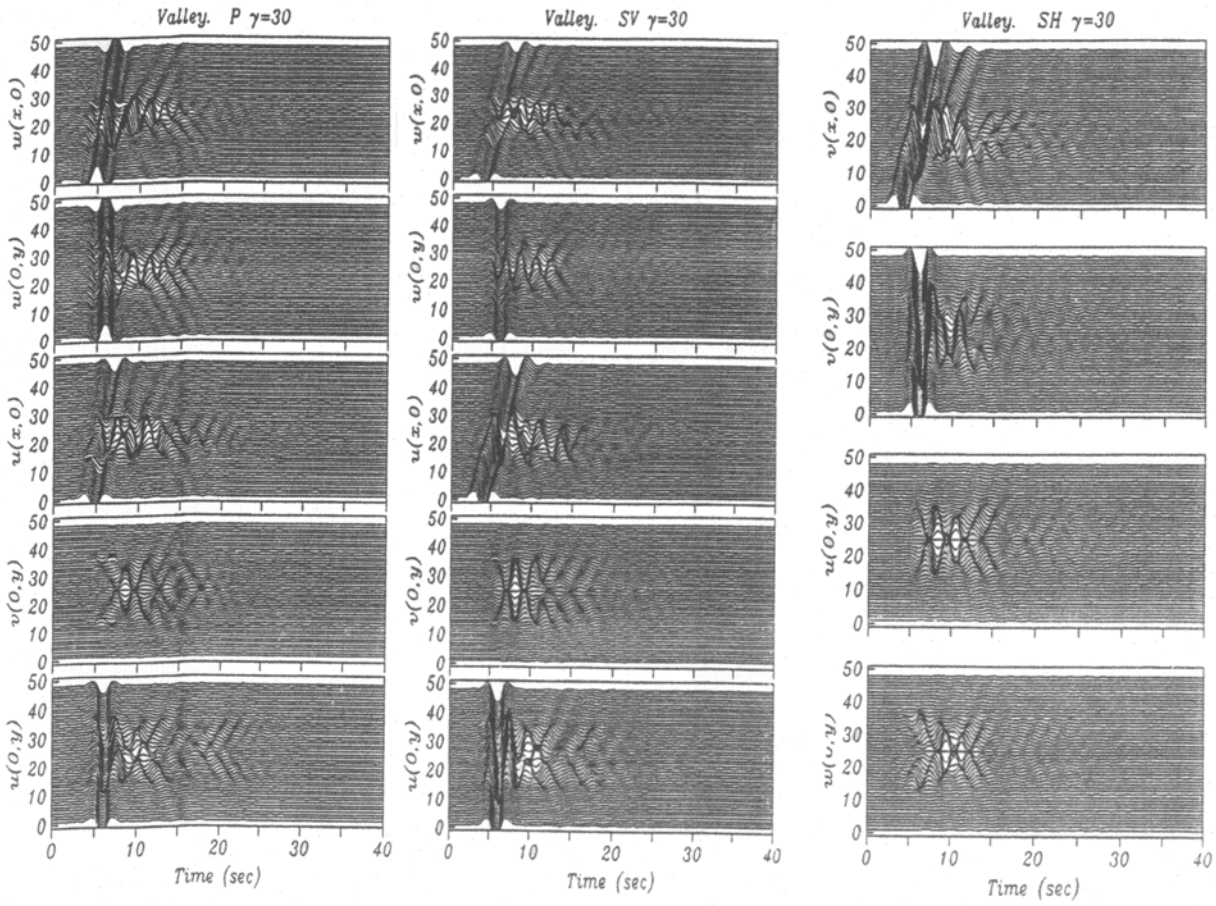

(b)

Fig. 9 (a) Perspective view of the basement of an irregular valley with P, SH, SV and Rayleigh wave incidence; azimuth $\phi = 0$; incidence angle γ with respect to the vertical for body forces, b) Synthetic seismograms for displacements u, v and w at 48 receivers, equally spaced along the x or y axes; the incident waveform is a Ricker wavelet with characteristic period of $t_p = 3$ s (redrawn from Sánchez-Sesma and Luzón, 1995)

Figure 9a shows a perspective of the basement of an irregular valley under incident P, SH, SV and Rayleigh waves. Material properties are $\beta_R = 1$ km/s, $\beta_E = 2$ km/s, $\nu_R = 0.35$, $\nu_E = 0.25$, and $\rho_R = 0.8\rho_E$, where subscripts R and E stand for the soft inclusion and the half-space, respectively.

The width of the valley is 8 km in the *y* direction, its depth is about 1 km, and a quality factor of 100 was assumed. Figure 9b depicts the synthetic seismograms obtained with the IBEM for the P, SV and SH cases, with an azimuth of 0 degrees and an incidence angle of 30 degrees with respect to the vertical. The results present very interesting patterns of interference of the refracted waves inside the basin, and in some cases, significant emission of waves is observed. Incident P and SV waves produce forward and backward scattering of Rayleigh waves by late emission, after refracted waves bounce back and forth in the sediment. Meanwhile, the SH incidence shows significant late emission of scattered SH pulses as a consequence of the shape of the valley, in which refracted waves of Love and Rayleigh types are generated continuously at the edge. One interesting finding for soft, shallow alluvial valleys is a mechanism of coupling of the 1D response and the locally generated surface waves. It is found that the lateral resonances are strongly coupled with the 1D response (Sánchez-Sesma et al., 1993b). The resonant frequencies may be predicted by using an asymptotic semi-classic approach (Rial, 1989).

3. Asymptotic Methods

When the high-frequency behavior is of interest, diffraction can be ignored and optics may be used. Ray theory is based upon the asymptotic behavior of wave solutions in high frequency, so that geometrical methods can be used (e.g., Cerveny, 1985; Lee and Langston, 1983; Sánchez-Sesma et al., 1988b).

The use of Ray methods presents problems associated with its geometrical nature that sometimes give rise to singularities or caustics. To approximately overcome them, a regularized form has been proposed, that uses Gaussian beams. Gaussian beams are solutions of an asymptotic form of wave equation that allows for some lateral variation, and thus, some "artificial" diffraction that smoothes out the discontinuities and eliminates singularities, is introduced (e.g., Nowack and Aki, 1984; Cerveny, 1985; Alvarez et al., 1991). The technique has been used by Yomogida and Aki (1985) to model long-period surface waves, in which the horizontal propagation and smoothing lateral effects were accounted for with Gaussian beams, whereas the vertical variation was considered using the normal modes. This approach assumes smooth variation along the propagation. An extension of these ideas has been proposed by Kato et al. (1993) and applied to model 3D large-scale sedimentary settings.

EXPERIMENTAL METHODS

Records of earthquakes are of great value to understand site effects and the response of structures. Sometimes, the site of interest has already suffered a destructive earthquake, and detailed macroseismic observations are available. However, the rare occurrence of intermediate and strong earthquakes makes the evaluation of site-specific transfer functions for the use in design directly from earthquake records difficult. Engineers and scientists have tried to overcome this lack of strong motion data by recording and analyzing weak motions (from microtremors, microseisms and aftershocks) or effects due to explosions, in order to estimate the site-specific transfer functions experimentally (see, e.g., Kanai, 1983, and Bard, 1999).

Microtemors provide a constant excitation, from which some properties of site response like predominant period, relative amplification, directional resonances, etc. can be characterized. Accounts of the technique and its application to some sites are the works by Dravinski et al. (1991), Morales et al. (1991), Lermo and Chávez-García (1994), Chávez-García et al. (1996), and Trifunac and Todorovska (2000b). Unfortunately, a problem arises because there may not be any similarity of spectra of recorded earthquakes and of measured microtremors at some sites. Udwadia and Trifunac (1973) pointed out that the differences might be attributed to the fact that recorded waves associated to strong and weak motion: (1) are of different types; and (2) have different propagation paths.

The technique proposed by Nakamura (1989) uses the horizontal to vertical (H/V) spectral ratio of weak motion records with very interesting findings. Although there is some discussion on the interpretation of their results (e.g., Lachet and Bard, 1994; Field and Jacob, 1995), Horike et al. (2001) have shown that the microtremor H/V ratios are either in agreement with or a little smaller than the earthquake ratios, and that sharp peaks in the microtremor H/V ratios can be chosen as the resonance frequency of a site, when the value of the peak is large (at least 4 to 5).

Aftershocks frequently occur following destructive earthquakes, and can provide valuable information on the reoccurrence of site effects (Trifunac and Todorovska, 2000a). Amplification of

ground motion due to geological and soil conditions may be extrapolated by means of linear methods. However, recent analysis by Trifunac et al. (1999) with data from aftershocks of the Northridge earthquake concluded that, although the characteristics of site-specific amplification functions can be measured by analyzing aftershocks or small earthquake records, the success rate of predicting the prominent peaks during future earthquakes is less than 50%, and that the successful predictions are limited to small amplitude motions only.

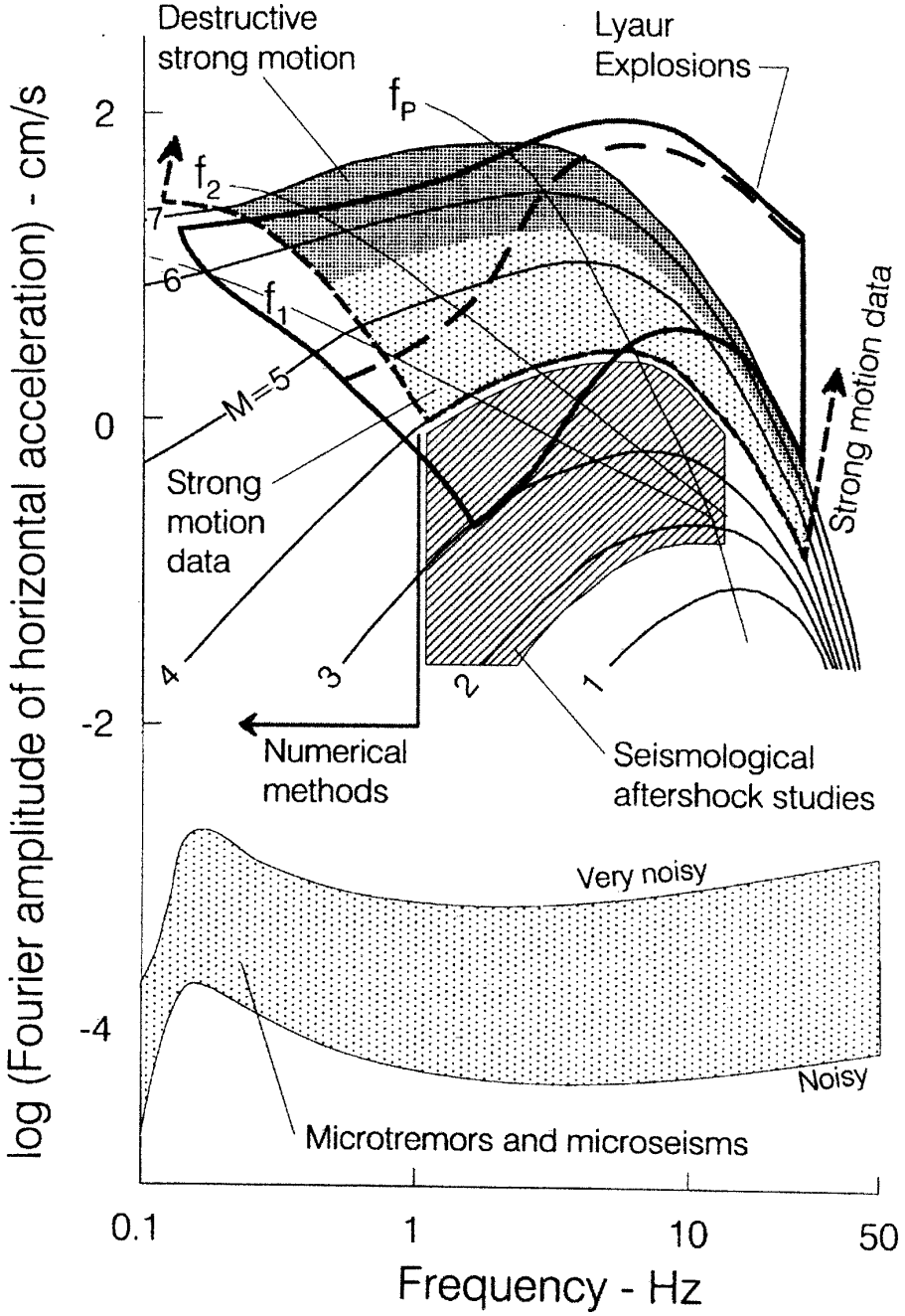

Fig. 10 Comparison of Fourier spectrum amplitudes of strong and weak motions; for the recorded strong motion, epicentral distance $R = 10$ km, focal depth $H = 5$ km and 0.5 probability of exceedance was taken for geological and soil "rock" sites; 10 calibration explosions at the Lyaur testing range were used (after Negmatullaev et al., 1999)

Recordings from distant nuclear explosions have been used to study local amplification of incident waves (e.g., Rogers et al., 1984). However, explosions have more rapid energy release than earthquakes and higher stress changes in a smaller source region. In a recent work, Negmatullaev et al. (1999) compared strong motion data of controlled explosions, detonated in arrays, with those of strong earthquake shaking and other published explosion data. They compared the Fourier amplitude spectra

with estimates by recent empirical scaling laws for strong ground motion, in the near-field of earthquakes, and suggested that such explosions can offer powerful possibilities for testing of almost full-scale structures. This is shown in Figure 10 where the upper gray shaded area stands for the amplitude spectra of recorded strong ground acceleration from both, destructive and non-destructive earthquakes, the area enclosed by a heavy line is for spectra from calibration explosions, spectra of typical seismological aftershock studies are in the hatched region, and spectra of microtremor and microseism noise are in the lower gray zone. The continuous lines labeled 1–7 show smoothed Fourier spectra of ground acceleration based on empirical scaling laws; f_1 and f_2 are corner frequencies (Trifunac, 1993), and f_p is the magnitude-dependent frequency of the spectral maximum.

A class of studies that begins to widen the scope in the study of near-surface propagation of seismic waves, including their amplification, attenuation and scattering, relies on data gathered from deep borehole seismometer arrays. Abercrombie (1995a, 1995b) has compared records and spectra up and downhole for several local events, thus showing that almost a half of the amplitude attenuation for those earthquakes occurs around the upper 300 m.

HYBRID METHODS

The so-called "hybrid" methods use the combinations of different techniques or the adaptation of approaches originally devised to study other problems.

A good example of this kind of methods is the successful combination of normal modes and finite differences (Fäh et al., 1993a, 1993b). In this approach, realistic sources can be assumed, and the waves they produce, are propagated to the site using normal mode theory. Then, the solution obtained at this step is used as the input for another method, finite differences in this case. An interesting example was computed with the IBEM by Luzón et al. (1995). They used as input data a seismogram at the surface, but outside an alluvial valley computed by Fäh (1992). The combination of finite and boundary elements has been used for wave propagation studies by Beskos and Spyrakos (1984), Kobayashi et al. (1986), Mossesian and Dravinski (1987), and Bielak et al. (1991).

In the framework of the source method (an IBEM with least squares), Benites and Aki (1989) computed the Green's functions by using expansions in terms of Gaussian beams. This approach allowed them to study some heterogeneous media. A similar but more complex idea is the combination of surface waves with BEM, as it has been proposed by Hisada et al. (1993) to model 3D alluvial valleys. In this approach, the Green's functions are computed using normal mode theory for long distances and the discrete wave number near the source points. A much-simplified approach was proposed by Rodríguez-Zúñiga et al. (1995). They neglected the interaction of the three-dimensional basin with the sediments, assuming that the motion is given at the basin interface. In some cases, simplifying assumptions are in order, and fast procedures can be devised. Such is the case for triangularly-shaped alluvial valleys (Paolucci et al., 1992), in which the geometry allows for explicit computation of Green's functions for a related configuration.

A promising technique that combines Ricatti method and IBEM, is currently being developed by Haines and Benites (personal communication) after the proposal of Haines (1989). In this approach, the geologically complex medium is assumed to be embedded into a bedrock half-space, upon the incidence of seismic waves. The wave equation in the complex medium is expressed in terms of generalized curvilinear coordinates, choosing one of them as the preferred propagation direction, in analogy to the Cartesian coordinate z (or r) in the reflectivity method (Kennett, 1983; see also Aki and Richards, 1980). In the other reference direction, the wavefield is expanded into basis functions, commonly Fourier components. This form of the wave equation yields non-linear differential equations of the Ricatti type (Haines, 1989), relating traction and displacement fields for each wavenumber, coupled at every point along the propagation coordinate. The wavefield scattered outside the complex medium, into the bedrock, is represented by a boundary integral scheme with artificial wave point source distribution along the boundary separating inner and outer media (e.g., Sánchez-Sesma and Esquivel, 1979). The weights of wave contribution of each wavenumber and the strength of each point source are found by matching boundary conditions in the least-squares sense.

CONCLUDING REMARKS

This rapid passage over some common methodologies to estimate local site effects on strong ground motion excludes many relevant techniques. The coverage is far from exhaustive. By example, an obvious absence is the effect of non-linear behavior of soils, including liquefaction.

Various analytical solutions and methods developed to study site effects were described. The interested reader may find in this short review a guide to pursue independent study.

Finite differences and finite elements methods are well-established techniques which can be used if the geometry and mechanical properties are well known and represented. Absorbing boundary conditions may be sufficient to reduce the models to a reasonable size.

Boundary element methods seem to be powerful tools for simulating wave propagation in homogeneous media with lateral irregularities. If detailed data of media properties are not available, reasonable estimates of ground motion can be obtained with BEM using simplified models. Indirect BEM is being applied to 2D and 3D configurations.

The various techniques have advantages and limitations, and the desired precision and availability of data should dictate the choice of method for a given problem.

ACKNOWLEDGEMENTS

This paper is dedicated to Prof. M. D. Trifunac on his 60th birthday. It is a small homage to both his multifarious contributions in Earthquake Engineering and Seismology and his dedication to the well-being of mankind. We are grateful to R. Vai for her critical reading of the manuscript and many valuable suggestions to improve it. Thanks are given to F. Chávez-García for his kind observations and to L. Ramírez for his help in the preparation of figures. V. Lobatón helped us to locate many references. This work was partially supported by ISMES, S.p.A., Italy and DGAPA-UNAM, Mexico, under Project IN104998.

REFERENCES

1. Abercrombie, R.E. (1995a). “Earthquake Locations Using Single-Station Deep Borehole Recordings: Implications for Microseismicity on the San Andreas Fault in Southern California”, J. Geophys. Res., Vol. 100, No. B12, pp. 24003-24014.
2. Abercrombie, R.E. (1995b). “Earthquake Source Scaling Relationship from 1 to 5 M_L Using Seismograms Recorded at 2.5-Km Depth”, J. Geophys. Res., Vol. 100, No. B12, pp. 24015-24036.
3. Aki, K. (1988). “Local Site Effects on Strong Ground Motion”, in “Earthquake Engineering and Soil Dynamics II - Recent Advances in Ground Motion Evaluation (edited by J.L. Von Thun)”, Geotechnical Special Publication No. 20, Am. Soc. Civil Eng., New York, U.S.A., pp. 103-155.
4. Aki, K. and Larner, K.L. (1970). “Surface Motion of a Layered Medium Having an Irregular Interface due to Incident Plane SH Waves”, J. Geophys. Res., Vol. 75, pp. 1921-1941.
5. Aki, K. and Richards, P.G. (1980). “Quantitative Seismology”, W.H. Freeman, San Francisco, U.S.A.
6. Alterman, Z. and Karal, F.C. (1968). “Propagation of Elastic Waves in Layered Media by Finite Difference Methods”, Bull. Seism. Soc. Am., Vol. 58, pp. 367-398.
7. Alvarez, D.A., Rodríguez, J.L. and Sánchez-Sesma, F.J. (1991). “Evaluación de la Respuesta Sísmica de Depósitos de Suelo Blando Mediante la Superposición de Haces Gaussianos”, Sismodinámica, Vol. 2, pp. 167-180.
8. Ávila, R., Suárez, M. and Sánchez-Sesma, F.J. (1993). “Simulación de la Propagación de Ondas Sísmicas en Configuraciones Irregulares con un Método Pseudoespectral”, Memorias Del X Congreso Nacional de Ingeniería Sísmica, Puerto Vallarta, Jalisco, México.
9. Bao, H., Bielak, J., Ghattas, O., Kallivokas, L.F., O’Hallaron, D.R., Shewchuk, J. and Xu, J. (1996). “Earthquake Ground Motion Modeling on Parallel Computers”, Proc. 1996 ACM/IEEE Supercomputing Conference, Pittsburgh, U.S.A.

10. Bao, H., Bielak, J., Ghattas, O., Kallivokas, L.F., O'Hallaron, D.R., Shewchuk, J. and Xu, J. (1998). "Large-Scale Simulation of Elastic Wave Propagation in Heterogeneous Media on Parallel Computers", Computer Meth. Appl. Mech. Eng., Vol. 152, pp. 85-102.
11. Bard, P.-Y. (1982). "Diffracted Waves and Displacement Field over Two-Dimensional Elevated Topographies", Geophys. J. Royal Astr. Soc., Vol. 71, pp. 731-760.
12. Bard, P.-Y. and Bouchon, M. (1980a). "The Seismic Response of Sediment-Filled Valleys, Part 1: The Case of Incident SH Waves", Bull. Seism. Soc. Am., Vol. 70, pp. 1263-1286.
13. Bard, P.-Y. and Bouchon, M. (1980b). "The Seismic Response of Sediment-Filled Valleys, Part 2: The Case of Incident P and SV waves", Bull. Seism. Soc. Am., Vol. 70, pp. 1921-1941.
14. Bard, P.-Y. and Tucker, B.E. (1985). "Ridge and Tunnel Effects: Comparing Observation with Theory", Bull. Seism. Soc. Am., Vol. 75, pp. 905-922.
15. Bard, P.-Y. (1999). "Microtremor Measurements: A Tool for Site Effect Estimation?", in "The Effects of the Surface Geology on Seismic Motion (edited by K. Irikura, K. Kudo, H. Okada, and T. Sasatami)", Balkema, Rotterdam, pp. 1251-1279.
16. Benites, R. and Aki, K. (1989). "Boundary Integral-Gaussian Beam Method for Seismic Wave Scattering: SH Waves in a Two-Dimensional Media", J. Acoust. Soc. Am., Vol. 86, pp. 375-386.
17. Beskos, D.E. and Spyrakos, C.C. (1984). "Dynamic Response of Strip Foundations by the Time Domain BEM-FEM Method", Dept. of Civil & Mineral Eng., University of Minnesota, Minneapolis, U.S.A.
18. Boore, D.M. (1972). "Finite Difference Methods for Seismic Wave Propagation in Heterogeneous Materials", in "Methods in Computational Physics, Vol. 11: Seismology (edited by B.A. Bolt)", Academic Press, New York, U.S.A.
19. Boore, D.M. (1983). "Stochastic Simulation of High-Frequency Ground Motions Based in Seismological Models of the Radiated Spectra", Bull. Seism. Soc. Am., Vol. 73, pp. 1865-1894.
20. Borcherdt, R.G. and Glassmoyer, G. (1992). "On the Characteristics of Local Geology and Their Influence on Ground Motions Generated by the Loma Prieta Earthquake in the San Francisco Bay Region, California", Bull. Seism. Soc. Am., Vol. 82, pp. 603-641.
21. Bouchon, M. (1973). "Effect of Topography on Surface Motion", Bull. Seism. Soc. Am., Vol. 63, pp. 615-632.
22. Bouchon, M. (1979). "Discrete Wave Number Representation of Elastic Wave Fields in Three-Space Dimensions", J. Geophys. Res., Vol. 84, No. B7, pp. 3609-3614.
23. Bouchon, M. (1985). "A Simple, Complete Numerical Solution to the Problem of Diffraction of SH Waves by an Irregular Surface", J. Acoust. Soc. Am., Vol. 77, pp. 1-5.
24. Bouchon, M. and Aki, K. (1977). "Discrete Wave-Number Representation of Seismic-Source Wave Fields", Bull. Seism. Soc. Am., Vol. 67, pp. 259-277.
25. Bouchon, M., Campillo, M. and Gaffet, S. (1989). "A Boundary Integral Equation-Discrete Wavenumber Representation Method to Study Wave Propagation in Multilayered Media Having Irregular Interfaces", Geophysics, Vol. 54, pp. 1134-1140.
26. Bouden, M., Khair, K.R. and Datta, S.K. (1990). "Ground Motion Amplification by Cylindrical Valleys Embedded in a Layered Medium", Earthquake Eng. Struct. Dyn., Vol. 19, pp. 497-512.
27. Bravo, M.A., Sánchez-Sesma, F.J. and Chávez-García, F.J. (1988). "Ground Motion on Stratified Alluvial Deposits for Incident SH Waves", Bull. Seism. Soc. Am., Vol. 78, pp. 436-450.
28. Brebbia, C.A. (1978). "The Boundary Element Method for Engineers", Pentech Press, London, U.K.
29. Brebbia, C.A. and Domínguez, J. (1992). "Boundary Elements: An Introductory Course", 2nd Edition, Comp. Mec. Publ., Southampton, U.K. & McGraw-Hill Book Co., New York, U.S.A.
30. Burridge, R., Mainardi, F. and Servizi, G. (1980). "Soil Amplification of Plane Seismic Waves", Phys. of the Earth and Planet. Int., Vol. 22, pp. 122-136.
31. Campillo, M. (1987). "Modeling of SH Wave Propagation in an Irregularly Layered Medium: Application to Seismic Profiles near a Dome", Geophys. Prospecting, Vol. 35, pp. 236-249.

32. Campillo, M. and Bouchon, M. (1985). "Synthetic SH Seismograms in a Laterally Varying Medium by the Discrete Wavenumber Method", Geophys. J. Royal Astr. Soc., Vol. 83, pp. 307-317.
33. Campillo, M., Bard, P.-Y., Nicollin, F. and Sánchez-Sesma, F.J. (1988). "The Incident Wavefield in Mexico City during the Great Michoacán Earthquake and its Interaction with the Deep Basin", Earthquake Spectra, Vol. 4, pp. 591-608.
34. Campillo, M., Sánchez-Sesma, F.J. and Aki, K. (1990). "Influence of Small Lateral Variations of a Soft Surficial Layer on Seismic Ground Motion", Soil Dyn. Earthquake Eng., Vol. 9, pp. 284-287.
35. Chávez-García, F.J., Sánchez, L.R. and Hatzfeld, D. (1996). "Topographic Site Effects and HVSR: A Comparison between Observation and Theory", Bull. Seism. Soc. Am., Vol. 86, pp. 1559-1573.
36. Chen, X.-F. (1990). "Seismogram Synthesis for Multi-Layered Media with Irregular Interfaces by Global Generalized Reflection/Transmission Matrices Method, I: Theory of 2-D SH Case", Bull. Seism. Soc. Am., Vol. 80, pp. 1696-1724.
37. Chen, X.-F. (1995). "Seismogram Synthesis for Multi-Layered Media with Irregular Interfaces by Global Generalized Reflection/Transmission Matrices Method, II: Applications for 2-D SH Case", Bull. Seism. Soc. Am, Vol. 85, pp. 1094-1106.
38. Chen, X.-F. (1996). "Seismogram Synthesis for Multi-Layered Media with Irregular Interfaces by Global Generalized Reflection/Transmission Matrices Method, III: Theory of 2-D P-SV Case", Bull. Seism. Soc. Am., Vol. 86, pp. 389-405.
39. Chen, X.-F. (1999). "Love Waves in Multi-Layered Media with Irregular Interfaces, Part I: Modal Solutions and Excitation Formulation", Bull. Seism. Soc. Am., Vol. 89, pp. 1519-1534.
40. Davis, L.L. and West, L.R. (1973). "Observed Effects of Topography on Ground Motion", Bull. Seism. Soc. Am., Vol. 63, pp. 283-298.
41. Dravinski, M. (1982). "Influence of Interface Depth upon Strong Ground Motion", Bull. Seism. Soc. Am., Vol. 72, pp. 597-614.
42. Dravinski, M. and Mossessian, T.K. (1987). "Scattering of Plane Harmonic P, SV and Rayleigh Waves by Dipping Layers of Arbitrary Shape", Bull. Seism. Soc. Am., Vol. 77, pp. 212-235.
43. Dravinski, M., Mossessian, T.K. and Eshraghi, H. (1991). "Predominant Motion of the Los Angeles Sedimentary Basin", Eng. Analysis with Boundary Elements, Vol. 8, pp. 206-214.
44. Duke, M. (1958). "Effects of Ground Destructiveness of Large Earthquakes", Proc. ASCE, Vol. 84, No. SM3.
45. Dunkin, J.W. (1965). "Computation of Modal Solutions in Layered, Elastic Media at High Frequencies", Bull. Seism. Soc. Am., Vol. 55, pp. 335-358.
46. Eshraghi, H. and Dravinski, M. (1989). "Scattering of Elastic Waves by Non Axisymmetric Three-Dimensional Dipping Layer", J. Num. Methods for Partial Differential Equations, Vol. 5, pp. 327-345.
47. Ewing, M., Jardetzky, W. and Press, F. (1957). "Elastic Waves in Layered Media", Mc-Graw Hill Book Co., New York, U.S.A.
48. Faccioli, E. (1991). "Seismic Amplification in the Presence of Geological and Topographic Irregularities (State of the Art Paper)", Proc. Second Int. Conf. on Recent Advances in Geotechnical Earthquake Eng. and Soil Dyn., St. Louis, Missouri, U.S.A., pp. 1779-1797.
49. Faccioli, E., Maggio, F., Quarteroni, A. and Tagliani, A. (1996). "Spectral Domain Decomposition Methods for the Solution of Acoustic and Elastic Wave Equations", Geophysics, Vol. 61, pp. 1160-1174.
50. Faccioli, E., Maggio, F., Paolucci, R. and Quarteroni, A. (1996). "2-D and 3-D Elastic Wave Propagation by a Pseudo-Spectral Domain Decomposition Method", Journal of Seismology, Vol. 1, pp. 237-251.
51. Fäh, D. (1992). "A Hybrid Technique for the Estimation of Strong Ground Motion in Sedimentary Basins", Ph.D. Thesis, Swiss Fed. Inst. Technology, Zurich, Switzerland.

52. Fäh, D., Iodice, C., Suhadolc, P. and Panza, G.F. (1993a). "A New Method for the Realistic Estimation of Seismic Ground Motion in Megacities: The Case of Rome", Earthquake Spectra, Vol. 9, pp. 643-688.
53. Fäh, D., Suhadolc, P. and Panza, G.F. (1993b). "Variability of Seismic Ground Motion in Complex Media: The Case of a Sedimentary Basin in the Friuli (Italy) Area", J. Appl. Geophys, Vol. 30, pp. 131-148.
54. Field, E.H. and Jacob, K.H. (1995). "A Comparison and Test of Various Site Response Estimation Techniques, Including Three That Are Not Reference Site Dependent", Bull. Seism. Soc. Am., Vol. 85, pp. 1127-1143.
55. Frankel, A. (1993). "Three-Dimensional Simulations of Ground Motion in the San Bernardino Valley, California, for Hypothetical Earthquakes on the San Andreas Fault", Bull. Seism. Soc. Am., Vol. 83, pp. 1020-1041.
56. Frankel, A. and Vidale, J. (1992). "A Three-Dimensional Simulation of Seismic Waves in the Santa Clara Valley, California, from a Loma Prieta Aftershock", Bull. Seism. Soc. Am., Vol. 82, pp. 2045-2074.
57. Furumura, K. and Takenaka, H. (1996). "2.5-D Modeling of Elastic Waves Using the Pseudospectral Method", Geophys. J. Int., Vol. 124, pp. 820-832.
58. Gaffet, S. and Bouchon, M. (1989). "Effects of Two-Dimensional Topographies Using the Discrete Wavenumber-Boundary Integral Equation Method in P-SV Cases", J. Acoust. Soc. Am., Vol. 85, pp. 2277-2283.
59. Geli, L., Bard, P.-Y. and Jullien, B. (1988). "The Effect of Topography on Earthquake Ground Motion: A Review and New Results", Bull. Seism. Soc. Am., Vol. 78, pp. 42-63.
60. Gil-Zepeda, A., Luzón, F., Aguirre, J., Morales, J., Sánchez-Sesma, F.J. and Ortiz-Alemán, C. (2001). "3D Seismic Response of the Deep Basement-Structure of the Granada Basin (Southern Spain)", Bull. Seism. Soc. Am., submitted.
61. Graves, R. (1998). "Three-Dimensional Finite-Difference Modeling of the San Andreas Fault: Source, Parametrization and Ground-Motion Levels", Bull. Seism. Soc. Am., Vol. 88, pp. 881-897.
62. Griffiths, D.W. and Bollinger, G.A. (1979). "The Effect of the Appalachian Mountain Topography on Seismic Waves", Bull. Seism. Soc. Am., Vol. 69, pp. 1081-1105.
63. Gutenberg, B. (1957). "Effects of Ground on Earthquake Motion", Bull. Seism. Soc. Am., Vol. 47, pp. 221-250.
64. Haines, A.J. (1989). "On the Structure of One-Way Elastic Wave Propagation and Exact Solutions to the Elastodynamic Equations: Theory for 2-Dimensional SH Waves", Monograph, DSIR, Wellington, New Zealand.
65. Hartzell, S.H. (1978). "Interpretation of Earthquake Strong Ground Motion and Implications for Earthquake Mechanism", Ph.D. Dissertation, University of California at San Diego, La Jolla, U.S.A.
66. Haskell, N.A. (1953). "The Dispersion of Surface Waves on Multilayered Media", Bull. Seism. Soc. Am., Vol. 43, pp. 17-34.
67. Haskell, N.A. (1960). "Crustal Reflection of Plane SH Waves", J. Geophys. Res., Vol. 65, pp. 4147-4150.
68. Haskell, N.A. (1962). "Crustal Reflection of Plane P and SV Waves", J. Geophys. Res., Vol. 67, pp. 4751-4767.
69. Hayashi, K., Burns, D.R. and Toksöz, M.N. (2001). "Discontinuous-Grid Finite-Difference Modeling Including Surface Topography", Bull. Seism. Soc. Am., Vol. 91, pp. 1750-1764.
70. Hisada, Y., Aki, K. and Teng, T.-L. (1993). "3-D Simulations of Surface Wave Propagation in the Kanto Sedimentary Basin, Japan, Part 2: Application of the Surface Wave BEM", Bull. Seism. Soc. Am., Vol. 83, pp. 1700-1720.
71. Hill, N.R. and Levander, A.R. (1984). "Resonances of Low-Velocity Layers with Lateral Variations", Bull. Seism. Soc. Am., Vol. 74, pp. 521-537.
72. Horike, M., Uebayashi, H. and Takeuchi, Y. (1990). "Seismic Response in Three-Dimensional Sedimentary Basin due to Plane S Wave Incidence", J. Phys. Earth, Vol. 38, pp. 261-284.

73. Horike, M., Zhao, B. and Kawase, H. (2001). "Comparison of Site Response Characteristics Inferred from Microtremors and Earthquake Shear Waves", Bull. Seism. Soc. Am., Vol. 91, pp. 1526-1536.
74. Hutchings, L. (1994). "Kinematic Earthquake Models and Synthesized Ground Motion Using Empirical Green's Functions", Bull. Seism. Soc. Am., Vol. 84, pp. 1028-1050.
75. Irikura, K. (1983). "Semi-Empirical Estimation of Strong Ground Motion during Large Earthquakes", Bull. Disaster Prev. Res. Inst., Vol. 33, pp. 63-104.
76. Jiang, T. and Kuribayashi, E. (1988). "The Three-Dimensional Resonance of Axisymmetric Sediment-Filled Valleys", Soils and Foundations, Vol. 28, pp. 130-146.
77. Jiang, T., Nishioka, S., Nagasaka, H. and Kuribayashi, E. (1993). "Three-Dimensional Reflectivity Method for Complicated Irregular Formations", Soil Dyn. Earthquake Eng., Vol. 12, pp. 173-182.
78. Joyner, W.B. (1975). "A Method for Calculating Nonlinear Seismic Response in Two Dimensions", Bull. Seism. Soc. Am., Vol. 65, pp. 1337-1357.
79. Joyner, W.B. and Chen, A.T.F. (1975). "Calculation of Nonlinear Ground Response in Earthquakes", Bull. Seism. Soc. Am., Vol. 65, pp. 1315-1336.
80. Kanai, K. (1949). "Relation between the Earthquake Damage of Non-wooden Buildings and the Nature of the Ground", Bull. Earthquake Res. Inst., Vol. 27, p. 97.
81. Kanai, K. (1951). "Relation between the Earthquake Damage of Non-wooden Buildings and the Nature of the Ground", Bull. Earthquake Res. Inst., Vol. 29, p. 209.
82. Kanai, K. (1983). "Engineering Seismology", University of Tokyo Press, Tokyo, Japan.
83. Kausel, E. and Roesset, J.M. (1981). "Stiffness Matrices for Layered Soils", Bull. Seism. Soc. Am., Vol. 71, pp. 1743-1761.
84. Kato, K., Aki, K. and Teng, T.-L. (1993). "3-D Simulations of Surface Wave Propagation in the Kanto Sedimentary Basin, Japan, Part 1: Application of the Surface Wave Gaussian Beam Method", Bull. Seism. Soc. Am., Vol. 83, pp. 1676-1699.
85. Kawano, M., Matsuda, S., Toyoda, K. and Yamada, J. (1994). "Seismic Response of Three-Dimensional Alluvial Deposit with Irregularities for Incident Wave Motion from a Point Source", Bull. Seism. Soc. Am., Vol. 84, pp. 1801-1814.
86. Kawase, H. (1988). "Time-Domain Response of a Semicircular Canyon for Incident SV, P, and Rayleigh Waves Calculated by the Discrete Wavenumber Boundary Element Method", Bull. Seism. Soc. Am., Vol. 78, pp. 1415-1437.
87. Kawase, H. and Aki, K. (1989). "A Study on the Response of a Soft Basin for Incident S, P and Rayleigh Waves with Special Reference to the Long Duration Observed in Mexico City", Bull. Seism. Soc. Am., Vol. 79, pp. 1361-1382.
88. Kawase, H., Sánchez-Sesma, F.J. and Aki, K. (1987). "Site Amplification Far beyond the Impedance Ratio for Incident SV Waves", EOS Trans., Am. Geophys. Union, Vol. 68, p. 1354.
89. Kelly, K.R. and Marfurt, K.J. (1990). "Numerical Modeling of Seismic Wave Propagation", Geophysics Reprint Series, No. 13, Soc. of Exploration Geophysics, Tulsa, U.S.A.
90. Kennett, B.L.N. (1983). "Seismic Wave Propagation in Stratified Media", Cambridge University Press, Cambridge, U.K.
91. Khair, K.R., Datta, S.K. and Shah, A.H. (1989). "Amplification of Obliquely Incident Seismic Waves by Cylindrical Alluvial Valleys of Arbitrary Cross-Sectional Shape, Part I: Incident P and SV Waves", Bull. Seism. Soc. Am., Vol. 79, pp. 610-630.
92. Kim, J. and Papageorgiou, A. (1993). "Discrete Wavenumber Boundary-Element Method for 3D Scattering Problems", J. Eng. Mech., ASCE, Vol. 119, pp. 603-624.
93. Kobayashi, S. (1987). "Elastodynamics", in "Boundary Element Methods in Mechanics (edited by D.E. Beskos)", North-Holland, Amsterdam, The Netherlands.
94. Kobayashi, S., Nishimura, N. and Mori, K. (1986). "Applications of Boundary Element-Finite Element Combined Method to Three-Dimensional Viscoelastic Problems", in "Boundary Elements (edited by D. Qinghua)", Pergamon Press, Oxford, U.K., pp. 67-74.

95. Komatitsch, D. and Vilotte, J.P. (1998). "The Spectral Element Method: An Efficient Tool to Simulate the Seismic Response of 2D and 3D Geological Structures", Bull. Seism. Soc. Am., Vol. 88, pp. 368-392.
96. Kosloff, R. and Baysal, E. (1982). "Forward Modeling by a Fourier Method", Geophysics, Vol. 52, pp. 1402-1412.
97. Lachet, C. and Bard, P.-Y. (1994). "Numerical and Theoretical Investigations on the Possibilities and Limitations of the "Nakamura's" Technique", J. Phys. Earth, Vol. 42, pp. 377-397.
98. Lee, J.J. and Langston, C.A. (1983). "Wave Propagation in a Three-Dimensional Circular Basin", Bull. Seism. Soc. Am., Vol. 73, pp. 1637-1655.
99. Lee, V.W. (1984). "Three-Dimensional Diffraction of Plane P, SV & SH Waves by a Hemispherical Alluvial Valley", Soil Dyn. Earthquake Eng., Vol. 3, pp. 133-144.
100. Lee, V.W. and Trifunac, M.D. (1979). "Response of Tunnels to Incident SH-Waves", J. Eng. Mech., ASCE, Vol. 105, pp. 643-659.
101. Lee, V.W. and Trifunac, M.D. (1982). "Body Wave Excitation of Embedded Hemisphere", J. Eng. Mech., ASCE, Vol. 108, pp. 546-563.
102. Lermo, J. and Chávez-García, F.J. (1994). "Are Microtremors Useful in Site Response Evaluation?", Bull. Seism. Soc. Am., Vol. 84, pp. 1350-1364.
103. Li, X., Bielak, J. and Ghattas, O. (1992). "Three-Dimensional Earthquake Response on a CM-2", Proc. 10th World Conf. Earthquake Eng., Madrid, Spain, Vol. 2, pp. 959-964.
104. Luco, J.E., Wong, H.L. and De Barros, F.C.P. (1990). "Three-Dimensional Response of a Cylindrical Canyon in a Layered Half-Space", Earthquake Eng. Struct. Dyn., Vol. 19, pp. 799-817.
105. Luzón, F., Aoi, S., Fäh, D. and Sánchez-Sesma, F.J. (1995). "Simulation of the Seismic Response of a 2D Sedimentary Basin: A Comparison between the Indirect Boundary Element Method and a Hybrid Technique", Bull. Seism. Soc. Am., Vol. 85, pp. 1501-1506.
106. Lysmer, J. and Drake, L.A. (1972). "A Finite Element Method for Seismology", in "Methods in Computational Physics, Vol. 11: Seismology (edited by B.A. Bolt)", Academic Press, New York, U.S.A.
107. Manolis, G.D. and Beskos, D.E. (1988). "Boundary Element Methods in Elastodynamics", Unwin Hyman Ltd., London, U.K.
108. Mateos, J.L., Flores, J., Novaro, O., Alvarez-Tostado, J.M. and Seligman, T.H. (1993b). "Generation of Inhomogeneous P Waves in a Layered Medium", Tectonophysics, Vol. 218, pp. 247-256.
109. MacDonald, H.M. (1902). "Electric Waves", Cambridge University Press, Cambridge, U.K.
110. Medvedev, S.V. (1955). "Ocenka Sizmicheskoi Balnoski u Zavisimosti ot Gruntovih Uslovi", Tr. Geofiz. Inst. AN SSSR, Vol. 4, p. 141.
111. Moczo, P., Labák, P., Kristek, J. and Hron, F. (1996). "Amplification and Differential Motion due to an antiplane 2D Resonance in the Sediment Valleys Embedded in a Layer over the Halfspace", Bull. Seism. Soc. Am., Vol. 86, pp. 1434-1446.
112. Moeen-Vaziri, N. and Trifunac, M.D. (1981). "A Note on the Vibration of a Semi-Circular Canal Excited by Plane SH-Wave", Bull. Indian Soc. Earthquake Tech., Vol. 18, No. 2, pp. 88-100.
113. Moeen-Vaziri, N. and Trifunac, M.D. (1985). "Scattering of Plane SH-Waves by Cylindrical Canals of Arbitrary Shape", Soil Dyn. Earthquake Eng., Vol. 4, pp. 18-23.
114. Moeen-Vaziri, N. and Trifunac, M.D. (1986). "Investigation of Scattering and Diffraction of Plane Seismic Waves through Two-Dimensional Inhomogeneities", Report 86-03, Dept. of Civil Eng., Univ. Southern Calif., Los Angeles, California, U.S.A.
115. Moeen-Vaziri, N. and Trifunac, M.D. (1988a). "Scattering and Diffraction of Plane SH-Waves by Two-Dimensional Inhomogeneities", Earthquake Eng. Struct. Dyn., Vol. 7, pp. 179-188.
116. Moeen-Vaziri, N. and Trifunac, M.D. (1988b). "Scattering and Diffraction of Plane SV-Waves by Two-Dimensional Inhomogeneities", Earthquake Eng. Struct. Dyn., Vol. 7, pp. 189-200.

117. Montalvo-Arrieta, J.C., Sánchez-Sesma, F.J. and Reinoso, E. (2002). "A Virtual Reference Site for the Valley of Mexico", Bull. Seism. Soc. Am., in press.
118. Morales, J., Vidal, F., Peña, J.A., Alguacil, G. and Ibáñez, J. (1991). "Microtremor Study in the Sediment Filled Basin of Zafarraya, Granada (Southern Spain)", Bull. Seism. Soc. Am., Vol. 81, pp. 687-693.
119. Mossessian, T.K. and Dravinski, M. (1990). "Amplification of Elastic Waves by a Three Dimensional Valley, Part 1: Steady State Response", Earthquake Eng. Struct. Dyn., Vol. 19, pp. 667-680.
120. Mossessian, T.K. and Dravinski, M. (1992). "A Hybrid Approach for Scattering of Elastic Waves by Three-Dimensional Irregularities of Arbitrary Shape", J. Phys. Earth, Vol. 40, pp. 241-261.
121. Mow, C.C. and Pao, Y.H. (1971). "The Diffraction of Elastic Waves and Dynamic Stress Concentrations", Report R-482-PR, The Rand Corporation, Santa Monica, California, U.S.A.
122. Nowack, R. and Aki, K. (1984). "The Two-Dimensional Gaussian Beam Synthetic Method: Testing and Application", J. Geophys. Res., Vol. 89, pp. 7797-7819.
123. Nakamura, Y. (1989). "A Method for Dynamic Characteristics Estimation of Subsurface Using Microtremor on the Ground Surface", QR of RTRI, Vol. 30, pp. 25-33.
124. Negmatullaev, S.Kh., Todorovska, M.I. and Trifunac, M.D. (1999). "Simulation of Strong Earthquake Ground Motion by Explosions - Experiments at the Lyaur Testing Range in Tajikistan", Soil Dyn. Earthquake Eng., Vol. 18, pp. 189-207.
125. Ohori, M., Koketsu, K. and Minami, T. (1992). "Seismic Responses of Three-Dimensional Sediment Filled Valleys due to Incident Plane Waves", J. Phys. Earth, Vol. 40, pp. 209-222.
126. Olsen, K.B. (2000). "Site Amplification in the Los Angeles Basin from Three-Dimensional Modeling of Ground Motion", Bull. Seism. Soc. Am., Vol. 90, pp. 77-94.
127. Olsen, K.B. and Schuster, G.T. (1991). "Seismic Hazard Analysis in Salt Lake Valley by Finite Difference Simulation of Three-Dimensional Elastic Wave Propagation", IBM Supercomputing Contest, pp. 135-165.
128. Olsen, K.B., Archuleta, R.J. and Matarese, J.R. (1995). "Three-Dimensional Simulation of a Magnitude 7.75 Earthquake on the San Andreas Fault", Science, Vol. 270, pp. 1628-1632.
129. Olsen, K.B., Matarese, J.R. and Archuleta, R.J. (1997). "Three-Dimensional Dynamic Simulation of the 1992 Landers Earthquake", Science, Vol. 278, pp. 834-837.
130. Ordaz, M., Arboleda, J. and Singh, S.K. (1995). "A Scheme of Random Summation of an Empirical Green's Function to Estimate Ground Motions from Future Large Earthquakes", Bull. Seism. Soc. Am., Vol. 85, pp. 1635-1647.
131. Ortiz-Alemán, C., Sánchez-Sesma, F.J., Rodríguez-Zúñiga, J.L. and Luzón, F. (1998). "Computing Topographical 3-D Site Effects Using a Fast IBEM/Conjugate Gradient Approach", Bull. Seism. Soc. Am., Vol. 88, pp. 393-399.
132. Paolucci, R., Suárez, M.M. and Sánchez-Sesma, F.J. (1992). "Fast Computation for a Class of Alluvial Valleys", Bull. Seism. Soc. Am., Vol. 82, pp. 2075-2086.
133. Paolucci, R., Faccioli, E. and Maggio, F. (1999). "3D Response Analysis of an Instrumented Hill at Matsuzaki, Japan, by a Spectral Method", Journal of Seismology, Vol. 3, pp. 191-209.
134. Papageorgiou, A.S. and Kim, J. (1993). "Propagation and Amplification of Seismic Waves in 2-D Valleys Excited by Obliquely Incident P- and SV-Waves", Earthquake Eng. Struct. Dyn., Vol. 22, pp. 167-182.
135. Pedersen, H.A., Sánchez-Sesma, F.J. and Campillo, M. (1994). "Three-Dimensional Scattering by Two-Dimensional Topographies", Bull. Seism. Soc. Am., Vol. 84, pp. 1169-1183.
136. Pérez-Rocha, L.E., Sánchez-Sesma, F.J. and Reinoso, E. (1991). "Three-Dimensional Site Effects in Mexico City: Evidence from Accelerometric Network Observations and Theoretical Results", Proc. 4th Int. Conf. Seismic Zonation, Earthquake Eng. Res. Inst., Stanford, California, U.S.A., Vol. 2, pp. 327-334.
137. Rial, J.A. (1989). "Seismic Wave Resonances in 3D Sedimentary Basins", Geophys. J. Int., Vol. 99, pp. 81-90.

138. Rial, J.A., Saltzman, N.G. and Ling, H. (1992). "Earthquake-Induced Resonance in Sedimentary Basins", American Scientist, Vol. 80, pp. 566-578.

139. Reid, H.F. (1910). "The California Earthquake of April 18, 1906", in "The Mechanics of the Earthquake, Vol. 2", Report of the State Earthquake Investigation Commission, Carnegie Institute of Washington, Washington, D.C., U.S.A.

140. Reinoso, E., Ordaz, M. and Sánchez-Sesma, F.J. (1990). "A Note on the Fast Computation of Response Spectra Estimates", Earthquake Eng. Struct. Dyn., Vol. 19, pp. 971-976.

141. Reinoso, E., Wrobel, L.C. and Power, H. (1994). "Preliminary Results of the Modeling of the Mexico City Valley with Two-Dimensional Boundary Element Method for the Scattering of SH Waves", Soil Dyn. Earthquake Eng., Vol. 12, pp. 457-468.

142. Rodríguez-Zúñiga, J.L., Sánchez-Sesma, F.J. and Pérez-Rocha, L.E. (1995). "Seismic Response of Shallow Three-Dimensional Valleys: The Use of Simplified Models", Bull. Seism. Soc. Am., Vol. 85, pp. 890-899.

143. Rogers, A.M., Borcherdt, R.D., Covington, P.A. and Perkins, D.M. (1984). "A Comparative Ground Motion Study near Los Angeles Using Recordings of Nevada Nuclear Tests and the 1971 San Fernando Earthquake", Bull. Seism. Soc. Am., Vol. 74, pp. 1925–1949.

144. Rovelli, A., Bonamassa, O., Cocco, M., Dibona, M. and Mazza, S. (1988). "Scaling Laws and Spectral Parameters of the Ground Motion in Active Extensional Areas in Italy", Bull. Seism. Soc. Am., Vol. 78, pp. 530-560.

145. Sánchez-Sesma, F.J. (1978). "Ground Motion Amplification due to Canyon of Arbitrary Shape", Proc. 2nd Int. Conf. on Microzonation, Vol. 2, pp. 729-742.

146. Sánchez-Sesma, F.J. (1983). "Diffraction of Elastic Waves by Three-Dimensional Surface Irregularities", Bull. Seism. Soc. Am., Vol. 73, pp. 1621-1636.

147. Sánchez-Sesma, F.J. (1985). "Diffraction of Elastic SH Waves by Wedges", Bull. Seism. Soc. Am., Vol. 75, pp. 1435-1446.

148. Sánchez-Sesma, F.J. (1987). "Site Effects on Strong Ground Motion", Soil Dyn. Earthquake Eng., Vol. 6, pp. 124-132.

149. Sánchez-Sesma, F.J. (1990). "Elementary Solutions for the Response of a Wedge-Shaped Medium to Incident SH and SV Waves", Bull. Seism. Soc. Am., Vol. 80, pp. 737-742.

150. Sánchez-Sesma, F.J. (1996). "Strong Ground Motions and Site Effects", in "Computer Analysis and Design of Earthquake Resistant Structures (edited by D.E. Beskos and S.A. Anagnostopoulos)", Comp. Mech. Publications, Southampton, U.K., pp. 201-239.

151. Sánchez-Sesma, F.J. and Campillo, M. (1991). "Diffraction of P, SV and Rayleigh Waves by Topographical Features: A Boundary Integral Formulation", Bull. Seism. Soc. Am., Vol. 81, pp. 2234-2253.

152. Sánchez-Sesma, F.J. and Campillo, M. (1993). "Topographic Effects for Incident P, SV and Rayleigh Waves", Tectonophysics, Vol. 218, pp. 113-125.

153. Sánchez-Sesma, F.J. and Esquivel, J. (1979). "Ground Motion on Alluvial Valleys under Incident Plane SH Waves", Bull. Seism. Soc. Am., Vol. 69, pp. 1107-1120.

154. Sánchez-Sesma, F.J. and Luzón, F. (1995). "Seismic Response of Three-Dimensional Alluvial Valleys for Incident P, S and Rayleigh Waves", Bull. Seism. Soc. Am., Vol. 85, pp. 269-284.

155. Sánchez-Sesma, F.J. and Luzón, F. (1996). "Can Horizontal P Waves Be Trapped and Resonate in a Shallow Sedimentary Basin?", Geophys. J. Int., Vol. 124, pp. 209-214.

156. Sánchez-Sesma, F.J. and Rosenblueth, E. (1979). "Ground Motion at Canyons of Arbitrary Shape under Incident SH Waves", Earthquake Eng. Struct. Dyn., Vol. 7, pp. 441-450.

157. Sánchez-Sesma, F.J. and Velázquez, S.A. (1987). "On the Seismic Response of a Dipping Layer", Wave Motion, Vol. 9, pp. 387-391.

158. Sánchez-Sesma, F.J., Chávez-Pérez, S. and Avilés, J. (1984). "Scattering of Elastic Waves by Three-Dimensional Topographies", Proc. 8th World Conf. Earthquake Eng., San Francisco, California, U.S.A., Vol. 2, pp. 639-646.

159. Sánchez-Sesma, F.J., Bravo, M.A. and Herrera, I. (1985). "Surface Motion of Topographical Irregularities for Incident P, SV and Rayleigh Waves", Bull. Seism. Soc. Am., Vol. 75, pp. 263-269.
160. Sánchez-Sesma, F.J., Chávez-Pérez, S., Suárez, M., Bravo, M.A. and Pérez-Rocha, L.E. (1988a). "On the Seismic Response of the Valley of Mexico", Earthquake Spectra, Vol. 4, pp. 569-589.
161. Sánchez-Sesma, F.J., Chávez-García, F.J. and Bravo, M.A. (1988b). "Seismic Response of a Class of Alluvial Valleys for Incident SH Waves", Bull. Seism. Soc. Am., Vol. 78, pp. 83-95.
162. Sánchez-Sesma, F.J., Campillo, M. and Irikura, K. (1989a). "A Note on the Rayleigh Hypothesis and the Aki-Larner Method", Bull. Seism. Soc. Am., Vol. 79, pp. 1995-1999.
163. Sánchez-Sesma, F.J., Pérez-Rocha, L.E. and Chávez-Pérez, S. (1989b). "Diffraction of Elastic Waves by Three-Dimensional Surface Irregularities, Part II", Bull. Seism. Soc. Am., Vol. 79, pp. 101-112.
164. Sánchez-Sesma, F.J., Ramos-Martínez, J. and Campillo, M. (1993a). "An Indirect Boundary Element Method Applied to Simulate the Seismic Response of Alluvial Valleys for Incident P, S and Rayleigh Waves", Earthquake Eng. Struct. Dyn., Vol. 22, pp. 279-295.
165. Sánchez-Sesma, F.J., Pérez-Rocha, L.E. and Reinoso, E. (1993b). "Ground Motion in Mexico City during the April 25, 1989, Guerrero Earthquake", Tectonophysics, Vol. 218, pp. 127-140.
166. Sánchez-Sesma, F.J., Vai, R., Castillo, J.M. and Luzón, F. (1995). "Seismic Response of Irregularly Stratified Media Using the Indirect Boundary Element Method", in "Soil Dynamics and Earthquake Engineering VII (edited by A.S. Cakmak and C.A. Brebbia)", Chania, Crete, Greece, pp. 225-233.
167. Sezawa, K. (1927). "Scattering of Elastic Waves and Some Allied Problems", Bull. Earthquake Res. Inst., Tokyo Univ., Japan, Vol. 3, p. 18.
168. Schenková, Z. and Zahradnik, J. (1996). "Interpretation of the Microtremor Spectra at the Zafarraya Basin, Southern Spain", Soil Dyn. Earthquake Eng., Vol. 15, pp. 69-73.
169. Shearer, P.M. and Orcutt, J.A. (1987). "Surface and Near Surface Effects on Seismic Waves: Theory and Borehole Seismometer Results", Bull. Seism. Soc. Am., Vol. 77, pp. 1168-1196.
170. Shinozaki, Y. and Yoshida, K. (1992). "Seismic Ground Motion in Three-Dimensional Sedimentary Basin", Special Seminar on Seismic Ground Motion in Sedimentary Basin, Disaster Prevention Research Institute, Kyoto University, Kyoto, Japan.
171. Smith, W.D. (1975). "The Application of Finite Element Analysis to Body Wave Propagation Problems", J. Geophys., Vol. 44, pp. 747-768.
172. Somerville, P.G., Sen, M.K. and Cohee, B. (1991). "Simulation of Strong Ground Motions Recorded during the 1985 Michoacan, Mexico, and Valparaiso, Chile Earthquakes", Bull. Seism. Soc. Am., Vol. 81, pp. 1-27.
173. Thomson, W.T. (1950). "Transmission of Elastic Waves through a Stratified Solid Medium", J. Appl. Phys., Vol. 21, pp. 89-93.
174. Todorovska, M.I. and Lee, V.W. (1990). "A Note on Response of Shallow Circular Valleys to Rayleigh Waves - Analytical Approach", Earthquake Eng. and Eng. Vibration, Vol. 10, pp. 21-34.
175. Todorovska, M.I. and Lee, V.W. (1991a). "Surface Motion of Circular Alluvial Valleys of Variable Depth for Incident Plane SH Waves", Soil Dyn. and Earthquake Eng., Vol. 10, pp. 192-200.
176. Todorovska, M.I. and Lee, V.W. (1991b). "A Note on Scattering of Rayleigh Waves by Shallow Circular Canyons: Analytical Approach", Bull. Indian Soc. of Earthquake Tech., Paper 306, Vol. 28, pp. 1-16.
177. Toshinawa, T. and Ohmachi, T. (1992). "Love Wave Propagation in a Three-Dimensional Sedimentary Basin", Bull. Seism. Soc. Am., Vol. 82, pp. 1661-1667.
178. Trifunac, M.D. (1971a). "Response Envelope Spectrum and Interpretation of Strong Earthquake Ground Motion", Bull. Seism. Soc. Am., Vol. 61, pp. 343-356.
179. Trifunac, M.D. (1971b). "Surface Motion of a Semi-Cylindrical Alluvial Valley for Incident Plane SH Waves", Bull. Seism. Soc. Am., Vol. 61, pp. 1755-1770.
180. Trifunac, M.D. (1973). "Scattering of Plane SH Waves by a Semi-Cylindrical Canyon", Earthquake Eng. Struct. Dyn., Vol. 1, pp. 267-281.

181. Trifunac, M.D. (1976a). "Preliminary Analysis of the Peaks of Strong Earthquake Ground Motion - Dependence of Peaks on Earthquake Magnitude, Epicentral Distance and the Recording Site Conditions", Bull. Seism. Soc. Am., Vol. 66, pp. 189-219.

182. Trifunac, M.D. (1976b). "A Note on the Range of Peak Amplitudes of Recorded Accelerations, Velocities and Displacements with Respect to the Modified Mercalli Intensity", Earthquake Notes, Vol. 47, No. 2, pp. 9-24.

183. Trifunac, M.D. (1976c). "Preliminary Empirical Model for Scaling Fourier Amplitude Spectra of Strong Ground Acceleration in Terms of Earthquake Magnitude, Source to Station Distance and Recording Site Conditions", Bull. Seism. Soc. Am., Vol. 66, pp. 1343-1373.

184. Trifunac, M.D. (1978). "Response Spectra of Earthquake Ground Motion", J. Eng. Mech., ASCE, Vol. 104, pp. 1081-1097.

185. Trifunac, M.D. (1979). "Preliminary Empirical Model for Scaling Fourier Amplitude Spectra of Strong Motion Acceleration in Terms of Modified Mercalli Intensity and Geological Site Conditions", Earthquake Eng. and Struct. Dyn., Vol. 7, pp. 63-74.

186. Trifunac, M.D. (1980). "Effects of Site Geology on Amplitude of Strong Motion", Proc. 7th World Conf. Earthquake Eng., Istanbul, Turkey, pp. 145-152.

187. Trifunac, M.D. (1987). "Influence of Local Soil and Geological Site Conditions on Fourier Spectrum Amplitudes of Recorded Strong Motion Accelerations", Report 87-04, Dept. of Civil Eng., Univ. Southern Calif., Los Angeles, California, U.S.A.

188. Trifunac, M.D. (1989). "Dependence of Fourier Spectrum Amplitudes of Recorded Strong Earthquake Accelerations on Magnitude, Local Soil Conditions and on Depth of Sediments", Earthquake Eng. Struct. Dyn., Vol. 18, pp. 999-1016.

189. Trifunac, M.D. (1990). "How to Model Amplification of Strong Earthquake Motions by Local Soil and Geologic Site Conditions", Earthquake Eng. Struct. Dyn., Vol. 19, pp. 833-846.

190. Trifunac, M.D. (1993). "Long Period Fourier Amplitude Spectra of Strong Motion Acceleration", Soil Dyn. Earthquake Eng., Vol. 12, pp. 363-382.

191. Trifunac, M.D. and Anderson, J.G. (1977). "Preliminary Empirical Models for Scaling Absolute Acceleration Spectra", Report 77-03, Dept. of Civil Eng., Univ. Southern Calif., Los Angeles, California, U.S.A.

192. Trifunac, M.D. and Brady, A.G. (1975a). "On the Correlation of Seismic Intensity Scales with the Peaks of Recorded Strong Ground Motion", Bull. Seism. Soc. Am., Vol. 65, pp. 139-162.

193. Trifunac, M.D. and Brady, A.G. (1975b). "A Study on the Duration of Strong Earthquake Ground Motion", Bull. Seism. Soc. Am., Vol. 65, pp. 581-626.

194. Trifunac, M.D. and Brady, A.G. (1975c). "Correlations of Peak Acceleration, Velocity and Displacement with Earthquake Magnitude, Epicentral Distance and Site Conditions", Earthquake Eng. and Struct. Dyn., Vol. 4, pp. 455-471.

195. Trifunac, M.D. and Hudson, D.E. (1971). "Analysis of the Pacoima Dam Accelerogram - San Fernando, California, Earthquake of 1971", Bull. Seism. Soc. Am., Vol. 61, pp. 1393-1411.

196. Trifunac, M.D. and Lee, V.W. (1978). "Dependence of the Fourier Amplitude Spectra of Strong Motion Acceleration on the Depth of Sedimentary Deposits", Report 78-14, Dept. of Civil Eng., Univ. Southern Calif., Los Angeles, California, U.S.A.

197. Trifunac, M.D. and Lee, V.W. (1989). "Empirical Models for Scaling Fourier Amplitude Spectra of Strong Ground Accelerations in Terms of Earthquake Magnitude, Source to Station Distance, Site Intensity and Recording Site Conditions", Soil Dyn. and Earthquake Eng., Vol. 8, pp. 110-125.

198. Trifunac, M.D. and Todorovska, M.I. (1998). "Damage Distribution during the 1994 Northridge, California, Earthquake Relative to Generalized Categories of Surficial Geology", Soil Dyn. Earthquake Eng., Vol. 17, pp. 239-253.

199. Trifunac, M.D. and Todorovska, M.I. (2000a). "Can Aftershock Studies Predict Site Amplification?: Northridge, CA, Earthquake of 17 January, 1994", Soil Dyn. and Earthquake Eng., Vol. 19, pp. 233-251.

200. Trifunac, M.D. and Todorovska, M.I. (2000b). "Long Period Microtremors, Microseisms and Earthquake Damage: Northridge, CA, Earthquake of 17 January, 1994", Soil Dyn. and Earthquake Eng., Vol. 19, pp. 253-267.

201. Trifunac, M.D. and Udwadia, F.E. (1974). "Variations of Strong Earthquake Ground Shaking in the Los Angeles Area", Bull. Seism. Soc. Am., Vol. 64, pp. 1429-1454.

202. Trifunac, M.D. and Westermo, B.D. (1977). "A Note on the Correlation of Frequency Dependent Duration of Strong Ground Motion with the Modified Mercalli Intensity and the Geological Conditions at the Recording Stations", Bull. Seism. Soc. Am., Vol. 67, pp. 917-927.

203. Trifunac, M.D., Hao, T.Y. and Todorovska, M.I. (1999). "On the Reoccurrence of Site Specific Response", Soil Dyn. and Earthquake Eng., Vol. 18, pp. 569–592.

204. Tucker, B.E., King, J.L., Hatzfeld, D. and Nersesov, I.L. (1984). "Observations of Hard-Rock Site Effects", Bull. Seism. Soc. Am., Vol. 74, pp. 121-136.

205. Udwadia, F.E and Trifunac, M.D. (1973). "Comparison of Earthquake and Microtremor Ground Motions in El Centro, California", Bull. Seism. Soc. Am., Vol. 63, pp. 1227–1253.

206. Udwadia, F.E. and Trifunac, M.D. (1974). "Characterization of Response Spectra through Statistics of Oscillator Response", Bull. Seism. Soc. Am., Vol. 64, pp. 205-219.

207. Vanmarcke, E.H. (1976). "Structural Response to Earthquakes", in "Seismic Risk and Engineering Decisions (edited by C. Lomnitz and E. Rosenblueth)", Elsevier Publishing Co., Amsterdam, pp. 287-337.

208. Vai, R., Castillo-Covarrubias, J.M., Sánchez-Sesma, F.J., Komatitsch, D. and Vilotte, J.-P. (1999). "Elastic Wave Propagation in an Irregularly Layered Medium", Soil Dyn. Earthquake Eng., Vol. 18, pp. 11-18.

209. Virieux, J. (1984). "SH-Wave Propagation in Heterogeneous Media: Velocity-Stress Finite-Difference Method", Geophysics, Vol. 49, pp. 1933-1942.

210. Virieux, J. (1986). "P-SV Wave Propagation in Heterogeneous Media: Velocity-Stress Finite-Difference Method", Geophysics, Vol. 51, pp. 889-901.

211. Wang, Y., Xu, J. and Schuster, G.T. (2001). "Viscoelastic Wave Simulation in Basins by a Variable-Grid Finite Difference Method", Bull. Seism. Soc. Am., Vol. 91, pp. 1741-1749.

212. Wong, H.L. (1979). "Diffraction of P, SV and Rayleigh Waves by Surface Topographies", Report CE 79-05, Department of Civil Engineering, University of Southern California, Los Angeles, California, U.S.A.

213. Wong, H.L. (1982). "Effect of Surface Topography on the Diffraction of P, SV and Rayleigh Waves", Bull. Seism. Soc. Am., Vol. 72, pp. 1167-1183.

214. Wong, H.L. and Jennings, P.C. (1975). "Effect of Canyon Topographies on Strong Ground Motion", Bull. Seism. Soc. Am., Vol. 65, pp. 1239-1257.

215. Wong, H.L. and Trifunac, M.D. (1974a). "Scattering of Plane SH Wave by a Semi-elliptical Canyon", Earthquake Eng. Struct. Dyn., Vol. 3, pp. 157-169.

216. Wong, H.L. and Trifunac, M.D. (1974b). "Surface Motion of a Semi-elliptical Alluvial Valley for Incident Plane SH Wave", Bull. Seism. Soc. Am., Vol. 64, pp. 1389-1403.

217. Wong, H.L. and Trifunac, M.D. (1977). "A Note on the Effects of Recording Site Conditions on Amplitudes of Strong Earthquake Ground Motions", Proc. 6th World Conf. Earthquake Eng., New Delhi, pp. 452-457.

218. Wong, H.L., Trifunac, M.D. and Westermo, B. (1977). "Effects of Surface and Subsurface Irregularities on the Amplitudes of Monochromatic Waves", Bull. Seism. Soc. Am., Vol. 67, pp. 353-368.

219. Yamanaka, H., Kazuoh, S. and Takanori, S. (1989). "Effects of Sedimentary Layers on Surface-Wave Propagation", Bull. Seism. Soc. Am., Vol. 79, pp. 631-644.

220. Yomogida, H. and Aki, K. (1985). "Waveform Synthesis of Surface Waves in a Laterally Heterogeneous Earth by the Gaussian Beam Method", J. Geophys. Res., Vol. 90, pp. 7665-7688.

221. Yomogida, K. and Etgen, J.T. (1993). "3-D Wave Propagation in the Los Angeles Basin for the Whittier-Narrows Earthquake", Bull. Seism. Soc. Am., Vol. 83, pp. 1325-1344.

222. Zhang, L. and Chopra, A.K. (1991). "Three-Dimensional Analysis of Spatially Varying Ground Motions around a Uniform Canyon in a Homogeneous Half-Space", Earthquake Eng. Struct. Dyn., Vol. 20, pp. 911-926.

223. Zhou, X. (1965). "Effect of Soil Classification on Structural Damage during Strong-Motion Earthquakes", Earthquake Eng. Research Report, Inst. Eng. Mechanics, Academia Sinica, Harbin, China, Vol. II, pp. 27-43.

224. Zienkiewicz, O.C. and Taylor, R.L. (1989). "The Finite Element Method, Vol. 1: Basic Formulation and Linear Problems", McGraw-Hill Book Co., London, U.K.

ISET Journal of Earthquake Technology, Paper No. 419, Vol. 39, No. 3, September 2002, pp. 91-103

A NOTE ON THE SIGNIFICANCE AND USES OF ELEMENTARY ANALYSES OF STRONG EARTHQUAKE GROUND MOTION

Ivanka Paskaleva
Scientific Director
Central Laboratory for Seismic Mechanics and Earthquake Engineering
Bulgarian Academy of Sciences, Academic G. Bonchev Street, Block 3, Sofia 1113, Bulgaria

ABSTRACT

The advanced theoretical and empirical models of strong ground earthquake motion are built on assumptions about the nature of strong ground motion that are drawn from elementary and direct studies of recorded strong ground motion. This brief note reviews selected published elementary studies, emphasizing their significance for the subsequent advanced studies, such as detailed regression models for peak amplitudes and response and Fourier spectra of strong motion. The illustrations are mostly from published work by Strong Motion Group at University of Southern California. They contributed many such elementary studies and have later used their findings in development of advanced regression models. Specifically, this note reviews observations on: the spatial attenuation of strong motion, the interpretation of its wave content, small versus large amplitudes, the strong motion magnitude scale, and the principles of empirical scaling of strong motion for use in earthquake engineering. It also presents selected examples of how the observational evidence, as recorded on accelerograms, has contributed towards creation of new and refinement of the existing theories.

KEYWORDS: Wave Content of Strong Motion, Spatial Attenuation of Strong Motion, Strong Motion Magnitude, Large versus Small Amplitudes of Ground Motion

INTRODUCTION

The state-of-the-art methodologies for engineering description of strong ground motion, for example the comprehensive empirical models for scaling peak amplitudes and response and Fourier spectra, and the methods for synthesis of artificial accelerograms, evolved over the past seventy years mainly due to the systematic efforts to record strong ground motion (Heck et al., 1936; Cloud and Carder, 1956; Halverson, 1970), and to analyze its physical nature. The success of the advanced methodologies in predicting the characteristics of possible future shaking depends significantly on the validity of the physical assumptions these methods are built on. For example, the empirical scaling models for peak amplitudes, spectra and duration of strong ground motion are based on assumptions about the functional relationship between the scaled quantities and various input parameters (such as the earthquake magnitude, source-to-site distance, local site condition, type of wave path, etc.), and the statistical regression gives only the coefficients in these assumed functional forms. The number of input parameters and the details of the assumed functional forms are eventually a compromise between the desired detail and what can be justified as statistically significant by the quantity and quality of the strong motion data available for the regression. As the strong motion data accumulated over the years, these models became more and more detailed.

The assumptions on the nature of strong ground motion and how it is affected by the earthquake source, propagation path characteristics and the local site geology, to be used for advanced studies, are drawn based on elementary analyses of recorded data, and on studies of analytical and numerical models for the range of parameters for which data is lacking or is insufficient. These elementary analyses are exploratory in nature, and often consist of various presentations of subsets of the data and visual observation of trends. While these types of analysis do not require any advanced mathematical skills, their success depends on the ingenuity of the ways the data is presented and on the experience of the analyst and his/her ability to "see" and interpret the trends (i.e. to see "the forest from the trees" and "the trees from the forest"). Nevertheless, these elementary studies are very powerful and important, firstly because their conclusions are based most directly and solely on observations, minimizing possible

artifacts from the method of analysis, and because they represent a necessary building block of many advanced studies to follow.

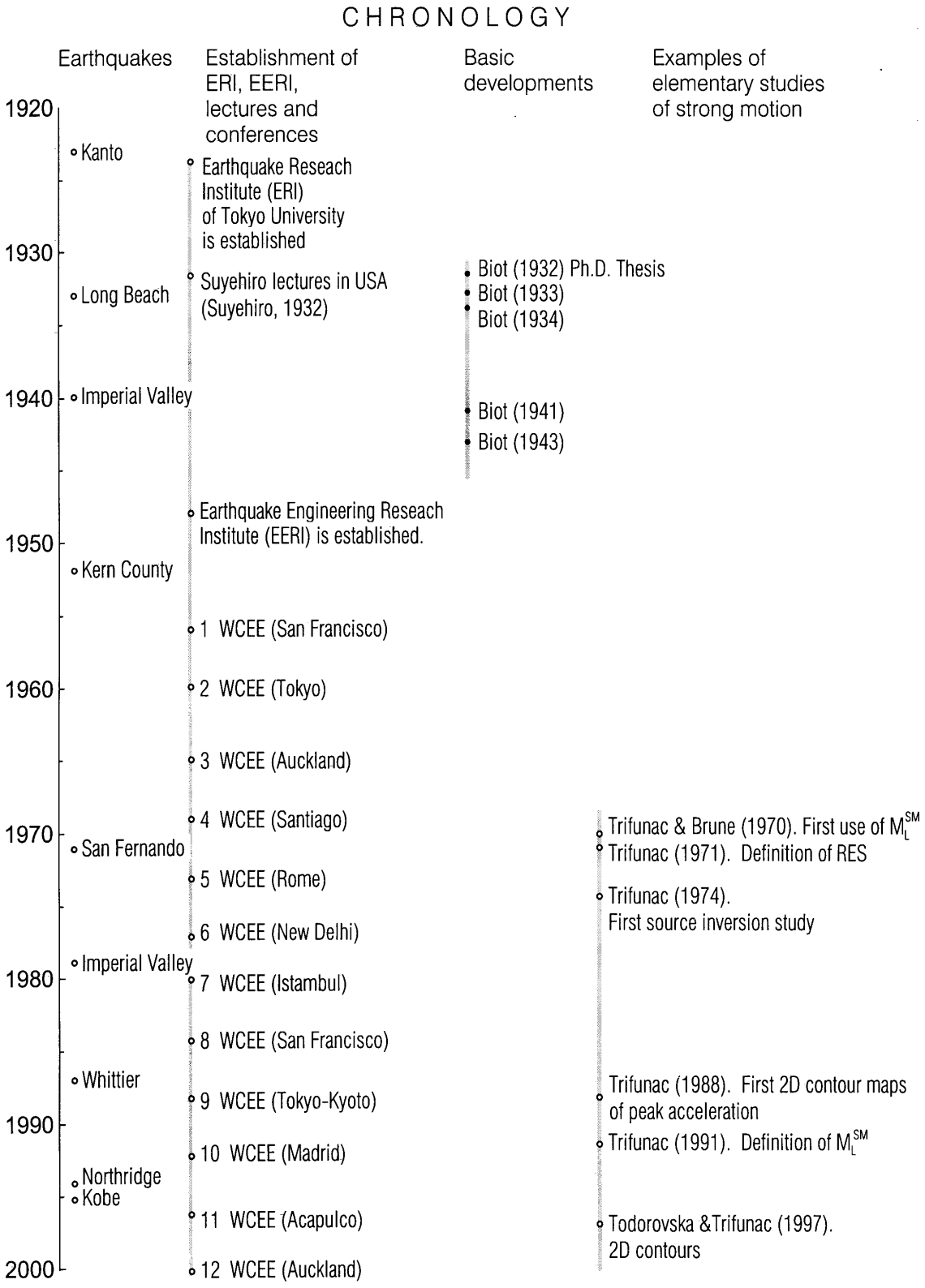

Fig. 1 Chronology of selected Trifunac's contributions to the analysis and interpretation of strong ground motion, relative to the years of occurrence of selected earthquakes, the establishment of ERI and EERI, the World Conferences on Earthquake Engineering, and the formulation of the response spectrum method in 1932 by Biot, which marked the beginning of the modern earthquake engineering

The aim of this brief note is to discuss published elementary studies of the nature of strong earthquake ground motion, with an emphasis on their importance for advanced regression analyses. The most successful empirical scaling models are those that use meticulously researched functional forms, based on physically sound interpretation of the theory and careful and comprehensive verification in terms of a large volume of recorded data. There are many excellent examples of published regression models of strong ground motion, but their review or even modest discussion are beyond the scope of this brief note. This note focuses only on selected most direct and elementary analyses of strong ground motion, citing examples mostly from the work of the Strong Motion Research Group at the University of Southern California (USC). The reason for this is that this group has contributed extensively to development of empirical scaling models of strong motion, so that the ideas and interpretations in the reviewed elementary studies in this note can be followed through their eventual application.

Specifically, this note reviews observations on: the spatial attenuation of strong motion, the interpretation of its wave content, small versus large amplitudes, the strong motion magnitude scale, and the principles of empirical scaling of strong motion for use in earthquake engineering. It also presents selected examples of how the observational evidence, as recorded on accelerograms, has contributed towards creation of new and refinement of the existing theories. The obvious need for continued and comprehensive observation of strong earthquake motions, in structures and in soils, will be emphasized to illustrate the quantity and quality of data that is needed to guide future theoretical and empirical developments in description and prediction of strong ground motion for engineering design.

ENGINEERING AND DESCRIPTIVE ANALYSES OF RECORDED MOTIONS

The modern era of earthquake engineering began with the second chapter of Biot's Ph.D. dissertation at California Institute of Technology in 1932, entitled "Vibration of Buildings during Earthquakes" (Biot, 1932). Biot's ideas were further refined in Biot (1933, 1934), and fully developed into the general theory of response spectrum superposition method in Biot (1941, 1942) (see Figure 1 for the chronology of his contributions relative to the times of significant (from engineering point of view) earthquakes, and the times of the World Conferences on Earthquake Engineering). It is remarkable that Biot was able to formulate so simple and ingenious methodology (still representing the basis for earthquake resistant design today, seventy years later), before any strong motion data were recorded in Southern California. By the time Biot presented his last two papers on earthquake engineering in 1941 and 1942, there were only five strong motion records (Long Beach, 1933, Ferndale, 1937, 1938, and El Centro, 1940, all in California; and Helena, 1935, in Montana).

Many studies of the basic properties of strong motion and of its scaling for engineering applications have been motivated by or can be traced back to either speculative comments or to intuitive discussions in Biot (1941, 1942) papers. Those roots and early formative concepts will be illustrated in some of the following examples.

In the late 1930s, the first recorded accelerograms were analyzed to describe the maximum response of a family of single-degree-of freedom representations of structures. Response spectra were computed with mechanical spectrum analyzers (torsional pendulum; Biot, 1941), for the purpose of developing "standard" response spectrum shapes to be used in design practice. The difficulty at that time was that the number of recorded strong motion accelerograms was small (Long Beach, 1933; Helena, 1935; Ferndale 1937, 1938; El Centro, 1940), and the fluctuations of the computed spectra were so large that only preliminary "spectral shapes" could be considered (Biot, 1942) for design.

Little changed until 1971. The seismic activity in Southern California was relatively low, and the number of recording instruments was small, resulting in slow accumulation of recorded accelerograms (Figure 2, Trifunac and Todorovska, 2001a). Examples of the first well-recorded earthquakes, with multiple triggered stations close to the causative faults, are the 1966 Parkfield (Housner and Trifunac, 1967; Hudson et al., 1969) and the 1971 San Fernando (Trifunac and Hudson, 1971) earthquakes in California. The Parkfield earthquake was recorded by five strong motion accelerographs (Trifunac and Udwadia, 1974), while the San Fernando earthquake produced 94 free-field and building basement records (Figure 2, Trifunac, 1974). An analysis of the Parkfield data suggested that "important structures to be located close to a fault … should be designed to withstand a 10 inch displacement pulse without serious consequences. … Also of special engineering significance was the fact that the earthquake ground motion of 40 to 50 percent of g … can be recorded near a surface fault" (Housner and Trifunac, 1967).

These estimates were soon exceeded during the San Fernando earthquake in 1971, with long period peak displacement approaching 50 cm (20 in) and peak ground acceleration exceeding 1.25g, at the Pacoima dam site (Trifunac and Hudson, 1971). This "large" peak acceleration revived the debates on how large peak accelerations are in the vicinity of causative faults (Ambraseys, 1973), but eventually and following other later recordings of even larger peak accelerations, its significance was reduced to a "normal" data point (Trifunac, 1976a).

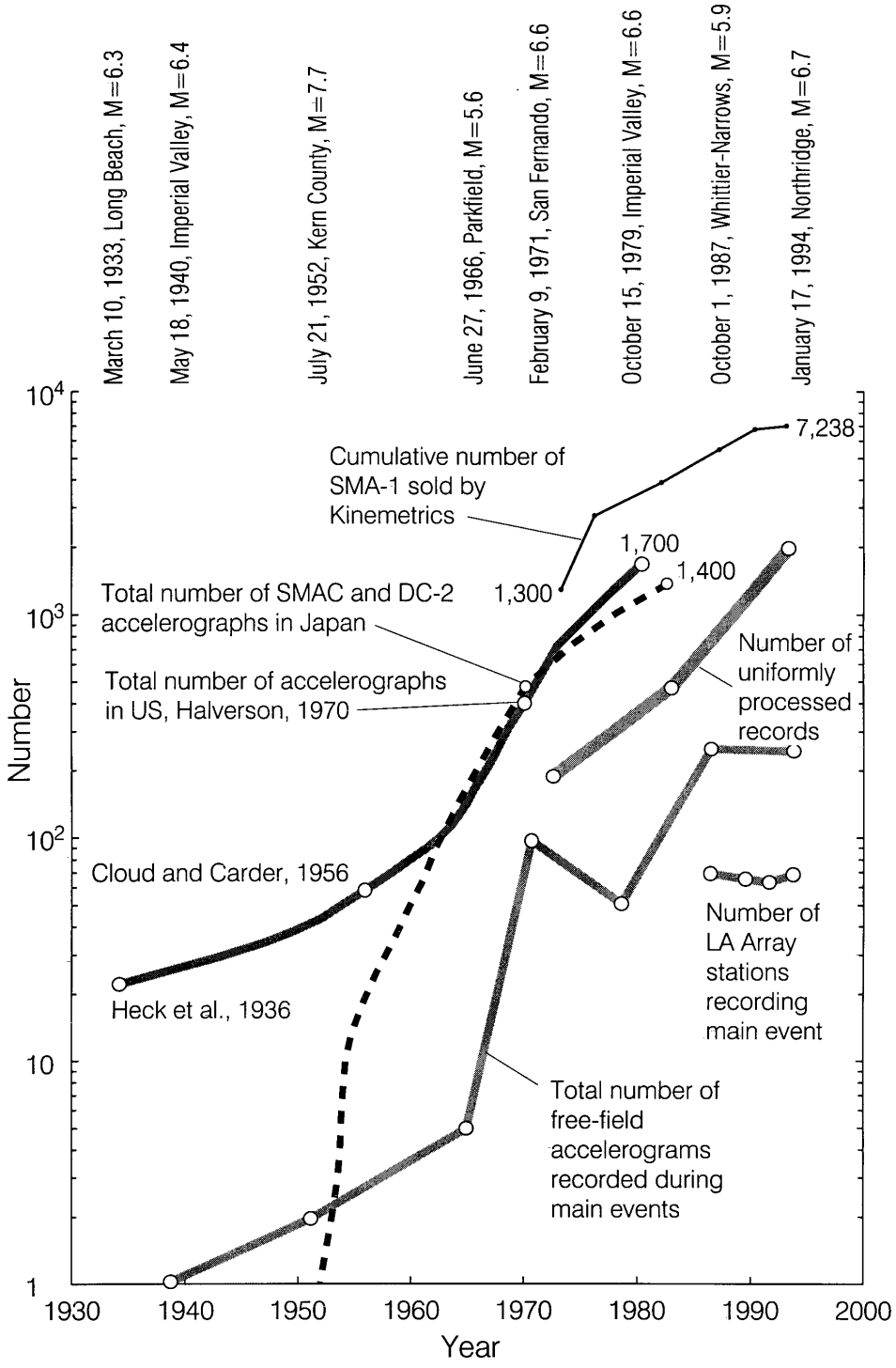

Fig. 2 Cumulative number of strong motion accelerographs in California and in Japan up to 1980, of uniformly processed three-component strong motion records used in three generations of comprehensive empirical scaling studies (Lee and Trifunac, 1995a,1995b), and of the total number of recorded "free-field" records of main earthquake events

With the accumulation of recorded and uniformly processed (Trifunac et al., 1971, 1972a, 1972b) strong motion accelerograms (Figure 2), the emphasis in publications describing the nature of recorded peak amplitudes gradually shifted to the analysis of their spatial variations and attenuation (Todorovska and Trifunac, 1977a, 1977b; Scientists from USGS and SCEC, 1994), as discussed in the following.

SPATIAL ATTENUATION EFFECTS

Since the 1940s, many empirical studies were carried out to develop empirical scaling laws to predict peak amplitudes of strong motion for use in engineering design. Many of these early scaling laws are reviewed in Trifunac and Brady (1975a), and subsequent papers on this subject are cited in Lee et al. (1995a,1995b). A common characteristic of all these empirical equations is the large uncertainty of the estimates, typically by about a factor of 2. In these papers, peak acceleration, velocity or displacement are plotted versus some representative source-to-site distance, and the differences due to the source radiation pattern and different propagation paths are viewed as "random" fluctuations of the data.

The deployment of the Los Angeles and Vicinity Strong Motion Network in 1979/1980 (Trifunac and Todorovska, 2001a), and the first significant recordings of the 1987 Whittier-Narrows earthquake, which triggered most stations of this network, started to change this simplified picture. For the first time, it became possible to plot contour maps showing attenuations of various strong motion parameters (Trifunac, 1988). In 1994, following the Northridge, California, earthquake, such maps could be presented for peak accelerations (Trifunac et al., 1994), peak velocities and surface strains (Trifunac et al., 1996; Trifunac and Lee, 1996), amplitudes and polarity of the peaks of strong motion (Todorovska and Trifunac, 1997a), the distribution of pseudo spectral velocity (Todorovska and Trifunac, 1997b), of duration of strong motion, of energy of strong motion, and of its average and maximum power (Trifunac et al., 2001).

The seemingly large fluctuations of strong motion amplitudes (Trifunac, 1976a) have influenced the development of stochastic representations of ground motion, and the use of the concept of coherence, which describes the degree of variability of strong motion with respect to separation distance. For example, for surface soils with shear wave velocity of 250 m/s and 65 m separation distance, the published values of coherency may be 0.5 at 1 Hz and 0.07 at 2 Hz. The contour maps of various peak amplitudes of strong motion and of their associated spectral amplitudes for the Northridge earthquake, however, show an entirely different picture of "slowly and continuously" changing peak amplitudes, over distances large relative to the wavelengths involved. Based on these observations, Todorovska and Trifunac (1997a) conclude that "Using stochastic representation and analysis of response seems convenient, because it takes advantage of the significant body of knowledge on stochastic processes in other fields. However, by assuming random nature of strong ground motion this approach reduces or eliminates the opportunities for further understanding and discovery of the true physical nature of the processes involved." There is no doubt that recording strong motion with dense arrays is invaluable for quantification of all characterizations of spatial randomness of strong motion.

An example of how detailed two-dimensional maps of peak amplitudes of strong motion (Todorovska and Trifunac, 1976a), and of the spectral amplitudes, can influence the development of the next generation empirical scaling equations is provided in the reports by Lee et al. (1995a, 1995b). These reports show how the attenuation laws for strong motion amplitudes can be refined to include path dependency, and how this reduces the scatter of the regression model.

The stochastic method of analysis and interpretation of strong ground motion and of the response of structures can be traced back to the studies of Kanai and his coworkers in Japan (Kanai, 1957; Tajimi, 1960), Rosenblueth (1956) in Mexico, Bolotin (1960) in Soviet Union, Bycroft (1960) in Canada, and Goodman et al. (1958) and Caughey and Stumpf (1961) in U.S., for example. It is based on evolves from the classical papers by Rice (1944, 1945) and Cartwright and Longuet-Higins (1956), and has been fully developed for stationary response of linear structures (Gupta and Trifunac, 1996), when the basic description of strong motion is viewed through its power spectrum density. However, for non-linear response, this body of theory breaks down, and new approaches must be developed with focus on what governs non-linear and damaging response. The short and impulsive nature of the largest peaks of velocity of ground motion, may offer the simplest and the most direct way to describe design power and design energy the structure can take before collapse (Trifunac et al., 2001). This however calls for new scaling of strong motion in terms of the power associated with one or several of the largest peaks of

ground velocity. Thus, the discovery that the peaks of strong motion and their polarity change slowly and continuously over large areas (Todorovska and Trifunac, 1997a) may change significantly the way we characterize amplitudes and frequency content of strong motion. In particular, it will change the way we specify excitation of structures which are long and which have multiple support points (bridges, dams, tunnels,…).

ANALYSIS OF THE NATURE OF RECORDED STRONG MOTION WAVES

With proper spatial and temporal scaling, the classical seismological theory of linear elastic wave propagation in layered and inhomogeneous medium is directly applicable to strong earthquake ground motion (Trifunac, 1971a, 1971b, 1973, 1974). In other words, recorded strong motion consists of body, surface and scattered (coda) waves. During most shallow and surface earthquakes, with focal depths less than 20 km (typical of Southern California), in the near-field and in the areas close to the fault, the bulk of wave energy arrives at the building site "horizontally". This has been first demonstrated for strong motion accelerograms by Trifunac (1971a), and has led directly to the development of a sequence of comprehensive methods for synthetic construction of artificial translational accelerograms (Trifunac, 1971b), torsional and rocking accelerograms (Lee and Trifunac 1985, 1987), curvograms (Trifunac, 1990), and time histories of strain associated with strong motion (Lee, 1990). Thus, a sequence of papers by Trifunac in 1971, is an example of how simple and direct analyses of the nature of strong motion via multiple filters can lead to the development of a realistic and physically sound method for synthesis of artificial accelerograms.

First studies of the effects of local soil and geologic site conditions (Kanai, 1983) have considered site models, which are excited by vertically incident shear waves. Such one-dimensional models are still used in many engineering analyses today, but those are not capable of providing a basis for the analysis of wave passage effects, and are associated with the torsional and rocking excitations, accompanying non-vertical incidence of body waves and surface waves. With interpretation of the wave content of strong motion and subsequent development of artificial accelerograms, it is now possible to excite soil-structure systems with most realistic and general ground motions (Todorovska et al., 1995).

Comprehensive studies of the frequency-dependent duration of strong motion are capable of identifying the nature of the waves scattered by and reflected from an interface between sediments and basement rock and from the edges of alluvial valleys (Novikova and Trifunac, 1993a, 1993b, 1994a, 1994b, 1994c), and of the duration of fault motion in California (Trifunac and Novikova, 1995). These studies suggest deterministic and identifiable dependence of the duration of strong motion on the chosen scaling variables up to frequencies of 6 to 7 Hz. Beyond about 7 Hz, the integral measures of duration (Trifunac and Brady, 1975b; Trifunac and Novikova, 1994) suggest that the strong motion consists of randomly scattered waves.

Combined with the results of Todorovska and Trifunac (1997a) on spatially coherent peak accelerations, velocities and displacements, these results suggest that for frequencies up to about 7 Hz, the largest peaks of strong motion can propagate in a deterministic fashion over great distances and through irregular geology. It appears that irregular geology acts as a complex, yet predictable and certainly not as a strong randomizing, agent for the waves longer than about 100 m. Since the large pulses of strong motion velocity can be related to the destructive power of waves incident upon structures and their foundations (Trifunac et al., 2001), it is clear that new scaling and attenuation equations will have to be developed to quantify this power for use in engineering design.

LARGE VERSUS SMALL AMPLITUDES OF GROUND MOTION

Strong earthquake ground motion is a rare event, which cannot be predicted in time or space, making it difficult to organize experiments and tests of theoretical calculations and of model-based simulations. To study amplification of strong motion waves by soft sediments and surface soils, for example, it has been suggested that microtremors and microseisms (which shake the ground continuously) could be used (Kanai, 1983). The amplitudes of microseisms and microtremors depend on the location, and are usually larger in metropolitan areas and close to the seashore. Their amplitudes are 10^5 to 10^8 times smaller than the amplitudes of a destructive strong motion (e.g. Trifunac and Todorovska, 2000a).

The usefulness of microtremors for site amplification studies has been a controversial subject, even in the approximately linear range of response of shallow surface soil layers (Kanai, 1983; Trifunac and Udwadia, 1974, 1977; Udwadia and Trifunac, 1972, 1973), but microtremors continue to be used in engineering site amplification studies. Part of the difficulty in interpreting and predicting the site amplification function is that the observed amplification does not always reoccur during the next strong motion shaking (Trifunac et al., 1999). A more serious problem is that the destructive strong earthquake shaking leads to non-linear soil response (Trifunac and Todorovska, 1996a), which can shift or completely change the shape of the site amplification function versus frequency, as determined from linear response (Trifunac and Todorovska, 2000b). Microtremor waves have been used by some researchers to estimate the amplification of strong motion waves, but it is generally acknowledged that their nature and propagation paths are different from those of strong motion waves.

Detailed spatial correlation studies of observed damage, reported site intensities, and recorded strong motion amplitudes, following Northridge, California earthquake of 1994, have shown that if microtremor studies are to be used to predict local site amplification, this may be possible only in the zones of essentially linear response of surface soil, that is, where strong motion amplitudes are small (Trifunac and Todorovska, 2000a, 2000b). In the zone of strong motion, where buildings and underground pipes get damaged, so far, neither microtremors nor aftershocks and small earthquake records could be used to predict spatial variations and amplifications in the presence of non-linear soil response.

STRONG MOTION MAGNITUDE, M_L^{SM}

Since 1935, the local magnitude scale M_L (Richter, 1935) has been one of the most useful and physically meaningful indicators of the earthquake size for scaling of strong ground motion. This is because it is measured at small epicentral distances (less than 600 km) and because it samples the amplitudes of ground motion at periods near 1 s, which is near the "center" of the largest amplitudes of the spectrum of strong ground motion (typically in the range between 0.1 and 25 Hz).

The local magnitude scale saturates near M_L = 6.5, because the corner frequency of the Fourier amplitude spectra of source displacement shifts to frequencies smaller than 1 Hz. In their quest for an ideal, single parameter scaling of the size of an earthquake source, seismologists first proposed to use the surface wave magnitude, M_s (Gutenberg, 1945), and more recently, the moment magnitude, M_w (Hanks and Kanamori, 1979). The surface wave magnitude samples the amplitudes of 20 s period Rayleigh waves, at teleseismic distances, while M_w is computed via empirical scaling equation from the seismic moment $M_0 = \mu \bar{u} A$, where μ is the rigidity of the rocks in the source region, $\bar{u}$ is the average dislocation, and A is the area of the fault. Magnitude M_w is then equal to $(\log_{10} M_0 - 16)/1.5$. Magnitudes M_s and M_w have become popular in geotechnical earthquake engineering, in spite of their dubious ability to scale the spectral amplitudes of strong motion for periods between 0.04 and 10 s. M_s samples 20 s period teleseismic Rayleigh waves and M_w samples periods $T \to \infty$, and so both of these magnitudes sample spectral amplitudes which are far outside the frequency range of a typical strong ground motion. If the strong motion spectrum had a constant or well-defined and stable shape (Trifunac, 1993a, 1994a), all magnitude scales could be equally useful and reliable. Since this spectrum has variable shape (Trifunac, 1994b), and because in the near-field, its shape is significantly different from that in the far-field, it is seen that for engineering scaling of strong motion, M_L is physically the most meaningful scale (Trifunac, 1991a).

The response of a Wood-Anderson torsional seismometer (Richter, 1935) can be calculated by numerical integration of its differential equation of motion, when subjected to excitation by a recorded strong motion accelerogram. Thus, recorded strong motion accelerograms can be used to compute the local magnitude scale, M_L^{SM}. This approach was first proposed in the study of aftershocks of the Imperial Valley, California, earthquake of 1940 (Trifunac and Brune, 1970), but the general definition and calibration of M_L^{SM} were presented by Trifunac (1991a, 1991b). A related correlation of seismoscope response with earthquake magnitude and Modified Mercalli Intensity was presented by Trifunac and Brady (1975c). Calibration of M_L^{SM} for attenuation of strong motion in South-Eastern Europe was

presented by Lee et al. (1990), and its relationship to other magnitudes, as determined by regional seismological stations in South-Eastern and Central Europe, was presented by Trifunac and Herak (1992). Examples of computing M_L^{SM} for the Dharamshala, 1986, earthquake in India, and the Loma Prieta, 1989, earthquake can be found in Trifunac (1993b, 1994c).

Systematic studies of the trends of the differences between M_L^{SM} and M_L (Trifunac, 1991b) can be used to understand the changes in spectral amplitudes of near-field and far-field strong motions. This helps in understanding and improving the ideas on how to develop empirical scaling equations for prediction of strong motion amplitudes. Studies of the differences in M_L^{SM} between different tectonic provinces, and of strong motion accelerograms recorded on geologic strata of different ages (Lee et al., 1990), help in the process of learning how to use empirical equations for scaling strong motion amplitudes, developed in one region (e.g., Southern California), for empirical predictions in another region. Finally, comparison and quantitative correlation of M_L^{SM} with regionally computed magnitude scales (Trifunac and Herak, 1992) helps in relative calibration of the regional magnitude scales, and thus is a step toward homogenizing earthquake catalogues for future seismic hazard studies.

SCALING OF STRONG MOTION FOR ENGINEERING DESIGN

The oldest and still commonly used scaling parameter of strong ground motion, used to quantify engineering design spectra for earthquake-resistant design calculations, is the peak ground acceleration. The idea that a standard shape of response spectrum should be established and that its amplitudes can be scaled by the representative value of ground acceleration can be traced back to the work of Biot. In his 1941 paper, he states: "…for design purposes standard spectrum should be established, giving the equivalent acceleration as a function of the frequency. These standard curves would be the envelopes of a collection of earthquake spectrums and could be made to depend on the nature and magnitude of the damping and on the location."

With the accumulation of strong motion data by the 1970s, and with an improved understanding of the spectral character of the earthquake source (Trifunac, 1972a, 1972b, 1976b, 1993a, 1994b), it is now possible to select physically meaningful parameters for scaling of strong motion for structural (Trifunac, 1991c, 1992, 1994b) and for geotechnical earthquake engineering design (Trifunac, 1995).

Up until late 1960's and early 1970's, peak acceleration was used for essentially all scalings of strong motion in engineering design. It is the directly measurable quantity (from any analog record) and its measurement does not require data processing or use of computers. Since the absolute acceleration spectrum converges to the peak acceleration of ground motion, when the oscillator period approaches zero, peak acceleration is also convenient to use for scaling the standard design spectrum amplitudes. Today, however, it is recognized that better and physically more meaningful scaling parameters or functions should be selected, on the basis of the nature of the phenomenon, which is being analyzed (Trifunac, 1992). For example, peak ground velocity should be used for estimation and mapping of peak strains in the soil (e.g., Todorovska et al., 1995; Todorovska and Trifunac, 1996). Peak ground velocity is further ideal for elementary scaling of damage potential of strong motion (Trifunac and Todorovska, 1997a, 1997b; Trifunac et al., 2001). For rational development of spectral shapes, representative for a given area and optimized for geometrical and temporal characteristics of locally contributing earthquake sources, Uniform Hazard Spectrum (UHS) scaling is most suitable, when the design methodology can be carried out using equivalent linear response representation (Todorovska et al., 1995). For non-linear design of earthquake-resistant structures in the near field, at present, the most promising elementary tool appears to be the peak power of strong motion, combined with the total incident wave energy (Trifunac et al., 2001).

SUMMARY AND CONCLUSIONS

This brief note presented examples of selected published elementary studies of engineering interpretation of strong earthquake ground motion, based directly on recorded accelerograms. It cited examples of studies that: (1) systematically describe the basic properties of the recorded motion, (2) describe the two-dimensional variations of the attenuation (enabling interpretation of its dependence on the geology along the propagation path), (3) interpret the time series of recorded accelerograms to identify

the wave content, (4) interpret amplification of strong motion via recordings of small amplitude motions (such as microtremors and microseisms), (5) measure the "size" of earthquakes via strong motion magnitude, and (6) present the prelude to empirical scaling models of strong motion amplitudes.

It is concluded that such studies and their findings must continue to play a central role in guiding theoretical and empirical modeling of strong ground motion in adopting realistic and significant assumptions about the nature of strong motion and its representation for engineering practice. It is hoped that more rigorous and denser future observations of strong motion will generate data for further new and more comprehensive descriptions of its properties.

REFERENCES

1. Ambraseys, N.N. (1973). "Dynamics of Response of Foundation Materials in Epicentral Regions in Strong Earthquakes", Proc. Fifth World Conf. on Earthquake Engineering, Rome, Italy, Vol. 1, pp. CXXVI-CXLVIII.
2. Biot, M.A. (1932). "Vibrations of Building during Earthquake, Chapter II in Ph.D. Thesis No. 259 entitled "Transient Oscillations in Elastic Systems", Aeronautics Department, Calif. Inst. of Tech., Pasadena, California, U.S.A.
3. Biot, M.A. (1933). "Theory of Elastic Systems Vibrating under Transient Impulse with an Application to Earthquake-Proof Buildings", Proc. National Academy of Sciences, Vol. 19, No. 2, pp. 262-268.
4. Biot, M.A. (1934). "Theory of Vibration of Buildings during Earthquake", Zeitschrift Für Angewandte Matematik and Mechanik, Vol. 14, No. 4, pp. 213-223.
5. Biot, M.A. (1941). "A Mechanical Analyzer for the Prediction of Earthquake Stresses", Bull. Seism. Soc. Am., Vol. 31, No. 2, pp. 151-171.
6. Biot, M.A. (1942). "Analytical and Experimental Methods in Engineering Seismology", ASCE Transactions, Vol. 108, pp. 365-408.
7. Bolotin, V.V. (1960). "Statistical Theory of the Aseismic Design of Structures", Proc. Second World Conf. on Earthquake Engineering, Tokyo, Japan, Vol. 2, pp. 1365-1374.
8. Bycroft, G.N. (1960). "White Noise Representation of Earthquakes", Proc. ASCE, Vol. 86, No. EM2, pp. 1-14.
9. Cartwright, D.E. and Longuet-Higgins, M.S. (1956). "The Statistical Distribution of Maxima for a Random Function", Proc. Royal Soc. of London, Ser. A327, pp. 212-232.
10. Caughey, T.K. and Stumpf, H.J. (1961). "Transient Response of a Dynamic System under Random Excitation", J. Applied Mech., ASME, Vol. 28, pp. 563-566.
11. Cloud, W.K. and Carder, D.S. (1956). "The Strong Motion Program of the Coast and Geodetic Survey", Proceedings of the First World Conference on Earthquake Engineering, Berkeley, California, Vol. 2, pp. 1-10.
12. Goodman, L.E., Rosenblueth, E. and Newmark, N.M. (1958). "Aseismic Design of Firmly Founded Elastic Structures", Trans. ASCE, Vol. 120, pp. 782-802.
13. Gupta, I.D. and Trifunac, M.D. (1996). "Investigation of Nonstationarity in Stochastic Seismic Response of Structures", Report CE 96-01, Dept. of Civil Eng., Univ. of Southern California, Los Angeles, California, U.S.A.
14. Gutenberg, B. (1945). "Amplitudes of Surface Waves and Magnitudes of Shallow Earthquakes", Bull. Seism. Soc. Am., Vol. 35, pp. 3-12.
15. Hanks, T.C. and Kanamori, H. (1979). "A Moment Magnitude Scale", J. Geophys. Res., Vol. 84, pp. 2348-2350.
16. Halverson, H.T. (1970). "Modern Trends in Strong Movement (Strong Motion) Instrumentation", in "Dynamic Waves in Civil Engineering (eds. D.A. Howells, I.P. Haigh, C. Taylor)", Wiley-lnterscience, London, U.K., pp. 341-363.
17. Heck, N.H., McComb, H.E. and Ulrich, F.P. (1936). "Strong-Motion Program and Tiltmeters", Chapter 2 in "Earthquake Investigations in California 1934-35", Special Publication No. 201, U.S. Department of Commerce. Coast and Geodetic Survey, pp. 4-30.

18. Housner, G.W. and Trifunac, M.D. (1967). "Analysis of Accelerograms - Parkfield Earthquake", Bull. Seism. Soc. Am., Vol. 57, pp. 1193-1220.
19. Hudson, D.E., Nigam, N.C. and Trifunac, M.D. (1969). "Analysis of Strong Motion Accelerograph Records", Fourth World Conference on Earthquake Engineering, Santiago, Chile, Vol. I, pp. 1-17.
20. Kanai, K. (1957). "Semi-empirical Formula for the Seismic Characteristics of Ground", Bull. Earthquake Res. Inst., Univ. of Tokyo, Japan, Vol. 35, pp. 308-325.
21. Kanai, K. (1983). "Engineering Seismology", Univ. of Tokyo Press, Japan.
22. Lee, V.W. (1990). "Surface Strains Associated with Strong Earthquake Shaking", Proc. Japan Soc. Civil Eng., Vol. 14, pp. 187-194.
23. Lee, V.W. and Trifunac, M.D. (1985). "Torsional Accelerograms", Soil Dynamics and Earthquake Engineering, Vol. 4, No. 3, pp. 132-139.
24. Lee, V.W. and Trifunac, M.D. (1987). "Rocking Strong Earthquake Accelerations", Soil Dynamics and Earthquake Eng., Vol. 6, No. 2, pp. 75-89.
25. Lee, V.W. and Trifunac, M.D. (1995a). "Frequency-Dependent Attenuation Function and Fourier Amplitude Spectra of Strong Earthquake Ground Motion in California", Report CE 95-03, Dept. of Civil Eng., Univ. of Southern California, Los Angeles, California, U.S.A.
26. Lee, V.W. and Trifunac, M.D. (1995b). "Pseudo Relative Velocity Spectra of Strong Earthquake Ground Motion in California", Report CE 95-04, Dept. of Civil Eng., Univ. Southern California, Los Angeles, California, U.S.A.
27. Lee, V.W., Trifunac, M.D., Herak, M., Zivčić, M. and Herak, D. (1990). "M_L^{SM} in Yugoslavia", Earthquake Eng. and Structural Dynamics, Vol. 19, No. 8, pp. 1167-1179.
28. Lee, V.W., Trifunac, M.D., Todorovska, M.I. and Novikova, E.I. (1995). "Empirical Equations Describing Attenuation of the Peaks of Strong Ground Motion, in terms of Magnitude, Distance, Path Effects and Site Conditions", Report CE 95-02, Dept. of Civil Eng., Univ. of Southern California, Los Angeles, California, U.S.A.
29. Novikova, E.I. and Trifunac, M.D. (1993a). "Modified Mercalli Intensity and the Geometry of the Sedimentary Basin as the Scaling Parameters of the Frequency Dependent Duration of Strong Motion", Soil Dynamics and Earthquake Eng., Vol. 12, No. 4, pp. 209-225.
30. Novikova, E.I. and Trifunac, M.D. (1993b). "Duration of Strong Earthquake Ground Motion: Physical Basis and Empirical Equations", Report CE 93-02, Dept. of Civil Eng., Univ. of Southern California, Los Angeles, California, U.S.A.
31. Novikova, E.I. and Trifunac, M.D. (1994a). "Duration of Strong Ground Motion in Terms of Earthquake Magnitude, Epicentral Distance, Site Conditions and Site Geometry", Earthquake Eng. and Structural Dynamics, Vol. 23, No. 9, pp. 1023-1043.
32. Novikova, E.I. and Trifunac, M.D. (1994b). "Influence of Geometry of Sedimentary Basins on the Frequency Dependent Duration of Strong Ground Motion", Earthquake Eng. and Engineering Vibration, Vol. 14, No. 2, pp. 7-44.
33. Novikova, E.I. and Trifunac, M.D. (1994c). "Empirical Models of Duration of Strong Earthquake Ground Motion Based on the Modified Mercalli Intensity", Report CE 94-01, Dept. of Civil Eng., Univ. of Southern California, Los Angeles, California, U.S.A.
34. Rice, S.O. (1944). "Mathematical Analysis of Random Noise", Bell System Tech. J., Vol. 23, pp. 282-332.
35. Rice, S.O. (1945). "Mathematical Analysis of Random Noise", Bell System Tech. J., Vol. 24, pp. 46-156.
36. Richter, C.F. (1935). "An Instrumental Earthquake Scale", Bull Seism. Soc. Amer., Vol. 25, pp. 1-32.
37. Rosenblueth, E. (1956). "Some Applications of Probability Theory in Aseismic Design", Proc. First World Conference on Earthquake Eng., Vol. 8, pp. 1-18.
38. Scientists from USGS and SCEC (1994). "The Magnitude 6.7, Northridge, California Earthquake of January 17, 1994", Science, Vol. 266, pp. 389-397.

39. Tajimi, H. (1960). "A Statistical Method for Determining the Maximum Response of a Building Structure during an Earthquake", Proc. Second World Conf. on Earthquake Eng., Tokyo, Japan, Vol. A-2, pp. 781-797.
40. Todorovska, M.I. and Trifunac, M.D. (1996). "Hazard Mapping of Normalized Peak Strain in Soil during Earthquakes – Microzonation of a Metropolitan Area", Soil Dyn. and Earthquake Eng., Vol. 15, No. 5, pp. 321-329.
41. Todorovska, M.I. and Trifunac, M.D. (1997a). "Amplitudes, Polarity and Time of Peaks of Strong Ground Motion during 1994 Northridge, California Earthquake", Soil Dynamics Earthquake Eng., Vol. 16, No. 4, pp. 235-258.
42. Todorovska, M.I. and Trifunac, M.D. (1997b). "Distribution of Pseudo Spectral Velocity during the Northridge, California, Earthquake of 17 January, 1994", Soil Dynamics and Earthquake Eng., Vol. 16, No. 3, pp. 173-192.
43. Todorovska, M.I., Gupta, I.D., Gupta, V.K., Lee, V.W. and Trifunac, M.D. (1995). "Selected Topics in Probabilistic Seismic Hazard Analysis", Report CE 95-08, Dept. of Civil Eng., Univ. of Southern California, Los Angeles, California, U.S.A.
44. Trifunac, M.D. (1971a). "Response Envelope Spectrum and Interpretation of Strong Earthquake Ground Motion", Bull. Seism. Soc. Am., Vol. 61, pp. 343-356.
45. Trifunac, M.D. (1971b). "A Method for Synthesizing Realistic Strong Ground Motion", Bull. Seism. Soc. Am., Vol. 61, pp. 1739-1753.
46. Trifunac, M.D. (1972a). "Stress Estimates for San Fernando, California Earthquake of February 9, 1971: Main Event and Thirteen Aftershocks", Bull. Seism. Soc. Am., Vol. 62, pp. 721-750.
47. Trifunac, M.D. (1972b). "Tectonic Stress and Source Mechanism of the Imperial Valley, California Earthquake of 1940", Bull. Seism. Soc. Am., Vol. 62, pp. 1283-1302.
48. Trifunac, M.D. (1973). "Analysis of Strong Earthquake Ground Motion for Prediction of Response Spectra", Earthquake Engineering and Struct. Dynamics, Vol. 2, No. 1, pp. 59-69.
49. Trifunac, M.D. (1974). "A Three-Dimensional Dislocation Model for the San Fernando, California, Earthquake of February 9, 1971", Bull. Seism. Soc. Am., Vol. 64, pp. 149-172.
50. Trifunac, M.D. (1976a). "Preliminary Analysis of the Peaks of Strong Earthquake Ground Motion - Dependence of Peaks on Earthquake Magnitude, Epicentral Distance and the Recording Site Conditions", Bull. Seism. Soc. Am., Vol. 66, pp. 189-219.
51. Trifunac, M.D. (1976b). "Preliminary Empirical Model for Scaling Fourier Amplitude Spectra of Strong Ground Acceleration in Terms of Earthquake Magnitude, Source to Station Distance and Recording Site Conditions", Bull. Seism. Soc. Am., Vol. 66, pp. 1343-1373.
52. Trifunac, M.D. (1988). "A Note on Peak Accelerations during 1 and 4 October, 1987 Earthquakes in Los Angeles, California", Earthquake Spectra, Vol. 4, No. 1, pp. 101-113.
53. Trifunac, M.D. (1990). "Curvograms of Strong Ground Motion", J. Eng. Mech. Div., ASCE, Vol. 116, No. 6, pp. 1426-1432.
54. Trifunac, M.D. (1991a). "M_L^{SM}", Soil Dyn. and Earthquake Eng., Vol. 10, No. 1, pp. 17-25.
55. Trifunac, M.D. (1991b). "A Note on the Differences in Magnitudes Estimated from Strong Motion Data and from Wood-Anderson Seismometer", Soil Dynamics and Earthquake Eng., Vol. 10, No. 8, pp. 423-428.
56. Trifunac, M.D. (1991c). "Recording and Interpreting Strong Earthquake Accelerograms", Proc. First Int. Conf. on Seismology and Earthquake Eng., Tehran, I.R. Iran, Vol. III, pp. 55-73.
57. Trifunac, M.D. (1992). "Should Peak Accelerations be Used to Scale Design Spectrum Amplitudes?", 10th World Conf. Earthquake Eng., Madrid, Spain, Vol. 10, pp. 5817-5822.
58. Trifunac, M.D. (1993a). "Long Period Fourier Amplitude Spectra of Strong Motion Acceleration", Soil Dynamics and Earthquake Eng., Vol. 12, No. 6, pp. 363-382.
59. Trifunac, M.D. (1993b). "An Example of Computing M_L^{SM} for Dharamshala Earthquake in India", Bull. Ind. Soc. Earthq. Tech., Vol. 30, No. 1, pp. 19-25.
60. Trifunac, M.D. (1994a). "Q and High Frequency Strong Motion Spectra", Soil Dynamics and Earthquake Eng., Vol. 13, No. 3, pp. 149-161.

61. Trifunac, M.D. (1994b). "Earthquake Source Variables for Scaling Spectral and Temporal Characteristics of Strong Ground Motion", 10th European Conf. Earthquake Eng., Vienna, Austria, Vol. 4, pp. 2585-2590.
62. Trifunac, M.D. (1994c). "M_L^{SM} of the 1989 Loma Prieta Earthquake", Soil Dynamics and Earthquake Eng., Vol. 13, No. 5, pp. 313-316.
63. Trifunac, M.D. (1995). "Scaling Earthquake Motion in Geotechnical Design", Third International Conference on Recent Advances in Geotechnical Earthquake Eng. and Soil Dynamics, St. Louis, Missouri, U.S.A., Vol. II, pp. 607-612.
64. Trifunac, M.D. and Brady, A.G. (1975a). "Correlations of Peak Acceleration, Velocity and Displacement with Earthquake Magnitude, Epicentral Distance and Site Conditions", Earthquake Engineering and Struct. Dynamics, Vol. 4, pp. 455-471.
65. Trifunac, M.D. and Brady, A.G. (1975b). "A Study on the Duration of Strong Earthquake Ground Motion", Bull. Seism. Soc. Am., Vol. 65, pp. 581-626.
66. Trifunac, M.D. and Brady, A.G. (1975c). "On the Correlation of Seismoscope Response with Earthquake Magnitude and Modified Mercalli Intensity", Bull. Seism. Soc. Am., Vol. 65, pp. 307-321.
67. Trifunac, M.D. and Brune, J.N. (1970). "Complexity of Energy Release during the Imperial Valley, California Earthquake 1940", Bull. Seism. Soc. Am., Vol. 60, pp. 137-160.
68. Trifunac, M.D. and Herak, D. (1992). "Relationship of M_L^{SM} and Magnitudes Determined by Regional Seismological Stations in Southeastern and Central Europe", Soil Dynamics and Earthquake Eng., Vol. 11, No. 4, pp. 229-241.
69. Trifunac, M.D. and Hudson, D.E. (1971). "Analysis of the Pacoima Dam Accelerogram, San Fernando, California Earthquake of 1971", Bull. Seism. Soc. Am., Vol. 61, pp. 1393-1411.
70. Trifunac, M.D. and Lee, V.W. (1996). "Peak Surface Strains during Strong Earthquake Motion", Soil Dynamics and Earthquake Eng., Vol. 15, No. 5, pp. 311-319.
71. Trifunac, M.D. and Novikova, E.I. (1994). "State of the Art Review on Strong Motion Duration", 10th European Conf. on Earthquake Eng., Vienna, Austria, Vol. 1, pp. 203-208.
72. Trifunac, M.D. and Novikova, E.I. (1995). "Duration of Earthquake Fault Motion in California", Earthquake Eng. and Structural Dynamics, Vol. 24, No. 6, pp. 781-799.
73. Trifunac, M.D. and Todorovska, M.I. (1996a). "Nonlinear Soil Response - 1994 Northridge California, Earthquake", J. Geotechnical Eng., ASCE, Vol. 122, No. 9, pp. 725-735.
74. Trifunac, M.D. and Todorovska, M.I. (1996b). "Hazard Mapping of Normalized Peak Strain in Soil during Earthquakes – Microzonation of a Metropolitan Area", Soil Dynamics and Earthquake Eng., Vol. 15, No. 5, pp. 321-329.
75. Trifunac, M.D. and Todorovska, M.I. (1997a). "Northridge, California, Earthquake of January 17, 1994: Density of Red-Tagged Buildings versus Peak Horizontal Velocity and Site Intensity of Strong Motion", Soil Dynamics and Earthquake Eng., Vol. 16, No. 3, pp. 209-222.
76. Trifunac, M.D. and Todorovska, M.I. (1997b). "Northridge, California, Earthquake of 17 January 1994: Density of Pipe Breaks and Surface Strains", Soil Dynamics and Earthquake Eng., Vol. 16, No. 3, pp. 193-207.
77. Trifunac, M.D. and Todorovska, M.I. (2000a). "Long Period Microtremors, Microseisms and Earthquake Damage: Northridge, California, Earthquake of 1994", Soil Dynamics and Earthquake Eng., Vol. 19, No. 4, pp. 253-267.
78. Trifunac, M.D. and Todorovska, M.I. (2000b). "Can Aftershock Studies Predict Site Amplification Factors? Northridge, California, Earthquake of 17 January, 1994", Soil Dynamics and Earthquake Eng., Vol. 19, No. 4, pp. 233-251.
79. Trifunac, M.D. and Todorovska, M.I. (2001). "Evolution of Accelerographs, Data Processing, Strong Motion Arrays and Amplitude and Spatial Resolution in Recording Strong Earthquake Motion", Soil Dynamics and Earthquake Eng., Vol. 21, No. 6, pp. 537-555.
80. Trifunac, M.D. and Udwadia, F.E. (1974). "Variations of Strong Earthquake Ground Shaking in the Los Angeles Area", Bull. Seism. Soc. Am., Vol. 64, pp. 1429-1454.

81. Trifunac, M.D. and Udwadia, F.E. (1974). "Parkfield, California, Earthquake of June 27, 1966: A Three-Dimensional Moving Dislocation", Bull. Seism. Soc. Am., Vol. 64, pp. 511-533.
82. Trifunac, M.D. and Udwadia, F.E. (1977). "Problems in the Construction of Microzoning Maps", Sixth World Conference Earthquake Engineering, New Delhi, Vol. I, pp. 735-741.
83. Trifunac, M.D. and Todorovska, M.I. (1996b). "Hazard Mapping of Normalized Peak Strain in Soil during Earthquakes – Microzonation of a Metropolitan Area", Soil Dynamics and Earthquake Eng., Vol. 15, No. 5, pp. 321-329.
84. Trifunac, M.D., Hao, T.Y. and Todorovska, M.I. (1999). "On Reoccurrence of Site Specific Response", Soil Dynamics and Earthquake Eng., Vol. 18, No. 8, pp. 564-592.
85. Trifunac, M.D., Hao, T.Y. and Todorovska, M.I. (2001). "On Energy Flow in Earthquake Response", Report CE 01-03, Dept. of Civil Engineering, University of Southern California, Los Angeles, California, U.S.A.
86. Trifunac, M.D., Hudson, D.E., Brady, A.G. and Vijayaraghavan, A. (1971). "Strong-Motion Earthquake Accelerograms, II: Corrected Accelerograms and Integrated Velocity and Displacement Curves", Report EERL 71-51, Earthquake Engineering Research Laboratory, California Institute of Technology, Pasadena, U.S.A.
87. Trifunac, M.D., Hudson, D.E. and Brady, A.G. (1972a). "Strong-Motion Accelerograms, III: Response Spectra", Report EERL 72-80, Earthquake Engineering Research Laboratory, California Institute of Technology, Pasadena, U.S.A.
88. Trifunac, M.D., Hudson, D.E., Udwadia, F.E., Brady, A.G. and Vijayaraghavan, A. (1972b). "Strong-Motion Earthquake Accelerograms, IV: Fourier Spectra", Report EERL 72-100, Earthquake Engineering Research Laboratory, California Institute of Technology, Pasadena, U.S.A.
89. Trifunac, M.D., Todorovska, M.I. and Ivanovic, S.S. (1994). "A Note on Distribution of Uncorrected Peak Ground Accelerations during Northridge, California, Earthquake of 17 January 1994", Soil Dynamics and Earthquake Eng., Vol. 13, No. 3, pp. 187-196.
90. Trifunac, M.D., Todorovska, M.I. and Ivanovic, S.S. (1996). "Peak Velocities, and Peak Surface Strains during Northridge, California, Earthquake of 17 January 1994", Soil Dynamics and Earthquake Eng., Vol. 15, No. 5, pp. 301-310.
91. Udwadia, F.E. and Trifunac, M.D. (1972). "Studies of Strong Earthquake Motions and Microtremor Processes", International Conference of Microzonation, Seattle, Washington, U.S.A., Vol. 1, pp. 319-334.
92. Udwadia, F.E. and Trifunac, M.D. (1973). "Comparison of Earthquake and Microtremor Ground Motions in El Centro, California", Bull. Seism. Soc. Am., Vol. 63, No. 4, pp. 1227-1253.

ISET Journal of Earthquake Technology, Paper No. 425, Vol. 39, No. 4, December 2002, pp. 219-254

EMPIRICAL SCALING OF STRONG EARTHQUAKE GROUND MOTION - PART I: ATTENUATION AND SCALING OF RESPONSE SPECTRA

V.W. Lee
Civil Engineering Department
University of Southern California
Los Angeles, California, U.S.A.

ABSTRACT

Three generations of empirical scaling equations, developed by the Strong Motion Research Group at University of Southern California in the 1970's, 1980's and 1990's, for the attenuation and scaling of spectral amplitudes of strong ground motion are reviewed. Semi-theoretical extrapolation functions for extending these empirical scaling equations to high and low frequencies are also presented. For brevity, only equations and illustrations which describe the relative response spectrum amplitudes are shown, but the methods and procedures presented are also applicable to scaling of Fourier amplitude spectra, for which complete corresponding references are also included.

KEYWORDS: PSV, Attenuation, Earthquake Source, Path Type, Local Geology and Soil

INTRODUCTION

In this paper, a review of selected scaling methods for the estimation of spectral amplitudes of strong earthquake ground motion will be presented. Since late 1960's, this work has advanced so much that at present, very detailed scaling equations are available for empirical estimation of strong motion amplitudes in California. For studies dealing with source mechanism and prediction of synthetic strong ground motion, the Fourier amplitude spectra are required (e.g., Lee and Trifunac, 1993; Trifunac, 1973, 1976b, 1989a, 1989b, 1989c, 1991a, 1993a; Trifunac and Lee, 1978, 1980, 1989a). For engineering estimation of the response of structures, several forms of relative response spectra are used (Trifunac, 1977a, 1977b, 1991a, 1994e; Trifunac and Anderson, 1978a, 1978b, 1978c; Trifunac and Gupta, 1991; Trifunac and Lee, 1989b). For simplicity and brevity in the following, empirical scaling of pseudo relative velocity (PSV) spectrum only will be described. *Mutatis mutandis* most of the methods will be applicable also for the scaling of Fourier spectrum amplitudes.

This paper is divided into four parts. The first part reviews the first generation of direct scaling equations of PSV amplitudes, and is based on the paper by Trifunac (1978). The second part introduces frequency-dependent attenuation equations and dependence of the direct scaling equations on local soil and local geologic site conditions. It also presents two parallel approaches, one based on magnitude and the other on intensity scale. This part is based on the papers by Trifunac and Lee (1985a, 1985b, 1985c, 1987). In the third part, direct scaling equations for PSV amplitudes which have been refined during the early 1990's and the new scaling models, as described in the reports by Lee and Trifunac (1995a, 1995b), are presented. Finally in the fourth part, the methods for extrapolation of spectral amplitudes to long $(T > 10 \text{ s})$ and short $(T < 0.04 \text{ s})$ periods (Trifunac, 1993a, 1993b, 1994a, 1994b, 1994c, 1994d, 1995a, 1995b) will be summarized.

The concept of response spectrum was introduced into earthquake engineering by Biot (1932, 1933, 1934, 1941, 1942) and Benioff (1934). Following the gradual accumulation of strong motion recordings since 1934, the response spectrum method for the design of earthquake-resistant structures (Hudson et al., 1972) is now a part of or is being introduced into many modern earthquake design codes (Newmark et al., 1977).

There are difficulties which result from the oversimplified methodology associated with the common response spectrum approach. Some are caused by the lack of information contained in the response spectrum or result from its definition, which is the maximum amplitude of the entire time-history response to ground motion. Many details on the duration of strong shaking (Trifunac and Brady, 1975a; Trifunac and Novikova, 1994) and on the number and the distribution of peak amplitudes in the response

are essentially eliminated (Gupta and Trifunac, 1988a, 1990a, 1990b, 1991a, 1991b). Other problems occur because the response analysis is linear. This makes the estimates of more realistic non-linear response difficult. In a non-linear progressively deteriorating structural system, strong shaking with same peak amplitudes may result in no damage, partial damage or total damage, depending on whether a structure was strained through one, several or many cycles of non-linear response. In spite of these and other well-known difficulties, the simplified response spectrum approach has gained considerable popularity among the engineering profession. If used judiciously and with awareness of its limitations, it may offer convenient and simple means for the design of earthquake-resistant structures.

The physical phenomena which cause strong shaking are described by parameters related to the earthquake source mechanism (seismic moment, fault geometry, dislocation amplitudes, stress drop, radiation pattern, etc.) and the transmission path. For engineering analyses, however, at present one still has to use less sophisticated parameters to describe strong shaking; e.g., earthquake magnitude (Trifunac, 1991b), epicentral distance, site conditions, Modified Mercalli Intensity (Trifunac, 1977c; Trifunac and Todorovska, 1989a, 1989b; Trifunac and Zivčić, 1991; Trifunac et al., 1988, 1991; Trifunac and Brady, 1975b, 1975c; Wong and Trifunac, 1979). This is because those simple parameters are readily available and can be processed to yield desired statistical or deterministic estimates of future earthquake shaking.

Different types of response spectra are calculated from strong-motion accelerograms (Hudson et al., 1972). In this paper, we begin by reviewing briefly the absolute acceleration spectrum, SA, which represents the maximum absolute acceleration of a single-degree-of-freedom system, with prescribed fraction of critical damping, during the excitation by a strong-motion accelerogram. The scaling of the absolute acceleration spectra, SA, can be considered in terms of two groups of parameters. The first group will consist of earthquake magnitude, M, epicentral distance, R, recording site conditions, s ($s = 0$ will be assigned to alluvium sites, $s = 2$ to hard basement rock sites, and $s = 1$ to intermediate sites; see Trifunac (1990a)), component direction ($v = 0$ for horizontal, and $v = 1$ for vertical motion), and a parameter, p, which will describe approximately the distribution of the spectral amplitudes. The second group will consist of the Modified Mercalli Intensity (MMI) in place of M, and the epicentral distance, R, will be deliberately omitted to avoid explicit emphasis on the rate of attenuation of MMI in California. While this omission will increase the scatter of the observed spectral amplitudes with respect to the assumed empirical model, it will permit the use of the derived correlations outside California, at least formally.

Following the first recordings of strong ground motion in 1934, 1940 and 1952, and the early systematic calculations of response spectrum amplitudes (Alford et al., 1951), it became possible to study the shape of response spectra. This led to the early development of "standard" spectral shapes for use in design. This concept was first proposed by Biot (1942) and carried out in the late 1950's (Housner, 1970), and extends to the present through cycles driven by the availability of new data. The early work was usually characterized by the fixed shape of response spectrum whose amplitude depended on a single scaling parameter. Though spectra were also developed (Veletsos et al., 1965) for scaling in terms of peak acceleration, peak velocity and peak displacement, the direct availability of peak acceleration amplitudes from recorded accelerograms and the lack of accurate and uniformly processed peak velocities and peak displacements (Trifunac, 1976a, 1976c) meant that most of the design spectra were essentially scaled by the peak acceleration alone (Trifunac and Brady, 1975d, 1975e; Trifunac and Lee, 1992). It was recognized that the shape of response spectra should depend on such parameters as earthquake magnitude, and source-to-station distance, but the data available in the mid- and late 1950's did not allow more refined analyses.

With the availability of additional strong motion recordings in the mid 1960's and early 1970's, it became possible to improve upon these early studies. One example of such an improved set of fixed shape absolute acceleration spectra was developed for the design of nuclear power plants (Nuclear Regulatory Commission Guide 1.60 spectra; see Newmark et al. (1973), Trifunac and Anderson (1977)). These spectra were still scaled by peak acceleration amplitudes, and the effects of magnitude, source-to-station distance, attenuation with distance and site conditions were introduced only through the modification of peak acceleration.

Observed damage from earthquake shaking depends on the geologic and local soil conditions. Numerous attempts have been made to relate this observation to the recorded strong-motion accelerations (Duke, 1958), and to the recordings on more sensitive seismological instruments (Gutenberg, 1957;

Borcherdt and Gibbs, 1976). With the exception of the work by Gutenberg (1957), most studies dealing with these effects attempted to relate the variations in damage to peak accelerations or peak velocity only, and thus explicitly or implicitly ignored the frequency-dependent nature of this problem.

Seed et al. (1974) presented one of the firs6t studies of the frequency-dependent variations of spectrum shape. In their analysis, the dependence of the spectral amplitudes on site conditions was investigated by carrying out four independent statistical analyses. The explicit dependence of spectrum shapes on magnitude and source-to-station distance were eliminated, however, by normalization of all spectral amplitudes to peak acceleration.

After the completion of the first phase of the uniform data processing effort (Trifunac, 1977d), it became possible to develop first multi-dimensional regression analyses of the shape and amplitudes of response spectra, as those depend not only on the recording site conditions, but also on other important parameters describing the strong ground motion. The first and pioneering studies on how the Fourier amplitude spectra depend on such scaling parameters (Trifunac, 1976b), have shown that similar correlations for absolute acceleration and other response spectra will produce equally valuable results.

FIRST DIRECT SCALING EQUATIONS FOR PSEUDO RELATIVE VELOCITY

The experience gained from the first direct scaling of the Fourier amplitude spectra (Trifunac, 1976b) and later of absolute acceleration spectra (Trifunac and Anderson, 1977) was next applied to direct scaling of PSV spectra. The database for this analysis resulted from recordings of 57 earthquakes whose magnitudes ranged from 3.0 to 7.7. Sixty-three percent of this data has been recorded on alluvium sites, 23% on "intermediate sites", and only 8% on basement rock sites. This site classification was proposed by Trifunac (see Trifunac and Brady (1975b)) to characterize roughly the geologic environment of the recording station. It has been designed for use with geologic maps, and for alluvium and sedimentary deposits with depths measured in thousands of feet (not hundreds of feet). For geological site characterization, ideally a site should be classified either as alluvium site $(s = 0)$ or as basement rock site $(s = 2)$. However, recognizing that in some cases, it may be difficult to make a choice in a complex geologic environment or that insufficient or no data are available on site characteristics, "intermediate" $(s = 1)$ site classification has been introduced and assigned to 23% of 187 records.

1. Direct Scaling of PSV Spectra in Terms of Magnitude and Source-to-Station Distance

For scaling of PSV spectra in terms of magnitude M, epicentral distance R, recording site conditions s, component direction v, and a parameter, p, which approximately determines the fraction of spectral amplitudes smaller than the selected spectra $\mathrm{PSV}(T)_p$, we employed (Trifunac, 1978)

$$\log[\mathrm{PSV}(T)_p] = M + \log A_0(R) - a(T)p - b(T)M - c(T) - d(T)s - e(T)v - f(T)M^2 - g(T)R \quad (1)$$

The functional form of Equation (1) has been motivated by the pioneering work of Trifuanc (1976b) and by the definition of local magnitude scale which states that the logarithm of peak amplitude on a standard instrument corrected for distance attenuation $[\log A_0(R)]$ is equal to the magnitude (Richter, 1958; Trifunac, 1991b). The terms $a(T)p + b(T)M + c(T) + d(T)s + e(T)v + f(T)M^2 + g(T)R$ then represent an empirical correction that depends on $M, p, s, v,$ and R. The term $a(T)p$, in which p is not probability, but a parameter related to probability of exceedance (Trifunac and Anderson, 1978a), approximates the distribution of observed amplitudes of $\mathrm{PSV}(T)$ about Equation (1) when $0.1 \le p \le 0.9$. The terms $b(T)M$ and $f(T)M^2$ model the diminishing growth of spectral amplitudes with increasing magnitude (Trifunac, 1973, 1976a, 1976b). Functions $d(T)$ and $e(T)$ model the frequency-dependent differences in spectral amplitudes for: (1) alluvium relative to basement rock sites; and (2) horizontal relative to vertical ground motion. Anelastic and scattering attenuation of amplitude with distance is often described by $\exp(-\pi R/(TQ\beta))$, where Q is the quality factor of the medium and β is the shear wave velocity (Trifunac, 1994b). The physical meaning of $g(T)$ in Equation (1) is then that it corresponds to $(\pi/TQ\beta) \times \log e$.

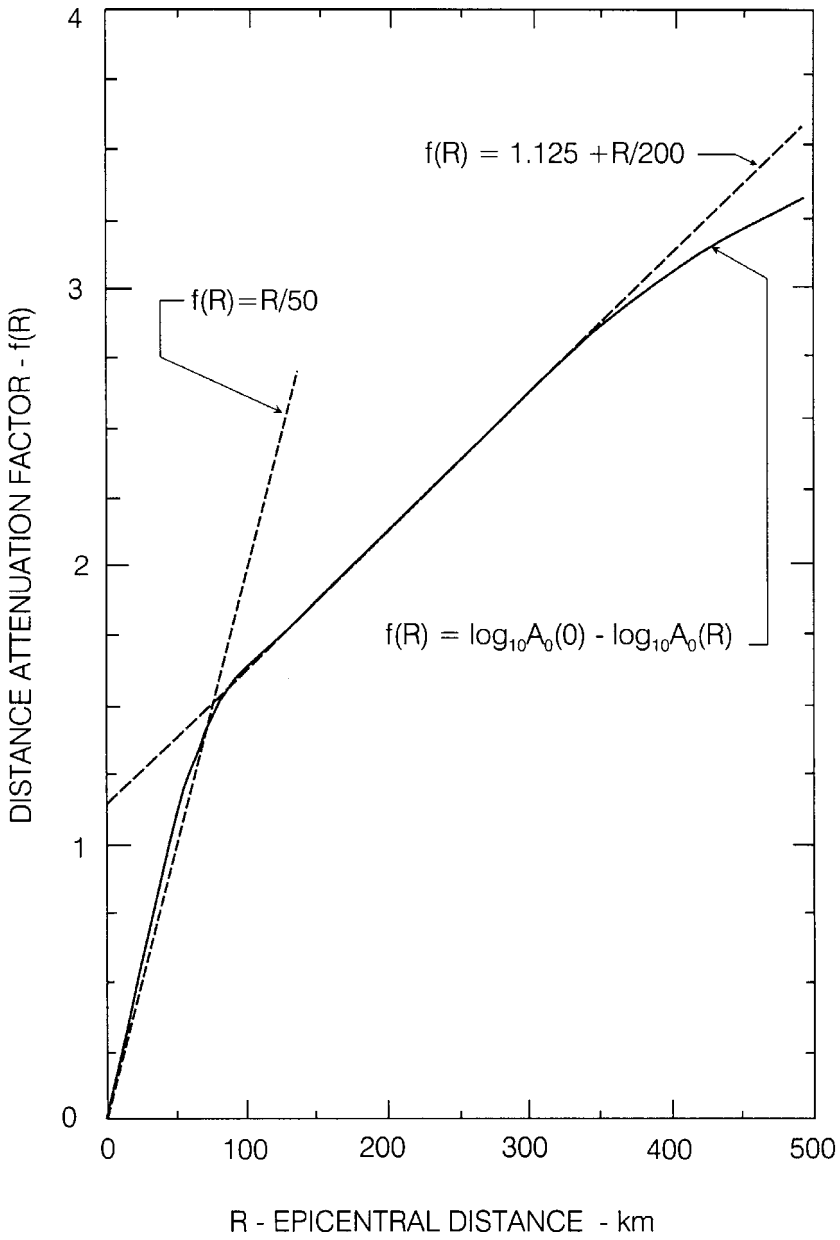

Fig. 1 Distance attenuation factor $f(R)$

The amplitude attenuation with distance has been modeled by the term $\log A_0(R)$. Figure 1 presents the plot of $f(R)$ defined so that

$$\log A_0(R) = \log A_0(R=0) - f(R) \tag{2}$$

and shows that $f(R)$ can be approximated by $R/50$ for $R \le 75\,\text{km}$ and by $1.125 + R/200$ for $350 \ge R \ge 75\,\text{km}$.

The change in slope at $R = 75$ km results from slower attenuation of surface waves with distance $\left(\sim 1/R^{1/2}\right)$, from the fact that in this distance range, surface waves emerge as the main contributors to strong shaking, and from strong reflections off the Moho discontinuity. The near- and intermediate-field terms of strong motion amplitudes attenuate like $1/R^4$ to $1/R^2$, while the amplitudes of body waves diminish as $1/R$. Thus, $f(R)$ [i.e., $\log A_0(R)$] represents an empirical description of how strong motion amplitudes decay with distance. The fact that $\log A_0(R)$ results from observations of actual wave attenuation with distance in California, suggests that this description of the changes of strong motion amplitudes with distance may be easier to justify on physical grounds than the frequently used

expressions of the form $(R+a)^{-n}$, in which a is some constant. There are several obvious disadvantages in using $(R+a)^{-n}$. First, for $R << a$, it tends to a constant a^{-n} for all frequencies of motion. This may lead to difficulties in modeling the near-field terms that attenuate like $1/R^2$ and $1/R^4$. Secondly, $(R+a)^{-n}$ experiences a rapid change of slope near $R=a$, from zero to $-n$. Finally, for $R >> a$, the values of n usually between 1 and 2 lead to too rapid amplitude attenuation with distance that is incompatible with surface wave attenuation (Trifunac and Lee, 1985a, 1990; Lee and Trifunac, 1995a).

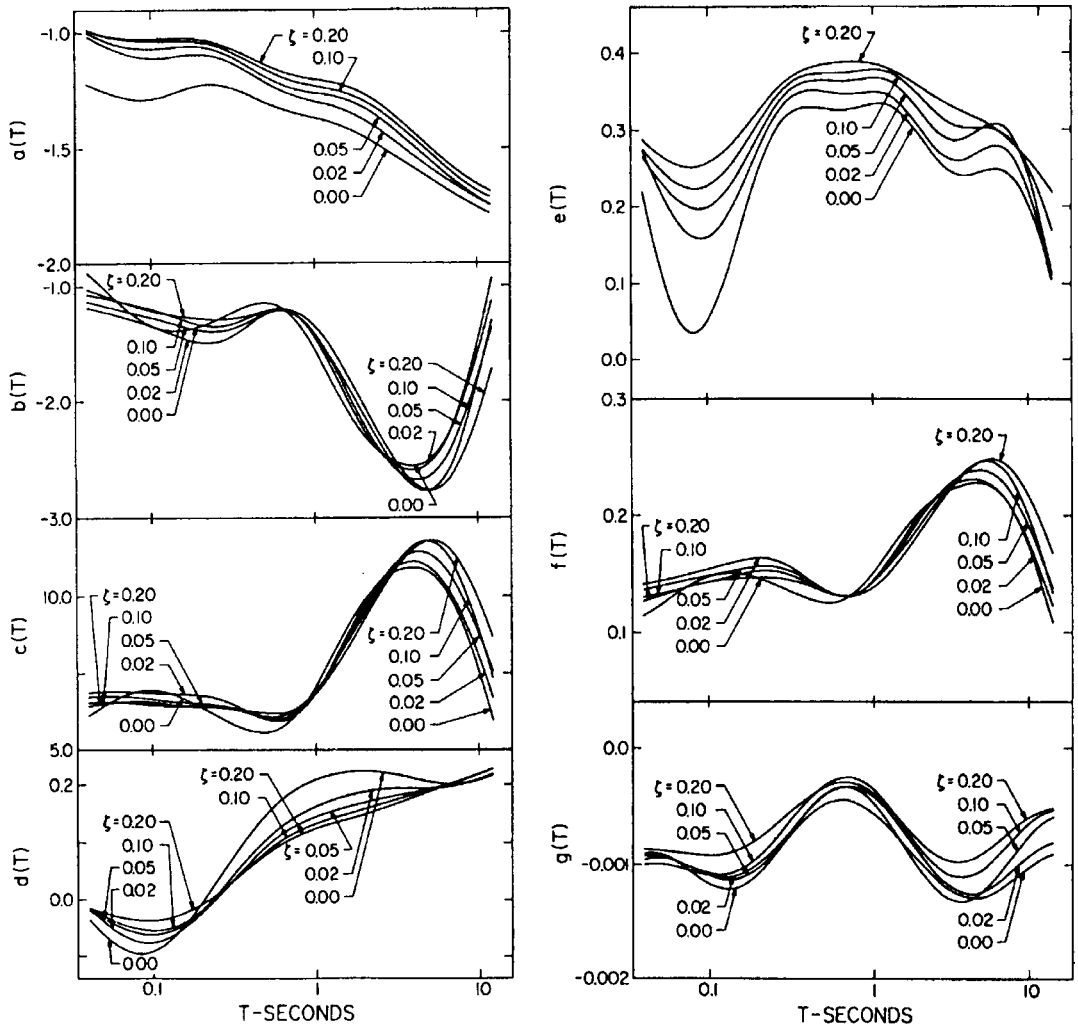

Fig. 2 Functions $a(T)$, $b(T)$,...$f(T)$ and $g(T)$

To compute the coefficient functions $a(T)$, $b(T)$, ..., Trifunac (1978) partitioned all data into four groups corresponding to the magnitude ranges $4.0-4.9$, $5.0-5.9$, $6.0-6.9$, and $7.0-7.9$. Each of these groups was next sub-divided into three sub-groups corresponding to the site classification, s. Depending on whether the recording component is horizontal or vertical, each of these sub-groups was finally divided into two parts corresponding to $v=0$ and 1. Within each of these parts, n data points with amplitudes equal to $\log[\mathrm{PSV}(T)]-M-\log A_0(R)$ were arranged so that the numerical values decreased monotonically. Then, if m = integer part of (pn), in which $0.05 \le p \le 0.95$, the $m-$th data point represents an estimate for an upper bound on $\log[\mathrm{PSV}(T)]-M-\log A_0(R)$, so that $100p$ percent of the corresponding data is less than that value. For actual regression calculations, at most 19 values of p equal to 0.05, 0.10, 0.15, ... 0.90 and 0.95 were used. The advantage of this approach was that it eliminated strong dependence of the final regression model on the earthquakes that contributed most to the available data.

Figure 2 presents the amplitudes of $a(T)$, $b(T)$, ... and $g(T)$ for $\zeta = 0.0, 0.02, 0.05, 0.10,$ and 0.20 plotted versus T, the undamped period of the single-degree-of-freedom oscillator. Here, ζ represents a fraction of critical damping.

Many features of functions $a(T)$ through $g(T)$ are similar to those found for the scaling of absolute acceleration spectra (Trifunac and Anderson, 1977). The amplitudes of $b(T)$ and $c(T)$, however, differ because of the normalization factors and the units employed in those two analyses, and because $\mathrm{PSV}(T)/\mathrm{SA}(T) \approx T/2\pi$. Figures 3 and 4 present examples of PSV spectra for $R = 0, \zeta = 0.02,$ and $p = 0.5$ in Equation (1).

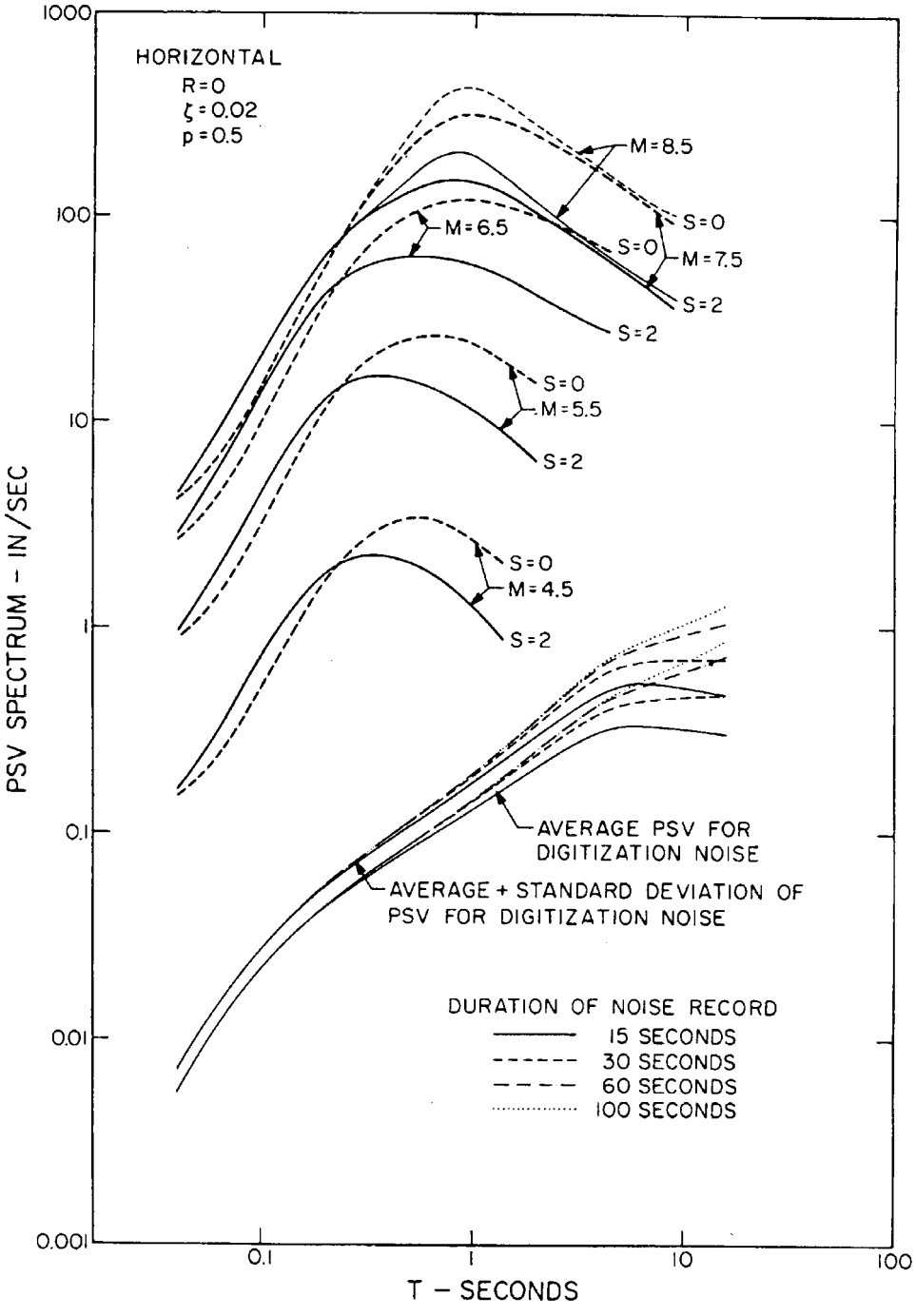

Fig. 3 Horizontal PSV spectra for $M = 4.5$ through 8.5, and for $s = 0$ and 2

The use of Equation (1) is constrained to the interval $M_{\min} \le M \le M_{\max}$, in which $M_{\min} = -b(T)/2f(T)$ and $M_{\max} = 1 - b(T)/(2f(T))$. For $M \ge M_{\max}$, M is to be replaced by $M_{\max}$,

and for $M < M_{\min}$, M is to be replaced by $M_{\min}$, only in the terms $b(T)M$ and $f(T)M^2$. This leads to linear growth of $\log[\mathrm{PSV}(T)_p]$ with respect to M for $M \le M_{\min}$, to parabolic growth for $M_{\min} \le M \le M_{\max}$, and to constant amplitudes for $M \ge M_{\max}$ which are equal to the amplitudes for $M = M_{\max}$.

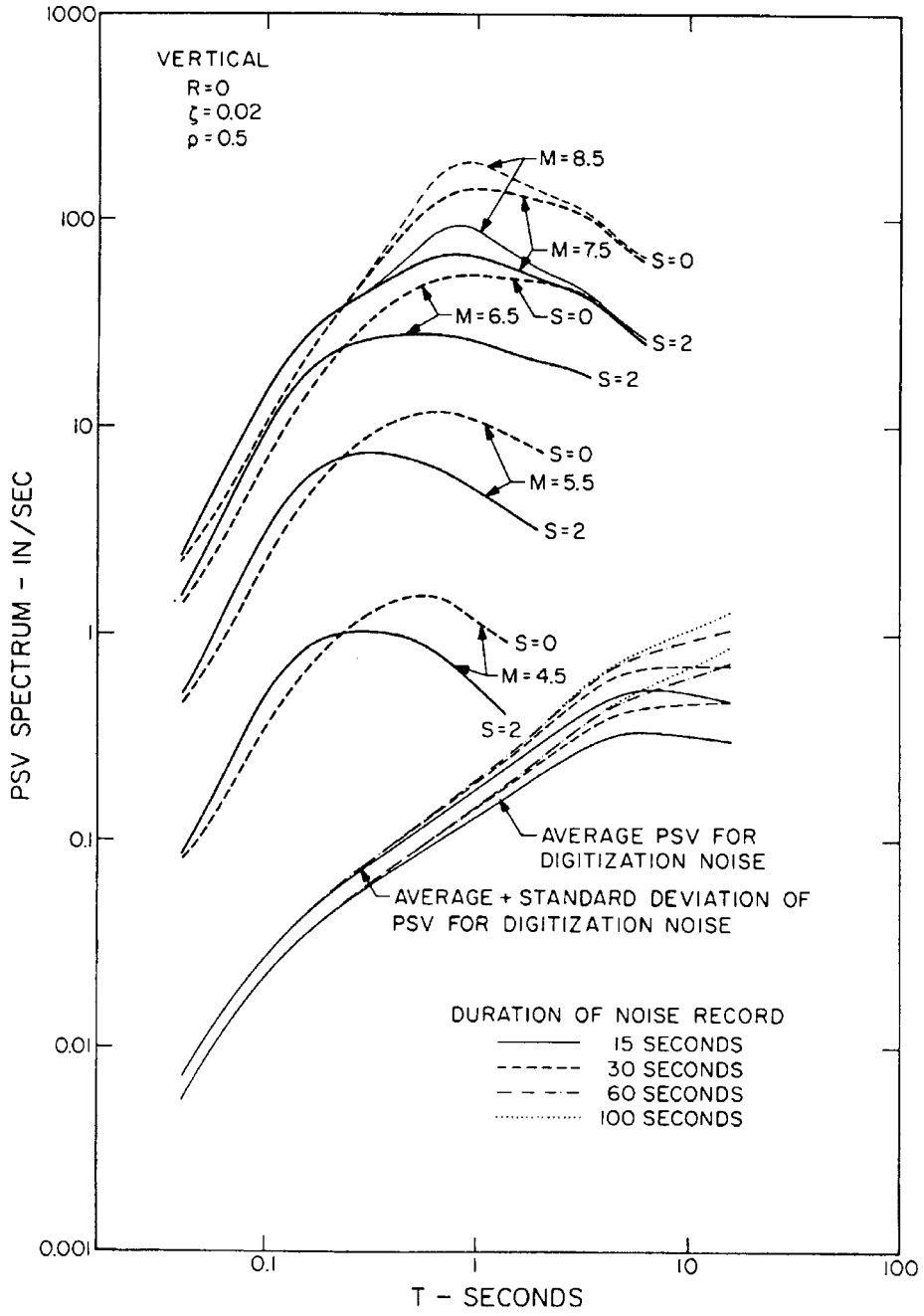

Fig. 4 Vertical PSV spectra for $M = 4.5$ through 8.5, and for $s = 0$ and 2

This type of growth for $\log[\mathrm{PSV}(T)_p]$ with respect to magnitude has been selected to model the effects of diminishing rate of growth of strong motion amplitudes with fault dimensions for large earthquakes with M between about 7.5 and 8.5. Though the precise nature of the growth of spectral amplitudes with M is difficult to decipher from the currently available data, the observations and the spectra of strong shaking so far do not contradict this form of Equation (1). The result of this analysis then is to suggest that the PSV amplitudes essentially cease to grow for $M \approx 7.5$.

Figures 3 and 4 further show the average and average plus one standard deviation of spectral amplitudes for the combined recording and data processing noise (Trifunac and Todorovska, 2001a,

2001b). This noise diminishes the signal-to-noise ratio in many recorded accelerograms for $T > 2$ s and thus the quality of $a(T)$ through $g(T)$ in the same period range. Consequently, the use of Equation (1) is not recommended for periods longer than those for which selected spectral amplitudes have been plotted in Figures 3 and 4.

The shapes of all response spectra should depend on earthquake magnitude, and this dependence is such as to enhance the long period motions for larger magnitudes. Figures 5 and 6 show that this is the case for PSV spectra (normalized to one for $T = 0.04$ s).

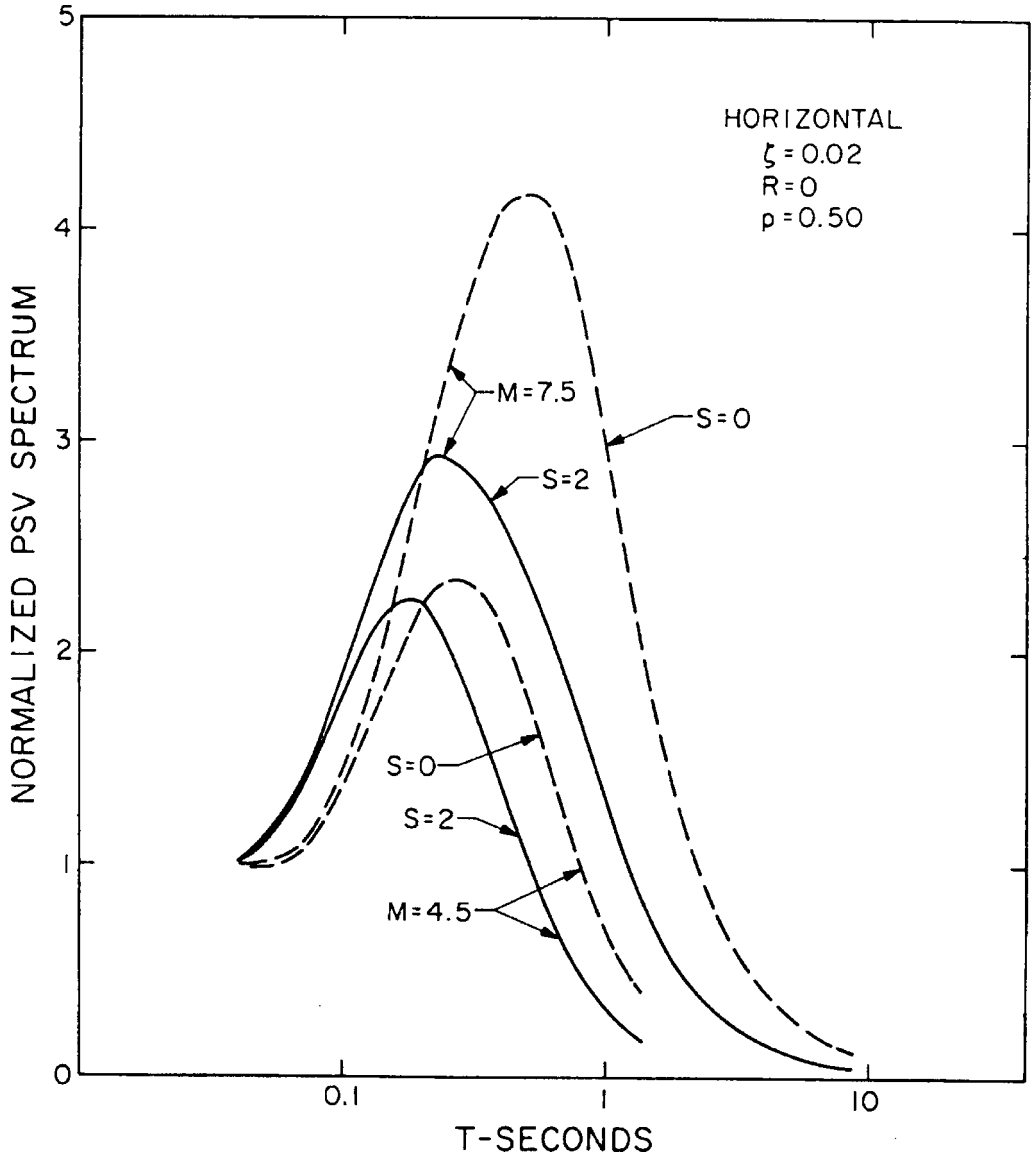

Fig. 5 Change of normalized horizontal PSV spectra with respect to magnitude M and site conditions s

2. Scaling of PSV Spectra in Terms of Modified Mercalli Intensity (MMI)

To scale PSV spectra in terms of MMI, in Equation (1), one can replace M by I_{MM} and delete the terms $\log A_0(R)$ and $g(T)R$ to get (Trifunac, 1979)

$$\log\left[\mathrm{PSV}(T), {}_p\right] = a(T)p + b(T)I_{MM} + c(T) + d(r)s + e(T)v \tag{3}$$

in which I_{MM} represents discrete levels on MMI scale; p, s, v, and $a(T)$ through $e(T)$ have the same meaning as in Equation (1).

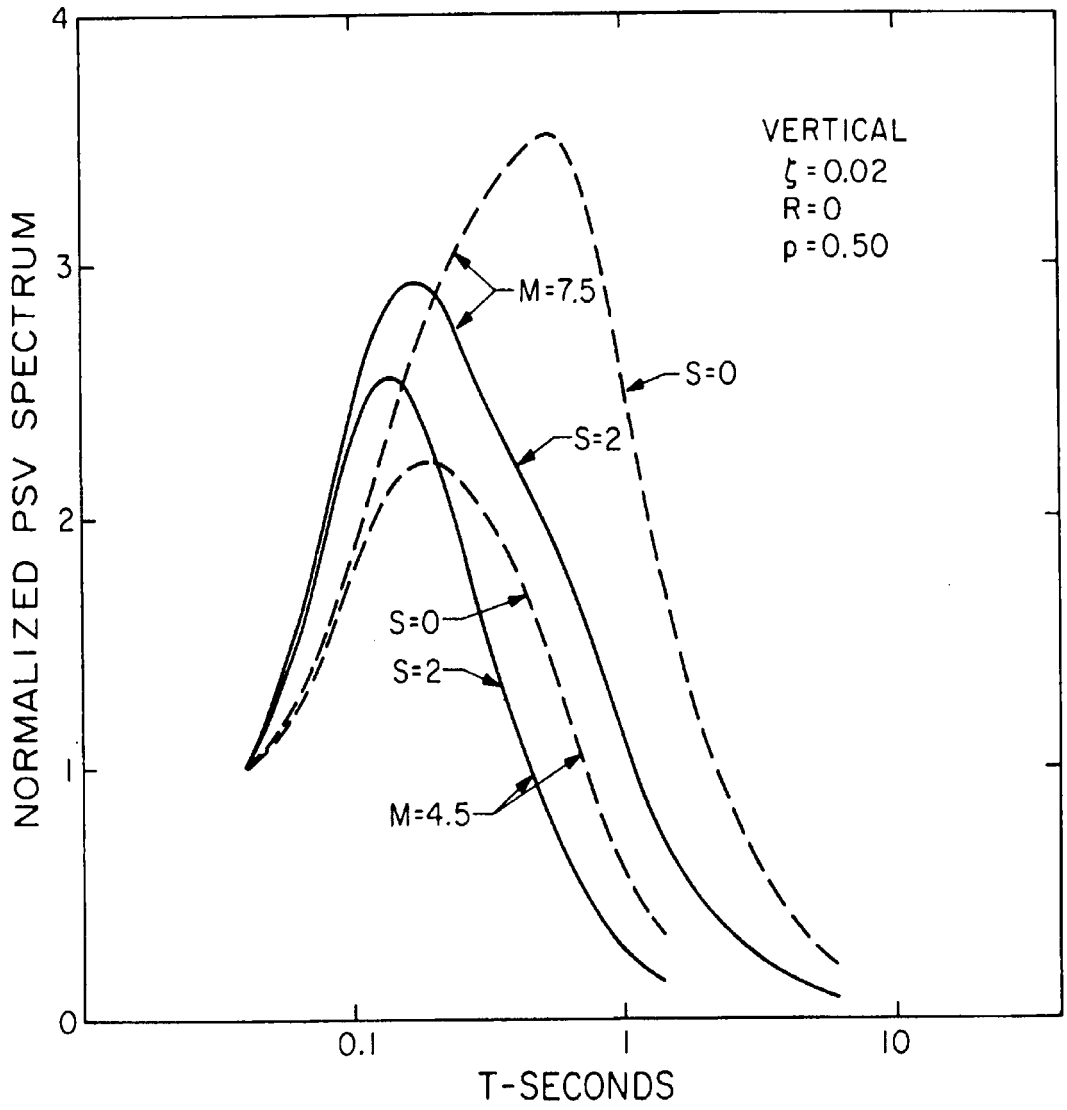

Fig. 6 Change of normalized vertical PSV spectra with respect to magnitude M and site conditions s

Through the use of regression analysis identical to that which was employed for scaling of absolute acceleration spectra and similar to that described previously for scaling in terms of M and R, it is possible to compute $a(T)$ through $e(T)$. The results are then as shown in Figure 7 for $\zeta = 0.00,\ 0.02,\ 0.05,\ 0.10,$ and 0.20.

Examples of using Equation (3) for MMI = IV through VIII, for $s = 0$ and 2, for $\zeta = 0.02$ and for $p = 0.5$ are shown in Figure 8 for horizontal and in Figure 9 for vertical PSV spectra. As in Figures 3 and 4, the amplitudes of recording and processing noise are also shown. For the spectra of intensities MMI $\leq$ VI, it is seen that the signal-to-noise ratio is small for periods longer than 2-3 s. Consequently, the coefficients $a(T)$ through $e(T)$ in this period range may be affected by this low signal-to-noise ratio, and Equation (3) should not be used in this range. This has been shown in Figures 8 and 9 by terminating spectral amplitudes for MMI = IV and VI at periods shorter than 12 s.

Equation (3) applies to MMI range from IV to VIII only, since it is in this range of intensities that the strong-motion data are currently available. For illustration only, Figures 8 and 9 also show (in light lines) the amplitudes of PSV spectra that result from extrapolating to MMI levels X and XII. By extrapolating to MMI = XII and by comparing the spectral amplitudes with the largest estimates of strong shaking from Equation (1), it is possible to test at least the consistency between the extrapolated maxima computed from Equations (1) and (3). Such a test was performed, and this showed that Equation (3), if extrapolated beyond I_{MM} = VIII, yields reasonable estimates of PSV spectral amplitudes for intermediate and low

frequencies. An example of this is presented in Figure 10 where extrapolated PSV spectra (smooth light lines) have been plotted for $\zeta = 0.0, 0.02, 0.05, 0.10,$ and $0.20,$ for $p = 0.1$ and $0.9,$ and for MMI = X and $s = 2,$ the conditions that correspond to the site where the Pacoima Dam accelerogram was recorded during the San Fernando, California, earthquake of 1971.

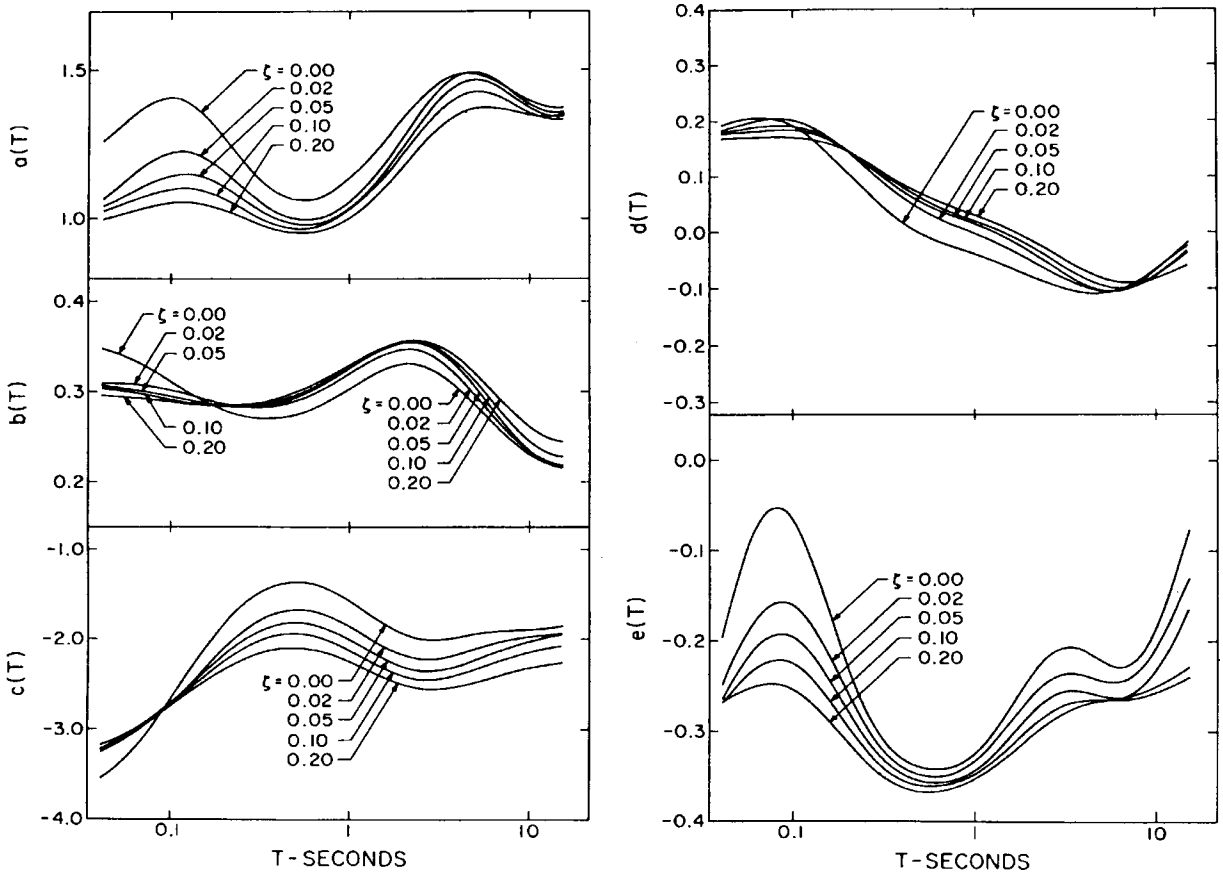

Fig. 7 Functions $a(T)$, $b(T)$, $c(T)$, $d(T)$ and $e(T)$

FREQUENCY-DEPENDENT ATTENUATION AND SIMULTANEOUS TREATMENT OF GEOLOGIC AND SOIL SITE CONDITIONS

The regression analysis of pseudo relative velocity spectra from strong-motion earthquake acceleration records belonging to the first generation of our empirical scaling equations has been outlined in the preceding section (Trifunac, 1978, 1979). There, it was shown that the response spectra of strong motion acceleration can be scaled directly in terms of earthquake magnitude, M, Richter's attenuation function, $A_0(R)$, epicentral distance, R, geological site condition, s, and the component direction, v, without any consideration of peak accelerations. Trifunac and Anderson (1977) used the same scaling function (as for Fourier spectra) to scale absolute acceleration spectra, SA. The same methodology was used to develop analogous functionals for scaling of pseudo relative velocity and relative velocity spectra, PSV and SV (Trifunac and Anderson, 1978a, 1978b). Subsequently, Trifunac and Lee (1979) refined the above analyses by introducing a measure of the depth of sedimentary deposits beneath the recording station, h, as a site characteristic to replace the scaling parameter for site conditions, s. The scaling function then became (Equation (1) of Trifunac and Lee, 1979):

$$\log_{10}[\mathrm{PSV}(T)] = M + \log_{10} A_0(R) - b(T)M - c(T) - d(T)h - e(T)v - f(T)M^2 - g(T)R \qquad (4)$$

In this equation, $\mathrm{PSV}(T)$ is the PSV amplitude at period T, and $\log_{10} A_0(R)$ represents the empirically determined function, describing the overall attenuation of amplitudes with epicentral distance, R (Richter, 1958). h is the site parameter described above. v is the parameter describing the component

of motion. The scaling functions $b(T)$ through $g(T)$ were determined through the regression analyses at 91 periods, T, between 0.04 s and 15 s.

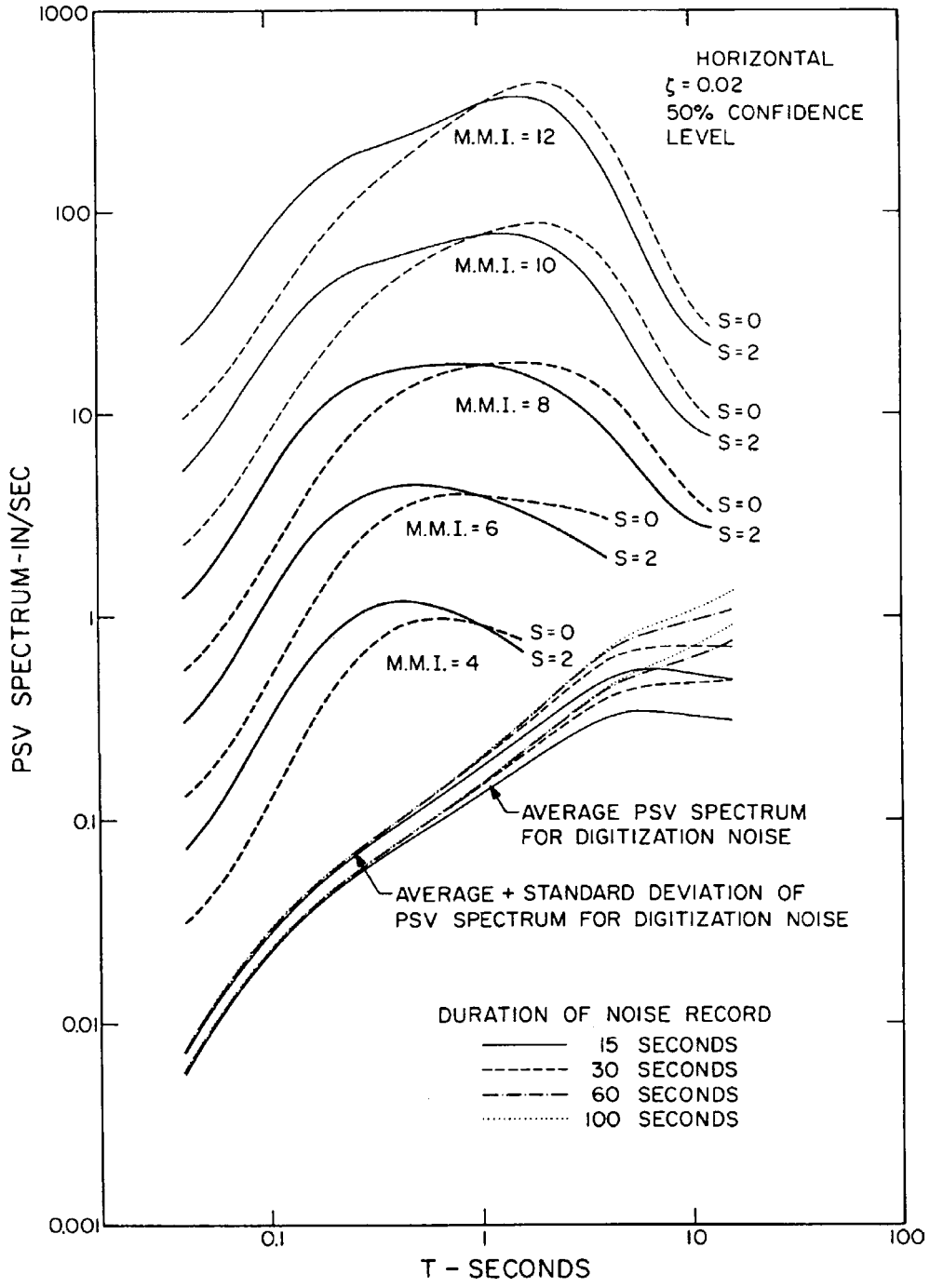

Fig. 8 Horizontal PSV spectra for MMI = IV through XII, and for $s = 0$ and 2

1. Scaling of PSV(T) in Terms of M, R, H, S, h and v

1.1 New Regression Analysis (Second Generation of Empirical Scaling Equations)

The first series of regression analyses (during 1970's) of the pseudo relative velocity spectra, PSV(T), were carried out for 186 free-field records corresponding to a total of 558 components of data from 57 earthquakes (starting with the Long Beach earthquake in 1933 and ending with the San Fernando earthquake in 1971). The expanded database, which we assembled in early 1980's, consisted of 438 three-component free-field records (1314 components of acceleration) from 104 earthquakes. Most of these earthquakes occurred in the regions of northern and southern California up to the year 1981. With

this new database, Trifunac and Lee (1985a) developed the first frequency-dependent attenuation function, $Att(\Delta, M, T)$, as a function of the "representative" distance Δ from the source to the site, magnitude M and period of the motion T. For a complete description of this attenuation function, the reader is referred to the above reference. Using the same function, Trifunac and Lee (1985b) presented the scaling functions for estimating the Fourier spectral amplitudes, FS(T).

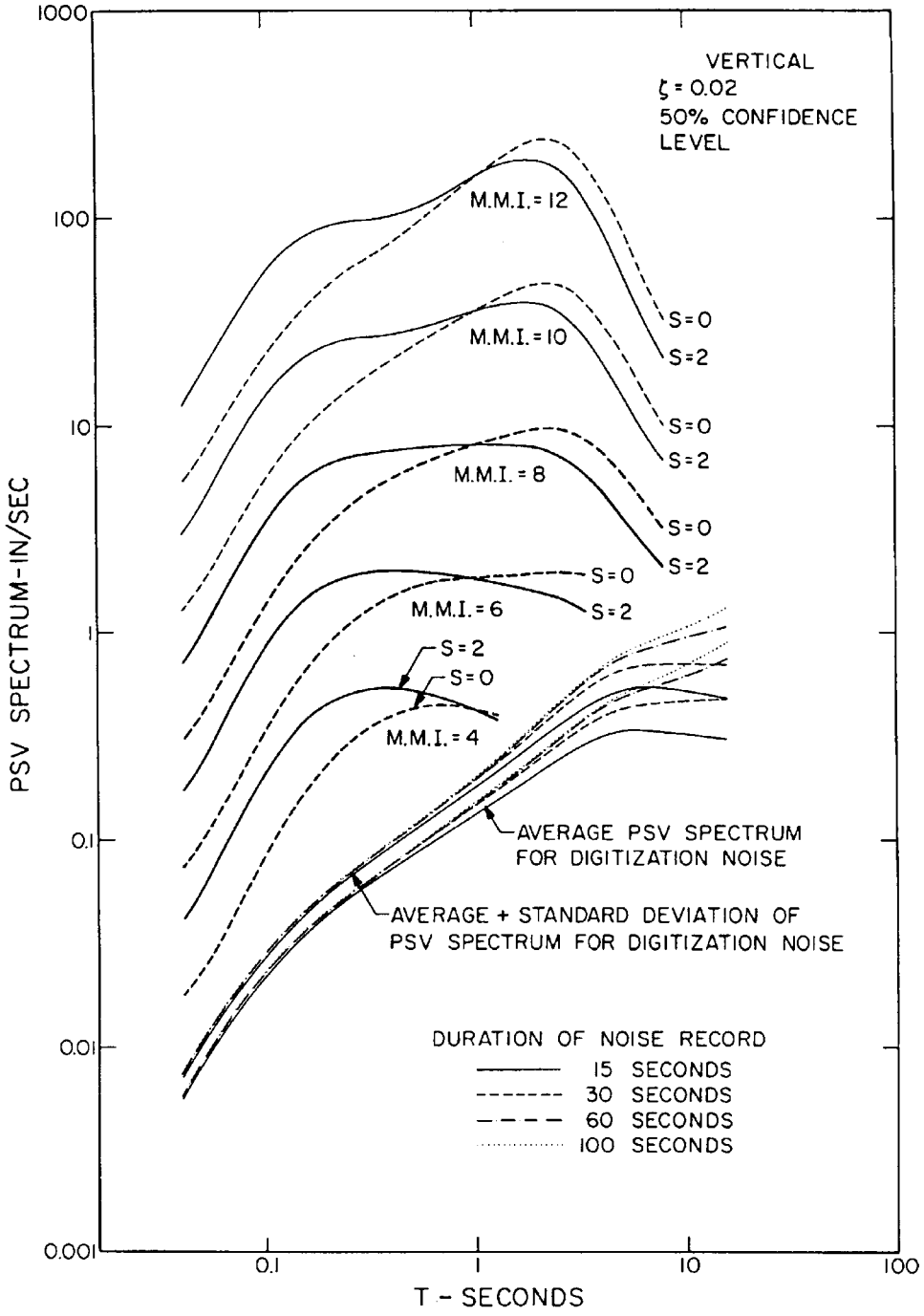

Fig. 9 Vertical PSV spectra for MMI = IV through XII, and for $s = 0$ and 2

Following these new ideas, the dependence of the PSV amplitudes of strong motion at a particular period, T, could be presented in exactly the same form. The scaling equation then became

$$\log_{10}[\mathrm{PSV}(T)] = M + Att(\Delta, M, T) + b_1(T)M + b_2(T)h + b_3(T)v + b_4(T)\Delta/100 + b_5(T) + b_6(T)M^2 \quad (5)$$

Equation (5) is of the same form as in our preceding analyses of spectral amplitudes, but with the old attenuation function $\log_{10} A_0(R)$ replaced by $Att(\Delta, M, T)$.

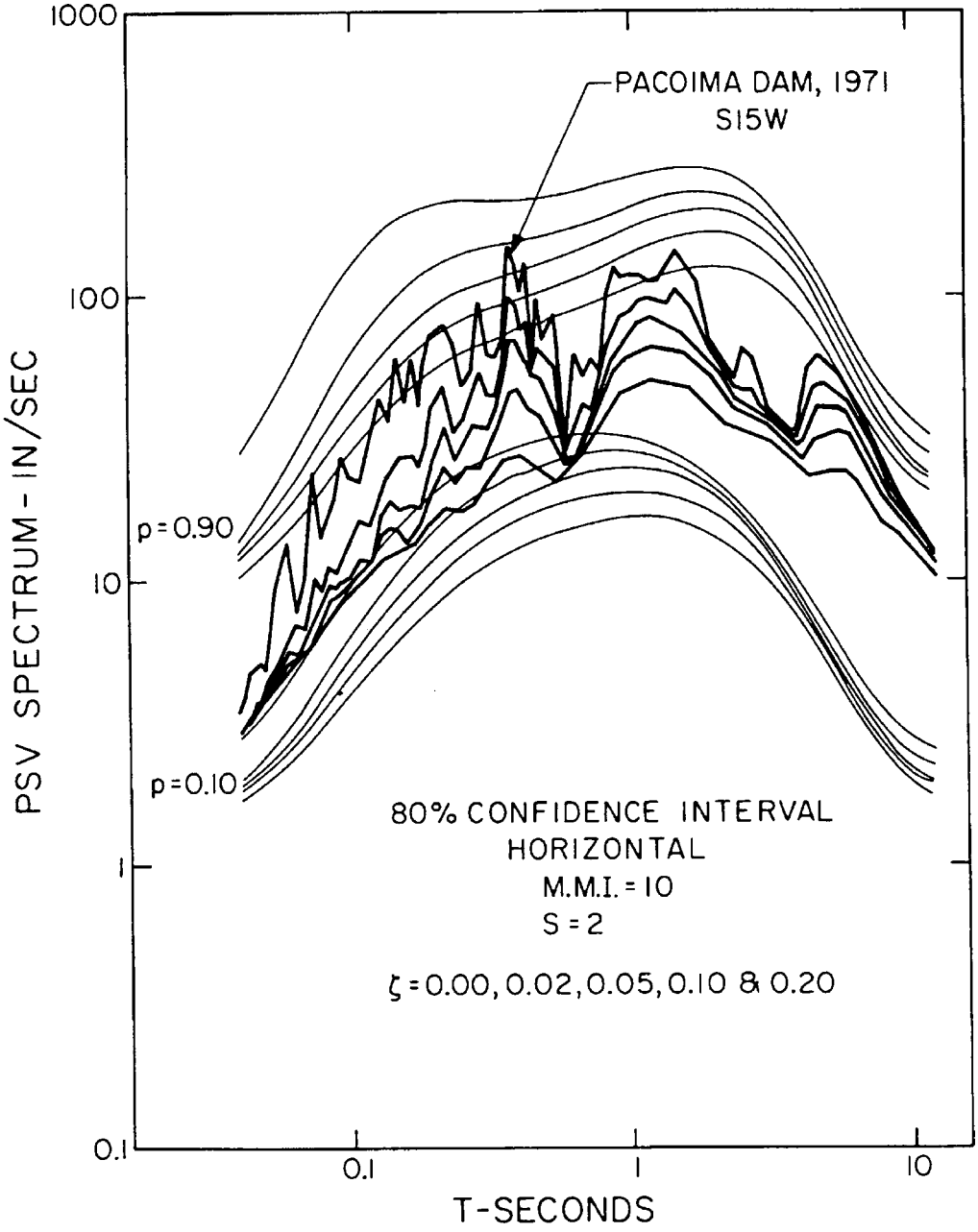

Fig. 10 Comparison of recorded (heavy lines) and computed (light lines) PSV spectra for 80% confidence interval

The new frequency-dependent attenuation function (Trifunac and Lee, 1985a) is

$$Att(\Delta, M, T) = Att_0(T)\log_{10}\Delta \tag{6a}$$

where $Att_0(T)$ is a parabola for $T < 1.8$ s and a constant for $T > 1.8$ s, as follows:

$$Att_0(T) = \begin{cases} -0.732025 & T > 1.8\ s \\ a + b\log_{10} T + c(\log_{10} T)^2 & T < 1.8\ s \end{cases} \tag{6b}$$

with $a = -0.767093$, $b = 0.271556$ and $c = -0.52564$ (see Figure 9.8 in Trifunac and Lee, 1985a). Δ is given by

$$\Delta = S\left(\ln\frac{R^2+H^2+S^2}{R^2+H^2+S_0^2}\right)^{-1/2} \tag{6c}$$

where

$$S = 0.2 + 8.51(M-3) \tag{6d}$$

M is magnitude, and S_0 is defined as the correlation radius of the source function. S_0 can be approximated by $S_0 = C_s T/2$, where C_s is the shear wave velocity. The equations above result from Model III, selected by Trifunac and Lee (1985a) as the most suitable description of the frequency-dependent attenuation function.

The scaling functions $b_1(T)$ through $b_6(T)$ are determined through regression analysis. The data is first screened to minimize a possible bias in the model, which could result from uneven distribution of data among the different magnitude ranges and site conditions, or from excessive contribution to the database from several abundantly recorded earthquakes. All procedures in data preparation and selection, and the form of the regression analysis employed here are the same as in Trifunac and Lee (1985a), and thus, their description will not be repeated.

During the regression analysis, it was found that the linear term in Δ in Equation (5), namely $b_4(T)\Delta/100$, results in the coefficient $b_4(T)$ being insignificant for most of the periods. Subsequently, this term was deleted, and the scaling equation (Equation (5)) became

$$\log_{10}\left[\mathrm{PSV}(T)\right] = M + \mathrm{Att}(\Delta, M, T) + b_1(T)M + b_2(T)h + b_3(T)v + b_5(T) + b_6(T)M^2 \tag{7}$$

The resulting "coefficients" $b_i(T)$ at each period T, resulting from linear regression, will be denoted by $\hat{b}_1(T)$ through $\hat{b}_6(T)$, respectively. The regression analysis was carried out separately for 5 sets of pseudo relative velocity amplitudes corresponding to 5 different values of critical damping, $\zeta = 0.0,\ 0.02,\ 0.05,\ 0.10$ and 0.20.

If $\hat{b}_1(T)$ through $\hat{b}_6(T)$ represent the best estimates of the functions $b_1(T)$ through $b_6(T)$, then $\log_{10}\hat{\mathrm{PSV}}(T)$ represents the best estimate of $\log_{10}\mathrm{PSV}(T)$ at the same period T, where

$$\log_{10}\left[\hat{\mathrm{PSV}}(T)\right] = M + \mathrm{Att}(\Delta, M, T) + \hat{b}_1(T)M + \hat{b}_2(T)h + \hat{b}_3(T)v + \hat{b}_5(T) + \hat{b}_6(T)M^2 \tag{8}$$

For given values of T, h, v, and Δ, $\log_{10}[\mathrm{PSV}(T)]$ represents a parabola, when plotted versus M. Following all preceding analyses, it was again assumed that Equation (8) applies only in the range $M_{\min} \le M \le M_{\max}$, where

$$M_{\min} = -\hat{b}_1(T)/\left(2\hat{b}_6(T)\right) \text{ and } M_{\max} = -\left(1+\hat{b}_1(T)\right)/\left(2\hat{b}_6(T)\right) \tag{9}$$

For $M \le M_{\min}$, M is used only in the first term of Equation (8), and $M_{\min}$ is used with $\hat{b}_1(T)$ and $\hat{b}_6(T)$. For $M \ge M_{\max}$, $M_{\max}$ is used in all the terms of M. In other words, Equation (8) is modified to

$$\log_{10}\hat{\mathrm{PSV}}(T) = \mathrm{Att}(\Delta, M, T) + \begin{cases} M + \hat{b}_1(T)M_{\min} + \hat{b}_2(T)h + \hat{b}_3(T)v + \hat{b}_5(T) + \hat{b}_6(T)M_{\min}^2, & M \le M_{\min} \\ M + \hat{b}_1(T)M + \hat{b}_2(T)h + \hat{b}_3(T)v + \hat{b}_5(T) + \hat{b}_6(T)M^2, & M_{\min} \le M \le M_{\max} \\ M_{\max} + \hat{b}_1(T)M_{\max} + \hat{b}_2(T)h + \hat{b}_3(T)v + \hat{b}_5(T) + \hat{b}_6(T)M_{\max}^2, & M_{\max} \le M \end{cases} \tag{10}$$

This will result in linear growth of $\log_{10}\mathrm{PSV}(T)$ with M for $M \le M_{\min}$, in parabolic growth for $M_{\min} \le M \le M_{\max}$, and in a constant value of $\mathrm{PSV}(T)$ corresponding to $M_{\max}$, for $M \ge M_{\max}$.

Table 1(a): PSV Regression Coefficients; Mag-Depth Model

$$\log_{10}\mathrm{PSV}(T) = M + \mathrm{Att}(\Delta, M, T) + b_1(T)M + b_2(T)h + b_3(T)v + b_5(T) + b_6(T)M^2$$

	Period, T (s)											
	0.040	0.065	0.110	0.190	0.340	0.500	0.900	1.600	2.800	4.400	7.500	14.00
$\zeta = 0.00$												
$b_1(T)$	-0.021	-0.018	0.070	0.237	0.408	0.505	0.651	0.786	0.839	0.747	0.407	-0.276
$b_2(T)$	0.039	0.030	0.027	0.035	0.052	0.063	0.076	0.088	0.097	0.095	0.079	0.046
$b_3(T)$	-0.076	-0.024	-0.002	-0.029	-0.090	-0.130	-0.153	-0.125	-0.100	-0.108	-0.121	-0.091
$b_5(T)$	-1.580	-1.465	-1.747	-2.470	-3.345	-3.877	-4.627	-5.205	-5.341	-4.924	-3.693	-1.442
$b_6(T)$	-0.041	0.045	-0.054	-0.066	-0.076	-0.082	-0.091	-0.101	-0.108	-0.106	-0.086	-0.038
$M_{\min}$	0.000	0.000	0.648	1.795	2.684	3.079	3.577	3.891	3.884	3.524	2.366	0.000
$M_{\max}$	11.939	10.911	9.907	9.371	9.263	9.177	9.071	8.842	8.514	8.241	8.180	9.526
$\zeta = 0.02$												
$b_1(T)$	-0.036	-0.009	0.121	0.331	0.497	0.555	0.638	0.768	0.852	0.780	0.407	-0.097
$b_2(T)$	0.039	0.032	0.028	0.034	0.047	0.055	0.066	0.079	0.093	0.095	0.083	0.051
$b_3(T)$	-0.104	-0.061	-0.037	-0.049	-0.097	-0.134	-0.160	-0.135	-0.110	-0.115	-0.127	-0.102
$b_5(T)$	-1.630	-1.571	-1.954	-2.786	-3.645	-4.067	-4.632	-5.186	-5.400	-5.046	-3.951	-2.066
$b_6(T)$	-0.040	0.049	-0.064	-0.079	-0.089	-0.090	-0.094	-0.102	-0.112	-0.110	-0.092	0.052
$M_{\min}$	0.000	0.000	0.945	2.095	2.792	3.083	3.394	3.765	3.804	3.545	2.603	0.000
$M_{\max}$	12.050	10.112	8.758	8.424	8.410	8.639	8.713	8.667	8.268	8.091	8.038	8.683
$\zeta = 0.05$												
$b_1(T)$	-0.040	-0.003	0.131	0.344	0.517	0.571	0.628	0.728	0.807	0.764	0.538	0.092
$b_2(T)$	0.042	0.037	0.032	0.034	0.044	0.052	0.065	0.078	0.090	0.091	0.080	0.053
$b_3(T)$	-0.101	-0.072	-1.054	-0.062	-0.103	-0.140	-0.168	-0.143	-0.114	-0.117	-0.131	-1.113
$b_5(T)$	-1.697	-1.672	-2.060	-2.889	-3.750	-4.154	-4.638	-5.099	-5.296	-5.026	-4.167	-2.723
$b_6(T)$	-0.038	0.049	-0.065	-0.082	-0.092	-0.094	-0.094	-0.101	-0.109	-0.110	-0.097	0.068
$M_{\min}$	0.000	0.000	1.008	2.098	2.810	3.037	3.340	3.604	3.702	3.473	2.773	0.676
$M_{\max}$	12.632	10.173	8.700	8.195	8.245	8.356	8.660	8.554	8.289	8.018	7.928	8.029
$\zeta = 0.10$												
$b_1(T)$	0.007	-0.016	0.128	0.334	0.508	0.558	0.603	0.700	0.787	0.762	0.581	0.241
$b_2(T)$	0.043	0.038	0.033	0.035	0.044	0.052	0.064	0.076	0.087	0.089	0.079	0.049
$b_3(T)$	-0.105	-0.080	-0.062	-0.067	-0.107	-0.144	-0.175	-0.153	-0.123	-0.124	-0.138	-0.132
$b_5(T)$	-1.867	-1.809	-2.160	-2.960	-3.795	-4.171	-4.605	-5.047	-5.265	-5.044	-4.336	-3.229
$b_6(T)$	-0.041	0.049	-0.064	-0.081	-0.092	-0.094	-0.094	-0.100	-0.109	-0.111	-0.102	-0.079
$M_{\min}$	0.085	0.163	1.000	2.062	2.761	2.968	3.207	3.500	3.610	3.432	2.848	1.525
$M_{\max}$	12.280	10.367	8.813	8.235	8.196	8.287	8.527	8.500	8.197	7.937	7.750	7.854
$\zeta = 0.20$												
$b_1(T)$	0.092	0.063	0.136	0.315	0.473	0.520	0.555	0.637	0.732	0.739	0.616	0.338
$b_2(T)$	0.046	0.042	0.038	0.039	0.046	0.053	0.063	0.074	0.087	0.091	0.081	0.049
$b_3(T)$	-0.094	-0.085	-0.078	-0.082	-0.110	-0.139	-0.170	-0.157	-0.128	-0.120	-0.131	-0.150
$b_5(T)$	-2.151	-2.044	-2.322	-3.035	-3.803	-4.150	-4.528	-4.906	-5.144	-5.036	-4.511	-3.575
$b_6(T)$	-0.048	0.052	-0.063	-0.079	-0.089	-0.091	-0.091	-0.096	-0.106	-0.111	-0.105	-0.088
$M_{\min}$	0.958	0.606	1.079	1.994	2.657	2.857	3.049	3.318	3.453	3.329	2.933	1.920
$M_{\max}$	11.375	10.221	9.016	8.323	8.275	8.352	8.544	8.526	8.170	7.833	7.695	7.602

With $\mathrm{PSV}(T)$ being the pseudo relative velocity response spectrum amplitudes computed from recorded accelerograms, the residuals $\varepsilon(T)$ were calculated from

$$\varepsilon(T) = \log_{10}\mathrm{PSV}(T) - \log_{10}\hat{\mathrm{PSV}}(T) \tag{11}$$

These residuals describe the distribution of the observed $\mathrm{PSV}(T)$ about the estimated $\hat{\mathrm{PSV}}(T)$. It is assumed that the residuals, $\varepsilon(T)$, can be described by the following probability distribution function of the form

$$p(\varepsilon, T) = \left[1 - \exp\left(-\exp\left(\alpha(T)\varepsilon(T) + \beta(T)\right)\right)\right]^{N(T)} \tag{12}$$

where, $p(\varepsilon, T)$ represents the probability that $\log_{10}\left[\mathrm{PSV}(T)\right] - \log_{10}\left[\hat{\mathrm{PSV}}(T)\right] \le \varepsilon(T)$. $\alpha(T)$, $\beta(T)$ and $N(T)$ are parameters of the distribution function. The integer power $N(T)$ is estimated from the empirical equation

$$N(T) = \min(10, [25/T]) \tag{13}$$

where, $[25/T]$ is the integral part of $25/T$. The parameters $\alpha(T)$ and $\beta(T)$ can then be estimated from the following equation, which is derived from Equation (12):

$$\ln\left(-\ln\left(1-p^{1/N(T)}\right)\right) = \alpha(T)\varepsilon(T) + \beta(T) \tag{14}$$

For a given residual value $\varepsilon(T)$ at a particular period T, the actual probability $p^*(\varepsilon, T)$ that $\varepsilon(T)$ will not be exceeded, can be evaluated by finding the fraction or residuals $\varepsilon(T)$ (computed from the database at that particular period) which are smaller than the given value. Using Equation (12), the estimated probability $\hat{p}(\varepsilon, T)$ that $\varepsilon(T)$ will not be exceeded, can also be evaluated and compared with the above fractions. The Kolmogorov-Smirnov, $KS(T)$, test and the χ^2 statistic, $\chi^2(T)$, can be computed to test for the goodness-of-fit of the distribution function in Equation (12).

Table 1(b): PSV Residuals Probability Coefficients (Equation (12)) and Goodness-of-Fit Statistics; Mag-Depth Model

$$\log_{10} \mathrm{PSV}(T) = M + \mathrm{Att}(\Delta, M, T) + \hat{b}_1(T)M + \hat{b}_2(T)h + \hat{b}_3(T)v + \hat{b}_5(T) + \hat{b}_6(T)M^2 + \varepsilon(T)$$

	Period, T (s)											
	0.040	0.065	0.110	0.190	0.340	0.500	0.900	1.600	2.800	4.400	7.500	14.00
ζ = 0.00												
$\alpha(T)$	1.258	1.259	1.224	1.212	1.258	1.297	1.296	1.235	1.327	1.673	2.373	3.216
$\beta(T)$	1.027	1.006	1.006	1.007	1.000	0.998	1.013	1.018	0.935	0.767	0.492	0.197
$N(T)$	10	10	10	10	10	10	10	10	9	6	3	2
$\chi^2(T)$	7.082	7.305	7.932	8.732	9.581	9.905	10.040	9.632	9.340	9.645	10.662	12.244
$KS(T)$	0.029	0.028	0.028	0.031	0.034	0.036	0.036	0.037	0.041	0.046	0.052	0.058
ζ = 0.02												
$\alpha(T)$	1.316	1.334	1.290	1.252	1.279	1.316	1.317	1.253	1.340	1.696	2.441	3.377
$\beta(T)$	1.027	1.008	1.008	1.010	1.002	0.999	1.014	1.019	0.935	0.767	0.492	0.197
$N(T)$	10	10	10	10	10	10	10	10	9	6	3	2
$\chi^2(T)$	6.469	7.455	8.893	10.657	11.502	11.011	9.430	8.484	8.648	9.331	11.005	14.718
$KS(T)$	0.028	0.028	0.030	0.034	0.038	0.039	0.038	0.037	0.040	0.044	0.050	0.057
ζ = 0.05												
$\alpha(T)$	1.320	1.360	1.324	1.273	1.282	1.315	1.321	1.263	1.358	1.731	2.520	3.526
$\beta(T)$	1.028	1.008	1.008	1.010	1.003	1.000	1.014	1.018	0.934	0.767	0.494	0.200
$N(T)$	10	10	10	10	10	10	10	10	9	6	3	2
$\chi^2(T)$	5.817	6.723	8.450	10.117	10.566	10.250	10.033	10.752	11.395	11.192	10.455	10.164
$KS(T)$	0.026	0.028	0.031	0.034	0.037	0.038	0.039	0.041	0.045	0.048	0.050	0.051
ζ = 0.10												
$\alpha(T)$	1.326	1.382	1.356	1.302	1.296	1.318	1.312	1.258	1.376	1.772	2.573	3.558
$\beta(T)$	1.028	1.009	1.009	1.011.	1.003	1.001	1.015	1.018	0.932	0.766	0.496	0.210
$N(T)$	10	10	10	10	10	10	10	10	9	6	3	2
$\chi^2(T)$	5.224	6.504	8.149	9.531	9.910	9.715	9.476	9.314	8.660	8.267	9.518	14.031
$KS(T)$	0.025	0.027	0.030	0.034	0.038	0.039	0.037	0.036	0.039	0.045	0.050	0.052
ζ = 0.20												
$\alpha(T)$	1.307	1.377	1.368	1.325	1.312	1.321	1.307	1.277	1.432	1.848	2.646	3.618
$\beta(T)$	1.028	1.010	1.010	1.011	1.003	1.001	1.016	1.019	0.933	0.767	0.500	0.218
$N(T)$	10	10	10	10	10	10	10	10	9	6	3	2
$\chi^2(T)$	5.127	6.602	8.300	9.740	10.685	10.873	10.512	9.950	9.756	9.605	8.770	6.936
$KS(T)$	0.026	0.029	0.034	0.037	0.039	0.039	0.039	0.038	0.040	0.043	0.047	0.049

1.2 Results of the Regression Analysis

Table 1 gives, for 12 points between $T = 0.04$ and $T = 14$ s, the amplitudes of the smoothed regression coefficients $\hat{b}_1(T)$, $\hat{b}_2(T)$, $\hat{b}_3(T)$, $\hat{b}_5(T)$, $\hat{b}_6(T)$ (note that $b_4(T)$ has been deleted), $\hat{M}_{\min}(T)$, $\hat{M}_{\max}(T)$, the smoothed amplitudes of $N(T)$, $\hat{\alpha}(T)$, $\hat{\beta}(T)$ in Equation (12), and the χ^2 and Kolmogorov-Smirnov statistics. The 12 periods used appear to be sufficient for most practical

computations, since the smoothness of PSV is such that almost any interpolation scheme will yield adequate estimates of their amplitudes at any period in the range $0.04-15$ s.

Table 2(a): PSV Regression Coefficients; MMI-Depth Model

$$\log_{10}\mathrm{PSV}(T)=b_1(T)I_{MM}+b_2(T)h+b_3(T)v+b_4(T)$$

	Period, T (s)											
	0.040	0.065	0.110	0.190	0.340	0.500	0.900	1.600	2.800	4.400	7.500	14.00
$\zeta = 0.00$												
$b_1(T)$	0.223	0.231	0.257	0.297	0.332	0.341	0.335	0.315	0.283	0.248	0.201	-0.145
$b_2(T)$	-0.027	-0.023	0.009	0.017	0.050	0.069	0.088	0.096	0.097	0.089	0.070	0.036
$b_3(T)$	-0.061	-0.029	-0.015	-0.045	-0.109	-0.139	-0.135	-0.099	-0.082	-0.039	-0.107	-0.115
$b_4(T)$	-1.715	-1.464	-1.278	-1.284	-1.435	-1.524	-1.551	-1.434	-1.207	-0.983	-0.757	-0.612
$\zeta = 0.02$												
$b_1(T)$	0.208	0.213	0.241	0.289	0.333	0.348	0.347	0.328	0.294	0.259	0.211	0.158
$b_2(T)$	-0.023	-0.026	-0.020	0.001	0.033	0.054	0.076	0.086	0.090	0.086	0.070	0.036
$b_3(T)$	-0.093	-0.066	-0.048	-0.067	-0.122	-0.152	-0.153	-0.117	-0.093	-0.099	-0.120	-0.132
$b_4(T)$	-1.766	-1.540	-1.393	-1.441	-1.625	-1.726	-1.756	-1.630	-1.383	-1.142	-0.900	-0.747
$\zeta = 0.05$												
$b_1(T)$	0.213	0.215	0.238	0.283	0.328	0.344	0.347	0.333	0.305	0.271	0.223	0.168
$b_2(T)$	-0.024	-0.025	-0.019	0.000	0.031	0.050	0.071	0.083	0.088	0.086	0.072	0.041
$b_3(T)$	-0.101	-0.080	-0.064	-0.077	-0.126	-0.155	-0.163	-0.134	-0.112	-0.116	-0.135	-0.148
$b_4(T)$	-1.824	-1.607	-1.466	-1.513	-1.694	-1.798	-1.845	-1.746	-1.521	-1.286	-1.040	-0.876
$\zeta = 0.10$												
$b_1(T)$	0.219	0.219	0.239	0.281	0.324	0.340	0.345	0.333	0.308	0.278	0.235	0.185
$b_2(T)$	-0.025	-0.023	-0.017	-0.001	-0.027	0.046	0.069	0.082	0.086	0.083	0.070	0.043
$b_3(T)$	-0.102	-0.087	-0.075	-0.086	-0.129	-0.157	-0.165	-0.137	-0.114	-0.117	-0.139	-0.158
$b_4(T)$	-1.882	-1.682	-1.551	-1.597	-1-769	-1.869	-1.921	-1.838	-1.634	-1.417	-1.190	-1.039
$\zeta = 0.20$												
$b_1(T)$	0.226	0.228	0.245	0.280	0.319	0.335	0.343	0.331	0.308	0.282	0.245	0.199
$b_2(T)$	-0.022	-0.024	-0.018	0.000	0.027	0.043	0.062	0.073	0.079	0.079	0.068	0.043
$b_3(T)$	-0.102	-0.093	-0.086	-0.096	-0.132	-0.157	-0.168	-0.143	-0.117	-0.117	-0.140	-0.161
$b_4(T)$	-1.960	-1.791	-1.675	-1.708	-1.862	-1.956	-2.004	-1.920	-1.735	-1.550	-1.355	-1.205

2. Scaling of $\mathrm{PSV}(T)$ in Terms of M, R, H, S, s and v

Sub-section 1 above characterized the local geology by the approximate overall depth of sedimentary deposits beneath the recording station, h, in km. As it has been noted previously, while the depth of sediments at each recording station represents a preferable site characterization, in many instances, little may be known about such depth at some sites, and so, the scaling of PSV amplitudes at any such site using depth, h, would become impossible. The site characterization in terms of $s = 0, 1$ and 2, which can be determined from knowledge of surface geology only, thus remains a useful approach to the scaling of PSV amplitudes. For a description of the distribution of data in the database (of early 1980's) among the different site conditions, and for the associated regression analyses, the reader is referred to Trifunac and Lee (1985b, 1985c).

3. Scaling of $\mathrm{PSV}(T)$ in Terms of MMI, h and v

3.1 The Scaling Relation

Sub-sections 1 and 2 above presented the description of the empirical models for scaling pseudo relative velocity spectra from strong-motion earthquake acceleration in terms of earthquake magnitude, source-to-station representative distance, and a parametric characterization of local geology at the recording station. Following the approach of Trifunac and Lee (1985b) for the scaling of Fourier amplitude spectra, Sub-sections 3 and 4 summarize the extension of the method outlined above to the scaling of pseudo relative velocity spectra in terms of Modified Mercalli Intensity (MMI) at the site.

The scaling equation becomes (Equation (4) of Trifunac and Lee (1979))

$$\log_{10}[\mathrm{PSV}(T)]=b(T)I_{MM}+c(T)+d(T)h+e(T)v \tag{15}$$

with I_{MM} denoting the reported discrete levels of the MMI scale at the recording station, and with all other parameters defined as above.

Table 2(b): PSV Residuals Probability Coefficients (Equation (12)) and Goodness-of-Fit Statistics; MMI-Depth Model

$$\log_{10}\mathrm{PSV}(T) = \hat{b}_1(T) I_{MM} + \hat{b}_2(T) h + \hat{b}_3(T) v + \hat{b}_4(T) + \varepsilon(T)$$

	Period, T (s)											
	0.040	0.065	0.110	0.190	0.340	0.500	0.900	1.600	2.800	4.400	7.500	14.00
$\zeta = 0.00$												
$\alpha(T)$	1.061	1.096	1.126	1.167	1.194	1.181	1.055	1.055	1.219	1.605	2.288	3.066
$\beta(T)$	1.006	0.987	0.988	0.991	0.984	0.982	0.998	1.004	0.919	0.752	0.484	0.204
$N(T)$	10	10	10	10	10	10	10	10	9	6	3	2
$\chi^2(T)$	6.623	6.878	6.162	5.342	5.695	6.804	9.229	11.205	11.654	11.103	10.743	12.511
$KS(T)$	0.029	0.030	0.028	0.026	0.027	0.030	0.037	0.044	0.046	0.046	0.048	0.057
$\zeta = 0.0$												
$\alpha(T)$	1.139	1.159	1.165	1.193	1.236	1.241	1.183	1.121	1.267	1.653	2.359	3.176
$\beta(T)$	1.006	0.988	0.988	0.990	0.983	0.981	0.998	1.004	0.918	0.751	0.482	0.201
$N(T)$	10	10	10	10	10	10	10	10	9	6	3	2
$\chi^2(T)$	6.993	6.994	6.332	5.340	4.813	5.254	7.703	11.571	14.225	13.897	10.959	7.452
$KS(T)$	0.026	0.028	0.028	0.026	0.026	0.028	0.036	0.046	0.052	0.053	0.051	0.053
$\zeta = 0.05$												
$\alpha(T)$	1.176	1.194	1.186	1.202	1.249	1.264	1.217	1.152	1.295	1.688	2.413	3.249
$\beta(T)$	1.005	0.988	0.989	0.990	0.982	0.981	0.999	1.005	0.918	0.750	0.480	0.199
$N(T)$	10	10	10	10	10	10	10	10	9	6	3	2
$\chi^2(T)$	6.204	6.645	6.978	6.765	6.353	6.669	8.840	12.064	13.805	13.170	10.981	9.395
$KS(T)$	0.026	0.028	0.029	0.028	0.028	0.031	0.038	0.047	0.052	0.051	0.048	0.048
$\zeta = 0.10$												
$\alpha(T)$	1.211	1.231	1.215	1.216	1.256	1.276	1.244	1.195	1.341	1.725	2.425	3.231
$\beta(T)$	1.004	0.988	0.989	0.991	0.983	0.982	1.000	1.006	0.919	0.749	0.477	0.192
$N(T)$	10	10	10	10	10	10	10	10	9	6	3	2
$\chi^2(T)$	5.610	6.922	8.055	7.692	6.527	6.895	10.477	14.973	15.972	13.727	10.199	8.859
$KS(T)$	0.033	0.032	0.031	0.030	0.029	0.031	0.038	0.046	0.050	0.049	0.047	0.048
$\zeta = 0.20$												
$\alpha(T)$	1.251	1.277	1.259	1.250	1.277	1.290	1.254	1.220	1.394	1.787	2.458	3.190
$\beta(T)$	1.004	0.988	0.990	0.991	0.983	0.982	1.000	1.006	0.918	0.748	0.473	0.185
$N(T)$	10	10	10	10	10	10	10	10	9	6	3	2
$\chi^2(T)$	6.768	7.540	7.114	5.810	5.839	7.512	11.826	15.594	16.616	15.203	11.806	7.674
$KS(T)$	0.037	0.037	0.033	0.027	0.025	0.028	0.040	0.053	0.059	0.056	0.050	0.049

The analysis was next carried out on the database with 438 free-field records from 104 earthquakes. The estimated MMI levels at some of the 438 free-field sites were used in addition to the reported MMI levels, which for the most part were available only for the original 186 free-field sites. The estimated MMI levels have been calculated by using the scaling equation

$$I_{MM} = 1.5M - A - B\ln\Delta - C\Delta/100 - Ds \tag{16}$$

with the procedure, as described in Lee and Trifunac (1985).

The scaling of pseudo relative velocity spectra now takes the form

$$\log_{10}[\mathrm{PSV}(T)] = b_1(T)\hat{I}_{MM} + b_2(T) h + b_3(T) v + b_4(T) \tag{17}$$

where $\hat{I}_{MM}$ is the estimated MMI level at the site from Equation (16), or the reported MMI level there, if available.

The scaling functions $b_1(T)$ through $b_4(T)$ have been determined through the regression analysis of the database. The fitted coefficients at each period T resulting from linear regression are denoted by $\hat{b}_1(T)$, $\hat{b}_2(T)$, $\hat{b}_3(T)$ and $\hat{b}_4(T)$.

3.2 Results of the Regression Analysis

Substitution of the coefficients $\hat{b}_1(T)$, $\hat{b}_2(T)$ into Equation (17) gives $\hat{\mathrm{PSV}}(T)$:

$$\log_{10}\hat{\mathrm{PSV}}(T) = \hat{b}_1(T)I_{MM} + \hat{b}_2(T)h + \hat{b}_3(T)v + \hat{b}_4(T) \tag{18}$$

where, $\log_{10}\hat{\mathrm{PSV}}(T)$ represents the estimate of the logarithm of the pseudo relative velocity spectrum at period T for this model. We recall Equation (8):

$$\log_{10}[\mathrm{PSV}(T)] = M + \mathrm{Att}(\Delta, M, T) + \hat{b}_1(T)M + \hat{b}_2(T)h + \hat{b}_3(T)v + \hat{b}_5(T) + \hat{b}_6(T)M^2 \tag{19}$$

which corresponds to the scaling of $\mathrm{PSV}(T)$ in terms of magnitude M, and "representative" source-to-station distance Δ. Trifunac and Lee (1985a, 1985b, 1985c, 1987) have described the resemblance in shape, of the function $\hat{b}_1(T)$ for intensity I_{MM} in (18), and M in Equation (19). The same holds true for the scaling function $\hat{b}_2(T)$ for h, and $\hat{b}_3(T)$ for v in both equations. This resemblance is obvious, even though, unlike in Equation (19), the explicit dependence of $\mathrm{PSV}(T)$ on "representative" source-to-station distance, Δ, is omitted from Equation (18). As pointed out previously (Trifunac and Lee, 1979), Equation (18) is intended to be in such simple form. Including the explicit dependence of $\mathrm{PSV}(T)$ on epicentral distance, R, or on "representative" source-to-station distance, Δ, as in $\mathrm{Att}(\Delta, M, T)$, would decrease the uncertainties associated with the estimation of $\mathrm{PSV}(T)$ in Equation (19), but then, this equation would only be applicable to those regions which have similar intensity attenuation with distance, as in California, where over 90% of the records in the database have been recorded.

With $\mathrm{PSV}(T)$ being the pseudo relative velocity with the damping value $\zeta = 0$, and computed from recorded accelerograms, the residuals, $\varepsilon(T)$, were calculated from Equation (11). It is assumed here again that the residuals, $\varepsilon(T)$ can be described by the distribution function of the form given by Equation (12). The probability $p(\varepsilon, T)$ at period T that $\log_{10}\mathrm{PSV}(T) - \log_{10}\hat{\mathrm{PSV}}(T) \le \varepsilon(T)$, is then given by Equation (12), with $\alpha(T)$ and $\beta(T)$ being the parameters to be determined. The integer power $N(T)$ in Equation (12) was estimated from the empirical equation, Equation (13).

For a given residue $\varepsilon(T)$ at a particular period T, the actual probability $p^*(\varepsilon, T)$ that $\varepsilon(T)$ will not be exceeded, the corresponding estimated probability $\hat{p}(\varepsilon, T)$, the Kolmogorov-Smirnov statistic, $KS(T)$, and the χ^2 statistic, $\chi^2(T)$, are all computed as in Sub-section 1 above, where a complete description of the steps and formulae involved are also described.

Tables 2(a) and 2(b) give, for 12 periods between $T = 0.04$ s and $T = 14$ s, the amplitudes of the smoothed regression coefficients $\hat{b}_1(T)$ through $\hat{b}_4(T)$, the discrete values $N(T)$, the smoothed coefficients $\hat{\alpha}(T)$ and $\hat{\beta}(T)$ in Equation (12), and the $\chi^2(T)$ and $KS(T)$ statistics.

4. Scaling of $\mathrm{PSV}(T)$ in Terms of MMI, *s* and *v*

Next, the description of the empirical model of scaling pseudo relative velocity spectra, computed from strong ground motion, in terms of Modified Mercalli Intensity (MMI) at a site and a description of local site geology can be considered. As in Sub-section 2 above, this analysis replaces the depth of sedimentary deposits h, used for the site characterization in Sub-section 3, by the corresponding site parameter s $(s = 0, 1 \text{ and } 2)$. The scaling relation and the results of regression analysis can be found in Trifuanc and Lee (1985c).

FREQUENCY-PATH-DEPENDENT ATTENUATION AND SIMULTANEOUS TREATMENT OF GEOLOGICAL AND SOIL SITE CONDITIONS

Starting in early 1990's, the frequency and magnitude-dependent attenuation equations of Trifunac and Lee (1985a) were further improved to include variations among selected "typical" wave paths. This enabled development of, so far the most advanced (third generation), empirical scaling equations of peak amplitudes (Lee et al., 1995) and spectra (Lee and Trifunac, 1995a, 1995b) of recorded strong ground motion. These developments were made possible by rapid increase in the number and quality of uniformly processed strong motion data.

1. The New (Current) Strong Motion Database

By late-1993, strong motion database grew to over 1926 free-field records from 297 earthquakes and aftershocks. This corresponds to over 3800 horizontal components and 1900 vertical components.

For each record in this database, the following information has been collected: (1) coordinates (latitude and longitude) and address of the recording site, (2) epicentral, R, and hypocentral, D, distances, (3) component orientation, (4) local geological site classification, s, (5) depth of sediments, h, from the surface to geological basement rock beneath the site, (6) local soil type, s_L, representative of the top 100 m - 200 m beneath the surface (Trifunac, 1990a), where $s_L = 0$ for hard "rock" soil sites, $s_L = 1$ for stiff soil sites, $s_L = 2$ for deep soil sites, (7) average soil velocity, V_L, in the top 30 m beneath the surface (if this is not available, a soil velocity type, S_T, is used instead, such that for $V_L > .75$ km/s, $.75 \geq V_L > .36$ km/s, $.36 \geq V_L > .18$ km/s, and $V_L \leq .18$ km/s, it is assigned to indicator variables A, B, C or D, respectively), (8) r (or $100r$), the ratio (or percentage), $0 \leq r \leq 1$, of the wave path through geological basement rock to the total path, measured along the surface from the earthquake epicenter to the recording site, and (9) the generalized path type classification, describing different types of wave paths between the sources and stations. At present, we consider eight such categories. Figure 11 shows a plot of the schematic representations of the ``geometry'' of these path types.

With the above set of parameters available at each of the recording sites, scaling equations were developed by regression analyses of peak accelerations, velocities and displacements (Lee et al., 1995), and of the duration of strong ground motion (Novikova and Trifunac, 1995). A new frequency-dependent attenuation function and empirical scaling equations for Fourier amplitudes were also developed (Lee and Trifunac, 1995a). The new frequency-dependent attenuation function describes the attenuation of the Fourier amplitudes at each period from the source to the site. It takes the form (Trifunac and Lee, 1990)

$$\mathrm{Att}(\Delta, M, T) = \begin{cases} A_0(T)\log(\Delta/L), & R \leq R_{\max} \\ A_0(T)\log(\Delta_{\max}/L) - (R - R_{\max})/200, & R > R_{\max} \end{cases} \tag{20}$$

with Δ, R, $\Delta_{\max}$, $R_{\max}$ defined as in the previous sections. The new parameter, $L = L(M)$, represents the length of the earthquake fault. It is approximately equal to $L = .01 \times 10^{0.5M}$ km (Trifunac, 1993a, 1993b). Δ/L is thus a dimensionless representative source-to-station distance.

At present, not all path types (Figure 11) have sufficient data to allow independent analyses. To ensure that the regression results are significant, several path types that are "similar" or "comparable", have been lumped into the following six groups: "0" includes all path types; "1" includes path type 1; "2" includes path types 2 and 6, "3" includes path types 3 and 7; "4" includes path types 4, 5 and 8; and "5" includes the path through rock only (path type 4). Regression analyses were then performed for each of the path groups (0 to 5) separately.

2. New Scaling Equations of PSV Spectra

We illustrate here only the scaling equations for the regression of pseudo relative velocity (PSV) spectral amplitudes in terms of magnitude, site geology, local soil types, and percentage of rock along the wave path from source to station.

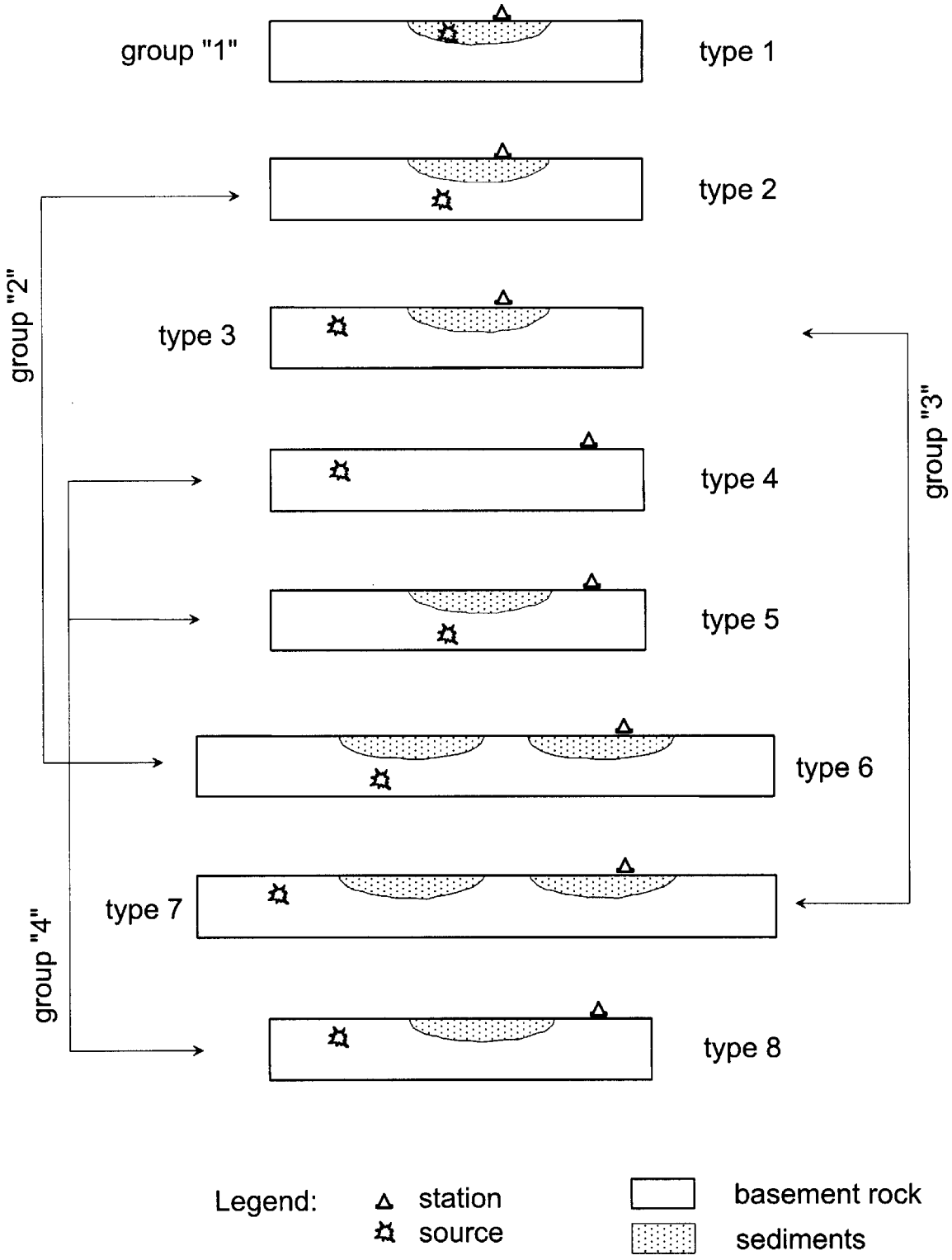

Fig. 11 Schematic representation of eight different path types for seismic waves propagating from source to the recording station (grouping of these eight path types into path groups, "1", "2", "3", …, is also shown)

Regression equations of similar form were previously used for the analyses of peak acceleration, velocity and displacement (Lee et al., 1995). The same equations were used for the analyses of Fourier spectral amplitudes, $FS(T)$ (Lee and Trifunac, 1995a). The reader is referred to the above two reports for additional detailed description of the equations and of the steps involved in the execution of the regression analyses and development of the scaling models. The equations used for the four scaling models are:

Model (i): Mag-site + soil + % rock path multi-step model

$$\log \mathrm{PSV}(T) = \begin{cases} M + \mathsf{A}_0(T)\log(\Delta/L) + b_1(T)M + b_2(T)a + b_3(T)v + b_4(T) + b_5(T)M^2 \\ \quad + \sum_i b_6^{(i)}(T)S_L^{(i)} + \left(b_{70}(T)r + b_{71}(T)(1-r)\right)R & R \le R_{\max} \\ M + \mathsf{A}_0(T)\log(\Delta_{\max}/L) + b_1(T)M + b_2(T)a + b_3(T)v + b_4(T) + b_5(T)M^2 \\ \quad + \sum_i b_6^{(i)}(T)S_L^{(i)} + \left(b_{70}(T)r + b_{71}(T)(1-r)\right)R_{\max} - (R - R_{\max})/200 & R > R_{\max} \end{cases} \quad (21)$$

Model (ii): Mag-depth + soil + % rock path multi-step model

$$\log \mathrm{PSV}(T) = \begin{cases} M + \mathsf{A}_0(T)\log(\Delta/L) + b_1(T)M + b_2(T)h + b_3(T)v + b_4(T) + b_5(T)M^2 \\ \quad + \sum_i b_6^{(i)}(T)S_L^{(i)} + \left(b_{70}(T)r + b_{71}(T)(1-r)\right)R & R \le R_{\max} \\ M + \mathsf{A}_0(T)\log(\Delta_{\max}/L) + b_1(T)M + b_2(T)h + b_3(T)v + b_4(T) + b_5(T)M^2 \\ \quad + \sum_i b_6^{(i)}(T)S_L^{(i)} + \left(b_{70}(T)r + b_{71}(T)(1-r)\right)R_{\max} - (R - R_{\max})/200 & R > R_{\max} \end{cases} \quad (22)$$

Model (iii): Mag-site + no soil + % rock path multi-step model

$$\log \mathrm{PSV}(T) = \begin{cases} M + \mathsf{A}_0(T)\log(\Delta/L) + b_1(T)M + b_2(T)s + b_3(T)v + b_4(T) + b_5(T)M^2 \\ \quad + \left(b_{70}(T)r + b_{71}(T)(1-r)\right)R & R \le R_{\max} \\ M + \mathsf{A}_0(T)\log(\Delta_{\max}/L) + b_1(T)M + b_2(T)s + b_3(T)v + b_4(T) + b_5(T)M^2 \\ \quad + \left(b_{70}(T)r + b_{71}(T)(1-r)\right)R_{\max} - (R - R_{\max})/200 & R > R_{\max} \end{cases} \quad (23)$$

Model (iv): Mag-depth + no soil + % rock path multi-step model

$$\log \mathrm{PSV}(T) = \begin{cases} M + \mathsf{A}_0(T)\log(\Delta/L) + b_1(T)M + b_2(T)h + b_3(T)v + b_4(T) + b_5(T)M^2 \\ \quad + \left(b_{70}(T)r + b_{71}(T)(1-r)\right)R & R \le R_{\max} \\ M + \mathsf{A}_0(T)\log(\Delta_{\max}/L) + b_1(T)M + b_2(T)h + b_3(T)v + b_4(T) + b_5(T)M^2 \\ \quad + \left(b_{70}(T)r + b_{71}(T)(1-r)\right)R_{\max} - (R - R_{\max})/200 & R > R_{\max} \end{cases} \quad (24)$$

The frequency-dependent attenuation function, $\mathsf{A}_0(T)\log(\Delta/L)$, used in each of the four models, is the function previously determined for the corresponding model in the regression of Fourier spectral amplitudes (Lee and Trifunac, 1995a). In Lee and Trifunac (1995a), notation $b_0(T)\log(\Delta/L)$ was used, to distinguish this from the similar terms in the second generation scaling models. The scaling functions $b_1(T)$ through $b_{71}(T)$ for each of the regression models were determined through regression analyses, using the new database of calculated $\mathrm{PSV}(T)$ amplitudes of over 1900 free-field records, at 91 discrete periods T, ranging from 0.04 sec to 15 sec, and for damping ratio $\zeta = 0.05$.

Description of the detailed steps of regression analyses, and illustration of numerous tables and figures resulting from the above models, is far too voluminous to be included in this review. The reader may peruse the reports by Lee and Trifunac (1995a, 1995b) for further details.

EXTENSION OF EMPIRICAL SCALING EQUATIONS TO HIGH AND LOW FREQUENCIES

The spectrum amplitudes described by detailed empirical scaling equations (Lee, 1989, 1990, 1991) are needed in computation of uniform hazard in terms of relative response spectra, in the probabilistic site specific analyses leading to seismic micro- and macro-zonation (Trifunac, 1988, 1989d, 1990b). Response spectra are also used in probabilistic determination of envelopes of shear forces and of bending moments

in engineering design (Amini and Trifuanc, 1985; Gupta and Trifunac, 1988a, 1988b, 1990a, 1990b, 1991a, 1991b; Todorovska, 1994a, 1994b, 1994c), and in estimation of losses for buildings exposed to strong shaking (Jordanovski et al., 1993). In all this work, spectral amplitudes need to be specified in a broad frequency band, which is broader than the band where the empirical scaling equations are valid.

In this section, a method for extension of the empirical scaling equations for response spectrum amplitudes, to periods longer than several seconds and shorter than 0.04 s, is reviewed. The proposed extension functions for long periods will match with the empirical response spectral amplitudes at the frequencies where the empirical scaling equations are still valid, and will be consistent with other independent observations and estimates of strong motion.

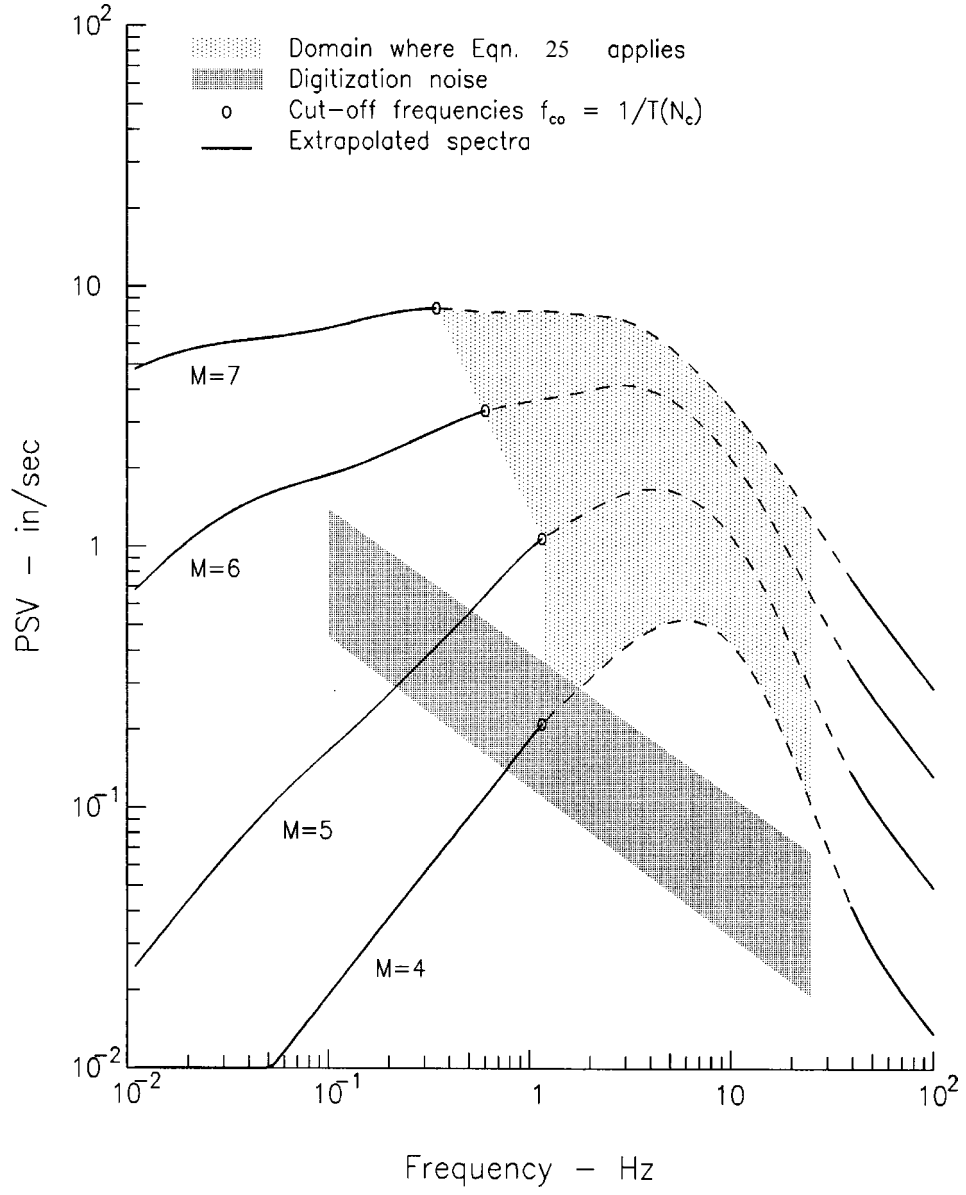

Fig. 12 PSV spectra versus frequency for damping ratio $\zeta = 0.05$ and probability of exceedance 0.5; the site is at epicentral distance $R = 10$ km and on rock $(h = 0)$, the source is at $H = 5$ km depth, and with magnitudes $M = 4$, 5, 6 and 7 (Equation (25) is valid inside the light shaded region for frequencies between corner frequency $f_{c0} = 1/T$ and 25 Hz; the extrapolation beyond this zone (heavy solid lines) is as proposed in this paper; the processing and digitization noise amplitudes are shown by the darker shaded zone increasing from ~10^{-1} to ~1 in/sec for frequencies decreasing from 10 to 0.1 Hz)

1. Empirical Scaling Equations

As we have shown in the previous sections, the empirical scaling equations for PSV spectral amplitudes employ scaling parameters, which depended on the earthquake source, propagation path and local site conditions. A typical equation is of the form

$$\log_{10}[\mathrm{PSV}(T)] = f(M, \Delta, T, v, h, s_L) \tag{25}$$

where, M is the earthquake magnitude, Δ is the representative source-to-station distance, T is the period of motion, and $v = 0$ for horizontal and $v = 1$ for vertical motion. h represents the depth of sediments, and s_L is the soil classification parameter. Those describe the local site conditions (Trifunac, 1990a). When some of these parameters are not available, other related equations can be employed. For example, in place of M, the site intensity may be used.

Our ability to develop empirical scaling equations for $\mathrm{PSV}(T)$ is limited by the quality and quantity of recorded strong motion data. As we have illustrated above, the preliminary scaling equations may be developed with several hundred recorded accelerograms. Frequency-dependent attenuation might be formulated with at least 500-600 records. More detailed scaling models will require at least one or two thousand records. The useful frequency range will depend on the characteristics of the recording transducers and on the digitization and processing techniques. Today, uniformly processed high quality strong motion data is available for periods between 0.04 and several seconds. This is illustrated in Figure 12, where the domain where Equation (25) applies, is indicated by the lightly shaded zone. This zone is bounded by spectra for $M = 4$ and $M = 7$, and lies between $T = 0.04$ s and T_c (cut-off period, increasing from 0.90 s for $M = 3$ and 4 to 7.5 s for $M = 7$ (Trifunac, 1993a)). The dark shaded zone, extending from $\sim 10^{-1}$ in/s near $T = 0.04$ s to ~ 1 in/s near $T = 10$ s, represents the amplitudes of the recording and processing noise (Trifunac and Todorovska, 2001a).

2. Long Period Extension

To extend $\mathrm{PSV}(T)$ amplitudes to long periods, we consider two extreme situations. One is referred to as "far-field", in which it will be assumed that $(R^2 + H^2)^{1/2} >> L$, and the other is called "near-field" for $(R^2 + H^2)^{1/2} \le L, W$. Here, L is the fault length, and W is the fault width. Finally, to compute $\mathrm{PSV}(T)$ at any distance, we specify the weighting functions that measure the relative contribution of the "near-field" and "far-field" terms to the complete ground motion and to the corresponding $\mathrm{PSV}(T)$ spectra.

The method will be identical to the one proposed for extrapolation of Fourier amplitude spectra to long periods (Trifunac, 1993a). In the first step, appropriate spectrum shape functions $\left(\frac{2\pi}{T}\,{}_F X_r(T,\zeta) \text{ and } \frac{2\pi}{T}\,{}_N X_r(T,\zeta)\right)$ are chosen. The amplitudes of these functions are next determined to agree with $\mathrm{PSV}(T)$ amplitudes computed from regression equations, like Equation (25), at $T = T_c$. No attempt has been made to match the slopes of $\mathrm{PSV}(T)$ for $T \le T_c$ with $\frac{2\pi}{T}\,{}_F X_r(T,\zeta)$ or $\frac{2\pi}{T}\,{}_N X_r(T,\zeta)$ for $T \ge T_c$. Finally, the success of the extrapolation can be tested by comparing the results with other independent estimates of the appropriate scaling parameters or function amplitudes, as $T \to \infty$.

2.1 Far-Field Extension

Let $\left|{}_F X_r(T,\zeta)\right|_{\max}$ be the peak of relative response of a single-degree-of-freedom system with frequency $\omega = 2\pi/T$, and fraction of critical damping ζ. To develop a functional form of $\left|{}_F X_r(T,\zeta)\right|_{\max}$, which can be used to extend the PSV spectra in the "far-field" and for large T, Trifunac (1995a) considers a pulse,

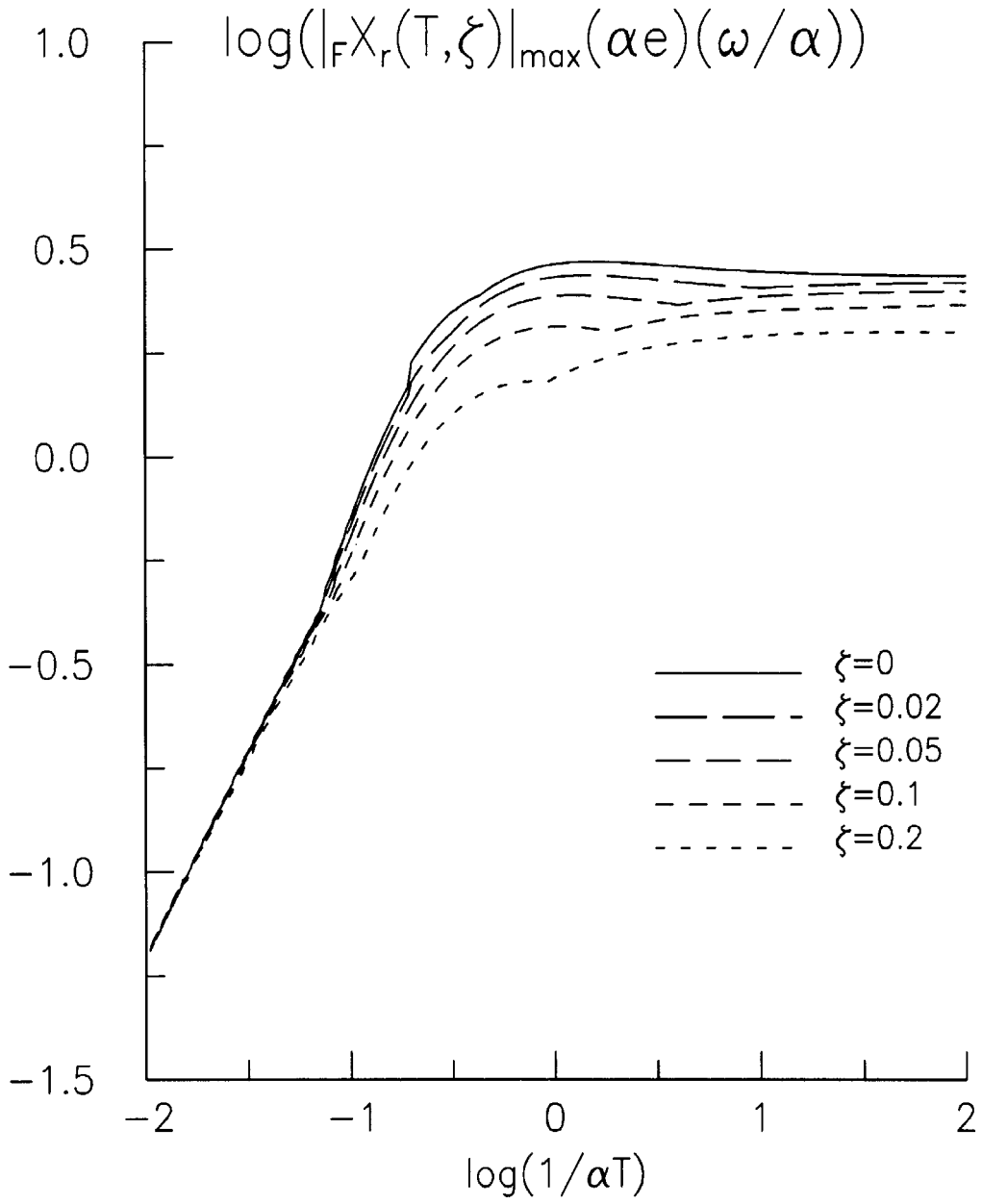

Fig. 13 Normalized amplitudes of pseudo velocity $|_F X_r(T,\zeta)|_{\max} \alpha e\left(\frac{\omega}{\alpha T}\right)$, versus dimensionless frequency $1/\alpha T$ for $\zeta = 0, 0.02, 0.05, 0.1$ and 0.2 (the ground displacement, $d_F(t)$, is the far-field pulse, with corner frequency α)

$$d_F(t) \sim d_{F,\max}\, \alpha e t e^{-\alpha t} \tag{26}$$

The actual ground motion is more complicated and cannot be described in detail by Equation (26); but the advantage of using this equation is that $d_F(t)$ can be related in a simple and direct way to the basic parameters governing the earthquake source.

Figure 13 shows the logarithm of the normalized (for peak value of the ground displacement $d_F(t)$ equal to one) pseudo relative velocity spectrum PSV. In terms of the dimensionless variables, PSV is equal to $|_F X_r(T,\zeta)|_{\max}(\alpha e)(\omega/\alpha)$. It is plotted versus $\log_{10}\frac{1}{\alpha T}$, for five damping values, ζ = 0.0, 0.02, 0.05, 0.1 and 0.2. For $\alpha T > 2.34$, the PSV spectra diminish like $1/(\alpha T)$. For $\alpha T < 2.34$, the PSV amplitudes are essentially constant.

To extend the Pseudo Relative Velocity Spectrum $\mathrm{PSV}(T)$, described by Equation (25), beyond the period T_c, we use the functional form of $|_F X_r(T,\zeta)|_{\max}(e\omega)$, and scale it by $d_{F,\max}$ such that at T_c

$$|_F X_r(T_c,\zeta)|_{\max} \frac{2\pi e}{T_c} d_{F,\max} = \mathrm{PSV}(T_c) \tag{27}$$

Then,

$$d_{F,\max} = \frac{T_c}{2\pi e} \frac{\mathrm{PSV}(T_c)}{|_F X_r(T_c,\zeta)|_{\max}} \tag{28}$$

2.2 Near-Field Extension

To find $|_N X_r(T,\zeta)|_{\max}$, which can represent the long period PSV spectral amplitudes in the near-field for $T > T_c$, Trifunac (1995a) considers

$$d_N(t) = d_{N,\max}\left(1 - e^{-t/\tau}\right) \tag{29}$$

Here, $d_{N,\max}$ represents the static permanent displacement at a station caused by an earthquake, t is time, and τ is the characteristic time. The details of actual ground motion are more complicated, but, for very long period oscillators, Equation (29) should give approximate estimates of the relative response.

Figure 14 shows the normalized (for $d_{N,\max} = 1$) spectra $\mathrm{PSV} \equiv |_N X_r(T,\zeta)|_{\max}(\omega\tau)$, plotted versus $\log_{10}\left(\frac{\tau}{T}\right)$. For $\frac{\tau}{T} < 0.2$, the PSV spectra for near-field displacement diminish like $\frac{\tau}{T}$. For $\frac{\tau}{T} > 0.2$, the PSV amplitudes are essentially constant.

To extend the PSV amplitudes to $T > T_c$, Trifunac (1995a) writes

$$\frac{2\pi\tau}{T_c}|_N X_r(T_c,\zeta)|_{\max} d_{N,\max} = \mathrm{PSV}(T_c) \tag{30}$$

and

$$d_{N,\max} = \frac{\mathrm{PSV}(T_c)}{|_N X_r(T_c,\zeta)|_{\max}} \frac{T_c}{2\pi\tau} \tag{31}$$

Here, $d_{N,\max}$ represents an estimate of the permanent ground displacement at the site, where $\mathrm{PSV}(T_c)$ has been computed.

2.3 Transition between Near-Field and Far-Field Spectra

To provide a continuous transition between $\mathrm{PSV}_{NF}(T) \equiv |_N X_r(T,\zeta)|_{\max} \frac{2\pi}{T}\tau d_{N,\max}$ and $\mathrm{PSV}_{FF}(T) \equiv |_F X_r(T,\zeta)|_{\max} e\frac{2\pi}{T} d_{F,\max}$, and to complete a representation for use in engineering applications, Trifunac (1995a) uses the results of Jovanovich et al. (1974). They showed that the error in approximating the static displacement field following an earthquake by a point source is typically less than 5 percent at distances greater than $4L$, where L is the source length. We define the distance S_1, between the station and the "top" of the vertical fault with "dimension" S and at depth H, as

$$S_1 = \begin{cases} \left[R^2 + (H-S)^2\right]^{1/2}, & H \geq S \\ R, & H < S \end{cases} \tag{32}$$

Here, $S = 0.01\times 10^{.5M}$, when $S \leq 30$ km, $S = 30$ km for larger events, and then, $\mathrm{PSV}_{NF}(T)$ and $\mathrm{PSV}_{FF}(T)$ can be combined as follows:

$$\mathrm{PSV}(T) = \mathrm{PSV}_{NF}(T)e^{-\left(\frac{3S_1}{4S}\right)} + \mathrm{PSV}_{FF}(T)\left(1 - e^{-\left(\frac{3S_1}{4S}\right)}\right), \quad T > T_c \tag{33}$$

In the above, $3/4$ is used to scale S_1/S, so that when $S_1/S = 4$, the exponent is equal to 3, $\left(e^{-3} \sim 0.05\right)$. For $T < T_c$, equations of the type of Equation (25) apply (Lee, 1989, 1990, 1991, 1993).

For $f < f_{co}\left(= 1/T_c\right)$, the heavy solid lines in Figure 12 show $\mathrm{PSV}(T)$ computed from Equation (33). For $R = 10$ km, $H = 5$ km, and $M = 4$ (bottom heavy solid line), since S_1 and Δ are both greater than $4S$, $\mathrm{PSV}_{FF}(T)$ contributes mainly to $\mathrm{PSV}(T)$, and so, $\mathrm{PSV}(T) \sim 1/T$. For $M \geq 7$, S_1 and Δ are smaller than $4S$, and the amplitudes of $\mathrm{PSV}(T)$ shown in Figure 12 are dominated by the flat portion of $\left|{}_N X_r(T,\zeta)\right|_{\max} e\frac{2\pi}{T} d_{N,\max}$ (see Figure 14), for T near and shorter than $\sim 5\tau$. For $M = 5$ and 6, the spectra, $\mathrm{PSV}(T)$, display progressively changing slope for $f < 1/\tau$. With increasing M (increasing S), this slope decreases from -1 towards 0, as M goes from 4 to 7, in the period (frequency) range shown in Figure 12.

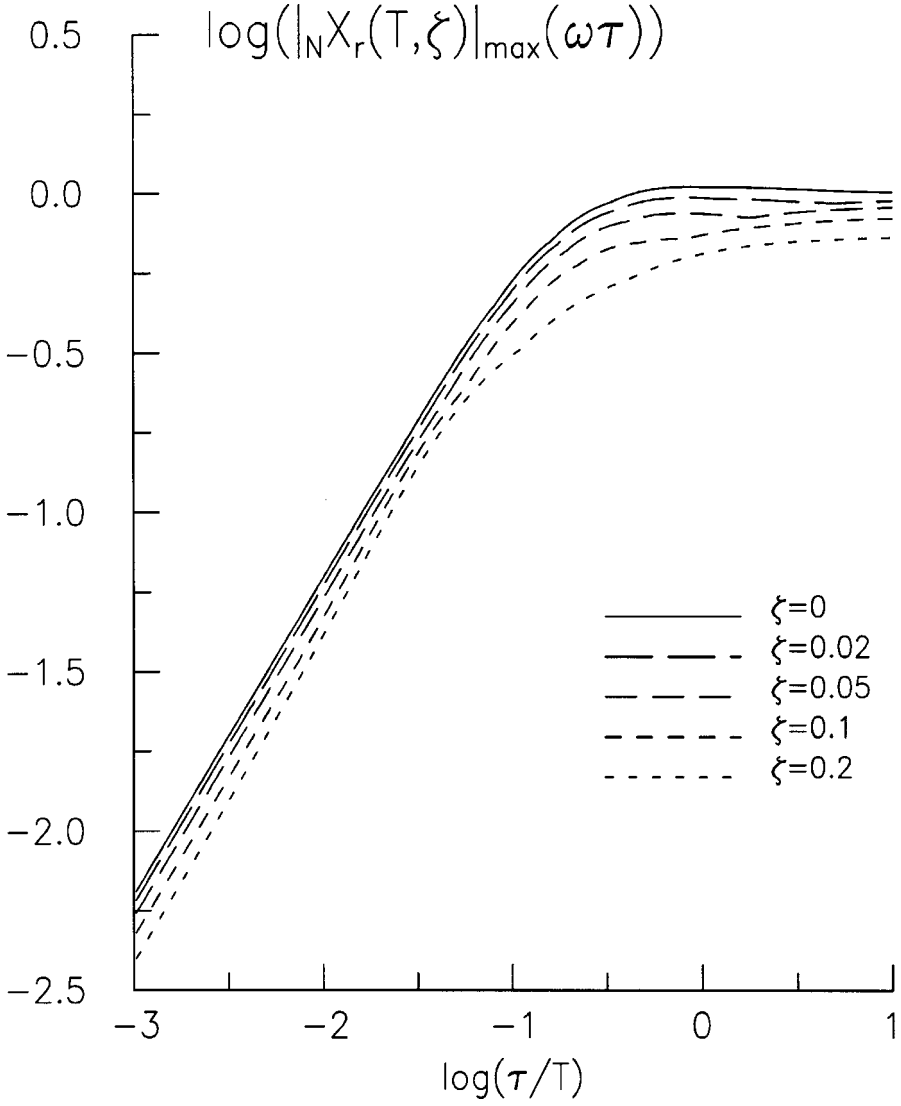

Fig. 14 $\left|{}_N X_r(T,\zeta)\right|_{\max}(\omega\tau)$, normalized PSV spectra versus dimensionless frequency $\frac{\tau}{T}$ for $\zeta = 0, 0.02, 0.05, 0.1$ and 0.2 (τ is the characteristic source time, and the displacement, $d_N(t)$, is the near-field displacement)

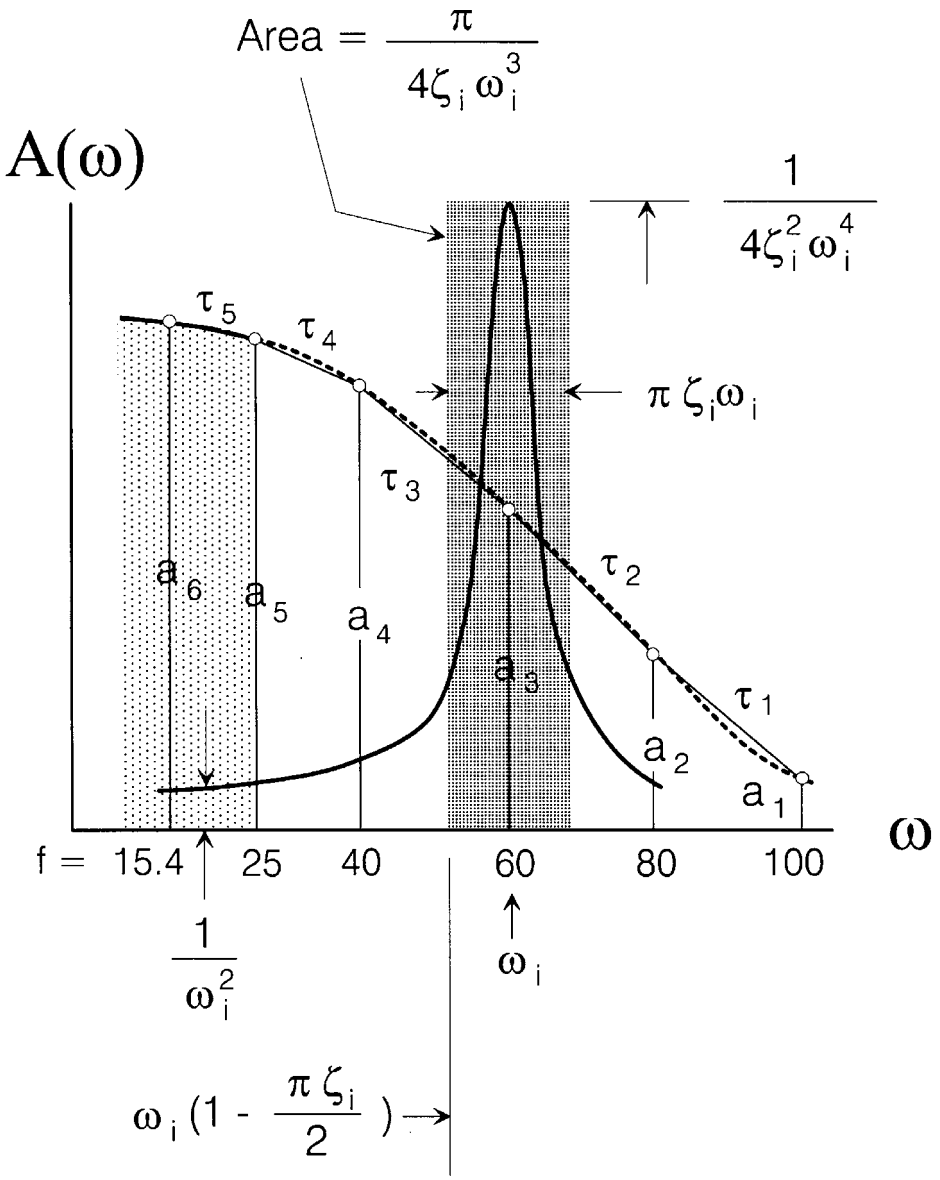

Fig. 15 Fourier amplitude spectra of strong motion acceleration $A(\omega)$ with amplitudes a_5, a_4,...a_1 at $f = 25$, 40, 60, 80 and 100 Hz (the mean square interval is shown by shaded rectangle; estimates of τ_Q in the respective frequency intervals are shown by τ_1 through τ_4 (from Trifunac (1995b))

3. Short Period Extension

To extrapolate the $\mathrm{PSV}(T)$ spectral amplitudes to periods shorter than $1/25$ s, it is necessary to employ the properties of the Fourier amplitude spectra at high frequencies (Trifunac, 1994a, 1994b). Then, using expressions for the expected values of the peaks of a random function, which is characterized by a narrow (peaked) transfer function, it is possible to derive the functional form for the extrapolation equations.

3.1 Fourier Amplitude Spectra of Strong Motion Acceleration at High Frequencies

In the real earth, noticeable attenuation takes place for frequencies higher than 1 to 10 Hz, and may be described empirically by $e^{-\pi\tau_Q f}$, where $\tau_Q = \Delta/(Q\beta)$ (Δ is the distance travelled by the wave, β is the velocity of shear waves, and Q is the attenuation quality factor).

From average travel times in Southern California, for short distances, the average shear wave velocity can be approximated by $\beta \sim 3.35 + .00175\ \Delta$, and then, Q can be computed from τ_Q versus frequency. The results show Q increasing proportionally with f for $f > 20$ Hz. For $\Delta < 100$ km and for $f > 20$ Hz, the average Q can be approximated by (Trifunac, 1994b)

$$Q \approx \left(0.367\Delta - 0.0014\Delta^2\right) f \tag{34}$$

Also,

$$\tau_Q \approx \frac{1}{\left(1.23 - 0.00405\Delta\right) f} \tag{35}$$

3.2 Extrapolation Equations

Trifunac (1995b) uses the results of Rice (1944, 1945) and of Cartwright and Longuet-Higgins (1956) for a functional relationship between the expected peak amplitudes of random functions and of their characterization in terms of their root-mean-square amplitude, r_{rms}, and the width, ε, of their energy spectrum. For a time-segment containing N peaks, the expected peak amplitude of response function $r(t)$, $r_{\max}$, can be approximated by

$$E\left[r_{\max}\right] \approx \bar{r}\left[\ln\left(1-\varepsilon^2\right)^{1/2} N\right]^{1/2} \tag{36}$$

where, $\bar{r}$ is the root mean square amplitude of all the peaks of $r(t)$. For intermediate and small ε, it can be shown that $\bar{r} \sim \sqrt{2} r_{\text{rms}}$, where r_{rms} is the root-mean-square value of $r(t)$. To extrapolate the response spectrum amplitudes from $\text{SD}\left(T = \frac{1}{25}\right)$ to $\text{SD}(T)$ for $25 < \frac{1}{T} < 100$ Hz, Trifunac (1995b) writes

$$\rho_{2,1} = \frac{E\left[{}_2 r_{\max}\right]}{E\left[{}_1 r_{\max}\right]} \tag{37}$$

$$\rho_{2,1} \approx \frac{\bar{r}_2\left[\ln\left(1-\varepsilon_2^2\right)^{1/2} N_2\right]^{1/2}}{\bar{r}_1\left[\ln\left(1-\varepsilon_1^2\right)^{1/2} N_1\right]^{1/2}} \tag{38}$$

where, the subscripts 1 and 2 refer to $r_1(t)$ and $r_2(t)$, evaluated for two different oscillator frequencies, f_1 and f_2.

Assuming that ε does not change significantly, as the frequency f changes from f_1 to f_2, this suggests that $\ln\left(1-\varepsilon_1^2\right)^{1/2} N_1 \sim \ln\left(1-\varepsilon_2^2\right)^{1/2} N_2$, and so,

$$\rho_{2,1} \approx \bar{r}_2 / \bar{r}_1 \tag{39}$$

Using the mean square approximation (Figure 15), this can be evaluated numerically,

$$\rho_{i+1,i}^2 \approx \frac{\dfrac{1}{\omega_{i+1}^4}\displaystyle\int_0^{\omega_{i+1}-\zeta_{i+1}\omega_{i+1}\pi/2} \left|A(\omega)\right|^2 d\omega + \dfrac{a_k^2 \pi}{4\zeta_{i+1}\omega_{i+1}^3}}{\dfrac{1}{\omega_i^4}\displaystyle\int_0^{\omega_i-\zeta_i\omega_i\pi/2} \left|A(\omega)\right|^2 d\omega + \dfrac{a_{k+1}^2 \pi}{4\zeta_i\omega_i^3}} \tag{40}$$

where, a_k amplitudes are as denoted in Figure 15.

Since $\text{PSV}(T) = \frac{2\pi}{T}\text{SD}(T)$,

$$\mathrm{PSV}(T_{i+1}) \approx \mathrm{PSV}(T_i)\frac{T_i}{T_{i+1}}\rho_{i+1,i} \tag{41}$$

where, $T_i = 1/f_i$. In Equation (40), the term, $\pi a_k^2/(4\zeta_i\omega_i^3)$, dominates for $f \le 10-20$ Hz. For higher frequencies, as $f \to \infty$, this term becomes negligible, and $\rho_{i+1,i} \to 1$ (Figure 16).

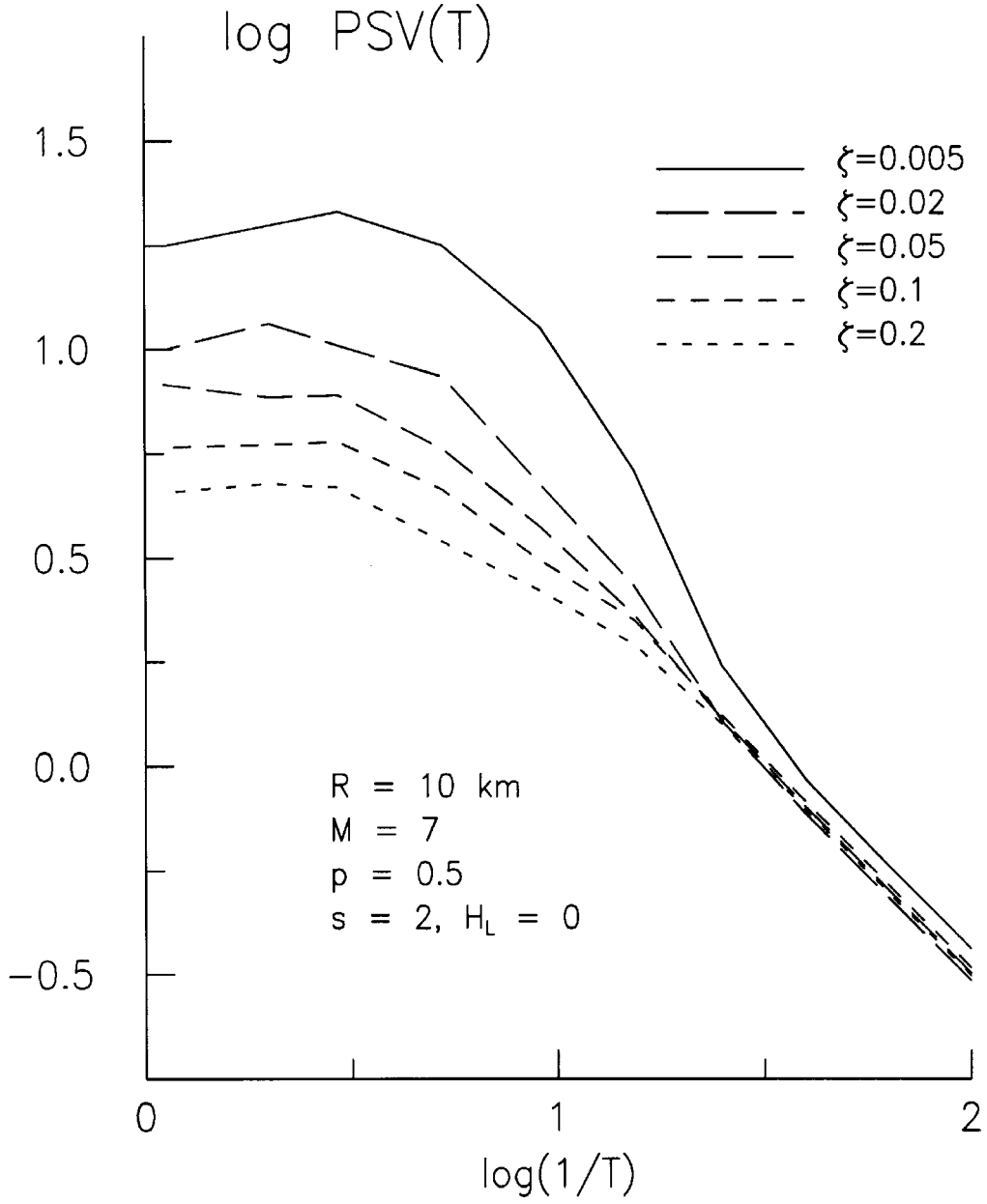

Fig. 16 An example of using Equation (41) to extrapolate response spectra $\mathrm{PSV}(T)$ to periods $T < 1/25$ s

4. DISCUSSION

The largest uncertainties are believed to exist near T_c, where the empirical scaling models approach the recording and processing noise. The tests performed so far suggest that the resulting $\mathrm{PSV}(T)$ are very realistic for $3.5 < M < 7$ and for horizontal ground motion. The slopes and amplitudes of empirically computed $\mathrm{FS}(T)$ (Trifunac, 1993a, 1993b) and $\mathrm{PSV}(T)$ for vertical motions suggest that near $T = T_c$, our empirical models may not be reliable for $M > 6.5$. To understand these amplitudes, we

need more recorded accelerograms for $M > 7$, and so, we must patiently wait for this data to become available.

Extrapolation of $\mathrm{PSV}(T)$ by Equation (33) from T_c towards $T \to \infty$ agrees favorably with the known trends of seismic moment M_o, peak ground displacements, and of the average dislocation amplitudes, $\bar{u}$, versus earthquake magnitude. Since the corner frequency in Fourier spectrum amplitudes, $1/\tau$, in the near-field ground motion is $\sim v/r$, where v is the dislocation velocity (typically between 2 and 3 km/s), and r is the representative source dimension, it is seen that τ can be larger than T_c. This is so, assuming that, for the frequencies considered here, the rupture occurs as a "smooth" process. Many studies have suggested that the faults slip irregularly, with large dislocations distributed at several or at many "hot" spots with large dislocation amplitudes, thus making larger events look like a sequence of smaller events. While this faulting behavior can affect τ appreciably, we do not have at present, reliable data to introduce and to verify such behavior.

The highly "local" nature of strong motion recording, local in the sense of the proximity to the fault (often less than, say 50 km), and the fact that it is $\bar{u}$ and not the overall source magnitude or moment and long source dimensions (L) that govern the near-field strong motion amplitudes, all agree with the observed trends of strong motion amplitudes predicted by the above outlined approach.

REFERENCES

1. Alford, J.L., Housner, G.W. and Martel, R.R. (1951). "Spectrum Analysis of Strong-Motion Earthquakes", Earthquake Eng. Res. Lab., Calif. Inst. of Tech., Pasadena, U.S.A.
2. Amini, A. and Trifunac, M.D. (1985). "Statistical Extension of Response Spectrum Superposition", Int. J. Soil Dynam. Earthquake Engg., Vol. 4, No. 2, pp. 54-63.
3. Benioff, H. (1934). "The Physical Evaluation of Seismic Destructiveness", Bull. Seism. Soc. Amer., Vol. 24, pp. 398-403.
4. Biot, M.A. (1932). "Vibrations of Building during Earthquake", Chapter II in Ph.D. Thesis No. 259 entitled "Transient Oscillations in Elastic System", Aeronautics Department, Calif. Inst. of Tech., Pasadena, California, U.S.A.
5. Biot, M.S. (1933). "Theory of Elastic Systems Vibrating under Transient Impulse with an Application to Earthquake-Proof Buildings", Proc. National Academy of Sciences, Vol. 19, No. 2, pp. 262-268.
6. Biot, M.A. (1934). "Theory of Vibration of Building during Earthquake", Zeitschrift *für* Angewandte Matematik und Mechanik, Vol. 14, No. 4, pp. 213-223.
7. Biot, M.A. (1941). "A Mechanical Analyzer for the Prediction of Earthquake Stresses", Bull. Seism. Soc. Amer., Vol. 31, pp. 151-171.
8. Biot, M.A. (1942). "Analytical and Experimental Methods in Engineering Seismology", ASCE Transactions, Vol. 108, pp. 365-408.
9. Borcherdt, R. and Gibbs, J.F. (1976). "Effects of Local Geological Conditions in the San Francisco Bay Region on Ground Motions and Intensities of the 1906 Earthquake", Bull. Seism. Soc. Amer., Vol. 66, pp. 467-500.
10. Cartwright, D.E. and Longuet-Higgins, M.S. (1956). "The Statistical Distribution of Maxima of a Random Function", Proc. Royal Soc. London, Ser. A327, pp. 212-232.
11. Duke, C.M. (1958). "Bibliography of Effects of Soil Conditions on Earthquake Damage", Earthquake Engg. Res. Inst.
12. Gutenberg, B. (1957). "Effects of Ground on Earthquake Motion", Bull. Seism. Soc. Amer., Vol. 47, pp. 221-250.
13. Gupta, I.D. and Trifunac, M.D. (1988a). "Order Statistics of Peaks in Earthquake Response", ASCE J. Engng Mech., Vol. 114, No. 10, pp. 1605-1627.
14. Gupta, I.D. and Trifunac, M.D. (1988b). "Attenuation of Intensity with Epicentral Distance in India", Int. J. Soil Dynamics and Earthquake Eng., Vol. 7, pp. 162-169.

15. Gupta, I.D. and Trifunac, M.D. (1990a). "Probabilistic Spectrum Superposition for Response Analysis Including the Effects of Soil-Structure Interaction", J. Prob. Engg. Mech., Vol. 5, No. 1, pp. 9-18.
16. Gupta, V.K. and Trifunac, M.D. (1990b). "Response of Multistoried Buildings to Ground Translation and Rocking during Earthquakes", J. Prob. Engg. Mech., Vol. 5, No. 3, pp. 138-145.
17. Gupta, V.K. and Trifunac, M.D. (1991a). "Seismic Response of Multistoried Buildings Including the Effects of Soil-Structure Interaction", Soil Dynam. and Earthquake Engg., Vol. 10, No. 8, pp. 414-422.
18. Gupta, V.K. and Trifunac, M.D. (1991b). "Effects of Ground Rocking on Dynamic Response of Multistoried Buildings during Earthquakes", Structural Engg./Earthquake Engg., JSCE, Vol. 8, No. 2, pp. 43-50.
19. Housner, G.W. (1970). "Design Spectrum", Chapter 5 in "Earthquake Engineering (edited by R.L. Wiegel)", Prentice-Hall.
20. Hudson, D.E., Trifunac, M.D. and Brady, A.G. (1972). "Strong-Motion Accelerograms III, Response Spectra", Report EERL 72-80, Earthqu. Engng Res. Lab., Calif. Inst. of Tech., Pasadena, U.S.A.
21. Jordanovski, L.R., Todorovska, M.I. and Trifunac, M.D. (1993). "Total Loss in a Building Exposed to Earthquake Hazard, Part I: The Model; Part II: A Hypothetical Example", Europ. Earthqu. Engng, Vol. VI, No. 3, pp. 14-32.
22. Jovanovich, D., Husseini, M.I. and Chinnery, M.A. (1974). "Elastic Dislocations in a Layered Half Space - I. Basic Theory and Numerical Methods; II. The Point Source", Geoph. J. Royal Astr. Soc., Vol. 39, pp. 205-239.
23. Lee, V.W. (1989). "Empirical Scaling of Pseudo Relative Velocity Spectra of Recorded Strong Earthquake Motion in Terms of Magnitude and Both Local Soil and Geologic Site Classifications", Earthqu. Engng and Engng Vib., Vol. 9, No. 3, pp. 9-29.
24. Lee, V.W. (1990). "Scaling PSV Spectra in Terms of Site Intensity, and Both Local Soil and Geological Site Classifications", Europ. Earthqu. Engng, Vol. IV, No. 1, pp. 3-12.
25. Lee, V.W. (1991). "Correlation of Pseudo Relative Velocity Spectra with Site Intensity, Local Soil Classification and Depth of Sediments", Soil Dynam. Earthqu. Engng., Vol. 10, No. 3, pp. 141-151.
26. Lee, V.W. (1993). "Scaling PSV from Earthquake Magnitude, Local Soil and Geological Depth of Sediments", ASCE J. Geotech. Engng, Vol. 119, No. 1, pp. 108-126.
27. Lee, V.W. and Trifunac, M.D. (1985). "Attenuation of Modified Mercalli Intensity for Small Epicentral Distance in California", Report CE 85-01, Dept. of Civil Eng., Univ. of Southern California, Los Angeles, California, U.S.A.
28. Lee, V.W. and Trifunac, M.D. (1993). "Empirical Scaling of Fourier Amplitude Spectra in Former Yugoslavia", Europ. Earthqu. Engng, Vol. VII, No. 2, pp. 47-61.
29. Lee, V.W. and Trifunac, M.D. (1995a). "Frequency Dependent Attenuation Function and Fourier Amplitude Spectra of Strong Earthquake Ground Motion in California", Report CE 95-03, Dept. of Civil Eng., Univ. of Southern California, Los Angeles, California, U.S.A.
30. Lee, V.W. and Trifunac, M.D. (1995b). "Pseudo Relative Velocity Spectra of Strong Earthquake Ground Motion in California", Report CE 95-04, Dept. of Civil Eng., Univ. of Southern California, Los Angeles, California, U.S.A.
31. Lee, V.W., Trifunac, M.D., Todorovska, M.I. and Novikova, E.I. (1995). "Empirical Equations Describing Attenuation of the Peaks of Strong Ground Motion, in Terms of Magnitude, Distance, Path Effects, and Site Conditions", Report CE 95-02, Dept. of Civil Eng., Univ. of Southern California, Los Angeles, California, U.S.A.
32. Newmark, N.M., Degenkolb, H.J., Chopra, A.K., Veletsos, A.S., Rosenblueth, E. and Sharpe, R.L. (1977). "Seismic Design and Analysis Provisions for the United States", Proc. Sixth World Conf. Earthqu. Engng, New Delhi, Vol. II, pp. 1986-1991.
33. Novikova, E.I. and Trifunac, M.D. (1995). "Frequency Dependent Duration of Strong Earthquake Ground Motion: Updated Empirical Equations", Report CE 95-01, Dept. of Civil Eng., Univ. Southern California, Los Angeles, California, U.S.A.

34. Rice, S.O. (1944). "Mathematical Analysis of Random Noise", Bell System Tech. J., Vol. 23, pp. 282-332.
35. Rice, S.O. (1945). "Mathematical Analysis of Random Noise", Bell System Tech. J., Vol. 24, pp. 46-156.
36. Richter, C.F. (1958). "Elementary Seismology", Freeman and Co., San Francisco.
37. Seed, H.B., Ugas, C. and Lysmer, J. (1974). "Site Dependent Spectra for Earthquake Resistant Design", Report EERC 74-12, Earthqu. Engng Res. Center, U.C. Berkeley, U.S.A.
38. Todorovska, M.I. (1994a). "A Note on Distribution of Amplitudes of Peaks in Structural Response including Uncertainties of the Exciting Ground Motion and of the Structural Model", Soil Dynam. Earthqu. Engng, Vol. 14, No. 3, pp. 211-217.
39. Todorovska, M.I. (1994b). "Order Statistics of Functionals of Strong Motion", Soil Dynam. Earthqu. Engng, Vol. 13, No. 3, pp. 149-161.
40. Todorovska, M.I. (1994c). "Comparison of Response Spectrum Amplitudes from Earthquakes with Lognormally and Exponentially Distributed Return Period", Soil Dynam. Earthqu. Engng., Vol. 13, No. 1, pp. 97-116.
41. Trifunac, M.D. (1973). "Analysis of Strong Earthquake Ground Motion for Prediction of Response Spectra", Int. J. Earthqu. Engng Struct. Dynam., Vol. 2, No. 1, pp. 59-69.
42. Trifunac, M.D. (1976a). "Preliminary Analysis of the Peaks of Strong Earthquake Ground Motion - Dependence of Peaks on Earthquake Magnitude, Epicentral Distance and Recording Site Conditions", Bull. Seism. Soc. Amer., Vol. 66, pp. 189-219.
43. Trifunac, M.D. (1976b). "Preliminary Empirical Model for Scaling Fourier Amplitude Spectra of Strong Ground Acceleration in Terms of Earthquake Magnitude, Source to Station Distance and Recording Site Conditions", Bull. Seism. Soc. Amer., Vol. 68, pp. 1345-1373.
44. Trifunac, M.D. (1976c). "A Note on the Range of Peak Amplitudes of Recorded Accelerations, Velocities and Displacements with Respect to the Modified Mercalli Intensity", Earthquake Notes, Vol. 47, No. 1, pp. 9-24.
45. Trifunac, M.D. (1977a). "Statistical Analysis of the Computed Response of Structural Response Recorders (S.R.R.) for Accelerograms Recorded in the United States of America", Sixth World Conference Earthquake Engineering, New Delhi, Vol. III, pp. 2956-2961.
46. Trifunac, M.D. (1977b). "Forecasting the Spectral Amplitudes of Strong Earthquake Ground Motion", Sixth World Conference Earthquake Engineering, New Delhi, Vol. I, pp. 139-152.
47. Trifunac, M.D. (1977c). "An Instrumental Comparison of the Modified Mercalli (M.M.I.) and Medvedev-Karnik-Sponheuer (M.K.S.) Intensity Scales", Sixth World Conference Earthquake Engineering, New Delhi, Vol. I, pp. 715-721.
48. Trifunac, M.D. (1977d). "Uniformly Processed Strong Earthquake Ground Accelerations in the Western United States of America for the Period from 1933 to 1971; Pseudo Relative Velocity Spectra and Processing Noise", Report CE 77-04, Dept. of Civil Eng., Univ. of Southern California, Los Angeles, California, U.S.A.
49. Trifunac, M.D. (1978). "Response Spectra of Earthquake Ground Motion", ASCE J. Eng. Mech., Vol. 104, No. EM5, pp. 1081-1097.
50. Trifunac, M.D. (1979). "Preliminary Empirical Model for Scaling Fourier Amplitude Spectra of Strong Motion Acceleration in Terms of Modified Mercalli Intensity and Geologic Site Conditions", Int. J. Earthqu. Engng and Struct. Dynam., Vol. 7, pp. 63-74.
51. Trifunac, M.D. (1988). "Seismic Microzonation Mapping via Uniform Risk Spectra", Proc. 9th World Conf. Earthqu. Engng, Tokyo-Kyoto, Japan, Vol. VII, pp. 75-80.
52. Trifunac, M.D. (1989a). "Dependence of Fourier Spectrum Amplitudes of Recorded Strong Earthquake Accelerations on Magnitude, Local Soil Conditions and on Depth of Sediments", Int. J. Earthquake Eng. Structural Dyn., Vol. 18, No. 7, pp. 999-1016.
53. Trifunac, M.D. (1989b). "Empirical Scaling of Fourier Spectrum Amplitudes of Recorded Strong Earthquake Accelerations in Terms of Magnitude and Local Soil and Geologic Site Conditions", Earthquake Eng. Eng. Vibration, Vol. 9, No. 2, pp. 23-44.

54. Trifunac, M.D. (1989c). "Scaling Strong Motion Fourier Spectra by Modified Mercalli Intensity, Local Soil and Geologic Site Conditions", Structural Eng./Earthquake Eng., JSCE, Vol. 6, No. 2, pp. 217-224.
55. Trifunac, M.D. (1989d). "Threshold Magnitudes Which Exceed the Expected Ground Motion during the Next 50 Years in a Metropolitan Area", Geofizika, Vol. 6, pp. 1-12.
56. Trifunac, M.D. (1990a). "How to Model Amplification of Strong Earthquake Motions by Local Soil and Geologic Site Conditions", Earthqu. Engng Struct. Dynam., Vol. 19, No. 6, pp. 833-846.
57. Trifunac, M.D. (1990b). "A Microzonation Method Based on Uniform Risk Spectra", Soil Dynam. Earthqu. Engng, Vol. 9, No. 1, pp. 34-43.
58. Trifunac, M.D. (1991a). "Empirical Scaling of Fourier Spectrum Amplitudes of Recorded Strong Earthquake Accelerations in Terms of Modified Mercalli Intensity, Local Soil Conditions and Depth of Sediments", Int. J. Soil Dynamics Earthquake Eng., Vol. 10, No.1, pp. 65-72.
59. Trifunac, M.D. (1991b). "M_L^{SM}", Int. J. Soil Dynam. Earthqu. Engng, Vol. 10, No. 1, pp. 17-25.
60. Trifunac, M.D. (1993a). "Long Period Fourier Amplitude Spectra of Strong Motion Acceleration", Soil Dynam. Earthqu. Engng, Vol. 12, No. 6, pp. 363-382.
61. Trifunac, M.D. (1993b). "Broad Band Extension of Fourier Amplitude Spectra of Strong Motion Acceleration", Report CE 93-01, Dept. of Civil Eng., Univ. of Southern California, Los Angeles, California, U.S.A.
62. Trifunac, M.D. (1994a). "Fourier Amplitude Spectra of Strong Motion Acceleration: Extension to High and Low Frequencies", Earthqu. Engng Struct. Dynam., Vol. 23, No. 4, pp. 389-411.
63. Trifunac, M.D. (1994b). "Q and High Frequency Strong Motion Spectra", Soil Dynam. Earthqu. Engng, Vol. 13, No. 4, pp. 149-161.
64. Trifunac, M.D. (1994c). "Earthquake Source Variables for Scaling Spectral and Temporal Characteristics of Strong Ground Motion", Proc. 10th Europ. Conf. Earthqu. Eng., Vienna, Austria, Vol. 4, pp. 2585-2590.
65. Trifunac, M.D. (1994d). "Response Spectra of Strong Motion Acceleration: Extension to High and Low Frequencies", Proc. 10th Europ. Conf. Earthqu. Eng., Vienna, Austria. Vol. 1, pp. 203-208.
66. Trifunac, M.D. (1994e). "Broad Band Extension of Pseudo Relative Velocity Spectra of Strong Motion", Report CE 94-02, Dept. of Civil Eng., Univ. Southern California, Los Angeles, California, U.S.A.
67. Trifunac, M.D. (1995a). "Pseudo Relative Velocity Spectra of Earthquake Ground Motion at Long Periods", Soil Dynam. Earthqu. Engng, Vol. 14, No. 5, pp. 331-346.
68. Trifunac, M.D. (1995b). "Pseudo Relative Velocity Spectra of Earthquake Ground Motion at High Frequencies", Earthqu. Engng Struct. Dynam., Vol. 24, No. 8, pp. 1113-1130.
69. Trifunac, M.D. and Anderson, J.G. (1977). "Preliminary Empirical Models for Scaling Absolute Acceleration Spectra", Report CE 77-03, Dept. of Civil Eng., Univ. of Southern California, Los Angeles, California, U.S.A.
70. Trifunac, M.D. and Anderson, J.G. (1978a). "Preliminary Empirical Models for Scaling Pseudo Relative Velocity Spectra", Report CE 78-04, Dept. of Civil Eng., Univ. of Southern California, Los Angeles, California, U.S.A.
71. Trifunac, M.D. and Anderson, J.G. (1978b). "Preliminary Models for Scaling Relative Velocity Spectra", Report CE 78-05, Dept. of Civil Eng., Univ. of Southern California, Los Angeles, California, U.S.A.
72. Trifunac, M.D. and Anderson, J.C. (1978c). "Estimation of Relative Velocity Spectra", Proc. 6th Symp. Earthquake Engineering, University of Roorkee, India.
73. Trifunac, M.D. and Brady, A.G. (1975a). "A Study on the Duration of Strong Earthquake Ground Motion", Bull. Seism. Soc. Amer., Vol. 65, pp. 581-626.
74. Trifunac, M.D. and Brady, A.G (1975b). "On the Correlation of Seismic Intensity Scales with the Peaks of Recorded Strong Ground Motion", Bull. Seism. Soc. Amer., Vol. 65, pp. 139-162.

75. Trifunac, M.D. and Brady, A.G. (1975c). "On the Correlation of Seismoscope Response with Earthquake Magnitude and Modified Mercalli Intensity", Bull. Seism. Soc. Amer., Vol. 65, pp. 307-321.
76. Trifunac, M.D. and Brady, A.G. (1975d). "Correlations of Peak Acceleration, Velocity and Displacement with Earthquake Magnitude, Epicentral Distance and Site Conditions", Int. J. Earthquake Engineering Struct. Dynamics, Vol. 4, pp. 455-471.
77. Trifunac, M.D. and Brady, A.G. (1975e). "On the Correlation of Peak Accelerations of Strong-Motion with Earthquake Magnitude, Epicentral Distance and Site Conditions" Proc. U.S. National Conference Earthquake Engineering, Ann Arbor, Michigan, U.S.A., pp. 43-52.
78. Trifunac, M.D. and Gupta, V.K. (1991). "Pseudo Relative Acceleration Spectrum", ASCE J. Engineering Mech., Vol. 117, No. 4, pp. 924-927.
79. Trifunac, M.D. and Lee, V.W. (1978). "Dependence of Fourier Amplitude Spectra of Strong Motion Acceleration on the Depth of Sedimentary Deposits", Report CE 78-14, Dept. of Civil Eng., Univ. of Southern California, Los Angeles, California, U.S.A.
80. Trifunac, M.D. and Lee, V.W. (1979). "Dependence of Pseudo Relative Velocity Spectra of Strong Motion Acceleration on the Depth of Sedimentary Deposits", Report CE 79-02, Dept. of Civil Eng., Univ. of Southern California, Los Angeles, California, U.S.A.
81. Trifunac, M.D. and Lee, V.W. (1980). "Fourier Amplitude Spectra of Strong Motion Acceleration", Bulletin EAEE, Vol. 6, pp. 2-18.
82. Trifunac, M.D. and Lee, V.W. (1985a). "Frequency Dependent Attenuation of Strong Earthquake Ground Motion", Report CE 85-02, Dept. of Civil Eng., Univ. of Southern California, Los Angeles, California, U.S.A.
83. Trifunac, M.D. and Lee, V.W. (1985b). "Preliminary Empirical Model for Scaling Fourier Amplitude Spectra of Strong Ground Acceleration in Terms of Earthquake Magnitude, Source to Station Distance, Site Intensity and Recording site Conditions", Report CE 85-03, Dept. of Civil Eng., Univ. of Southern California, Los Angeles, California, U.S.A.
84. Trifunac, M.D and Lee, V.W. (1985c). "Preliminary Empirical Model for Scaling Pseudo Relative Velocity Spectra of Strong Earthquake Acceleration in Terms of Magnitude, Distance, Site Intensity and Recording Site Conditions", Report CE 85-04, Dept. of Civil Eng., Univ. of Southern California, Los Angeles, California, U.S.A.
85. Trifunac, M.D. and Lee, V.W. (1987). "Direct Empirical Scaling of Response Spectral Amplitudes from Various Site and Earthquake Parameters", Report NUREG/CE-4903, U.S. Nuclear Regulatory Commission, Vol. 1.
86. Trifunac, M.D. and Lee, V.W. (1989a). "Empirical Models for Scaling Fourier Amplitude Spectra of Strong Ground Acceleration in Terms of Earthquake Magnitude, Source to Station Distance, Site Intensity and Recording Site Conditions", Int. J. Soil Dynamics Earthquake Eng., Vol. 8, No. 3, pp. 110-125.
87. Trifunac, M.D. and Lee, V.W. (1989b). "Empirical Models for Scaling Pseudo Relative Velocity Spectra of Strong Earthquake Accelerations in Terms of Magnitude, Distance, Site Intensity and Recording Site Conditions", Int. J. Soil Dynamics Earthquake Eng., Vol. 8, No. 3, pp. 126-144.
88. Trifunac, M.D. and Lee, V.W. (1990). "Frequency Dependent Attenuation of Strong Earthquake Ground Motion", Int. J. Soil Dynam. Earthqu. Engng, Vol. 9, No. 1, pp. 3-15.
89. Trifunac, M.D. and Lee, V.W. (1992). "A Note on Scaling Peak Acceleration, Velocity and Displacement of Strong Earthquake Shaking by Modified Mercalli Intensity (MMI) and Site Soil and Geologic Conditions", Soil Dynamics Earthquake Eng., Vol. 11, No. 2, pp. 101-110.
90. Trifunac, M.D. and Novikova, E.I. (1994). "State of the Art Review of Strong Motion Duration", Proc. 10th Europ. Conf. Earthqu. Eng., Vienna, Austria, Vol. 1, pp. 131-140.
91. Trifunac, M.D. and Todorovska, M.I. (1989a). "Attenuation of Seismic Intensity in Albania and Yugoslavia", Int. J. Struct. Dynamics Earthquake Eng., Vol. 10, No. 5, pp. 617-631.
92. Trifunac, M.D. and Todorovska, M.I. (1989b). "Methodology for Selection of Earthquake Design Motions for Important Engineering Structures", Report CE 89-01, Dept. of Civil Eng., Univ. Southern Calif., Los Angeles, California, U.S.A.

93. Trifunac, M.D. and Todorovska, M.I. (2001a). "A Note on the Useable Range in Accelerographs Recording Translation", Soil Dynamics Earthquake Eng., Vol. 21, No. 4, pp. 275-286.
94. Trifunac, M.D. and Todorovska, M.I. (2001b). "Evolution of Accelerographs, Data Processing, Strong Motion Arrays and Amplitude and Spatial Resolution in Recording Strong Earthquake Motion", Soil Dynamics Earthquake Eng., Vol. 21, No. 6, pp. 537-555.
95. Trifunac, M.D. and Živčič, M. (1991). "A Note on Instrumental Comparison of the Modified Mercalli Intensity (MMI) in the Western United States and the Mercalli-Cancani-Sieberg (MCS) Intensity in Yugoslavia", European Earthquake Eng., Vol. V, No. 1, pp. 2-26.
96. Trifunac, M.D., Lee, V.W., Cao, H. and Todorovska, M.I. (1988). "Attenuation of Seismic Intensity in Balkan Countries", Report CE 88-01, Dept. of Civil Eng., Univ. of Southern Calif., Los Angeles, California, U.S.A.
97. Trifunac, M.D., Lee, V.W., Živčič, M. and Manic, M. (1991). "On the Correlation of Mercalli-Cancani-Sieberg Intensity Scale in Yugoslavia with the Peaks of Recorded Strong Earthquake Ground Motion", European Earthquake Eng., Vol. V, No. 1, pp. 27-33.
98. Veletsos, A.S., Newmark, N.M. and Chelapati, C.V. (1965). "Deformation Spectra for Elastic and Elastoplastic Systems Subjected to Ground Shock and Earthquake Motions", Proc. Third World Conf. Earthqu. Engng, New Zealand, Vol. II, pp. 663-680.
99. Wong, H.L. and Trifunac, M.D. (1979). "A Comparison of the Modified Mercalli (MMI) and the Japanese Meteorological Agency (JMA) Intensity Scales", Earthquake Engineering Struct. Dynamics, Vol. 7, No. 8, pp. 75-83.

ISET Journal of Earthquake Technology, Paper No. 426, Vol. 39, No.4, December 2002, pp. 255-271

EMPIRICAL SCALING OF STRONG EARTHQUAKE GROUND MOTION - PART II: DURATION OF STRONG MOTION

V.W. Lee
Civil Engineering Department
University of Southern California
Los Angeles, California, U.S.A.

ABSTRACT

Definitions of duration are reviewed, with emphasis on the one, which is used in most studies. In this definition, the duration is related to the rate of energy input into structures. Next, the physical parameters of the earthquake source and propagation path, and regional geologic and local soil characteristics, are discussed, as those influence the duration of strong motion. Finally, scaling models are illustrated, obtained from regression analyses of strong motion recordings in the western USA.

KEYWORDS: Duration, Energy, Rupture, Path and Regional Effects

INTRODUCTION

The duration of strong earthquake ground motion determines the rate of energy input into a structure, and should be considered in all analyses of linear and non-linear structural response. It has an important role in the analysis of liquefaction (Trifunac, 1995) and of permanent displacements of soils, and in the procedures and algorithms for probabilistic assessment of structural response to earthquakes. For example, studies of the statistical distribution of peaks in structural response (Udwadia and Trifunac, 1974; Amini and Trifunac, 1985; Gupta and Trifunac, 1991) require that the duration of shaking is specified. These studies determine the probabilities of exceedance of given levels of displacement, shear force or overturning moment, for a given number of times, at any level of a multistory building. The duration of strong shaking is also required for generation of site-specific artificial accelerograms (Lee and Trifunac, 1985, 1987; Wong and Trifunac, 1979).

The importance of the duration of shaking for non-linear response has been recognized, but it is still not used in the building design codes. The fatigue and non-linear yielding effects are thus ignored, or are considered in a simplified way. Clear and direct definitions of duration, and scaling models relating it to the earthquake source parameters (Trifunac et al., 2001), the propagation path characteristics, and the regional geologic and local soil conditions at the site, are required to incorporate the duration in analyses and design of structures.

In this paper, selected empirical regression equations of the duration of strong earthquake ground motion, in terms of earthquake magnitude, M, epicentral distance, Δ, site intensity I_{MM}, and the region specific propagation parameters, will be illustrated. A variety of such models were reviewed elsewhere (Trifunac and Westermo, 1976a, 1976b, 1977a, 1977b, 1978, 1982; Westermo and Trifunac, 1978, 1979; Novikova and Trifunac, 1993a, 1993b, 1993c, 1994a, 1994b, 1994c, 1995a, 1995b, 1995c; Novikova et al., 1993, 1995; Trifunac and Novikova, 1994, 1995). In this paper, we emphasize new, recent models, which use detailed characterization of the recording site conditions.

DEFINITIONS OF STRONG MOTION DURATION

The first studies of strong motion duration did not present its quantitative definition or dependence on magnitude and epicentral distance. In studies that followed, the duration was defined as the time interval between the first and the last time when the acceleration exceeds the level of 0.05g (bracketed duration, Page et al. (1972)), or the time interval during which 90% of the total energy is recorded at the station (Trifunac and Brady, 1975). Kawashima and Aizawa (1989) refined the definition of bracketed duration, and introduced normalized duration (elapsed time between the first and the last acceleration excursion

greater than μ times the peak acceleration). Mohraz and Peng (1989) introduced the structural frequency and damping into the definition, and used a low-pass filter for computing the duration.

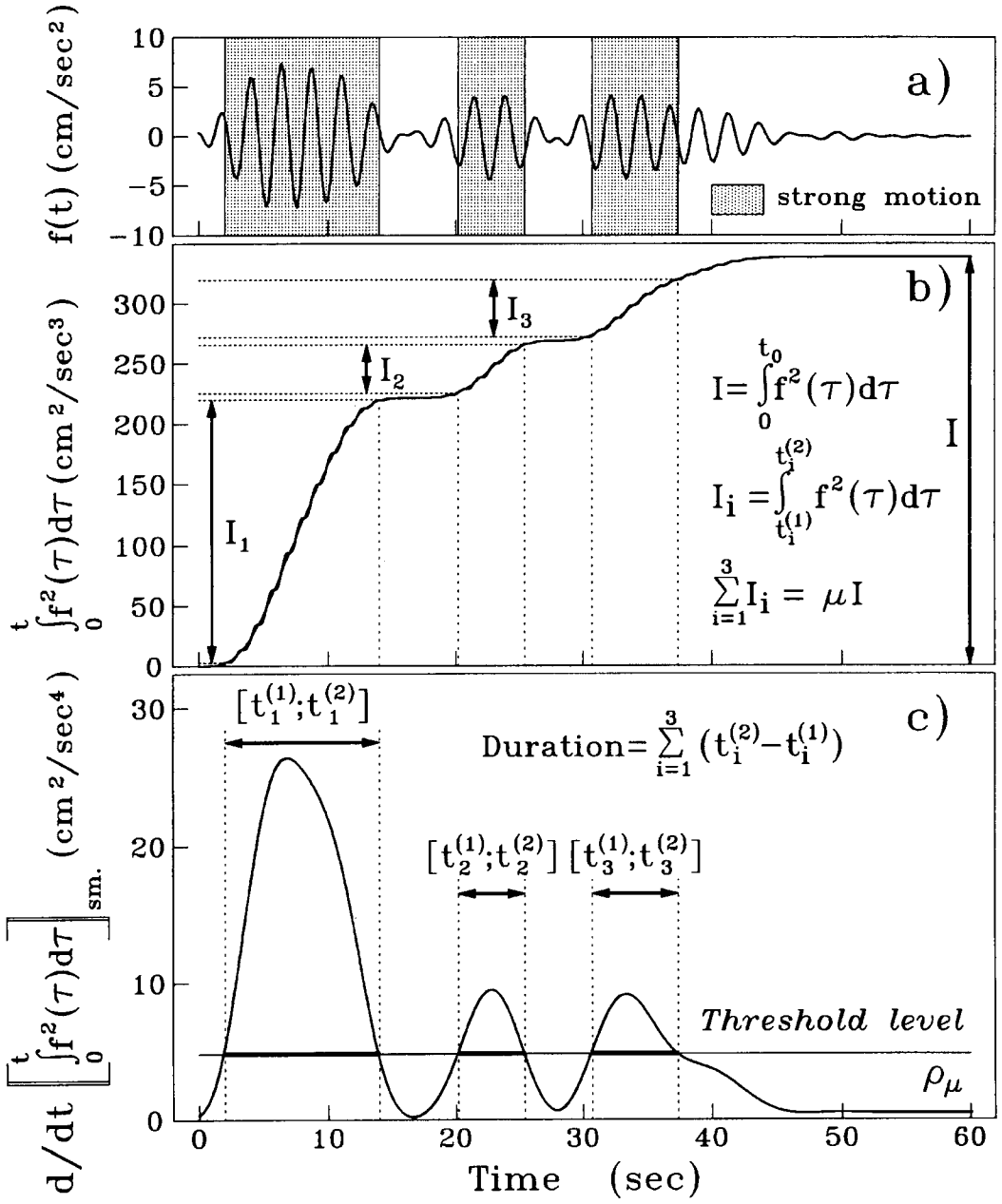

Fig. 1 The definition of duration for an acceleration component, (band-pass filtered, central frequency 0.37 Hz): a) time history $f(t)$ (the strong motion intervals are shaded); b) $\int_0^t f^2(\tau)d\tau$; c) the derivative of the integral of $f^2(t)$ after smoothing and the threshold level ρ_μ (the time intervals giving contribution to duration with $\mu = 0.9$ are highlighted)

The studies of Trifunac and Westermo (1977a, 1977b, 1982), Westermo and Trifunac (1978, 1979), and Novikova and Trifunac (1993a, 1993b, 1993c, 1994a, 1994b, 1994c, 1995a, 1995b, 1995c), use a definition that is related to the energy input in structures (Trifunac et al., 2001). This energy is proportional to $\int_0^\infty a^2(t)dt$. Next, the seismic wave energy radiated from the earthquake source is proportional to $\int_0^\infty v^2(t)dt$, where $v(t)$ is the ground velocity. In the statistics of the peak amplitudes of a random function, $f(t)$, the expected value of the peaks depends on the number of peaks, N, which is

proportional to the duration of strong motion, and on $\left[(1/T)\int_0^T f^2(t)dt\right]^{1/2}$, the root-mean-square of $f(t)$. A common feature in the above functionals is the integral of the form $\int f^2(t)dt$, a monotonically increasing function of time, and proportional to the work during response. It is natural then to associate the duration of strong motion with the time interval during which most of this work (e.g., 90 percent) is realized.

The studies of Novikova and Trifunac (1993a, 1993b, 1993c, 1994a, 1994b, 1994c, 1995a, 1995b, 1995c) consider dependence of duration on frequency. This is done by filtering the signal into 12 frequency bands (also called channels), with central frequencies from f_0 = 0.075 Hz to f_0 = 21 Hz. For each channel independently, the strong motion duration is evaluated, and it is analyzed how it depends on the earthquake parameters, on the propagation path characteristics, and on the local conditions at the site. Figure 1 illustrates how the duration of a function $f(t)$ is calculated for a frequency channel ($f(t)$ can be ground displacement, velocity or acceleration). The duration is the sum of the lengths of the strong "pulses" of $f(t)$. The beginning and end of the pulses is determined from the condition that the integral $\int_0^\infty a^2(t)dt$ gains 90% of its final value (Figure 1). This condition is equivalent to the time derivative of the same integral being greater than a threshold level (the duration is evaluated using smoothed $\int_0^\infty f^2(\tau)d\tau$). The duration evaluated by this procedure directly from the recorded motion is referred to as "observed" duration.

One feature of the above definition is that only the strong pulses contribute to the duration. Other physically related definitions (Trifunac and Brady, 1975; McCann and Shah, 1979) consider the strong motion interval to be continuous. Another feature is that the duration evaluated by the above procedure is not related to absolute levels of motion. The knowledge of the frequency-dependent duration in this "relative" sense, combined with the information about the Fourier spectral amplitudes (Trifunac, 1991, 1993, 1994a, 1994b, 1994c), provides a complete description of strong motion.

SCALING PARAMETERS

The duration of strong ground motion may be represented by the sum,

$$dur = \tau_0 + \tau_\Delta + \tau_{\text{region}} \tag{1}$$

where, dur is the total duration of acceleration, velocity or displacement, τ_0 stands for the duration of the rupture process at the source, τ_Δ represents the increase in duration due to propagation path effects, and τ_{region} describes the prolongation effects caused by the geometry of the regional geologic features and of the local soil at the recording site.

1. Duration of Rupture, τ_0

The duration of the rupture process, τ_0, depends on the amount of released energy (magnitude M), the geometry of the ruptured area, fault length and width (L and W), the speed of the rupture process (dislocation velocity, v), and on the shear wave velocity in the medium, β (Trifunac and Novikova, 1995).

The frequency dependence of τ_0 on magnitude M can be modeled by a quadratic function,

$$\tau_0 \approx a_1 + a_2 \cdot M + a_3 \cdot M^2 \tag{2}$$

where, a_i $(i = 1 \text{ to } 3)$ are regression coefficients. Although an exponential function would be more "natural", this quadratic expression is preferred (Novikova and Trifunac, 1993a). The duration of the rupture process, estimated from the duration of high-frequency radiations from the source, can be approximated by $\tau_0 = \alpha \exp(\gamma M)$, where $\alpha \approx .01$ and $\gamma \approx 1$. This can be compared with other estimates of different durations of the earthquake source (Trifunac and Novikova, 1995; Trifunac and Todorovska, 2002).

The duration of faulting is

$$\tau_1 \approx L/v + 0.5W/\beta \tag{3}$$

where, W is the fault width, L is the fault length, v is average velocity of dislocation, and β is the shear wave velocity in the medium surrounding the source. τ_1 can be computed from estimates of L, W, v and β, but can also be evaluated from $f_1 = 1/\tau_1$, where f_1 is one of the two corner frequencies in the low-frequency part of the Fourier spectrum of strong motion acceleration (Trifunac, 1993).

Near long and narrow faults, it is useful to work with the time it takes the dislocation to reach its ultimate amplitude, $\bar{u}$. Designating this time by T_0, it can be shown that $T_0 \approx \dfrac{\bar{u}\mu}{\sigma\beta}$ (Trifunac, 1994b, 1998). Here, μ is the rigidity, and σ is the effective stress (Trifunac, 1993, 1994b, 1998). Another "local" estimate of duration of faulting corresponds to the time it takes the dislocation to spread over the entire fault width, $\tau_2 \approx W/v$. This is related to another corner frequency in the Fourier amplitude spectrum, $f_2 = 1/\tau_2$ (Trifunac, 1993, 1998).

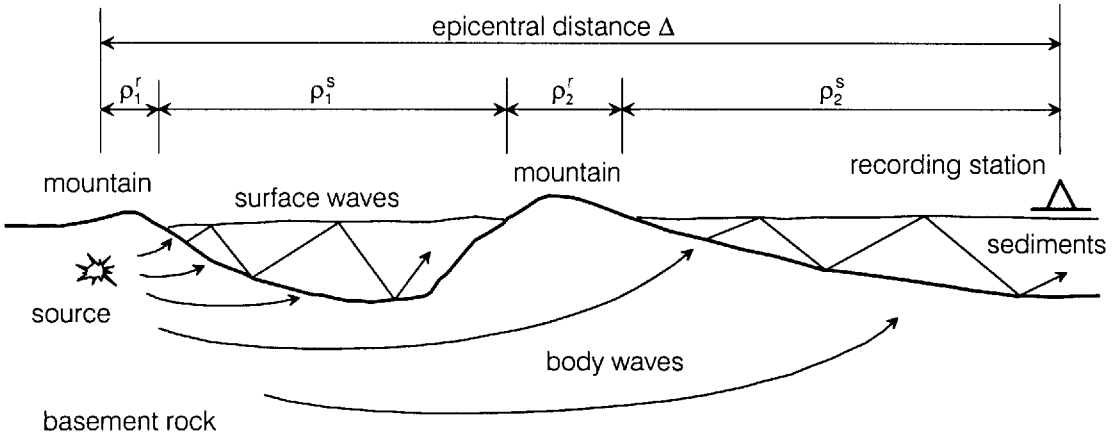

Fig. 2 The strong motion energy reaches the station in form of the surface waves and body wave

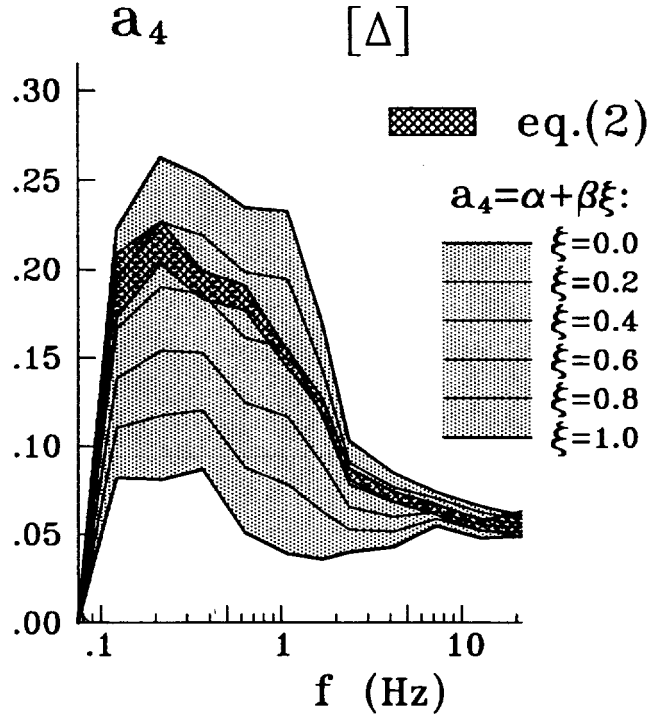

Fig. 3 "σ-interval" of the coefficient $a_4(f)$ in Equation (4) (cross-hatched area), and the coefficient a_4 with linear dependence of a_4 on the hardness of the propagation path, ξ (shaded zone)

2. Propagation Path Effects, τ_Δ

The second term in Equation (1), τ_Δ, describes the prolongations due to the distance traveled. It can be modeled by

$$\tau_\Delta(f) = a_4(f) \cdot \Delta \tag{4}$$

where, Δ is the epicentral distance, and f is the frequency.

This form has the interpretation that the duration of strong motion increases with the distance traveled due to dispersion of the strong motion waves (Figure 2). At its maximum (Figure 3, near frequency 0.2 Hz), the value of 0.2 corresponds to the increase of duration by 2 sec per 10 km of epicentral distance, and at $f \approx$ 15 to 20 Hz, this value drops to 0.5 sec per 10 km. At low and intermediate frequencies, the main contribution to strong ground motion comes from surface waves, and the increase of the duration with distance can be explained by the dispersion of those waves, travelling through irregular, but generally "layered" structure of the upper crust (Trifunac, 1971). If $c_{min}(f)$ and $c_{max}(f)$ are the effective minimum and maximum phase velocities of the surface waves, and v_{min} and v_{max} are the lowest and the highest shear wave velocities in the layered half-space, then

$$a_4(f) \approx \frac{1}{c_{\min}(f)} - \frac{1}{c_{\max}(f)} < \frac{1}{v_{\min}} - \frac{1}{v_{\max}} \tag{5}$$

For long surface waves, only one mode of propagation is possible (at the local distances), and for a narrow frequency band, only minor dispersion occurs; so, $a_4(f) \to 0$ as $f \to 0$. Increasing f introduces additional modes; the variety of possible phase velocities increases, and $a_4(f)$ grows. Further increase in frequency causes concentration of the phase velocities of different modes at the smallest shear wave velocity of the region. Then, $c_{min}(f)$ ($\approx v_{min}$) and $c_{max}(f)$ decrease, and so does $a_4(f)$. For high frequencies (f > 5 to 10 Hz), a_4 does not depend on frequency. The nature of the broadening of the strong motion pulses with distance differs here from the dispersive nature of the low-frequency wave propagation. For high frequencies, the strong motion appears to consist primarily of scattered body waves (Sato, 1989).

The propagation path effects depend on the percentage of the path traveled through rocks or through soft sediments. Using a map that shows the distribution of basement rocks on the earth's surface, we can characterize "hardness" of the transmission path for each pair source-station by the ratio of the portion of epicentral distance covered by rocks, as seen on the surface, to the total epicentral distance, $(\rho_1^r + \rho_2^r)/\Delta$ (Figure 2). We denote this ratio by ξ, and call paths with high ratio ξ as "hard" and with low ratio ξ as "soft". It may be assumed that $a_4 = \alpha + \beta\xi$, that is, the "prolongation due to propagation" coefficient is a linear function of the "hardness" of the path ξ (the regression analysis of this modified model gives practically the same results for all other scaling coefficients, as for the model in which ξ is ignored). The resulting dependence of a_4 on frequency is shown in Figure 3. The interval $a_4 \pm \sigma_4$ where β = 0, is shown for comparison. As expected, a_4 [$\xi \approx 0$] > a_4 [all cases] > [$\xi \approx 1$].

The sum, $\tau_0 + \tau_\Delta$, represents the duration observed at the sites located on basement rock, and is called here as “basic duration”. It serves as a basis for developing more "complete" accounting for prolongation of duration at the sites located on sediments.

3. Regional Effects, τ_{region}

Deviations from a uniform horizontally layered crust model occur everywhere along the path of the waves propagating from the fault to the recording site. For the San Fernando, 1971, California, earthquake, for example, substantial deviations from a multi-layered model dominate in the whole region shaken by this event. These deviations occur due to the topography of the basement rock, so that the several upper kilometers of the crust can be viewed as a collection of sedimentary basins separated by irregularly shaped basement rock “barriers”. These barriers can be recognized on the surface as mountains, coupling geological and topographical irregularities (Figure 2). The influence of such structures on the propagating waves can be understood by studying idealized sedimentary basins (Todorovska and Lee, 1990, 1991a, 1991b), by generalization to arbitrarily shaped layers (Moeen-Vaziri and Trifunac, 1988a, 1988b), and by interpretation of recorded data and numerical modeling of the wave propagation.

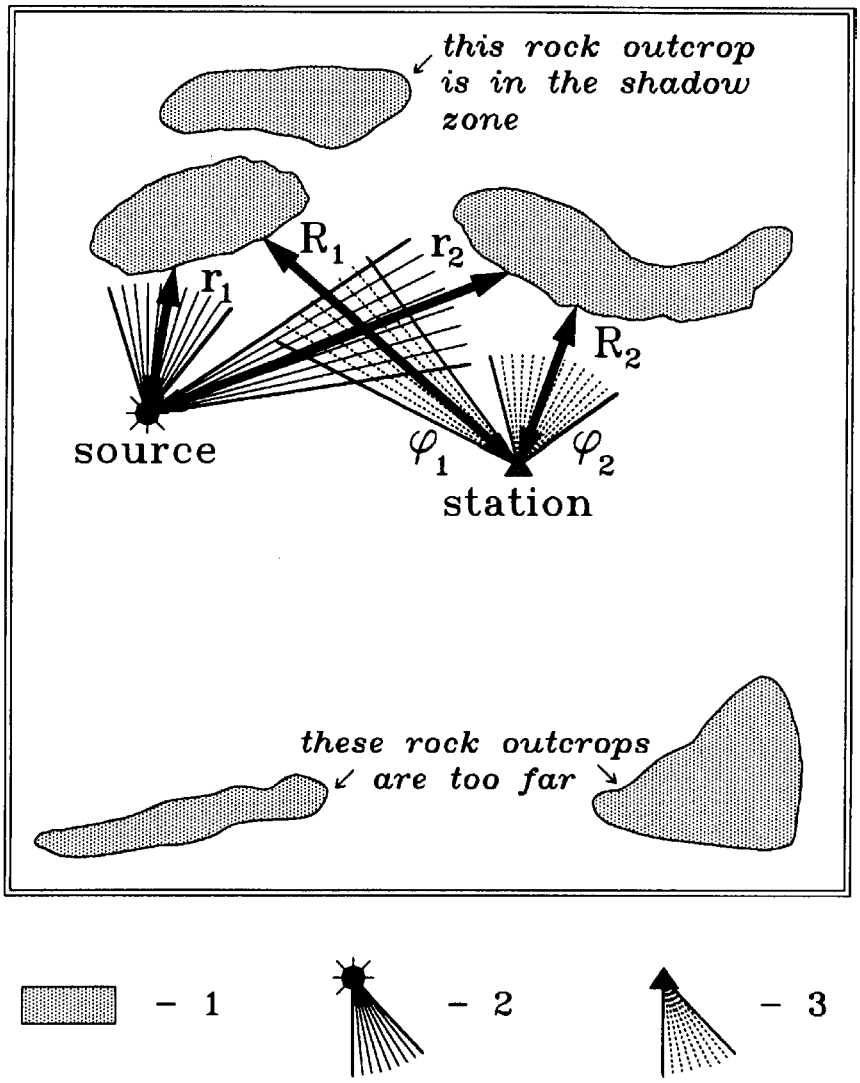

Fig. 4 A representation of R and φ ("1" shows the basements rocks on the earth's surface; "2" is the angle, subtended at the source by the rocks from which reflection occurs; the solid lines represent the direct waves; "3" is the angle, subtended at the recording station by the surface of the rocks from which reflection occurs; the dashed lines represent the waves reflected by the rock towards the station)

The reflection of waves back into the valley, and the conversion of body waves into "surface" waves at the boundaries of a sedimentary basin, suggest that the parameters describing some horizontal dimension of sedimentary basins should play a role in the description of the duration. The resulting prolongation of motion at stations, which are situated on sediments, has been studied by Novikova and Trifunac, while considering two parameters. One is the horizontal distance R (Figures 4 and 5) from the station to the basement rocks, appearing on the surface and producing reflections. The second parameter, φ, is the angle with which the reflecting surface of the rocks can be seen from the station. This parameter describes the "efficiency" of these reflections.

To scale the prolongation of motion in terms of R and φ, Novikova and Trifunac considered the energy of the waves reflected by individual "rocks" towards the station. The resulting equation ("energy equation"), however, is too complex to be considered in this review. Instead, we describe a simplification that ignores the geometrical spreading and attenuation. Then, the "energy equation" can be simplified to (Novikova and Trifunac, 1994a, 1994b)

$$R\varphi = \sum_i R_i \varphi_i \tag{6}$$

which states that the reflecting surface of the "fictitious" rock should be equal to the sum of the reflecting surfaces of the individual rocks.

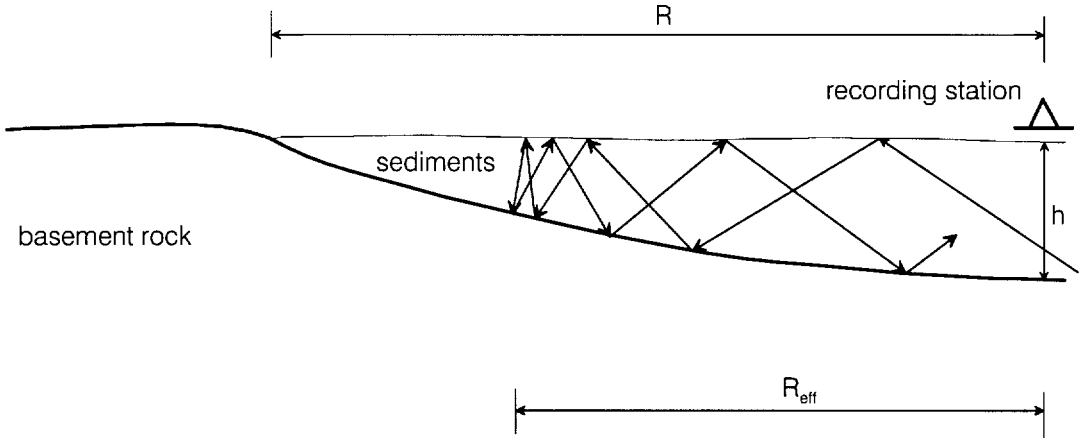

Fig. 5 Reflection of trapped waves from the edge of a sedimentary valley (h is the depth of sediments under the station, R is the distance to the reflecting rock, as it is seen on the earth's surface, and R_{eff} is the "effective" distance from the station to the region where the reflection actually occurs)

A pulse, reflected by a rock in the direction of the station, spends more time in the medium than a direct pulse; it travels distance $R_i + r_i$, and arrives at the station later. The "fictitious" rock has to be positioned at such a distance R from the station, that the delay of the pulses, reflected by it, represents some "proper" combination of the delays of pulses, coming from the individual rocks. The simplified "delay equation" is of the form (Novikova and Trifunac, 1994b)

$$R = \sum_i R_i \frac{R_i \varphi_i}{\sum_j R_j \varphi_j} \tag{7}$$

The increase of φ leads also to an increase of the duration of the reflected pulses, because a larger reflecting surface increases the azimuth and time windows of the sampled wave train. This suggests that τ_{region} is an increasing function of φ. The presently available data suggest that the dependence of τ_{region} on φ can be approximated by a linear function.

The dependence of τ_{region} on R is more complex. For small R, the time intervals, which correspond to the initial pulse (of duration dur_1) and to the reflected pulse (of duration dur_2), will be observed at the station almost simultaneously, without producing significant increase in the duration. For larger R, the time delay between the two pulses causes a complete separation of the corresponding intervals of strong motion, and the total duration is longer and equal to $dur_1 + dur_2$. Further increase of R causes an increase of the time, the reflected waves spend travelling through a dispersive medium. This causes increase of dur_2, and results in further prolongation of the total duration, $dur_1 + dur_2$. For large R, the second pulse, generated by reflection from a remote rock, experiences strong attenuation, and is so weak that it cannot be noticed relative to the background noise of the scattered waves. Therefore, two ranges of horizontal characteristic dimension exist: "small" R, where duration grows with increasing R, and "large" R, where the effect is opposite. A simple way to describe such dependence on R is to use,

$$\tau_{\text{region}}(R) = const_1 + const_2 R + const_3 R^2 \tag{8}$$

for some $const_i$, $i = 1,2,3$ (different at different frequency bands). We expect that $const_3 < 0$.

The depth of sediments, h, plays an important role in scaling various characteristics of strong earthquake ground motion (Trifunac and Lee, 1990; Lee, 1991). Studies of the influence of the depth of

sediments on the duration of strong motion were also performed. In the more recent studies, a parabolic dependence has been assumed

$$\tau_{\text{region}}(h) = const_4 + const_5 h + const_6 h^2 \tag{9}$$

where, $const_i$, $i = 4,5,6$ depend on frequency. $\tau_{\text{region}}(h)$ should be similar to $\tau_{\text{region}}(R)$, with the difference in scale, since h describes the dimension perpendicular to the predominant direction of the strong motion wave propagation. The wave cannot penetrate to the edge of the shallowing basin, and refracts and reflects back into the valley (see Figure 5). The length of this "penetration" depends on the geometry of the basin, on the wavelength of the wave, and on the incident angle. The "effective" horizontal distance, R_{eff}, from the station to the region of reflection, is difficult to be determined, and so, Novikova and Trifunac employed R and h in all equations, and accounted for the reduction of distance via empirical regression coefficients. Fixing the horizontal dimension, R, and changing the depth of the sediments, h, changes R_{eff} also. The appropriate way to account for this coupling is to combine these effects by adding a coupling term. Recalling the contribution from the angle of reflection φ, the final form of $\tau_{\text{region}}(R, h, \varphi)$ becomes

$$\begin{aligned}\tau_{\text{region}}(R,h,\varphi) = a_5 \cdot h + a_6 \cdot R + a_7 \cdot hR \\ + a_8 \cdot R^2 + a_9 \cdot h^2 + a_{10} \cdot \varphi\end{aligned} \tag{10}$$

where, a_i, i = 5 to 10 are regression coefficients. The numbering of these and of all other coefficients in this paper has been chosen to maintain consistency with all previous works on this subject (Novikova and Trifunac, 1993a, 1993b, 1993c, 1994a, 1994b).

4. Effects of the Local Soil

At high frequencies (short wave lengths), τ_{region} should include additional terms representing the effects of local soil conditions. For consistency and continuity with previous work of Novikova and Trifunac, the soil conditions can be characterized by the parameter s_L only (s_L = 0 for "rock", s_L = 1 for stiff soil sites, and s_L = 2 for deep soil sites (Trifunac, 1990)). In future, when more site-specific data becomes available, it will be possible to refine this classification and to consider more continuous soil site variables.

In the present database, any attempt to include s_L in the equations dealing with parameters h, R and φ, fails because of instability of the solution of the regression equations (due to the lack of data on s_L). At the present time, the effects of the local soil conditions can be studied, if the geology of the recording site is modeled in a simplified manner, using qualitative variable s (s = 0 for sediments, s = 2 for basement rock, and s = 1 for intermediate sites, see Trifunac (1990)). In this paper, we illustrate a duration model, where both "geological" parameter s (characterizing a site on the scale of kilometers) and local soil conditions parameter s_L (geotechnical description on a scale of tens of meters) are used simultaneously.

REGRESSION MODELS

1. Modeling in Terms of Magnitude, Epicentral Distance and Geometry of a Sedimentary Valley

A variety of regression models of the duration of strong ground motion have been presented by Novikova and Trifunac (1993a, 1993b, 1993c, 1994a, 1994b, 1994c, 1995a, 1995b, 1995c). Most of these are constructed starting with the "basic" model, which scales the duration in terms of the earthquake magnitude and the epicentral distance. The "basic" duration is a sum of τ_0 and τ_Δ, the duration of the rupture process and the prolongation due to propagation path effects, as discussed in the previous section. A more complete description also considers regional effects, as included in the function τ_{region}. In what follows, we illustrate a model, which uses the most "complete" representation, given by Equation (10). In this model, the duration at frequency f is represented by

$$\begin{Bmatrix} dur^{(h)}(f) \\ dur^{(v)}(f) \end{Bmatrix} = \begin{Bmatrix} a_1^{(h)}(f) \\ a_1^{(v)}(f) \end{Bmatrix} + a_2(f)\cdot\bar{M} + a_3(f)\cdot\bar{M}^2 + a_4(f)\cdot\Delta + \begin{Bmatrix} \left[a_5^{(h)}(f)\cdot h + a_6^{(h)}(f)\cdot R + a_7^{(h)}(f)\cdot hR + a_8^{(h)}(f)\cdot R^2 + a_9^{(h)}(f)\cdot h^2 + a_{10}^{(h)}(f)\cdot\varphi \right] \\ \left[a_5^{(v)}(f)\cdot h + a_6^{(v)}(f)\cdot R + a_7^{(v)}(f)\cdot hR + a_8^{(v)}(f)\cdot R^2 + a_9^{(v)}(f)\cdot h^2 + a_{10}^{(v)}(f)\cdot\varphi \right] \end{Bmatrix} \quad (11)$$

where, the epicentral distance, Δ, the depth of sediments, h, and the distance to the reflecting rocks, R, are measured in kilometers. The angle φ is measured in degrees, and $\bar{M} = \max\{M, M_{\min}(f)\}$, where $M_{\min}(f) = \dfrac{-a_2(f)}{2a_3(f)}$. $\bar{M}$ is introduced to keep the duration of strong motion a non-decreasing function of magnitude. The expression in the square bracket in Equation (11) represents the frequency-dependent term τ_{region}, when it is given by Equation (10), and $\left[\tau_{\text{region}}(f)\right] = \max\{0, \tau_{\text{region}}(f)\}$. The values of R, h and φ are assumed to be zero, if the station is located on rock. Two different sets of coefficients, $\{a_i^{(h)}(f),\ i = 1,5 \text{ to } 10\}$ for the horizontal components, and $\{a_i^{(v)}(f),\ i = 1,5 \text{ to } 10\}$ for the vertical ones, are considered.

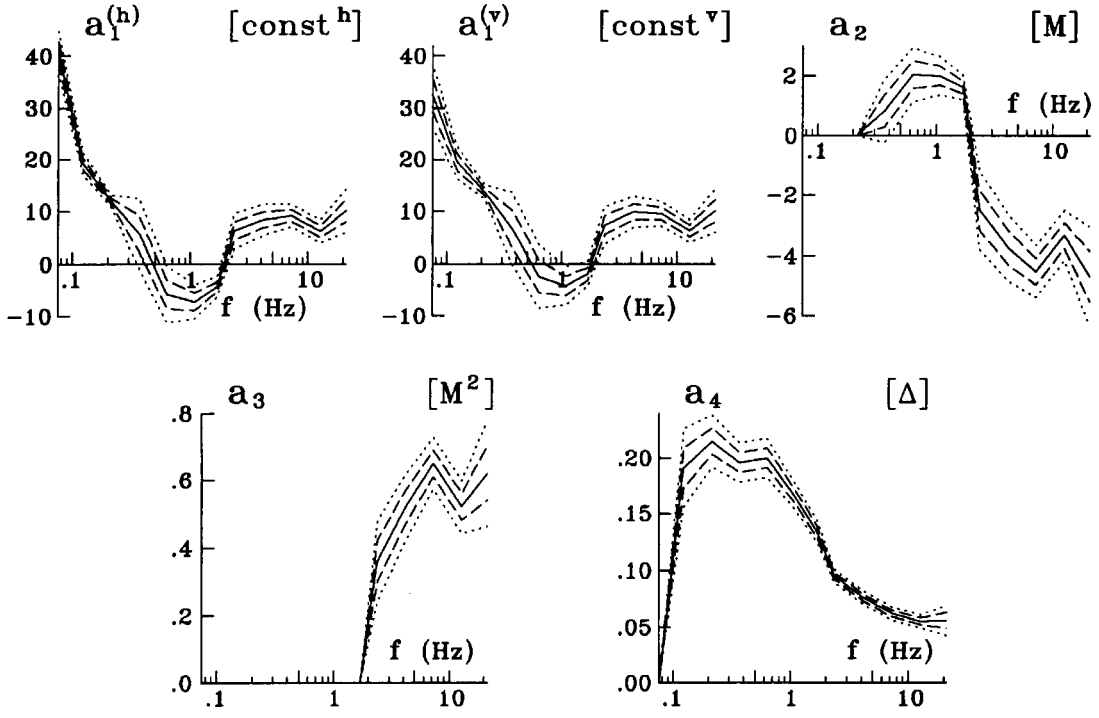

Fig. 6(a) Coefficients a_1 through a_4 in Equation (11), versus central frequency of the channels (solid lines) (the dashed lines indicate the "σ-intervals" and the dotted lines indicate the 95% confidence intervals)

Figures 6(a) and 6(b) show the dependence of the coefficients of the regression model on frequency (solid lines), and their reliability in terms of the "σ-interval" and the 95% confidence interval. The coefficients $\{a_i(f),\ i = 1 \text{ to } 4\}$ show how the duration depends on the magnitude and on the epicentral distance. No dependence of the duration on magnitude M can be detected at low frequencies, because

the dimension of the source is smaller than the wavelength of the seismic waves at these frequencies. As the frequency increases, first linear, and then quadratic dependence on M can be observed.

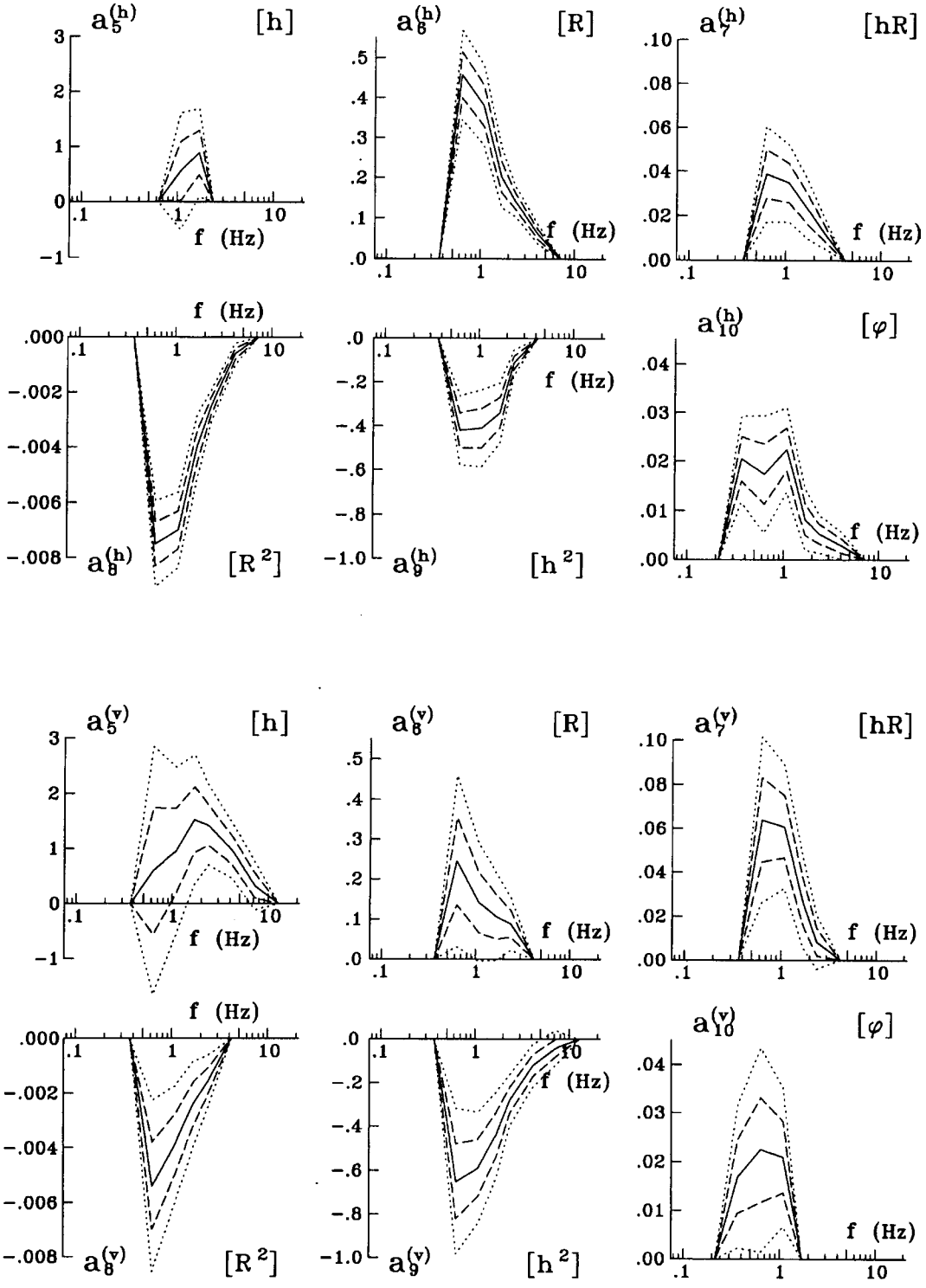

Fig. 6(b) Coefficients a_5 through a_{10} in Equation (11), versus central frequency of the channels (solid lines) (the dashed lines indicate the "σ-intervals" and the dotted lines indicate the 95% confidence intervals)

The coefficients $\{a_i(f), i = 5 \text{ to } 10\}$ describe the influence of the geometry of the sedimentary basin. The coefficient $a_{10}(f)$ represents the "strength" of the horizontal reflections, measured by the angle φ. The coefficients scaling the contributions of the quadratic terms R^2 and h^2 are negative. Thus, the duration increases for intermediate values of R and h, and there is no increase for small or large R and

h. Figure 7 shows isolines (in seconds) of the positive contribution to the overall duration, predicted by Equation (11), made by the following sum of terms involving R and h:

$$\begin{Bmatrix} \tau^{(h)}_{\text{region}}(R,h) \\ \tau^{(v)}_{\text{region}}(R,h) \end{Bmatrix} = \tag{12}$$

$$\begin{Bmatrix} \left[\begin{matrix} a_5^{(h)} \cdot h + a_6^{(h)} \cdot R + a_7^{(h)} \cdot hR \\ + a_8^{(h)} \cdot R^2 + a_9^{(h)} \cdot h^2 \end{matrix} \right] \\ \left[\begin{matrix} a_5^{(v)} \cdot h + a_6^{(v)} \cdot R + a_7^{(v)} \cdot hR \\ + a_8^{(v)} \cdot R^2 + a_9^{(v)} \cdot h^2 \end{matrix} \right] \end{Bmatrix}$$

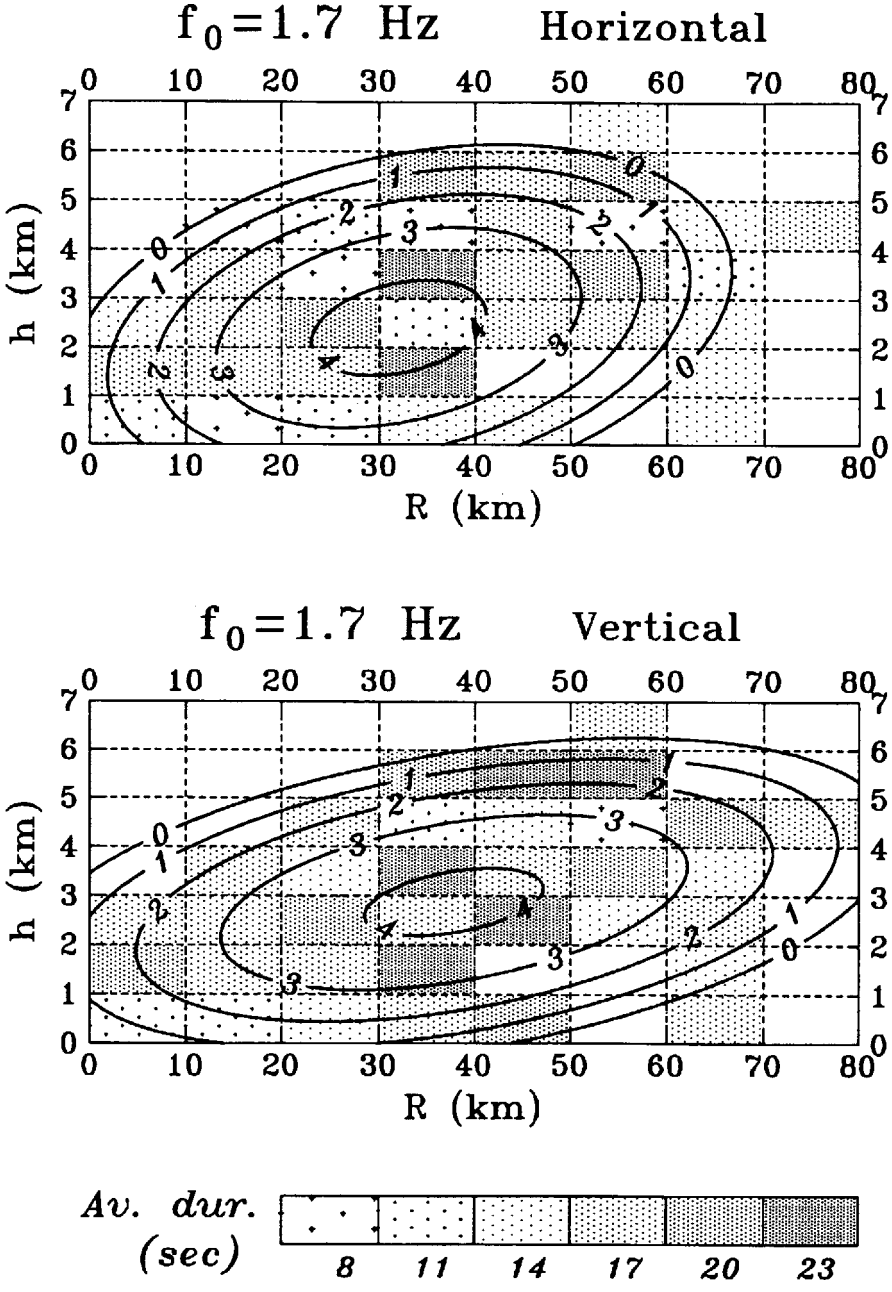

Fig. 7 Isolines of prolongation of motion (in seconds) defined by Equation (12) (the observed duration is shown averaged over ranges of R and h, as specified by the dashed mesh)

Figure 7 also shows the observed duration, averaged over the ranges of R and h. The darker shade corresponds to longer observed durations. The coefficients representing the prolongation of motion by the specific shape of the valley, are distinct from zero in the intermediate frequency range only. At low frequencies ($f \leq 0.3$ Hz), all the coefficients $\{a_i(f),\ i = 5 \text{ to } 10\}$ are equal to zero, and no influence of the sedimentary basin can be noticed. At channel # 4 ($f_0 = 0.37$ Hz), the prolongation is expressed by a term involving φ only. The angle of effective reflection, φ, appears to be more sensitive to long waves. At $f = 0.63$ to 2.5 Hz, the geometrical properties of the sedimentary basin "work" in full strength, and all the terms in τ_{region} have non-zero values. It is interesting to notice that the range of parameters R and h where $\tau_{\text{region}}\ (R, h) > 0$, preserves itself for both components in the frequency range $f = 0.63$-2.5 Hz. This effect may be similar in nature to the independence of the amplification factor from the frequency of motion inside the interval $f_2 < f < f_1$ (Trifunac, 1990). Inside the frequency range where $\tau_{\text{region}}\ (R, h) > 0$, the value of $\tau_{\text{region}}\ (R, h)$, however, does depend on frequency. The maximum possible contribution of $\tau_{\text{region}}\ (R, h)$ changes from 7.5 s to 2.5 s for the horizontal components, and from 5 s to 3.5 s for the vertical component, when the frequency changes from 0.63 Hz to 2.5 Hz. After the transition range (4.2 to 7.2 Hz), where some effects of the geometry of the sedimentary basin can still be noticed, the short wave range ($f > 5.0$ to 8.5 Hz) sets in. For these frequencies, no influence on the duration by the presence of a sedimentary basin can be observed.

We consider next the differences between the coefficients for the horizontal $\{a_i^{(h)}(f),\ i = 5 \text{ to } 10\}$ and vertical $\{a_i^{(v)}(f),\ i = 5 \text{ to } 10\}$ components. The coefficients, $a_6^{(h)}(f)$ and $a_8^{(h)}(f)$, which scale the influence of the parameter R on the horizontal component of motion, are better defined and can be followed in a wider frequency range than their vertical counterparts, $a_6^{(v)}(f)$ and $a_8^{(v)}(f)$. Conversely, the coefficients that describe the contribution of the depth of sediments h to the duration of the horizontal component, i.e. $a_5^{(h)}(f)$ and $a_7^{(h)}(f)$, have larger variances, and are distinct from zero in a narrower frequency range, compared to $a_5^{(v)}(f)$ and $a_7^{(v)}(f)$. Thus, the strong motion duration of the horizontal components appears to be more sensitive to the horizontal characteristic dimension R, while the duration of the vertical component "feels" the depth of sediments under the station, h, better, than it "feels" R. The parameter R describes the geometry of the basin on a large scale, while h gives a more local description in terms of the depth of sediments right under the recording station.

The angle φ with which the reflecting rocks are "seen" from the station, is a measure of the contributions to the duration from the horizontal reflections. The characteristic "dimension" of these reflections is described by R. Both φ– and R–related coefficients are better defined for the horizontal components. The typical values obtained for $a_0(f)$ give an increase in duration by about 2 s for $f \approx 0.37$ to 1.1 Hz, and by about 0.5 s and less for $f \approx 2.5$ to 1.1 Hz, per each 100° of φ.

2. Modeling in Terms of Magnitude, Epicentral Distance and Geological and Local Soil Conditions

To examine the influence of the local soil conditions on the duration of strong ground motion, the sites are divided into three groups according to the value of the soil parameter s_L. Deep soil sites have $s_L = 2$, stiff soil is designated as $s_L = 1$, and $s_L = 0$ stands for a "rock" site. Following Novikova and Trifunac (1994a), the qualitative indicator variables ("geological" parameter s, and "local" soil parameter s_L) are included in the model equation in the form, $a_{11}(f) \cdot S_L^{(1)} + a_{12}(f) \cdot S_L^{(2)} + a_{13}(f) \cdot S^{(1)} + a_{14}(f) \cdot S^{(0)}$, where $S^{(1)}$ and $S^{(0)}$ are indicator variables for $s = 1$ and $s = 0$ ($s = 0$ for sediments, $s = 2$ for basement rock, and $s = 1$ for intermediate sites), and $S_L^{(1)}$ and $S_L^{(2)}$ are the indicator variables for $s_L = 1$ and $s_L = 2$. However, a substantial reduction in the number of available data points (because of the lack of information about S_L for many sites), causes instability in the regression analysis. Therefore, Novikova and Trifunac reduced the number of unknown coefficients (to "improve" numerical stability) by treating the parameter s as a regular quantitative "continuous" variable.

The model that follows is then

$$\begin{Bmatrix} dur^{(h)}(f) \\ dur^{(v)}(f) \end{Bmatrix} =$$

$$\max\left[\left(\begin{Bmatrix} a_1^h(f) \\ a_1^v(f) \end{Bmatrix} + a_2(f)\cdot M\right), 1\right] \qquad (13)$$

$$+a_4(f)\cdot\Delta + a_{15}(f)\cdot(2-s)$$

$$+a_{11}(f)\cdot S_L^{(1)} + a_{12}(f)\cdot S_L^{(2)}$$

To avoid negative values of the duration, at locations close to a source, for small magnitude events, it is assumed that the duration at the source should not be less than 1 s. The reason to consider the term $a_{15}(f)\cdot(2 - s)$ instead of $a_{15}(f)\cdot s$ is that it is convenient to have basement rock as a reference, and to deal with positive a_{15}, if the duration on sediments is longer than that on the rock sites.

The results of the regression analysis with Equation (13) are shown in Figures 8(a) and 8(b). The coefficient $a_{15}(f)$, responsible for scaling the influence of the epicentral distance Δ, does not change, when compared to other related models. The coefficients $a_1(f)$ and $a_2(f)$ have different meanings now due to a linear approximation of τ_0. For low frequencies (f_0 = 0.37 Hz), the duration of motion on sediments (s = 0) is about 4 s longer, than that on rock sites. At high frequencies, $a_{15}(f)$ is not well defined (the condition $|\sigma_{15}(f)/a_{12}(f)| < 1$ is hardly satisfied). The inequality shows that the duration of strong motion is longer on deep soil (s_L = 2) and shorter on "rock" sites (s_L = 0), with stiff sites being in the middle. Also, the influence of the local soil conditions on the duration can be noticed at higher frequencies, compared to the influence of the geological conditions.

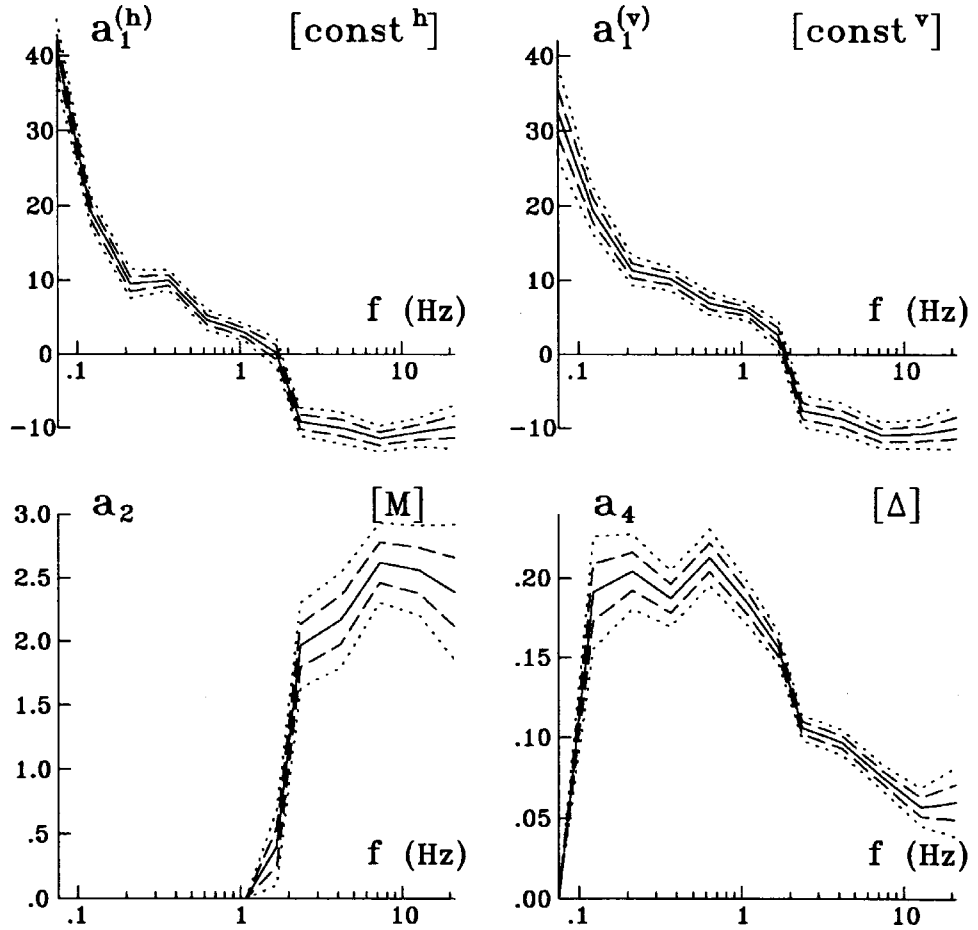

Fig. 8(a) The coefficients $a_1(f)$, $a_2(f)$ and $a_4(f)$, in the model in Equation (13) plotted versus central frequency of the channel (solid lines) (the dashed lines indicate the "σ – intervals", and the dotted lines indicate the 95% confidence intervals)

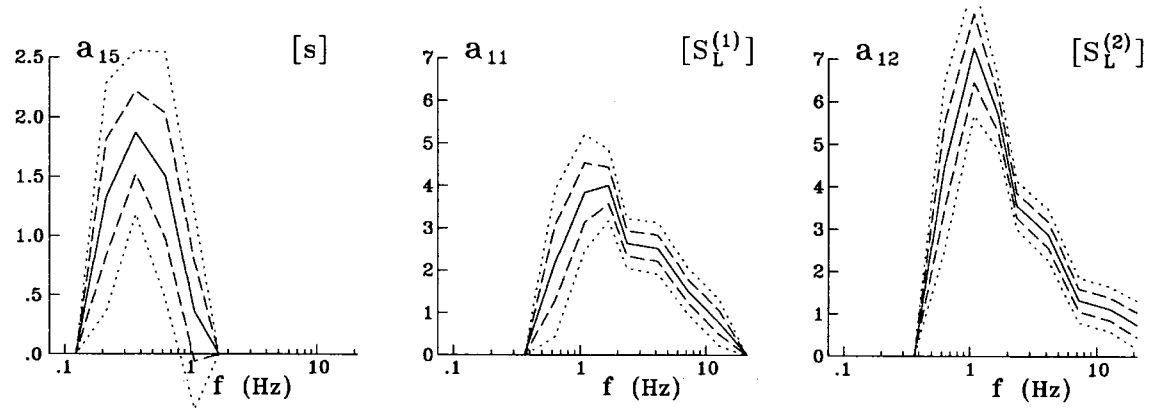

Fig. 8(b) The coefficients $a_{15}(f)$, $a_{11}(f)$ and $a_{12}(f)$ in the model in Equation (13) plotted versus central frequency of the channel (solid lines) (the dashed lines indicate the "σ-intervals", and the dotted lines indicate the 95% confidence intervals)

DISCUSSION AND CONCLUSIONS

The models reviewed in this paper suggest the physical mechanisms, which may be responsible for the prolongation of strong ground motion at sites located on sediments. However, the prolongation mechanisms discussed here (e.g., reflection of the waves at the boundaries of a valley back inside the valley) represent only one possible way to interpret these observations.

Consider, for example, the case shown in Figure 2. The earthquake source generates body (and surface) seismic waves. Some body waves penetrate deep into the crust, and reach the recording station from below. Some body waves are converted into surface waves at the first boundary rock-sediments, at a distance ρ_1^r from the source. Together with the surface waves generated in the epicentral region, these waves propagate through the sedimentary valley, and reach the boundary at epicentral distance $\rho_1^r + \rho_1^s$. There, they are partially reflected back into the valley (this surface wave energy is "trapped" in the valley), and partially continue to propagate away from the source in the form of body and surface waves. Similar processes of surface-body wave conversions and reflections from the edges of the valley repeat in each sufficiently deep alluvial valley. As a result, a complex picture of overlapping strong motion pulses consisting of body and surface waves is recorded at the station.

When the three-dimensional geometry of the region is irregular, and when many factors contribute to the formation of the signal at the location of the station, it is difficult to decide how to describe these factors by using just a few parameters which can be included in the regression analysis. For example, Novikova and Trifunac considered the percentage of epicentral distance covered by rocks on the earth surface $\xi = \left(\rho_1^r + \rho_2^r\right)/\Delta$, and looked at $\tau_\Delta = \left(a_4^{(1)} + a_4^{(2)}\xi\right)\cdot\Delta$ instead of $\tau_\Delta = a_4 \cdot \Delta$. It appears that, per each 10 km of epicentral distance at frequencies near 0.3 Hz, the motion is prolonged by 2.5 s if $\xi = 0$ (the direct surface path from the source to the station does not cross any rocks), and by only 0.8 s if $\xi = 1$ (the epicenter and the station are located in the same rock outcrop). We explain this by dispersion along the path through alluvium. Choosing ξ as one of the parameters describing the geometry of the region is only an approximation. If the deep source and the recording station are separated by several valleys, the strong motion energy observed at the site could be coming from direct body waves and from surface waves generated at the edges of the valley, where the station is located. In this case, one might consider the percentage of path covered by alluvium valleys located far from the station. If the source in Figure 2 is shifted to a greater depth, this parameter can be expressed as the ratio ρ_2^s/Δ. Another parameter, useful in the consideration of shallow sources, is the number of boundaries rock-sediments and sediments-rock, crossed by the waves on their way to the recording station. It may influence, not only the duration of strong motion, but also the amplitude of Fourier spectrum observed at the site. Large number of boundaries would weaken the signal. Also, the presence of several valleys reduces the amplitudes of strong motion, because some energy is "trapped" in these valleys and cannot reach the recording station.

When a detailed description of the geological conditions at the site is not available, the parameter s can be used instead. The importance of considering the local soil together with the geological site conditions was also demonstrated. The influence of the geological and soil site conditions on the duration of strong ground motion prevails at different frequencies. The duration can be prolonged by 3.5 sec at a site located on a deep sedimentary layer at frequencies about 0.5 Hz, and by as much as 5 to 6 sec due to the presence of soft soil underneath the station at frequency of about 1 Hz.

The results of this and of all cited works can be used for the prediction of the duration of shaking expected during future earthquakes, when the parameters of the shock (M and Δ, or I_{MM}) and the site (R, φ and h, or s and s_L) can be specified. However, we note that the equations and the regression coefficients can be employed for such a prediction, only in the region where the data were recorded (western U.S., and primarily southern California). A different geological environment may be associated with different earthquake mechanism, distribution of hypocentral depths of the sources, velocities and attenuation factors, thus changing the values of the regression coefficients (Novikova et al., 1993).

REFERENCES

1. Amini, A. and Trifunac, M.D. (1985). "Statistical Extension of Response Spectrum Superposition", Int. J. Soil Dynam. Earthqu. Engng, Vol. 4, No. 2, pp. 54-63.
2. Gupta, V.K. and Trifunac, M.D. (1991). "Effect of Ground Rocking on Dynamic Response of Multistoried Building during Earthquakes", Struct. Engng/Earthqu. Engng, JSCE, Vol. 8, pp. 43-50.
3. Kawashima, K. and Aizawa, K. (1989). "Bracketed and Normalized Durations of Earthquake Ground Acceleration", Earthqu. Engng Struct. Dynam., Vol. 18, pp. 1041-1051.
4. Lee, V.W. and Trifunac, M.D. (1985). "Torsional Accelerograms", Int. J. Soil Dynam. Earthqu. Engng, Vol. 4, No. 3, pp. 132-139.
5. Lee, V.W. and Trifunac, M.D. (1987). "Rocking Strong Earthquake Accelerations", Int. J. Soil Dynam. Earthqu. Engng, Vol. 6, pp. 75-89.
6. Lee, V.W. (1991). "Correlation of Pseudo Relative Velocity Spectra with Site Intensity, Local Soil Classification and Depth of Sediments", Int. J. Soil Dynam. Earthqu. Engng, Vol. 10, pp. 141-151.
7. McCann, M.W. and Shah, H.C. (1979). "Determining Strong-Motion Duration of Earthquakes", Bull. Seism. Soc. Amer., Vol. 69, pp. 1253-1265.
8. Mohraz, B. and Peng, M.-M. (1989). "Use of a Low-Pass Filter in Determining the Duration of Strong Ground Motion", Publication PVP-182, Pressure Vessels and Piping Division, ASME, New York, U.S.A., pp. 197-200.
9. Moeen-Vaziri, N. and Trifunac, M.D. (1988a). "Scattering and Diffraction of Plane P- and SH-Waves by Two-Dimensional Inhomogeneities: Part I", Int. J. Soil Dynam. Earthqu. Engng, Vol. 7, No. 4, pp. 179-188.
10. Moeen-Vaziri, N. and Trifunac, M.D. (1988b). "Scattering and Diffraction of Plane P- and SV-Waves by Two-Dimensional Inhomogeneities: Part II", Int. J. Soil Dynam. Earthqu. Engng, Vol. 7, No. 4, pp. 189-200.
11. Novikova, E.I. and Trifunac, M.D. (1993a). "Duration of Strong Ground Motion: Physical Basis and Empirical Equations", Report CE 93-02, Dept. of Civil Eng., Univ. of Southern California, Los Angeles, California, U.S.A.
12. Novikova, E.I. and Trifunac, M.D. (1993b). "Modified Mercalli Intensity Scaling of the Frequency Dependent Duration of Strong Ground Motion", Soil Dynam. Earthqu. Engng, Vol. 12, No. 5, pp. 309-322.
13. Novikova, E.I. and Trifunac, M.D. (1993c). "Modified Mercalli Intensity and the Geometry of the Sedimentary Basin as Scaling Parameters of the Frequency Dependent Duration of Strong Ground Motion", Soil Dynam. Earthqu. Engng, Vol. 12, No. 4, pp. 209-225.
14. Novikova, E.I. and Trifunac, M.D. (1994a). "Duration of Strong Ground Motion in Terms of Earthquake Magnitude, Epicentral Distance, Site Conditions and Site Geometry", Earthqu. Engng Struct. Dynam., Vol. 23, No. 9, pp. 1023-1043.

15. Novikova, E.I. and Trifunac, M.D. (1994b). "Influence of Geometry of Sedimentary Basins on the Frequency Dependent Duration of Strong Ground Motion", Earthqu. Engng. Engng. Vibrat., Vol. 14, No. 2, pp. 7-44.
16. Novikova, E.I. and Trifunac, M.D. (1994c). "Empirical Models of the Duration of Strong Earthquake Ground Motion Based on the Modified Mercalli Intensity", Report CE 94-01, Dept. of Civil Eng., Univ. Southern California, Los Angeles, California, U.S.A.
17. Novikova, E.I. and Trifunac, M.D. (1995a). "Frequency Dependent Duration of Strong Earthquake Ground Motion on the Territory of Former Yugoslavia, Part 1: Magnitude Models", European Earthquake Eng., Vol. VIII, No. 3, pp. 11-25.
18. Novikova, E.I. and Trifunac, M.D. (1995b). "Frequency Dependent Duration of Strong Earthquake Ground Motion: Updated Empirical Equations", Report CE 95-01, Dept. of Civil Eng., Univ. Southern California, Los Angeles, California, U.S.A.
19. Novikova, E.I., Todorovska, M.I. and Trifunac, M.D. (1993). "A Preliminary Study of the Duration of Strong Earthquake Ground Motion on the Territory of Former Yugoslavia", Report CE 93-09, Dept. of Civil Eng., Univ. of Southern California, Los Angeles, California, U.S.A.
20. Novikova, E.I., Todorovska, M.I. and Trifunac, M.D. (1995). "Frequency Dependent Duration of Strong Earthquake Ground Motion on the Territory of Former Yugoslavia, Part II: Local Intensity Models", European Earthquake Eng., Vol. VIII, No. 3, pp. 26-37.
21. Page, R.A., Boore, D.M., Joyner, W.B. and Coulter, H.W. (1972). "Ground Motion Values for Use in the Seismic Design of the Trans-Alaska Pipeline System", USGS Circular 672.
22. Sato, H. (1989). "Broadening of Seismogram Envelops in the Randomly Inhomogeneous Lithosphere Based on the Parabolic Approximation: Southeastern Honshu", Japan. J. Geophys. Res., Vol. 94, No. 17, pp. 17735-17747.
23. Todorovska, M.I. and Lee, V.W. (1990). "A Note on Response of Shallow Circular Valleys to Rayleigh Waves: Analytical Approach", Earthqu Engng Engng Vibrat., Vol. 10, pp. 21-34.
24. Todorovska, M.I. and Lee, V.W. (1991a). "Surface Motion of Shallow Circular Alluvial Valleys for Incident Plane SH Waves - Analytical Solution", Int. J. Soil Dynam. Earthqu. Engng, Vol. 10, pp. 192-200.
25. Todorovska, M.I. and Lee, V.W. (1991b). "A Note on Scattering of Rayleigh Waves by Shallow Circular Canyons: Analytical Approach", Bull. Indian Soc. Earthqu. Tech., Vol. 28, No. 2, pp. 1-16.
26. Trifunac, M.D. (1971). "Response Envelope Spectrum in Interpretation of Strong Ground Motion", Bull. Seism. Soc. Amer., Vol. 61, pp. 343-356.
27. Trifunac, M.D. (1990). "How to Model Amplification of Strong Earthquake Motions by Local Soil and Geological Site Conditions", Earthqu. Engng Struct. Dynam., Vol. 19, pp. 833-846.
28. Trifunac, M.D. (1991). "Empirical Scaling of Fourier Spectrum Amplitudes of Recorded Strong Earthquake Accelerations in Terms of Modified Mercalli Intensity, Local Soil Conditions, and Depth of Sediments", Soil Dynam. Earthqu. Engng, Vol. 10, No. 1, pp. 65-72.
29. Trifunac, M.D. (1993). "Long Period Fourier Amplitude Spectra of Strong Motion Acceleration", Soil Dynam. Earthqu. Engng, Vol. 12, No. 6, pp. 363-382.
30. Trifunac, M.D. (1994a). "Fourier Amplitude Spectra of Strong Motion Acceleration: Extension of High and Low Frequencies", Earthqu. Engng Struct. Dynam., Vol. 23, No. 4, pp. 384-411.
31. Trifunac, M.D. (1994b). "Similarity of Strong Motion Earthquakes in California", European Earthqu. Engng., Vol. VIII, No. 1, pp. 38-48.
32. Trifunac, M.D. (1994c). "Q and High Frequency Strong Motion Spectra", Soil Dynam. Earthqu. Engng., Vol. 13, No. 3, pp. 149-161.
33. Trifunac, M.D. (1995). "Empirical Criteria for Liquefaction in Sands via Standard Penetration Tests and Seismic Wave Energy", Soil Dynamics Earthquake Eng., Vol. 14, No. 4, pp. 419-426.
34. Trifunac, M.D. (1998). "Stresses and Intermediate Frequencies of Strong Motion Acceleration", Geofizika, Vol. 14, pp. 1-27.
35. Trifunac, M.D. and Brady, A.G. (1975). "A Study on the Duration of Strong Earthquake Ground Motion", Bull. Seism. Soc. Amer., Vol. 65, pp. 581-626.

36. Trifunac, M.D. and Lee, V.W. (1990). "Frequency Dependent Attenuation of Strong Earthquake Ground Motion", Int. J. Soil Dynam. Earthqu. Engng, Vol. 9, pp. 3-15.
37. Trifunac, M.D. and Novikova, E.I. (1994). "State of the Art Review on Strong Motion Duration", 10th European Conf. Earthquake Eng., Vienna, Austria, Vol. 1, pp. 131-140.
38. Trifunac, M.D. and Novikova, E.I. (1995). "Duration of Earthquake Fault Motion in California", Earthquake Eng. Structural Dynamics, Vol. 24, No. 6, pp. 781-799.
39. Trifunac, M.D. and Todorovska, M.I. (2002). "A Note on the Differences in Tsunami Source Parameters for Submarine Slides and Earthquakes", Soil Dynamics Earthquake Eng., Vol. 22, No. 2, pp. 143-155.
40. Trifunac, M.D. and Westermo, B. (1976a). "Dependence of Duration of Strong Earthquake Ground Motion on Magnitude, Epicentral Distance, Geologic Conditions at the Recording Station and Frequency of Motion", Report CE 76-02, Dept. of Civil Eng., University of Southern Calif., Los Angeles, California, U.S.A.
41. Trifunac, M.D. and Westermo, B. (1976b). "Correlations of Frequency Dependent Duration of Strong Earthquake Ground Motion with the Modified Mercalli Intensity and the Geologic Conditions at the Recording Stations", Report CE 76-03, Dept. of Civil Eng., University of Southern Calif., Los Angeles, California, U.S.A.
42. Trifunac, M.D. and Westermo, B. (1977a). "Recent Development in the Analysis of the Duration of Strong Earthquake Ground Motion", Sixth World Conference Earthquake Engineering, New Delhi, India, Vol. I, pp. 365-371.
43. Trifunac, M.D. and Westermo, B. (1977b). "A Note on the Correlation of Frequency-Dependent Duration of Strong Earthquake Ground Motion with the Modified Mercalli Intensity and the Geological Conditions at the Recording Stations", Bull. Seism. Soc. Amer., Vol. 67, pp. 917-927.
44. Trifunac, M.D. and Westermo, B. (1978). "A Note on the Dependence of the Duration of Strong Earthquake Ground Motion on Magnitude, Epicentral Distance, Geologic Conditions at the Recording Station and Frequency of Motion", Bull. Inst. Earthquake Engineering Seism., University "Kiril i Metodij", Skopje, Yugoslavia.
45. Trifunac, M.D. and Westermo, B. (1982). "Duration of Strong Earthquake Shaking", Int. J. Soil Dynam. Earthqu. Engng, Vol. 2, pp. 117-121.
46. Trifunac, M.D., Hao, T.Y. and Todorovska, M.I. (2001). "On Energy Flow in Earthquake Response", Report CE 01-03, Dept. of Civil Eng., Univ. of Southern California, Los Angeles, California, U.S.A.
47. Udwadia, F.E. and Trifunac, M.D. (1974). "Characterization of Response Spectra through the Statistics of Oscillator Response", Bull. Seism. Soc. Amer., Vol. 64, pp. 205-219.
48. Westermo, B.D. and Trifunac, M.D. (1978). "Correlations of the Frequency Dependent Duration of Strong Earthquake Ground Motion with the Magnitude, Epicentral Distance, and the Depth of Sediments at the Recording Site", Report CE 78-12, Dept. of Civil Eng., Univ. of Southern California, Los Angeles, California, U.S.A.
49. Westermo, B.D. and Trifunac, M.D. (1979). "Correlations of the Frequency Dependent Duration of Strong Ground Motion with the Modified Mercalli Intensity and the Depth of Sediments at the Recording Site", Report CE 79-01, Dept. of Civil Eng., Univ. of Southern California, Los Angeles, California, U.S.A.
50. Wong, H.L. and Trifunac, M.D. (1979). "Generation of Artificial Strong Motion Accelerograms", Earthqu. Engng Struct. Dynam., Vol. 7, pp. 509-527.

ISET Journal of Earthquake Technology, Paper No. 427, Vol. 39, No. 4, December 2002, pp. 273-310

EMPIRICAL SCALING OF STRONG EARTHQUAKE GROUND MOTION - PART III: SYNTHETIC STRONG MOTION

V.W. Lee
Civil Engineering Department
University of Southern California
Los Angeles, California, U.S.A.

ABSTRACT

A comprehensive and general method for the prediction of strong motion amplitudes, developed by Strong Motion Research Group at University of Southern California, is reviewed. It uses synthetic translational accelerograms and the theory of linear wave propagation to predict all other components of strong motion: rotations (torsion and rocking), strains and curvatures. It gives site-specific synthetic motions which have realistic non-stationary frequency content, site-specific dispersion properties, and amplitudes and the duration which are compatible with empirical scaling equations developed for the estimation of strong motion in California.

KEYWORDS: Dispersion, Rayleigh and Love Modes, Translation, Torsion, Rocking

INTRODUCTION

For many applications, it is necessary to estimate future shaking at a particular site which is outside the range of strong-motion parameters for which the existing recorded data is available. This happens, in particular, in those parts of the world where recorded data is not yet available. Considerable variability in the characteristics of recorded strong-motions recorded under similar conditions, may require a characterization of future shaking in terms of an ensemble of accelerograms rather than in terms of just one or two "typical" records. In many earthquake engineering analyses, particularly those which deal with the non-linear response of structures, the entire analysis must be performed in the time domain, because the superposition techniques do not apply. This and many related situations have thus created a need for the development of techniques for the generation of synthetic (artificial) strong-motion time histories that simulate realistic ground motions. In this work, we will review the only complete and comprehensive family of papers which outline the methods for generation of artificial time histories of (1) translational acceleration, (2) rotational acceleration (torsion and rocking), (3) surface strain, and (4) surface curvature.

Apparent irregularity of early recorded accelerograms and the limited number of records in the 1950's have led investigators to explore the possibility of modeling strong ground shaking by means of random time functions of simple but known properties. Housner (1955), for example, assumed that an accelerogram could be modeled by a series of one-cycle sine-wave pulses; others used a series of pulses distributed randomly in time (Goodman et al., 1955; Rosenblueth, 1956; Bycroft, 1960; Rosenblueth and Bustamante, 1962). On the basis of such artificial time functions of known statistical properties, it became clear (Bolotin, 1960) that the nonstationarity of ground motion can influence structural response significantly. This prompted the development of methods for the construction of artificial accelerograms by using nonstationary random time series (e.g., Bogdanoff et al., 1961; Amin and Ang, 1966; Goto and Toki, 1969). The nonstationarity in these models was achieved typically by (a) multiplying stationary random time series by a nonstationary envelope function, (b) changing the frequency content of an artificial accelerogram as a function of time, and by (c) superimposing simple earthquake sources with some phase delays in time (e.g., Rascon and Cornell, 1969) to represent the propagation of a simple earthquake source (e.g., Honda, 1957) by means of radiated P and S waves only.

Observational studies of strong ground motion in the 1970's showed that a typical strong motion record consists of near-field, intermediate-field, body and surface waves contributing different amounts to the total result, depending on the earthquake source mechanism and on the wave path (Trifunac, 1971a, 1971b; Trifunac, 1972a, 1972b; Trifunac, 1973). Empirical studies of spectral characteristics (Trifunac, 1976, 1979a, 1979b, 1993, 1994, 1995a, 1995b; Trifunac and Anderson, 1977; Trifunac and Lee, 1978, 1985) and frequency-dependent duration (Trifunac and Westermo, 1976a, 1976b; Trifunac and Novikova,

1994, 1995) have further shown the nature of the dependence of strong motion on the geologic environment of the recording station. Consequently, realistic artificial accelerograms must have nonstationary frequency, amplitude and duration characteristics that agree with the trends present in the recorded accelerograms.

In choosing a suitable accelerogram for a particular analysis, many factors must be taken into account, for example, the distance between the source and the site, the size of the earthquake, and the geology surrounding the site. The recorded accelerograms cannot be modified in a simple way to satisfy the requirements at all sites (Lee and Trifunac, 1989), and thus, site-dependent artificial accelerograms are needed.

The majority of the proposed methods for the generation of synthetic accelerograms fall into two categories: (1) methods that utilize random functions, and (2) methods that involve source mechanism and wave propagation models. Using the former methods, the resulting accelerograms do not always have a correct frequency content for engineering applications, and the frequency characteristics of the time record are often uniform from beginning to the end of the record. For a recorded accelerogram, the frequency contained in the beginning of the record (during the arrival of body and high-frequency surface waves) is generally higher. Using the latter methods, a more physically consistent record can be generated, but it is impossible to model all the details of the source as well as of the wave path adequately for the complete frequency range of interest (e.g., 0.5-30 Hz). Because of the simplifications, the generated records often lack proper high-frequency characteristics, when compared with the recorded accelerograms.

This work reviews a unique and comprehensive group of methods for constructing synthetic accelerograms, which have a given Fourier amplitude spectrum, $F(\omega)$, and a given duration. The Fourier amplitude spectrum and the duration can be obtained from correlations with the earthquake parameters. The times of arrival of the waves can be derived from the dispersive properties of the site. This introduces the specific characteristics of each site into the resulting artificial records of strong motion.

GENERATION OF SYNTHETIC TRANSLATIONAL ACCELEROGRAMS

The synthetic translational components of acceleration are constructed to have a required Fourier amplitude spectrum, $FS(\omega)$, and a given duration, $D(\omega)$, at the site. For completeness in this presentation, a review of the method first proposed by Trifunac (1971b), and later refined by Wong and Trifunac (1978, 1979), for the generation of synthetic accelerograms is briefly summarized as follows.

1. Dispersion Curves at a Site

For a given site, a profile with equivalent layered medium is first determined. A model can have L layers. For each layer i, with $i = 1$ to L, the parameters h_i, α_i, β_i and ρ_i must be specified, where $h_i =$ thickness of the $i-$th layer, $\alpha_i = P-$wave velocity, $\beta_i = S-$wave velocity, and $\rho_i =$ density of the medium, with the bottom $(i = L)$ medium of infinite thickness.

In such a medium, surface waves will travel in a dispersive manner, and this will, in general, depend on (1) the material properties of the medium, (2) the frequency of the wave motion, and on (3) the thicknesses of different layers.

Through calculations for the group and phase velocities of the Rayleigh and Love surface waves, the dispersion curves can be evaluated. The results will be given for each mode of Rayleigh and Love surface waves separately, and will consist of phase and group velocities, $C_m(\omega_n)$ and $U_m(\omega_n)$, for a given set of selected frequencies, ω_n, $n = 1, 2, ..., N$.

2. Arrival Times

Once the dispersion curves have been computed, the arrival time of the $m-$th mode at frequency ω_n can be written as

$$t^*_{nm}(R) = R/U_m(\omega_n) \tag{1}$$

where, R is the epicentral distance from the source to the site. For computational efficiency, Equation (1) will be assumed to hold not only at frequency ω_n, but at a frequency band $\omega_n \pm \Delta\omega_n$, which is narrow enough for $U_m(\omega)$ to be assumed constant.

3. Contribution of the Modes at a Given Frequency Band

Within the frequency band $\omega_n \pm \Delta\omega_n$, the $m-$th mode of surface waves is assumed to have a Fourier transform

$$A_{nm}(\omega) = \begin{cases} \dfrac{\pi}{2} A_{nm} e^{-i\left[(\omega-\omega_n)t^*_{nm}+\phi_n\right]} & |\omega-\omega_n| \le \Delta\omega_n \\ 0 & \text{otherwise} \end{cases}$$
$$A_{nm}(-\omega) = A^*_{nm}(\omega) \tag{2}$$

where, ϕ_n is the phase. It is introduced to model the source randomness and other effects along the path. t^*_{nm} is the arrival time of the $m-$th mode given in Equation (1). A_{nm} is the relative amplitude of the $m-$th mode. The phase ϕ_n will be assumed to be a random number between $-\pi$ and π. The relative amplitude A_{nm} will be described in the next section.

The inverse transform of (2) is given by

$$a_{nm}(t) = \frac{1}{2\pi}\int_{-\infty}^{\infty} A_{nm}(\omega) e^{i\omega t} d\omega, \tag{3a}$$

which can be calculated to be

$$a_{nm}(t) = A_{nm}\frac{\sin\Delta\omega_n(t-t^*_{nm})}{(t-t^*_{nm})}\cos(\omega_n t+\phi_n) \tag{3b}$$

This represents the contribution of the $m-$th mode at the given frequency band. The total contribution of all the modes is then given by

$$a_n(t) = \sum_{m=1}^{M}\alpha_n a_{nm}(t) = \sum_{m=1}^{M}\alpha_n A_{nm}\frac{\sin\Delta\omega_n(t-t^*_{nm})}{(t-t^*_{nm})}\cos(\omega_n t+\phi_n), \tag{3c}$$

where, M is the total number of wave modes, and α_n is the scaling factor used to determine the final amplitude of $FS(\omega_n)$, as described in the next sub-section.

4. Determination of A_{nm} and α_n

Relative amplitudes of different modes of surface waves, A_{nm}, depend on the source mechanism and the propagation path, and are difficult to be estimated in a general case. Hence, it is useful to estimate these amplitudes empirically on the basis of previous acceleration recordings.

The following empirical equations for A_{nm} have been suggested by Trifunac (1971b)

$$A_{nm}(\omega_n) = A_1(m)A_2(\omega_n) \tag{4}$$

where,

$$A_1(m) = \left|\exp\left(-(m-m_0)^2/2C_0^2\right) + C_R X_m\right| \tag{5}$$

and

$$A_2(\omega_n) = \left|B_0\exp\left(-(\omega_n-\omega_p)^2/2\omega_B^2\right) + B_R X_n\right| \tag{6}$$

with X_m and X_n being random numbers between -1 and 1, and the values of other constants are suggested in Table 1.

Table 1: Empirical Scaling Coefficients for Equations (5) and (6) (from Trifunac, 1971a, 1971b)

Mode	C_0	m_o	C_R	B_0	ω_p	ω_B	B_R
1	3	5	0.2	1.5	10	5	0.1
2	3	5	0.2	1.5	10	5	0.1
3	3	5	0.2	1.5	10	5	0.1
4	3	5	0.2	2.0	25	15	0.1
5	3	5	0.2	2.0	25	15	0.1
6	3	6	0.2	3.0	30	10	0.3
7	3	7	0.2	1.5	30	5	0.25

The scaling factor α_n is next determined, by using the empirically determined Fourier amplitudes. The Fourier amplitude of $a_n(t)$ in Equation (3c) is given by

$$\left|A_n(\omega)\right| = \begin{cases} \left|\sum_{m=1}^{M} \frac{\pi}{2}\alpha_n A_{nm} \exp\left[-i\left((\omega-\omega_n)t_{nm}^* - \phi_n\right)\right]\right|, & \left|\omega-\omega_m\right| < \Delta\omega_n \\ 0 & \text{otherwise} \end{cases} \tag{7}$$

for $0 \le \omega < \infty$, and $\left|A_n(-\omega)\right| = \left|A_n(\omega)\right|$.

It is seen that the amplitude $\left|A_n(\omega)\right|$ is defined only over the narrow band of width $2\Delta\omega_n$. Its mean amplitude over this band is given by

$$\overline{\left|A_n(\omega)\right|} = \frac{1}{2\Delta\omega_n}\int_{\omega_n-\Delta\omega_n}^{\omega_n+\Delta\omega_n}\left|A_n(\omega)\right|d\omega \tag{8}$$

which should agree with the empirically estimated Fourier amplitude, $\hat{FS}(\omega_n)$,

$$\overline{\left|A_n(\omega)\right|} = \hat{FS}(\omega_n) \tag{9}$$

Combining Equations (7), (8) and (9), α_n becomes

$$\alpha_n = \frac{2\Delta\omega_n \hat{FS}(\omega_n)}{\frac{\pi}{2}\int_{\omega_n-\Delta\omega_n}^{\omega_n+\Delta\omega_n}\left|\sum_{m=1}^{M} A_{nm}\exp\left[-i\left((\omega-\omega_n)t_{nm}^* - \phi_n\right)\right]\right|d\omega} \tag{10}$$

The Fourier amplitude $\hat{FS}(\omega_n)$ at frequency ω_n may be estimated from empirical scaling equations, by using the earthquake parameters specified at the site. These parameters may include a suitable combination of the following: M = local magnitude M_L or surface wave magnitude M_S (Richter, 1958), R = epicentral distance, MMI = modified Mercalli intensity at the site, s = geological site classification (s = 0, 1 or 2), S_L = geotechnical site classification, h = depth of sediments, and v = component direction ($v = 0$: horizontal; $v = 1$: vertical).

5. The Total Accelerogram

The total accelerogram can be expressed as

$$a(t) = \sum_{n=1}^{N} a_n(t) \tag{11}$$

where, N is the total number of frequency bands. From Equation (3), (11) becomes

$$a(t) = \sum_{n=1}^{N} \left(\sum_{m=1}^{M} A_{nm} \frac{\sin \Delta\omega_n \left(t - t^*_{nm}\right)}{t - t^*_{nm}} \right) \alpha_n \cos\left(\omega_n t + \phi_n\right) \tag{12}$$

One final property, the duration or 'length' of $a(t)$, will be determined by using the empirical results on strong motion duration (Trifunac and Brady, 1975; Trifunac and Novikova, 1994) and the first and last arrival times of the waves.

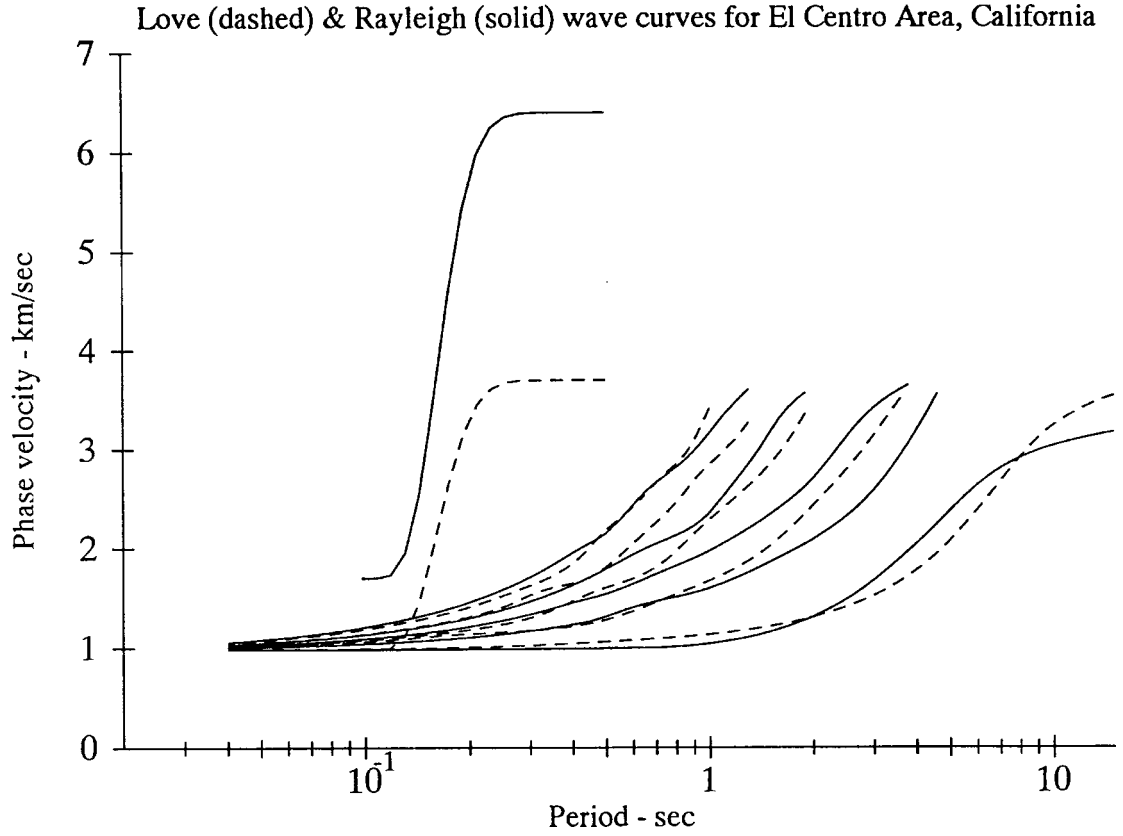

Fig. 1 Love and Rayleigh waves curves for El Centro Area, California: phase velocity

6. Example of Synthetic Accelerograms

To illustrate synthetic accelerograms, we choose the site at Westmoreland in Imperial Valley, California. Dispersion curves for this site were computed assuming the properties of layered medium in Table 2.

Table 2: Properties of the Layered Medium Adopted to Represent the Site Properties in the Area of Westmoreland in Imperial Valley, California

Layer #	Depth (km)	P-Wave Velocity (km/sec)	S-Wave Velocity (km/sec)	Density (gm/cm^3)
1	0.18	1.70	1.98	1.28
2	0.55	1.96	1.13	1.36
3	0.98	2.71	1.57	1.59
4	1.19	3.76	2.17	1.91
5	2.68	4.69	2.71	2.19
6	∞	6.40	3.70	2.71

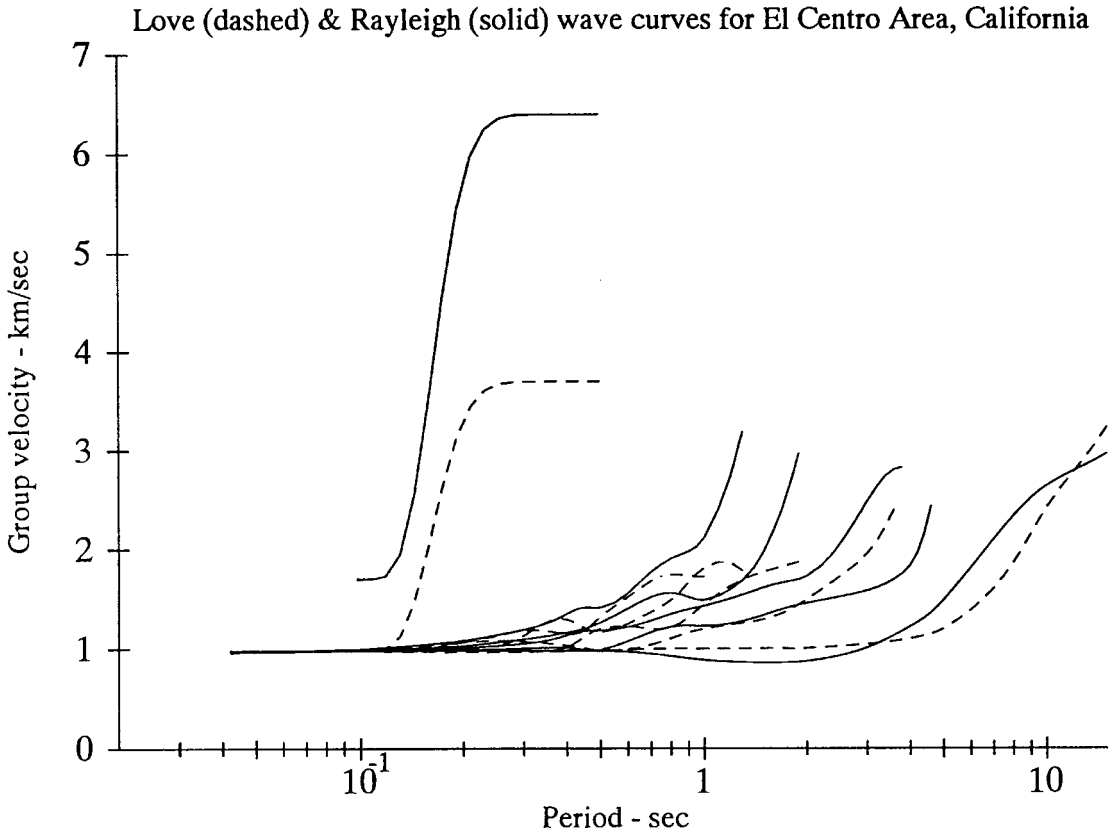

Fig. 2 Love and Rayleigh waves curves for El Centro Area, California: group velocity

Figure 1 shows the Rayleigh- and Love-wave phase velocities (in km/sec) versus the period of the waves (in seconds). The 5 solid curves are for the first 5 modes of the Rayleigh waves. Mode 1 is the rightmost solid curve, and mode 5 is next to the leftmost solid curve, with the intermediate modes in between. The same holds for the modes of Love waves. At low periods, all the curves approach the minimum $S-$wave velocity (0.98 km/s at this site). Figure 2 shows the corresponding group velocity curves. The two curves at the extreme left in Figures 1 and 2 approximately model the arrival of the wave components associated with the incident P and S waves.

The following earthquake parameters are chosen for this site, as input for the computer program SYNACC (Wong and Trifunac, 1978): earthquake magnitude, $M = 6.5$, epicentral distance, D = 10.0 km, confidence level, $p = 0.5$, site condition, s = 0 (alluvium), and component direction, v = 0 (horizontal).

Figure 3 shows a plot of the synthetic translational acceleration, and the velocity and displacement time-histories calculated from it. Figure 4 presents the corresponding response and Fourier spectra.

THE TORSIONAL COMPONENT OF EARTHQUAKE GROUND MOTIONS

The importance of torsional and rocking excitations has been indicated by the studies of Dravinski and Trifunac (1979, 1980), Kobori and Shinozaki (1975), Luco (1976), Bielak (1978), Lee (1979), Gupta and Trifunac (1987, 1988, 1990a, 1990b, 1990c, 1991), Todorovska and Lee (1989), and Todorovska and Trifunac (1989, 1990a, 1990b, 1992, 1993). With the slow development of strong-motion instruments that record rotational components of strong motions (Hudson, 1983; Trifunac and Todorovska, 2001), it becomes necessary to explore the possibility of estimating those in terms of the corresponding translational components of strong shaking.

By considering the horizontal propagation of plane waves with constant velocity C, Newmark (1969) estimated the contribution to the displacements of building foundation, resulting from torsional earthquake ground motions. Tso and Hsu (1978) used a similar approach, in addition to assuming that the motions also included plane non-dispersive waves. Nathan and MacKenzie (1975) discussed the possible

averaging effects of foundation sizes on the resulting torsional excitations of buildings. These investigations, however, failed to consider the dependence of the phase velocity on the frequencies of the incoming Love waves. Their assumption that the incoming waves are of constant phase velocity at all frequencies, makes their results useless. Lee and Trifunac (1985) included the effects of wave dispersion and transient arrivals in the estimation of torsional accelerograms in an elastic layered half-space. The earlier work of Trifunac (1982) in calculating the torsional component of incident plane SH-waves was extended to enable the calculation of torsion from surface Love waves.

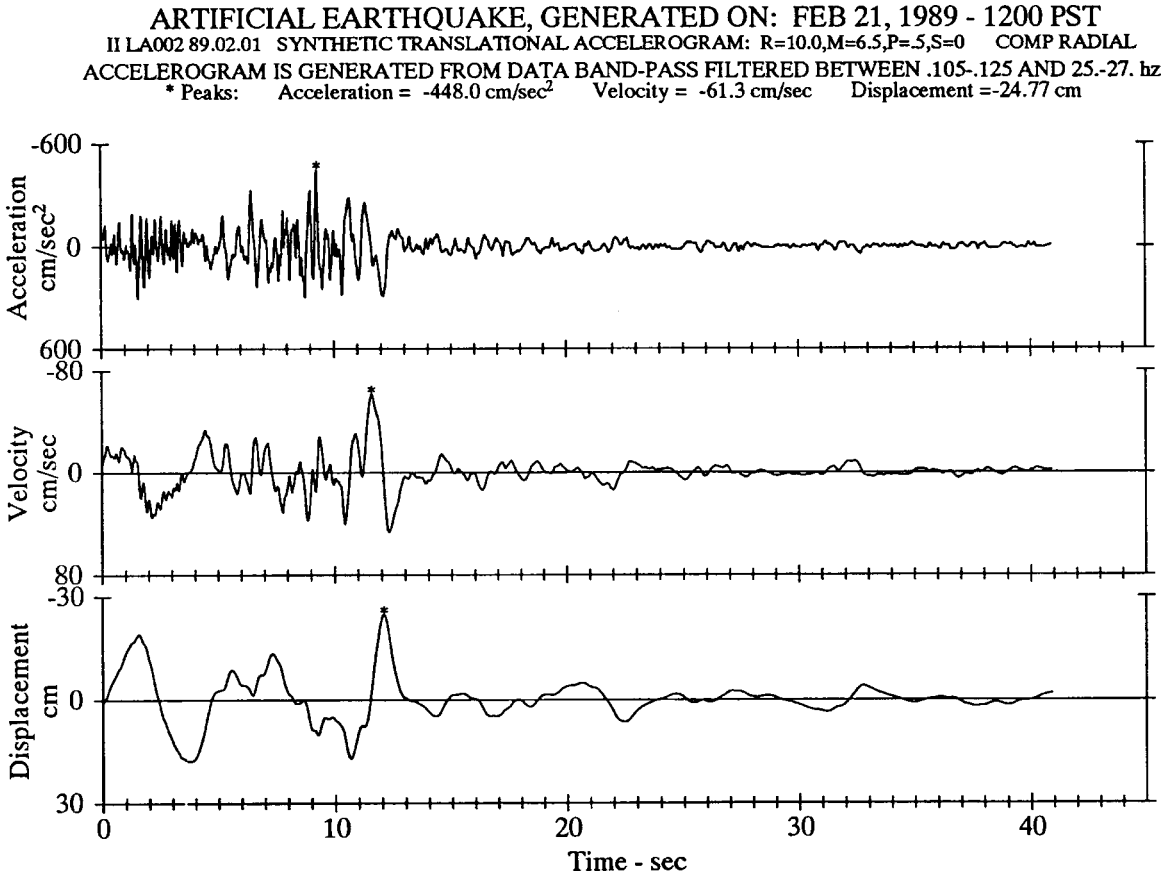

Fig. 3 Artificial earthquake synthetic translational accelerogram

1. The Torsional Motion of Incident Waves

Figure 5 shows the rectangular coordinate system (x_1, x_2, x_3) with the incident and reflected plane SH-waves, in the presence of the stress-free boundary $(x_2 = 0)$, at the surface of the elastic, homogeneous and isotropic half space $(x_2 \le 0)$. The particle motions of the waves are in the x_3 – direction.

The incident SH-wave is assumed to have amplitude A_0 and angle of incidence θ_0 (Figure 5). The reflected wave will also have amplitude A_0 and the same angle of reflection θ_0. The resulting motion is

$$\begin{aligned} u_3 &= \left[A_0 e^{ik(x_1 \sin\theta_0 + x_2 \cos\theta_0)} + A_0 e^{ik(x_1 \sin\theta_0 - x_2 \cos\theta_0)}\right] e^{-i\omega t} \\ &= 2A_0 \cos(kx_2 \cos\theta_0) e^{ikx_1 \sin\theta_0} e^{-i\omega t} \end{aligned} \tag{13}$$

with ω being the frequency of the incoming wave, with velocity β, and $k = \omega/\beta$, the corresponding wave number. The torsional component of motion associated with the SH-waves at the half-space surface $(x_2 = 0)$ is (Trifunac, 1982):

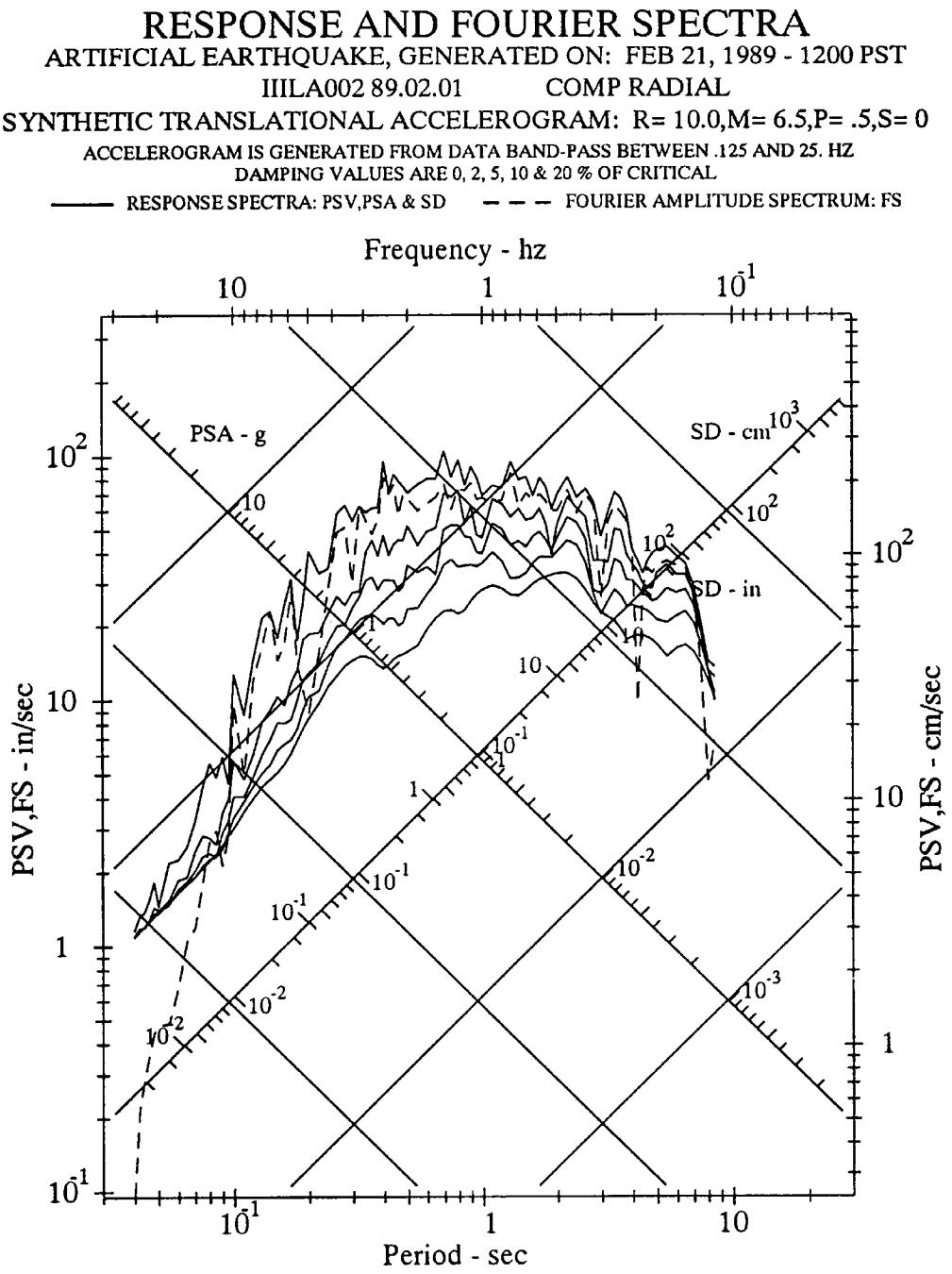

Fig. 4 Artificial earthquake synthetic translational response and Fourier spectra

$$
\begin{aligned}
\psi_{13}\big|_{x_2=0} &= \left(\frac{1}{2}\tilde{\Delta}\times\tilde{u}\right)\times\hat{e}_2 = -\frac{1}{2}\frac{\partial u_3}{\partial x_1} \\
&= -A_0 ik\sin\theta_0 e^{ikx_1\sin\theta_0} \\
&= -\frac{1}{2}ik\sin\theta_0 u_3 \\
&= \frac{k\sin\theta_0}{2}u_3 e^{-i\pi/2}
\end{aligned}
\tag{14}
$$

It is seen that the torsional motion has a phase shift of $-\pi/2$ relative to the translational motion. From Equation (14), one can define the amplitude ratio,

$$\left|\frac{\psi_{13}}{u_3}\right| = \frac{k\sin\theta_0}{2} = \frac{1}{2}\frac{\omega}{\beta}\sin\theta_0 = \frac{1}{2}\frac{\omega}{c_x} \tag{15}$$

where, $c_x = \beta/\sin\theta_0$ is the phase velocity in the horizontal (x_1) direction. Including the phase shift, Equation (14) can be rewritten as

$$\psi_{13}\Big|_{x_2=0} = \frac{1}{2}\frac{\omega}{c_x}u_3 e^{-i\pi/2} \tag{16}$$

which shows that at the ground surface $(x_2 = 0)$, the amplitude of torsional motion increases linearly with frequency, ω.

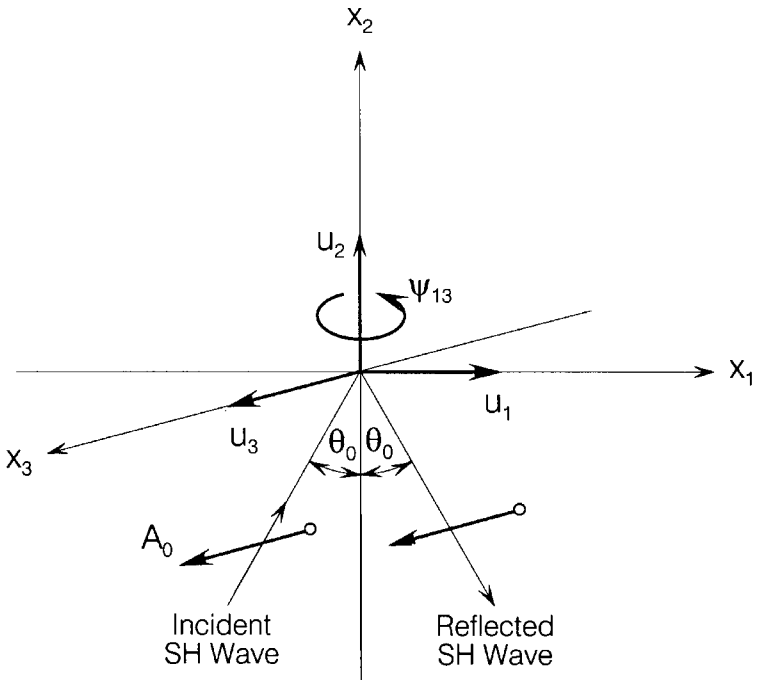

Fig. 5 Incident SH wave on half-space

2. Estimation of Synthetic Torsional Motion

Recording of the rotational components of strong motion is at present limited only to a few experimental programs (Shibata et al., 1976; Trifunac and Todorovska, 2001). It is not very likely that a significant amount of such data will, in the near future, be available for empirical and theoretical analyses. It thus becomes necessary to explore the possibility of estimating torsional acceleration in terms of the corresponding translational components of strong motion, along with the information on the types and the direction of approach of the incident waves.

Expressing the strong earthquake translational ground motion in terms of the Fourier amplitude spectrum, the Fourier amplitude spectrum of the corresponding torsional motion can be estimated by using Equation (16). By employing this result in conjunction with the method for the synthesis of artificial translational accelerograms, as described in the previous section, the complete time-history of synthetic torsional motion can be constructed.

From Equation (2), the $m-$th mode of surface waves, within the frequency band $\omega_n \pm \Delta\omega_n$, has the Fourier transform of the translational motion given by

$$A_{nm}(\omega) = \begin{cases} \dfrac{\pi}{2} A_{nm} e^{-i\left[(\omega-\omega_n)t^*_{nm}+\phi_0\right]} & |\omega-\omega_n| \le \Delta\omega_n \\ 0 & \text{otherwise} \end{cases}$$

and (17)

$$A_{nm}(-\omega) = A^*_{nm}(\omega)$$

The corresponding Fourier transform of the rotational motion is thus given by

$$\Psi_{nm}(\omega)=\begin{cases}\dfrac{\omega\pi}{4C_{nm}}A_{nm}e^{-i\left[(\omega-\omega_n)t^*_{nm}+\phi_n+\pi/2\right]} & |\omega-\omega_n|\le\Delta\omega_n\\ 0 & \text{otherwise}\end{cases} \tag{18}$$

where, $C_{nm}=C_m(\omega_n)$ is the phase velocity of the $m-$th mode of surface Love waves, assumed to be constant within the frequency band $\omega_n\pm\Delta\omega_n$. The total contribution from all the modes of Love waves to the rotational motion in this frequency band is

$$\Psi_n(\omega)=\begin{cases}\dfrac{\alpha_n\omega\pi}{4}\sum_{m=1}^{M}\dfrac{A_{nm}}{C_{nm}}e^{-i\left[(\omega-\omega_n)t^*_{nm}+\phi_n+\pi/2\right]} & |\omega-\omega_n|\le\Delta\omega_n\\ 0 & \text{otherwise}\end{cases} \tag{19}$$

where, α_n is the scaling factor, as given in Equation (10).

The total Fourier transform of the rotational accelerogram is then given by

$$\Psi(\omega)=\sum_{n=1}^{N}\Psi_n(\omega) \tag{20}$$

where, N is the total number of frequency bands considered. The ratio of the Fourier amplitude of the rotational acceleration to that of the translational motion thus takes the form

$$\left|\frac{\Psi(\omega)}{A(\omega)}\right|=\left|\frac{\Psi_n(\omega)}{A_n(\omega)}\right| \tag{21}$$

for the frequencies within the frequency band $\omega_n\pm\Delta\omega_n$. On simplifying, Equation (21) takes the form

$$\left|\frac{\Psi(\omega)}{A(\omega)}\right|=\frac{\omega}{2}\left|\frac{\sum_{m=1}^{M}\dfrac{A_{nm}}{C_{nm}}e^{-(\omega-\omega_n)t^*_{nm}}}{\sum_{m=1}^{N}A_{nm}e^{-(\omega-\omega_n)t^*_{nm}}}\right|;\ |\omega-\omega_n|\le\Delta\omega_n \tag{22}$$

and, in particular for $\omega=\omega_n$,

$$\left|\frac{\Psi(\omega)}{A(\omega)}\right|_{\omega=\omega_n}=\frac{\omega_n}{2}\frac{\sum_{m=1}^{M}A_{nm}/C_{nm}}{\sum_{m=1}^{M}A_{nm}} \tag{23}$$

An asymptotic expansion of Equation (23) for large and small frequencies is possible. At the high-frequency end, the phase velocities of all modes of surface waves approach $\beta_{\min}$, the minimum shear wave velocity in the layered model. Thus

$$\left|\frac{\Psi(\omega)}{A(\omega)}\right|\sim\frac{\omega_n}{2}\left|\frac{\sum_{m=1}^{M}A_{nm}/\beta_{\min}}{\sum_{m=1}^{M}A_{nm}}\right|=\frac{\omega_n}{2\beta_{\min}} \tag{24}$$

$$\text{as } \omega_n\to\infty$$

At the low-frequency end, essentially the only mode present in the layered model is the first mode, and its phase velocity approaches $\beta_{\max}$, the maximum shear wave velocity in the layered medium. Thus,

$$\left|\frac{\Psi(\omega)}{A(\omega)}\right|\sim\frac{\omega_n}{2}\left|\frac{A_{n1}/\beta_{\max}}{A_{n1}}\right|=\frac{\omega_n}{2\beta_{\max}} \tag{25}$$

$$\text{as } \omega_n\to 0$$

It is noted that from the dimensional analysis point of view, Equations (24) and (25) agree with the equations proposed by Newmark (1969). However, it is seen that the "velocity" representing the overall

average trend of the ratio $|\Psi(\omega)/A(\omega)|$ is not constant. It changes from $\beta_{min}\,(\text{for } \omega \to \infty)$ to $\beta_{max}\,(\text{for } \omega \to 0)$, the velocity in the half-space beneath the surface layers.

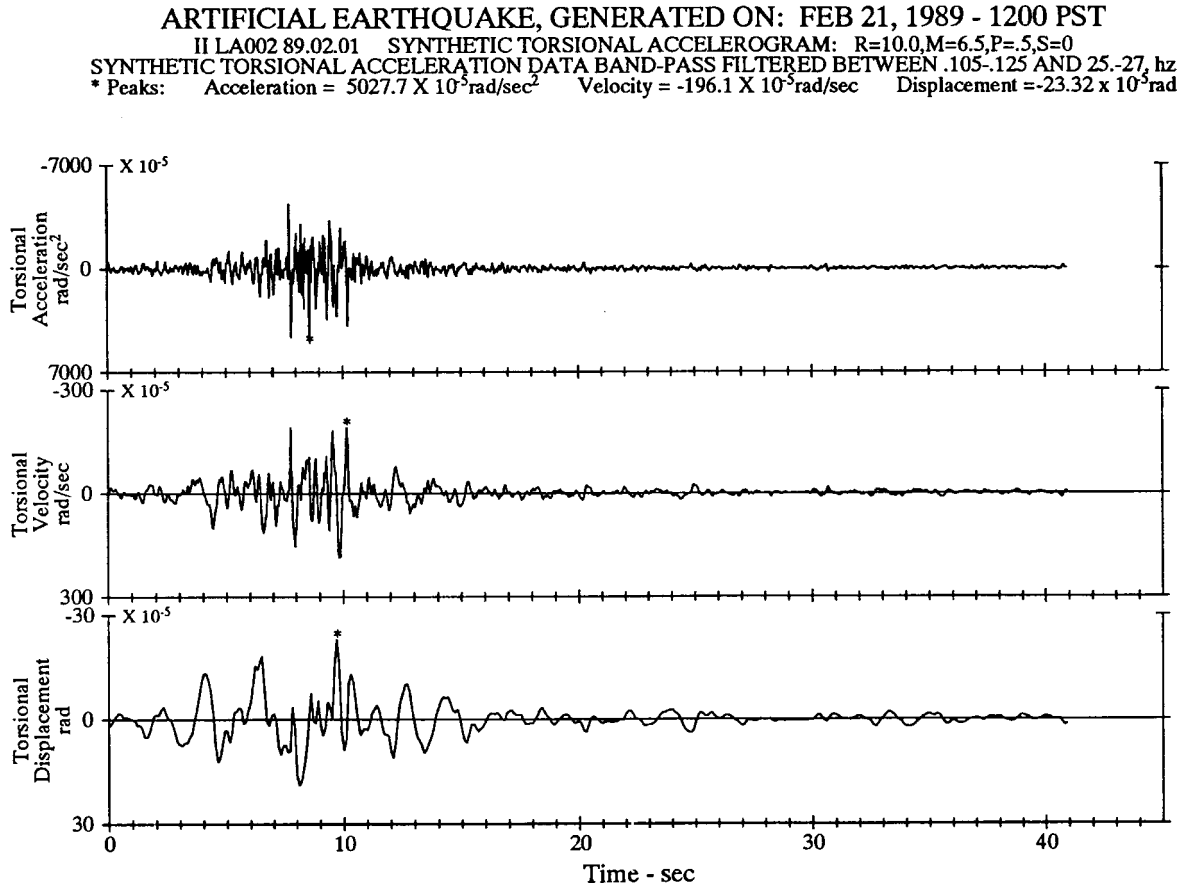

Fig. 6 Artificial earthquake synthetic torsional accelerogram

3. Examples of Synthetic Torsion

Following the analysis in the previous sections, one can generate the translational (horizontal and vertical) and torsional accelerograms simultaneously. For illustration, the same site at Westmoreland in Imperial Valley is used, as in Sub-section 6 of the previous section. Thus, the same dispersion curves for this site are used here.

Figure 6 gives a plot of the synthetic torsional acceleration, velocity and displacement, with units in rad/s^2, rad/s and rad, respectively. Figure 7 presents the corresponding torsional response and Fourier spectra. As in the case of the response spectra for the translational accelerogram, the torsional response spectra represent the maximum torsional response of single-degree-of-freedom systems of specified natural periods and damping ratios, when subjected to the torsional accelerogram as input. The units for torsional displacement, SD, pseudo relative velocity, PSV, and relative pseudo acceleration, PSA, are rad, rad/s, and rad/s^2, respectively.

Figure 8 shows the ratio of torsional to translational response for different periods and damping ratios. As indicated by Equation (16), the ratio is high at the high-frequency (short-period) end, and decreases almost linearly towards the low-frequency (long-period) end. The Fourier spectrum (dashed line) also starts out with the large ratio at the high-frequency end, and progressively decreases to the small ratios at the low-frequency (long-period) end. The five solid curves correspond to the damping values of 0, 2, 5, 10 and 20% of critical. At the high-frequency end, the zero damping curve has a higher ratio than the 2, 5, 10 and 20% curves. The ratios for all five damping ratios decrease progressively with decreasing frequency (increasing period), with the order of the ratios switched at the low-frequency end, so that the 20% damping curve ends up with the highest ratio, followed by 10%, 5%, 2% and 0% curves, with the ratio for the Fourier spectrum being the lowest on average.

Figure 9 shows the ratios of torsional to translational Fourier spectrum amplitudes, as calculated from Equation (23). The dashed line joining the high- and low-frequency asymptotic limits, connects the amplitudes given by Equations (24) and (25). Comparison with Figure 8 shows that this straight line approximates the overall trend of the ratios of torsional to translational spectral amplitudes very well.

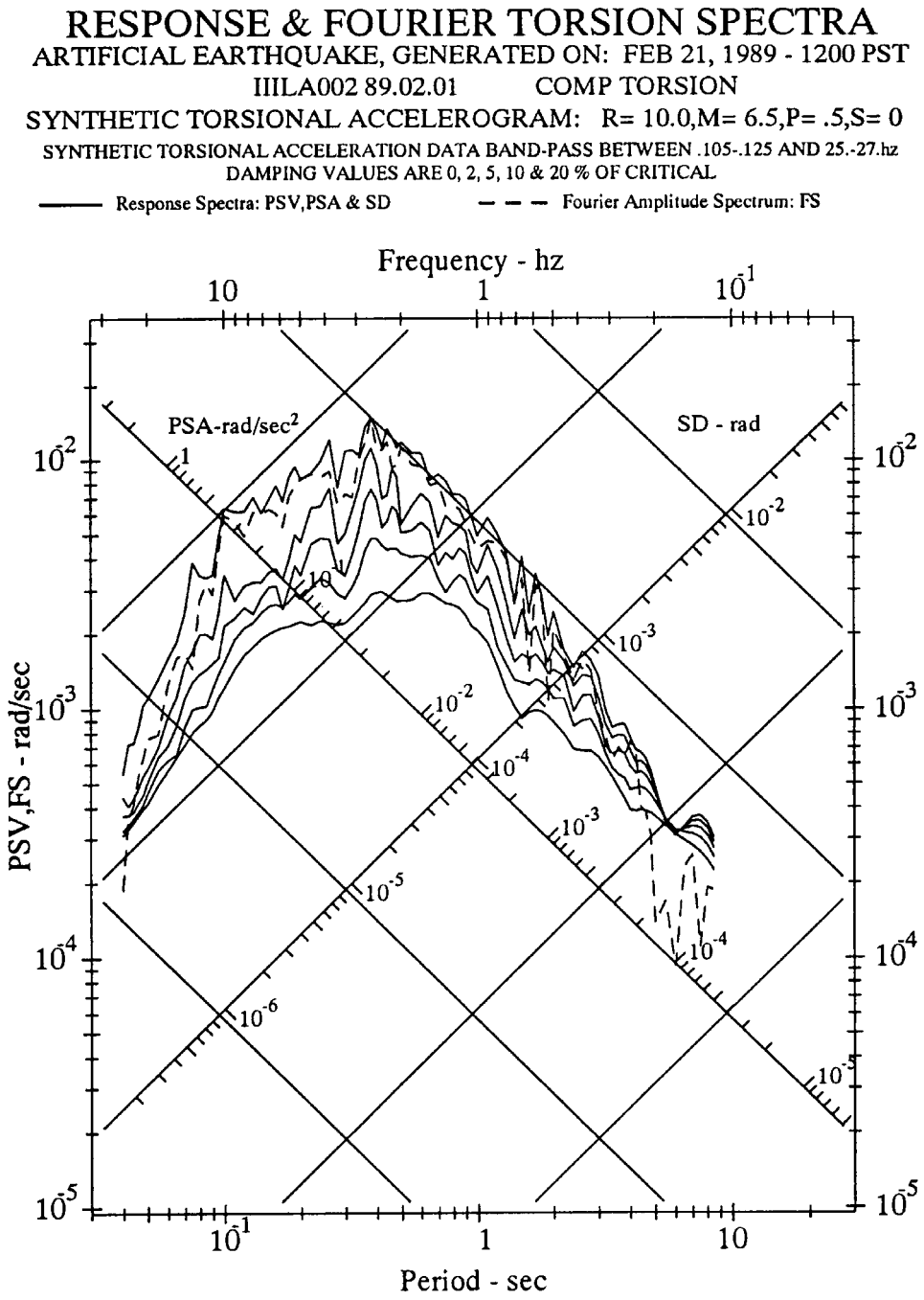

Fig. 7 Artificial earthquake synthetic torsional response and Fourier spectra

THE ROCKING COMPONENT OF STRONG EARTHQUAKE GROUND MOTION

The rotational components of strong earthquake ground motions have been studied by a number of investigators since the 1970's (Lee, 1979; Trifunac, 1982). Yim et al. (1980), and Koh and Spanos (1984) studied the rocking response of rigid structures to strong ground motion. Ishiyama (1982) investigated the motions and overturning of a rigid body in response to earthquake excitations, both experimentally and theoretically. Psycharis (1983) studied the rocking, toppling and uplift of flexible structures due to earthquake motions. Similar studies were carried out by Kato et al. (1984), and by Baba and Nakashima (1984).

As in the case of torsional motions, the development of strong-motion instruments to record the rocking components of earthquake ground motions is slow. It is again necessary to estimate these motions in terms of the corresponding translational components of strong shaking. For this purpose, the earlier work of Trifunac (1982) on calculating the rocking angles associated with incident plane P- and SV-waves was extended by Lee and Trifunac (1987) to calculate the rocking component of motion associated with incoming P-, SV- and Rayleigh waves.

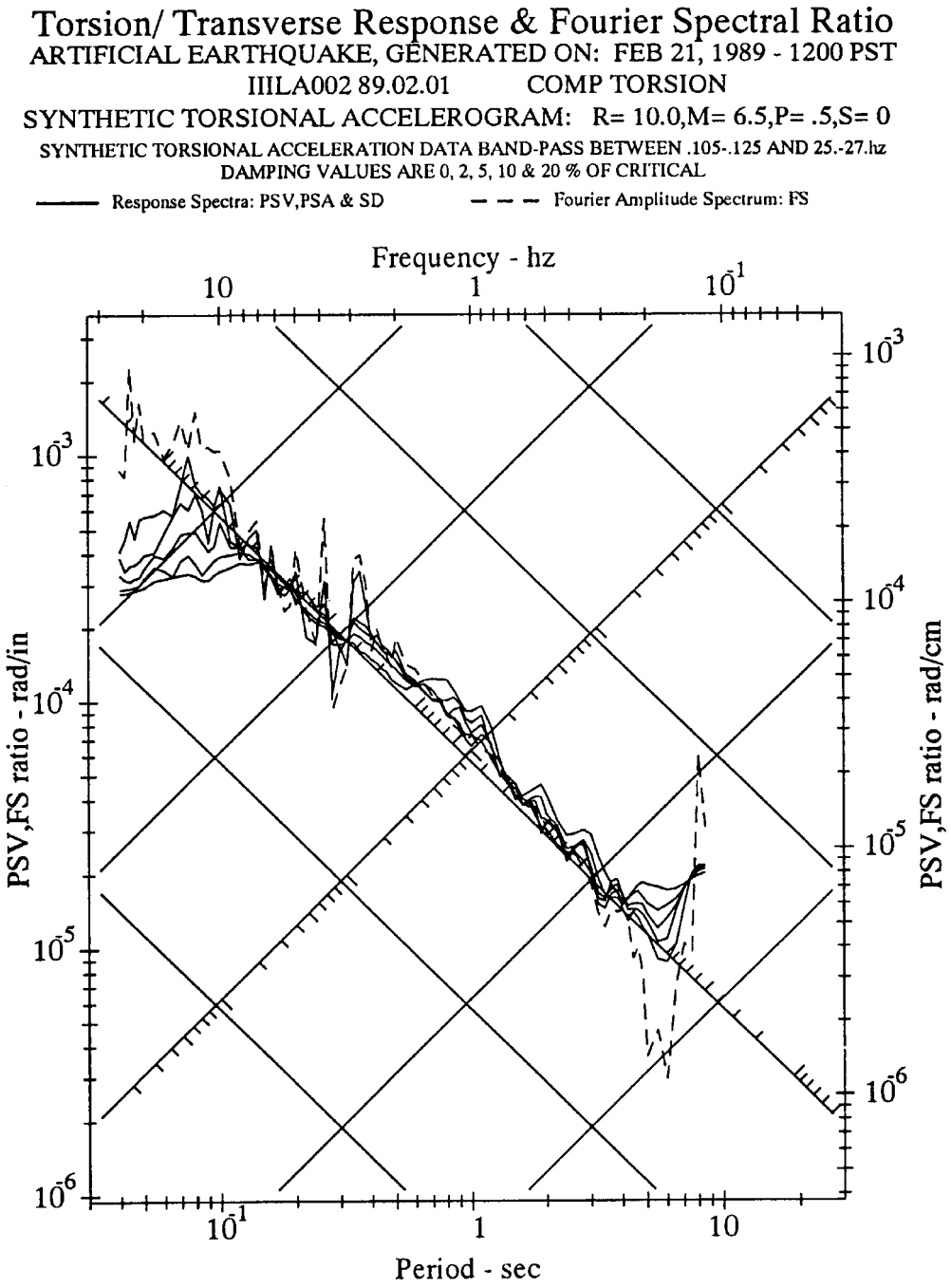

Fig. 8 Artificial earthquake synthetic torsion/transverse response and Fourier spectral ratio

1. The Rocking Motion Associated with Incident Waves

The following describes estimation of the rocking component from the known translational components of motion. Estimating the rocking from incident P- and SV-waves has been reviewed by Trifunac (1982).

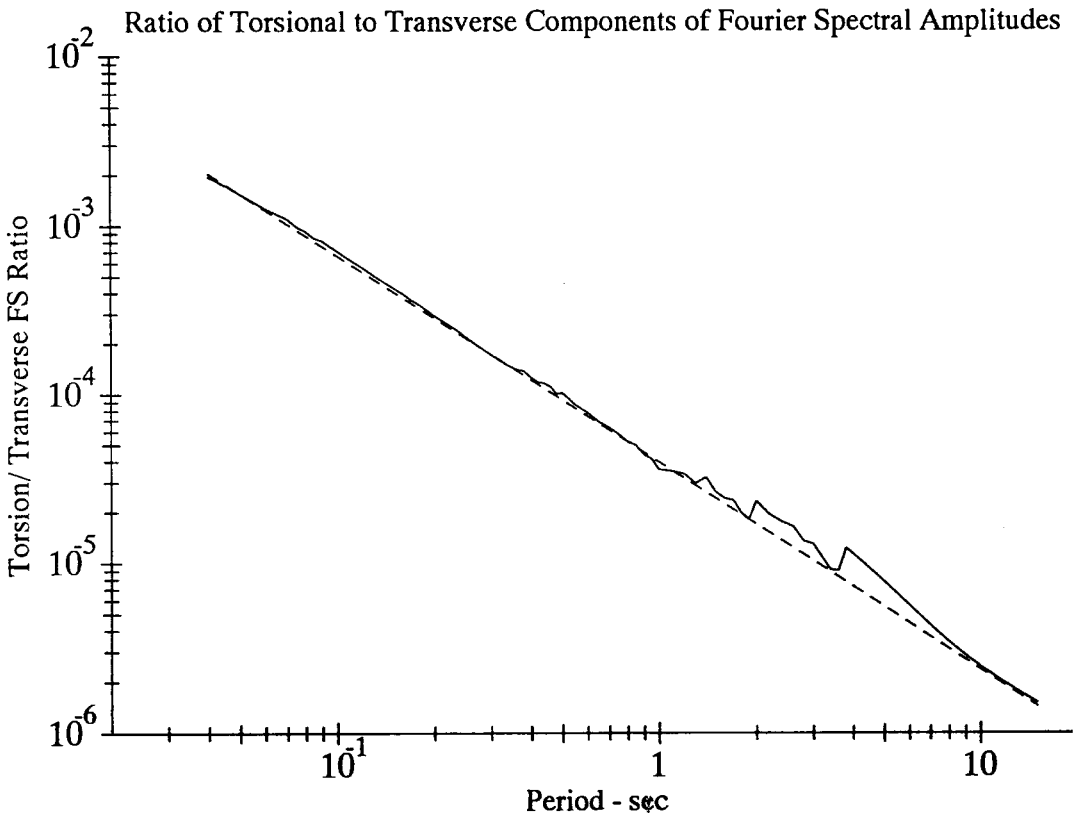

Fig. 9 Artificial earthquake synthetic torsion/transverse Fourier spectral ratio

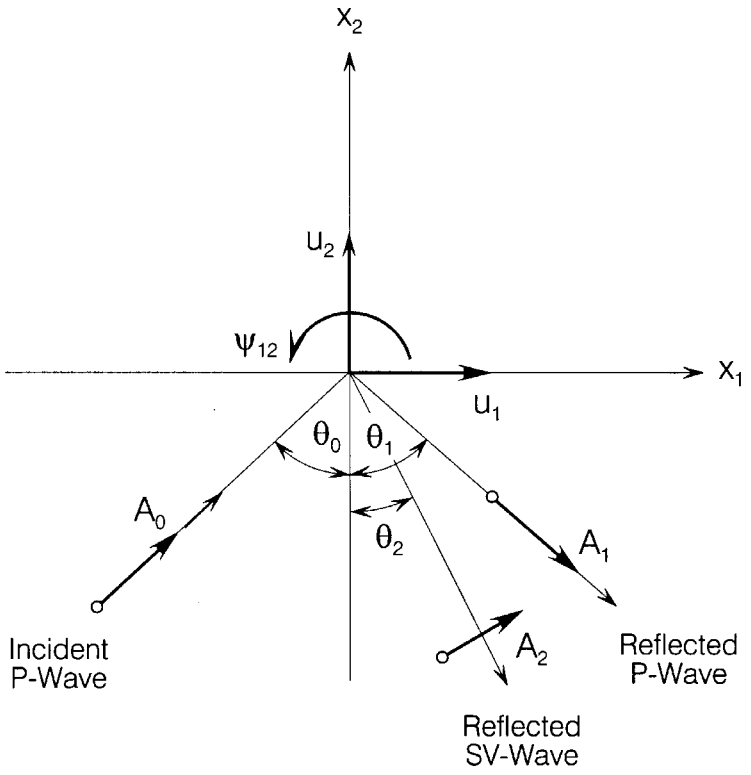

Fig. 10 Incident P-wave on half-space

1.1 Incident P-Waves

Figure 10 shows the coordinate system (x_1, x_2) and the incident and reflected rays associated with incident plane P-waves in an elastic homogeneous and isotropic half-space $(x_2 \le 0)$. The amplitudes of the incident and reflected P-waves, and reflected SV-waves are A_0, A_1, and A_2, respectively. Two components of motion at the surface $(x_2 = 0)$ are

$$u_1 = \left(A_0 \sin\theta_0 + A_1 \sin\theta_1 + A_2 \cos\theta_2\right) \exp\left[i\left(k_\alpha x_1 \sin\theta_0 - \omega t\right)\right] \tag{26}$$

$$u_2 = \left(A_0 \cos\theta_0 - A_1 \cos\theta_1 + A_2 \sin\theta_2\right) \exp\left[i\left(k_\alpha x_1 \sin\theta_0 - \omega t\right)\right] \tag{27}$$

and the rocking component about the x_3 – direction is given by

$$\psi_{12} = \frac{1}{2}\left(\frac{\partial u_2}{\partial x_1} - \frac{\partial u_1}{\partial x_2}\right) = \frac{i}{2} A_2 k_\beta \exp\left[i\left(k_\alpha x_1 \sin\theta_0 - \omega t\right)\right] \tag{28}$$

where, k_α and k_β are

$$k_\alpha = \omega/\alpha, \quad k_\beta = \omega/\beta \tag{29}$$

with ω being the circular frequency, and α and β, the respective velocities of P- and SV-waves. In the above and subsequent equations, t represents time and $i \equiv \sqrt{-1}$. Trifunac (1982) further showed that

$$\left|\psi_{12}/u_2\right| = \left(\beta/\alpha\right)\left(\omega/C_\alpha\right) \tag{30}$$

thus expressing rocking in terms of the translation, u_2. Here, C_α is the horizontal phase velocity.

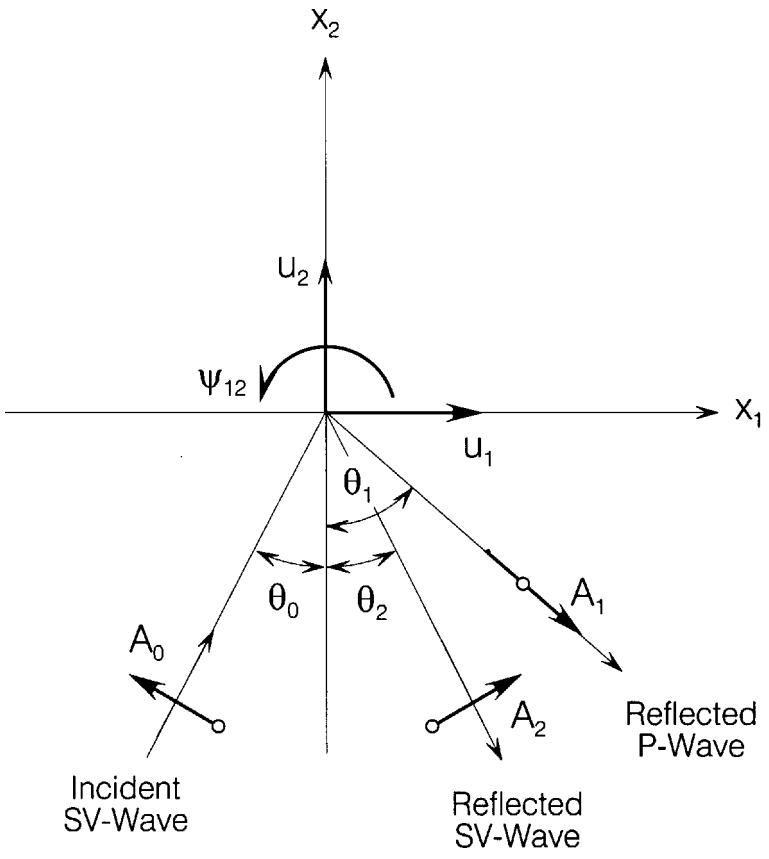

Fig. 11 Incident SV-wave on half-space

1.2 Incident SV-Waves

Figure 11 shows the coordinate system (x_1, x_2) and the incident and reflected rays associated with plane SV-waves. The amplitudes of the incident SV-waves and reflected P- and SV-waves are A_0, A_1 and A_2, respectively. The two translational, u_1 and u_2, and rocking, ψ_{12}, components of motions are

$$u_1 = \left(-A_0 \cos\theta_0 + A_1 \sin\theta_1 + A_2 \cos\theta_2\right) \exp\left[i\left(k_\beta x_1 \sin\theta_0 - \omega t\right)\right] \tag{31a}$$

$$u_2 = \left(A_0 \sin\theta_0 - A_1 \cos\theta_1 + A_2 \sin\theta_2\right) \exp\left[i\left(k_\beta x_1 \sin\theta_0 - \omega t\right)\right] \tag{31b}$$

and

$$\psi_{12} = \frac{1}{2}\left(\frac{\partial u_2}{\partial x_1} - \frac{\partial u_1}{\partial x_2}\right) = \frac{ik_\beta}{2}\left(A_0 + A_2\right) \exp\left[i\left(k_\beta x_1 \sin\theta_0 - \omega t\right)\right] \tag{32}$$

The ratio,

$$\left|\psi_{12}/u_2\right| = \omega/C_\alpha \tag{33}$$

gives the rocking component ψ_{12} in terms of the translational component u_2.

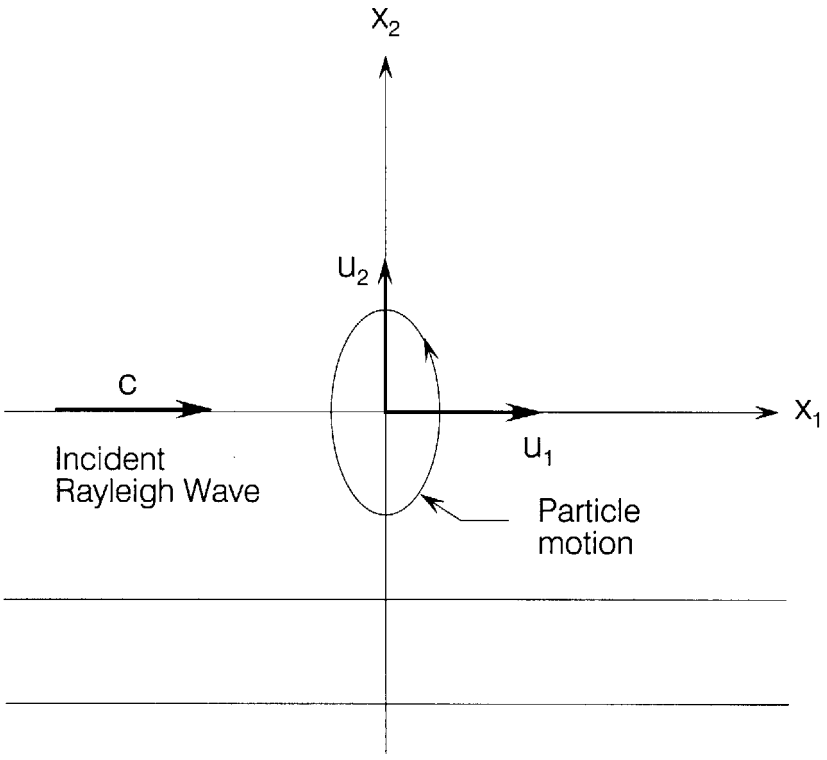

Fig. 12 Incident Rayleigh wave on half-space

1.3 Rayleigh Waves

Figure 12 shows the coordinate system (x_1, x_2) for the half-space with L layers, with the last (L-th) layer extending to $x_2 = -\infty$. Using Lamé potentials, Φ and Ψ, the Rayleigh waves in the top layer are given by

$$\Phi = \left[A_1 \exp(ikrx_2) + A_2 \exp(-ikrx_2)\right] \exp(ik(x_1 - ct)) \tag{34a}$$

and

$$\Psi = \left[B_1 \exp(iksx_2) + B_2 \exp(-iksx_2)\right] \exp(ik(x_1 - ct)) \tag{34b}$$

where, $k = \omega/c$ is the wave number, c is the phase velocity in the x_1 – direction, A_1, A_2, B_1 and B_2, are the amplitudes to be determined, and r and s are defined by

$$r^2 = \left(c^2/\alpha^2 - 1\right) \tag{35a}$$

$$s^2 = \left(c^2/\beta^2 - 1\right) \tag{35b}$$

The two components of displacement are given by

$$u_1 = \frac{\partial \Phi}{\partial x_1} + \frac{\partial \Psi}{\partial x_2} \tag{36a}$$

and

$$u_2 = \frac{\partial \Phi}{\partial x_2} - \frac{\partial \Psi}{\partial x_1} \tag{36b}$$

Using Equations (34a) and (34b), this gives

$$u_1 = ik\left[A_1 \exp(ikrx_2) + A_2 \exp(-ikrx_2) + sB_1 \exp(iksx_2) - sB_2 \exp(-iksx_2)\right]\exp(ik(x_1 - ct)) \tag{37a}$$

and

$$u_2 = ik\left[rA_1 \exp(ikrx_2) - rA_2 \exp(-ikrx_2) + B_1 \exp(iksx_2) - B_2 \exp(-iksx_2)\right]\exp(ik(x_1 - ct)) \tag{37b}$$

From

$$\frac{\partial u_1}{\partial x_2} = -k^2\left[rA_1 \exp(ikrx_2) - rA_2 \exp(-ikr_2) + s^2 B_1 \exp(iksx_2) + s^2 B_2 \exp(-iksx_2)\right]* \exp(ik(x_1 - ct)) \tag{38a}$$

and

$$\frac{\partial u_2}{\partial x_1} = -k^2\left[rA_1 \exp(ikrx_2) - rA_2 \exp(-ikrx_2) - B_1 \exp(iksx_2) - B_2 \exp(-iksx_2)\right]* \exp(ik(x_1 - ct)) \tag{38b}$$

the rocking component is

$$\psi_{12} = \frac{1}{2}\left(\frac{\partial u_2}{\partial x_1} - \frac{\partial u_1}{\partial x_2}\right) = \frac{k^2\left(1 + s^2\right)}{2} \times \left[B_1 \exp(iksx_2) + B_2 \exp(-iksx_2)\right]\exp(ik(x_1 - ct)) \tag{39}$$

At the surface of the half-space $(x_2 = 0)$, this reduces to

$$\psi_{12} = \frac{k^2\left(1 + s^2\right)}{2}(B_1 + B_2)\exp(ik(x_1 - ct)) \tag{40}$$

Equation (40) can be simplified further. The potentials Φ and Ψ in Equation (34) also satisfy the stress-free boundary conditions at the surface of the half-space $(x_2 = 0)$:

$$\sigma_{22} = \sigma_{12} = 0 \tag{41}$$

where, σ_{22} is the normal stress, and σ_{12} is the shear stress. Those are given by

$$\sigma_{22} = \lambda\Delta^2\Phi + 2\mu\frac{\partial^2 \Phi}{\partial x_2^2} - 2\mu\frac{\partial^2 \Psi}{\partial x_1 \partial x_2} \tag{42a}$$

and

$$\sigma_{12} = 2\mu\frac{\partial^2 \Phi}{\partial x_1 \partial x_2} + \mu\left(\frac{\partial^2 \Phi}{\partial x_2^2} - \frac{\partial^2 \Psi}{\partial x_1^2}\right) \tag{42b}$$

with λ and μ being the Lamé constants. Using the expressions for Φ and Ψ in Equation (34) to calculate σ_{12} and setting it to zero at $x_2 = 0$ gives

$$-2r(A_1 - A_2) + (1 - s^2)(B_1 + B_2) = 0 \tag{43}$$

Also, from Equation (37), the displacement u_2 at $x_2 = 0$ is

$$u_2\big|_{x_2=0} = ik(r(A_1 - A_2) - (B_1 + B_2)) \tag{44}$$

Combining Equations (43) and (44) gives

$$u_2\Big|_{x_2=0} = \frac{-ik}{2}(1 + s^2)(B_1 + B_2)\exp(ik(x_1 - ct)) \tag{45}$$

from which the rocking at the surface $(x_2 = 0)$ is (see Equation (40)):

$$\psi_{12} = iku_2 = i\omega u_2 / c \tag{46}$$

This is a very simple result, as in the case of incident P-waves (Equation (30)) or incident SV-waves (Equation (33)). Equation (46) will be used in conjunction with our method for the synthesis of artificial translational accelerograms to construct the time-history of rocking.

The simple relations between rocking ψ_{12} and displacement u_2 in all of the above three cases (plane P-, SV-waves, and surface Rayleigh waves) is a consequence of a more fundamental principle satisfied by elastic waves in general. Starting with the Φ and Ψ potentials, the two components of displacement, u_1 and u_2, are given by Equation (36). At the surface of the half space $(x_2 = 0)$, the boundary condition $\sigma_{12} = 0$ implies that (Equation (42))

$$2\frac{\partial^2 \Phi}{\partial x_1 \partial x_2} + \frac{\partial^2 \Psi}{\partial x_2^2} - \frac{\partial^2 \Psi}{\partial x_1^2} = 0 \tag{47a}$$

or

$$\frac{\partial}{\partial x_2}\left(\frac{\partial \Phi}{\partial x_1} + \frac{\partial \Psi}{\partial x_2}\right) + \frac{\partial}{\partial x_1}\left(\frac{\partial \Phi}{\partial x_2} - \frac{\partial \Psi}{\partial x_1}\right) = 0 \tag{47b}$$

so that Equation (36) shows that this is equivalent to

$$\left(\frac{\partial u_1}{\partial x_2} + \frac{\partial u_2}{\partial x_1}\right)\Big|_{x_2=0} = 0 \tag{48}$$

The rocking ψ_{12} at the surface $(x_2 = 0)$ then becomes

$$\psi_{12} = \frac{1}{2}\left(\frac{\partial u_2}{\partial x_1} - \frac{\partial u_1}{\partial x_2}\right) = \frac{\partial u_2}{\partial x_1} = -\frac{\partial u_1}{\partial x_2} \tag{49}$$

Thus, if the waves have the displacement u_2 given by

$$u_2 = f(x_2)\exp(ik(x_1 - ct)) \tag{50}$$

for a general function $f(x_2)$, such that the wave equations are satisfied, then from Equation (49)

$$\psi_{12} = iku_2 \tag{51}$$

which is the simple relation previously obtained for all three cases. Similar conclusion can be drawn for the torsional motions also.

2. Estimation of Synthetic Rocking

From the preceding analysis, it is seen that the rocking component of motion, ψ_{12}, can be related to the translational component, u_2, of the Rayleigh surface waves in the layered half-space. Equation (46) further shows that at the ground surface $(x_2 = 0)$, the amplitudes of rocking increase linearly with frequency ω. Similar results have been previously observed for the case of torsional motion, where it

was shown that the torsional component of motion, ψ_{13}, is associated with the translational component, u_3, of the Love waves at $x_2 = 0$

$$\Psi_{13} = \frac{-i}{2} k u_3 = -\frac{i}{2}\frac{\omega}{c} u_3 \tag{52}$$

where, c is the phase velocity of Love waves. The same estimation steps can thus be carried over from torsion to rocking. Starting from the $m-$th mode of surface waves within the frequency band $\omega_n \pm \Delta\omega_n$, the Fourier transform of the vertical translation, $\mathsf{A}_{nm}(\omega)$, is given by (Lee and Trifunac, 1987)

$$\mathsf{A}_{nm}(\omega) = \begin{cases} \pi \big/ 2 A_{nm} e^{-i\left[(\omega-\omega_n)t^*_{nm}+\phi_n\right]} & |\omega - \omega_n| \le \Delta\omega_n \\ 0 & \text{otherwise} \end{cases} \tag{53a}$$

and

$$\mathsf{A}_{nm}(-\omega) = \mathsf{A}^*_{nm}(\omega) \tag{53b}$$

where, $\mathsf{A}^*_{nm}(\omega)$ is the complex conjugate of $\mathsf{A}_{nm}(\omega)$. A_{nm} is the relative amplitude of the $m-$th mode, given by the empirical equations suggested by Trifunac (1971b), and has been used in the synthesis of artificial accelerograms for both the translational components and torsional component. t^*_{nm} is the arrival time of the $m-$th mode defined earlier. ϕ_n is the phase of the wave at the given frequency band, introduced to include the effects of source and other miscellaneous effects along the propagation path. It is assumed to be a random number between $-\pi$ and π.

The corresponding Fourier transform of the $m-$th mode of rocking, $\Psi_{nm}(\omega)$, in the frequency band, $2\Delta\omega_n$, is

$$\Psi_{nm}(\omega) = \begin{cases} \left(i\pi\omega/2C_{nm}\right) A_{nm} e^{-i\left[(\omega-\omega_n)t^*_{nm}+\phi_n\right]} & |\omega - \omega_n| \le \Delta\omega_n \\ 0 & \text{otherwise} \end{cases} \tag{54}$$

where, $C_{nm} = C_{nm}(\omega_n)$ is the phase velocity of the $m-$th mode of Rayleigh waves, assumed to be constant within the frequency band $\omega_n \pm \Delta\omega_n$. Combining all of the *M* modes of Rayleigh waves gives the Fourier transform of vertical displacement, $\mathsf{A}_n(\omega)$, at the frequency band as

$$\mathsf{A}_n(\omega) = \sum_{m=1}^{M} \mathsf{A}_{nm}(\omega) \tag{55}$$

Note that for the Fourier transform of horizontal displacements, this will include both the modes of Love and Rayleigh waves in the band $2\Delta\omega_n$, and with relative contributions determined from the angles between x_1 and x_3 axes relative to the azimuth of wave arrival. Similarly, the total rocking, $\Psi_n(\omega)$, at the frequency band $2\Delta\omega_n$ is

$$\Psi_n(\omega) = \sum_{m=1}^{M} \psi_{nm}(\omega) \tag{56}$$

The total Fourier transforms of vertical displacement, $\mathsf{A}(\omega)$, and rocking, $\Psi(\omega)$, then become

$$\mathsf{A}(\omega) = \sum_{n=1}^{N} \alpha_n \mathsf{A}_n(\omega) \tag{57a}$$

and

$$\Psi(\omega) = \sum_{n=1}^{N} \alpha_n \Psi_n(\omega) \tag{57b}$$

where, N is the total number of frequency bands considered. α_n is the scaling factor determined so that the Fourier amplitude of vertical displacement at frequency ω_n will match with the corresponding actual or estimated component of Fourier amplitude $|FS(\omega_n)|$ at the site. The actual Fourier amplitudes are those calculated from the actual accelerogram recorded at the site. The estimated Fourier amplitudes are those calculated from the empirical models for scaling Fourier amplitude spectra of strong ground acceleration in terms of the earthquake magnitude, source-to-station distance, site intensity, and recording site conditions.

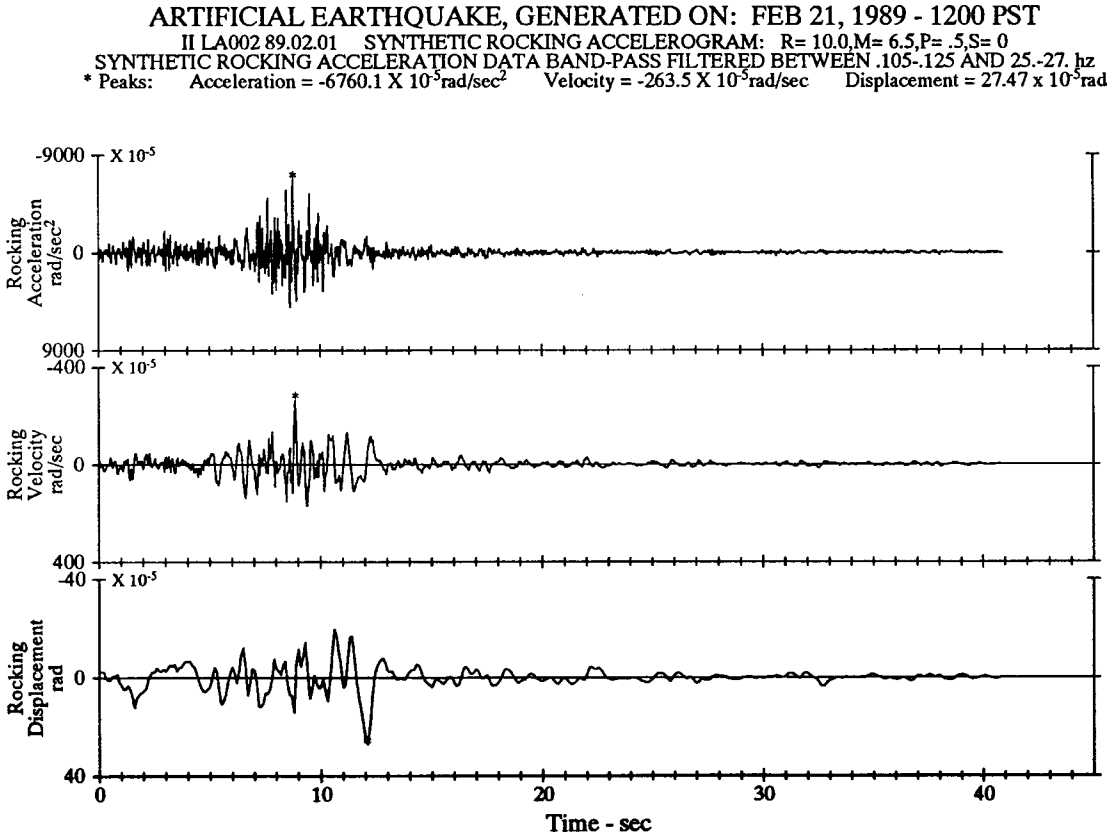

Fig. 13 Artificial earthquake synthetic rocking accelerogram

The ratio of the Fourier amplitude of rocking acceleration to that of vertical translation is

$$\left|\frac{\Psi(\omega)}{A(\omega)}\right| \cong \left|\frac{\Psi_n(\omega)}{A_n(\omega)}\right|, \quad |\omega - \omega_n| \le \Delta\omega_n \tag{58}$$

Using Equations (53) through (56), this becomes

$$\left|\frac{\Psi(\omega)}{A(\omega)}\right| = \omega \left|\frac{\sum_{m=1}^{M} \frac{A_{nm}}{C_{nm}} e^{-i(\omega-\omega_n)t^*_{nm}}}{\sum_{m=1}^{M} A_{nm} e^{-i(\omega-\omega_n)t^*_{nm}}}\right|, \quad |\omega - \omega_n| \le \Delta\omega_n \tag{59}$$

and, in particular for $\omega = \omega_n$,

$$\left|\frac{\Psi(\omega)}{A(\omega)}\right| = \omega_n \left|\frac{\sum_{m=1}^{M} A_{nm}/C_{nm}}{\sum_{m=1}^{M} A_{nm}}\right| \tag{60}$$

Note that except for the factor of 1/2, the same empirical relation was obtained for the ratio of Fourier amplitude of torsional to Fourier amplitude of horizontal accelerations.

As for torsional motions, the asymptotic expansion of Equation (60) for large and small frequencies is possible here. At the high-frequency end, the phase velocities of all modes of Rayleigh surface waves approach $\beta_{\min}$, the minimum shear wave velocity in the layered half-space model. Thus,

$$\left|\frac{\Psi(\omega_n)}{A(\omega_n)}\right| \sim \omega_n \frac{\sum_{m=1}^{M} A_{nm}/\beta_{\min}}{\sum_{m=1}^{M} A_{nm}} = \frac{\omega_n}{\beta_{\min}} \qquad \text{as } \omega_n \to \infty \tag{61}$$

At the low-frequency end, the only mode present in the layered medium is the first mode, and its phase velocity approaches $\beta_{\max}$, the largest (usually for half-space) shear wave velocity in the layered model. Thus,

$$\left|\frac{\Psi(\omega_n)}{A(\omega_n)}\right| \sim \omega_n \left|\frac{A_{n1}/\beta_{\max}}{A_{n1}}\right| = \omega_n/\beta_{\max} \qquad \text{as } \omega_n \to \infty \tag{62}$$

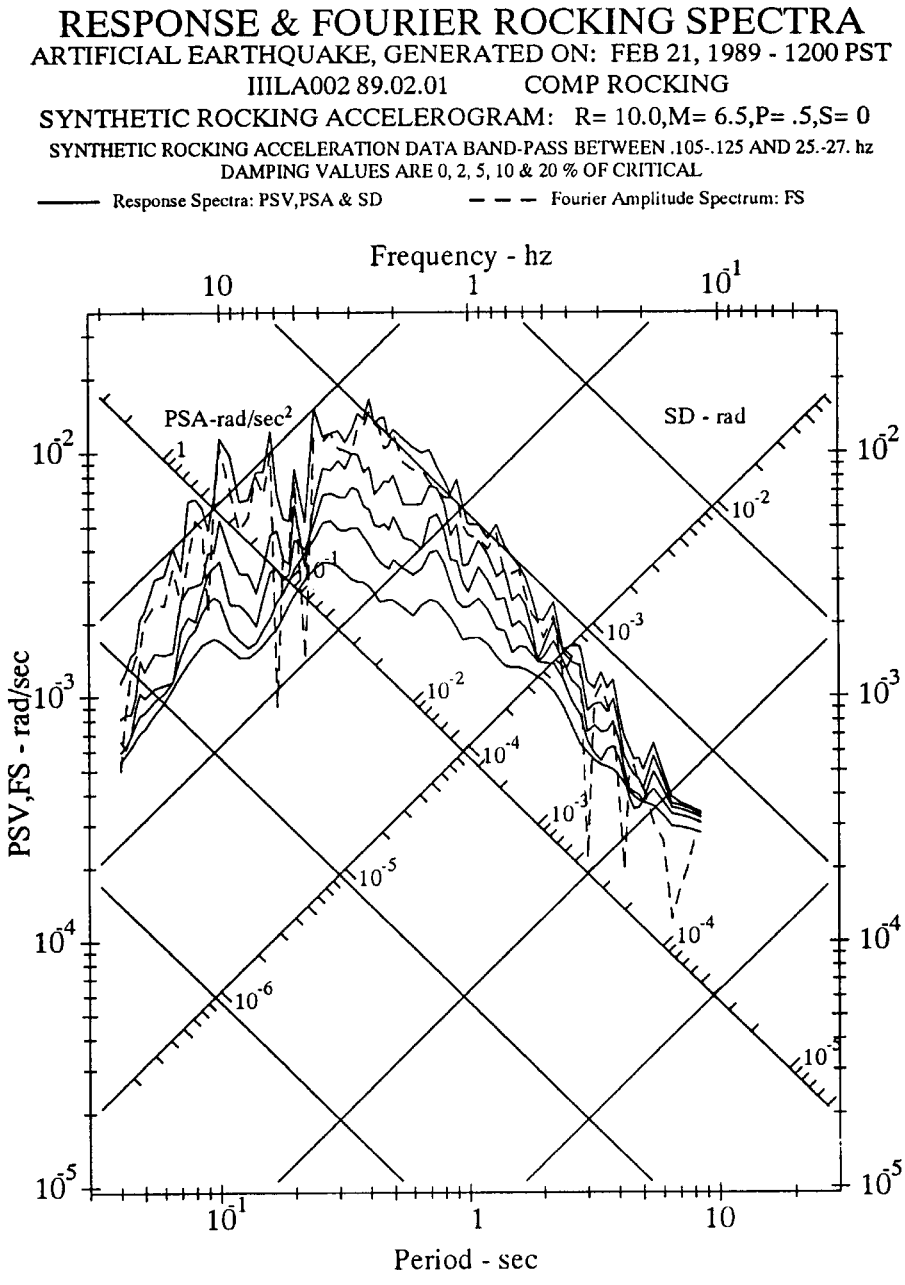

Fig. 14 Artificial earthquake synthetic rocking response and Fourier spectra

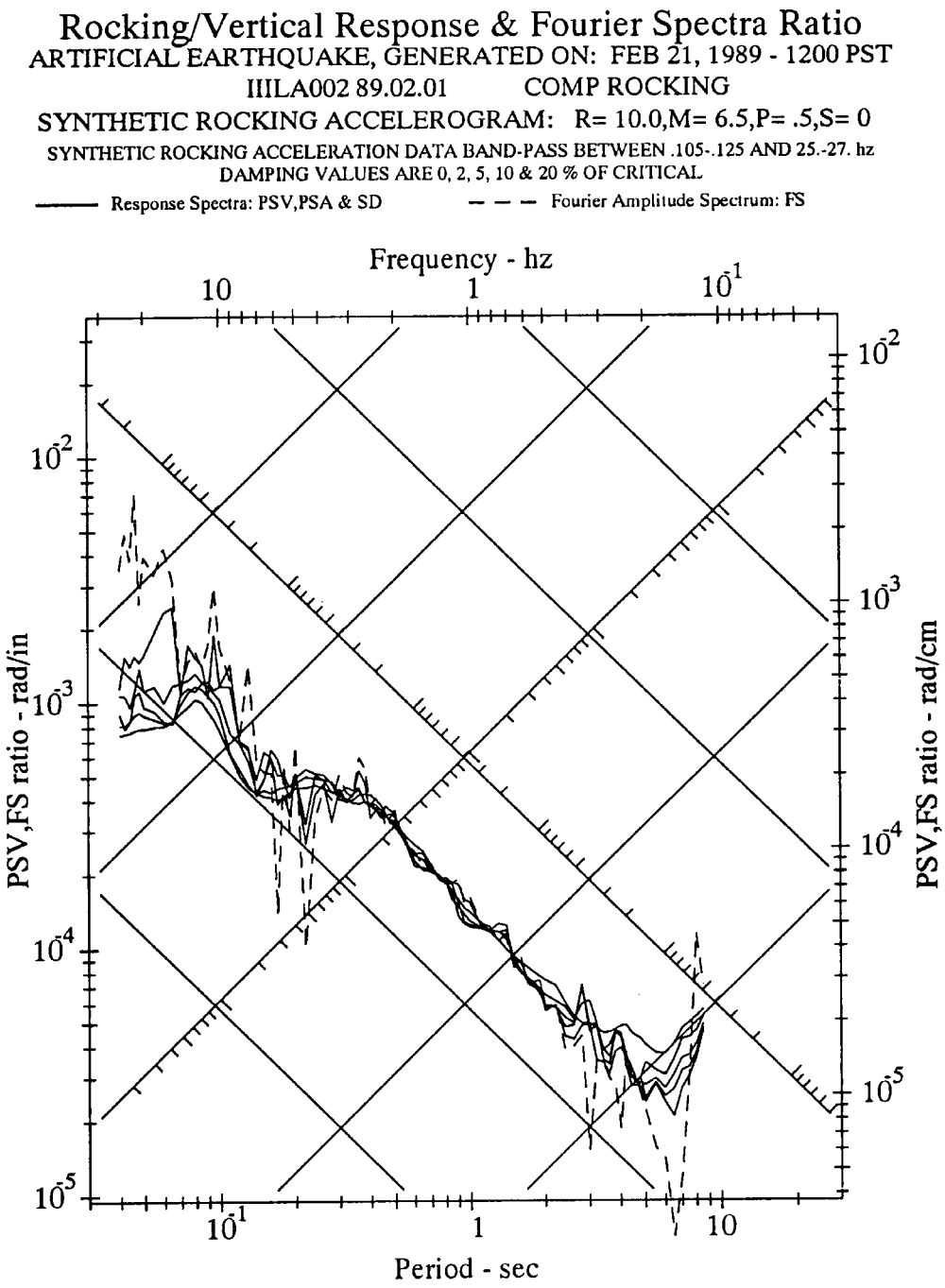

Fig. 15 Artificial earthquake synthetic rocking/vertical response and Fourier spectral ratio

3. Examples of Synthetic Rocking

Following the analysis in the previous sections, one can readily generate the translational (horizontal: radial, transverse; and vertical), torsional and rocking accelerograms simultaneously. As in Sub-section 3 of the previous section, the same site at Westmoreland in Imperial Valley, and the same dispersion curves are used in the following examples.

Figure 13 shows a plot of the synthetic rocking motions. It presents examples of the rocking acceleration, velocity and displacement in rad/s^2, rad/s, and rad, respectively. Figure 14 gives the corresponding rocking response and Fourier spectra. It represents the maximum rocking responses of over 80 single-degree-of-freedom systems, with natural periods in the range 0.04-8 s and with 5 damping ratios $(\zeta = 0,\ 0.02,\ 0.05,\ 0.10 \text{ and } 0.20)$, when subjected to the corresponding rocking accelerograms. The units for the rocking displacement, SD, pseudo relative velocity, PSV, and pseudo acceleration, PSA, responses are rad, rad/s, and rad/s^2, respectively. Figure 15 shows the ratio of rocking to vertical

translational response. As indicated in Equation (46), this ratio tends to vary linearly with frequency, or inversely with period.

SURFACE STRAINS OF EARTHQUAKE GROUND MOTIONS

Expressions for surface strains in an elastic half-space associated with incident plane (P, SV and SH) body waves are given in Trifunac (1979b). Those associated with the Rayleigh and Love surface waves are given in Lee (1990).

Studies of earthquake-induced damage to engineered structures show that there are cases of damages, which result from the differential motions caused by large strains associated with ground shaking (Trifunac, 1979b, 1997). In some cases, these strains are superimposed on the dynamic responses, and only contribute to the resultant total vibrations. In other cases, when the characteristic frequencies of the system differ from the principal frequency content of strong motion, these local strains may affect the structural systems in a quasi-static manner. Long underground pipelines and railroad tracks may buckle, and bridges may collapse because of the excessive differential support motions, due to excessive local strains associated with earthquake ground shaking (Trifunac and Todorovska, 1997a, 1997b; Trifunac et al., 1996). Studies of the responses of long structures excited by ground shaking (Kojić et al., 1988; Todorovska and Trifunac, 1989, 1990a, 1990b; Trifunac and Todorovska, 1997a) have demonstrated the need for detailed description of motions at various points of single (or multiple) foundation(s), with emphasis on the differential motions associated with large surface strains.

1. The Surface Strains Associated with Incident Waves

This sub-section is devoted to estimation of the surface strains from the known translational components of motion (Trifunac, 1979b; Lee, 1990). Referring to Figures 10 and 11 for incident P- and SV-waves, and Figure 5 for incident SH-waves, the surface strains at $x_2 = 0,$ associated with incident P- and SV-waves, are

$$\varepsilon_{x_1} = u_{1,1} = ik_\alpha \sin\theta_0 u_1 \tag{63a}$$

$$\varepsilon_{x_2} = u_{2,2} = ik_\alpha \left(\frac{2}{(\alpha/\beta)^2} - 1 \right) \sin\theta_0 u_1 \tag{63b}$$

and

$$\varepsilon_{x_1 x_2} = 1/2\left(u_{1,2} + u_{2,1}\right) = 0 \tag{63c}$$

Those associated with incident plane SH-waves are

$$\varepsilon_{x_1} = \varepsilon_{x_2} = 0 \tag{64a}$$

$$\varepsilon_{x_1 x_3} = 1/2\left(u_{1,3} + u_{3,1}\right) = (1/2)u_{3,1} = (1/2)ik_\beta \sin\theta_0 u_3 \tag{64b}$$

Lee (1990) showed that similar expressions for surface strains can also be derived for the Rayleigh and Love waves. Referring to Equations (34)-(37) for the Φ and Ψ potentials, and the horizontal (x_1) and vertical (x_2) components of displacements associated with Rayleigh waves, the associated surface strains at $x_2 = 0$ are

$$\varepsilon_{x_1} = u_{1,1} = -k^2\left[A_1 + A_2 + s\left(B_1 - B_2\right)\right]\exp\left(ik\left(x_1 - ct\right)\right) \tag{65a}$$

$$\varepsilon_{x_2} = u_{2,2} = -k^2\left[r\left(A_1 + A_2\right) - s\left(B_1 - B_2\right)\right]\exp\left(ik\left(x_1 - ct\right)\right) \tag{65b}$$

where, $c\left(< \beta < \alpha\right)$ is the phase velocity of the surface waves in the $x_1 -$direction; $k = \omega/c$ is the corresponding wave number; and r and s are, respectively, numbers given by (Equation (35))

$$r = \left(c^2/\alpha^2 - 1\right)^{1/2} \tag{66a}$$

$$s = \left(c^2/\beta^2 - 1\right)^{1/2} \tag{66b}$$

Recall from Equation (37a) that the horizontal component of displacement at the surface $(x_2 = 0)$ is given by

$$u_1 = ik\left[A_1 + A_2 + s(B_1 - B_2)\right]\exp(ik(x_1 - ct)) \tag{67}$$

It is clear from Equations (65a) and (67) that for Rayleigh waves, the surface normal strain in the horizontal (x_1) direction at $x_2 = 0$ is

$$\varepsilon_{x_1} = u_{1,1} = iku_1 \tag{68}$$

The surface normal strain, ε_{x_2}, in the vertical (x_2) direction at $x_2 = 0$ can also be expressed in terms of u_1. Recalling the stress-free boundary conditions at the half-space surface (Equation (41)),

$$\sigma_{22} = \sigma_{12} = 0 \tag{69}$$

and, from Equation (42), expressing the stresses in terms of the potentials at $x_2 = 0$ gives

$$(1 - s^2)(A_1 + A_2) + 2s(B_1 - B_2) = 0 \tag{70a}$$

$$-2r(A_1 - A_2) + (1 - s^2)(B_1 + B_2) = 0 \tag{70b}$$

Using Equation (70a), Equations (67) and (65b) can be rewritten as

$$u_1 = ik\left(\frac{1 + s^2}{2}\right)(A_1 + A_2)\exp(ik(x_1 - ct)) \tag{71a}$$

$$\varepsilon_{x_2} = -k^2\left(r^2 + \frac{(1 - s^2)}{2}\right)(A_1 + A_2)\exp(ik(x_1 - ct)) \tag{71b}$$

Using the expressions for r and s in Equation (66), Equation (71) can be further simplified to

$$u_1 = ik\frac{c^2}{2\beta^2}(A_1 + A_2)\exp(ik(x_1 - ct)) \tag{72a}$$

$$\varepsilon_{x_2} = -k^2\left(c^2/\alpha^2 - c^2/2\beta^2\right)(A_1 + A_2)\exp(ik(x_1 - ct)) \tag{72b}$$

from which it follows that

$$\varepsilon_{x_2} = ik\left[\frac{2}{(\alpha/\beta)^2} - 1\right]u_1 \tag{73}$$

This is of the same form as Equation (63b), for incident plane P- and SV-waves. For $\nu = 0.25$, $(\alpha/\beta)^2 = 3$, and thus, Equation (73) takes the form

$$\varepsilon_{x_2} = -\frac{ik}{3}u_1 \tag{74}$$

The surface shear strains, $\varepsilon_{x_2x_1}$ and $\varepsilon_{x_2x_3}$, are both zero, because the corresponding shear stresses, $\tau_{x_2x_1}$ and $\tau_{x_2x_3}$, vanish at the half-space surface $(x_2 = 0)$.

Similar expressions for surface strains associated with Love waves can be derived. Starting with the anti-plane displacement, u_3, in the top layer of the layered half-space,

$$u_3 = \left(B_1 e^{iksx_2} + B_2 e^{-iksx_2}\right)\exp(ik(x_1 - ct)) \tag{75}$$

the associated surface strains are given by

$$\varepsilon_{x_1x_3} = \frac{1}{2}(u_{1,3} + u_{3,1}) = \frac{1}{2}u_{3,1} = \frac{1}{2}iku_3 \tag{76a}$$

$$\varepsilon_{x_2x_3} = \frac{1}{2}(u_{2,3} + u_{3,2}) = (1/2)u_{3,2} = 0 \tag{76b}$$

$$\varepsilon_{x_3x_3} = u_{3,3} = 0 \tag{76c}$$

The surface shear strain $\varepsilon_{x_2x_3}$ is zero, because the corresponding shear stress $\tau_{x_2x_3}$ vanishes at the half-space surface.

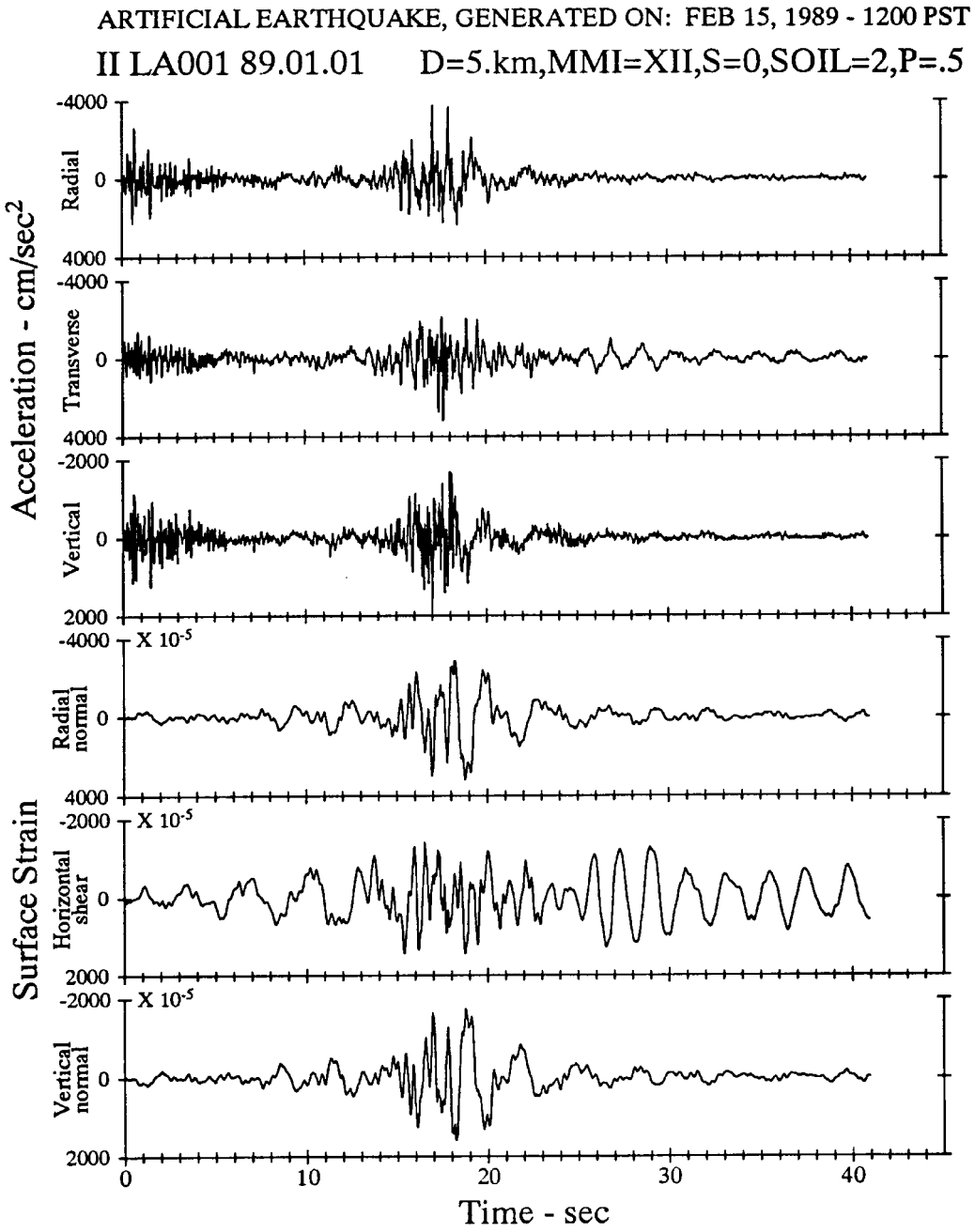

Fig. 16 Artificial earthquake synthetic acceleration and surface strain accelerogram: LA001

2. Estimation of Synthetic Strain

From the preceding analysis, it is seen that the surface strains associated with strong earthquake motions are related to the translational components of body Rayleigh and Love waves in the half-space. The three non-vanishing components of surface strains, ε_{x_1} (Equation (68)), ε_{x_2} (Equation (73)) and $\varepsilon_{x_1x_3}$ (Equation (76a)), have amplitudes, which all increase linearly with wave number k and hence with frequency ω .

From Equation (2), the $m-$th mode of acceleration of horizontal motion $\ddot{u}_1$ for Rayleigh waves has Fourier transform, within frequency band $\omega_n \pm \Delta\omega_n$, as

$$\mathsf{A}_{nm}(\omega) = \begin{cases} (\pi/2) A_{nm} e^{-i\left[(\omega-\omega_n)t^*_{nm}+\phi_n\right]} & |\omega-\omega_n| \le \Delta\omega_n \\ 0 & \text{otherwise} \end{cases}$$

and (77)

$$\mathsf{A}_{nm}(-\omega) = \mathsf{A}^*_{nm}(\omega)$$

where, $\mathsf{A}^*_{nm}(\omega)$ is the complex conjugate of $\mathsf{A}_{nm}(\omega)$. The corresponding Fourier transform of the in-plane displacement of horizontal motion, u_1, denoted by $\mathsf{U}_{nm}(\omega)$, is then

$$\mathsf{A}_{nm}(\omega) = \frac{-\mathsf{A}_{nm}(\omega)}{\omega^2} = \begin{cases} -\dfrac{\pi}{2\omega^2} A_{nm} e^{-i\left[(\omega-\omega_n)t^*_{nm}+\phi_n\right]} & |\omega-\omega_n| \le \Delta\omega_n \\ 0 & \text{otherwise} \end{cases} \tag{78}$$

Similar expressions can be written for the Fourier transform of the anti-plane displacement of horizontal motion, u_3, for Love waves. From this, on using Equations (68), (73) and (76a), the Fourier transforms of the $m-$th mode of strains $\varepsilon_{11,nm}(\omega)$, $\varepsilon_{22,nm}(\omega)$ and $\varepsilon_{13,nm}(\omega)$ (respectively for $\varepsilon_{x_1x_1}(t)$, $\varepsilon_{x_2x_2}(t)$, and $\varepsilon_{x_1x_3}(t)$), in the same frequency band $\omega_n \pm \Delta\omega_n$, become

$$\mathrm{E}_{11,nm}(\omega) = \frac{i\omega}{C_{nm}} \mathsf{U}_{nm}(\omega) = \frac{-i}{\omega C_{nm}} \mathsf{A}_{nm}(\omega) \tag{79a}$$

$$\mathrm{E}_{22,nm}(\omega) = \frac{i\omega}{C_{nm}} \left(\frac{2}{(\alpha/\beta)^2} - 1 \right) \mathsf{U}_{nm}(\omega) = \frac{-i}{\omega C_{nm}} \left(\frac{2}{(\alpha/\beta)^2} - 1 \right) \mathsf{A}_{nm}(\omega) \tag{79b}$$

$$\mathrm{E}_{13,nm}(\omega) = \frac{1}{2} \frac{i\omega}{C_{nm}} \mathsf{U}_{nm}(\omega) = \frac{-i}{2\omega C_{nm}} \mathsf{A}_{nm}(\omega) \tag{79c}$$

where, $C_{nm} = C_m(\omega_n)$ is the phase velocity of the $m-$th mode of Rayleigh waves in Equations (79a) and (79b), and $\mathsf{U}_{nm}(\omega)$ is the transform of displacement $u_1(t)$. In Equation (79c), $C_{nm} = C_m(\omega_n)$ is for the Love waves, with $\mathsf{U}_{nm}(\omega)$ being the transform of the corresponding anti-plane displacement $u_3(t)$. Those are assumed to be constant within the frequency band $\omega_n \pm \Delta\omega_n$.

As in the generation of torsion and rocking time-histories, the total contribution from all the modes of surface and body waves in the same frequency band takes the form

$$\mathrm{E}_{ij,n}(\omega) = \begin{cases} -\dfrac{i\pi}{2\omega} f_{ij} \alpha_n \sum_{m=1}^{M} A_{nm} e^{-i\left[(\omega-\omega_n)t^*_{nm}+\phi_n\right]} & |\omega-\omega_n| \le \Delta\omega_n \\ 0 & \text{otherwise} \end{cases} \tag{80}$$

where,

$$f_{ij} = \begin{cases} 1 & i=j=1, \text{ for Rayleigh waves} \\ \dfrac{2}{(\alpha/\beta)^2} - 1 & i=j=2, \text{ for Rayleigh waves} \\ 1/2 & i=1,\ j=3, \text{ for Love waves} \\ 0 & \text{otherwise} \end{cases} \tag{81}$$

and α_n is the scaling factor, as given by Equation (10). For $i = j = 1$ and $i = j = 2$, the contribution of surface waves comes only from the Rayleigh waves, and for $i = 1,\ j = 3,$ the contribution is from the Love waves. The total Fourier transform of the strain time-history is then

$$\mathrm{E}_{ij}(\omega) = \sum_{n=1}^{N} \mathrm{E}_{ij,n}(\omega) \tag{82}$$

where, N is the total number of frequency bands used.

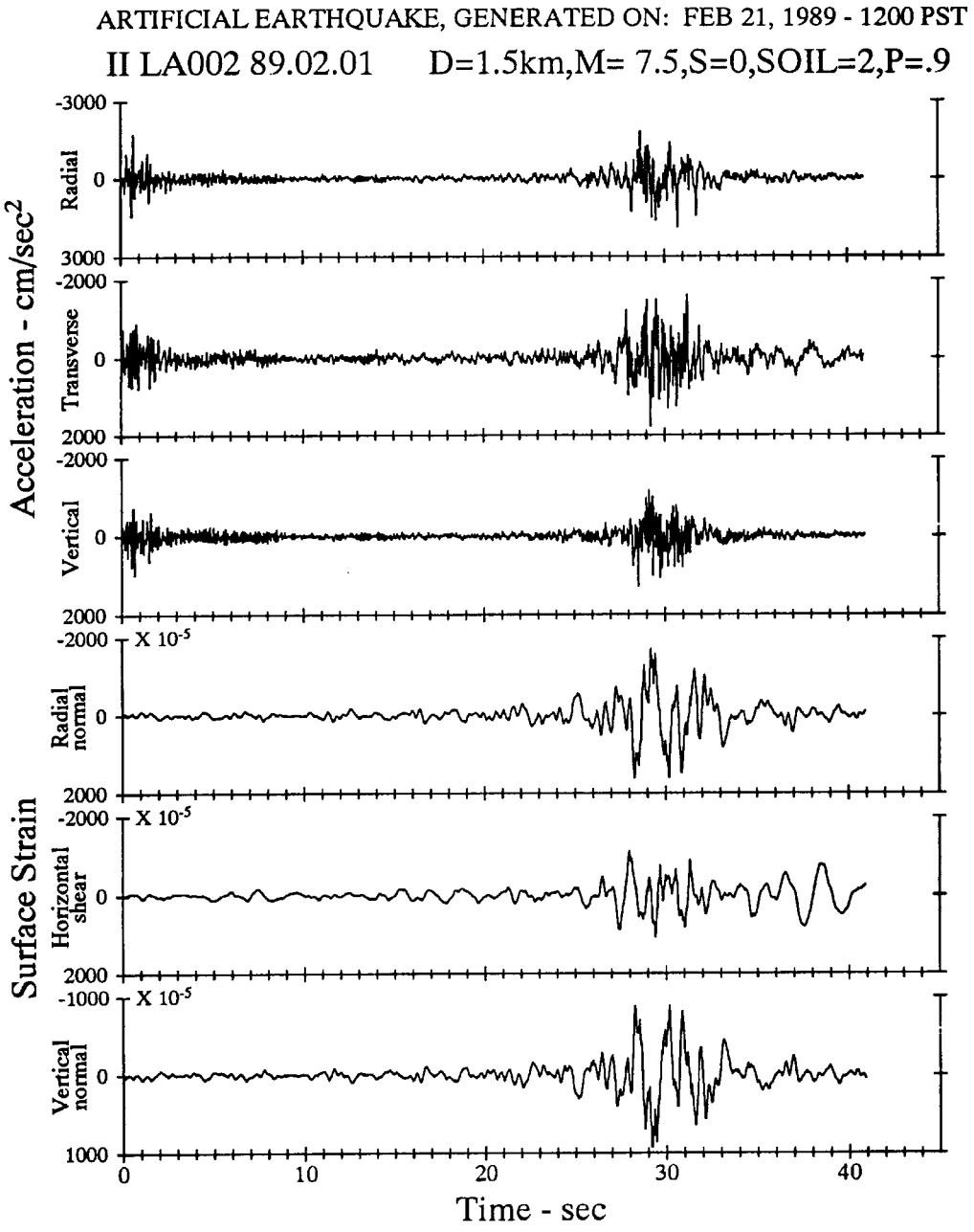

Fig. 17 Artificial earthquake synthetic acceleration and surface strain accelerogram: LA002

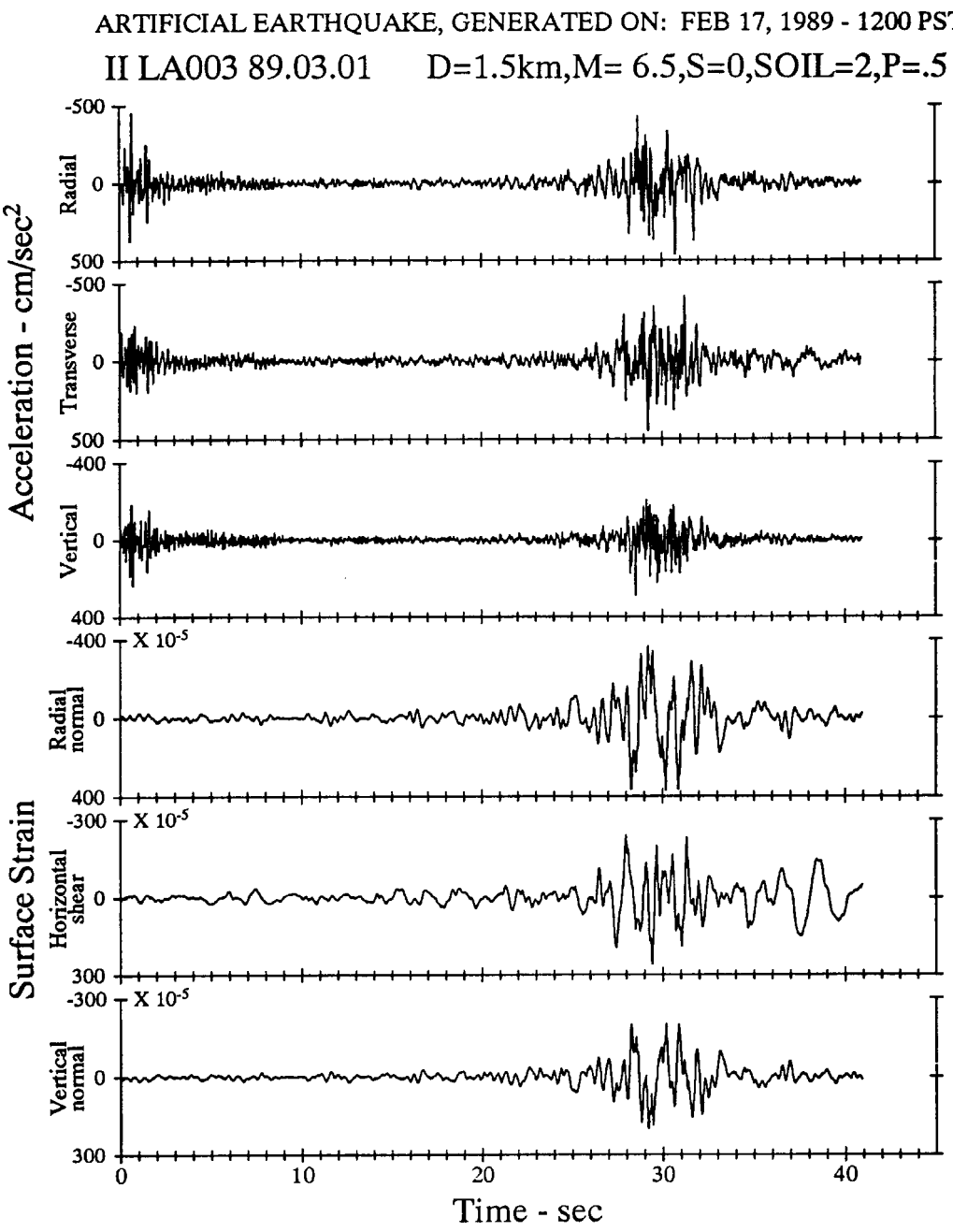

Fig. 18 Artificial earthquake synthetic acceleration and surface strain accelerogram: LA003

3. Examples of Synthetic Strains

We have earlier presented examples for the local site geology and dispersion of the surface waves for a site in Westmoreland, Imperial Valley, California. To illustrate "large" strains, we modify this "site" (see Table 2) to have a 50 m layer with shear wave velocity of 50 m/s at the top, and a second 130 m layer with shear wave velocity of 300 m/s (Table 3). For depths greater than 180 m, we adopt the material properties, as in Table 2. For long period motions, the dispersion curves for this modified model would be identical to those in Figures 1 and 2. For short periods and layer properties as in Table 3, the phase and group velocities would be reduced from 0.98 km/s to 0.05 km/s. The modified site will exemplify "soft" soil and geologic conditions in which, as implied by Equations (80) and (81), the strains can be "large". We also consider large amplitudes of strong shaking, in the immediate vicinity of the epicenter. Figure 16 presents an example computed for the site intensity, $MMI = XII$, source at epicentral distance of 5 km for $s = 0$ (site on alluvium) and $s_L = 2$ (deep soil site), and for $p = 0.5$, where p is the probability of

exceedance for the derived spectrum (Trifunac, 1989a, 1989b). These conditions result in peak accelerations (37.3 m/s^2 for radial, 31.9 m/s^2 for transverse, and 18.5 m/s^2 for vertical ground motions) larger than what has been recorded so far, and thus illustrate extreme response amplitudes and the associated strains. The resulting peak strains are, respectively, 0.03, 0.01 and 0.02. Because the strains are proportional to ku, the overall appearance of strain versus time is similar to that of the ground motion velocity. Figure 17 shows another example for M = 7.5, 1.5 km epicentral distance, $s = 0$, $s_L = 2$, and $p = 0.9$. The radial, transverse and vertical peak accelerations, respectively equal to 19.0 m/s^2, 17.86 m/s^2, and 12.9 m/s^2, lead to the corresponding peak strains equal to 0.017, 0.011, and 0.009. These examples have been chosen to illustrate the extreme cases. Considering the local geologic cross-section, as given in Table 2, M = 6.5, $s = 0$, $s_L = 2$, and $p = 0.5$ would result in peak accelerations equal to 4.59 m/s^2, 4.48 m/s^2, and 2.91 m/s^2, for example. Then, the associated strains would equal only to 3.7 x 10^{-3}, 2.6 x 10^{-3}, and 2.0 x 10^{-3}, for $\varepsilon_{x_1x_1}$, $\varepsilon_{x_1x_3}$ and $\varepsilon_{x_2x_2}$, respectively (Figure 18).

Table 3: Same as Table 2 Except for a Modification in the Top 180 m of Layer 1, to Illustrate the Effects for a "Soft" Site

Layer	h_i (km)	α (km/s)	β_i (km/s)	ρ_i (g/cm^3)
1a	0.05	0.105	0.05	1.20
1b	0.13	0.60	0.30	1.28
2	0.55	1.96	1.13	1.36
3	0.98	2.71	1.57	1.59
4	1.19	3.76	2.17	1.91
5	2.68	4.69	2.71	2.19
6	∞	6.40	3.70	2.71

The above examples illustrate the possible strain amplitudes implied by the linear theory, but those cannot be taken to be "average" or "typical" estimates, for magnitudes, site intensities, or local conditions considered. In general, the strain amplitudes will increase with overall increase in the strong motion amplitudes, and with decrease of shear wave velocities of soil and sedimentary layers near the ground surface. Time-dependence of strain components near the ground surface is roughly proportional to that of the corresponding components of ground velocity, and thus, the peak strains will also increase with the peak ground velocity.

It is seen that by using the linear theory of wave propagation, the strain amplitudes can be evaluated exactly in three-dimensions. When the local geologic conditions are too complex to model the near-surface motions by the equivalent parallel layer models, the method presented here can be modified to give again the exact representation of near-surface strains, but in terms of other than the rectangular Cartesian coordinate system (Moeen-Vaziri and Trifunac, 1988a, 1988b; Lee and Wu, 1994a, 1994b; Manoogian and Lee, 1996).

Many engineering inferences on linear and non-linear strains in rock and in soil, during the passage of seismic waves, are limited by the assumption that the incident energy arrives vertically in a one-dimensional wave propagation model. The method presented here should help in the development of input motions and input strains for modeling three-dimensional non-linear responses of soft and water-saturated soils, and for full and direct estimation of strains in the linear response range.

CURVOGRAMS OF EARTHQUAKE GROUND MOTION

Analyses of the effects of strong earthquake shaking on engineered structures are performed for dynamic forces that result from strong motion accelerations. However, pseudo-static deformations that result from wave passage under long structures may also contribute forces, which, in certain cases, may be larger than the dynamic forces (Kojić et al., 1988; Todorovska and Lee, 1989; Todorovska and Trifunac, 1989, 1990a, 1990b). Such loadings and the resulting response of structures depend on the

nature of ground waves, inhomogeneities in the soil, sediments or rock under the foundation, the surface topography near structure, and on the nature of the structure-foundation system.

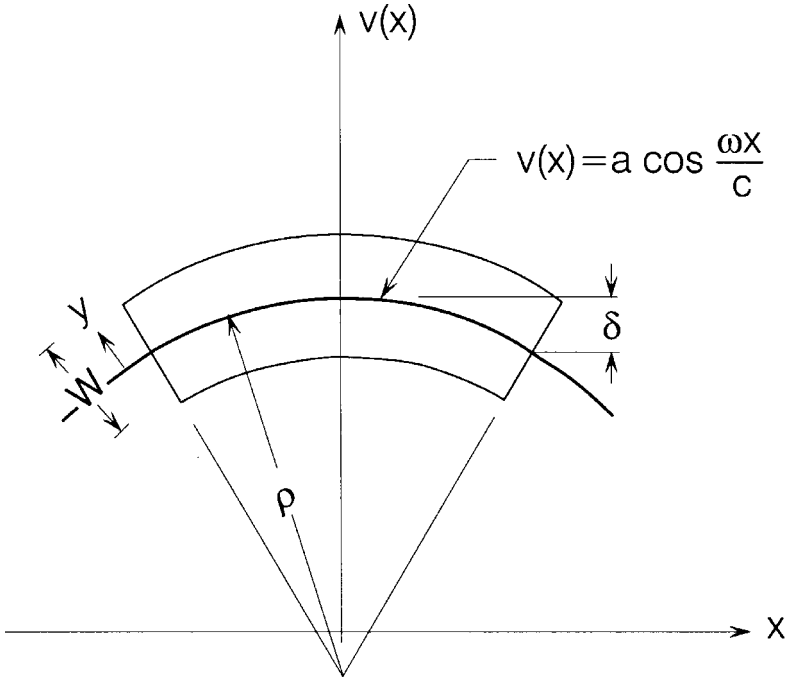

Fig. 19 Curvature

For ground waves that are long relative to the plan dimensions of a structure, it is possible to describe the strong ground motion in terms of the translational and rotational components of ground motion (Gupta and Trifunac, 1987, 1988; Lee and Trifunac, 1985, 1987; Trifunac, 1982). For short ground waves with wave lengths comparable to or shorter than the structural dimensions, the details of the wave passage analysis must be worked out to obtain realistic response analyses (Kojić et al., 1988; Todorovska and Trifunac, 1990b). In this work, we consider an intermediate case in which the ground waves have wave lengths at least two-three times longer than the structural dimensions, and are long enough to approximate the resulting pseudo-static deformations of the foundation system during the wave passage by an equivalent segment of circular arc. This is illustrated in Figure 19, which shows the plan view of a rectangular foundation deformed into bending by the passing ground wave. Since the significance of such a deformation for structural response can be evaluated with sufficient accuracy, if the radius of curvature of ground deformation is known, in this section, we present a method for evaluating the curvograms (plots of curvature versus time) on ground surface. Trifunac (1990) extended the method for generation of synthetic translational (Trifunac, 1971b; Wong and Trifunac, 1978, 1979), rocking (Lee and Trifunac, 1987), torsional (Lee and Trifunac, 1985) accelerograms, and strain (Lee, 1990) time histories, to obtain curvograms of strong motion.

Let x_1, x_2 and x_3 be the radial, vertical and transverse coordinates. Let c be the apparent phase velocity of wave motion in the radial (x_1) direction. Let u_1, u_2 and u_3 be the displacements in the x_1, x_2 and x_3 directions. Then, the curvature in the vertical plane, $k_2(t)$, is

$$k_2(t) = \frac{\partial^2 u_2 / \partial x_1^2}{\left[1 + (\partial u_2 / \partial x_1)^2\right]^{3/2}} \approx \frac{\partial^2 u_2}{\partial x_1^2} \tag{83}$$

For Rayleigh waves propagating along the ground surface, we have

$$u_2 = U_2(z) e^{ik(x_1 - ct)} \tag{84}$$

so

$$\frac{\partial^2 u_2}{\partial x_1^2} = -k^2 u_2 = -\frac{\omega^2 u_2}{c^2} \tag{85a}$$

and

$$\ddot{u}_2 = \frac{\partial^2 u_2}{\partial t_1^2} = -\omega^2 u_2 \tag{85b}$$

or

$$k_2(t) \approx \frac{\partial^2 u_2}{\partial x_1^2} = \frac{\ddot{u}_2}{c^2} \quad \text{(vertical)} \tag{86a}$$

Likewise, we have

$$k_3(t) \approx \frac{\partial^2 u_3}{\partial x_1^2} = \frac{\ddot{u}_3}{c^2} \quad \text{(transverse)} \tag{86b}$$

$$k_1(t) \equiv 0 \quad \text{(radial)} \tag{86c}$$

as discussed in Trifunac (1990).

1. Estimation of Synthetic Curvograms

From the preceding analysis, it is seen that the curvatures of motion are related to the accelerations, $\ddot{u}_2(t)$ or $\ddot{u}_3(t)$, corresponding to the translational components of motion. As before (by using Equation (2)), we start with the $m-$th mode of surface waves within the frequency band $\omega_n \pm \Delta\omega_n$, associated with the acceleration of vertical motion, $\ddot{u}_2(t)$, whose Fourier transform is given by

$$\mathsf{A}_{nm}(\omega) = \begin{cases} \dfrac{\pi}{2} A_{nm} e^{-i(\omega-\omega_n)t^*_{nm} + i\phi_n} & |\omega - \omega_n| \le \Delta\omega_n \\ 0 & \text{otherwise} \end{cases} \tag{87}$$

and

$$\mathsf{A}_{nm}(-\omega) = \mathsf{A}^*_{nm}(\omega) \tag{88}$$

The inverse transform of Equation (83) is (from Equation (3b))

$$a_{nm}(t) = A_{nm} \frac{\sin \Delta\omega_n (t - t^*_{nm})}{t - t^*_{nm}} \cos(\omega_n t + \phi_n) \tag{89}$$

This represents the contribution of the $m-$th mode of surface waves to acceleration in the frequency band $\omega_n \pm \Delta\omega_n$. The corresponding component of curvature is

$$k_{nm}(t) = \frac{a_{nm}(t)}{C^2_{nm}} = \frac{A_{nm}}{C^2_{nm}} \frac{\sin \Delta\omega_n (t - t^*_{nm})}{t - t^*_{nm}} \cos(\omega_n t + \phi_n) \tag{90}$$

where, as before, $C_{nm} = C_m(\omega_n)$ is the phase velocity of the $m-$th mode of surface waves. The total contributions, $a_n(t)$ and $k_n(t)$, from all modes of surface and body waves in the frequency band $\omega_n \pm \Delta\omega_n$, to acceleration and curvature are, respectively,

$$a_n(t) = \alpha_n \sum_{m=1}^{M} a_{nm}(t) = \alpha_n \sum_{m=1}^{M} A_{nm} \frac{\sin \Delta\omega_n (t - t^*_{nm})}{t - t^*_{nm}} \cos(\omega_n t + \phi_n) \tag{91a}$$

$$k_n(t) = \alpha_n \sum_{m=1}^{M} \frac{a_{nm}(t)}{C^2_{nm}} = \alpha_n \sum_{m=1}^{M} \frac{A_{nm}}{C^2_{nm}} \frac{\sin \Delta\omega_n (t - t^*_{nm})}{t - t^*_{nm}} \cos(\omega_n t + \phi_n) \tag{91b}$$

Recalling that α_n is the scaling factor, as given in Equation (10), the time histories of acceleration and curvature are given by

$$a_i(t) = \sum_{n=1}^{N} a_n(t) = \sum_{n=1}^{N} \alpha_n \left(\sum_{m=1}^{M} A_{nm} \frac{\sin \Delta\omega_n (t - t^*_{nm})}{t - t^*_{nm}} \right) \cos(\omega_n t + \phi_n) \tag{92a}$$

$$k_i(t) = \sum_{n=1}^{N} k_n(t) = \sum_{n=1}^{N} \alpha_n \left(\sum_{m=1}^{M} \frac{A_{nm}}{C^2_{nm}} \frac{\sin \Delta\omega_n (t - t^*_{nm})}{t - t^*_{nm}} \right) \cos(\omega_n t + \phi_n) \tag{92b}$$

with $i = 2$ for the vertical curvature $(k_2(t))$, and $i = 3$ for the transverse curvature $(k_3(t))$. It may be recalled that $k_1(t) \equiv 0$.

By using the corresponding Rayleigh wave phase velocities $C_{nm} = C_m(\omega_n)$ for vertical curvature, and Love wave phase velocities for transverse curvature, their time histories can be computed.

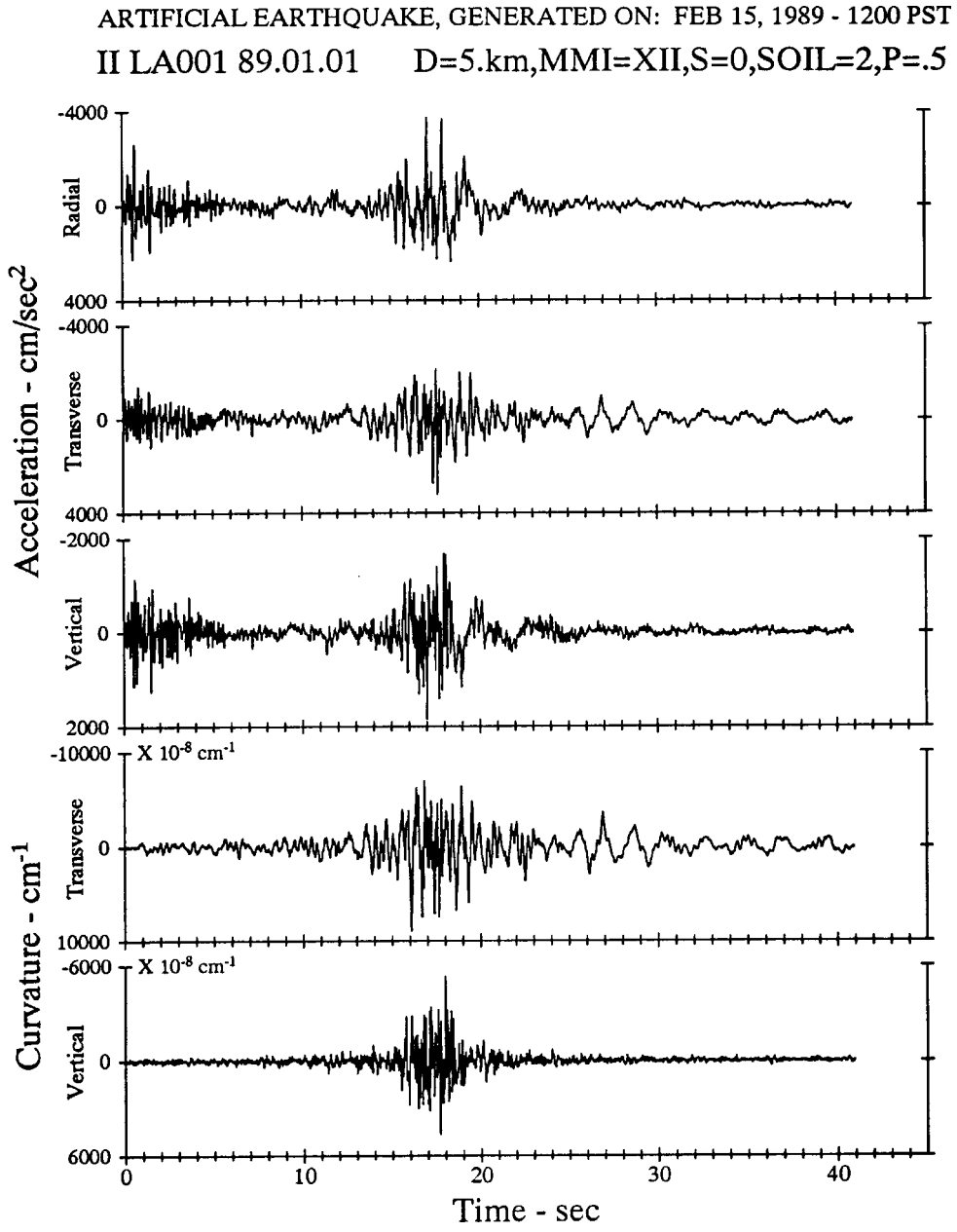

Fig. 20 Artificial earthquake synthetic acceleration and curvature accelerogram: LA001

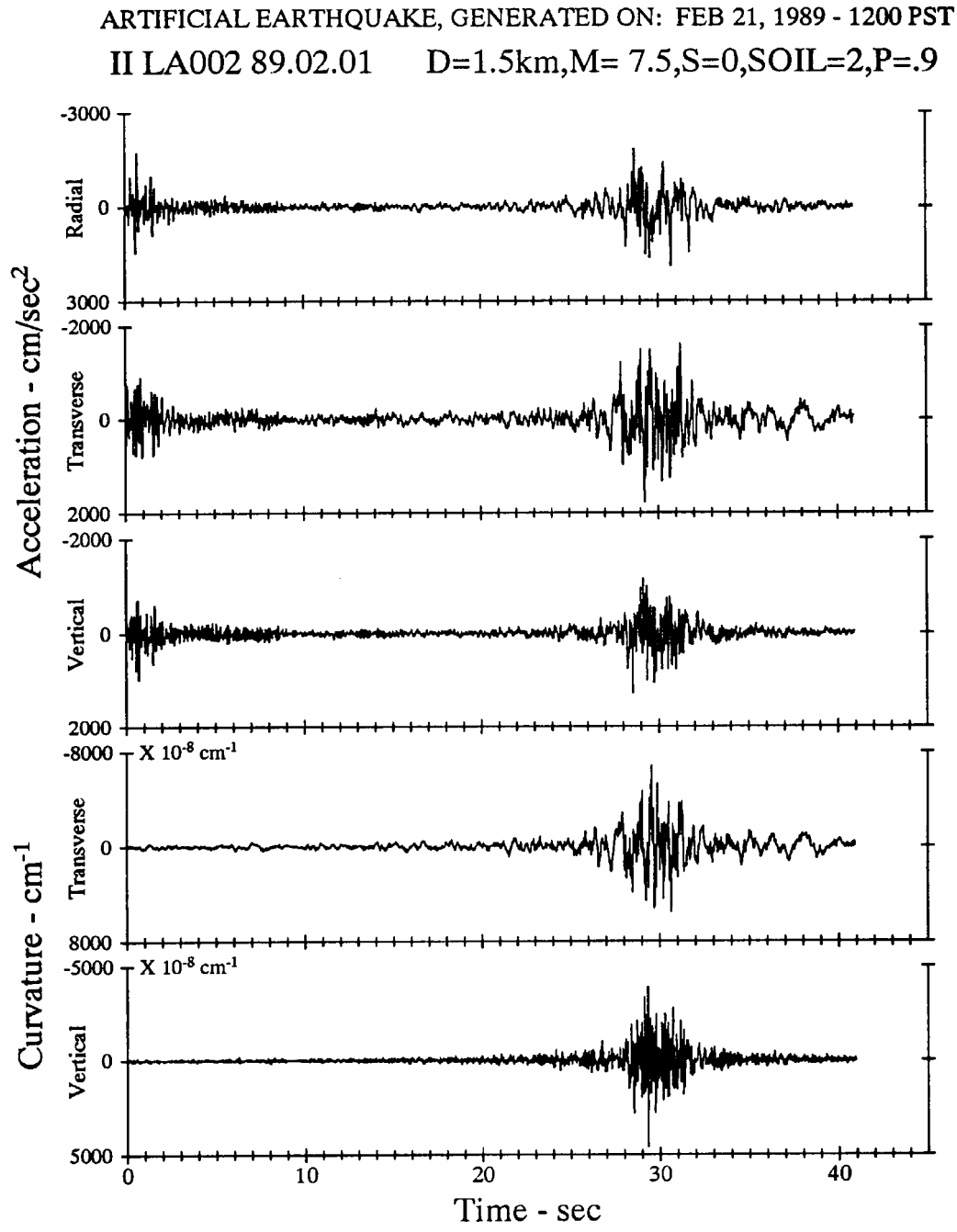

Fig. 21 Artificial earthquake synthetic acceleration and curvature accelerogram: LA002

3. Examples of Synthetic Curvograms

To illustrate the appearance of synthetic curvograms, we consider again the site at Westmoreland in Imperial Valley, California. The local geology and the associated dispersion curves for this site have been used in the preceding sections dealing with the translational, rocking, and torsional accelerograms. For continuity and comparison with the earlier analyses, we consider this site again (Tables 2 and 3). From Equations (86a) and (86b), it is seen that the largest curvature (smallest radius) will be associated with large peak accelerations and with small c, i.e., with "soft" layers near the surface. Thus, in the first example, we consider the site intensity $MMI = XII$ for a source at distance $R = 5$ km. We also assume that the site is on sediments $(s = 0)$ and on deep soil $(s_L = 2)$ (Trifunac, 1989a, 1989b), and compute empirical Fourier spectrum amplitudes, assuming 50% probability of exceedance $(p = 0.5)$. To model $s = 0$ and $s_L = 2$ site conditions, we modify the top layer (in Table 2) to consist of two layers of

thickness 50 m and 130 m, and with shear wave velocities of 50 and 300 m/s, respectively (Table 3). For depths greater than 180 m, we assume the values given in Table 2. Figure 20 shows the resulting radial, transverse, and vertical accelerograms, and the associated transverse and vertical curvograms. The smallest radii of curvature corresponding to $k_{2,\max} = 0.54 \times 10^{-4}\,\mathrm{cm}^{-1}$ and $k_{3,\max} = 0.89 \times 10^{-4}\,\mathrm{cm}^{-1}$ are $\rho_{2,\min} = 185$ m and $\rho_{3,\min} = 112$ m, respectively.

Figure 21 illustrates similar results, but for scaling in terms of magnitude (Trifunac, 1989a). For $M = 7.5,\ R = 1.5$ km, and $p = 0.9,$ the peak curvatures are $k_{2,\max} = 0.46 \times 10^{-4}\,\mathrm{cm}^{-1}$ and $k_{3,\max} = 0.68 \times 10^{-4}\,\mathrm{cm}^{-1},$ and the corresponding radii of curvature are $\rho_{2,\min} = 217$ m and $\rho_{3,\min} = 147$ m.

CONCLUSIONS

A comprehensive method for synthesizing realistic strong motion accelerograms (translations and rotations), strains and curvatures for use in engineering design has been presented. The advantages of this method are that the results are consistent with all known characteristics of the recorded strong shaking. In particular, these accelerograms have non-stationary characteristics in time, which are derived from the known dispersive properties of earthquake waves guided through shallow low-velocity layers of the earth's crust. These dispersive characteristics can be introduced directly as an input into the computer program, and thus can portray directly the geologic environment of each specific site. Other scaling functionals, required for the synthesis of artificial accelerograms presented here, are: (i) the Fourier amplitude spectrum, and (ii) the frequency-dependent duration of strong shaking. These two functionals can be estimated via the empirical scaling relations developed either in terms of earthquake magnitude or in terms of Modified Mercalli Intensity.

It has been shown how the rocking and torsional accelerograms can be generated from the synthetic translational accelerograms, by applying the straightforward exact physical principles of elastic wave propagation. The rotational accelerograms obtained in this way have realistic physical properties, and should resemble actual rotational ground motions, as long as the synthetic translational accelerograms from which those are derived, have such corresponding physical properties.

Using the linear theory of wave propagation, the strain amplitudes can be evaluated exactly in three-dimensions. When local geologic conditions are too complex to model near-surface motions by the equivalent parallel layer models, the method presented here can be modified to give again the exact representation of near-surface translations, rotations, and strains (e.g., see Moeen-Vaziri and Trifunac (1988a, 1988b)).

The above examples illustrate the strain amplitudes implied by the linear theory, and cannot be taken to be "average" or "typical" estimates, for magnitudes, site intensities, or local conditions considered. In general, the strain amplitudes will increase with an overall increase in the strong motion amplitudes, and with a decrease in shear wave velocities of soil and sedimentary layers near the ground surface. Time-dependence of strain components near the ground surface is roughly proportional to the corresponding components of ground velocity, and thus, peak strains will also increase with peak ground velocity.

Finally, the above examples show that the radii of curvature in the range of one to several hundred meters may occur for very large accelerations (1-3 g), near epicenter, and when the local soil and geologic conditions are characterized by very low wave velocities (e.g., 50 m/s). Such conditions correspond only to the instances of exciting very large amplitudes of waves with short wave lengths, and can be expected to occur for soft soil and geologic site conditions near epicenters of earthquakes with high stress drop.

REFERENCES

1. Amin, M. and Ang., A.H.S. (1966). "A Nonstationary Stochastic Model for Strong Motion Earthquakes", Report 306, Struct. Research Series, Dept. of Civil Engng, Univ. of Illinois, Illinois, U.S.A.
2. Baba, K. and Nakashima, H. (1984). "Seismic Response of Uplifting Shear Wall-Flexural Frame Interaction Systems", Proc. 8th World Conf. Earthqu. Engng., Vol. IV, pp. 259-266.

3. Bielak, J. (1978). "Dynamic Response of Nonlinear Building-Foundation System", Earthqu. Engng. Struct. Dynam., Vol. 6, pp. 17-30.
4. Bogdanoff, J.L., Goldberg, J.E. and Bernard, M.C. (1961). "Response of a Simple Structure to a Random Earthquake-Like Disturbance", Bull. Seism. Soc. Amer., Vol. 51, pp. 293-310.
5. Bolotin, V.V. (1960). "Statistical Theory of Aseismic Design of Structures", Proc. 2nd World Conf. Earthqu. Engng, Japan, pp. 1365-1374.
6. Bycroft, G.N. (1960). "White-Noise Representation of Earthquakes", J. Eng. Mech. Div., ASCE, Vol. 86, pp. 1-16.
7. Dravinski, M. and Trifunac, M.D. (1979). "Static, Dynamic and Rotational Components of Strong Shaking near Faults", Report CE 79-06, Dept. of Civil Eng., Univ. of Southern California, Los Angeles, California, U.S.A.
8. Dravinski, M. and Trifunac, M.D. (1980). "Response of Layer to Strike-Slip Vertical Fault", Proc. Engineering Mech. Div., ASCE, No. EM4, pp. 609-621.
9. Goodman, L.E., Rosenblueth, E. and Newmark, N.M. (1955). "Aseismic Design of Firmly Founded Elastic Structures", Trans. ASCE, Vol. 120, pp. 782-802.
10. Goto, H. and Toki, K. (1969). "Structural Response to Nonstationary Random Excitation", Proc. 4th World Conf. Earthqu. Engng, Santiago, Chile.
11. Gupta, I.D. and Trifunac, M.D. (1987). "A Note on Contribution of Torsional Excitation to Earthquake Response of Simple Symmetric Buildings", Earthqu. Engng and Engng Vibrat., Vol. 7, No. 3, pp. 27-46.
12. Gupta, I.D. and Trifunac, M.D. (1988). "A Note on Contribution of Rocking Excitation to Earthquake Response of Simple Buildings", Bull. Indian Soc. Earthquake Tech., Vol. 25, No. 2, pp. 73-83.
13. Gupta, V.K. and Trifunac, M.D. (1990a). "Response of Multistoried Buildings to Ground Translation and Rocking during Earthquakes", J. Prob. Engng Mech., Vol. 5, No. 3, pp. 138-145.
14. Gupta, V.K. and Trifunac, M.D. (1990b). "A Note on Contributions of Ground Torsion to Seismic Response of Symmetric Multistoried Buildings", Earthqu. Engng Engng Vib., Vol. 10, No. 3, pp. 27-40.
15. Gupta, V.K. and Trifunac, M.D. (1990c). "Response of Multistoried Buildings to Ground Translation and Torsion during Earthquakes", Europ. Earthqu. Engng, Vol. IV, No. 1, pp. 34-42.
16. Gupta, V.K. and Trifunac, M.D. (1991). "Effects of Ground Rocking on Dynamic Response of Multistoried Buildings during Earthquakes", Struct. Engng/Earthqu. Engng, JSCE, Vol. 8, No. 2, pp. 43-50.
17. Honda, H. (1957). "The Mechanism of Earthquakes", Geophys. Inst., Tohoku Univ., Vol. 9, No. 5, pp. 1-46.
18. Housner, G.W. (1955). "Properties of Strong Ground Motion Earthquakes", Bull. Seism. Soc. Amer., Vol. 45, pp. 187-218.
19. Hudson, D.E. (1983). "Strong Motion Instrumentation Systems", Proc. Golden Anniversary Workshop Strong Motion Seism., Univ. of Southern California, Los Angeles, California, U.S.A., pp. 73-86.
20. Ishiyama, Y. (1982). "Motions of Rigid Bodies and Criteria for Overturning by Earthquake Excitations", Earthqu. Engng Struct. Dynam., Vol. 10, No. 5, pp. 635-650.
21. Kato, D., Katsumata, H. and Aoyama, H. (1984). "Effect of Wall Base Rotation on Behavior of Reinforced Concrete Frame-Wall Buildings", Proc. 8th World Conf. Earthqu. Engng, Vol. IV, pp. 243-247.
22. Kobori, T. and Shinozaki, I. (1975). "Torsional Vibration of Structure due to Obliquely Incident SH Waves", Proc. 5th European Conf. Earthqu. Engng, Vol. 1, Paper No. 22, pp. 1-5.
23. Kojić, S., Lee, V.W. and Trifunac, M.D. (1988). "Earthquake Response of Arch Dams to Nonuniform Canyon Motion", Report CE 88-03, Dept. of Civil Eng., Univ. of Southern California, Los Angeles, California, U.S.A.
24. Koh, A.S. and Spanos, P.-T.D. (1984). "Seismically Induced Rocking of Rigid Structures", Proc. 8th World Conf. Earthqu. Engng, Vol. IV, pp. 251-258.

25. Lee, V.W. (1979). "Investigation of Three-Dimensional Soil-Structure Interaction", Report CE 79-11, Dept. of Civil Eng., Univ. of Southern California, Los Angeles, California, U.S.A.
26. Lee, V.W. (1990). "Surface Strains Associated with Strong Earthquake Shaking", Proc. JSCE, No. 422/I-14, pp. 187-194.
27. Lee, V.W. and Trifunac, M.D. (1985). "Torsional Accelerograms", Int. J. Soil Dynam. Earthqu. Engng, Vol. 4, No. 3, pp. 132-139.
28. Lee, V.W. and Trifunac, M.D. (1987). "Rocking Strong Earthquake Accelerations", Int. J. Soil Dynam. Earthqu. Engng, Vol. 6, No. 2, pp. 75-89.
29. Lee, V.W. and Trifunac, M.D. (1989). "A Note on Filtering Strong Motion Accelerograms to Produce Response Spectra of Specified Shape and Amplitude", Europ. Earthqu. Engng, Vol. VIII, No. 2, pp. 38-45.
30. Lee, V.W. and Wu, X. (1994a). "Application of the Weighted Residual Method to Diffraction by 2-D Canyons of Arbitrary Shape, I: Incident SH Waves", Soil Dynam. Earthqu. Engng, Vol. 13, No. 5, pp. 355-364.
31. Lee, V.W. and Wu, X. (1994b). "Application of the Weighted Residual Method to Diffraction by 2-D Canyons of Arbitrary Shape, II: Incident P, SV and Rayleigh Waves", Soil Dynam. Earthqu. Engng, Vol. 13, No. 5, pp. 355-364.
32. Luco, J.E. (1976). "Torsional Response of Structures for SH Waves: The Case of Hemispherical Foundation", Bull. Seism. Soc. Amer., Vol. 66, pp. 109-123.
33. Manoogian, M.E. and Lee, V.W. (1996). "Diffraction of SH Waves by Sub-surface Inclusion of Arbitrary Shape", ASCE J. Eng. Mech., Vol. 122, No. 2, pp. 123-129.
34. Moeen-Vaziri, N. and Trifunac, M.D. (1988a). "Scattering and Diffraction of Plane SH-Waves by Two-Dimensional Inhomogeneities", Soil Dynam. Earthqu. Engng, Vol. 7, No. 4, pp. 179-188.
35. Moeen-Vaziri, N. and Trifunac, M.D. (1988b). "Scattering and Diffraction of Plane P and SV Waves by Two-Dimensional Inhomogeneities", Soil Dynam. Earthqu. Engng, Vol. 7, No. 4, pp. 189-200.
36. Nathan, N.D. and MacKenzie, J.R. (1975). "Rotational Components of Earthquake Motions", Can. J. Civil Eng., Vol. 2, pp. 430-436.
37. Newmark, N.M. (1969). "Torsion in Symmetrical Buildings", Proc. 4th World Conf. Earthqu. Engng, Santiago, Chile, A3.19-A3.32.
38. Psycharis, I.N. (1983). "Dynamics of Flexible Systems with Partial Lift-off", Earthqu. Engng Struct. Dynam., Vol. 11, pp. 501-523.
39. Rascon, O.A. and Cornell, A.C. (1969). "A Physically Based Model to Simulate Strong Earthquake Records on Firm Ground", Proc. 4th World Conf. Earthqu. Engng, Santiago, Chile.
40. Richter, C.F. (1958). "Elementary Seismology", Freeman and Co., San Francisco, U.S.A.
41. Rosenblueth, E. (1956). "Some Applications of Probability Theory on Aseismic Design", Proc. World Conf. Earthqu. Engng, Berkeley, California, U.S.A., No. 8, pp. 1-18.
42. Rosenblueth, E. and Bustamante, J.E. (1962). "Distribution of Structural Response to Earthquakes", J. Eng. Mech. Div., ASCE, Vol. 88, pp. 75-106.
43. Shibata, H., Shigeta, T. and Sone, A. (1976). "A Note on Some Results of Observation of Torsional Ground Motions and Their Response Analysis", Bull. Earthqu. Resist. Struct. Res. Center, Vol. 10, pp. 43-47.
44. Todorovska, M.I. and Lee, V.W. (1989). "Seismic Waves in Buildings with Shear Walls or Central Core", ASCE J. Eng. Mech., Vol. 115, No. 12, pp. 2659-2686.
45. Todorovska, M.I. and Trifunac, M.D. (1989). "Antiplane Earthquake Waves in Long Structures", ASCE J. Eng. Mech., Vol. 115, No. 2, pp. 2687-2708.
46. Todorovska, M.I. and Trifunac, M.D. (1990a). "Propagation of Earthquake Waves in Buildings with Soft First Floor", ASCE J. Eng. Mech., Vol. 116, No. 4, pp. 892-900.
47. Todorovska, M.I. and Trifunac, M.D. (1990b). "A Note on Excitation of Long Structures by Ground Waves", ASCE J. Eng. Mech., Vol. 116, No. 4, pp. 952-964.

48. Todorovska, M.I. and Trifunac, M.D. (1992). "Effect of Input Base Rocking on the Relative Response of Long Buildings on Embedded Foundations", Europ. Earthqu. Engng, Vol. VI, No. 1, pp. 36-46.
49. Todorovska, M.I. and Trifunac, M.D. (1993). "The Effects of Wave Passage on the Response of Base-Isolated Buildings on Rigid Embedded Foundations", Report CE 93-10, Dept. of Civil Eng., Univ. of Southern California, Los Angeles, California, U.S.A.
50. Trifunac, M.D. (1971a). "Response Envelope Spectrum and Interpretation of Strong Earthquake Ground Motion", Bull. Seism. Soc. Amer., Vol. 61, pp. 343-356.
51. Trifunac, M.D. (1971b). "A Method for Synthesizing Realistic Strong Ground Motion", Bull. Seism. Soc. Amer., Vol. 61, pp. 1755-1770.
52. Trifunac, M.D. (1972a). "Stress Estimates for San Fernando, California, Earthquake of 9 February 1971: Main Event and Thirteen Aftershocks", Bull. Seism. Soc. Amer., Vol. 62, pp. 721-750.
53. Trifunac, M.D. (1972b). "Tectonic Stress and Source Mechanism of the Imperial Valley, California, Earthquake of 1940", Bull. Seism. Soc. Amer., Vol. 62, pp. 1283-1302.
54. Trifunac, M.D. (1973). "Analysis of Strong Earthquake Ground Motion for Prediction of Response Spectra", Earthqu. Engng Struct. Dynam., Vol. 2, No. 1, pp. 59-69.
55. Trifunac, M.D. (1976). "Preliminary Empirical Model for Scaling Fourier Amplitude Spectra of Strong Ground Acceleration in Terms of Earthquake Magnitude, Source to Station Distance and Recording Site Conditions", Bull. Seism. Soc. Amer., Vol. 66, pp. 1343-1373.
56. Trifunac, M.D. (1979a). "Preliminary Empirical Model for Scaling Fourier Amplitude Spectra of Strong Motion Acceleration in Terms of Modified Mercalli Intensity and Geologic Site Conditions", Earthqu. Engng Struct. Dynam., Vol. 7, pp. 63-74.
57. Trifunac, M.D. (1979b). "A Note on Surface Strains Associated with Incident Body Waves", Bull. EAEE, Vol. 5, pp. 5-95.
58. Trifunac, M.D. (1982). "A Note on Rotational Components of Earthquake Motions for Incident Body Waves", Soil Dynam. Earthqu. Engng, Vol. 1, No. 1, pp. 11-19.
59. Trifunac, M.D. (1989a). "Dependence of Fourier Spectrum Amplitudes of Recorded Strong Earthquake Accelerations on Magnitude, Local Soil Conditions and on Depth of Sediments", Earthqu. Engng Struct. Dynam., Vol. 18, No. 7, pp. 999-1016.
60. Trifunac, M.D. (1989b). "Empirical Scaling of Fourier Spectrum Amplitudes of Recorded Strong Earthquake Accelerations in Terms of Magnitude and Local Soil and Geologic Conditions", Earthqu. Engng Engng Vib., Vol. 9, No. 2, pp. 23-44.
61. Trifunac, M.D. (1990). "Curvograms of Strong Ground Motion", ASCE J. Eng. Mech., Vol. 116, No. 6, pp. 1426-1432.
62. Trifunac, M.D. (1993). "Long Period Fourier Amplitude Spectra of Strong Motion Acceleration", Soil Dynam. Earthqu. Engng, Vol. 12, No. 6, pp. 363-382.
63. Trifunac, M.D. (1994). "Q and High Frequency Strong Motion Spectra", Soil Dynam. Earthqu. Engng, Vol. 13, No. 3, pp. 149-161.
64. Trifunac, M.D. (1995a). "Pseudo Relative Velocity Spectra of Earthquake Ground Motion at Long Periods", Soil Dynam. Earthqu. Engng, Vol. 14, No. 5, pp. 331-346.
65. Trifunac, M.D. (1995b). "Pseudo Relative Velocity Spectra of Earthquake Ground Motion at High Frequencies", Earthqu. Engng Struct. Dynam., Vol. 24, No. 8, pp. 1113-1130.
66. Trifunac, M.D. (1997). "Differential Earthquake Motion of Building Foundations", J. Structural Eng., ASCE, Vol. 123, No. 4, pp. 414-422.
67. Trifunac, M.D. and Brady, A.G. (1975). "A Study on the Duration of Strong Earthquake Ground Motion", Bull. Seism. Soc. Amer., Vol. 65, pp. 581-626.
68. Trifunac, M.D. and Anderson, J.G. (1977). "Preliminary Empirical Models for Scaling Absolute Acceleration Spectra", Report CE 76-03, Dept. of Civil Eng., Univ. of Southern California, Los Angeles, California, U.S.A.

69. Trifunac, M.D. and Lee, V.W. (1978). "Dependence of the Fourier Amplitude Spectra of Strong Motion Acceleration on the Depth of Sedimentary Deposits", Report CE 78-14, Dept. of Civil Eng., Univ. of Southern California, Los Angeles, California, U.S.A.
70. Trifunac, M.D. and Lee, V.W. (1985). "Preliminary Empirical Model for Scaling Fourier Amplitude Spectra of Strong Ground Acceleration in Terms of Earthquake Magnitude, Source to Station Distance, Site Intensity and Recording Site Conditions", Report CE 85-03, Dept. of Civil Eng., Univ. of Southern California, Los Angeles, California, U.S.A.
71. Trifunac, M.D. and Novikova, E.I. (1994). "State of the Art Review on Strong Motion Duration", 10th Europ. Conf. Earthqu. Engng, Vienna, Austria. Vol. 1, pp. 131-140.
72. Trifunac, M.D. and Novikova, E.I. (1995). "Duration of Earthquake Fault Motion in California", Earthqu. Engng Struct. Dynam., Vol. 24, No. 6, pp. 781-799.
73. Trifunac, M.D. and Todorovska, M.I. (1997a). "Response Spectra and Differential Motion of Columns", Earthquake Eng. Structural Dyn., Vol. 26, No. 2, pp. 251-268.
74. Trifunac, M.D. and Todorovska, M.I. (1997b). "Northridge, California, Earthquake of 17 January 1994: Density of Pipe Breaks and Surface Strains", Soil Dynamics Earthquake Eng., Vol. 16, No. 3, pp. 193-207.
75. Trifunac, M.D. and Todorovska, M.I. (2001). "A Note on Useable Dynamic Range in Accelerographs Recording Translation", Soil Dynamics Earthquake Eng., Vol. 21, No. 4, pp. 275-286.
76. Trifunac, M.D., Todorovska, M.I. and Ivanovic, S.S. (1996). "Peak Velocities, and Peak Surface Strains during Northridge, California, Earthquake of 17 January 1994", Soil Dynamics Earthquake Eng., Vol. 15, No. 5, pp. 301-310.
77. Trifunac, M.D. and Westermo, B.D. (1976a). "Dependence of Duration of Strong Earthquake Ground Motion on Magnitude, Epicentral Distance, Geologic Conditions at the Recording Station and Frequency of Motion", Report CE 76-02, Dept. of Civil Eng., Univ. of Southern California, Los Angeles, California, U.S.A.
78. Trifunac, M.D. and Westermo, B.D. (1976b). "Correlations of Frequency Dependent Duration of Strong Earthquake Ground Motion with the Modified Mercalli Intensity and the Geologic Conditions at the Recording Stations", Report CE 77-03, Dept. of Civil Eng., Univ. of Southern California, Los Angeles, California, U.S.A.
79. Tso, W.K. and Hsu, T.I. (1978). "Torsional Spectrum for Earthquake Motions", Earthqu. Engng Struct. Dynam., Vol. 6, pp. 375-382.
80. Wong, H.L. and Trifunac, M.D. (1978). "Synthesizing Realistic Strong Motion Accelerograms", Report CE 78-07, Dept. of Civil Eng., Univ. of Southern California, Los Angeles, California, U.S.A.
81. Wong, H.L. and Trifunac, M.D. (1979). "Generation of Artificial Strong Motion Accelerograms", Earthquake Engineering Structural Dynamics, Vol. 7, pp. 509-527.
82. Yim, C.S., Chopra, A.K. and Penzien, J. (1980). "Rocking Response of Rigid Blocks to Earthquakes", Earthqu. Engng Struct. Dynam., Vol. 8, No. 6, pp. 565-587.

ISET Journal of Earthquake Technology, Paper No. 428, Vol. 39, No. 4, December 2002, pp. 311-346

THE STATE OF THE ART IN SEISMIC HAZARD ANALYSIS

I.D. Gupta
Central Water & Power Research Station
Khadakwasla, Pune-411024

ABSTRACT

The seismic hazard analysis is concerned with getting an estimate of the strong-motion parameters at a site for the purpose of earthquake resistant design or seismic safety assessment. For generalized applications, seismic hazard analysis can also be used to prepare macro or micro zoning maps of an area by estimating the strong-motion parameters for a closely spaced grid of sites. Two basic methodologies used for the purpose are the "deterministic" and the "probabilistic" seismic hazard analysis (PSHA) approaches. In the deterministic approach, the strong-motion parameters are estimated for the maximum credible earthquake, assumed to occur at the closest possible distance from the site of interest, without considering the likelihood of its occurrence during a specified exposure period. On the other hand, the probabilistic approach integrates the effects of all the earthquakes expected to occur at different locations during a specified life period, with the associated uncertainties and randomness taken into account. The present paper gives a critical and detailed description of both deterministic and probabilistic approaches for seismic hazard analyses. A large number of example results are presented to illustrate the implementations of the two approaches. The results of the probabilistic approach are able to account for the effects of all the controlling factors in a balanced way, and can thus be considered more reliable. The advantages quoted in favour of using the deterministic approach can simply be achieved via de-aggregation of the probabilistic hazard analysis.

KEYWORDS: Seismic Hazard, Deterministic Approach, Probabilistic Approach, Uniform Risk Spectra, Hazard De-aggregation

INTRODUCTION

The seismic hazard analysis refers to the estimation of some measure of the strong earthquake ground motion expected to occur at a selected site. This is necessary for the purpose of evolving earthquake resistant design of a new structure or for estimating the safety of an existing structure of importance, like dams, nuclear power plants, long-span bridges, high-rise buildings, etc. at that site. In earthquake engineering and related areas, it is customary to distinguish between earthquake hazard and earthquake risk, although the semantics of these two words is the same. Earthquake hazard is used to describe the severity of ground motion at a site (Anderson and Trifunac, 1977, 1978a), regardless of the consequences, while the risk refers to the consequences (Jordanovski et al., 1991, 1993). To be consistent with this terminology, in this paper, the term hazard is used to describe the ground motion and the structural response with no regard to the consequences.

By taking into account all the available database on seismicity, tectonics, geology and attenuation characteristics of the seismic waves in an area of interest, the seismic hazard analysis is used to provide an estimate of the site-specific design ground motion at the site of a structure (Dravinski et al., 1980; Westermo et al., 1980). One important application of hazard analysis is the preparation of seismic zoning maps for generalized applications (Lee and Trifunac, 1987; Trifunac, 1989a, 1990a; Anderson and Trifunac, 1977, 1978a, 1978b). By estimating the amplitudes of a parameter describing the ground motion or the earthquake effect at a closely spaced grid of sites covering the complete area of a big city or an entire state, zoning maps can be developed by contouring the sub-areas with equal hazard. Such maps find useful applications in the earthquake-resistant design of common types of structures, for which it is not possible to carry out the detailed site-specific studies. The zoning maps are also useful for land-use planning, assessing the needs for remedial measures, and estimation of possible economical losses during future earthquakes (Trifunac, 1989b; Trifunac and Todorovska, 1998).

The seismic hazard at a site can be described by a variety of parameters of ground shaking. Before the actual instrumental measurements of strong ground motion became available, various intensity scales

(MMI, MKS, etc.) based on the description of observed damages were used to describe the severity of ground motion. Intensity data are (and should be) still used as a supplement to the instrumental recordings. More recently, peak ground acceleration, and to a much lesser extent the peak velocity and displacement, had been popular instrumental measurements of ground motion. Most of the existing code provisions and design procedures have been developed in terms of peak acceleration and a normalized standard spectral shape (IAEE, 1984). However, to account for the effects of earthquake magnitude and distance on the spectral shape, one should define directly the spectral amplitudes at different frequencies by using the frequency-dependent scaling equations for the spectral amplitudes (Lee, 1987). For the seismic zoning, one should thus prepare a separate zoning map in terms of the response spectrum amplitude at each frequency (Trifunac, 1989a, 1990a). In addition, there may be other derived parameters like peak strain or liquefaction potential, for example, to quantify the seismic hazard and preparation of zoning maps (Todorovska and Trifunac, 1996a, 1996b, 1999).

There are two basic philosophies for the seismic hazard analysis, viz., deterministic and probabilistic. The former proposes design for the maximum earthquake, that is the one that will produce most severe ground motion at a site. The latter advocates that likelihood of occurrence should also be considered in view of the fact that the life of a structure is very short compared to the recurrence intervals of large events. The first basic step in seismic hazard analysis is to collect the input data on tectonics and seismicity and on ground motion scaling models. One should then decide the methodology of hazard analysis, which may be deterministic (scenario earthquake) or probabilistic (an ensemble of earthquakes). The hazard may be characterized in terms of a variety of ground motion parameters (e.g., peak amplitudes, duration of shaking, Fourier and response spectra, differential motions, artificial time histories, etc.) or the effects of ground shaking on structure (displacement, shear and bending moment envelopes) and site response (liquefaction occurrence, slope stability, permanent displacements, etc.). However, the present paper addresses mainly the issue of estimating the strong-motion parameters of interest for earthquake-resistant design and seismic safety assessment purposes.

The deterministic approach for seismic hazard analysis is not well documented in literature, and it is practised differently in different parts of the world and even in different application areas. In its most commonly used form, the deterministic method first assesses the maximum possible earthquake magnitude for each of the seismic sources (important faults or seismic provinces) within an areas of about 300 km radius around the site of a structure of interest. Then, by assuming each of these earthquakes to occur at a location that places the focus at the minimum possible distance to the site, the ground motion is predicted by using an empirical attenuation relation or some other appropriate technique.

The probabilistic seismic hazard methodology involves integrating the probabilities of experiencing a particular level of a selected strong motion parameter due to the total seismicity expected to occur in the area (about 300 km radius) of a site of interest during a specified life period (Cornell, 1968; Anderson and Trifunac, 1977, 1978a). This approach is able to consider the inherent random uncertainties and scattering present in the input database as well as in the attenuation characteristics of ground motion parameters (Lee and Trifunac, 1985; Gupta, 1991). It is thus able to provide the estimate of ground motion with a specified confidence level (probability of not exceeding). The probabilistic approach is convenient to compare risks in various parts of a country and to compare the earthquake risk with other natural and man-made hazards. For example, the design loads should be such that the risk of damage is equal throughout the country, and that it is comparable to other risks that we are prepared to take (e.g.; risk of a traffic accident, or a plane crash, or damage from floods and cyclones). The probabilistic approach opens the possibility for risk-benefit analyses and respective design motions. The motivation for such a design principle is that, at the time of construction or strengthening, if it is invested in strength beyond that required just to prevent collapse (e.g., by codes), the monetary losses during future likely earthquakes may be reduced significantly.

The strong motion parameters in both deterministic and probabilistic methodologies are commonly estimated from empirical attenuation relations in terms of earthquake magnitude, distance and soil and geologic site conditions. Where instrumentally recorded data are lacking, the scaling of strong motion parameters in terms of site intensity (e.g., Modified Mercalli) scale can also be used. Therefore, this paper first describes the attenuation and scaling relations for the peak acceleration and the response spectral amplitudes, which are the strong motion parameters used commonly to obtain the design response spectrum. The deterministic and probabilistic formulations of seismic hazard analysis are presented next. The deterministic methodology basically aims at finding the combination of the maximum possible

magnitude and the corresponding distance which would generate the highest level of ground motion at a site of interest. The probabilistic approach, on the other hand, is based on the total expected seismicity (number of earthquakes of different magnitudes) during a specified life period with its proper spatial distribution with respect to the site of interest. Various approaches to define this seismicity are reviewed briefly in the paper. Example results are presented to highlight the salient features of the probabilistic approach vis-a-vis the deterministic approach. An example of the seismic zoning via probabilistic seismic hazard analysis (PSHA) approach is also presented for the purpose of illustration.

ATTENUATION AND SCALING RELATIONS

For quantifying the seismic hazard at a site or to prepare a seismic zoning map, one needs to know the attenuation and scaling characteristics of the various strong motion parameters with distance, earthquake size and the geological conditions. Though the acceleration time-histories provide the most comprehensive description of the ground motion, due to stochastic nature of the time-history amplitudes, it is not feasible to develop the attenuation relations directly for them. Till recent past, the attenuation relations were most commonly developed for the peak ground acceleration, which was used to scale a normalized standard spectral shape (Biot, 1942; Housner, 1959; Newmark and Hall, 1969; Seed et al., 1976; Mohraz, 1976). However, this approach suffers from several drawbacks and is unable to represent various characteristics of the response spectra in a realistic way (Trifunac, 1992; Gupta, 2002). To improve upon the use of standard spectrum and peak acceleration, Trifunac and co-workers in 1977-1979 were the first investigators to develop direct scaling relations for the response spectral amplitudes at different periods. These studies were motivated by the development of similar relations earlier for the Fourier Spectrum (FS) amplitudes by Trifunac (1976). Use of such relations made it possible to incorporate in a very realistic way, the effects of earthquake size, distance, component of motion and the geological condition on the Fourier and response spectrum amplitudes and shapes. Once the response or Fourier spectrum is obtained, the design accelerograms can be synthesized to be compatible with these spectra (Tsai, 1972; Wong and Trifunac, 1979; Lee and Trifunac, 1989; Gupta and Joshi, 1993; etc.).

A large number of frequency-dependent attenuation relations have been developed by different investigators, several of which are listed in Douglas (2001). The fundamental requirements for such an attenuation relationship are that it should represent, at each frequency, the magnitude and distance saturations and the variation in geometrical spreading with distance in a realistic way. Many of the available relations do not satisfy one or the other of these requirements. The distance variation of the geometrical attenuation is neglected by most of the published relationships. Due to predominance of different types of waves at near and long distances, this variation is very important. Since mid-seventies, Trifunac and co-workers have developed several generations of the frequency-dependent attenuation relations, which have considered all of the above mentioned requirements in a very comprehensive and physically sound way. A brief review on these relations is, therefore, presented in the following.

The first generation of frequency-dependent attenuation relations due to Trifunac and co-workers were based on a uniformly processed strong motion database (Trifunac, 1977) of 186 records with a total of 558 components of motions from 57 earthquakes with $M = 3.0$ to 7.7, where M refers to M_L up to around magnitude 6.5 and to M_S for higher magnitudes. This database was first used by Trifunac (1976) to develop the attenuation relations for Fourier spectrum (FS) amplitudes at wave-periods between 0.04 and 15.0 s, in terms of earthquake magnitude M, epicentral distance R, component direction v ($v = 0$ for horizontal and 1 for vertical), and the geological condition beneath and surrounding the recording site, defined by parameter s ($s = 0$ for alluvium, 1 for intermediate and 2 for basement rock sites). Trifunac and Anderson (1977, 1978a, 1978b) developed similar relations for the absolute spectrum acceleration (SA), relative spectrum velocity (SV) and the relative pseudo spectrum velocity (PSV) for five values of damping ratio $\zeta = 0.0$, 0.02, 0.05, 0.10 and 0.20. Trifunac and Lee (1978, 1979) developed the attenuation relations for FS and PSV amplitudes with the site geological condition defined by the depth of sedimentary deposits, h (in km), rather than by the scaling parameter s.

In early 1980's, the strong motion database in California region expanded to 438 free-field records, i.e. a total of 1314 components of acceleration from 104 earthquakes. With this new database, Trifunac and Lee (1985a, 1990) developed the first frequency-dependent attenuation function, $Att(\Delta, M, T)$, as a

function of the "representative" distance Δ from the source to the site, magnitude M and period of the motion, T. Using this attenuation function, Trifunac and Lee (1985b, 1985c) presented the second generation of scaling functions for estimating FS and PSV spectral amplitudes, wherein the site geological condition was represented in terms of either s or h. These as well as the previous attenuation relations did not include the effect of local soil site condition defined by shallow alluvium and soft deposits of a few tens of meters. Therefore, using the same database of 438 records, Trifunac (1987, 1989c, 1989d) and Lee (1987, 1989, 1993) developed respectively for FS and PSV spectra, the updated attenuation relations including the effects of local soil site condition along with the geological condition on a broader scale, defined by s or h. Following Seed's (1976) classification, the local soil condition in these relations was defined by the variable s_L = 0, 1 and 2, for rock, stiff-soil and deep-soil sites, respectively.

For example, the empirical attenuation relation, when the geological condition is specified by depth of sedimentary deposits, h, is as follows (Lee, 1987):

$$\begin{aligned}\log \text{PSV}(T) = M + Att(\Delta, M, T) + b_1(T)M + b_2(T)h + b_3(T)v + b_4(T)hv \\ + b_5(T) + b_6(T)M^2 + b_7^{(1)}(T)S_L^{(1)} + b_7^{(2)}(T)S_L^{(2)}\end{aligned} \tag{1}$$

Here, $b_1(T)$ through $b_7(T)$ are the scaling coefficients, determined by regression analysis of spectral amplitudes of recorded accelerograms, for different periods and damping values, and parameters $S_L^{(1)}$ and $S_L^{(2)}$ are the indicator variables used to define the soil condition,

$$S_L^{(1)} = \begin{cases} 1 \text{ if } s_L = 1 \text{ (stiff soil)} \\ 0 \text{ otherwise} \end{cases}; \quad S_L^{(2)} = \begin{cases} 1 \text{ if } s_L = 2 \text{ (deep soil)} \\ 0 \text{ otherwise} \end{cases} \tag{2}$$

The function $Att(\Delta, M, T)$, which defines the frequency-dependent attenuation, is given by (Trifunac and Lee, 1990),

$$Att(\Delta, M, T) = \begin{cases} A_0(T)\log\Delta & ; R \le R_0 \\ A_0(T)\log\Delta - \dfrac{(R - R_0)}{200} & ; R \ge R_0 \end{cases} \tag{3}$$

with

$$A_0(T) = \begin{cases} -0.0732 & ; T \ge 1.8 \text{ s} \\ -0.767 + 0.272\log T - 0.526(\log T)^2 & ; T \le 1.8 \text{ s} \end{cases}$$

where Δ is a representative source-to-site distance, defined as

$$\Delta = S\left(\ln\frac{R^2 + H^2 + S^2}{R^2 + H^2 + S_0^2}\right)^{-\frac{1}{2}} \tag{4}$$

In this expression, R is the epicentral distance and H is the focal depth. R_0 is a transition distance (about 150 km for $T < 0.05$ s and ≈ 50 km for $T > 1$ s), and Δ_0 is the value of Δ for $R = R_0$. Function $Att(\Delta, M, T)$ depends on magnitude M implicitly through S, which is a measure of the source dimension,

$$S = 0.2 + 8.51(M - 3); \quad M > 3 \tag{5}$$

S_0 represents the coherence radius of the source and is approximately given by $S_0 \sim \beta T/2$, where β is the shear wave velocity in the source region, and T is the wave period.

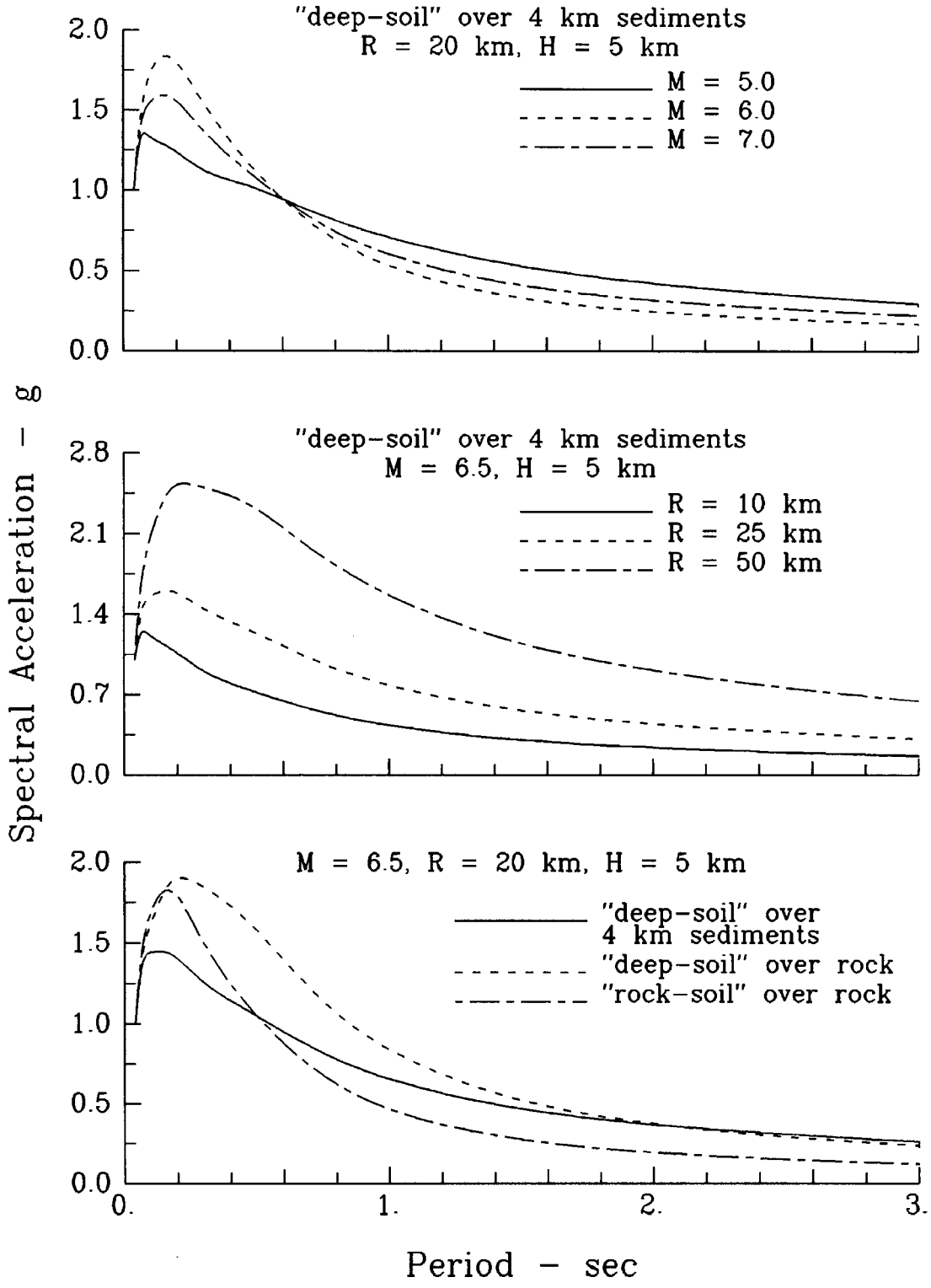

Fig. 1 Illustration of the effects of earthquake magnitude, source-to-site distance and the local soil and regional geological conditions on the normalized PSA spectra

The empirical attenuation relation, when the geological condition is defined by parameter $s = 0$, 1 and 2, is as follows (Lee, 1987):

$$\begin{aligned}\log \text{PSV}(T) = {} & M + Att(\Delta, M, T) + b_1(T)M + b_2^{(1)}(T)S^{(1)} + b_2^{(2)}(T)S^{(2)} \\ & + b_3(T)v + b_4^{(1)}(T)S^{(1)}v + b_4^{(2)}(T)S^{(2)}v + b_5(T) + b_6(T)M^2 + b_7^{(1)}(T)S_L^{(1)} + b_7^{(2)}(T)S_L^{(2)}\end{aligned} \tag{6}$$

where $S^{(1)}$ and $S^{(2)}$ are the indicator variables defining the site geological condition,

$$S^{(1)} = \begin{cases} 1 \text{ if } s = 1 \text{ (intermediate geology)} \\ 0 \text{ otherwise} \end{cases}; \quad S^{(2)} = \begin{cases} 1 \text{ if } s = 2 \text{ (basement rock)} \\ 0 \text{ otherwise} \end{cases} \tag{7}$$

With $\overline{\text{PSV}}(T)$ as the spectrum amplitudes estimated using Equation (1) or (6), and $\text{PSV}(T)$ the spectrum amplitudes computed from recorded accelerograms, the residuals $\varepsilon(T) = \log \text{PSV}(T) - \log \overline{\text{PSV}}(T)$ are described by the following probability distribution

$$p(\varepsilon, T) = \left[1 - \exp\left(-\exp\left(\alpha(T)\varepsilon(T) + \beta(T)\right)\right)\right]^{n(T)} \tag{8}$$

Here, $p(\varepsilon, T)$ is the probability that $\log \text{PSV}(T) - \log \overline{\text{PSV}}(T) \le \varepsilon(T)$, and $\alpha(T)$, $\beta(T)$ and $n(T)$ are parameters of the distribution, which are found from a regression analysis of the observed residuals. Thus, the probability that a given spectral amplitude $\text{PSV}(T)$ will be exceeded due to magnitude M at distance R is given by

$$q\left(\text{PSV}(T) \mid M, R\right) = 1 - p(\varepsilon, T) \tag{9}$$

It will be shown later that this probability of exceedance is one of the basic inputs required for the probabilistic seismic hazard model.

The attenuation relations of Equations (1) and (6) can be used along with Equation (8) to evaluate the $\text{PSV}(T)$ spectrum with any desired confidence level (probability of not exceeding) for given values of magnitude, distance, soil condition and regional geology, expressed in terms of depth of sedimentary deposits or qualitatively as alluvium $(s = 0)$, rock $(s = 2)$ or intermediate type $(s = 1)$. The pseudo acceleration spectrum, $\text{PSA}(T)$ can be obtained from the pseudo velocity spectrum, by using the following relationship

$$\text{PSA}(T) = \frac{2\pi}{T} \text{PSV}(T) \tag{10}$$

Using the foregoing attenuation relations, the 5% damped pseudo acceleration spectra have been computed for various earthquake parameters and different soil and geological conditions. These spectra, normalized to an acceleration of unity at 0.04 s period, are plotted in Figures 1(a) to 1(c). Results in Figure 1(a) reveal that with increase in design earthquake magnitude, the ground motion at a site is characterized by increasing contents of long and intermediate period waves. From Figure 1(b), it is seen that with increase in source-to-site distance, the high frequency (low-period) components of ground motion are attenuated more compared to the long period components. Thus, the spectra for larger magnitudes at longer distances have relatively higher contents of intermediate and long-period motions, which is similar to the effect of alluvium and soft sedimentary deposits at the recording site. On the other hand, spectra of small magnitudes at close distances contain more of low-period waves, which is similar to the effect of hard rock condition at the recording site. Thus, to obtain realistic site specific response spectra, it is essential to consider the frequency-dependent scaling effects of earthquake magnitude and distance, in addition to that of the soil condition (Trifunac, 1990b; Gupta and Joshi, 1996). Figure 1(c) exhibits the effects of the local soil and the surrounding geological conditions on the response spectral shapes. It is seen that the spectrum on a soil site overlying directly on the basement rock or that on thick sedimentary deposits may be quite different from the spectrum on a rock site. Thus, both local soil and site geological conditions play important role in deciding the shape and amplitudes of the response spectrum at a site. The use of direct scaling relations for the spectral amplitudes provides a simple way to quantify these effects in a realistic way.

Parallel with the development of attenuation relations in terms of earthquake magnitude and distance, Trifunac and co-workers have also developed scaling relations in terms of site intensity on Modified Mercalli Intensity (MMI) scale. For areas lacking in instrumentally recorded strong-motion data, these relations may find very useful applications for seismic hazard analysis. Based on the first data set of 186 records, Trifunac (1979) and Trifunac and Anderson (1977, 1978a, 1978b) developed the scaling

relations for FS, SA, SV and PSV spectral amplitudes, with the site geological condition described by parameter s. Trifunac and Lee (1978, 1979) developed relations for FS and PSV, with geological condition in terms of the depth of sedimentary deposits, h, in km. With the expanded database of 438 records, Trifunac and Lee (1985b, 1985c) developed improved scaling relations, with geological conditions described by either parameter s or the depth of sedimentary deposits, h. Also, similar to the attenuation relations in terms of magnitude, these relations were further improved to include the effect of the local soil condition along with the geological condition of the site and the surrounding area. Trifunac (1987, 1991) developed the scaling relations for FS, and Lee (1987, 1990, 1991) for the PSV spectral amplitudes. As the expressions for both FS and PSV relations are identical, only the PSV relations are presented here as follows:

$$\begin{aligned}\log \overline{\mathrm{PSV}}(T) = {} & b_1(T) I_1 + b_2(T) h + b_3(T) v + b_4(T) hv \\ & + b_5(T) + b_7^{(1)}(T) S_L^{(1)} + b_7^{(2)}(T) S_L^{(2)}\end{aligned} \tag{11}$$

and

$$\begin{aligned}\log \overline{\mathrm{PSV}}(T) = {} & b_1(T) I + b_2^{(1)}(T) S^{(1)} + b_2^{(2)}(T) S^{(2)} + b_3(T) v + b_4^{(1)}(T) S^{(1)} v \\ & + b_4^{(2)}(T) S^{(2)} v + b_5(T) + b_7^{(1)}(T) S_L^{(1)} + b_7^{(2)}(T) S_L^{(2)}\end{aligned} \tag{12}$$

Various parameters in these expressions have the same meaning as described before for the attenuation relations in terms of magnitude and distance. The distributions of the residuals have been also defined in a similar way by Equation (8), which can be used to compute the spectral amplitudes with different confidence levels or to obtain the probability that a specified amplitude $\mathrm{PSV}(T)$ will be exceeded due to site intensity I_1. The site intensity due to an earthquake with epicentral intensity I_0 at distance R can also be described in a probabilistic way (Anderson, 1978; Gupta and Trifunac, 1988; Trifunac and Todorovska, 1989; Gupta et al., 1999).

DETERMINISTIC METHODOLOGY

The deterministic methodology aims at finding the maximum possible ground motion at a site by taking into account the seismotectonic setup of the area around the site and the available data on past earthquakes in the area (Krinitzsky, 1995; Romeo and Prestininzi, 2000). For this purpose, first the magnitude of the largest possible earthquake (also termed as maximum credible earthquake) is estimated for each of the seismic sources (faults or tectonic provinces) identified in an area of about 300 km radius around the site of interest. The commonly used forms of seismic sources are the line, area, dipping plane, and the volume sources. The point source is also used sometimes when the epicenters are concentrated in a very small area far away from the site of interest. The maximum magnitude in each of the sources is assumed to occur at the closest possible distance from the site. Out of all the sources, the magnitude and distance combination which gives the largest ground motion amplitude at the site is used in the deterministic method. Most commonly, the ground motion is estimated by using an empirical attenuation relation as described in the previous section. In some cases, the ground motion may also be evaluated by using empirical Green's function or stochastic seismological source model approaches (Hartzell, 1982; Hadley and Helmberger, 1980; Irikura and Muramatu, 1982; Boore and Atkinson, 1987; Gupta and Rambabu, 1996; etc.). Thus, the most important aspect of the deterministic methodology is to estimate the maximum magnitude, $M_{\max}$, for each seismic source. However, no widely accepted method exists for estimating $M_{\max}$ at present. Various methods in vogue can be grouped into two main categories: deterministic and probabilistic, which are described briefly in the following.

1. Deterministic Estimation of $M_{\max}$

The deterministic method most often used to find the maximum magnitude, $M_{\max}$, is based on the empirical regression relationships between the magnitude and various tectonic and fault rupture parameters like length, area and dislocation. Figures 2(a) and 2(b) show the relationships developed by different investigators in terms of the fault length and the fault area, respectively. It may be noted that the

sub-surface rupture length $\left(\overline{L}\right)$ can be determined more accurately from the spread of aftershock activity, and is thus considered more appropriate compared to the estimates based on surface rupture length $\left(L\right)$. The surface rupture may vary widely with geologic condition and hypocentral depth. The relationships in terms of rupture area are characterized by smaller variations compared to the rupture length relations. However, it is very difficult to predict the rupture scenario for a future earthquake, to have reliable prediction of magnitude by this method.

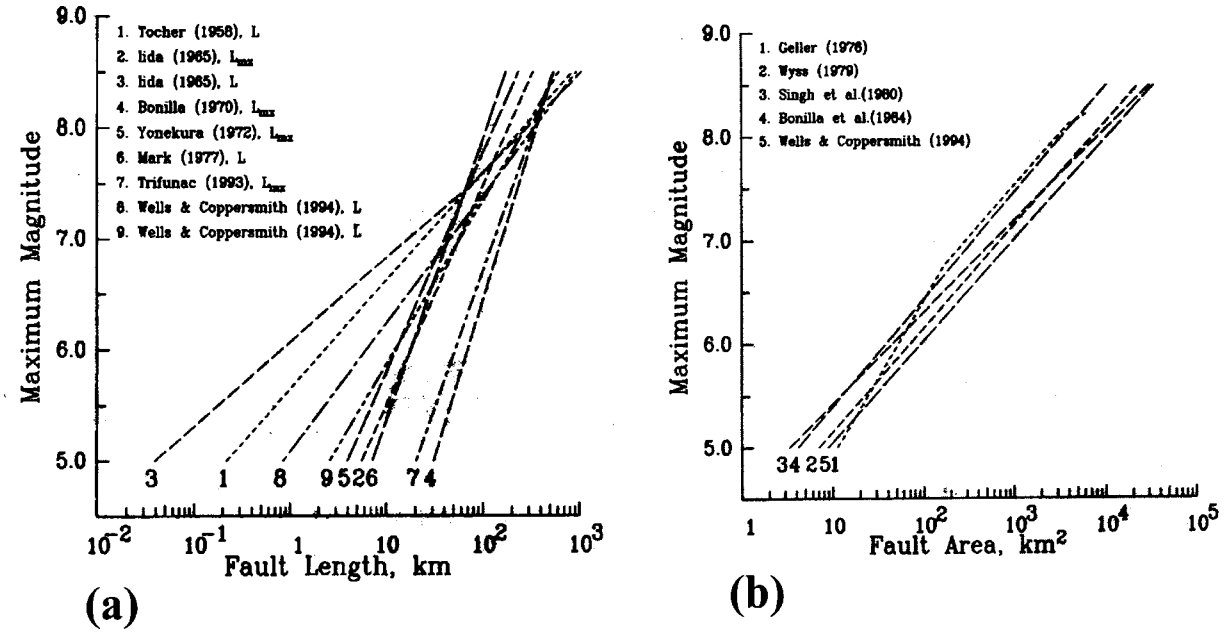

Fig. 2 Comparison of several empirical relationships used to find the maximum magnitude from (a) the fault rupture length and (b) the fault rupture area

$M_{\max}$ can also be related to the strain rate or the rate of seismic-moment release (Smith, 1976; Anderson and Luco, 1983; Papastamatiou, 1980; Wesnousky, 1986). If $M_0\left(M\right)$ is the seismic moment corresponding to a magnitude M, and $n\left(M\right)dM$ is the long-term average rate of occurrence of seismic events within a small magnitude interval of dM centered at magnitude M, the seismic moment rate $\dot{M}_0$ can be defined as

$$\dot{M}_0 = \int_{-\infty}^{\infty} M_0\left(M\right) n\left(M\right) dM \tag{13}$$

The seismic moment can be determined from earthquake magnitude using the following form of empirical relationship,

$$\log M_0 = c + dM \tag{14}$$

Hanks and Kanamori (1979) have proposed $c = 16.0$ and $d = 1.5$. The quantity $n\left(M\right)$ is an occurrence rate density function defined from the number, $N\left(M\right)$, of earthquakes per year with magnitude greater than or equal to M as

$$n\left(M\right) = -\frac{dN\left(M\right)}{dM} \tag{15}$$

Assuming that $N\left(M\right)$ can be defined by the Gutenberg-Richter's (Gutenberg and Richter, 1954) frequency-magnitude relationship truncated at the maximum magnitude $M_{\max}$, Smith (1976) has derived the following expression for estimating $M_{\max}$ from a knowledge of the moment rate $\dot{M}_0$,

$$M_{\max} = \frac{\log\left[\left(\frac{d}{d-b}\right)T\dot{M}_0\right] - c}{d} \tag{16}$$

Constant b in this expression is the slope of the Gutenberg-Richter's relationship, and this determines the proportion of large earthquakes relative to small earthquakes in a region. The term $T\dot{M}_0$ represents the cumulative moment of all the earthquakes in a time interval T, which should be the average recurrence period of $M_{\max}$. The moment rate $\dot{M}_0$ can be estimated from the geological slip rate, $\dot{u}$, and the total fault rupture area, A, as $\dot{M}_0 = \mu A\dot{u}$, where μ is the shear modulus of the rock at the fault. To use Equation (16), the recurrence interval for the maximum earthquake could approximately be estimated from the paleoseismic investigations. Though microfracturing studies of rock in laboratory and observations of earthquake sequences have led several investigators to suggest a possible relationship between b-value and seismotectonic data (Scholz, 1968; Wyss and Brune, 1968), it is not possible to estimate it from the geological data alone. It, therefore, becomes necessary to estimate this parameter from actual earthquake sequences (Esteva, 1969; Trifunac, 1994, 1998). Microearthquakes, main shocks, aftershocks, and earthquake swarms occurring within the region of interest or within geotectonically similar regions may give statistically significant estimate of b. However, the basic data on seismic slip rate (tectonic minus creep rate) may not be readily available in most cases to use this method.

To illustrate the applicability of the above method, a rough estimate of the maximum magnitude is made for the Himalayan region. From west to east, the entire Himalaya has a length of about 2500 km, and the width of the associated seismic source is about 100 km. The source of major earthquakes along the Himalaya has been postulated as a gently dipping detachment plane, north of the main boundary fault (MBF), at a depth of about 20 to 30 km (Seeber and Armbruster, 1981). Thus, the total rupture plane of the Himalaya has an area (A) of about 2.5 x 10^5 km^2. From a knowledge of the crustal model (Khattri et al., 1994), the shear modulus, μ, for the Himalayan rocks can be taken as 3.4 x 10^{11} dyne/cm^2. Also, after accounting for the trans-Himalayan deformations, the long-term average of the slip rate, $\dot{u}$, along the Himalayan detachment plane is corroborated to be only about 15 mm/year (Bilham and Gaur, 2000). This gives the moment rate $\dot{M}_0 = \mu A\dot{u}$ as 1.275 x 10^{27}dyne-cm/year. An analysis of instrumentally recorded data in the recent past suggests a b-value of about 0.9 for the Himalayan region. Thus, assuming that the recurrence period for largest earthquakes with magnitude 8(+) anywhere in the Himalaya is about 40 years, Equation (16) predicts $M_{\max}$ for such an earthquake as 8.7. This value is quite consistent with the four largest earthquakes known to have occurred in different parts of the Himalaya during the known past. However, the complete length of the Himalaya is segregated by transverse faults into independent segments not exceeding about 100 to 150 km of length. The moment rate $\dot{M}_0$ for such a segment of about 150 km would be 7.65 x 10^{25} dyne-cm/year. For $M_{\max}$ = 8.7, the expression of Equation (16) predicts an average recurrence period of about 587 years for any specified segment of the Himalaya. Thus, for the regions lacking in recorded earthquake data, information on geological slip rates, if available accurately, can be used to arrive at the maximum earthquake magnitude.

Another class of deterministic procedures is based on extrapolation of frequency-magnitude curves, derived from a short record of historical earthquakes. Though the linear extrapolation may be very conservative compared to truncated or exponential fall-off terminations (Wesnousky, 1994), it is used commonly due to lack of the exact knowledge about the non-linear nature for the large "characteristic earthquakes". Further, an extrapolation for a recurrence interval of 500 to 1000 years is used commonly, whereas the actual recurrence period may sometimes be quite different. When the available data are not adequate to define the frequency-magnitude relationship for a seismic source, the maximum earthquake magnitude is sometimes also found simply by adding an increment to the largest historical earthquake. Magnitude units of 0.5 or 1.0 are often added to get an estimate of $M_{\max}$ in many applications.

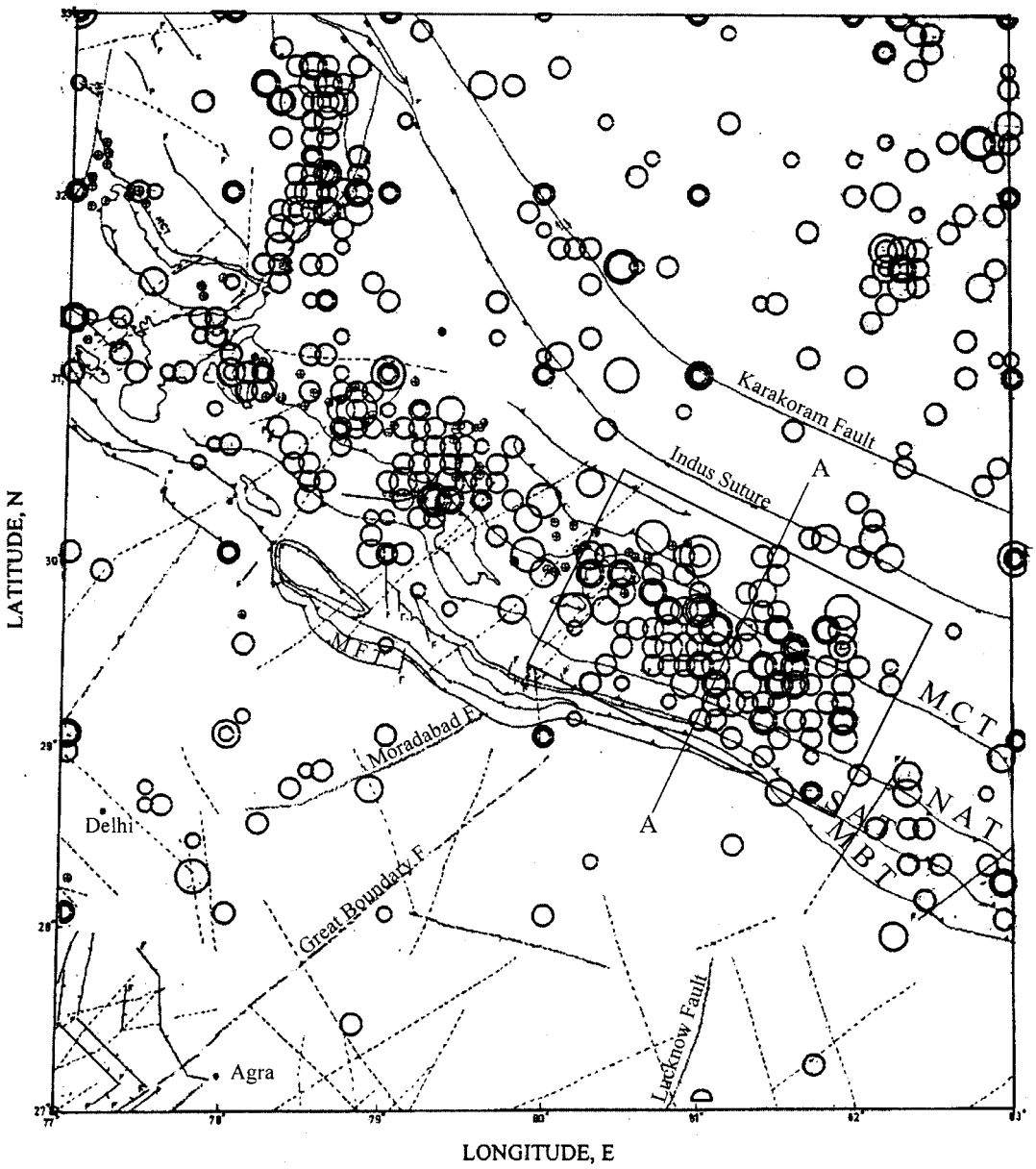

Fig. 3 Major tectonic features and the distribution of epicenters of available data on past earthquakes in a typical segment of the Himalayan region, used to compute the example results

2. Probabilistic Estimation of $M_{\max}$

The oldest probabilistic approach to find $M_{\max}$ is the use of extreme-value statistics, which was probably applied in seismology for the first time by Nordquist (1945), who used Gumbel Type-I distribution. Epstein and Lomnitz (1966) proved that the Gumbel Type-I distribution can be derived directly from the assumption that seismic events follow the Poisson distribution and the Gutenberg-Richter frequency-magnitude relationship. Use of several other extreme-value distributions has been introduced in seismology by different investigators to obtain the expected maximum magnitude for a desired return period. Gupta et al. (1988, 1994) have made a comparative study of several important extreme-value distributions and have also proposed the use of Log-Pearson Type-3 distribution for earthquake data. Such distributions have the advantage over the extrapolation of magnitude-frequency relation that they do not need data on smaller magnitudes, which are generally not reported completely for a sufficiently long time interval. The extreme-value distributions are fitted to the maximum magnitude observed per unit interval of time, commonly taken as one year. However, the available data are generally not complete even for the annual maximum magnitudes for the pre-instrumental period, and

also for the recent periods for areas with low level of seismicity and inadequate instrumentation. The estimates of the maximum magnitude from the extreme-value distributions depend on the assumed recurrence period, which may generally be associated with large uncertainty. Thus, conventionally, the extreme-value statistics does not predict M_{max} in an absolute way from a given data base.

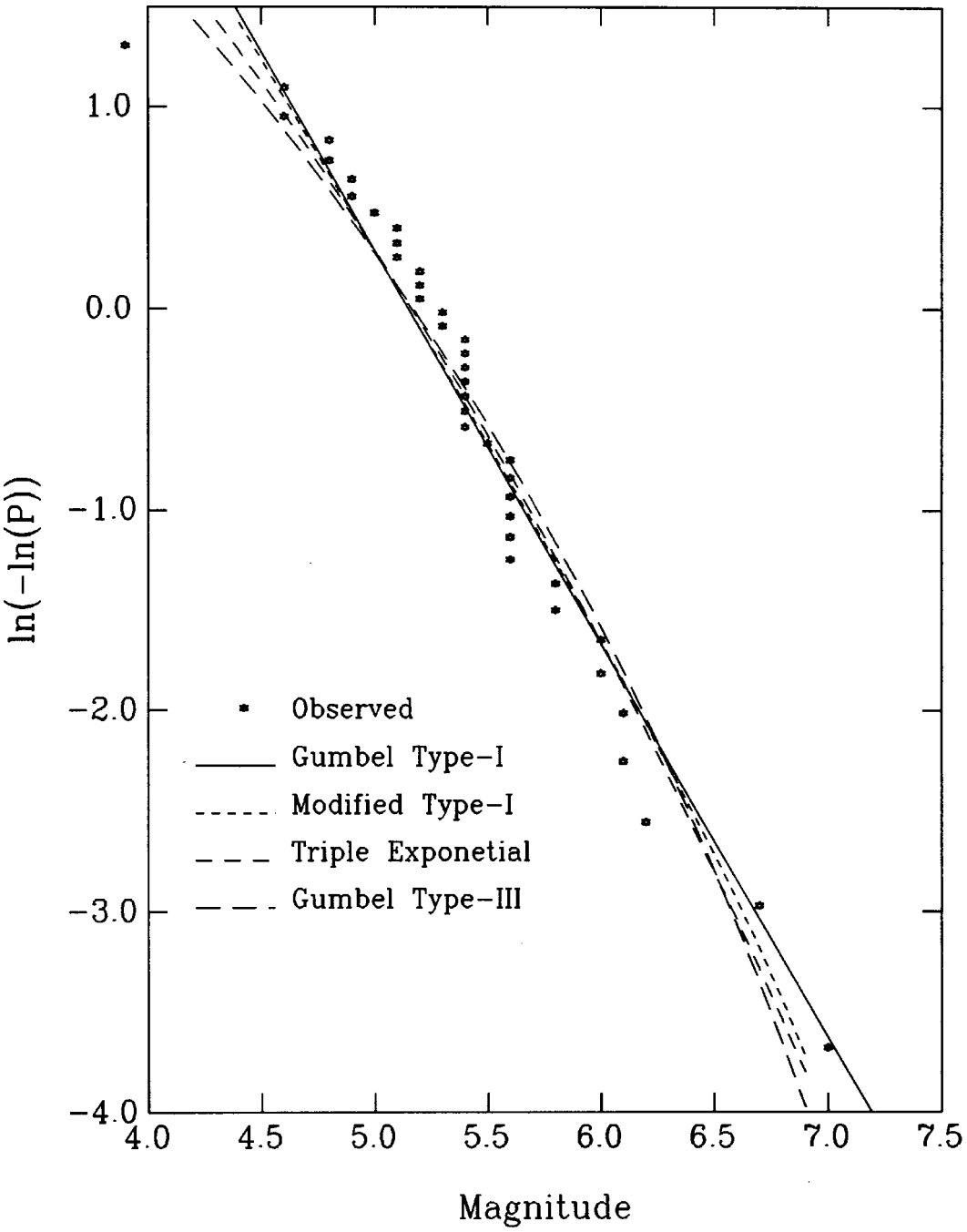

Fig. 4 Fitting of four commonly used extreme-value distributions to the available data on annual maximum magnitudes for the period 1963 to 2001 in the area of Figure 3

A more comprehensive probabilistic approach for estimating the maximum regional magnitude, M_{max}, was suggested by Kijko and Sellevoll (1989), which has been further refined recently by Kijko and Graham (1998) to consider the uncertainties in the input magnitude data. To describe the earthquake magnitude, they have used a doubly truncated exponential probability distribution function with lower cut-off magnitude M_{min}, an upper bound magnitude M_{max}, and a statistical parameter $\beta = b \ln 10$, where b is the Gutenberg-Richter's parameter. This has been then used to define the probability distribution of the maximum magnitude for a period of T years of observation. By constraining the

observed largest magnitude to be the expected value of the largest observed magnitude, Kijko (1983) has obtained an estimator for M_{max}, which requires knowledge of the mean seismic activity rate λ and the parameter β (or *b*). To estimate M_{max}, Kijko and co-workers have developed a joint maximum-likelihood function using mixed data files, consisting of an incomplete part of the earthquake catalogue containing only large historical events for a very long period and the complete part of the catalogue for a short recent period. The incomplete part is described by extreme-value distribution based on the doubly truncated magnitude distribution defined in terms of parameter β, and the complete part by the Poisson probability density function with mean occurrence rate λ. The possible standard deviations in the apparent magnitude values are accounted in these distributions by defining their Bayesian forms (Kijko and Graham, 1998). By including the expression for M_{max} into the maximum likelihood function for parameters β and λ, an iterative procedure is used to get the maximum likelihood estimate of M_{max} along with parameters β and λ.

To illustrate the application of the probabilistic method for estimation of M_{max}, a typical segment of the Himalayan region as shown in Figure 3 has been considered. The catalogue of past earthquakes for this area has been compiled for the period 1764 to 2001 from different published sources. However, to use the conventional extreme-value distribution, data on even annual maximum magnitudes is complete for a period of only 39 years from 1963 to 2001. Four different extreme-value distributions, viz., Gumbel Type-I and III (Gumbel, 1958), Modified Type-I (Chen and Lin, 1973) and Triple-exponential (Kijko and Sellevoll, 1981) distributions, are fitted to these data as shown in Figure 4. On the other hand, to apply the method of Kijko and co-workers based on a joint maximum likelihood function using mixed data files, the entire catalogue has been used. The part of the catalogue upto 1962 is treated as incomplete, which contains 17 of the largest seismic events with threshold magnitude as 5.7. The standard deviation of the magnitude for all these events is assumed to be 0.4. The subsequent part of the catalogue is considered complete and is divided into three periods as 1963 to 1971, 1972 to 1981, and 1982 to 2001, with threshold magnitudes as 5.1, 4.6 and 4.1, respectively. The corresponding uncertainties in the magnitude estimation are taken as 0.3, 0.2 and 0.2, respectively. The minimum magnitude, M_{min}, is taken as 3.8. The largest known earthquake in the area is with magnitude 7.5. Using these data, the maximum likelihood estimate $\hat{M}_{max}$ of the largest earthquake magnitude is obtained as 7.8 ± 0.57. The maximum likelihood estimates of parameters β and λ are found to be $\hat{\beta} = 2.22 \pm 0.07$ and $\hat{\lambda} = 27.05 \pm 1.59$. The expected recurrence period for the maximum magnitude is found to be 1298 years. The average values of the maximum magnitude for this recurrence period as obtained from other conventional extreme-value distributions shown in Figure 4 are: 8.8 (Gumbel Type-I), 7.6 (Modified Type-I), 7.5 (Gumbel Type-III) and 8.1 (Triple-exponential). The results of different extreme-value distributions are seen to vary widely and cannot be relied upon, because no constraint is applied to define the maximum magnitude in these distributions as has been done in the maximum-likelihood method of Kijko and co-workers.

PSHA METHODOLOGY

The results of the deterministic approach based on a single earthquake at a fixed distance from a selected site are not always able to ensure the intended conservatism for all the structures covering a wide range of frequencies. This is because the ground motion in different frequency ranges may be dominated by earthquakes of different magnitudes and distances. Thus, to get a reliable estimation of the seismic hazard at a site, it is necessary to consider the effects of all the earthquakes of different magnitudes with their proper spatial distribution around the site of interest (Cornell, 1968; Anderson and Trifunac, 1977, 1978a), and not just a single earthquake. Also, the random uncertainties in specifying the input parameters should be taken into account (Lee and Trifunac, 1985). The probabilistic seismic hazard analysis (PSHA) methodology provides a means to consider the effect of the total expected seismicity over a specified exposure period, and also the random nature of earthquake occurrences and attenuation of seismic waves with distance.

1. Theoretical Formulation

The PSHA approach is based on defining a composite probability distribution function for a selected strong-motion parameter at a site of interest due to the total expected seismicity in the area around the site during a specified exposure period. The four basic types of input to be specified and appropriately modelled for this purpose are: (i) the earthquake sources contributing to the hazard (e.g., within 300 km radius around the site), (ii) the expected total seismicity in each source, (iii) the site characteristics (e.g., geological and soil conditions), and (iv) the conditional probability that the strong motion parameter exceeds a specified level upon the occurrence of a particular earthquake. There should be a balance in the details of these inputs. The detail that significantly influences the outcome should be captured, but only if it can be obtained with reasonable accuracy and reliability. Complicated models of earthquake occurrence, which may require specification of parameters that cannot be obtained with reasonable accuracy from available data, should be avoided. The same is true for ground motion modelling; only the details that can be extracted from available strong motion data with sufficient statistical significance should be included. Another example is the modelling of geometry of the earthquake source zones. Close to the site, areal and volume zones should be used and the size of the rupture should not be neglected, while distant source zones can be modelled as line or point sources.

In actual calculations, the earthquake size is discretized, and all the earthquakes within a small magnitude interval centered around magnitude M_j are represented by M_j. The possible locations of ruptures are also discretized by distances R_i. Thus, the pair (i, j) indicates an earthquake of magnitude M_j occurring at distance R_i from the site of interest. For each such pair, the average rate of occurrence of earthquakes per year, v_{ij}, needs to be assigned. This rate depends on the rate for the entire source zone and on the probability distribution of ruptures within the zone. Then, assuming the earthquake occurrence at a location to follow the Poisson distribution, the expected number of earthquakes with magnitude M_j occurring at distance R_i from the site during a time interval of Y years is given by $n_{ij}(Y) = v_{ij}.Y$. Let X be the random variable representing a strong motion parameter (e.g., peak amplitude, spectral amplitude or site intensity), and let x be a possible level of X. Also, let $q\left(x \middle| M_j, R_i\right)$ be the conditional probability that value x will be exceeded due to an earthquake of type (i, j). The expected number of times for which $X > x$ occurs due to earthquakes of type (i, j), is equal to $q\left(x \middle| M_j, R_i\right).n_{ij}(Y)$, and the expected number of times for which $X > x$ occurs due to any type of earthquakes, is given by (Anderson and Trifunac, 1977, 1978a)

$$N_E(x) = \sum_{i=1}^{I}\sum_{j=1}^{J} q\left(x \middle| M_j,\ R_i\right).n_{ij}(Y) \tag{17}$$

The occurrence of the event $X > x$ from earthquakes of type (i, j) is a selective Poissonian process, and that from all possible earthquakes is also Poissonian (as the sum of Poissonian random variables) with parameter $N_E(x)$. Thus, the probability of $X > x$ (i.e., amplitude x is exceeded) is given by

$$P(X > x) = 1.0 - \exp\{-N_E(x)\} = 1.0 - \exp\left\{-\sum_{i=1}^{I}\sum_{j=1}^{J} q\left(x \middle| M_j, R_i\right).n_{ij}(Y)\right\} \tag{18}$$

The plots of x versus $P(X > x)$ for different exposure periods are commonly termed as "hazard curves". In many studies, the hazard curve is computed only for one year to define the annual probability of exceedance. In practical applications, the value x is determined by considering the annual probability of exceedance of the order of 1.0×10^{-5} to 1.0×10^{-3}. However, this commonly adopted practice does not provide a direct idea about the probability of exceeding value x during a specified exposure period. Therefore, in this paper, all the example results will be presented for a specified confidence level over a given exposure period.

The theoretical formulation of Equation (18) is based on the assumption that the earthquakes occur at a constant rate in time. However, it is applicable to earthquake occurrences with time-varying rate also,

provided that the total number of earthquakes, $n_{ij}(Y)$, are estimated by taking such time-dependence into account (Lee, 1992; Todorovska, 1994). Two important examples of the time-dependent activity rate are the occurrence of large characteristic earthquakes and the aftershock sequences. After a large earthquake, it takes time to accumulate the required strain energy to cause another similar earthquake at the same location (David et al., 1989). Therefore, the occurrence rate should be small soon after the occurrence of a large earthquake. However, as the elapsed time, T_o, since the previous event approaches the average return period of such an event, the occurrence rate should increase. Thus, the Poissonian model overestimates the hazard soon after the occurrence of a large earthquake, and may underestimate the hazard when the next earthquake is due or overdue. Processes of earthquake occurrence that satisfy all the Poissonian assumptions, but the one for constant rate, are of the type of "nonhomogeneous Poissonian processes". Such processes are normally specified by the hazard rate $h(t)$, which can be used to evaluate the conditional expected number of earthquakes $n_{ij}(Y|T_o)$, given the elapsed time, T_o, since the last large earthquake as

$$n_{ij}(Y|T_o) = \int_{T_o}^{T_o+Y} h(t)dt \tag{19}$$

Several investigators (Nishenko and Buland, 1987; Jara and Rosenblueth, 1988) have shown that the characteristic earthquakes along the plate boundaries can be described well by the lognormally distributed interoccurrence time period, the hazard rate for which is given by

$$h(t) = \frac{f(t)}{1-F(t)} \tag{20}$$

Here, $f(t)$ is the lognormal density function and $F(t)$ the corresponding distribution function for the interoccurrence time *t*. These are defined as

$$f(t) = \frac{1}{\sqrt{2\pi}\zeta t} e^{-\frac{1}{2}\left(\frac{\ln t-\lambda}{\zeta}\right)^2};\ 0 \le t \le \infty \tag{21}$$

and

$$F(t) = \Phi\left(\frac{\ln t-\lambda}{\zeta}\right) \tag{22}$$

where λ and ζ are respectively the mean and standard deviation of $\ln t$, with $\Phi(\cdot)$ as the distribution function for the standard normal density function with zero mean and unit standard deviation.

The aftershock activity following a large main earthquake can be modelled as a nonhomogeneous Poisson process in time by the modified Omori's law as (Utsu, 1961)

$$n(t) = \frac{K}{(t+c)^p} \tag{23}$$

where, $n(t)$ is the rate of occurrence of aftershocks at time t after the main shock, and K, c and p are constants. Assuming the magnitude distribution to follow the Gutenberg-Richter's frequency-magnitude relationship, the occurrence rate, $\lambda(t, M_j)$, of aftershocks with magnitude M_j or greater at time t, while following a main shock of magnitude M_m, can be obtained as

$$\lambda(t, M_j) = n(t)10^{b(M_m-M_j)} \tag{24}$$

By integrating it over time and suitably distributing the resulting numbers in space, one can get the numbers n_{ij} required in the PSHA formulation.

In addition to the Poissonian occurrences, earthquakes may sometimes be postulated to occur as a result of some triggering mechanism (e.g., earth tides; Trifunac, 1970), or deterministically at certain locations in a source zone (e.g., earthquake prediction). The above probabilistic formulation can also be extended to incorporate the contributions of such events occurring in a "literal" way (Anderson and

Trifunac, 1977, 1978a; Lee and Trifunac, 1985). If $n^*_{kl}(Y)$ is the total number of such deterministic events over a time interval of Y years, the probability of $X > x$ due to these earthquakes alone is given by

$$P^*(X > x) = 1.0 - \exp\left\{\sum_{k=1}^{K}\sum_{l=1}^{L} \ln\left[1 - q\left(x \middle| M_l, R_k\right)\right] \cdot n_{kl}(Y)\right\} \tag{25}$$

The combined probability that $X > x$ from Poissonian as well as deterministic earthquakes, can be written as (Anderson and Trifunac, 1978a)

$$P^+(X > x) = 1.0 - \exp\left\{-\sum_{i=1}^{I}\sum_{j=1}^{J} q\left(x \middle| M_j, R_i\right) \cdot n_{ij}(Y)\right\} \times \exp\left\{\sum_{k=1}^{K}\sum_{l=1}^{L} \ln\left[1 - q\left(x \middle| M_l, R_k\right)\right] n_{kl}(Y)\right\} \tag{26}$$

The expression of Equation (18) or (26) can be used to compute the value, x, of a strong-motion parameter X with any desired confidence level p (probability of not exceeding). If X represents the response spectrum, $\mathrm{PSV}(T)$, or the Fourier spectrum, $\mathrm{FS}(T)$, amplitude at period T, then by computing the spectrum amplitudes at various periods with the same confidence level, it is possible to construct a complete spectrum having a constant probability of not exceeding. Such spectra were first proposed by Anderson and Trifunac (1977), and were termed as "Uniform Risk Spectra" or "Uniform Hazard Spectra". Such a spectrum has the property that it will not be exceeded with a desired confidence level, at any of the periods due to any of the earthquakes expected to occur anywhere in the region of a site of interest. Further, a uniform hazard spectrum is able to represent simultaneously and in a balanced way, the influence of the various contributing attenuation and amplification factors as well as relative contributions of all the regional earthquake sources.

Two basic input quantities required for the implementation of PSHA approach are the probability $q\left(x \middle| M_j, R_i\right)$ and the seismicity $n_{ij}(Y)$. $q\left(x \middle| M_j, R_i\right)$ defines the probability of exceeding a value x of the strong motion parameter of interest due to the magnitude and distance combination (M_j, R_i). It can be obtained from the probability distribution of the observed values of a strong-motion parameter around the expected value, as estimated from the empirical scaling relation (e.g., see Equation (9)). The seismicity $n_{ij}(Y)$ represents the total number of earthquakes expected to occur in Y years within a small magnitude range around magnitude M_j and a small distance range around distance R_i from a site of interest. This can be obtained by suitable spatial distribution of the total number, $\mathcal{N}(M_j)$, of earthquakes per year in the magnitude range M_j in each of the source zones identified in the region of the site. The evaluation of $\mathcal{N}(M_j)$ for a source zone is commonly based on fitting a magnitude recurrence relation to the available data on past earthquakes. When the data on past earthquakes is not adequate, the evaluation of seismicity can also be based on the long-term seismological slip rates. Both these approaches are described briefly in the following.

2. Evaluation of Seismicity from Past Earthquake Data

Evaluation of seismicity using available data on past earthquakes is most commonly based on the Gutenberg-Richter's (Gutenberg and Richter, 1954) recurrence relationship, according to which the yearly occurrence rate $N(M)$ of earthquakes with magnitude greater than or equal to M in a particular source zone can be described by

$$\log N(M) = a - bM \tag{27}$$

Here, a and b are constants specific to the source zone, and these can be estimated by a least square regression analysis of the past seismicity data. When the available data are not complete for a sufficiently long period of time to get statistically stable values of parameters a and b, one can also obtain these parameters from the maximum likelihood method of Kijko and co-workers, using mixed data files consisting of an extreme part for a very long historical period and the recent complete parts of the available earthquake catalogue. Once the relationship of Equation (27) has been defined for a particular

source zone, the number of earthquakes $\mathcal{N}(M_j)$ within magnitude range $(M_j - \delta M_j, M_j + \delta M_j)$ in that source zone can be obtained as

$$\mathcal{N}(M_j) = N(M_j - \delta M_j) - N(M_j + \delta M_j) \tag{28}$$

The magnitude recurrence model of earthquakes as defined by Equation (27) is quite suitable to describe the seismicity of large regions, which typically contain a number of faults. However, if it is intended to have the fault-specific sources, then it may be more appropriate to model the recurrence behaviour based on the characteristic earthquake model. In regions where repeated characteristic earthquakes have occurred during historical time, the seismicity data shows distinctly non-linear recurrence relationship (e.g., Schwartz and Coppersmith, 1984; Wesnousky, 1994; etc.). For practical applications, the earthquakes upto certain magnitude level (say, $M_{\max}$) can be defined by the exponentially decaying magnitude distribution of Equation (27) and by a uniform distribution in a narrow magnitude range (say, 0.5 magnitude unit) around the expected magnitude, M_{char}, of the characteristic earthquake (Youngs and Coppersmith, 1985). M_{char} and $M_{\max}$ may generally differ by magnitude units of 1.5 or so. As explained before, the number of characteristic earthquakes can be estimated by using Equation (19) with a lognormal density function for their interoccurrence time intervals.

The earthquake catalogues are generally incomplete for smaller magnitude earthquakes in the olden times due to inadequate instrumentation. However, due to short return periods of smaller magnitudes, their recurrence rates can be evaluated even from the most recent data for about 15-20 years. On the other hand, to get a reliable estimate for the occurrence rates of larger magnitude earthquakes with long return periods, one has to consider the data for a much longer period. Therefore, to minimize the effect of incompleteness in the available data base on the estimation of parameters a and b in Equation (27), Stepp (1973) introduced a statistical method based on the stability of the magnitude recurrence rate.

In Stepp's method, an available catalogue of earthquakes is grouped into magnitude ranges, say $\Delta M = 1$ unit, and in time intervals of about 5-10 years. The average number of events per year, $R(M)$, are then evaluated for each magnitude class for increasing time interval lengths, starting with the most recent time interval. The first window consists of the most recent years, say 5 years, the next window would consist of the recent 10 years, and so on. An analysis of the series of $R(M)$ obtained as above will show the length of the time window for which $R(M)$ becomes stationary for a given magnitude range. Thus, Stepp's method involves determining that fraction of the total time sample, in which the mean rate of occurrence, $R(M)$, is stable for each magnitude class. For this purpose, $R(M)$ is modelled as a Poisson point process in time, such that the standard deviation of $R(M)$ for a time interval of T years is given by

$$S_R = \sqrt{R(M)/T} \tag{29}$$

Assuming stationarity of $R(M)$, S_R will behave as $1/\sqrt{T}$. The plot of the standard deviation S_R as a function of T is known as the "completeness plot". For a particular magnitude class, the period of completeness is reflected in this plot by a distinct departure of the S_R values from the linearity of the $1/\sqrt{T}$ slope. This period, which should be a minimum for a stable $R(M)$, becomes successively longer with each higher magnitude class. A typical completeness plot for the available earthquake data for the region of Figure 3 is shown in Figure 5. Thus, to fit the relationship of Equation (27), the annual number of earthquakes in a particular magnitude range can be found by using the data for the period for which that magnitude range is recorded completely.

To consider the spatial distribution of the seismicity within a source zone, the entire source zone is divided into a large number of small source elements. The center of each of these elements is the possible location of earthquakes. Depending on the position of the element with respect to the zone boundaries, likelihood can be assigned that an earthquake of given size occurs in that element (e.g., larger magnitude earthquakes are less likely to initiate close to the zone boundary). On the basis of such likelihood, the

number $\mathcal{N}(M_j)$ for the source zone can be distributed among the source elements, to get the expected number, $n_{ij}(Y)$, of earthquakes of size M_j in the ith source element.

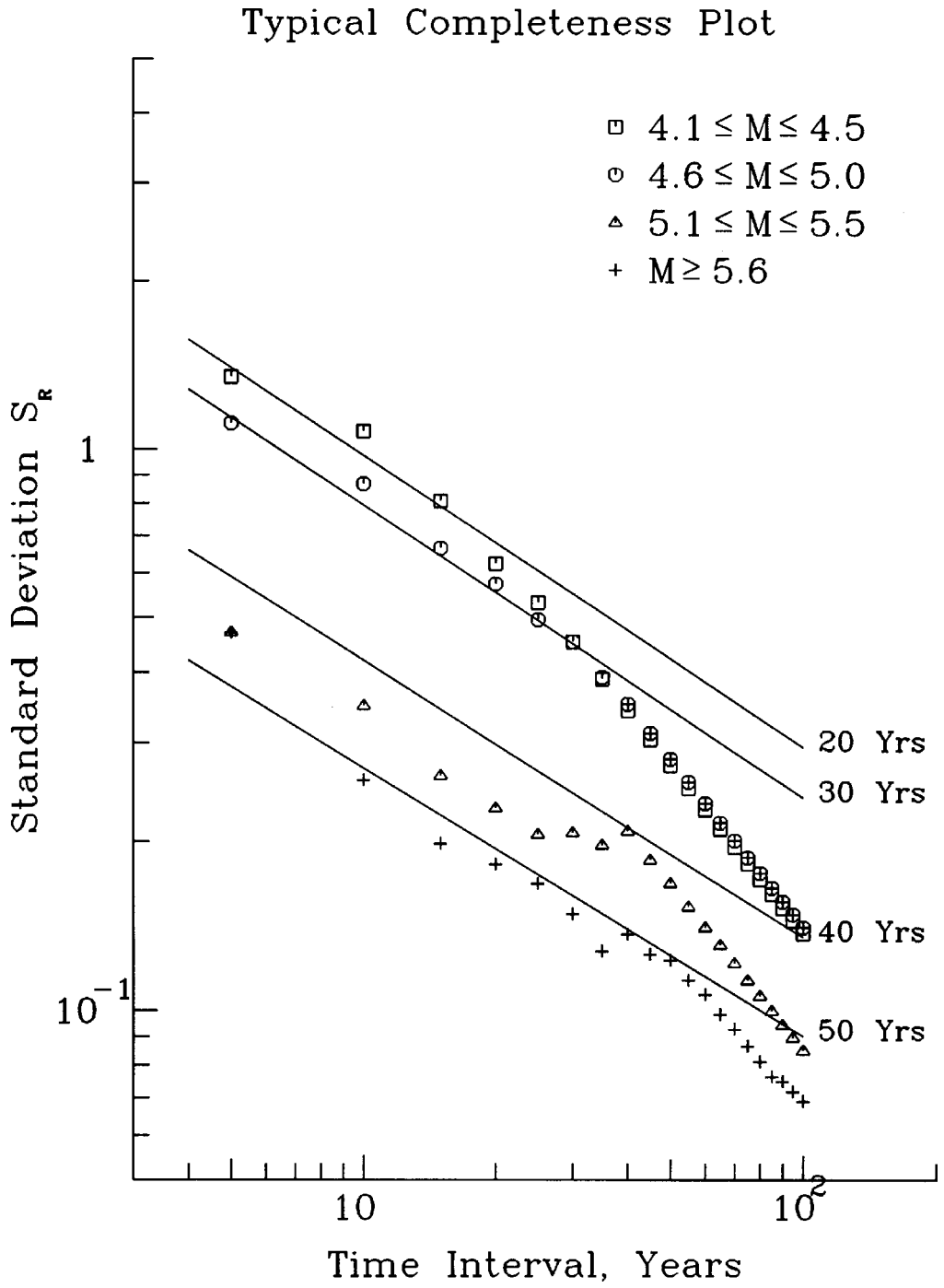

Fig. 5 A typical completeness plot for the available data on past earthquakes in the area of Figure 3 (the most recent time intervals for which different magnitude classes are recorded completely are also indicated in the figure)

3. Evaluation of Seismicity from Geological Data

The theoretical background used to develop the expression of Equation (16) to estimate the maximum magnitude, $M_{\max}$, from the moment rate can also be used to define a frequency-magnitude relationship, if $M_{\max}$ is assumed to be known. To illustrate this, the Gutenberg-Richter's recurrence relation, with upper bound magnitude as $M_{\max}$, can be written as

$$N(M) = K_0 10^a \left(10^{-bM} - 10^{-bM_{\max}}\right);\ K_0 = \left(1 - 10^{-bM_{\max}}\right)^{-1} \tag{30}$$

This gives the occurrence rate density function $n(M)$ as

$$n(M) = -\frac{dN(M)}{dM} = K_0 b 10^{a-bM} \ln 10 \tag{31}$$

Using this and $M_0(M)$ defined by Equation (14) in Equation (13), and performing the integration, one gets

$$\dot{M}_0(M) = \frac{K_0 b}{d-b} 10^a \left[M_0(M_{\max}) 10^{-bM_{\max}} - 10^c\right] \tag{32}$$

Substituting the value of 10^a from this expression into Equation (30) gives the mean occurrence rate for magnitudes greater than or equal to M as

$$N(M) = \frac{\dot{M}_0(d-b)}{b} \cdot \frac{10^{b(M_{\max}-M)} - 1}{M_0(M_{\max}) - 10^{c+bM_{\max}}} \tag{33}$$

Even for very small values of $M_{\max}$ (say, about 5.0), this expression can be simplified, without any significant effect on the final results, as follows:

$$N(M) = \frac{\dot{M}_0(d-b)}{b} \cdot \frac{10^{b(M_{\max}-M)}}{M_0(M_{\max})} \tag{34}$$

If, in addition, N_C number of characteristic earthquakes with magnitudes distributed uniformly in the interval $(M_{\text{char}} - \Delta M_{\text{char}}/2,\ M_{\text{char}} + \Delta M_{\text{char}}/2)$ also contribute to the moment release rate, $\dot{M}_0$ in this expression has to be replaced by $\dot{M}_0^{\text{char}}$, defined as

$$\dot{M}_0^{\text{char}} = \dot{M}_0 - \frac{N_C}{\Delta M_{\text{char}}} \cdot \frac{M_0(M_{\text{char}})}{d \ln 10} \left[10^{d\Delta M_{\text{char}}/2} - 10^{-d\Delta M_{\text{char}}/2}\right] \tag{35}$$

As described before for the estimation of $M_{\max}$, the moment rate $\dot{M}_0$ in the above expressions can be obtained from the total fault area (A), and the long term average of geological slip rate, $(\dot{u})$, as $\dot{M}_0 = \mu A \dot{u}$. However, parameter b has to be estimated from the available seismological data for the region of interest or another region with similar seismotectonic setup. Thus, the foregoing formulation can be used for evaluating the seismicity from the geologically determined slip rate. Slip-rate data is generally available for major faults in a region. These rates are primarily established from offsets of geological formations or geomorphic features (e.g., offsets of terraces and stream courses) along the faults and through detailed study of creep rates, trenching and age dating. Slip rates may also be determined from available geodetic measurements.

To illustrate the application of the above formulation for estimation of seismicity, let us consider a 150 km long segment of the Himalayan arc. The source of major earthquakes along this segment can be considered a gently dipping detachment plane of about 100 km width. Taking μ = 3.4 x 10^{11} dyne/cm^2 and $\dot{u}$ = 15 mm/year, as explained before, one gets $\dot{M} = \mu A \dot{u}$ = 7.65 x 10^{25} dyne-cm/year. For $M_{\max}$ as 8.0 and b as 0.9, Equation (34) then leads to the following frequency-magnitude relationship:

$$\log N(M) = 4.9 - 0.9M \tag{36}$$

This relation can be reconciled very well with the available data on past seismicity in different parts of the Himalaya. Thus, the information on geological slip rates can be used to obtain the earthquake recurrence relations for estimating the seismicity for the purpose of seismic hazard analysis.

UNCERTAINTIES IN SEISMIC HAZARD ANALYSIS

The foregoing PSHA formulation has accounted for the uncertainties related to the inherent random nature of the various input parameters used to describe the seismicity and the ground motion attenuation. For example, the random nature of earthquake recurrence is described by Poisson model, that of earthquake magnitudes by Gutenberg-Richter's relation, that of earthquake location by spatial distribution of the total number of earthquakes in a source zone, and that of the ground motion attenuation by the probability distribution about the mean attenuation law. Such random nature of the input parameters is commonly termed as the "aleatory" uncertainties, which are inherent to the physical processes generating the seismicity and the ground motion. These uncertainties cannot be thus eliminated completely, though it may be possible to minimize them by collecting more and good quality of data.

Further, the parameters describing the aleatory uncertainties may themselves be associated with some uncertainties due to limited amount of the available data used for their estimation. It is therefore necessary to describe these parameters by suitable probability distributions and to replace them by their Bayesian estimates. For example, if the parameters a and b in the Gutenberg-Richter's relationship are described respectively by probability density functions $f(a)$ and $f(b)$, the Bayesian estimate, $\hat{N}(M_j)$, of the number of earthquakes with magnitude M_j or more can be defined as

$$\hat{N}(M_j) = \int_{-\infty}^{\infty}\int_{-\infty}^{\infty} N(M_j|a,b) f(a) g(b) da db \tag{37}$$

Here, $N(M_j|a,b)$ is the number of earthquakes obtained from Equation (27) for specified values of parameters a and b. If μ_a and μ_b are the mean values and σ_a and σ_b the corresponding standard deviations of parameters a and b, then on assuming both a and b to follow the Gaussian probability distribution, the integral in Equation (37) can be evaluated to get

$$\hat{N}(M_j) = N(M_j) 10^{\frac{1}{2}\left(\sigma_a^2 + \sigma_b^2 M_j^2\right)\ln 10} \tag{38}$$

where $N(M_j)$ is the number of earthquakes obtained from Equation (27) by using mean values of a and b. Further, the upper-bound cut-off magnitude, $M_{\max}$, is also generally associated with large uncertainty, which can be described via some probability density function over the expected range of $M_{\max}$ (Lee and Trifunac, 1985). Thus, the expected number of earthquakes within magnitude interval $(M_j - \delta M_j, M_j + \delta M_j)$, with a, b and $M_{\max}$ all taken as random, can be estimated by multiplying $\hat{N}(M_j)$ obtained from Equation (38) with the probability that $M_j \le M_{\max}$, evaluated by assuming a probability density function for $M_{\max}$.

In addition to above, both probabilistic and deterministic approaches are subject to the uncertainties in modelling the seismic sources, seismic activity of each source, and the attenuation of strong motion parameters in an exact way (Abrahamson, 2000; Stepp and Wong, 2001). The seismic activity of a source zone refers to the maximum magnitude and its distance from a selected site in case of the deterministic approach, and the total seismicity for a specified time period with spatial distribution over the entire source zone in case of the PSHA approach. The modelling uncertainties are commonly termed as "epistemic" uncertainties, which are associated mainly with the lack of exact knowledge of the physical processes. Thus, at least in principle, it is possible to eliminate these uncertainties by collecting more data to arrive at the exact models for the seismic sources and the ground motion attenuation laws.

In the deterministic approach, the epistemic uncertainties may generally lead to several possible alternatives for the maximum credible earthquake magnitude, its source-to-site distance from the site of interest, and the ground motion attenuation relation, which in turn would lead to several different estimates of the ground motion. The effects of these uncertainties can be accounted for by defining a discrete probability density function for all the alternatives and by estimating the "mean" or "median" value of the ground motion parameter. In the PSHA approach, the "logic-tree" formulation is often used to incorporate the effects of both aleatory and epistemic uncertainties (Coppersmith and Youngs, 1986; SSHAC, 1997; Savy et al., 2002). The logic-tree methodology considers a large number of different

probabilistic models and model parameters, and computes the hazard for all the combinations of parameter values defined by the end branches of the logic-tree. Each of the input parameters is assigned an appropriate weight to define a discrete probability density function for the frequency, $N_E(x)$, of exceeding a value x of a strong motion parameter X, as defined by Equation (17). One can then obtain the various statistical estimates of the frequency of exceeding x; the most common among them is the expected (mean) value, defined as

$$\bar{N}_E(x) = \sum_{\theta_k} N_E(x|\theta_k) p(\theta_k) \tag{39}$$

where, $p(\theta_k)$ represents the discrete probability density function for the parameter set θ_k. The use of the hazard curve based on $\bar{N}_E(x)$ is able to consider the effect of all the uncertainties in the probabilistic estimation of the seismic hazard.

DE-AGGREGATION OF PROBABILISTIC SEISMIC HAZARD

The probabilistic seismic hazard analysis (PSHA) carries out integration over the total expected seismicity during a given exposure period to provide the estimate of a strong-motion parameter of interest with a specified confidence level. The PSHA is thus able to quantify and account for the random uncertainties associated with estimation of the seismicity and the attenuation characteristics of the region. However, the physical image of an earthquake in terms of magnitude and source-to-site distance is lost in the PSHA analysis. For physical interpretation of the results from PSHA and to take certain engineering decisions, it is desirable to have a representative earthquake which is compatible with the results of the PSHA method (Trifunac, 1989b). This could be achieved through the de-aggregation of the probabilistic seismic hazard, as described in the following (McGuire, 1995).

The basis of the PSHA methodology is the expression of Equation (19), which defines for a site of interest the probability of exceeding a value x of a selected strong-motion parameter X, due to the total expected seismicity in the area around the site during a specified exposure period. The seismicity refers to the number, $n_{ij}(Y)$, of earthquakes with magnitude M_j occurring at distance R_i. From Equation (18), one can estimate the value of the strong motion parameter X with a specified probability of exceedance p. If this value is represented by x_p, the de-aggregation of PSHA aims at finding the relative contribution of the earthquakes of type (i, j) to the probability of $X > x_p$. This is the same as the conditional probability of M_j and R_i, given that $X > x_p$, which can be defined as

$$f(M_j, R_i | X > x_p) = \frac{1.0 - \exp\{-q(x_p | M_j, R_i) n_{ij}(Y)\}}{1.0 - \exp\{-\sum_{i=1}^{I}\sum_{j=1}^{J} q(x_p | M_j, R_i) n_{ij}(Y)\}} \tag{40}$$

The numerator on the right hand side of this expression represents the probability of $X > x_p$ due to earthquakes of type (i, j), and the denominator represents the probability of $X > x_p$ due to all the expected earthquakes. The representative values of earthquake magnitude and distance can be obtained from this distribution as

$$\overline{M} = \sum_{i=1}^{I}\sum_{j=1}^{J} M_j f(M_j, R_i | X > x_p) \quad \text{and} \quad \overline{R} = \sum_{i=1}^{I}\sum_{j=1}^{J} R_i f(M_j, R_i | X > x_p) \tag{41}$$

The value of the strong-motion parameter X with probability of exceedance p, as obtained using these values of magnitude and distance, will be matching closely with the value x_p as obtained by the PSHA approach. $\overline{M}$ and $\overline{R}$ may thus be termed as hazard-consistent magnitude and distance, respectively (Ishikawa and Kameda, 1988; Kameda, 1994).

In principle, PSHA can be performed for any of the strong motion parameters. However, in practice, it is more often carried out for the peak ground acceleration and the response spectral amplitudes only.

Thus, the hazard-consistent magnitude and distance may be very handy for selecting ground motion characteristics like duration, nonstationarity, etc. for the purpose of generating spectrum-compatible design accelerograms. However, one basic problem with the de-aggregation of PSHA stems from the fact that to reproduce the amplitudes of a uniform hazard spectrum at different natural periods, the hazard-consistent magnitude and distance are found to vary significantly. Thus, in general, it is not possible to define a single representative earthquake, which can be consistent with an entire uniform hazard spectrum (Trifunac, 1989b).

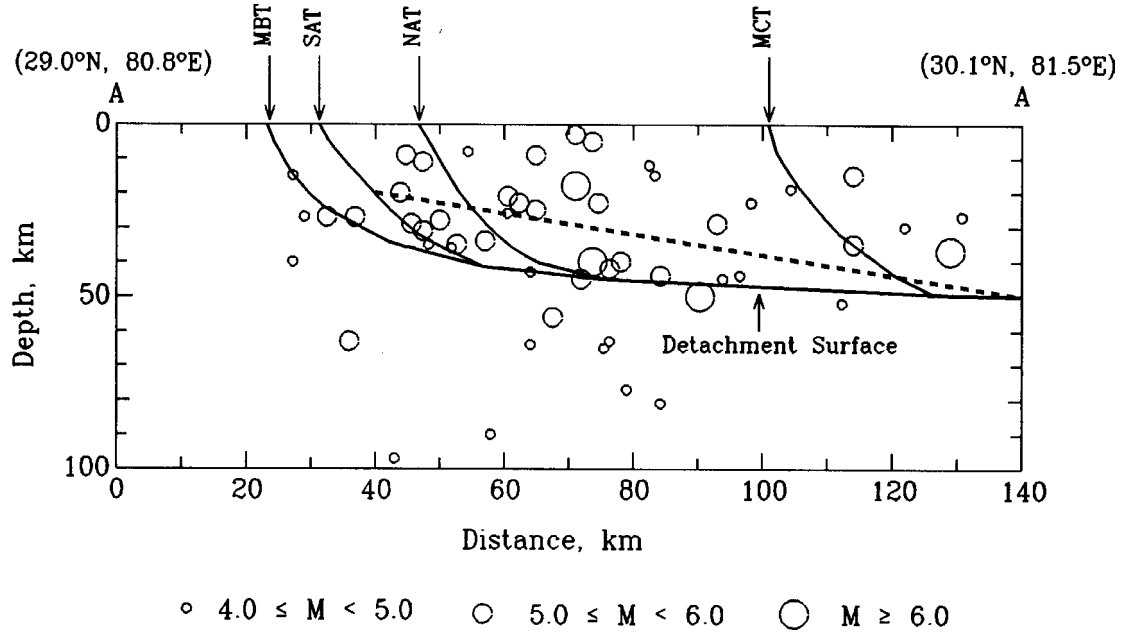

Fig. 6 The depth section along line A-A in Figure 3 of the available data on past earthquakes in an area of about 150 km long segment of the Himalayan arc (the possible location of the postulated Himalayan detachment plane is also shown in the figure)

EXAMPLE RESULTS

To illustrate how the results of probabilistic seismic hazard analysis (PSHA) are able to account for, in a realistic way, the effects of various seismotectonic and geological parameters, a 150 km long segment of the Himalayan arc around line A-A in Figure 3 has been considered as the seismic source. The depth section of the available past earthquake data in this source is shown in Figure 6. As mentioned before, major earthquakes in the Himalaya are associated with a gently dipping detachment surface north of the main boundary thrust (MBT) to which the various Himalayan thrusts join at steep angles (Seeber and Armbruster, 1981). The other thrusts north of MBT along section A-A in Figure 3 are the South Almora Thrust (SAT), North Almora Thrust (NAT) and the Main Central Thrust (MCT). It is seen that earthquakes with magnitude greater than or equal to 6.0 are mostly associated with the detachment surface as shown in Figure 6, whereas more of smaller magnitudes occur at shallower depths. Also, it is seen that there is a general decreasing trend in the number of earthquakes as one goes to the north from MBT. The example seismic source, which is about 150 km long and 100 km wide area of the crustal detachment surface along the Himalaya, has been idealized by a detachment plane, as shown in Figure 6 by a dashed line. A three-dimensional schematic of this seismic source is depicted in Figure 7.

The example results are computed in the form of pseudo acceleration spectra (PSA) with a damping ratio of 5%, by using the attenuation relations due to Lee (1987). To define the average seismicity of the above source, the moment rate $\dot{M}_o$ is taken as 1.0 x 10^{26} dyne-cm/year, $M_{\max}$ as 8.0, and the $b-$value as 0.9. The exposure time for estimating the total seismicity is taken as 100 years. From Equation (34), the Gutenberg-Richter's productivity coefficient a for these values works out to be 5.0. For the present computations, the lower threshold magnitude has been taken as 4.0, because smaller magnitudes are not expected to be of much engineering significance. To evaluate the total expected number of earthquakes $\mathcal{N}\left(M_j\right)$ in different magnitude intervals $\left(M_j-\delta M_j, M_j+\delta M_j\right)$, the magnitudes between the

minimum and the maximum values are discretized with interval $\delta M_j = 0.25$. To consider the spatial distribution of seismicity, numbers $\mathcal{N}\left(M_j\right)$ are distributed all over the surface projection of the detachment plane. For this purpose, the entire surface area is divided into small elements of 5 km x 5 km size as shown in Figure 7, and the epicenters are assumed to occur at the centers of these elements. In view of the observed spatial distribution of the past earthquakes, the probability of earthquake occurrences is assumed to decrease linearly to one half as one goes from the southern boundary to the northern boundary of the seismic source. The focal depth of earthquakes with magnitude 6.0 or more is taken as the depth of the detachment plane, whereas those with smaller magnitudes is assumed to be 10 km shallower. Thus, the presented example can be considered to represent a generalized situation for a 150 km long typical segment anywhere along the Himalaya. However, as the attenuation relations used are not specific to the Himalayan region, the conclusions drawn are to be considered of qualitative nature only.

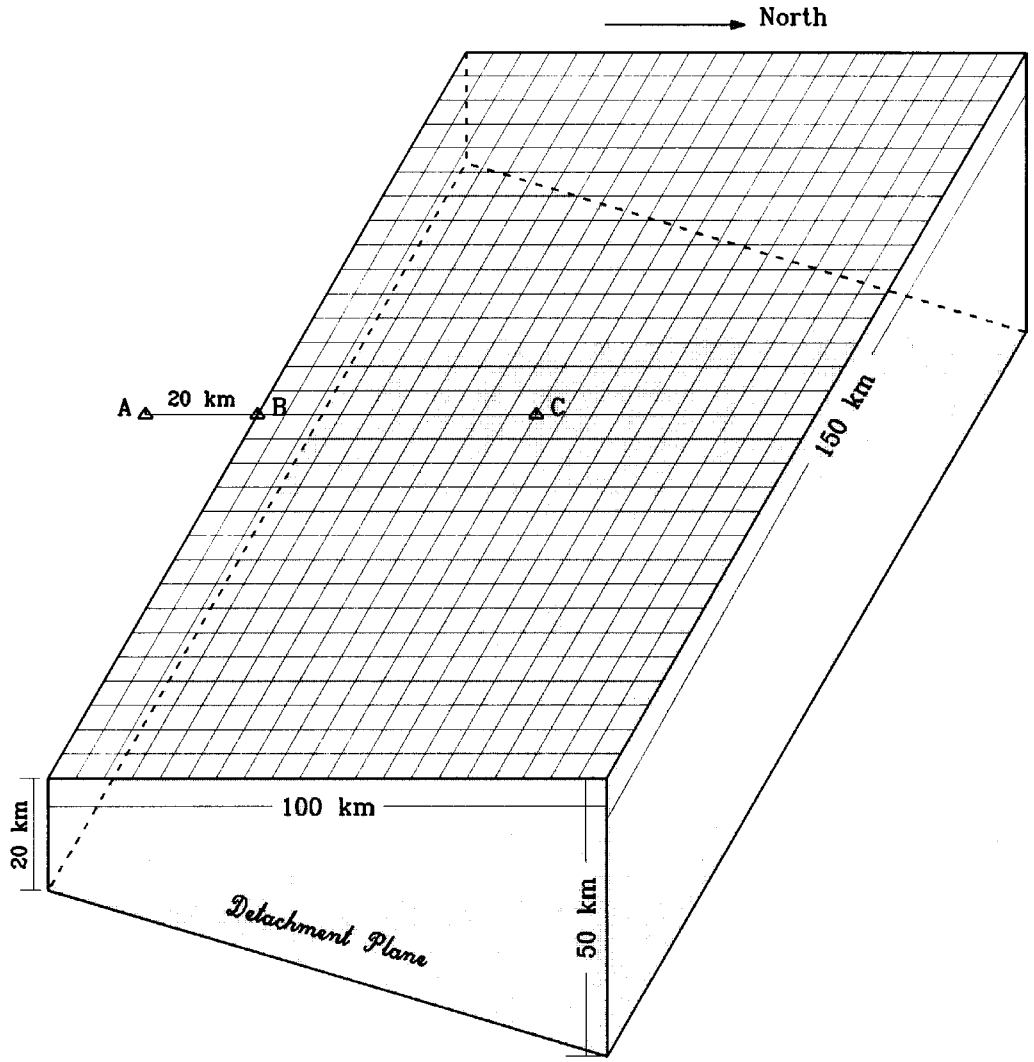

Fig. 7 An idealized schematic diagram of the seismic source (a detachment plane) indicated in Figure 6 by dashed line (example results are computed by discretizing the surface projection of the source plane into rectangular elements of 5 km x 5 km size)

First of all, to study the effect of the confidence level on the uniform hazard response spectrum, example results are computed for three different confidence levels of 0.1, 0.5 and 0.9 for site-A in Figure 7 at a distance of 20 km from the surface projection of the seismic source. To illustrate how the results of the deterministic approach compare with the results of PSHA approach, corresponding response spectra are also obtained for $M_{\max} = 8.0$ with focal depth of 20 km and distance as 20 km from site-A. Both these spectra are shown plotted in Figure 8, from which it may be inferred that, in general, it would not be

possible for any pair of M_{max} and its distance to match the results of the deterministic approach with those of the PSHA approach over the entire period range and for all the confidence levels. In the presented example, the PSHA spectra show narrower probability distribution, which is also seen to be shifted towards higher amplitudes. Thus, the common belief that deterministic approach is always more conservative is not true in general.

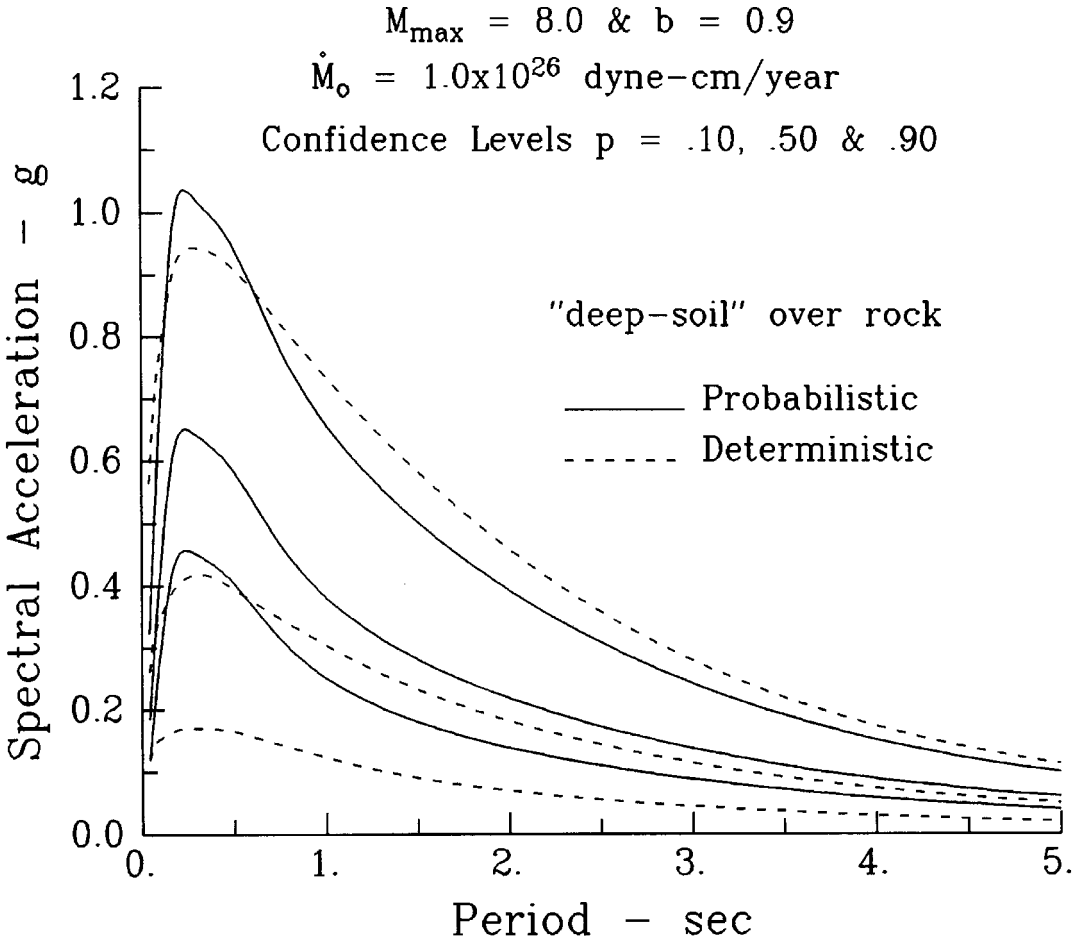

Fig. 8 Comparison of the response spectra of horizontal component of motion obtained by the PSHA and deterministic approaches for different confidence levels

Figure 9 shows the comparison between the probabilistic and deterministic spectra with a confidence level of 0.5 for the horizontal and vertical components of motion. For both the components, the spectra of PSHA approach are seen to be significantly higher in almost the entire period range. From the results in Figure 9, it is further observed that for deep-soil sites overlying the basement rock, the spectral amplitudes for vertical motion are comparable with the horizontal motion for periods greater than about 3.5 s. The conformity between the deterministic and the probabilistic spectra in this regard confirms the fact that the probabilistic spectra are able to take into account in a physical way the dependence on the various governing parameters. To illustrate further the physical nature of the PSHA approach, Figures 10 and 11 show the influence of the local soil condition and the depth of sediments underneath on the uniform hazard spectra. Figure 10 shows the spectra for "rock-soil" over rock and "deep-soil" over rock, where the latter parameter refers to geological basement rock (i.e., no sediments). Taking the "rock-soil" and rock as reference, it is seen that at longer periods, "deep-soil" amplifies the spectral amplitude, and at smaller periods, it attenuates the amplitudes. In most cases, "rock-soil" is found over rock and "deep-soil" over thick sediments. Uniform hazard spectra for these extreme conditions are shown in Figure 11. It is seen that at longer periods, the sediments further amplify the spectral amplitudes, whereas the amplitudes are practically same for smaller periods. Thus, compared to "deep-soil" over rock, the sediments also amplify the low-period amplitudes. It is thus established that the PSHA methodology is able to represent in a physically realistic way the influence of both the local soil and the surrounding geological condition.

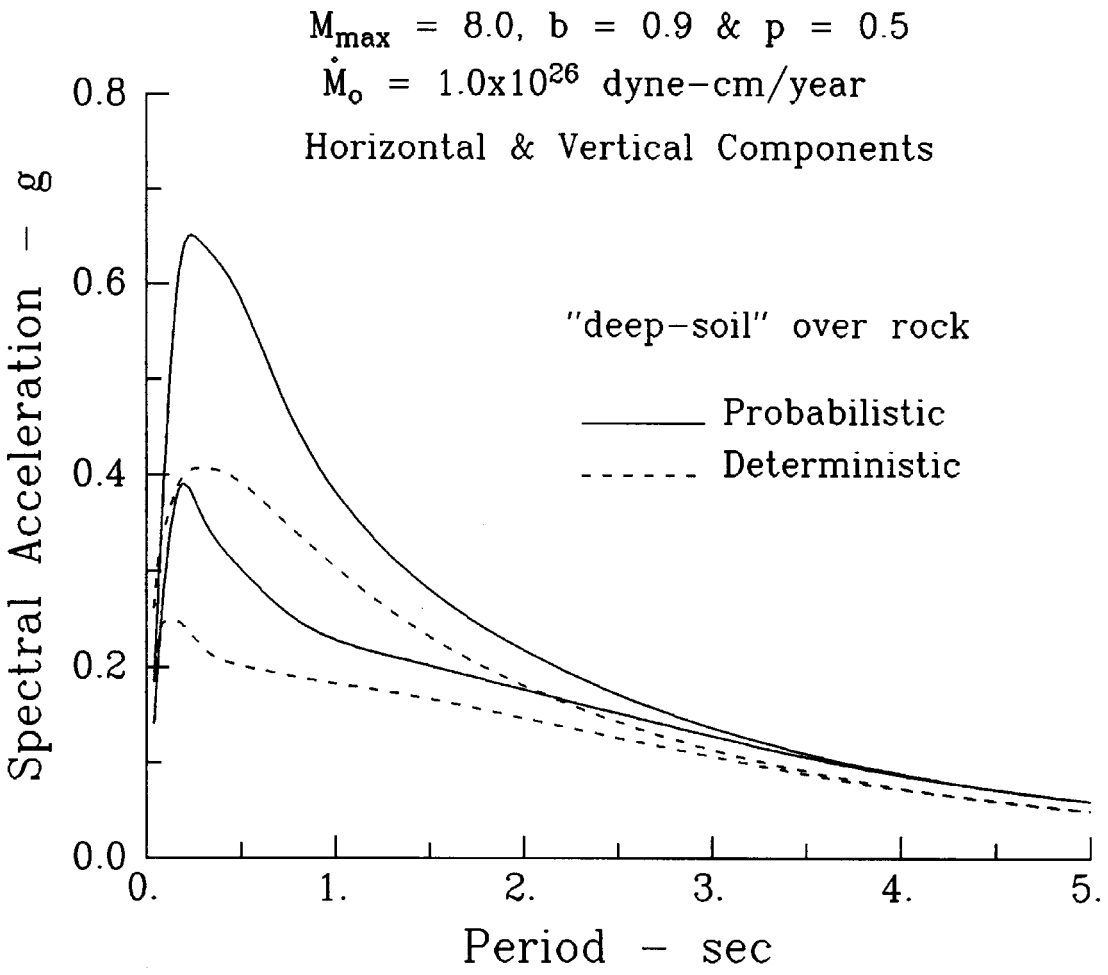

Fig. 9 Comparison of the response spectra obtained by the PSHA and deterministic approaches for the horizontal and vertical components of motion with a confidence level of 0.5

Next, to illustrate the effect of the spatial distribution of seismicity with respect to the site of interest, uniform hazard spectra are computed for three sites indicated by solid triangles A, B and C in Figure 7. Site-A is located at a distance of 20 km from the center of the southern boundary of the surface projection of the seismic source, site-B is located at the center of this boundary, and site-C lies at the center of the area of the surface projection. Thus, for sites-A to C, the distance from the seismic source is decreasing continuously. As described before, the spatial distribution of the seismicity is considered to be non-uniform in such a way that the probability of earthquake occurrences reduces linearly to one-half, as one goes from the southern boundary to the northern boundary of the seismic source. The focal depths for earthquakes with magnitudes greater than or equal to 6.0 are taken as the depth of the detachment plane shown in Figure 7, and those with smaller magnitudes as 10 km shallower. In addition, for the purpose of comparison, results are also computed for a uniform spatial distribution of the seismicity with a constant focal depth of 20 km for all the earthquakes. Both these results are presented in Figure 12, where thick curves correspond to the non-uniform and thin curves to the uniform distribution of the seismicity. It is seen that at the same site, the shape and the amplitudes of the uniform hazard spectrum may differ significantly with change in the spatial distribution of the seismicity. For the case of uniform distribution of seismicity, with decrease in the distance, the spectral amplitudes are seen to increase over the entire period range. However, this increase is not same at all the periods. On the other hand, for non-uniform distribution of seismicity, the variation in the response spectral amplitude is seen to be quite typical. For example, the response spectrum at site-B is higher over the entire period range than that at site-C, though site-C is closer to the seismic source.

The PSHA approach can also be used to prepare the seismic zoning maps for an area. Seismic zoning can be done on a macro or a micro scale, depending on the size of the area (a whole region or a whole country versus a metropolitan area, for example). The strong-motion parameters used for seismic zoning may also vary widely, such as the Modified Mercalli Intensity (Gupta et al., 2002), peak acceleration

(Algermissen and Perkins, 1976; Khattri et al., 1984; Gupta and Joshi, 2001), peak strain in soils (Todorovska and Trifunac, 1996b), probability of liquefaction (Trifunac and Todorovska, 1999), or the response spectral amplitudes at different natural periods (Lee and Trifunac, 1987; Trifunac, 1988, 1990a). However, the most widely used parameter is the peak ground acceleration. The zoning maps prepared for different parts of the world under the Global Seismic Hazard Analysis Program (GSHAP), which are compiled in a special issue of Annali de Geofisica (December 1999), are also in terms of the peak acceleration. In case of the spectral amplitudes, several zoning maps are required to be prepared for different natural periods and damping ratios, so that the complete spectrum can be constructed by reading the spectral amplitude at each period for a specified damping ratio. In addition, for any of the strong-motion parameters, the zoning maps may be prepared for different confidence levels and exposure periods. To illustrate the application of the PSHA approach to prepare the seismic zoning maps and to highlight the important characteristics of such maps, typical zoning maps in terms of the PSA amplitudes are presented for an area having the geometry and the seismicity similar to that of the Maharashtra state.

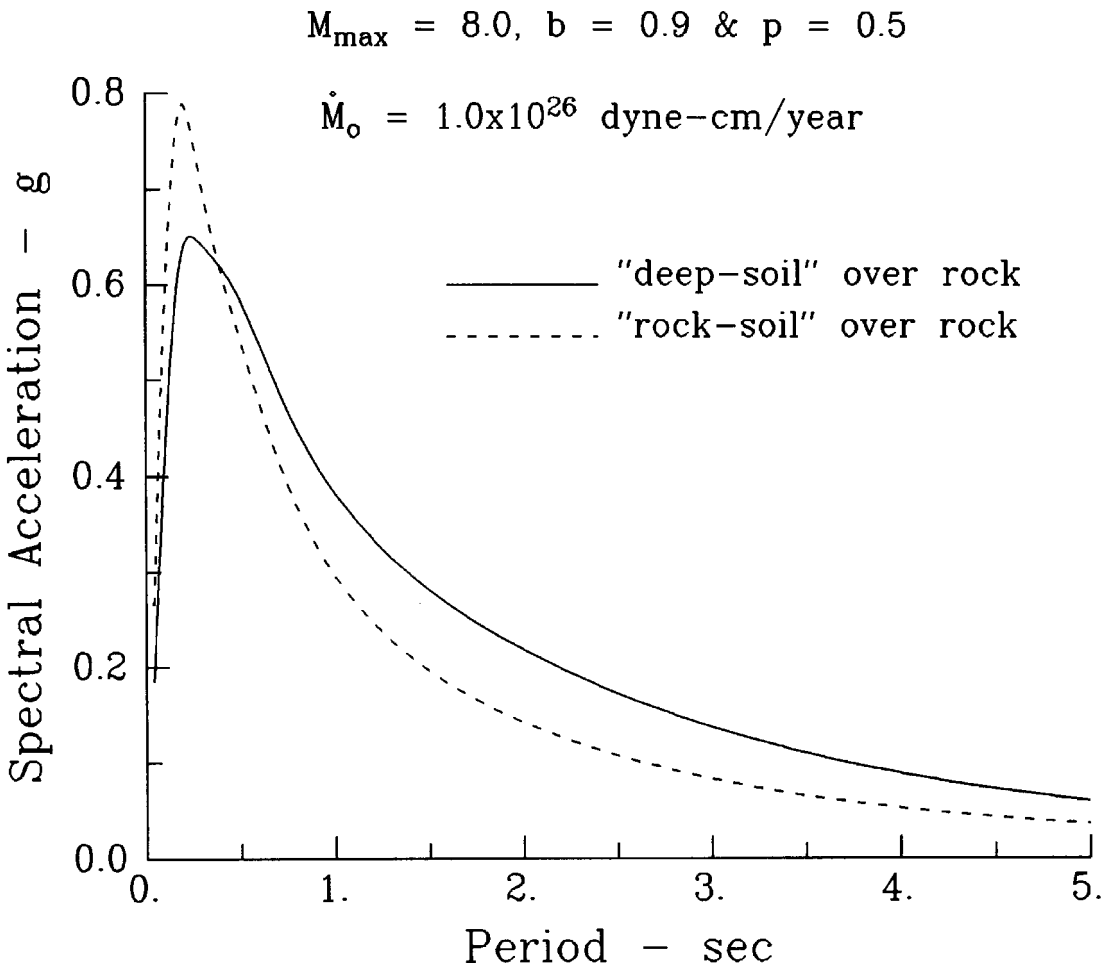

Fig. 10 Illustration of the effect of local soil condition on the uniform hazard response spectra

From a knowledge of the tectonic features and the distribution of the epicenters of available data on past earthquakes, the seismicity of the Maharashtra state and adjoining areas can be defined by twelve (area type) seismic sources with diffused seismicity, as shown in Figure 13 (Gupta et al., 2002). The values of the parameters a and b in the Gutenberg-Richter's relationship and the expected M_{max} for all the seismic sources are taken from Gupta et al. (2002). For the PSHA computations, the seismicity is defined by discretizing the magnitude into seven intervals, with central magnitudes M_j as 3.0, 3.6, 4.2, 4.8, 5.4, 6.0 and 6.6 (with δM_j taken uniformly equal to 0.3 for all the intervals). The exposure period has been considered as 100 years, and the spatial distribution of the total expected seismicity is assumed to be uniform in each of the seismic source areas. To prepare the seismic zoning maps, the entire area of Maharashtra state is defined by a grid of 1728 sites with 0.125^0 latitude and 0.125^0 longitude spacings. Using the contributions from all the earthquakes within 300 km of each of these sites,

PSA amplitudes are computed for four natural periods equal to 0.04, 0.19, 0.9 and 2.8 s, and two confidence levels equal to 0.5 and 0.84. The site soil and the geological conditions are both taken to be as hard rock type for the computation of these results. The zoning maps thus obtained for confidence levels of 0.50 and 0.84 are shown plotted in Figures 14 and 15, respectively. It is seen that in addition to the confidence level, the distribution of seismic hazard changes with the natural period, and hence a single zoning map in terms of peak ground acceleration does not provide a realistic picture of hazard to structures with different natural periods. The maps like those in Figures 14 and 15 are able to consider simultaneously and in a balanced way, the effects of all the parameters like level of seismicity, spatial distribution of seismicity, local soil and geological conditions, and the attenuation characteristics of the strong-motion parameters. The variation in any of these governing parameters is manifested by corresponding changes in the distribution of seismic hazard. The PSHA methodology is also able to consider the uncertainties in the input parameters and the random scattering in the data.

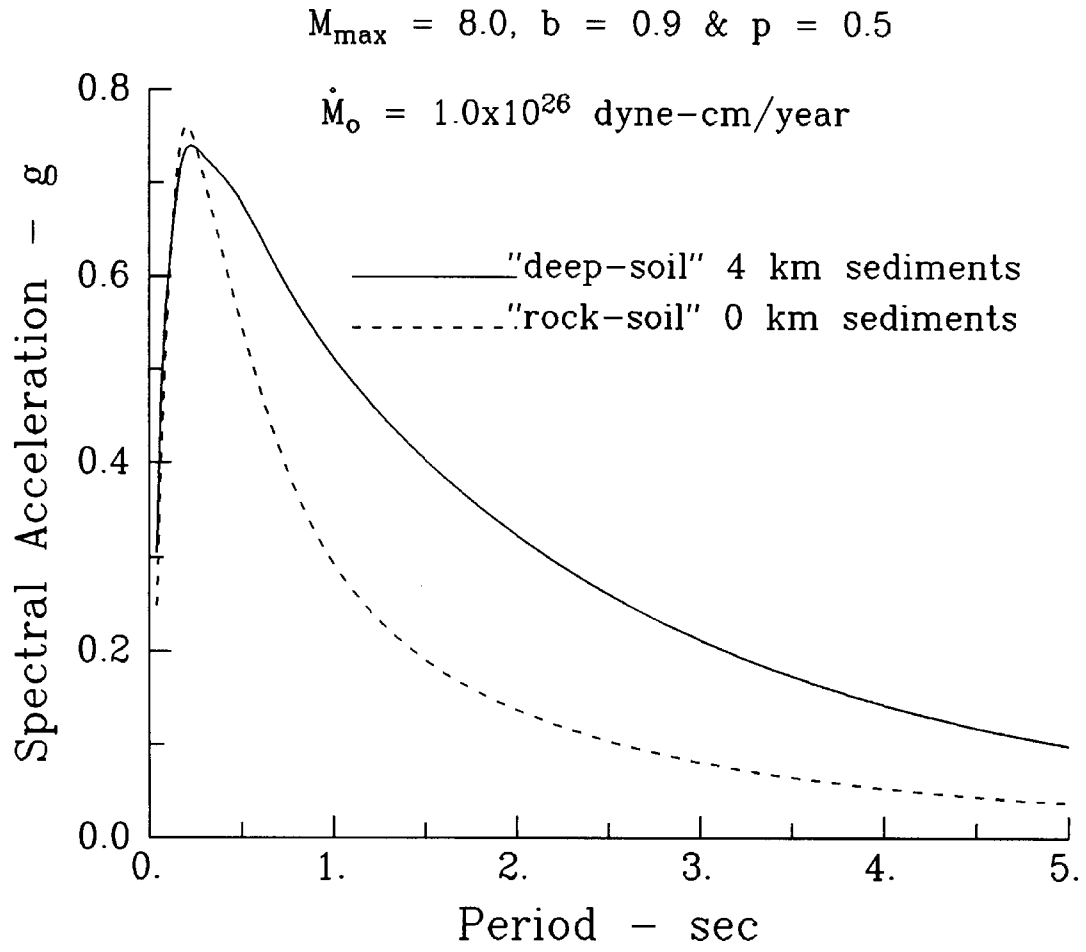

Fig. 11 Comparison of the uniform hazard response spectra for two extreme site conditions defined by hard rock and deep-soil overlying thick sediments

DISCUSSION AND CONCLUSIONS

The present paper has described the current state-of-the-art approaches for the deterministic and the probabilistic seismic hazard analyses. The basic inputs required for both the approaches are the same, which include data on past seismicity, knowledge of the tectonic features, information on site soil condition and the underlying geology of the surrounding area, and the attenuation characteristics of the strong-motion parameter to be used for quantifying the hazard. The first step of analysis is also the same in both the approaches, wherein all possible seismic source zones are identified on the basis of available data on tectonic features and the spatial distribution of the epicenters of past earthquakes. Then, in the deterministic seismic hazard analysis (DSHA), the maximum possible earthquake is estimated for each of the seismic sources. This earthquake, commonly termed as maximum credible earthquake (MCE), is

assumed to occur at a location in the particular seismic source zone, which minimizes its distance from the site of interest. For each of these MCEs, the value of the associated strong-motion parameter at the selected site is most commonly estimated by using an appropriate empirical attenuation relationship. The MCE that produces the largest value of the strong-motion parameter is considered for practical applications, with the conviction that it will never be exceeded.

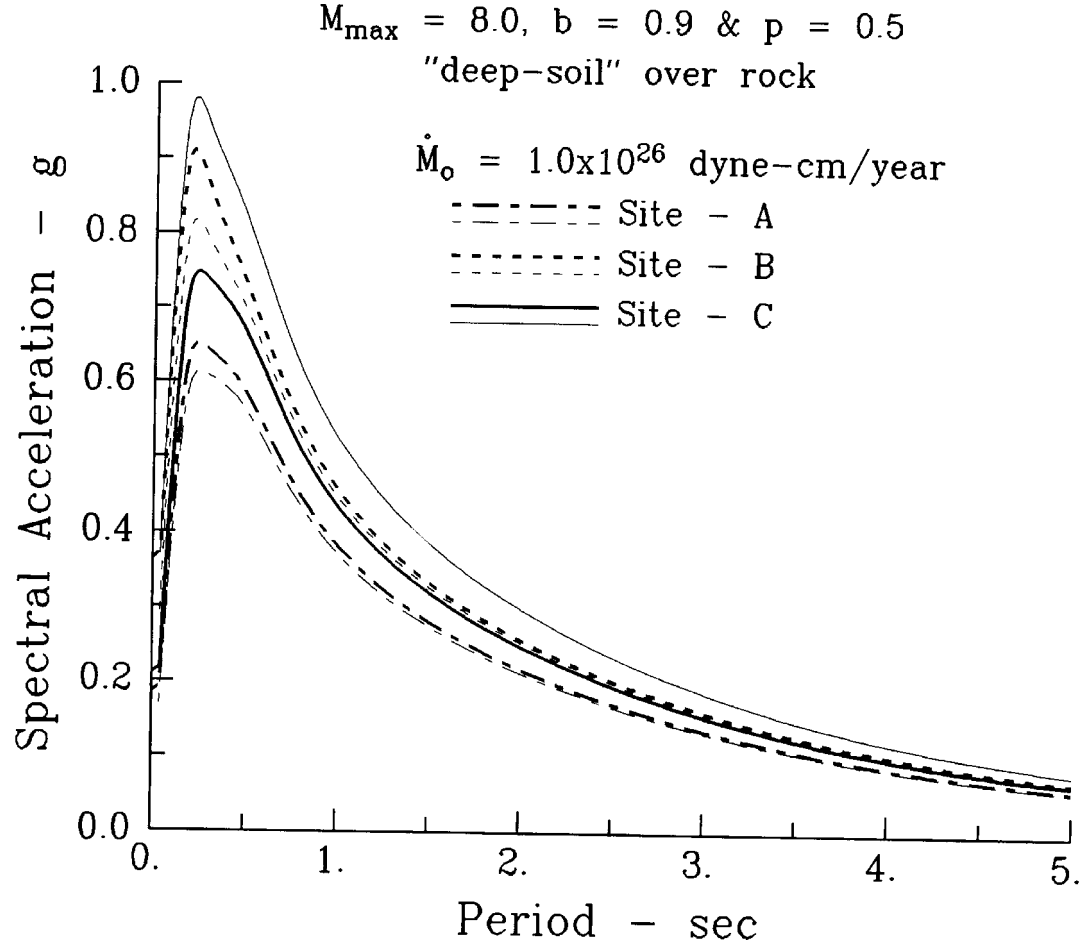

Fig. 12 Illustration of the changes in uniform hazard response spectra with the changes in the spatial distribution of the seismicity (the thick curves correspond to a nonuniform and thin curves to a uniform spatial distribution of the seismicity)

However, the DSHA approach lacks a rational scientific basis and may not always ensure the intended conservatism. The database used and each step of analysis are generally associated with large uncertainties, and thus, selecting the most pessimistic scenario is neither likely to represent reality nor is a good engineering decision. Further, one might be prepared to take at least the same amount of risk in case of earthquakes, to which he is prone in the daily walk of life. However, the DSHA does not provide a means to quantify this risk. In the PSHA approach, the maximum possible earthquake in each seismic source is assigned a finite probability of occurrence during a specified time interval, to account for the fact that the recurrence interval of such an event is normally much longer than the time periods of interest in practical applications. In addition, the total expected numbers of earthquakes with different lower magnitudes during a specified time interval are also considered as per the Gutenberg-Richter's relationship. To account for the random spatial distribution of all these earthquakes for each of the sources, they are distributed appropriately within the entire source zone. Then, a strong-motion parameter of interest is estimated at the selected site with a desired confidence level by defining a composite probability distribution function as a result of the total expected seismicity in all the source zones, with the observed scattering in the strong motion parameter taken into account. Thus, by incorporating the effects of various random uncertainties in the input parameters, the probabilistic seismic hazard analysis (PSHA) approach provides an avenue to arrive at more objective and cost-effective engineering decisions. If desired for some engineering applications, a single pair of magnitude and distance, which can

reproduce the results of the PSHA for a selected site, can also be obtained by de-aggregation of the probabilistic seismic hazard.

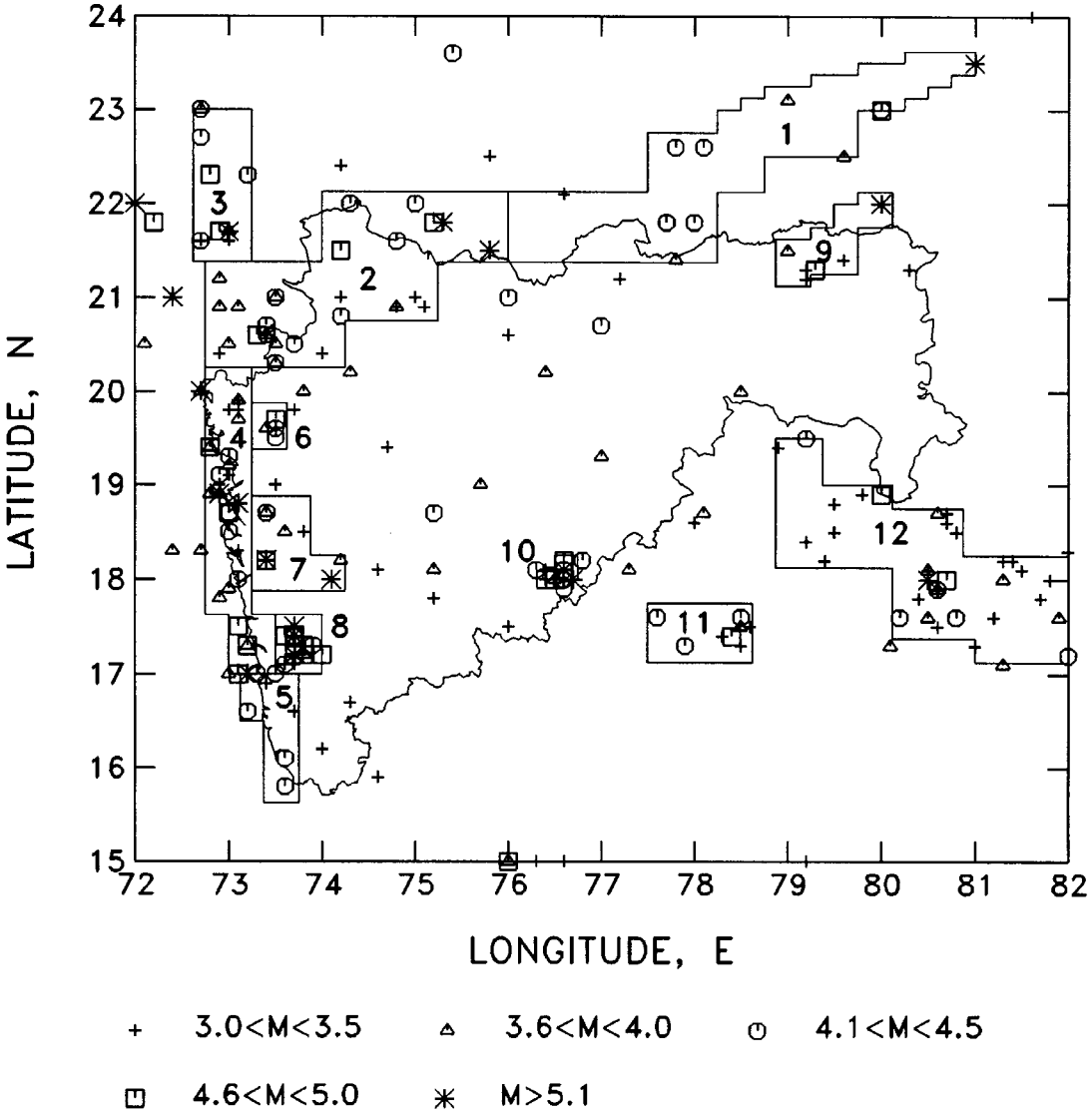

Fig. 13 Twelve possible seismic sources and the distribution of epicenters of available data on past earthquakes in the state of Maharashtra and its adjoining areas

In most of the practical applications, exact knowledge of seismic source geometries, fault rupture scenarios, recurrence model for seismic activity rate, and the attenuation relations for the strong motion parameters is lacking, which makes it difficult to arrive at an unequivocal single representation of seismic sources, their seismicity and the ground motion attenuation. For any particular case, several widely differing and competing alternatives may thus be proposed by different investigators (epistemic uncertainties). As there is no simple way to select the optimum and the most effective alternative, the "mean" or "median" value of the strong motion parameter obtained from several physically plausible models is recommended to be used to get an unbiased estimate of the probabilistic seismic hazard. The DSHA approach can also incorporate the effects of the epistemic uncertainties by computing the mean and median values by considering all possible alternatives regarding the maximum magnitude and its closest distance from a selected site, as well as the ground motion attenuation relation. However, the aleatory uncertainties related to the random nature of the various input parameters are not considered in the deterministic formulation.

Further, it may be noted that the seismic hazard at a site for different frequency ranges is governed by earthquakes with different magnitude and distance combinations. Thus, a single deterministic pair of magnitude and distance is unable to provide the design response spectrum with a desired confidence level for all the natural periods. Also, the results of DSHA approach are, in general, very sensitive to the

choice of the MCE magnitude and its distance, which makes it very difficult to arrive at a stable and reliable estimate. The uniform hazard response spectrum computed by the PSHA approach has the property that with a specified confidence level, it will not be exceeded at any of the periods due to any of the earthquakes expected during a given time interval, thus taking the randomness of earthquake occurrences in space, time and magnitude into account. The paper has also illustrated the use of the PSHA approach to prepare probabilistic seismic zoning maps for the spectral amplitudes at different natural periods with a specified confidence level and a given exposure time. Such maps are able to portray in a balanced way the effects of all the governing factors related to seismicity and the geology on the strong-motion parameter of zoning.

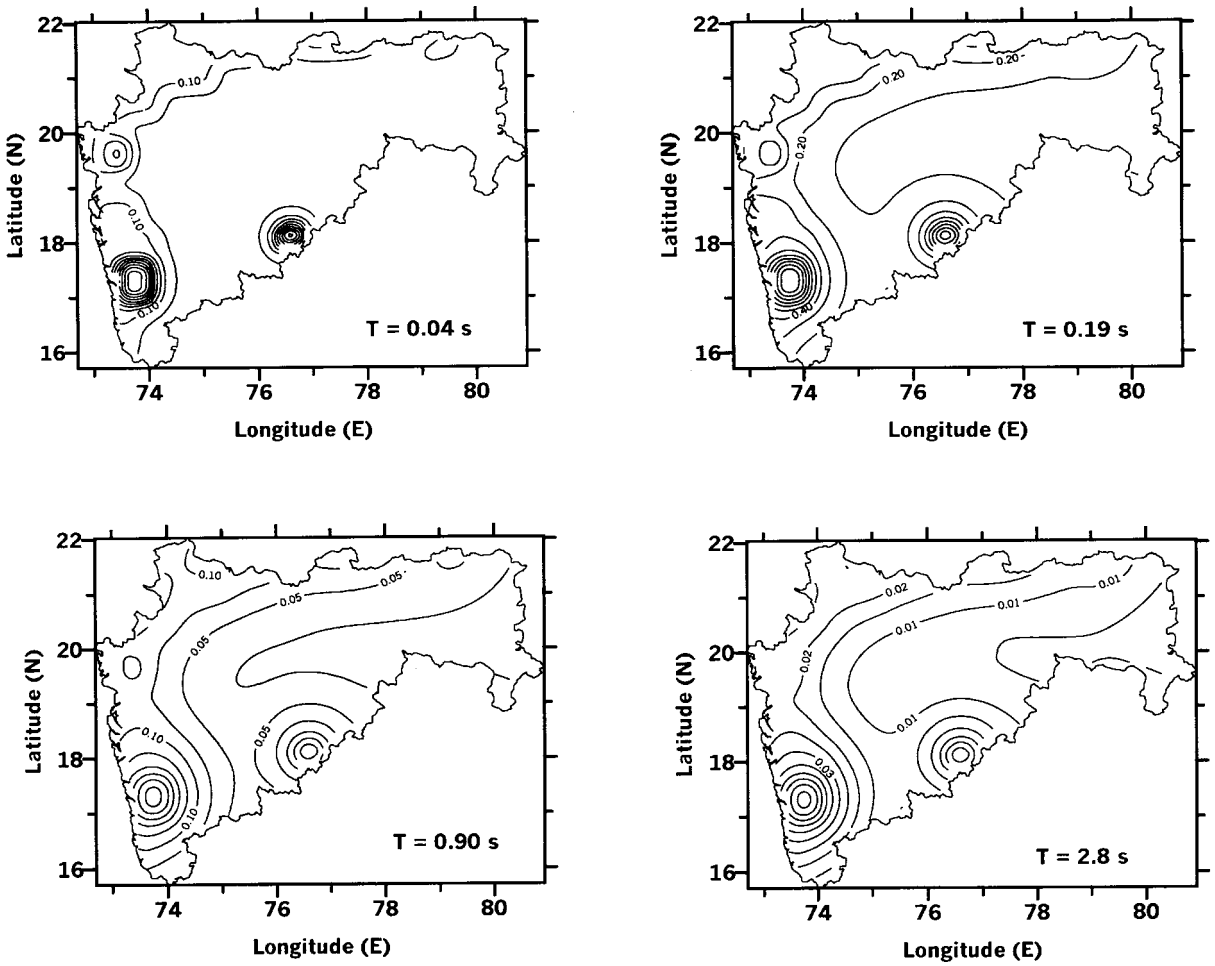

Fig. 14 Seismic zoning maps with a confidence level of 0.50 and exposure time of 100 years for the state of Maharashtra in terms of PSA amplitudes at four natural periods

Though it may be difficult to establish an approach to seismic hazard assessment that will be the ideal tool for all situations (Bommer, 2002), in view of the above discussion, it may be concluded that the PSHA approach should be a preferred choice. Acknowledging the fact that the basic purpose of both DSHA and PSHA approaches is to facilitate engineering designs and decisions, and not to predict the actual earthquakes and ground motions, it is concluded that the PSHA approach provides a scientifically more sound method for seismic hazard analysis.

ACKNOWLEDGEMENTS

The author is grateful to Mrs. V.M. Bendre, Director, Central Water and Power Research Station, Pune for showing very keen interest in the present research work and for according her permission for publication of this paper.

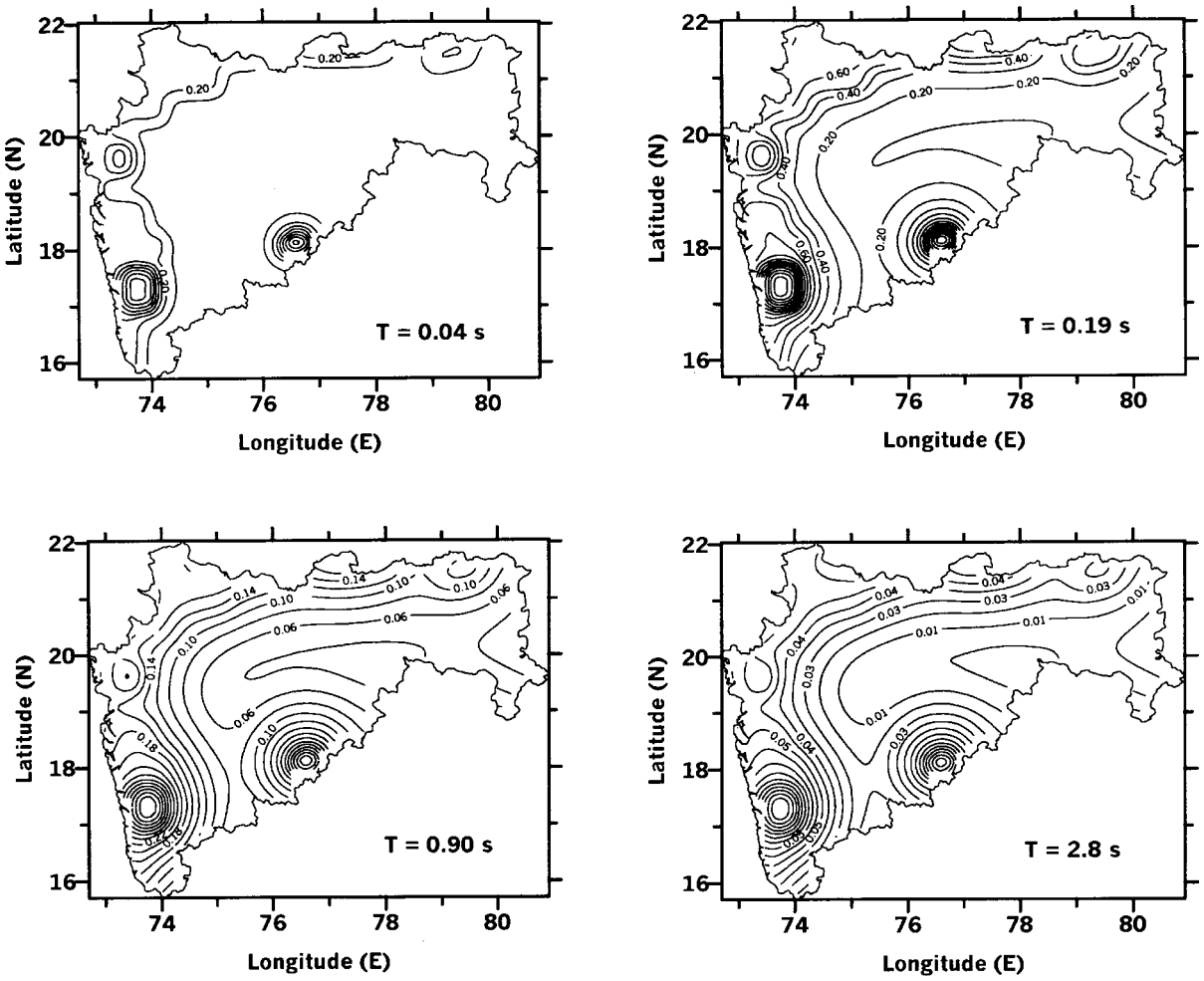

Fig. 15 Seismic zoning maps with a confidence level of 0.84 and exposure time of 100 years for the state of Maharashtra in terms of PSA amplitudes at four natural periods

REFERENCES

1. Abrahamson, N.A. (2000). "Treatment of Variability and Uncertainty in Numerical and Empirical Methods for Ground Motion Estimation", Proc. 2nd US-Japan Workshop on Performance-Based Earthq. Eng. Methodology for Reinforced Concrete Building Structures, Sapporo, Japan, pp. 63-73.
2. Algermissen, S.T. and Perkins, D.M. (1976). "A Probabilistic Estimate of Maximum Acceleration in Rock in the Contiguous United States", Open-File Report 76-416, U.S. Geological Survey.
3. Anderson, J.G. (1978). "On the Attenuation of Modified Mercalli Intensity with Distance in the United States", Bull. Seism. Soc. Am., Vol. 68, pp. 1147-1179.
4. Anderson, J.G. and Luco, J.E. (1983). "Consequence of Slip Rate Constraints on Earthquake Occurrence Relations", Bull. Seism. Soc. Am., Vol. 73, pp. 471-496.
5. Anderson, J.G. and Trifunac, M.D. (1977a). "Uniform Risk Functionals for Characterisation of Strong Earthquake Ground Motion", Report CE 77-02, Dept. of Civil Eng., University of Southern California, Los Angeles, California, U.S.A.
6. Anderson, J.G. and Trifunac, M.D. (1977b). "Uniform Risk Functionals for Characterisation of Strong Earthquake Ground Motion", Proc. Second Annual ASCE EMD Specialty Conference, North Carolina State Univ., Raleigh, N.C., U.S.A., pp. 332-335.
7. Anderson, J.G. and Trifunac, M.D. (1978a). "Uniform Risk Functionals for Characterization of Strong Earthquake Ground Motion", Bull. Seism. Soc. Am., Vol. 68, pp. 205-218.

8. Anderson, J.G. and Trifunac, M.D. (1978b). "Application of Seismic Risk Procedures to Problems in Microzonation", Proc. 2nd Int. Conf. on Microzonation for Safer Construction, Research and Applications, Vol. I, pp. 559-569.
9. Anderson, J.G. and Trifunac, M.D. (1979). "A Note on Probabilistic Computation of Earthquake Response Spectrum Amplitudes", Nuclear Engineering and Design, Vol. 51, pp. 285-294.
10. Anderson, J.G., Lee, V.W. and Trifunac, M.D. (1987). "Methods for Introduction of Geological Data into Characterisation of Active Faults and Seismicity and Upgrading of the Uniform Risk Spectrum Technique", U.S. Nuclear Regulatory Commission, Report NUREG/CR-4903.
11. Bilham, R. and Gaur, V.K. (2000). "Geodetic Contributions to the Study of Seismotectonics in India", Current Science, Vol. 79, pp. 1259-1269.
12. Biot, M.A. (1942). "Analytical and Experimental Methods in Engineering Seismology", ASCE Transactions, Vol. 5, pp. 365-408.
13. Bommer, J.J. (2002). "Deterministic versus Probabilistic Seismic Hazard Assessment: An Exaggerated and Obstructive Dichotomy", Jour. Earthq. Eng., Vol. 6, Special Issue 1, pp. 43-73.
14. Bonilla, M.G. and Buchanon, J.M. (1970). "Interim Report on World-Wide Historic Surface Faulting", Open-File Report 70-34, U.S. Geological Survey.
15. Bonilla, M.G., Markad, R.K. and Lienkaemper, J.J. (1984). "Statistical Relations among Earthquake Magnitude, Surface Rupture Length, and Surface Rupture Displacement", Bull. Seism. Soc. Am., Vol. 74, pp. 2379-2411.
16. Boore, D.M. and Atkinson, B.M. (1987). "Stochastic Prediction of Ground Motion and Spectral Response at Hard-Rock Sites in Eastern North America", Bull. Seism. Soc. Am., Vol. 77, pp. 440-467.
17. Chen, P.S. and Lin, P.H. (1973). "An Application of Theory of Extreme Values to Moderate and Long-Interval Earthquake Prediction", Acta Geophys., Vol. 16, p. 6.
18. Coppersmith, K.J. and Youngs, R.R. (1986). "Capturing Uncertainties in Probabilistic Seismic Hazard Assessments within Intraplate Environments", Proc. 3rd National Conf. on Earthq. Eng., Charleston, South Carolina, U.S.A., Vol. I, pp. 301-312.
19. Cornell, C.A. (1968). "Engineering Seismic Risk Analysis", Bull. Seism. Soc. Am., Vol. 58, No. 5, pp. 1583-1606.
20. David, P.M., Jackson, D.D. and Kagan, Y.Y. (1989). "The Longer It Has Been since the Last Earthquake, the Longer the Expected Time till the Next", Bull. Seism. Soc. Am., Vol. 79, No. 5, pp. 1439-1456.
21. Douglas, J. (2001). "A Comprehensive Worldwide Summary of Strong-Motion Attenuation Relationships for Peak Ground Acceleration and Spectral Ordinates (1969 to 2000)", ESEE Report 01-1, Civil Engineering Dept., Imperial College of Science, Technology and Medicine, London, U.K.
22. Dravinski, M., Trifunac, M.D. and Westermo, B.D. (1980). "Ratios of Uniform Risk Spectrum Amplitudes for Different Probabilities of Exceedance and for Shallow, Random Seismicity Surrounding the Site", Report CE 80-02, Dept. of Civil Eng., Univ. of Southern California, Los Angeles, California, U.S.A.
23. Epstein, B. and Lomnitz, C. (1966). "A Model for Occurrence of Large Earthquakes", Nature, Vol. 211, pp. 954-956.
24. Esteva, L. (1969). "Seismicity Prediction, A Bayesian Approach", Proc. 4th World Conf. Earthq. Eng., Santiago, Chile.
25. Geller, R.J. (1976). "Scaling Relations for Earthquake Source Parameters and Magnitude", Bull. Seism. Soc. Am., Vol. 66, pp. 1501-1523.
26. Gumbel, E.J. (1958). "Statistics of Extremes", Columbia Univ. Press, New York, U.S.A.
27. Gupta, I.D. (1991). "A Note on Computing Uniform Risk Spectra from Intensity Data on Earthquake Occurrence", Soil Dyn. Earthq. Eng., Vol. 10, No. 8, pp. 407-413.
28. Gupta, I.D. (2002). "Should Normalised Spectral Shapes be Used for Estimating Site-Specific Design Ground Motion?", Proc. 12th Symp. on Earthq. Eng., Indian Institute of Technology Roorkee, Roorkee, Vol. I, pp. 168-175.

29. Gupta, I.D. and Deshpande, V.C. (1994). "Application of Log-Pearson Type-3 Distribution for Evaluation of Design Earthquake Magnitude", Jour. Inst. Engineers (India), Civil Div., Vol. 75, pp. 129-134.
30. Gupta, I.D. and Joshi, R.G. (1993). "On Synthesizing Response Spectrum Compatible Accelerograms", European Earthq. Eng., Vol. 7, pp. 25-33.
31. Gupta, I.D. and Joshi, R.G. (1996). "Evaluation of Design Earthquake Ground Motion for Soil and Rock Sites", Proc. Workshop on Design Practices in Earthq. Geotech. Eng., Roorkee, pp. 58-87.
32. Gupta, I.D. and Joshi, R.G. (2001). "Probabilistic Seismic Zoning of Maharashtra State", Proc. Workshop on Seismicity of Western India with Special Reference to Recent Kutch Earthquake, Paper No. 1, Pune.
33. Gupta, I.D. and Rambabu, V. (1996). "Simulation of Design Response Spectra of Strong-Motion Acceleration in Koyna Dam Region Using Seismological Source Model Approach", Bull. Ind. Soc. Earthq. Tech., Vol. 33, No. 2, pp. 181-193.
34. Gupta, I.D. and Trifunac, M.D. (1988). "Attenuation of Intensity with Epicentral Distances in India", Soil Dyn. Earthq. Eng., Vol. 7, pp. 162-169.
35. Gupta, I.D., Joshi, R.G. and Rambabu, V. (2002). "An Example of Seismic Zoning Using PSHA Approach", MAEER's MIT Pune Jour., Vol. IX, No. 1-4, pp. 107-116.
36. Gupta, I.D., Nagle, B.R. and Pagare, V.S. (1988). "An Investigation for the Probabilities of Maximum Earthquake Magnitudes in Northwest Himalayan Region", Bull. Ind. Soc. Earthq. Tech., Vol. 25, pp. 11-22.
37. Gupta, I.D., Joshi, R.G., Rambabu, V. and Rame Gowda, B.M. (1999). "Attenuation of MMI with Distance in Peninsular India", European Earthq. Eng., Vol. 13, pp. 25-32.
38. Gutenberg, B. and Richter, C.F. (1954). "Seismicity of the Earth and Associated Phenomena", Princeton Univ. Press, Princeton, New Jersey, U.S.A.
39. Hadley, D.M. and Helmberger, D.V. (1980). "Simulation of Strong Ground Motions", Bull. Seism. Soc. Am., Vol. 70, pp. 610-617.
40. Hanks, T.C. and Kanamori, H. (1979). "A Moment Magnitude Scale", Jour. Geophys. Res., Vol. 84, pp. 2348-2350.
41. Hartzell, S.H. (1982). "Simulation of Ground Acceleration for May 1980 Mammoth Lakes, California Earthquakes", Bull. Seism. Soc. Am., Vol. 72, pp. 2381-2387.
42. Housner, G.W. (1959). "Behaviour of Structures during Earthquakes", Jour. Eng. Mech. Div., ASCE, Vol. 85, pp. 109-129.
43. IAEE (1984). "Earthquake Resistant Regulations, A World List-1984", International Association of Earthquake Engineering, Gakujutsu Bunken Fukyn-Kai, Tokyo, Japan.
44. Iida, K. (1965). "Earthquake Magnitude, Earthquake Fault, and Source Dimensions", Jour. Earthq. Sci., Nagoya Univ., Vol. 13, pp. 115-132.
45. Irikura, K. and Muramatu, I. (1982). "Synthesis of Strong Ground Motions from Large Earthquakes Using Observed Seismograms of Small Events", Proc. 3rd International Microzonation Conf., Seattle, U.S.A., pp. 447-458.
46. Ishikawa, Y. and Kameda, H. (1988). "Hazard Consistent Magnitude and Distance for Extended Seismic Risk Analysis", Proc. 9th World Conf. Earthq. Eng., Vol. 2, pp. 89-94.
47. Jara, J.M. and Rosenblueth, E. (1988). "Probability Distribution of Times between Characteristic Subduction Earthquakes", Earthq. Spectra, Vol. 4, pp. 449-531.
48. Jordanovski, L.R., Todorovska, M.I. and Trifunac, M.D. (1991). "A Model for Assessment of the Total Loss in a Building Exposed to Earthquake Hazard", Report CE 92-05, Dept. of Civil Eng., Univ. of Southern California, Los Angeles, California, U.S.A.
49. Jordanovski, L.R., Todorovska, M.I. and Trifunac, M.D. (1993). "Total Loss in a Building Exposed to Earthquake Hazard, Part I: The Model; Part II: A Hypothetical Example", European Earthq. Eng., Vol. VI, No. 3, pp. 14-32.
50. Kameda, H. (1994). "Probabilistic Seismic Hazard and Stochastic Ground Motions", Engineering Structures, Vol. 16, pp. 547-557.

51. Khattri, K.N., Rogers, A.M. and Algermissen, S.T. (1984). "A Seismic Hazard Map of India and Adjacent Areas", Tectonophysics, Vol. 108, pp. 93-134.
52. Khattri, K.N., Yu, G., Anderson, J.G., Brune, J.N. and Zeng, Y. (1994). "Seismic Hazard Estimation Using Modelling of Earthquake Strong Ground Motions: A Brief Analysis of 1991 Uttarkashi Earthquake, Himalaya and Prognostication for a Great Earthquake in the Region", Current Science, Vol. 67, No. 5, pp. 343-353.
53. Kijko, A. (1983). "A Modified Form of the First Gumbel Distribution Model for the Occurrence of Large Earthquakes", Acta Geophys., Vol. 31, pp. 27-39.
54. Kijko, A. and Graham, G. (1998). "Parametric-Historic Procedure for Probabilistic Seismic Hazard Analysis, Part I: Estimation of Maximum Regional Magnitude $M_{\max}$", Pure and Applied Geophysics, Vol. 152, pp. 413-442.
55. Kijko, A. and Sellevoll, M.A. (1981). "Triple-Exponential Distribution, A Modified Model for the Occurrence of Large Earthquakes", Bull. Seism. Soc. Am., Vol. 71, pp. 2097-2101.
56. Kijko, A. and Sellevoll, M.A. (1989). "Estimation of Earthquake Hazard Parameters from Incomplete Data Files, Part I: Utilization of Extreme and Complete Catalogues with Different Threshold Magnitudes", Bull. Seism. Soc. Am., Vol. 79, pp. 645-654.
57. Krinitzsky, E.L. (1995). "Deterministic versus Probabilistic Seismic Hazard Analysis for Critical Structures", Int. Jour. Eng. Geol., Vol. 40, pp. 1-7.
58. Lee, V.W. (1987). "Influence of Local Soil and Geologic Site Conditions on Pseudo Relative Velocity Response Spectrum Amplitudes of Recorded Strong Motion Accelerations", Report CE 87-05, Dept. of Civil Eng., Univ. of Southern California, Los Angeles, California, U.S.A.
59. Lee, V.W. (1989). "Empirical Scaling of Pseudo Relative Velocity Spectra of Recorded Strong Earthquake Motion in Terms of Magnitude, and Both Local Soil and Geologic Site Classifications", Earthq. Eng. Eng. Vib., Vol. 9, No. 3, pp. 9-29.
60. Lee, V.W. (1990). "Scaling PSV Spectra in Terms of Site Intensity, and Both Local Soil and Geological Site Classifications", European Earthq. Eng., Vol. IV, No. 1, pp. 3-12.
61. Lee, V.W. (1991). "Correlation of Pseudo Relative Velocity Spectra with Site Intensity, Local Soil Classification and Depth of Sediments", Soil Dyn. Earthq. Eng., Vol. 10, No. 3, pp. 141-151.
62. Lee, V.W. (1992). "On Strong Motion Uniform Risk Functionals Computed from General Probability Distributions of Earthquake Recurrences", Soil Dyn. Earthq. Eng., Vol. 11, pp. 357-367.
63. Lee, V.W. (1993). "Scaling PSV from Earthquake Magnitude, Local Soil and Geological Depth of Sediments", Jour. Geotech. Eng., ASCE, Vol. 119, No. 1, pp. 108-126.
64. Lee, V.W. and Trifunac, M.D. (1985). "Uniform Risk Spectra of Strong Earthquake Ground Motion: NEQRISK", Report CE 85-05, Dept. of Civil Eng., Univ. of Southern California, Los Angeles, California, U.S.A.
65. Lee, V.W. and Trifunac, M.D. (1987). "Microzonation of a Metropolitan Area", Report CE 87-02, Dept. of Civil Eng., Univ. of Southern California, Los Angeles, California, U.S.A.
66. Lee, V.W. and Trifunac, M.D. (1989). "A Note on Filtering Strong Motion Accelerograms to Produce Response Spectra of Specified Shape and Amplitude", European Earthquake Eng., Vol. VIII, No. 2, pp. 38-45.
67. Mark, R.K. (1977). "Application of Linear Statistical Model of Earthquake Magnitude versus Fault Length in Estimating Maximum Expectable Earthquakes", Geology, Vol. 5, pp. 464-466.
68. McGuire, R.K. (1995). "Probabilistic Seismic Hazard Analysis and Design Earthquakes: Closing the Loop", Bull. Seism. Soc. Am., Vol. 85, pp. 1275-1284.
69. Mohraz, B. (1976). "A Study of Earthquake Response Spectra for Different Geological Conditions", Bull. Seism. Soc. Am., Vol. 66, pp. 915-935.
70. Newmark, N.M. and Hall, W.J. (1969). "Seismic Design Criteria for Nuclear Reactor Facilities", Proc. 4th World Conf. Earthq. Eng., Vol. B-4, pp. 37-50.
71. Nishenko, S.P. and Buland, R.A. (1987). "A Generic Recurrence Time Distribution for Earthquake Forecasting", Bull. Seism. Soc. Am., Vol. 77, pp. 1382-1399.

72. Nordquist, J.M. (1945). "Theory of Largest Values Applied to Earthquake Magnitudes", Trans. Am. Geophys. Union, Vol. 26, pp. 29-31.

73. Papastamatiou, D. (1980). "Incorporation of Crustal Deformation to Seismic Hazard Analysis", Bull. Seism. Soc. Am., Vol. 70, pp. 1323-1335.

74. Romeo, R. and Prestininzi, A. (2000). "Probabilistic versus Deterministic Seismic Hazard Analysis: An Integrated Approach for Siting Problems", Soil Dyn. Earthq. Eng., Vol. 20, pp. 75-84.

75. Savy, J.B., Foxall, W., Abrahamson, N. and Bernreuter, D. (2002). "Guidance for Performing Probabilistic Seismic Hazard Analysis for a Nuclear Plant Site: Example Application to the Southeastern United States", Report NUREG/CR-6607, U.S. Nuclear Regulatory Commission, Washington, D.C., U.S.A.

76. Scholz, C.H. (1968). "The Frequency-Magnitude Relation of Microfracturing in Rock and its Relation to Earthquakes", Bull. Seism. Soc. Am., Vol. 58, pp. 399-415.

77. Schwartz, D.P. and Coppersmith, K.J. (1984). "Fault Behavior and Characteristic Earthquakes: Examples from the Wasatch and San Andreas Faults", J. Geophys. Res., Vol. 89, pp. 5681-5698.

78. Seeber, L. and Armbruster, J.G. (1981). "Great Detachment Earthquakes along the Himalayan Arc and Long Term Forecasting", in "Earthquake Prediction - An International Review", Maurice Ewing Series 4, Am. Geophys. Union, Washington, D.C., U.S.A., pp. 259-277.

79. Seed, H.B., Ugas, C. and Lysmer, J. (1976). "Site-Dependent Spectra for Earthquake Resistant Design", Bull. Seism. Soc. Am., Vol. 66, pp. 221-243.

80. Singh, S.K., Bazan, E. and Esteva, L. (1980). "Expected Earthquake Magnitude from a Fault", Bull. Seism. Soc. Am., Vol. 70, pp. 903-914.

81. Smith, S.W. (1976). "Determination of Maximum Earthquake Magnitude", Geophys. Res. Letters, Vol. 33, pp. 351-354.

82. SSHAC (1997). "Recommendations for Probabilistic Seismic Hazard Analysis: Guidance on Uncertainty and Use of Experts", Report NUREG/CR-6372, Senior Seismic Hazard Analysis Committee, U.S. Nuclear Regulatory Commission, Washington, D.C., U.S.A.

83. Stepp, J.C. (1973). "Analysis of Completeness of the Earthquake Sample in the Puget Sound Area", in "Seismic Zoning (edited by S.T. Harding)", NOAA Tech. Report ERL 267-ESL30, Boulder, Colorado, U.S.A.

84. Stepp, J.C. and Wong, I.G. (2001). "Probabilistic Seismic Hazard Analyses for Ground Motions and Fault Displacement at Yucca Mountain, Nevada", Earthquake Spectra, Vol. 17, No. 1, pp. 113-151.

85. Todorovska, M.I. (1994). "Comparison of Response Spectrum Amplitudes from Earthquakes with Lognormally and Exponentially Distributed Return Periods", Soil Dyn. Earthq. Eng., Vol. 13, pp. 97-116.

86. Todorovska, M.I. and Trifunac, M.D. (1996a). "A Seismic Hazard Model for Peak Strains in Soils during Strong Earthquake Shaking", Earthq. Eng. Eng. Vib., Vol. 16, Supplement, pp. 1-12.

87. Todorovska, M.I. and Trifunac, M.D. (1996b). "Hazard Mapping of Normalized Peak Strain in Soil during Earthquakes - Microzonation of a Metropolitan Area", Soil Dyn. Earthq. Eng., Vol. 15, No. 5, pp. 321-329.

88. Todorovska, M.I. and Trifunac, M.D. (1999). "Liquefaction Opportunity Mapping via Seismic Wave Energy", Jour. Geotech. Geoenvironmental Eng., ASCE, Vol. 125, No. 12, pp. 1032-1042.

89. Todorovska, M.I., Gupta, I.D., Gupta, V.K., Lee, V.W. and Trifunac, M.D. (1995). "Selected Topics in Probabilistic Seismic Hazard Analysis", Report CE 95-08, Dept. of Civil Eng., Univ. of Southern California, Los Angeles, California, U.S.A.

90. Tocher, D. (1958). "Earthquake Energy and Ground Breakage", Bull. Seism. Soc. Am., Vol. 48, pp. 147-153.

91. Trifunac, M.D. (1970). "On the Statistics and Possible Triggering Mechanism of Earthquakes in Southern California", Report EERL 70-03, Earthquake Eng. Research Lab., Calif. Inst. of Technology, Pasadena, California, U.S.A.

92. Trifunac, M.D. (1976). "Preliminary Empirical Model for Scaling Fourier Amplitude Spectra of Strong Ground Acceleration in Terms of Earthquake Magnitude, Source to Station Distance and Recording Site Conditions", Bull. Seism. Soc. Am., Vol. 66, pp. 1345-1373.
93. Trifunac, M.D. (1977). "Uniformly Processed Strong Earthquake Ground Accelerations in the Western United States of America for the Period from 1933 to 1971: Pseudo Relative Velocity Spectra and Processing Noise", Report CE 77-04, Dept. of Civil Eng., Univ. of Southern California, Los Angeles, California, U.S.A.
94. Trifunac, M.D. (1979). "Preliminary Empirical Model for Scaling Fourier Amplitude Spectra of Strong Motion Acceleration in Terms of Modified Mercalli Intensity and Geological Site Condition", Earthq. Eng. Struct. Dyn., Vol. 7, pp. 63-74.
95. Trifunac, M.D. (1987). "Influence of Local Soil and Geologic Site Conditions on Fourier Spectrum Amplitudes of Recorded Strong Motion Accelerations", Report CE 87-04, Dept. of Civil Eng., Univ. of Southern California, Los Angeles, California, U.S.A.
96. Trifunac, M.D. (1988). "Seismic Microzonation Mapping via Uniform Risk Spectra", Proc. 9th World Conf. Earthq. Eng., Vol. VII, pp. 75-80.
97. Trifunac, M.D. (1989a). "Seismic Microzonation", Proc. UNDRO Seminar on Lessons Learned from Earthquakes, Moscow, USSR, pp. 21-27.
98. Trifunac, M.D. (1989b). "Threshold Magnitudes Which Cause Ground Motion Exceeding the Values Expected during the Next 50 Years in a Metropolitan Area", Geofizika, Vol. 6, pp. 1-12.
99. Trifunac, M.D. (1989c). "Dependence of Fourier Spectrum Amplitudes of Recorded Strong Earthquake Accelerations on Magnitude, Local Soil Conditions and on Depth of Sediments", Earthq. Eng. Struct. Dyn., Vol. 18, pp. 999-1016.
100. Trifunac, M.D. (1989d). "Empirical Scaling of Fourier Spectrum Amplitudes of Recorded Strong Earthquake Accelerations in Terms of Magnitude and Local Soil and Geologic Conditions", Earthq. Eng. Eng. Vib., Vol. 9, No. 2, pp. 23-44.
101. Trifunac, M.D. (1990a). "A Microzonation Method Based on Uniform Risk Spectra", Soil Dyn. Earthq. Eng, Vol. 9, No. 1, pp. 34-43.
102. Trifunac, M.D. (1990b). "How to Model Amplification of Strong Earthquake Motions by Local Soil and Geologic Site Conditions", Earthq. Eng. Struct. Dyn., Vol. 19, No. 6, pp. 833-846.
103. Trifunac, M.D. (1991). "Empirical Scaling of Fourier Spectrum Amplitudes of Recorded Strong Earthquake Accelerations in Terms of Modified Mercalli Intensity, Local Soil Conditions and Depth of Sediments", Soil Dyn. Earthq. Eng., Vol. 10, No. 1, pp. 65-72.
104. Trifunac, M.D. (1992). "Should Peak Acceleration be Used to Scale Design Spectrum Amplitudes?", Proc. 10th World Conf. on Earthq. Eng., Madrid, Spain, Vol. 10, pp. 5817-5822.
105. Trifunac, M.D. (1993). "Broad Band Extension of Fourier Amplitude Spectra of Strong Motion Acceleration", Report CE 93-01, Dept. of Civil Eng., Univ. of Southern California, Los Angeles, California, U.S.A.
106. Trifunac, M.D. (1994). "Similarity of Strong Motion Earthquakes in California", European Earthquake Eng., Vol. VIII, No. 1, pp. 38-48.
107. Trifunac, M.D. (1998). "Stresses and Intermediate Frequencies of Strong Motion Acceleration", Geofizika, Vol. 14, pp. 1-27.
108. Trifunac, M.D. and Anderson, J.G. (1977). "Preliminary Empirical Models for Scaling Absolute Acceleration Spectra", Report CE 77-03, Dept. of Civil Eng., Univ. of Southern California, Los Angeles, California, U.S.A.
109. Trifunac, M.D. and Anderson, J.G. (1978a). "Preliminary Empirical Models for Scaling Pseudo Relative Velocity Spectra", Report CE 78-04, Dept. of Civil Eng., Univ. of Southern California, Los Angeles, California, U.S.A.
110. Trifunac, M.D. and Anderson, J.G. (1978b). "Preliminary Models for Scaling Relative Velocity Spectra", Report CE 78-05, Dept. of Civil Eng., Univ. of Southern California, Los Angeles, California, U.S.A.

111. Trifunac, M.D. and Lee, V.W. (1978). "Dependence of Fourier Amplitude Spectra of Strong Motion Acceleration on the Depth of Sedimentary Deposits", Report CE 78-14, Dept. of Civil Eng., Univ. of Southern California, Los Angeles, California, U.S.A.

112. Trifunac, M.D. and Lee, V.W. (1979). "Dependence of Pseudo Relative Velocity Spectra of Strong Motion Acceleration on the Depth of Sedimentary Deposits", Report CE 79-02, Dept. of Civil Eng., Univ. of Southern California, Los Angeles, California, U.S.A.

113. Trifunac, M.D. and Lee, V.W. (1985a). "Frequency Dependent Attenuation of Strong Earthquake Ground Motion", Report CE 85-02, Dept. of Civil Eng., Univ. of Southern California, Los Angeles, California, U.S.A.

114. Trifunac, M.D. and Lee, V.W. (1985b). "Preliminary Empirical Model for Scaling Fourier Amplitude Spectra of Strong Ground Acceleration in Terms of Earthquake Magnitude, Source to Station Distance, Site Intensity and Recording Site Conditions", Report CE 85-03, Dept. of Civil Eng., Univ. of Southern California, Los Angeles, California, U.S.A.

115. Trifunac, M.D. and Lee, V.W. (1985c). "Preliminary Empirical Model for Scaling Pseudo Relative Velocity Spectra of Strong Earthquake Acceleration in Terms of Magnitude, Distance, Site Intensity and Recording Site Conditions", Report CE 85-04, Dept. of Civil Eng., Univ. of Southern California, Los Angeles, California, U.S.A.

116. Trifunac, M.D. and Lee, V.W. (1990). "Frequency Dependent Attenuation of Strong Earthquake Ground Motion", Soil Dyn. Earthq. Eng, Vol. 9, No. 1, pp. 3-15.

117. Trifunac, M.D. and Todorovska, M.I. (1989). "Attenuation of Seismic Intensity in Albania and Yugoslavia", Earthq. Eng. Struct. Dyn., Vol. 18, pp. 617-631.

118. Trifunac, M.D. and Todorovska, M.I. (1998). "Comment on the Role of Earthquake Hazard Maps in Loss Estimation: A Study of the Northridge Earthquake", Earthq. Spectra, Vol. 14, No. 3, pp. 557-563.

119. Tsai, N.C. (1972). "Spectrum Compatible Motions for Design Purposes", Jour. Eng. Mech. Div., ASCE, Vol. 98, pp. 345-356.

120. Utsu, T. (1961). "A Statistical Study on the Occurrence of Aftershocks", Geophys. Mag., Vol. 30, pp. 521-605.

121. Wells, D.L. and Coppersmith, K.J. (1994). "New Empirical Relationships among Magnitude, Rupture Length, Rupture Width, Rupture Area, and Surface Displacement", Bull. Seism. Soc. Am., Vol. 84, pp. 974-1002.

122. Wesnousky, S.G. (1986). "Earthquakes, Quaternary Faults and Seismic Hazard in California", Jour. Geophys. Res., Vol. 91, pp. 12587-12631.

123. Wesnousky, S.G. (1994). "The Gutenberg-Richter or Characteristic Earthquake Distribution, Which Is It?", Bull. Seism. Soc. Am., Vol. 84, No. 6, pp. 1940-1959.

124. Westermo, B.D., Anderson, J.G., Trifunac, M.D. and Dravinski, M. (1980). "Seismic Risk Tables for Pseudo Relative Velocity Spectra in Regions with Shallow Seismicity", Report CE 80-01, Dept. of Civil Eng., Univ. of Southern California, Los Angeles, California, U.S.A.

125. Wong, H.L. and Trifunac, M.D. (1979). "Generation of Artificial Strong Motion Accelerograms", Earthq. Eng. Struct. Dyn., Vol. 7, pp. 509-527.

126. Wyss, M. (1979). "Estimating Maximum Expected Magnitude of Earthquakes from Fault Dimensions", Geology, Vol. 7, pp. 336-340.

127. Wyss, M. and Brune, J.N. (1968). "Seismic Moment, Stress, and Source Dimensions for Earthquakes in the California-Nevada Region", Jour. Geophys. Res., Vol. 73, pp. 4681-4694.

128. Yonekura, N. (1972). "A Review on Seismic Crustal Deformations in and near Japan", Bull. Dept. Geography, Univ. of Tokyo, Vol. 4, pp. 17-50.

129. Youngs, R.R. and Coppersmith, K.J. (1985). "Implications of Fault Slip Rates and Earthquake Recurrence Models to Probabilistic Seismic Hazard Estimates", Bull. Seism. Soc. Am., Vol. 75, No. 4, pp. 939-964.

ISET Journal of Earthquake Technology, Paper No. 429, Vol. 39, No. 4, December 2002, pp. 347-365

DEVELOPMENTS IN RESPONSE SPECTRUM -BASED STOCHASTIC RESPONSE OF STRUCTURAL SYSTEMS

Vinay K. Gupta
Department of Civil Engineering
IIT Kanpur, Kanpur-208016

ABSTRACT

Response spectra are commonly used for the estimation of the largest peak response of a linear structural system in a seismic environment. Traditionally, this has been done through the use of appropriate modal combination rules in case of multi-degree-of-freedom systems. While these methods do not consider uncertainty in response due to phasing in seismic waves, those also do not go beyond estimating the largest peak response, and have natural limitation of being applied accurately to only a few types of structural systems. This paper considers a review of alternative methods which have been developed since mid-1970's to give probabilistic estimates of response peaks, while continuing to use the information available through response spectra. These methods have the convenience of being applied in a variety of situations, do not usually suffer from the inaccuracies associated with the use of modal combination rules, and present state-of-the-art methodology in linear seismic response analysis. The limitations of various formulations proposed under these methods are identified, and future directions of required work are suggested.

KEYWORDS: Ground Motion Process, Response Spectrum-Based Characterization, Linear MDOF Systems, Peak Stochastic Response

INTRODUCTION

1. Seismic Response Analysis

Computation of the dynamic response of structures to earthquake ground motions involves, in general, three steps: (i) formulation and selection of the physical model, (ii) mathematical formulation of the governing equations, and (iii) computation of the response. The extent of rigour in each of these steps depends on the type of application, required output, and on the desired accuracy.

Formulation and selection of the physical model also depends on the past experience, with similar and related modeling, and has to represent, as realistically as possible, the desired characteristics of response. Arriving at the final model inevitably involves simplification of the complete full-scale structure. This may require iterations, involving verification via specific measurements on similar or related structures (e.g., see Trifunac and Todorovska, 1999a; Kojic et al., 1984a, 1984b, 1993), observation of general trends in full-scale structural response (Udwadia and Trifunac, 1974a; Trifunac et al., 2001a, 2001b, 2001c, 2002) or of selected features of full-scale response (Trifunac and Lee, 1979, 1986). Model geometry and its properties may be chosen suitably to study specific aspects of one versus two versus three-dimensional characteristics of response (e.g., see Kojic and Trifunac, 1988, 1989, 1991a, 1991b), or to isolate and emphasize the effects of the selected model properties (e.g., see Kashefi and Trifunac, 1986).

Mathematical formulation of the methods for computation of response of the chosen model can result in the selection of vibrational or wave propagation types of analyses. The wave propagation approach may be advantageous, particularly for impulsive excitations; but this has become obvious and has been used in earthquake engineering only recently (e.g., see Todorovska et al., 1988, 2001a, 2001b; Todorovska and Trifunac, 1989, 1990a, 1990b; Trifunac, 1997, 2000; Trifunac and Todorovska, 1997). The wave propagation method of analysis is essential in the study of soil-structure interaction effects, in the structural models supported by flexible foundations (Hayir et al., 2001; Todorovska and Trifunac, 2001; Todorovska et al., 2001c; Trifunac and Todorovska, 1999b). This method of solution, when combined with a finite element or finite difference formulation, also offers an excellent tool for solution of many problems involving irregular geometry and non-linear material properties.

Computation of the response usually involves direct integration of the differential equations in time domain, if the time-history of the excitation is known *a priori* (Trifunac, 2003). For linear problems which can use the superposition principle, this may be performed in frequency domain also. When there is uncertainty regarding the time-history of the excitation, stochastic methods of response estimation can be used. Though these methods have traditionally centered around the most elementary discrete representation of the structures, in terms of the single-degree-of-freedom (SDOF) or multi-degree-of-freedom (MDOF) systems, those can be extended to the continuum model representation also. The stochastic methods have been particularly helpful for evaluation of the relative significance and additional contributions (i) due to torsion and rocking in strong motion (e.g., see Gupta and Trifunac, 1987a, 1989, 1990d, 1991a, 1993), (ii) due to soil-structure interaction (e.g., see Gupta and Trifunac, 1987a, 1989), and (iii) in the description of relative amplitudes of all peaks of the response (e.g., see Udwadia and Trifunac, 1973a, 1973b; Amini and Trifunac, 1981, 1984; Gupta and Trifunac, 1992, 1998d). These methods have further enabled incorporation of the response into the general framework for characterization of seismic hazard (e.g., see Todorovska et al., 1995).

2. Response Spectrum-Based Techniques

As stated above, estimating the peak response of a linear structural system with known dynamic characteristics to a given description of the ground motion forms an important part of its overall seismic safety assessment. The ground motion can be described in form of a set of smooth, expected response spectra for various damping ratios. These spectra are obtained after the statistical processing of accelerograms pertaining to similar earthquake parameters and recorded in similar site conditions. Since a given response spectrum may be consistent with many ground acceleration time-histories, the computed structural response for the given spectrum is not unique. Thus, any response analysis should account for this inherent uncertainty, while being able to use some or all of the response spectrum ordinates.

Though various consistent time-histories may look different in detail, those cannot be distinguished from each other as regards their overall statistical properties. However, it is possible to completely describe a random process like this in a compact manner by a power spectral density function (PSDF). One may then estimate statistical variations in the largest structural response by working with the PSDF of the ground motion process and by using the stationary theory of random vibrations. Since ground motion processes are highly non-stationary, such a (time-independent) PSDF, even though it can be viewed as a 'temporally averaged' PSDF, fails to estimate peak parameters of the process correctly. Further, when such PSDF is used along with time-independent transfer functions of structural responses, the non-stationarity caused by sudden application of the excitation is not accounted for. This may lead to additional response errors, unless the system is very stiff and/or highly damped. It is possible to provide corrections for these errors by directly using the response spectrum ordinates in case of MDOF systems (e.g., see Amini and Trifunac, 1985; Gupta and Trifunac, 1987c), or by using a fictitious PSDF corresponding to an 'equivalent stationary' ground motion process (e.g., see Singh and Chu, 1976; Der Kiureghian, 1981; Shrikhande and Gupta, 1997a; Gupta and Trifunac, 1998a). In the former, simplifications lead to the development of modal combination rules (e.g., see Rosenblueth and Elorduy, 1969; Wilson et al., 1981; Singh and Mehta, 1983; Der Kiureghian and Nakamura, 1993; Gupta, 1996a), wherein the response spectra are used to predict the largest peak response for each mode of the structure, and then these individual modal maxima are combined to give the expected peak response. These simple methods however do not address the inherent uncertainty in the ground motion due to random phasing. They can also not be applied with consistent accuracy to different types of structural systems. In the case of 'fictitious' PSDF, one may either have compatibility with peak ground acceleration (PGA) or with a set of response spectrum ordinates. In case of compatibility with PGA, however, it is necessary to use the transient transfer functions to account for the non-stationarity caused by sudden application of the excitation.

Uncertainty due to random phasing may also be considered by modelling the nonstationarity in ground motions more explicitly and by using the transient transfer functions to describe the time-dependent harmonic response to a suddenly applied harmonic excitation. In most of the methods in this category, the ground motions are modeled as the envelope function modulated stationary processes. Formulations based on such a modelling (e.g., see Gasparini, 1979; To, 1982; Bucher, 1988; Borino et al., 1988; Sun and Kareem, 1989) are however complicated for practical design applications, and those have also been devoid of a framework to characterize the perceived seismic hazard at a site through the parameters of proposed models. On the other hand, the wavelet-based methods in this category (e.g., see

Basu and Gupta, 1997) can account for frequency non-stationarity (associated with arrival of different types of seismic waves at different times and the dispersion in these waves), besides using the efficient characterization of seismic hazard via spectrum-compatible wavelet functionals (see Mukherjee and Gupta, 2002).

This paper provides an overview of various PSDF-based and wavelet-based methods available for estimating peak structural response of linear MDOF systems in case of response spectrum-based characterization of seismic hazard. For facilitating a convenient comparison in case of PSDF-based methods, the problem is first formulated for the response of a symmetric shear building, and then various available formulations are analyzed. Possible directions are also identified for further research work. It is hoped that together with Gupta and Trifunac (1996), this review will also provide the reader a comprehensive general summary of methods available for estimation of maximum stochastic response by using response spectrum.

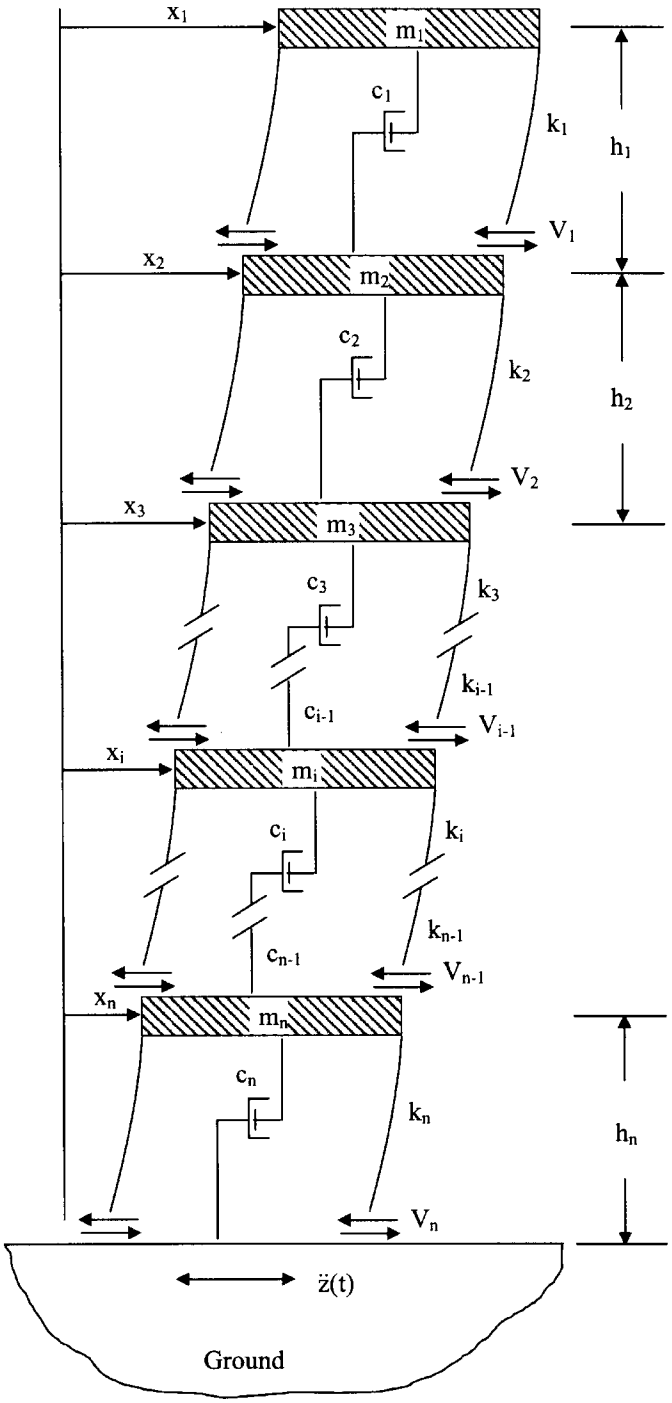

Fig. 1 Shear building model for *n*-storied building

FORMULATION OF PSDF-BASED METHODS

Consider a symmetric shear building, shown in Figure 1, where the lumped floor masses m_i, $i=1,2,...n$ are interconnected through massless column springs of stiffnesses k_i, $i=1,2,...n$, and the viscous dampers representing the interstory damping of magnitude c_i, $i=1,2,...n$. The n-coupled equations of motion for this system can be written as

$$[m]\{\ddot{x}\}+[c]\{\dot{x}\}+[k]\{x\}=-\ddot{z}[m]\{\Gamma\} \tag{1}$$

where $[m]$, $[c]$ and $[k]$ respectively are the $n\times n$ mass, damping and stiffness matrices in terms of m_i, c_i and k_i, $i=1,2,...n$; $\{\Gamma\}$ is the $n\times 1$ ground displacement influence vector; $\{x\}$ is the $n\times 1$ vector comprising of relative displacements $x_i(t)$, $i=1,2,...n$ of the floor masses; and, $\{\dot{x}\}\left(=\frac{d}{dt}\{x\}\right)$, $\{\ddot{x}\}\left(=\frac{d^2}{dt^2}\{x\}\right)$ are the time derivatives of $\{x\}$. Viscous damping, $[c]$ is assumed to be of such a form that it can be diagonalized by the transformation $[A]^T[c][A]$ where $[A]$ $(=[\{\phi^{(1)}\}\{\phi^{(2)}\}....\{\phi^{(n)}\}])$ is the $n\times n$ modal matrix of eigenvectors $\{\phi^{(j)}\}$, $j=1,2,..n$ obtained by solving the eigenvalue problem $\omega^2[m]\{\phi\}=[k]\{\phi\}$. The jth element of this diagonal form is denoted as $2\zeta_j\omega_j M_j$, where ω_j and ζ_j respectively are the eigenvalue and damping ratio corresponding to the eigenvector $\{\phi^{(j)}\}$, and $M_j=\{\phi^{(j)}\}^T[m]\{\phi^{(j)}\}$ is the jth modal mass. Premultiplying Equation (1) by $[A]^T$ and making normal mode decomposition of relative displacement by the transformation, $\{x(t)\}=[A]\{\xi(t)\}$, it follows that

$$[A]^T[m][A]\{\ddot{\xi}\}+[A]^T[c][A]\{\dot{\xi}\}+[A]^T[k][A]\{\xi\}=-\ddot{z}[A]^T[m]\{I\} \tag{2}$$

where $\{\xi(t)\}$ is the $n\times 1$ vector of normal coordinates. Since, $\{\phi^{(j)}\}^T[k]\{\phi^{(j)}\}=M_j\omega_j^2$, and the eigenvectors $\{\phi^{(j)}\}$, $j=1,2,...n$ are mutually orthogonal with respect to the matrices $[m]$ and $[k]$, following n decoupled equations can be obtained from Equation (2), each describing the motion in a specific mode,

$$\ddot{\xi}_j+2\zeta_j\omega_j\dot{\xi}_j+\omega_j^2\xi_j=-\alpha_j\ddot{z};\qquad j=1,2,...,n \tag{3}$$

where, $\alpha_j=\{\phi^{(j)}\}^T[m]\{\Gamma\}/M_j$ is the modal participation factor in the jth mode. Fourier transformation of Equation (3) into the frequency domain leads to

$$-\omega^2\Xi_j(\omega)+2\zeta_j\omega_j\Xi_j(\omega)i+\omega_j^2\Xi_j(\omega)=-\alpha_j Z(\omega) \tag{4}$$

where $i=\sqrt{-1}$, $\Xi_j(\omega)=\mathcal{F}(\xi_j(t))$ and $Z(\omega)=\mathcal{F}(\ddot{z}(t))$, the operator, $\mathcal{F}$ representing the Fourier transformation of time-dependent variable into its frequency domain counterpart. Solving for $\Xi_j(\omega)$ from Equation (4) and using the relation $\{x(t)\}=[A]\{\xi(t)\}$ in the frequency domain, i.e. $\{X(\omega)\}=[A]\{\Xi(\omega)\}$ where $\{X(\omega)\}=\mathcal{F}(\{x(t)\})$, the relative displacement of the ith floor, $X_i(\omega)$, can be expressed as

$$\begin{aligned}X_i(\omega)&=\sum_{j=1}^{n}A_{ij}\alpha_j H_j(\omega)Z(\omega)\\&=\sum_{j=1}^{n}\phi_i^{(j)}\alpha_j H_j(\omega)Z(\omega)\end{aligned} \tag{5}$$

where

$$H_j(\omega) = \frac{1}{\omega_j^2 - \omega^2 + 2i\zeta_j\omega_j\omega} \tag{6}$$

is the transfer function relating the relative displacement of the equivalent SDOF oscillator in the jth mode to the input base excitation, and $\phi_i^{(j)}$ is the ith element of the jth mode shape vector, $\{\phi^{(j)}\}$. Thus, on assuming stationarity in the excitation and the response, the PSDF, $S_{x_i}(\omega)$, of displacement of the ith floor, may be expressed as

$$S_{x_i}(\omega) = S_{\ddot{z}}(\omega)\sum_{j=1}^{n}[(\phi_i^{(j)})^2\alpha_j^2 \mid H_j(\omega)\mid^2 + \sum_{k=1,k\neq j}^{n}\phi_i^{(j)}\phi_i^{(k)}\alpha_j\alpha_k \mathrm{Re}(H_j(\omega)H_k^*(\omega))] \tag{7}$$

where, $S_{\ddot{z}}(\omega)$ is the PSDF of the input base excitation, $\ddot{z}(t)$. The double summation term in the above equation can be seen to represent the effects of interaction of the jth mode with the other $n-1$ modes of vibration. This can be further simplified by using the partial fractions for $\mathrm{Re}(H_j(\omega)H_k^*(\omega))$ (as in Gupta and Trifunac, 1990b) as

$$S_{x_i}(\omega) = S_{\ddot{z}}(\omega)\sum_{j=1}^{n}\mid H_j(\omega)\mid^2 [(\phi_i^{(j)})^2\alpha_j^2 + \sum_{k=1,k\neq j}^{n}\phi_i^{(j)}\phi_i^{(k)}\alpha_j\alpha_k\{C_{jk} + (1-\frac{\omega^2}{\omega_j^2})D_{jk}\}], \tag{8}$$

where, C_{jk} and D_{jk} are the coefficients given in terms of ζ_j, ζ_k and $\varrho = \omega_k/\omega_j$ as

$$C_{jk} = \frac{1}{B_{jk}}\Big[8\zeta_j(\zeta_j + \zeta_k\varrho)\{(1-\varrho^2)^2 - 4\varrho(\zeta_j - \zeta_k\varrho)(\zeta_k - \zeta_j\varrho)\}\Big] \tag{9}$$

$$D_{jk} = \frac{1}{B_{jk}}\Big[2(1-\varrho^2)\{4\varrho(\zeta_j - \zeta_k\varrho)(\zeta_k - \zeta_j\varrho) - (1-\varrho^2)^2\}\Big] \tag{10}$$

and

$$B_{jk} = 8\varrho^2\Big[(\zeta_j^2 + \zeta_k^2)(1-\varrho^2)^2 - 2(\zeta_k^2 - \zeta_j^2\varrho^2)(\zeta_j^2 - \zeta_k^2\varrho^2)\Big] + (1-\varrho^2)^4 \tag{11}$$

Generalizing Equation (8) for any response, $r(t)$ of a linear system, such that $r(t) = \sum_{j=1}^{n}\rho_j\xi_j(t)$, one can write

$$S_r(\omega) = S_{\ddot{z}}(\omega)\sum_{j=1}^{n}[\{\rho_j^2\alpha_j^2 + \sum_{k=1,k\neq j}^{n}\rho_j\rho_k\alpha_j\alpha_k(C_{jk} + D_{jk})\}\mid H_j(\omega)\mid^2 - \frac{\mid \omega H_j(\omega)\mid^2}{\omega_j^2}\sum_{k=1,k\neq j}^{n}\rho_j\rho_k\alpha_j\alpha_k D_{jk}] \tag{12}$$

as the spectral density function of $r(t)$. Here, ρ_j is the normalized amplitude of response, $r(t)$, in the jth mode of vibration, and is expressed as a linear combination of the elements of the jth mode shape, $\{\phi^{(j)}\}$. For example, it is equal to $\phi_i^{(j)}$ for the displacement response, and to $\sum_{l=1}^{i} m_l\omega_j^2\phi_l^{(j)}$ for the shear response at the ith floor level.

Taking moments of $S_r(\omega)$ about the origin leads to

$$\lambda_p = \int_0^\infty \omega^p S_r(\omega)\,\mathrm{d}\omega = \sum_{j=1}^{n}[\{\rho_j^2\alpha_j^2 + \sum_{k=1,k\neq j}^{n}\rho_j\rho_k\alpha_j\alpha_k(C_{jk} + D_{jk})\}\lambda_{p,j}^D - \frac{\lambda_{p,j}^V}{\omega_j^2}\sum_{k=1,k\neq j}^{n}\rho_j\rho_k\alpha_j\alpha_k D_{jk}], \quad p = 0, 1, 2,... \tag{13}$$

where

$$\lambda_{p,j}^{D} = \int_0^\infty S_{\ddot{z}}(\omega)\left|H_j(\omega)\right|^2 \omega^p \, d\omega, \quad p = 0,1,2,...$$

is the pth moment of the PSDF of displacement response of a SDOF oscillator with ω_j frequency and ζ_j damping ratio and subjected to the base acceleration, $\ddot{z}(t)$, and

$$\lambda_{p,j}^{V} = \lambda_{p+2,j}^{D} = \int_0^\infty S_{\ddot{z}}(\omega)\left|\omega H_j(\omega)\right|^2 \omega^p \, d\omega, \quad p = 0,1,2,...$$

is the pth moment of the PSDF for relative velocity response of this oscillator. Equation (13) can alternatively be put in the following form,

$$\lambda_p = \sum_{j=1}^{n} \rho_j^2 \alpha_j^2 \lambda_{p,j}^{D} (1 + \delta_{p,j}), \quad p = 0,1,2,... \tag{14}$$

where,

$$\delta_{p,j} = \sum_{k=1,k\neq j}^{n} \frac{\rho_k \alpha_k}{\rho_j \alpha_j} (C_{jk} + D_{jk}\gamma_{p,j}) \tag{15}$$

is the correction term accounting for the cross-correlation of the jth mode with the remaining $n-1$ modes. $\gamma_{p,j}$ is the multiplying factor for D_{jk}

$$\gamma_{p,j} = 1 - \frac{\lambda_{p,j}^{V}}{\omega_j^2 \lambda_{p,j}^{D}}. \tag{16}$$

For p = 0, this factor is a measure of the deviation of the rate of zero crossings of the displacement response of the SDOF system from what it would have been, had this system been subjected to an ideal white noise. For most excitation processes, this continuously decreases with the increasing natural period of the oscillator, remaining negative when the SDOF system is more flexible compared to the excitation process, and positive when the SDOF system is stiffer. It becomes zero near the dominant frequency of the ground motion. It may be noteworthy that the terms, 'C_{jk}' and '$D_{jk}\gamma_{p,j}$', in the expression for $\delta_{p,j}$ contribute to different types of cross-correlation. While 'C_{jk}' is important in case of closer spacing of jth and kth modes, '$D_{jk}\gamma_{p,j}$', becomes important when ω_j is not close to the dominant frequency of the ground motion. In case of the excitation being like a white noise over the frequencies of interest, the second term may be ignored without introducing significant error in $\delta_{p,j}$.

By calculating the required moments from Equation (13) or (14) for p = 0, 2 and 4, and then by multiplying the root-mean-square (r.m.s.) value with the stationary peak factor, the peak amplitude of the response, $r(t)$, of desired order and level of confidence can be determined (see Appendix A). The response process is however non-stationary, partly because the excitation process is non-stationary and partly because the excitation suddenly starts at zero time with finite operating time. This may significantly affect all three moments, λ_0, λ_2 and λ_4, and since the calculation of the r.m.s. value, r_{rms}, of $r(t)$ depends only on λ_0, r_{rms} needs to be corrected for nonstationarity by multiplication with a 'non-stationarity factor'. However, it may not be necessary to revise the peak factors, because the input parameters depend on the ratios of these moments, and it may be reasonable to assume that all the three moments are affected by nonstationarity to the same extent.

For better understanding, one can express r_{rms} as a SRSS combination of its contributions from different modes,

$$r_{\text{rms}}^2 = \sum_{j=1}^{n} r_{j,\text{rms}}^2 \tag{17}$$

where,

$$r_{j,\mathrm{rms}} = \rho_j \alpha_j \sqrt{\lambda_{0,j}^{D}(1+\delta_{0,j})} \tag{18}$$

is the r.m.s. value of $r(t)$, if the contribution of the jth mode only is considered. It may be noted that the term, $\sqrt{\lambda_{0,j}^{D}}$, represents the r.m.s. value of relative displacement response of the equivalent SDOF oscillator corresponding to the jth mode. This may alternatively be represented as $\mathrm{SD}_j \big/ \beta_j \eta_j^{(1)}$, where SD_j is the spectral displacement corresponding to the natural frequency ω_j and the damping ratio ζ_j, β_j is the 'non-stationarity factor' by which the r.m.s. value in the jth mode is modified, and $\eta_j^{(1)}$ is the (stationary) peak factor for the largest peak displacement response of the jth mode oscillator. This may be obtained from the knowledge of the moments in the jth mode and by using the expressions given in Appendix A. Then, one can modify the r.m.s. value to $\overline{r}_{\mathrm{rms}}$ by multiplying it with a factor, β. Thus, the ith peak value of $r(t)$ response, i.e. $\overline{r}_{\mathrm{peak}}^{(i)}$, is given by

$$\begin{aligned} \overline{r}_{\mathrm{peak}}^{(i)^2} &= \eta^{(i)^2} \overline{r}_{\mathrm{rms}}^2 \\ &= \beta^2 \eta^{(i)^2} r_{\mathrm{rms}}^2 \\ &= \sum_{j=1}^{n} \frac{\beta^2}{\beta_j^2} \frac{\eta^{(i)^2}}{\eta_j^{(1)^2}} \rho_j^2 \alpha_j^2 \mathrm{SD}_j^2 \left(1+\delta_{0,j}\right) \end{aligned} \tag{19}$$

where, $\eta^{(i)}$ is the (stationary) peak factor corresponding to the ith ordered peak of response, $r(t)$. Let $\overline{r}_{j,\max} = \rho_j \alpha_j \mathrm{SD}_j$ represent the maximum value of the response $r(t)$ in the jth mode, as obtained from the response spectrum curve. Then, $\overline{r}_{\mathrm{peak}}^{(i)}$ may be expressed as

$$\overline{r}_{\mathrm{peak}}^{(i)^2} = \sum_{j=1}^{n} \frac{\beta^2}{\beta_j^2} \frac{\eta^{(i)^2}}{\eta_j^{(1)^2}} \overline{r}_{j,\max}^2 \left(1+\delta_{0,j}\right) \tag{20}$$

Alternatively,

$$\overline{r}_{\mathrm{peak}}^{(i)^2} = \sum_{j=1}^{n} \overline{r}_{j,\mathrm{peak}}^{(i)^2} \tag{21}$$

becomes the familiar SRSS form for the peak response, with

$$\overline{r}_{j,\mathrm{peak}}^{(i)} = \frac{\beta}{\beta_j} \frac{\eta^{(i)}}{\eta_j^{(1)}} \overline{r}_{j,\max} \left(1+\delta_{0,j}\right)^{\frac{1}{2}} \tag{22}$$

representing the contribution of the jth mode to the ith peak response.

DISCUSSION OF PSDF-BASED METHODS

The above PSDF-based formulation for the ith peak response, in essence, has formed the basis of most response spectrum-based probabilistic approaches presented over the last two decades. There are three broad categories of these approaches.

1. Category I Methods

In this category, $S_{\ddot{z}}(\omega)$ is obtained from the Fourier transform $Z(\omega)$ of $\ddot{z}(t)$ by calculating the temporal PSDF, for several samples, with the knowledge of the ground motion duration, and then by averaging over the temporal PSDFs for these samples. Here, the ground motion duration, T_s, is taken as

the average length of the stationary segment of the sample time histories of excitation process. Thus, $S_{\ddot{z}}(\omega)$ may be expressed as

$$S_{\ddot{z}}(\omega) = \frac{E\left[\left|Z(\omega)\right|^2\right]}{\pi T_s} \tag{23}$$

where, $E[.]$ represents the expectation operator. Due to this idealization of input PSDF, the 'non-stationarity factors' account for both types of non-stationarity: (i) inherent non-stationarity in the excitation process, and (ii) that acquired by sudden application of the excitation process.

Amini and Trifunac (1985) assumed the cross-correlation between various modes to be negligible (i.e., $\delta_{0,j} = 0$), as in the case of the SRSS method (Goodman et al., 1953), and β_j to be same as β for all modes. This resulted in the following contribution of the jth mode,

$$\overline{r}_{j,\text{peak}}^{(i)} = \frac{\eta^{(i)}}{\eta_j^{(1)}} \overline{r}_{j,\max} \tag{24}$$

This formulation overestimates the higher order peak responses (for $i \geq 2$), and therefore, Gupta and Trifunac (1987c) proposed an improved estimation of $\eta^{(i)}$, using the concept of order statistics. They also proposed to include the effects of modal correlation in the calculation of $\eta^{(i)}$ and $\eta_j^{(i)}$, while assuming $\gamma_{p,j}$ to be zero. The formulation of Gupta and Trifunac (1987c) for negligible modal cross-correlation has been extended further as follows. Gupta and Trifunac (1987d) extended this to find the resultant response caused by the simultaneous excitation of all three translational components of ground motion. Gupta and Trifunac (1987b) obtained the response of simple symmetric buildings to torsional component of ground motion, and Gupta and Trifunac (1988a) obtained the response to simultaneous action of translational and rocking components of ground motion, while assuming those to be in phase. Gupta and Trifunac (1990a) extended the formulation of Gupta and Trifunac (1988a) to include the effects of relative deformations of foundation with respect to the surrounding soil, while assuming those to be in phase with the excitations, in case of significant soil-structure interaction effects.

Gupta and Trifunac (1990b) included the modal cross-correlation completely, while assuming the factor, β, to be same as in the case of negligible cross-correlation, i.e. by taking

$$\beta = \left[\frac{\sum_{j=1}^{n} (\overline{r}_{j,\max}/\eta_j^{(1)})^2}{\sum_{j=1}^{n} (\overline{r}_{j,\max}/\beta_j \eta_j^{(1)})^2} \right]^{1/2} \tag{25}$$

in Equation (22). They extended this approach to apply in case of simultaneous excitation of translational and rocking components of ground motion, with the two components assumed to be at a constant phase difference. Gupta and Trifunac (1990c) extended this to apply in case of simultaneous action of (i) translational and torsional, and (ii) translational, rocking and torsional components of ground motion for simple symmetric buildings, when constant phase differences may be assumed between the translational and rotational components. Gupta and Trifunac (1991b) extended the formulation of Gupta and Trifunac (1990b) to include the effects of dynamic soil-structure interaction (i) by modifying the Fourier spectra of and phase difference between the two components, and (ii) by estimating β from 'non-stationarity factors' associated with the fixed-base building response and soil rocking response to the translational component of motion.

It is implicitly assumed in Equation (25) that the extent to which non-stationarity affects the response in any mode is not influenced by the extent to which other modes correlate with this mode, and that this extent is same for all modes. The degree of non-stationarity may however be significantly different in various modal responses due to the different modal frequencies and damping ratios, unless the excitation process is very long, with a higher mode associated with reduced effect of non-stationarity. In view of this, Agarwal and Gupta (1995) used the assumption of $\beta_j = \beta$, as in Equation (24), for determining more accurate lateral-torsional response of torsionally coupled buildings. For simplicity, they assumed the response process in each mode to be truly narrow-banded, and thus considered $\gamma_{0,j}$ to be zero for all

modes (as in the case of the CQC method (Wilson et al., 1981)). This resulted in the following contribution of the jth mode,

$$\bar{r}_{j,\text{peak}}^{(i)} = \frac{\eta^{(i)}}{\eta_j^{(1)}} \bar{r}_{j,\max} \left(1 + \sum_{k=1,k\neq j}^{n} \frac{\rho_k \alpha_k}{\rho_j \alpha_j} C_{jk} \right)^{\frac{1}{2}} \tag{26}$$

The formulation of Agarwal and Gupta (1995) is thus expected to work better when the modal cross-correlation is primarily due to the closeness of interacting modes. By including $\gamma_{0,j}$ in Equation (26), this formulation can be generalized to other situations also.

It may be observed that the crucial element of the Category I methods is how β is estimated. β depends on the values of β_j, where β_j is expected to increase with the value of j. It may thus be expected that β lies somewhere in between β_1 and β_n, with a value closer to β_1, due to the dominance of lower modes in the total response. Further studies are however needed to explore whether a weighted sum of various β_j's or some other alternative will lead to further improvement in the approach of Agarwal and Gupta (1995). It is also noted that the methods in this category require the specification of Fourier spectrum along with the response spectra, which makes those unattractive without any obvious advantages in comparison to other PSDF-based methods.

2. Category II Methods

In the second category, the input PSDF is obtained in the same way as in the case of the first category of methods, but the 'non-stationarity factors' account only for the inherent non-stationarity in the ground motion process. The acquired non-stationarity in the response process is decoupled from the inherent non-stationarity, and is accounted for by the use of transient transfer function (instead of steady-state transfer function, as in Equation (6)). These methods require only the response spectrum ordinate at zero-period, i.e. PGA. On the other hand, those require more computationally-intensive non-stationary peak factors for the evolutionary processes, instead of the stationary peak factors applicable for stationary processes (see Appendix A for details).

Shrikhande and Gupta (1997a) proposed to replace the given non-stationary ground acceleration process by an equivalent stationary process. The PSDF of this equivalent process is obtained by scaling-up the PSDF described by Equation (23), so as to correspond to a specified value of PGA. They also proposed to use the transient transfer function, $\tilde{H}_j(\omega,t)$, in place of the steady-state transfer function, $H_j(\omega)$, in Equation (7). In view of this, the (evolutionary) spectral density of $r(t)$ becomes

$$S_r(\omega,t) = S_{\ddot{z}}(\omega) \sum_{j=1}^{n} [\rho_j^2 \alpha_j^2 \,|\, \tilde{H}_j(\omega,t)\,|^2 + \sum_{k=1,k\neq j}^{n} \rho_j \rho_k \alpha_j \alpha_k \text{Re}(\tilde{H}_j(\omega,t) \tilde{H}_k^*(\omega,t))] \tag{27}$$

To estimate the ordered peak response from $S_r(\omega,t)$, the order statistics approach of peak factors for stationary processes has been proposed to be extended to evolutionary processes in a simple, approximate, but computationally more intensive manner. Later, Shrikhande and Gupta (1999) have used this approach in formulating the seismic response of suspension bridges in case of significant soil-structure interaction and spatially varying ground motions.

The formulation of Shrikhande and Gupta (1997a) considered the use of a simpler form of $\tilde{H}_j(\omega,t)$ through the use of time-dependent damping ratio, $\zeta_j(t) = \zeta_j/[1-e^{-2\omega_j\zeta_j t}]$, in place of ζ_j. Gupta and Trifunac (2000) have identified situations where such a simplification may lead to large errors in response estimation, and thus, it is preferable to use the following exact form of $\tilde{H}_j(\omega,t)$ for more accurate results in all situations:

$$\tilde{H}_j(\omega,t) = H_j(\omega) \left[e^{-i\omega t} - e^{-\zeta_j \omega_j t} \left\{ \cos\omega_j t \sqrt{1-\zeta_j^2} + \frac{\zeta_j \omega_j - i\omega}{\omega_j \sqrt{1-\zeta_j^2}} \sin\omega_j t \sqrt{1-\zeta_j^2} \right\} \right] \tag{28}$$

Further, it will be useful to consider a more realistic energy distribution of the 'equivalent stationary' ground motion (as against the 'time-averaged' energy distribution), perhaps that based on the (truncated) Fourier transform of the stationary phase only (Udwadia and Trifunac, 1974b). It is obvious that if the PSDF of the 'equivalent stationary' motion does not correctly describe the instantaneous PSDF of the excitation in the neighbourhood of the instant when maximum response peak occurs, the resulting inaccuracy in the peak estimation may be substantial. This condition is usually difficult to satisfy, and therefore, the Category II methods are useful only when the non-stationarity due to finite operating time dominates over the inherent non-stationarity. This may happen when either the structural system is very flexible or the ground motion has a long stationary phase.

3. Category III Methods

In the third category of PSDF-based methods, PSDF of the ground excitation is taken to be spectrum-compatible PSDF, i.e. the PSDF that is compatible with the given response spectrum (see, for example, Kaul, 1978; Unruh and Kana, 1981; Christian, 1989; Gupta and Trifunac, 1998b). Alternatively, as shown by Gupta and Trifunac (1998b), strong motion duration in Equation (23) is taken to be frequency-dependent. Since a spectrum-compatible PSDF incorporates all effects of inherent and response non-stationarities for the responses of a set of SDOF oscillators of certain damping ratio, these methods do not require the use of 'non-stationarity factors'. Thus, contribution of the jth mode to the ith peak response becomes

$$\overline{r}_{j,\text{peak}}^{(i)} = \rho_j \alpha_j \eta^{(i)} \sqrt{\lambda_{0,j}^{D}(1+\delta_{0,j})} \tag{29}$$

Singh and Chu (1976) proposed the estimation of the largest peak only (i = 1), and used this approach for generating floor response spectra of a building. Der Kiureghian (1981) also proposed the estimation of largest peak only, but without requiring to calculate $S_{\ddot{z}}(\omega)$ from the given response spectrum. Instead, various moments involving $S_{\ddot{z}}(\omega)$ were directly expressed in form of response spectrum ordinates to calculate $\eta^{(1)}$ and $\lambda_{0,j}^{D}$. Further, $\gamma_{0,j}$ was taken as zero for all modes, thus including the cross-correlation only due to the closeness of interacting modes.

Gupta (1996b, 1997) used the spectrum-compatible PSDF-based approach for generating the floor response spectra. Dey and Gupta (1998, 1999), and Ray Chaudhuri and Gupta (2002a, 2002b) used this approach for calculating the seismic response of multiply-supported secondary systems. Gupta and Trifunac (1998a) proposed the use of the transient transfer function at $t = T$, i.e. $\tilde{H}_j(\omega, T)$, where T is the total duration of the excitation, in place of the steady-state transfer function, i.e. $H_j(\omega)$ ($\equiv \tilde{H}_j(\omega, \infty)$). This is due to the fact that the spectrum-compatible PSDF, they propose to use in their formulation, is obtained by using the transient transfer function at $t = T$ (Gupta and Trifunac, 1998b). If the spectrum-compatible PSDF is obtained by using the steady-state transfer function, as is the case with most other formulations, it becomes necessary to use the steady-state form for the modal transfer functions also (with no change in the assumed value of total duration). Using the spectrum-compatible PSDF of Gupta and Trifunac (1998b), Gupta and Trifunac (1999) have also proposed to estimate seismic response of non-classically damped MDOF systems.

Even though the Category III methods are simpler to use and are quite accurate, as regards the largest peak response, those require *a priori* the iterative computation of spectrum-compatible PSDF, corresponding to a particular response spectrum curve. Since the response spectrum curves for other damping ratios are not used in this process, the so-obtained PSDF is usually not compatible with the entire set of response spectrum curves. One may perhaps use the envelope PSDF (as used by Dey and Gupta, 1998) for conservative response estimates. One may also obtain PSDFs for spectra of different damping ratios through the use of transient transfer functions, and since these PSDFs differ little from each other, one may find an 'average' PSDF (see Shrikhande and Gupta, 1996). Such a PSDF will be useful in case of Category II methods, because of the need to use transient modal transfer functions in response calculations.

WAVELET-BASED METHODS

Wavelet-based methods using the response spectrum-based characterization of seismic hazard involve the calculation of spectrum-compatible wavelet functionals (as described in Mukherjee and Gupta, 2002), just as spectrum-compatible PSDF is calculated in the case of Category III PSDF-based methods. The difference here is that these functionals are made more realistic through an additional input of desired structure of non-stationarity (depending on the existing conditions of earthquake source mechanism, wave propagation, and local site effects) in form of the wavelet coefficients of a recorded accelerogram. Once the ground motion process is characterized in form of the statistical functionals of wavelet coefficients, instantaneous PSDF of the response process is obtained in terms of system properties and input functionals, and the ordered peak response is estimated as in the case of the Category II PSDF-based methods.

Let the ground acceleration process be assumed to be zero mean, locally Gaussian, and be characterized through the (spectrum-compatible) statistical functionals (Mukherjee and Gupta, 2000), $E[W_\psi^2 \ddot{z}(a_p, b_q)]$, where

$$W_\psi \ddot{z}(a_p, b_q) = \int_{-\infty}^{\infty} \ddot{z}(t) \psi_{a_p, b_q}(t) \mathrm{d}t \tag{30}$$

denotes the wavelet coefficient of $\ddot{z}(t)$ at scale parameter, a_p, and translation parameter, b_q, and

$$\psi_{a_p, b_q}(t) = \frac{1}{\sqrt{a_p}} \psi\left(\frac{t - b_q}{a_p}\right) \tag{31}$$

is the dilated and translated form of the mother wavelet, $\psi(t)$. As suggested by Basu and Gupta (1998), let $a_p = \sigma^p$ with $\sigma = 2^{1/4}$, $b_q = (q-1)\Delta b$ (Δb being the digitization interval), and

$$\psi(t) = \frac{1}{\pi\sqrt{(\sigma - 1)}} \frac{\sin \sigma\pi t - \sin \pi t}{t} \tag{32}$$

with Fourier transform

$$\begin{aligned} \hat{\psi}(\omega) &= \frac{1}{\sqrt{2(\sigma - 1)\pi}}, \quad \pi \le |\omega| \le \sigma\pi \\ &= 0 \qquad\qquad \text{otherwise} \end{aligned} \tag{33}$$

The instantaneous PSDF in this case may be expressed as (Basu and Gupta, 1997)

$$\begin{aligned} S_r(\omega, t)|_{t=b_q} = \sum_p \frac{K}{a_p} E[W_\psi^2 \ddot{z}(a_p, b_q)] \sum_{j=1}^{n} \Bigg[&\{\rho_j^2 \alpha_j^2 + \sum_{k=1, k\neq j}^{n} \rho_j \rho_k \alpha_j \alpha_k (C_{jk} + D_{jk})\} |H_j(\omega)|^2 \\ &- \frac{|\omega H_j(\omega)|^2}{\omega_j^2} \sum_{k=1, k\neq j}^{n} \rho_j \rho_k \alpha_j \alpha_k D_{jk} \Bigg] |\hat{\psi}_{a_p, b_q}(\omega)|^2 \end{aligned} \tag{34}$$

where,

$$K = \frac{1}{4\pi C_\psi} \left(\sigma - \frac{1}{\sigma}\right) \tag{35}$$

and

$$C_\psi = \int_{-\infty}^{\infty} \frac{|\hat{\psi}(\omega)|^2}{|\omega|} \mathrm{d}\omega \tag{36}$$

Accordingly, the instantaneous value of the sth moment may be obtained as

$$\lambda_s(t)\,|_{t=b_q} = \sum_p \frac{K}{(\sigma-1)\pi} E[W_\psi^2 \ddot{z}(a_p, b_q)] \sum_{j=1}^{n} \rho_j^2 \alpha_j^2 \lambda_{s,j}^{p,D} (1+\delta_{s,j}^{p}), \quad s = 0,1,2,... \tag{37}$$

where,

$$\delta_{s,j}^{p} = \sum_{k=1,k\neq j}^{n} \frac{\rho_k \alpha_k}{\rho_j \alpha_j} \left[C_{jk} + D_{jk} \left(1 - \frac{\lambda_{s,j}^{p,V}}{\omega_j^2 \lambda_{s,j}^{p,D}} \right) \right] \tag{38}$$

is the term accounting for the instantaneous cross-correlation of the jth mode with the remaining $n-1$ modes; and $\lambda_{s,j}^{p,D}$ and $\lambda_{s,j}^{p,V}$ respectively are the sth moments for the displacement and velocity responses of the jth mode oscillator for the pth band of energy (see Basu and Gupta, 1997, for the closed form expressions for these moments). The simplification achieved by ignoring $\delta_{s,j}^{p}$ is more accurate than that achieved by ignoring $\delta_{p,j}$ in Equation (14). In fact, this simplification leads to reasonably accurate results even when the natural frequencies of the structural system are closely spaced (Basu and Gupta, 1997). The wavelet-based approach has been extended to include the effects of soil-structure interaction in case of tanks (Chatterjee and Basu, 2001) and to the use of equivalent linearization in case of non-linear systems (Basu and Gupta, 1999a, 1999b, 2000, 2001).

CONCLUSIONS

It has been seen that there are various response spectrum-based formulations available for the stochastic estimation of the response of a MDOF system, and that each one of those caters to a different type of need. This need is usually dictated by the available input data, and by the balance the user wishes to adopt between the desired levels of accuracy and simplicity. On one hand, there are Category III PSDF-based methods that just require the response spectrum ordinates, while on the other, the Category I PSDF-based methods require specification of Fourier spectrum also, and the wavelet-based methods require the specification of a recorded time-history. Since all PSDF-based methods are based on the concept of a fictitious ground motion process, their utility is limited to finding the first few largest response peaks. For other response statistics, a more detailed description of excitation process is required. In such situations, though being computationally more intensive, the wavelet-based methods can be more useful. There is however a need to further reduce the number of input data points in the specification of the (spectrum-compatible) input process, and to apply wavelet-based approach to different types of structural systems. Also, specification of the input process in case of two or more response spectra (of different damping ratios) needs to be addressed.

To the extent that one may be interested in response peak amplitudes only, the Category III PSDF-based methods appear to be more accurate than the Category I methods (in tackling the effects of non-stationarity) and most convenient, amongst all methods discussed in this paper. Those however suffer from the limitation of being based on the response spectrum of a single value of damping ratio. Except for the idea of envelope PSDF used by some investigators, this problem has not received much attention so far. Further, since the use of transient transfer function may not usually be a computationally viable option, it needs to be seen whether the use of transfer function, $\bar{H}_j(\omega, T)$, is indeed a better option than $H_j(\omega)$, or there should be some other value of t at which the transient transfer function is to be evaluated. When the non-stationarity in response due to the short length of the excitation process is significant, compared to that due to the stationary phase being too short in the excitation process, it may be desirable to consider the transient transfer function. Then, the Category II PSDF-based methods requiring the input of Fourier spectrum and PGA only may be more convenient.

ACKNOWLEDGEMENTS

This paper is dedicated to Professor M.D. Trifunac in recognition of his leadership, invaluable contributions, and commitment to research in earthquake engineering. Among notable contributions, he deserves much of the credit for leading the efforts on simplifying the non-stationary analyses of structural

systems through the use of response spectra and on extending these analyses to estimate amplitudes of second largest and higher order peaks.

APPENDIX A: STATIONARY AND NON-STATIONARY PEAK FACTORS

1. Stationary Peak Factors

Consider a stationary, zero mean, and Gaussian process, $X(t)$, with PSDF $S_X(\omega)$ and duration T. Peak amplitude of desired order and level of confidence in this process may be estimated by computing the root-mean-square (r.m.s.) value as the square-root of the area under $S_X(\omega)$, and by multiplying this with the corresponding peak factor. The peak factor for the ith peak may be determined by using its probability density and cumulative probability functions given by (Gupta and Trifunac, 1988b)

$$p^{(i)}(\eta) = \frac{N!}{(N-i)!(i-1)!}\left[P(\eta)\right]^{i-1}\left[1-P(\eta)\right]^{N-i}p(\eta) \tag{A.1}$$

and

$$P^{(i)}(\eta) = \int_{\eta}^{\infty} p^{(i)}(u)\mathrm{d}u = \sum_{r=i}^{N!} \frac{N!}{(N-r)!r!}\left[P(\eta)\right]^{r}\left[1-P(\eta)\right]^{N-r} \tag{A.2}$$

Whereas the distribution function here can be used iteratively to obtain the peak factor for any desired confidence level, the density function can be used to find the peak factors for the expected and the most probable peak amplitudes. In Equations (A.1) and (A.2), $p(\eta)$ is the probability density function of the (unordered) peaks in $|X(t)|$ given by (Cartwright and Longuet-Higgins, 1956; Gupta, 1994)

$$p(\eta) = \frac{\sqrt{2}}{\sqrt{\pi}\,(1+\sqrt{1-\varepsilon^2})}\left[\varepsilon e^{-\eta^2/2\varepsilon^2} + (1-\varepsilon^2)^{1/2}\eta e^{-\eta^2/2}\int_{-\infty}^{\eta(1-\varepsilon^2)^{1/2}/\varepsilon} e^{-x^2/2}\mathrm{d}x\right];\ \eta \geq 0 \tag{A.3}$$

$P(\eta) = \int_{\eta}^{\infty} p(u)\mathrm{d}u$ is the cumulative probability function of these peaks, and N is the total number of these peaks given by

$$N = \frac{T}{2\pi}(1+\sqrt{1-\varepsilon^2})\left[\frac{\lambda_4}{\lambda_2}\right]^{1/2} \tag{A.4}$$

In Equation (A.3), ε is the band-width parameter of $S_X(\omega)$, and is given by

$$\varepsilon = \left[\frac{\lambda_0\lambda_4 - \lambda_2^2}{\lambda_0\lambda_4}\right]^{1/2} \tag{A.5}$$

where, in general, the nth moment, λ_n of the PSDF is defined by

$$\lambda_n = \int_0^{\infty} \omega^n S_X(\omega)\mathrm{d}\omega \qquad (n = 0,1,2,...) \tag{A.6}$$

For the 'expected' i th order peak amplitude, the peak factor, $\bar{\eta}^{(i)}$, is given by

$$\bar{\eta}^{(i)} = \int_{-\infty}^{\infty} u p^{(i)}(u)\mathrm{d}u \tag{A.7}$$

For an approximate and direct evaluation scheme using the numerical integration, Equation (A.7) may be written alternatively as

$$\bar{\eta}^{(i)} = \int_0^{\infty} P^{(i)}(u)\mathrm{d}u - \int_0^{\infty} \mathrm{d}(uP^{(i)}(u)) \tag{A.8}$$

and thus, $\bar{\eta}^{(i)}$ approximately becomes equal to [area under the $P^{(i)}(\eta)$ curve between η = 0 and $\eta_{\lim}$] minus [$\eta_{\lim}P^{(i)}(\eta)|_{\eta=\eta_{\lim}}$]. Here, $\eta_{\lim}$ is the value of η at which $P^{(i)}(\eta)$ becomes very small. This value may safely be taken as 9.0 for all orders of peaks (Gupta, 1994).

It may be noted that Equations (A.1) and (A.2) are for the N peaks (distributed as in Equation (A.3)) assumed to be statistically independent. As shown by Basu et al. (1996) and Gupta and Trifunac (1998c), this assumption gives reasonably good results for the expected values of first few ordered peaks.

2. Non-stationary Peak Factors

If the process, $X(t)$, is non-stationary with the PSDF, $S_X(\omega,t)$, we can obtain the instantaneous values of moments, band-width parameter, and number of peaks, as

$$\lambda_n(t) = \int_0^\infty \omega^n S_X(\omega,t)\mathrm{d}\omega \qquad (n = 0,1,2,...) \tag{A.9}$$

$$\varepsilon(t) = \left[\frac{\lambda_0(t)\lambda_4(t) - \lambda_2^2(t)}{\lambda_0(t)\lambda_4(t)}\right]^{1/2} \tag{A.10}$$

$$N(t) = \frac{T}{2\pi}\left(1+\sqrt{1-\varepsilon^2(t)}\right)\left[\frac{\lambda_4(t)}{\lambda_2(t)}\right]^{1/2} \tag{A.11}$$

Using these parameters, the ith largest peak value may be expressed, in case of evolutionary response processes, as (Shrikhande and Gupta, 1997a, 1997b)

$$X_{\text{peak}}^{(i)} = \left[\frac{1}{T}\int_0^T (\eta^{(i)}(t))^2\lambda_0(t)\mathrm{d}t\right]^{1/2} \tag{A.12}$$

where, $\eta^{(i)}(t)$ is the peak factor for the ith largest peak value in case of a fictitious stationary process having duration, T, and the band-width parameter and number of peaks respectively as $\varepsilon(t)$ and $N(t)$. $\eta^{(i)}(t)$ is to be evaluated by using Equation (A.1) or (A.2) for the same level of confidence, for which $X_{\text{peak}}^{(i)}$ is desired to be obtained. The integral in Equation (A.12) may be evaluated efficiently by means of any standard quadrature routine.

In a more generalized situation, as proposed by Basu and Gupta (1998), $X_{\text{peak}}^{(i)}$ may be estimated by estimating the largest peak amplitude via the first passage formulation (Vanmarcke, 1975) and by scaling this down to the higher order peak amplitudes via the order statistics formulation (Gupta and Trifunac, 1988b). For the largest peak, we use the expression of the probability that the process, $|X(t)|$, remains below the level, x, during the time interval, $(0,T)$, as

$$P_T(x) = \exp\left[-\int_0^T \alpha(t)\mathrm{d}t\right] \tag{A.13}$$

where

$$\alpha(t) = \frac{\Omega(t)}{\pi}\frac{1-\exp(-\sqrt{\pi/2}\mu^{1.2}(t)\frac{x}{\sigma(t)})}{1-\exp(-x^2/2\sigma^2(t))}e^{-x^2/2\sigma^2(t)} \tag{A.14}$$

with

$$\sigma(t) = \sqrt{\lambda_0(t)} \tag{A.15}$$

$$\Omega(t) = \sqrt{\frac{\lambda_2(t)}{\lambda_0(t)}} \tag{A.16}$$

$$\mu(t) = \sqrt{1 - \frac{\lambda_1^2(t)}{\lambda_0(t)\lambda_2(t)}} \tag{A.17}$$

For the ith largest peak ($i > 1$), we consider an equivalent stationary process which has the duration as

$$T^* = \frac{\int_0^T \Omega(t)\mathrm{d}t}{\Omega(t)|_{t=t_m}} \tag{A.18}$$

and the band-width parameter and number of peaks respectively as $\varepsilon(t)|_{t=t_m}$ and $N(t)|_{t=t_m}$, with t_m denoting the time-instant of occurrence of the largest mean-square response in the process. Corresponding to this process, (stationary) peak factors, $\eta^{(1)}(t)|_{t=t_m}$ and $\eta^{(i)}(t)|_{t=t_m}$, are determined for the largest peak and the ith largest peak respectively, and then, the largest peak amplitude estimated via Equation (A.13) is scaled down in the ratio, $\eta^{(i)}(t)|_{t=t_m} / \eta^{(1)}(t)|_{t=t_m}$.

REFERENCES

1. Agarwal, P. and Gupta, V.K. (1995). "A Stochastic Approach to the Response of Torsionally Coupled Multistoried Buildings", European Earthq. Eng., Vol. IX, No. 2, pp. 44–55.
2. Amini, A. and Trifunac, M.D. (1981). "Distribution of Peaks in Linear Earthquake Response", J. Eng. Mech. Div., Proc. ASCE, Vol. 107, No. EM1, pp. 207-227.
3. Amini, A. and Trifunac, M.D. (1984). "A Statistical Basis for Spectrum Superposition in Response to Earthquake Excitation", Proc. 8th World Conf. Earthq. Eng., San Francisco, California, U.S.A., Vol. IV, pp. 179–186.
4. Amini, A. and Trifunac, M.D. (1985). "Statistical Extension of Response Spectrum Superposition", Soil Dyn. Earthq. Eng., Vol. 4, No. 2, pp. 54–63.
5. Basu, B. and Gupta, V.K. (1997). "Non-stationary Seismic Response of MDOF Systems by Wavelet Transform", Earthq. Eng. Struct. Dyn., Vol. 26, pp. 1243–1258.
6. Basu, B. and Gupta, V.K. (1998). "Seismic Response of SDOF Systems by Wavelet Modelling of Nonstationary Processes", J. Eng. Mech. (ASCE), Vol. 124, No. 10, pp. 1142–1150.
7. Basu, B. and Gupta, V.K. (1999a). "Wavelet-Based Analysis of Non-stationary Response of a Slipping Foundation", J. Sound Vib., Vol. 222, No. 4, pp. 547–563.
8. Basu, B. and Gupta, V.K. (1999b). "On Equivalent Linearization Using Wavelet Transform", J. Vib. Acoust. (ASME), Vol. 121, No. 4, pp. 429–432.
9. Basu, B. and Gupta, V.K. (2000). "Wavelet-Based Non-stationary Response Analysis of a Friction Base-Isolated Structure", Earthq. Eng. Struct. Dyn., Vol. 29, pp. 1659–1676.
10. Basu, B. and Gupta, V.K. (2001). "Wavelet-Based Stochastic Seismic Response of a Duffing Oscillator", J. Sound Vib., Vol. 245, No. 2, pp. 251–260.
11. Basu, B., Gupta, V.K. and Kundu, D. (1996). "Ordered Peak Statistics through Digital Simulation", Earthq. Eng. Struct. Dyn., Vol. 25, pp. 1061–1073.
12. Borino, G., Di Paola, M. and Muscolino, G. (1988). "Non-stationary Spectral Moments of Base Excited MDOF Systems", Earthq. Eng. Struct. Dyn., Vol. 16, pp. 745–756.
13. Bucher, C.G. (1988). "Approximate Nonstationary Random Vibration Analysis for MDOF Systems", J. Appl. Mech. (ASME), Vol. 55, pp. 197–200.
14. Cartwright, D.E. and Longuet-Higgins, M.S. (1956). "The Statistical Distribution of Maxima of a Random Function", Proc. Roy. Soc. London, Vol. A 237, pp. 212–232.
15. Chatterjee, P. and Basu, B. (2001). "Non-stationary Seismic Response of Tanks with Soil Interaction by Wavelets", Earthq. Eng. Struct. Dyn., Vol. 30, pp. 1419–1437.
16. Christian, J.T. (1989). "Generating Seismic Design Power Spectral Density Functions", Earthq. Spectra, Vol. 5, No. 2, pp. 351–367.

17. Der Kiureghian, A. (1981). "A Response Spectrum Method for Random Vibration Analysis of MDF Systems", Earthq. Eng. Struct. Dyn., Vol. 9, pp. 419–435.
18. Der Kiureghian, A. and Nakamura, Y. (1993). "CQC Modal Combination Rule for High-Frequency Modes", Earthq. Eng. Struct. Dyn., Vol. 22, pp. 943–956.
19. Dey, A. and Gupta, V.K. (1998). "Response of Multiply Supported Secondary Systems to Earthquakes in Frequency Domain", Earthq. Eng. Struct. Dyn., Vol. 27, pp. 187–201.
20. Dey, A. and Gupta, V.K. (1999). "Stochastic Seismic Response of Multiply-Supported Secondary Systems in Flexible-Base Structures", Earthq. Eng. Struct. Dyn., Vol. 28, pp. 351–369.
21. Gasparini, D.A. (1979). "Response of MDOF Systems to Nonstationary Random Excitation", J. Eng. Mech. Div., Proc. ASCE, Vol. 105, No. EM1, pp. 13–27.
22. Goodman, L.E., Rosenblueth, E. and Newmark, N.M. (1953). "Aseismic Design of Firmly Founded Elastic Structures", Trans. ASCE, Vol. 120, pp. 782–802.
23. Gupta, V.K. (1994). "Stochastic Approach to Seismic Floor Spectra in Nuclear Power Plants", Report 94–02, Dept. of Civil Eng., I.I.T. Kanpur, Kanpur.
24. Gupta, V.K. (1996a). "A New Modal Combination Rule for the Building Response to Earthquakes", International Seminar Civil Eng. Practices Twentyfirst Century, Roorkee, Vol. III, pp. 1756–1764.
25. Gupta, V.K. (1996b). "A New Stochastic Approach for Seismic Floor Spectra Generation", Symposium Earthq. Effects Structures, Plant and Machinery, New Delhi, Vol. I, Part II-4, pp. 1–12.
26. Gupta, V.K. (1997). "Acceleration Transfer Function of Secondary Systems", J. Eng. Mech. (ASCE), Vol. 123, No. 7, pp. 678–685.
27. Gupta, I.D. and Trifunac, M.D. (1987a). "Statistical Analysis of Response Spectra Method in Earthquake Engineering", Report 87–03, Department of Civil Engineering, University of Southern California, Los Angeles, California, U.S.A.
28. Gupta, I.D. and Trifunac, M.D. (1987b). "A Note on Contribution of Torsional Excitation to Earthquake Response of Simple Symmetric Buildings", Earthq. Eng. Eng. Vib., Vol. 7, No. 3, pp. 27–46.
29. Gupta, I.D. and Trifunac, M.D. (1987c). "Order Statistics of Peaks in Earthquake Response of Multi-Degree-of-Freedom Systems", Earthq. Eng. Eng. Vib., Vol. 7, No. 4, pp. 15–50.
30. Gupta, I.D. and Trifunac, M.D. (1987d). "Order Statistics of Peaks of the Response to Multi-component Seismic Excitation", Bull. Indian Soc. Earthq. Tech., Vol. 24, No. 3–4, pp. 135–159.
31. Gupta, I.D. and Trifunac, M.D. (1988a). "A Note on Computing the Contribution of Rocking Excitation to Earthquake Response of Simple Buildings", Bull. Indian Soc. Earthq. Tech., Vol. 25, No. 2, pp. 73–89.
32. Gupta, I.D. and Trifunac, M.D. (1988b). "Order Statistics of Peaks in Earthquake Response", J. Eng. Mech. (ASCE), Vol. 114, No. 10, pp. 1605–1627.
33. Gupta, V.K. and Trifunac, M.D. (1989). "Investigation of Building Response to Translational and Rotational Earthquake Excitations", Report 89–02, Dept. Civil Eng., Univ. Southern California, Los Angeles, California, U.S.A.
34. Gupta, I.D. and Trifunac, M.D. (1990a). "Probabilistic Spectrum Superposition for Response Analysis Including the Effects of Soil-Structure Interaction", J. Probabilistic Eng. Mech., Vol. 5, pp. 9–18.
35. Gupta, V.K. and Trifunac, M.D. (1990b). "Response of Multistoried Buildings to Ground Translation and Rocking during Earthquakes", J. Probabilistic Eng. Mech., Vol. 5, pp. 138–145.
36. Gupta, V.K. and Trifunac, M.D. (1990c). "Response of Multistoried Buildings to Ground Translation and Torsion during Earthquakes", European Earthq. Eng., Vol. IV, No. 1, pp. 34–42.
37. Gupta, V.K. and Trifunac, M.D. (1990d). "A Note on Contributions of Ground Torsion to Seismic Response of Symmetric Multistoried Buildings", Earthquake Eng. Eng. Vib., Vol. 10, No. 3, pp. 27–40.
38. Gupta, V.K. and Trifunac, M.D. (1991a). "Effects of Ground Rocking on Dynamic Response of Multistoried Buildings during Earthquakes", Struct. Eng./Earthq. Eng. (JSCE), Vol. 8, No. 2, pp. 43–50.

39. Gupta, V.K. and Trifunac, M.D. (1991b). "Seismic Response of Multistoried Buildings Including the Effects of Soil-Structure Interaction", Soil Dyn. Earthq. Eng., Vol. 10, No. 8, pp. 414–422.
40. Gupta, V.K. and Trifunac, M.D. (1992). "Higher Order Peaks in Response of Multistoried Buildings", Proc. Tenth World Conference Earthq. Eng., Madrid, Spain, Vol. 7, pp. 3819–3824.
41. Gupta, V.K. and Trifunac, M.D. (1993). "A Note on the Effects of Ground Rocking in Response of Buildings during 1989 Loma Prieta Earthquake", Earthq. Eng. Eng. Vib., Vol. 13, No. 2, pp. 12–28.
42. Gupta, I.D. and Trifunac, M.D. (1996). "Investigation of Nonstationarity in Stochastic Seismic Response of Structures", Report 96–01, Dept. Civil Eng., Univ. Southern California, Los Angeles, California, U.S.A.
43. Gupta, I.D. and Trifunac, M.D. (1998a). "An Improved Probabilistic Spectrum Superposition", Soil Dyn. Earthq. Eng., Vol. 17, pp. 1–11.
44. Gupta, I.D. and Trifunac, M.D. (1998b). "Defining Equivalent Stationary PSDF to Account for Nonstationarity of Earthquake Ground Motion", Soil Dyn. Earthq. Eng., Vol. 17, pp. 89–99.
45. Gupta, I.D. and Trifunac, M.D. (1998c). "A Note on the Statistics of Ordered Peaks in Stationary Stochastic Processes", Soil Dyn. Earthq. Eng., Vol. 17, pp. 317–328.
46. Gupta, I.D. and Trifunac, M.D. (1998d). "A Note on Statistics of Level Crossings and Peak Amplitude in Stationary Stochastic Process", European Earthq. Eng., Vol. XII, No. 3, pp. 52–58.
47. Gupta, I.D. and Trifunac, M.D. (1999). "Statistics of Ordered Peaks in the Response of Non-classically Damped Structures", J. Probabilistic Eng. Mech., Vol. 14, pp. 329–337.
48. Gupta, I.D. and Trifunac, M.D. (2000). "A Note on the Nonstationarity of Seismic Response of Structures", Eng. Structures, Vol. 23, pp. 1567–1577.
49. Hayir, A., Todorovska, M.I. and Trifunac, M.D. (2001). "Antiplane Response of a Dike with Flexible Soil-Structure Interface to Incident SH-Waves", Soil Dyn. Earthq. Eng., Vol. 21, No. 7, pp. 603–613.
50. Kashefi, I. and Trifunac, M.D. (1986). "Investigation of Earthquake Response of Simple Bridge Structures", Report 86–02, Dept. Civil Eng., Univ. Southern California, Los Angeles, California, U.S.A.
51. Kaul, M.K. (1978). "Stochastic Characterization of Earthquake through Their Response Spectrum", Earthq. Eng. Struct. Dyn., Vol. 6, pp. 497–509.
52. Kojic, S. and Trifunac, M.D. (1988). "Earthquake Response of Arch Dams to Nonuniform Canyon Motion", Report 88–03, Dept. Civil Eng., Univ. Southern California, Los Angeles, California, U.S.A.
53. Kojic, S. and Trifunac, M.D. (1989). "Transient Pressures in Hydrotechnical Tunnels during Earthquakes", Earthq. Eng. Struct. Dyn., Vol. 16, No. 3, pp. 523–539.
54. Kojic, S. and Trifunac, M.D. (1991a). "Earthquake Stresses in Arch Dams: I — Theory and Antiplane Excitation", J. Eng. Mech. (ASCE), Vol. 117, No. 3, pp. 532–552.
55. Kojic, S. and Trifunac, M.D. (1991b). "Earthquake Stresses in Arch Dams: II — Excitation by SV, P and Rayleigh Waves", J. Eng. Mech. (ASCE), Vol. 117, No. 3, pp. 553–574.
56. Kojic, S., Trifunac, M.D. and Anderson, J.C. (1984a). "A Design Analysis of the Imperial County Services Building", 8th World Conference Earthquake Eng., San Francisco, California, U.S.A.
57. Kojic, S., Trifunac, M.D. and Anderson, J.C. (1984b). "A Post Earthquake Response Analysis of the Imperial County Services Building", Report 84–02, Dept. Civil Eng., Univ. Southern California, Los Angeles, California, U.S.A.
58. Kojic, S., Trifunac, M.D. and Anderson, J.C. (1993). "Earthquake Response of the Imperial County Services Building in El Centro", Earthq. Eng. Eng. Vib., Vol. 13, No. 4, pp. 47–72.
59. Mukherjee, S. and Gupta, V.K. (2002). "Wavelet-Based Characterization of Design Ground Motions", Earthq. Eng. Struct. Dyn., Vol. 31, pp. 1173–1190.
60. Ray Chaudhuri, S. and Gupta, V.K. (2002a). "A Response-Based Decoupling Criterion for Multiply-Supported Secondary Systems", Earthq. Eng. Struct. Dyn., Vol. 31, pp. 1541–1562.
61. Ray Chaudhuri, S. and Gupta, V.K. (2002b). "Variability in Seismic Response of Secondary Systems due to Uncertain Soil Properties", Eng. Structures, Vol. 24, pp. 1601–1613.

62. Rosenblueth, E. and Elorduy, J. (1969). "Response of Linear Systems to Certain Transient Disturbances", Proc. Fourth World Conference Earthq. Eng., Santiago, Chile, Vol. 1, Part A-1, pp. 185–196.
63. Shrikhande, M. and Gupta, V.K. (1996). "On Generating Ensemble of Design Spectrum-Compatible Accelerograms", European Earthq. Eng., Vol. X, No. 3, pp. 49–56.
64. Shrikhande, M. and Gupta, V.K. (1997a). "A Generalized Approach for the Seismic Response of Structural Systems", European Earthq. Eng., Vol. XI, No. 2, pp. 3–12.
65. Shrikhande, M. and Gupta, V.K. (1997b). "On Evolutionary Seismic Response and Peak Factors", Proc. Structural Eng. Convention 1997, Dept. Civil Eng., I.I.T. Madras, Chennai, pp. 511–517.
66. Shrikhande, M. and Gupta, V.K. (1999). "Dynamic Soil-Structure Interaction Effects on the Seismic Response of Suspension Bridges", Earthq. Eng. Struct. Dyn., Vol. 28, pp. 1383–1403.
67. Singh, M.P. and Chu, S.L. (1976). "Stochastic Considerations in Seismic Analysis of Structures", Earthq. Eng. Struct. Dyn., Vol. 4, pp. 295–307.
68. Singh, M.P. and Mehta, K.B. (1983). "Seismic Design Response by an Alternative SRSS Rule", Earthq. Eng. Struct. Dyn., Vol. 11, pp. 771–783.
69. Sun, W.J. and Kareem, A. (1989). "Response of MDOF Systems to Nonstationary Random Excitation", Eng. Structures, Vol. 11, pp. 83–91.
70. To, C.W.S. (1982). "Nonstationary Random Responses of a Multi-Degree-Freedom System by the Theory of Evolutionary Spectra", J. Sound Vib., Vol. 83, No. 2, pp. 273–291.
71. Todorovska, M.I. and Trifunac, M.D. (1989). "Antiplane Earthquake Waves in Long Structures", J. Eng. Mech. (ASCE), Vol. 115, No. 2, pp. 2687–2708.
72. Todorovska, M.I. and Trifunac, M.D. (1990a). "Propagation of Earthquake Waves in Buildings with Soft First Floor", J. Eng. Mech. (ASCE), Vol. 116, No. 4, pp. 892–900.
73. Todorovska, M.I. and Trifunac, M.D. (1990b). "Note on Excitation of Long Structures by Ground Waves", J. Eng. Mech. (ASCE), Vol. 116, No. 4, pp. 952–964 (with Errata in Vol. 116, p. 1671).
74. Todorovska, M.I. and Trifunac, M.D. (2001). "Flexible versus Rigid Foundation Models of Soil-Structure Interaction: Incident SH-Waves", Proc. 2nd U.S.-Japan Workshop on Soil-Structure Interaction, Tsukuba City, Japan.
75. Todorovska, M.I., Lee, V.W. and Trifunac, M.D. (1988). "Investigation of Earthquake Response of Long Buildings", Report 88–02, Dept. Civil Eng., Univ. Southern California, Los Angeles, California, U.S.A.
76. Todorovska, M.I., Gupta, I.D., Lee, V.W., Gupta, V.K. and Trifunac, M.D. (1995). "Selected Topics in Probabilistic Seismic Hazard Analysis", Report 95–08, Dept. Civil Eng., Univ. Southern California, Los Angeles, U.S.A.
77. Todorovska, M.I., Ivanovic, S.S. and Trifunac, M.D. (2001a). "Wave Propagation in a Seven-Story Reinforced Concrete Building, Part I: Theoretical Models", Soil Dyn. Earthq. Eng., Vol. 21, No. 3, pp. 211–223.
78. Todorovska, M.I., Ivanovic, S.S. and Trifunac, M.D. (2001b). "Wave Propagation in a Seven-Story Reinforced Concrete Building, Part II: Observed Wave Numbers", Soil Dyn. Earthq. Eng., Vol. 21, No. 3, pp. 225–236.
79. Todorovska, M.I., Hayir, A. and Trifunac, M.D. (2001c). "Antiplane Response of a Dike on Flexible Embedded Foundation to Incident SH-Waves", Soil Dyn. Earthq. Eng., Vol. 21, No. 7, pp. 593–601.
80. Trifunac, M.D. (1997). "Differential Earthquake Motion of Building Foundations", J. Struct. Eng. (ASCE), Vol. 123, No. 4, pp. 414–422.
81. Trifunac, M.D. (2000). "Comments on Seismic Soil-Structure Interaction in Buildings, I: Analytical Methods and II: Empirical Findings", J. Geotech. Geoenvironmental Eng. (ASCE), Vol. 126, No. 7, pp. 668–670.
82. Trifunac, M.D. (2003). "70-th Anniversary of Biot Spectrum", 23rd Annual ISET Lecture, ISET J. Earthq. Tech. (in press).

83. Trifunac, M.D. and Lee, V.W. (1979). "Time of Maximum Response of Single-Degree-of-Freedom Oscillator for Earthquake Excitation", Report 79–14, Dept. Civil Eng., Univ. Southern California, Los Angeles, U.S.A.
84. Trifunac, M.D. and Lee, V.W. (1986). "A Note on Time of Maximum Response of Single Degree of Freedom Oscillator to Earthquake Excitation", Soil Dyn. Earthq. Eng., Vol. 5, No. 2, pp. 119-129.
85. Trifunac, M.D. and Todorovska, M.I. (1997). "Response Spectra and Differential Motion of Columns", Earthq. Eng. Struct. Dyn., Vol. 26, No. 2, pp. 251–268.
86. Trifunac, M.D. and Todorovska, M.I. (1999a). "Recording and Interpreting Earthquake Response of Full-Scale Structures", Proc. NATO Advanced Workshop on Strong Motion Instrumentation for Civil Engineering Structures, Istanbul, Turkey.
87. Trifunac, M.D. and Todorovska, M.I. (1999b). "Relative Flexibility of a Building Foundation", in "Proc. UJNR Workshop on Soil-Structure Interaction, Sept. 22–23, 1998", Open File Report 99–142, U.S. Geological Survey, U.S. Dept. of Interior, U.S.A., Paper No. 17.
88. Trifunac, M.D., Hao, T.Y. and Todorovska, M.I. (2001a). "Response of a 14 Story Reinforced Concrete Structure to Excitation by Nine Earthquakes: 61 Years of Observation in the Hollywood Storage Building", Report 01–02, Dept. Civil Eng., Univ. Southern California, Los Angeles, California, U.S.A.
89. Trifunac, M.D., Ivanovic, S.S. and Todorovska, M.I. (2001b). "Apparent Periods of a Building, Part I: Fourier Analysis", J. Struct. Eng. (ASCE), Vol. 127, No. 5, pp. 517–526.
90. Trifunac, M.D., Ivanovic, S.S. and Todorovska, M.I. (2001c). "Apparent Periods of a Building, Part II: Time-Frequency Analysis", J. Struct. Eng. (ASCE), Vol. 127, No. 5, pp. 527–537.
91. Trifunac, M.D., Ivanovic, S.S. and Todorovska, M.I. (2002). "Wave Propagation in a Seven-Story Reinforced Concrete Building: III. Damage Detection via Changes in Wave Numbers", Soil Dyn. Earthq. Eng. (in press).
92. Udwadia, F.E. and Trifunac, M.D. (1973a). "The Fourier Transform, Response Spectra and Their Relationship through the Statistics of Oscillator Response", Report 73–01, Earthquake Engineering Research Laboratory, California Inst. Tech., Pasadena, U.S.A.
93. Udwadia, F.E. and Trifunac, M.D. (1973b). "Damped Fourier Spectrum and Response Spectra", Bull. Seism. Soc. Am., Vol. 63, pp. 1775–1783.
94. Udwadia, F.E. and Trifunac, M.D. (1974a). "Time and Amplitude Dependent Response of Structures", Earthq. Eng. Struct. Dyn., Vol. 2, pp. 359-378.
95. Udwadia, F.E. and Trifunac, M.D. (1974b). "Characterization of Response Spectra through the Statistics of Oscillator Response", Bull. Seism. Soc. Amer., Vol. 64, pp. 205–219.
96. Unruh, J.F. and Kana, D.D. (1981). "An Iterative Procedure for the Generation of Consistent Power/Response Spectrum", Nucl. Eng. Des., Vol. 66, pp. 427–435.
97. Vanmarcke, E.H. (1975). "On the Distribution of the First-Passage Time for Normal Stationary Random Processes", J. Appl. Mech., Trans. ASME, Vol. 42(E), pp. 215–220.
98. Wilson, E.L., Der Kiureghian, A. and Bayo, E.P. (1981). "A Replacement for the SRSS Method in Seismic Analysis", Earthq. Eng. Struct. Dyn., Vol. 9, pp. 187–194.

ISET Journal of Earthquake Technology, Paper No. 422, Vol. 39, No. 3, September 2002, pp. 139-165

FULL-SCALE EXPERIMENTAL STUDIES OF SOIL-STRUCTURE INTERACTION

Maria I. Todorovska
Research Associate Professor
Civil Engineering Department
University of Southern California
Los Angeles, CA 90089-2531, U.S.A.

ABSTRACT

This paper presents a review of the full-scale experimental studies of soil-structure interaction. It briefly reviews the early research on soil-structure interaction, starting from the 1930s, the studies of the Hollywood Storage Building in the U.S. (the first structure in California where earthquake strong motion was recorded in 1933), selected research on soil-structure interaction and full-scale testing from the 1970s to present, and experimental work on large model tests. It also presents examples of full-scale tests in actual structures, and an analysis of the trends in full-scale experimental studies of soil-structure interaction via the number of published journal and conference papers. It is concluded that monitoring of earthquake response in and around buildings and comprehensive full-scale tests of structures are the best experimental methods for investigating soil-structure interaction, because they are most complete, the boundary conditions are satisfied exactly, and the problems related to scaling and similarity laws are eliminated.

KEYWORDS: Soil-Structure Interaction, Full-Scale Testing, Large-Scale Tests, Hollywood Storage Building

INTRODUCTION

Soil-structure interaction is a collection of phenomena in the response of structures caused by the flexibility of the foundation soils, as well as in the response of soils caused by the presence of structures. In general, it lengthens the apparent system period, increases the relative contribution of the rocking component of ground motion to the total response, and usually reduces the maximum base shear (Todorovska and Trifunac, 1990a, 1991, 1992a, 1992b, 1993; Gupta and Trifunac, 1991). This reduction results from the scattering of the incident waves from the foundation, and from radiation of the structural vibration energy into the soil. When the soil surrounding the foundation experiences small to moderate levels of non-linear response, the soil-structure interaction can lead to significant absorption of the incident wave energy, thus reducing the available energy to excite the structure (Trifunac et al., 2001a).

The simplest soil-structure interaction models are those in which the structure is supported by a rigid foundation (Abdel-Ghaffar and Trifunac, 1977; Werner et al., 1977, 1979). These models require only six additional degrees-of-freedom (three translations and three rotations), but may be too simple for practical applications. Models with flexible foundations are rare (Iguchi and Luco, 1982; Hayir et al., 2001; Liou and Huang, 1994; Todorovska et al., 2001a, 2001b; Trifunac and Todorovska, 1999c; Wong et al., 1977) and difficult to validate against data (Trifunac et al., 1999).

Recorded strong motion in structures indicates that destructive shaking is often accompanied by non-linear response of the foundation soils (Luco et al., 1986; Trifunac and Todorovska, 1998; Trifunac et al., 1999, 2001b, 2001c), and that the time-dependent changes of the apparent frequencies of the response are often due to significant contribution of soil-structure interaction (Udwadia and Trifunac, 1974).

Contributions to the subject of soil-structure interaction have been reviewed on numerous occasions, during conferences devoted specifically to this subject (e.g., International Symposium on Soil-Structure Interaction, 1977), symposia following World Conferences on Earthquake Engineering (Ergunay and Erdik, 1981), and workshops (Celebi and Okawa, 1999). The subject has been reviewed in specialized reports (Luco, 1980) and researched in numerous doctoral dissertations (e.g., Merritt, 1953; Luco, 1969a; Lee, 1979), and books (Wolf, 1985, 1994).

Experimental studies of soil-structure interaction are best conducted in full-scale in actual buildings, during microtremors (Trifunac, 1970a, 1970b, 1972a), forced vibrations (Blume, 1936; Hudson, 1970), and earthquake excitation (Luco et al., 1987; Stewart and Stewart, 1997). The difficulties of conducting experiments in the laboratory are not only due to the similarity laws that have to be satisfied, but are mainly due to modeling the (semi-infinite) half-space boundary condition.

Experimental studies of soil-structure interaction have also been conducted in the laboratory, e.g., static and dynamic (shaking table) tests of soil structure interaction, and centrifuge experiments of soil-pile and soil-structure interaction. Since 1970s, the number of papers dealing with these subjects has grown steadily, producing a large volume of specialized research results (see, e.g., McLean and Ko, 1991, and Kimura et al., 1998), a comprehensive review of which would be more appropriate for a separate future paper, and is out of the scope of this paper.

This paper focuses on a review of the full-scale experimental studies of soil-structure interaction. First, it briefly reviews the early research on soil-structure interaction, starting from the early 1930s, and including the work of Suyehiro, Sezawa and Kanai, and Biot. This is followed by a review of studies of the Hollywood Storage Building in the U.S. (the first structure in California where earthquake strong motion was recorded in 1933), by a review of selected research on soil-structure interaction and full-scale testing from the 1970s to present, and by a review of experimental work on large model tests. Next, the paper reviews specific examples of full-scale tests in actual structures, to illustrate how such tests contribute towards formulation of models and assumptions. Finally, it presents an analysis of the trends in full-scale experimental studies of soil-structure interaction via the number of published journal and conference papers. The last section presents a discussion and the conclusions.

THE EARLY RESEARCH ON SOIL-STRUCTURE INTERACTION

We begin by reviewing the work of Suyehiro, Sezawa, Kanai and Biot – pioneers who contributed to the evolution of the concept of soil-structure interaction.

In the fall of 1931, Professor Kyoji Suyehiro visited the United States and presented a series of three lectures on Engineering Seismology (Suyehiro, 1932). His third lecture (III) entitled "Vibration of Buildings in an Earthquake" is of particular interest. In this lecture, Suyehiro discussed the response and observed damage of "rigid", "medium rigid" and "weak" buildings situated on "soft" (loose clay) and "rock" ground. He explained how the "rigid" building "moved as a rigid body on the ground-bed" and suffered little or no damage. In contrast, the "weak" buildings on "rock" ground were either damaged or destroyed. Searching for an explanation, Suyehiro states that "very probably the primary cause is the yielding of the ground-bed due to oscillation of the foundation…". He concluded, "such cushioning action of the ground at the time of an earthquake may serve more or less to relieve the destructive action of a strong earthquake in the case of masonry (i.e. rigid) buildings". These remarkable observations were confirmed many times by earthquake damage patterns seen since 1932. Suyehiro then describes microtremor measurements in the Earthquake Research Institute, in the building and on the adjacent ground. Professor Ishimoto performed these measurements in 1929 (see Figure 55 on Page 91 of Suyehiro's lectures). His investigation of the velocity of ripples on the ground is very useful in this connection. According to him, "on the surface of the ground where our Institute building stands, the P-wave has a velocity of above 120 m. per sec. and the S-wave about 65 m. per sec. Therefore, very probably, the wavelength of ripples having a period of 0.1 sec. is between 6.5 to 12.0 m.; hence, they are less than the linear dimensions of the building. Consequently, a building on soft ground is not sensitive to those quick and short ripples. It may also be mentioned that this fact may be attributed to a certain extent to another behavior of the vibration of soft ground, in which the amplitude of the component of a seismic vibration of very short period decreases quickly with depth. Therefore, foundations at some depth below the surface will be less affected by the rapid components of seismic vibrations."

It is fascinating to read how Suyehiro describes the scattering of short waves from a "rigid" foundation and the resulting averaging (smoothing) action of the foundation. "According to observations made by Professor Imamura on the vibration of the Diet Building during construction, some very rapid ripples, having a period of about 0.1 sec., disappeared in the motion of the foundation although the foundation moved about as much as the neighboring ground". In his published lectures, Suyehiro does not use the modern term "soil-structure-interaction", but it is obvious that one of the main topics of his lecture

III is in fact soil-structure-interaction. Of course, from today's viewpoint, his observations were intuitive and for the most part qualitative, but his insight and ability to interpret observations were remarkable.

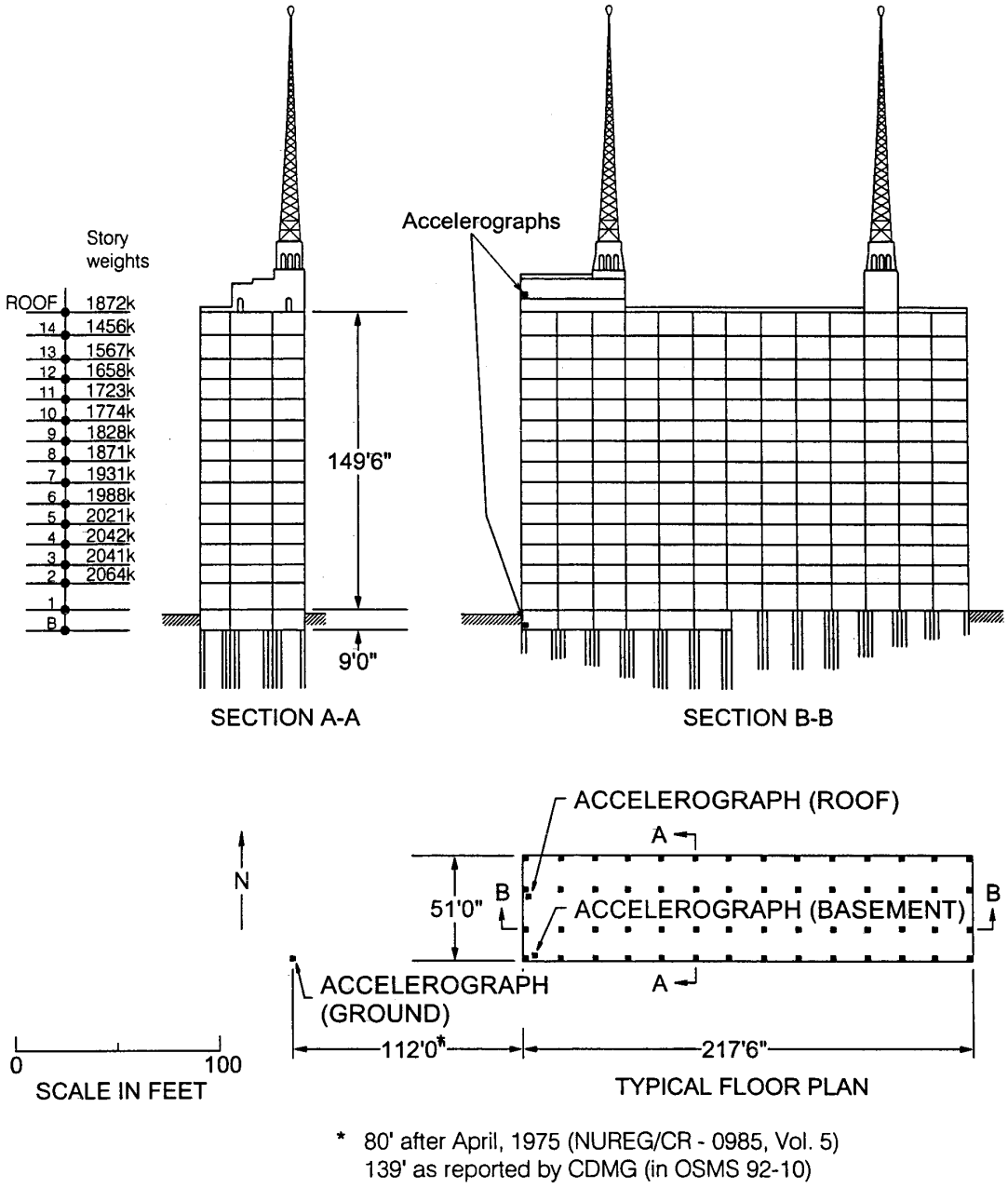

Fig. 1 A sketch of the Hollywood Storage Building in the early 1950s (the location of the strong motion accelerographs is indicated, one in the basement, one on the roof and one at a "free-field" site, 112 feet west of the south-west corner of the building) (after Duke et al., 1970)

Sezawa and Kanai (1935, 1936) also made pioneering studies of soil-structure-interaction. Their method was based on wave propagation, and even though they did not use the term "soil-structure-interaction", that is what they were studying. Their stated aim was to investigate the "decay of the seismic vibration of a simple or tall structure by dissipation of their energy into the ground". Summarizing this work and his observations over the span of 50 years, Kanai (1983) writes: "the excellent agreement between the calculated waveform and the observed seismograms seems to indicate that most of the vibrational damping of the buildings and dams during earthquakes occurred at the contact surface between the structure and the ground". To better appreciate the mathematical formulation and the physical insight of Sezawa's and Kanai's work, it is helpful to begin by reading Luco (1969b) and Trifunac (1972b).

During the 1950s, Kanai and co-workers carried out numerous tests on full-scale structures. They studied the influence of the ground stiffness on the response of structures (Kanai et al., 1953, 1955a, 1955b), using excitation by microtremors, vibration generators (Kanai et al., 1958a, 1958b), and earthquakes (Kanai et al., 1958c).

It is well known that "Earthquake Engineering as such could be considered to have been born with Biot's concept of a response of an idealized structure to ground motion" (Krishna, 1981). Here Krishna is referring to the second chapter in Biot's Ph.D. Dissertation, defended at Caltech in 1932, and entitled "Vibration of Buildings during Earthquakes" (Biot, 1932). These ideas were further refined and published during the following two years (Biot, 1933, 1934). Nine years later, Biot briefly returned to the subject of Earthquake Engineering, describing computation of response spectra by means of a mechanical analyzer (Biot, 1941a), and formulating the general theory and principles of response analysis and response spectrum superposition in Biot (1942).

It is not known that Biot was also working on the subject of soil-structure interaction. In an unpublished note (Biot, 1941b), he states "the problem is extremely complex because it involves a complete knowledge of the propagation and properties of the seismic waves in the strongly heterogeneous surface layers of the earth, as well as their diffraction and reflection by objects built on the surface… In the present investigation, we have attempted to answer the following question: What is the influence of the elasticity of the ground on the rocking motion of a building? How resistant is the surrounding soil to the rocking displacement of a foundation; what are the factors influencing this rigidity, and can we expect this effect to have a practical influence in the action of earthquakes on buildings? The problem is simplified by neglecting the radiation of elastic wave due to the rocking". The ideas and equations from this unpublished note appear in an abridged form in Section V entitled "Influence of Foundation on Motion of Blocks" of Biot's 1942 paper. One cannot but marvel how well Biot understood the physical nature of the problem, almost 30 years before the "modern" research started to evolve in the 1970s.

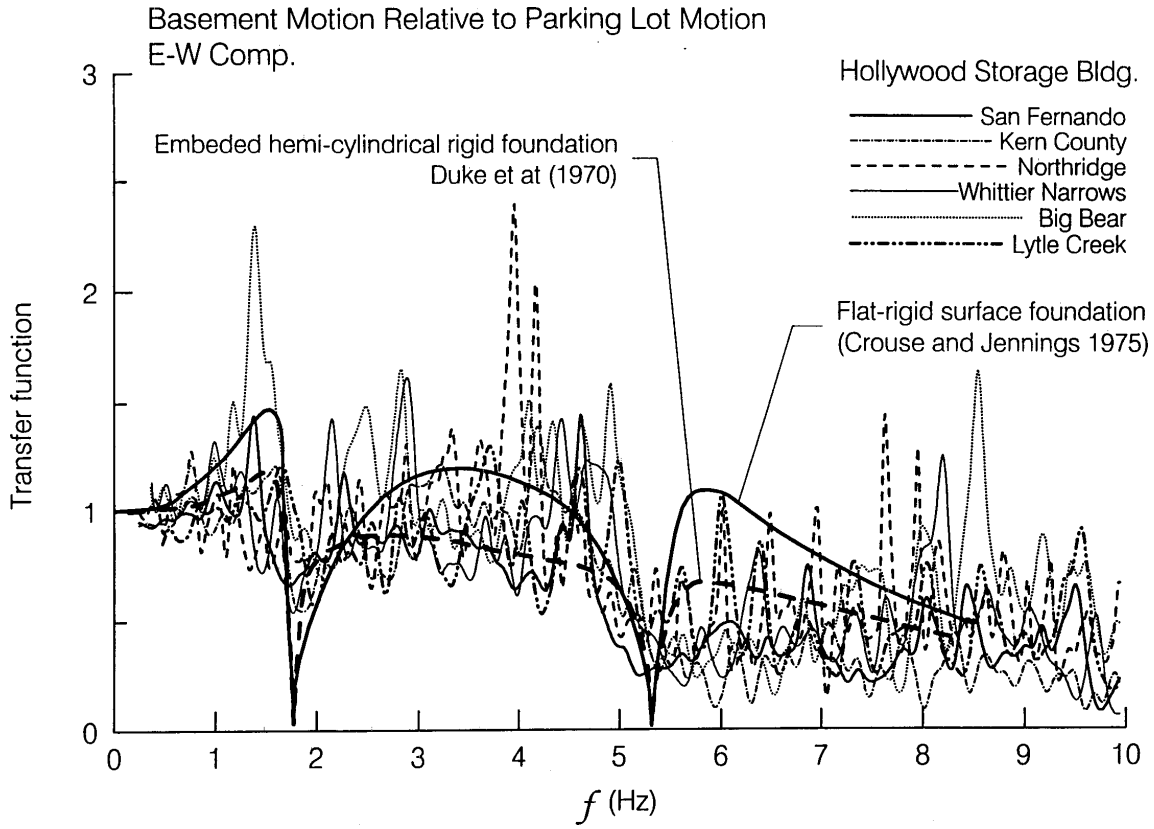

Fig. 2 E-W acceleration transfer-function between motion recorded at the basement of Hollywood Storage Building and at the "free-field" site (in the parking lot, about 100 feet west of the building, see Figure 1) during six earthquakes (the heavy solid and dashed lines correspond to two examples of theoretical transfer-functions (Crouse and Jennings, 1975))

STUDIES OF THE HOLLYWOOD STORAGE BUILDING

The Hollywood Storage Building (HSB, located at 1025 North Highland Ave. in Los Angeles, Figure 1) was the first structure in California equipped with permanent strong motion accelerographs in 1933 (the instrument in the parking lot was installed in December 1939; see Trifunac et al., 2001d). It is also the first building in California where strong motion was recorded (October, 1933), and also the first building for which it could be shown that both theoretical analysis and observation of soil-structure interaction are consistent (Figure 2; Duke et al., 1970). This building served as a testing ground for intuitive (Housner, 1957) and theoretical and quantitative (Duke et al., 1970) studies of soil-structure interaction. The data recorded in and near this building was also used in several other related studies, for example, on scattering of waves by a "rigid" foundation, the associated "filtering" of high frequency motions, and on the associated torsional excitation of the foundation (Cloud, 1978; Gupta and Trifunac, 1990; Shioya and Yamahara, 1980; Whitley et al., 1977). Since 1933, there were numerous triggers of the strong motion accelerographs in this building, but only a few, so far, have been processed and are available for analysis. This building was also studied using ambient and forced vibration tests (Carder, 1936, 1964).

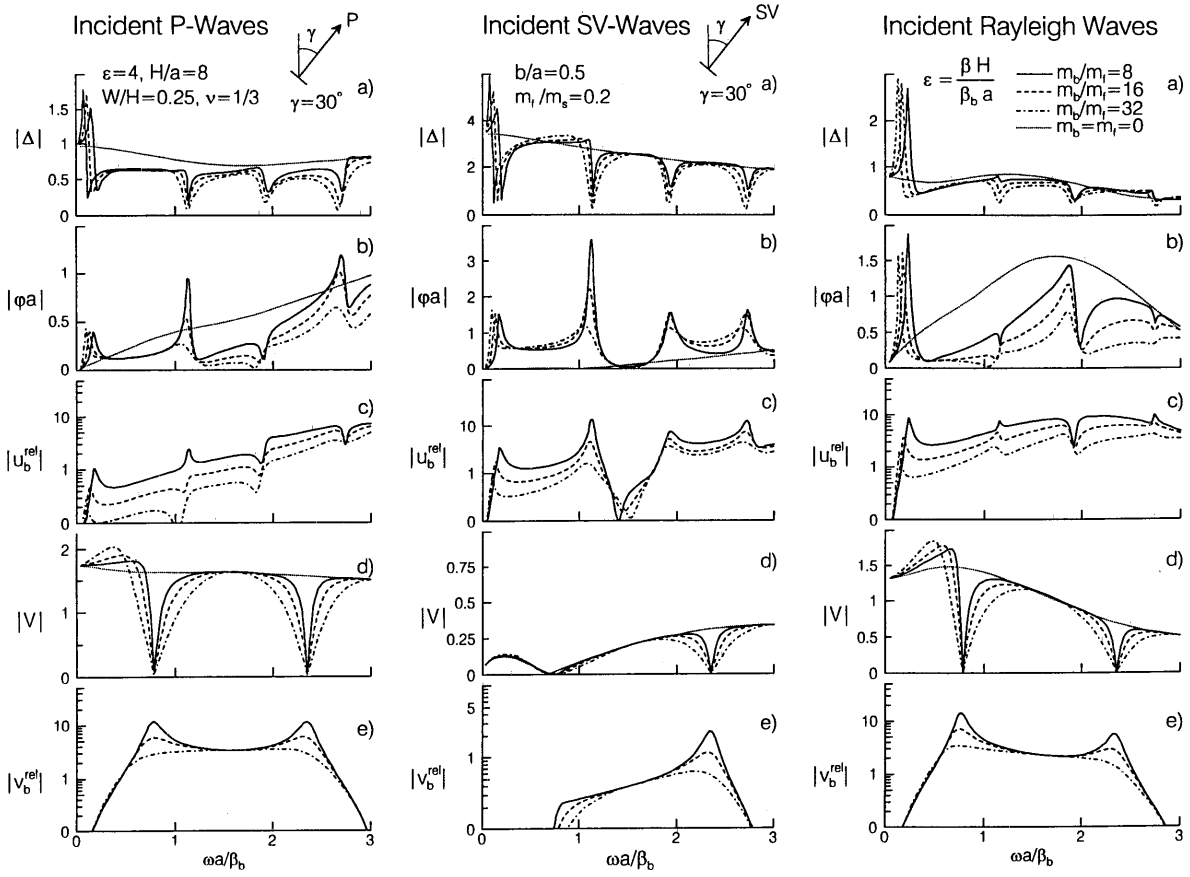

Fig. 3 Transfer-function amplitudes for (a) horizontal foundation motion, Δ, (b) foundation rocking, φa, (c) building relative horizontal motion, u_b, (d) vertical foundation motion, V, and (e) building relative vertical motion, v_b, versus dimensionless frequency, $\omega a/\beta_b$, for incident P-waves (left), SV-waves (center) and Rayleigh waves (right) (after Todorovska and Trifunac, 1990a) (W and H represent the width and height of the building, h and $2a$ represent embedment and width of the rigid foundation respectively, β and β_b are shear wave velocities in the soil and in the building, m_b is mass of the building, m_f is mass of the foundation and m_s is mass of soil replaced by the foundation, all per unit length of the 2D models)

Housner (1957) performed visual comparison of the accelerations recorded in the basement of this building and in the parking lot during the 1952 Kern County earthquake, as well as of the corresponding

response spectra (spectral velocity) computed by an analog computer (Housner and McCann, 1949). He concluded that, for this "relatively large, heavy and stiff" building, "there was not significant amount of ground coupling," and that "in order for the ground coupling to be significant, in engineering sense, the ground would have to be much softer than the so called soft alluvium on which the building rests." This often cited conclusion, as well as the inference made about differences in the stresses in the building along its long and short axes, should be taken with great caution, as they are based on inaccurately processed data, using the limited data processing technology available at that time, and on intuitive reasoning limited by the lack of analytical solutions for this problem at that time, which would have provided deeper insight into the problem and helped interpret the empirical data. More specifically, a recent comparison of the spectra that Housner (1957) used in his analysis revealed that there were significant errors in the response spectra he computed, for the longer periods for all components, and for all periods for the EW component of the motion recorded in the basement (approximately by a factor of two, see Trifunac et al., 2001d, which reviews data on nine earthquakes recorded in this building during the past 61 years of observation). These errors lead to an erroneous inference that there was a significant difference between the components of motion along the long axis recorded in the parking lot and in the basement, while there was no significant difference for the components along the short axis (see Figure 1). The conclusion that there was no significant coupling between the motion of the ground and of the building was based on the intuitive reasoning that "if the horizontal coupling were strong… the spectrum curve for zero damping would have a peak at the fundamental period of vibration (of the building)." Analytical solutions showed later that the transfer-function for the horizontal motion of the base actually has a zero or a local minimum at the natural period of vibration of the building (see Figure 3).

As illustrated above, studies of the effects of soil-structure interaction may be based on comparison of the motions recorded in the structure with those recorded at a "free-field site" (typically several hundred feet away from the structure). It is usually assumed that the "free-field" record approximates the motions in the absence of the structure (Trifunac, 1972b). The transfer-functions between the foundation motion and the corresponding motions at the "free field site" are then used in the analysis (Lee et al., 1982; Moslem and Trifunac, 1987). The first successful interpretation of observed data, using analysis of this type, was presented by Duke et al. (1970). They interpreted the EW recorded motions (along the longitudinal building direction, see Figure 1) of the Hollywood Storage Building in terms of an analytic solution of soil-structure interaction, with a rigid semi-cylindrical foundation, and for vertically incident SH waves (see the dashed line in Figure 2, Luco, 1969b). Duke et al. (1970) did not interpret the soil-structure interaction for NS (transverse) response, because at that time, a theoretical solution did not exist for in-plane motion. Figure 3 shows results for in-plane motion of a model similar to the two-dimensional model of Luco (1969b) and Trifunac (1972b), i.e. a shear wall supported by a cylindrical foundation embedded into an elastic homogeneous half-space, redrawn from Todorovska and Trifunac (1990a). It shows the foundation horizontal displacement, Δ, rocking angle, φ, relative horizontal displacement of the top of the shear wall, u_b^{rel}, foundation vertical motion, V, and relative vertical displacement of the top of the shear wall, v_b^{rel}, for incident unit amplitude P- and SV-waves with incident angle $\gamma = 30^{\circ}$ and Rayleigh waves with unit horizontal amplitude on the surface, and for different model parameters ($\varepsilon = \beta H/\beta_b\, a$, H/a, W/H, m_s/m_f, m_b/m_f, where a is the half width of the foundation, H and W are the shear wall height and width, and m_b, m_f and m_s are the mass of the shear-wall, foundation and soil replaced by the foundation). It is seen that, as for the solutions of Luco (1969b) and Trifunac (1972b) for SH wave excitation, Δ has minima at the natural frequencies of the building. However, for all other frequencies, the transfer-functions for Δ are complicated and different for different incoming waves and angles of wave incidence. Thus, selecting a simple model and formulating an interpretation in terms of transfer-functions of recorded horizontal motions only, is difficult. In contrast, transfer-functions for vertical motion (V) are simpler and more similar for all incident waves and incident angles. The transfer-functions of rocking motions are very dependent on the type of incident waves. Since actual strong motion consists of all body and surface waves, the observed transfer-functions for in-plane motion (assuming linear behavior of the foundation soils), would be more complicated and different from any of the Δ transfer-functions illustrated in Figure 3.

In the analysis of Duke et al. (1970) and Todorovska and Trifunac (1990a) (see Figure 3), it was assumed that the building foundation can be represented by a semi-cylindrical rigid mass. Clearly this is a very rough approximation for the foundation system of the Hollywood Storage Building, which is on Raymond concrete piles 12 ft to 30ft long (Figure 1). Thus, if this foundation is to be modeled by a rigid equivalent foundation, it would be good to select some more representative embedment ratios, as this affects the nature of the waves scattered from the foundation (Wong and Trifunac, 1974). It is more likely however that this foundation does not behave like a rigid body, especially for intermediate and high frequency waves (Trifunac et al., 1999). How to represent soil-structure interaction with flexible three-dimensional foundations has not been studied so far in sufficient detail to allow any definite interpretation, and so we leave this interesting topic for a future analysis. So far, there have been no dense arrays in building foundations that have recorded earthquake motion.

An example of an early analysis of the rocking period of a rigid building on flexible soil can be found in Biot (1942). Merritt and Housner (1954) also investigated the rocking motions, from which Housner (1957) concluded "significant effects could be expected only with exceptionally soft ground". It is interesting to note that Housner (1957) and Duke et al. (1970) papers appear to have left an impression on subsequent researchers, who state for example that the "evidence of soil structure interaction can be quantitatively detected in the frequency domain by the ratio $\left|\Delta + u_g^H\right| \ / \ \left|u_g^h\right|$" (e.g., Hradilek et al., 1973). Rocking and torsional contribution to interaction are rarely addressed in papers which aim to interpret earthquake accelerograms recorded in buildings.

Duke et al. (1970) concluded, "soil-structure interaction produced marked change in the horizontal base displacements, in the east-west direction...", with little or no rocking in this direction. For the north-south direction, the soil-structure interaction did not affect drastically the horizontal base displacements, but produced rocking of the foundation, as can be observed by analysis of the roof motion.

Other studies of Hollywood Storage Building were presented by Crouse and Jennings (1975) who compared strong motion records of the 1952 Kern County earthquake with a new set of records from the 1971 San Fernando earthquake, and by Serino and Fenves (1990) and Papageorgiou and Lin (1991), who analyzed its response after the Whittier-Narrows earthquake of 1987. Serino and Fenves (1990) used substructuring method (Chopra and Gutierez, 1973) and estimated the reduction of base shear, overturning moment and roof displacement of 3, 7 and zero percent for transverse direction, and 17, 15 and 19 percent for longitudinal direction, respectively. The studies of Crouse and Jennings (1995) and Papageorgiou and Lin (1991) are discussed in more detail in Trifunac et al. (2001d).

RESEARCH ON FULL-SCALE TESTING OF SOIL-STRUCTURE INTERACTION AFTER 1970

Journal and conference papers explicitly dealing with analysis of soil-structure interaction, in full-scale and in terms of recorded earthquake response, are rare. Examples include studies of a three-story long building founded on soft soil (Muria-Vila and Alcorta, 1992), a study of free-field motions surrounding a building, and of the motions of the building (Kashima and Kitagawa, 1988), creation of a database of earthquake records for response of a concrete tower (Ganev et al., 1993), and earthquake response analyses of simple bridges (Goel and Chopra, 1994; Werner et al., 1994), and of a caisson–type foundation of Sasame bridge (Kaino and Kikuchi, 1988). Analysis of earthquake records and identification of soil-structure interaction from recorded accelerograms in buildings is discussed in Safak (1992).

Full-scale tests of soil-structure interaction using periodic force excitation of structures are more common. The examples include tests of bridges (Crouse et al., 1987; Maragakis et al., 1996; Ventura et al., 1995), buildings with prefabricated panels (Petrovski, 1978; Erdik and Gulkan, 1984), a steel frame building (Shinozaki et al., 1994), tall concrete silo tower (Ellis, 1986), nuclear reactor buildings (Erdik et al., 1985; Mizuno and Tsushima, 1975; Casirati et al., 1988; and Iguchi et al., 1988), and foundations supported by piles (Urao et al., 1988; and Yahata et al., 1992). Wave motion resulting from soil-structure interaction during forced vibration tests of a nine-story reinforced concrete building (Luco et al., 1986, 1988) is described in Luco et al. (1975). Vibrations of a full-scale bridge structure excited by quickly released horizontal loads are described in Douglas et al. (1990) and in Richardson and Douglas (1993).

Non-linear response of the soil may cause significant changes in the apparent frequencies of the building-soil system (Trifunac et al., 2001a, 2001b), and this may lead to different results for small and large amplitudes of response (Luco et al., 1986). These differences can be quantified and interpreted by comparison of experimental results for small and large amplitudes of response (Trifunac, 1972a; Fukuoka, 1977; Ueshima, 1988; and Tobita et al., 2000).

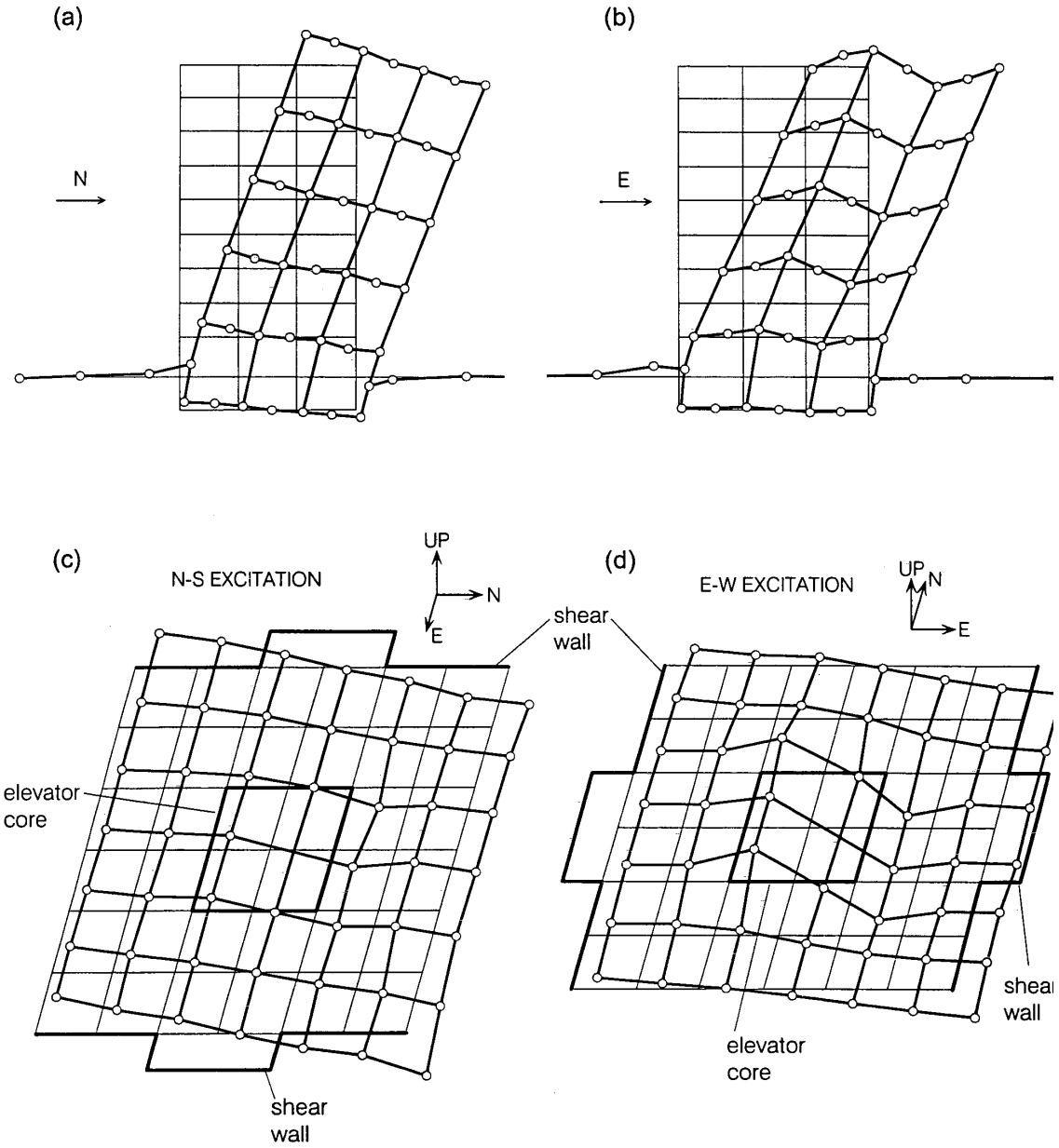

Fig. 4 Deformation of Millikan Library, a nine-story reinforced concrete building, excited at the roof by a shaker with two counter rotating masses (a) along the west shear wall during NS excitation, (b) along a section through the elevator core during EW excitation, (c) of the basement slab during NS excitation, and (d) of the basement slab during EW excitation (from Foutch et al., 1975)

LARGE MODEL TESTS

To understand soil-structure interaction and to validate different modeling and analysis methods, in-situ experimental investigations are essential. Because it is difficult to simulate half-space conditions in small specimens on shaking tables, a viable alternative is to construct scaled down models in seismically active areas. This approach offers numerous other advantages: choice of embedment depth, control of

backfill soil material, possibility to install detailed instrumentation, ability to control the surroundings of the site, etc. (Tang et al., 1989).

As the full-scale structures, large-scale models can be excited by periodic actuators or shakers (e.g., Petrovski, 1975; Mizuno, 1978; Hadjian et al., 1990; Luco and Wong, 1990; Fujimori et al., 1992; Inukai et al., 1992; Ohtsuka et al., 1992; Tuzuki et al., 1992; Uchiyama, 1992; de Barros and Luco, 1995), earthquakes (Iguchi et al., 1988a, 1988b; Wong and Luco, 1990), or by both (Tohma et al., 1985; Toki and Kiyono, 1992; Ganev et al., 1996; Ohtsuka et al., 1996). Small amplitude measurements during microtremor excitation can also be compared with results from forced vibration tests, and with response to earthquake excitation (Mizuno, 1980). Kitada et al. (1999) present a recent summary of large model testing in Japan.

A special category of full-scale experiments deals with soil-structure interaction characteristics of foundations for strong motion accelerographs. Because of their small dimensions, studies of these full-scale foundations give results analogous to those from in-situ tests of scaled models mentioned above (Crouse and Hushmand, 1990; Crouse et al., 1984; Ramirez-Centeno and Ruiz-Sandoval, 1996).

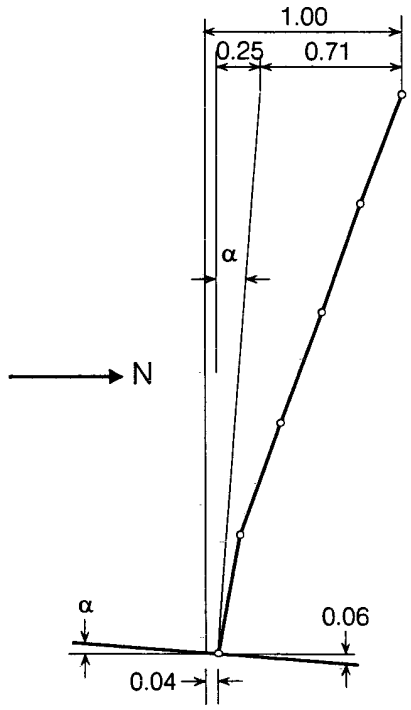

Fig. 5 Contributions of foundation translation and rocking to the roof motion of Millikan Library, for N-S shaking (from Foutch et al., 1975)

EXAMPLES OF FULL-SCALE TESTS IN ACTUAL STRUCTURES

In the following, we review several examples of full-scale tests in actual structures to illustrate how those tests can contribute towards formulation of realistic models and model assumptions.

1. Rigid versus Flexible Foundation Models

In dynamic analyses of soil-structure systems, it is convenient to assume that the foundation is rigid. This simplifies the analysis, and reduces the number of additional degrees-of-freedom required to include the soil-structure interaction, and thereby the number of simultaneous equations to be solved. However, the validity of this assumption must be carefully investigated, as it depends not only on the relative rigidity of the foundation and of the soil, but also on the type of structure and its overall rigidity, lateral load-resisting system and orientation. This can be illustrated by comparison of the NS and EW vibrations of Millikan Library in Pasadena, a nine-story reinforced concrete structure, studied by Luco et al. (1986). Even though the foundation system of this building is relatively flexible, for NS vibrations, the two symmetric shear walls at each end of the building (east and west) act to “stiffen” the foundation slab,

which allows rigid foundation representation (Figure 4, a and c). For EW vibrations, the building carries the lateral loads by an elevator core, which deforms the foundation slab in the middle, while the shear walls act as membranes providing axial constraints, but little bending stiffness (Figure 4, b and d), and thus, the foundation slab cannot be approximated by a rigid foundation model. The three-dimensional deformation shapes in Figure 4 show how this structure deforms while vibrating in NS and EW directions. These were measured during forced vibration tests of this building (Foutch et al., 1975), and were essential for this interpretation. Figure 5 shows schematically the relative contributions of the horizontal deformation of the soil (4 percent), the roof displacement resulting from rigid body rocking (25 percent), and the relative deformation of the building (71 percent), during steady state forced-vibrations in the NS direction (as in Figure 4a).

Recent ambient vibration tests in a seven-story reinforced concrete moment resistant frame building in Van Nuys, California showed that the foundation supported by piles deforms during passage of microtremor waves. It can be inferred that the same happens during the passage of strong motion waves that have much larger amplitude. A detailed ambient vibration survey of this symmetric structure on symmetric pile foundations showed that the center of torsion for this structure is outside the building plan, close to its south-east corner (Trifunac et al., 1999). Subsequent examination of the strong motion records in this building showed that this eccentricity may have been present in all post-1971 responses, and is due either to some asymmetry in the soil-pile system from the time of its construction in 1966, or to some partial damage from the 1971 San Fernando earthquake (Trifunac et al., 1999), or may be, to a large lateral heterogeneity in the soil.

Differential motions of building foundations (Trifunac, 1997) may reduce the translational response at the upper floors, but may lead to large additional shear forces and bending moments in the columns of the first floor, depending on the foundation design. The response spectrum method can be modified to include the consequences of such differential motions (Trifunac and Todorovska, 1997), but it is necessary to study this further via full-scale measurements during future strong earthquakes, and to correlate the theory with observations.

The assumption that foundations can be represented by rigid "slabs" seems to be implicit in most full-scale instrumentation programs for buildings where strong motion has been recorded so far. Technically, it should be easy to supplement the existing instrumentation to provide data on differential motion of building foundations. Ideally, this should be done first in instrumented buildings where strong motion has already been recorded during many past earthquakes, so that additional value can be added to the existing data, interpretation and analyses.

2. Surface versus Embedded Foundation Models

Following many ambient, forced vibration tests of and earthquakes recorded in Millikan Library (Figure 4) and apparent inconsistencies in the data and its interpretation, Luco et al. (1986) decided in the mid-1970s to develop a comprehensive theoretical model that includes the soil-structure interaction. When this model was completed, the comparison of the recorded motions with those predicted by the model showed that the foundation impedances, available at that time only for rigid surface foundations, were not adequate. This initiated work on refinement of the (rigid foundation) impedance functions to include explicitly the embedment. With the new impedance functions, there was an excellent agreement between the theoretical predictions and the measurements for the NS response. The report on this study could finally be completed, 10 years later (Luco et al., 1986).

3. Experimental Estimates of Impedance Functions

Let H_s and M_s be the horizontal force and moment with which the foundation and the soil interact, resulting from the flexibility of the soil, and let Δ and φ be the corresponding horizontal displacement and rocking angle of the foundation. These four variables are related by

$$H_s = GL\left(K_{HH}\Delta + K_{HM}\, L\varphi\right) \tag{2a}$$

$$M_s = GL^2\left(K_{MH}\Delta + K_{MM}\, L\varphi\right) \tag{2b}$$

where K_{HH}, $K_{HM} = K_{MH}$ and K_{MM} represent the normalized, complex, frequency-dependent impedance functions for the foundation assumed rigid, G is the reference shear modulus of the soil, and L is a characteristic length, which depends on the shape of the foundation.

Numerous analytical and numerical procedures have been developed for computation of frequency-dependent impedance functions. These procedures require simplified representation of the soil medium, usually in terms of parallel homogeneous layers and of infinite extent horizontally. Also, equivalent dynamic soil moduli must be specified on the basis of standard field and laboratory geotechnical tests. Carefully and well-designed full-scale experiments on structures are therefore invaluable to verify those methods and to evaluate the adequacy of the theoretical approximations and selection of the governing parameters.

Luco et al. (1986, 1988) and Wong et al. (1988), for example, have described forced vibration tests of Millikan Library, in which the response at the top of the structure and the translational and rocking response at the base can be used to calculate the force and the moment the foundation exerts on the soil. When the coupling impedances K_{MH} and K_{HM} are small, K_{HH} and K_{MM} can be approximated from experimental measurements. They found excellent agreement between theoretical and experimental estimates of rocking impedance functions, and not so good agreement for the corresponding horizontal impedance functions, particularly for the EW response. They concluded, "These discrepancies in the E-W direction are associated with the failure of the simple foundation model to account for the flexibility of the actual foundation and for the large radiation damping in horizontal vibrations obtained experimentally. It seems then, that if the foundation acts as a rigid body it is possible to predict quite accurately the effects of soil-structure interaction during forced vibration tests by use of simple models. Analytical models more complex than those used in this study may be required for highly flexible foundations" (Wong et al., 1988).

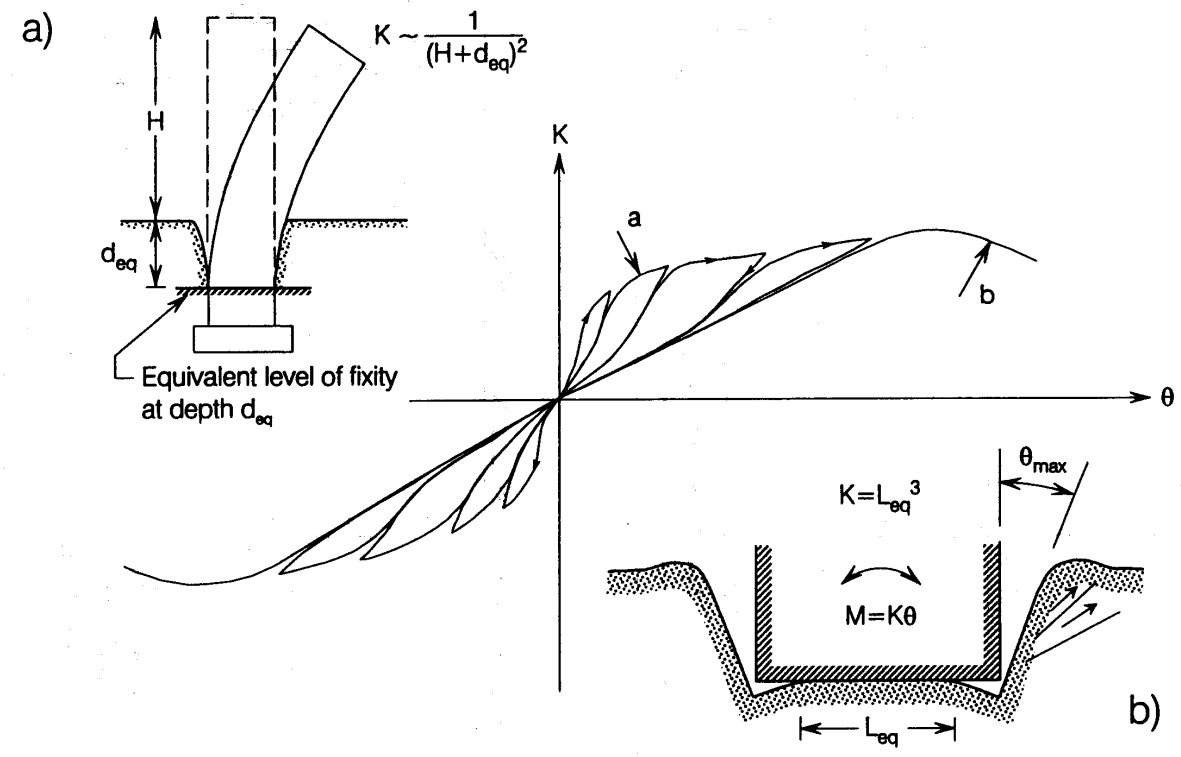

Fig. 6 (a) Non-linear changes in the rocking stiffness caused by passive soil pressure on the sidewalls of the building and variable equivalent depth of fixity d_{eq} (b) A schematic representation of "permanent" soil deformation after large rocking response (from Trifunac et al., 2001c)

4. Torsion

The torsional response in non-symmetric structures is caused by geometrical separation of the centers of mass and of rigidity. For symmetric structures, torsional response may occur because of asymmetry of the foundation system, the wave passage effects (Luco, 1976; Trifunac et al., 1999), accidental torsion (buildings are rarely perfectly symmetric), or from all of the above. Long and narrow symmetric buildings, for example, can experience significant torsional response and whipping (Todorovska and

Trifunac, 1989, 1990b), when excited by earthquake waves propagating along the longitudinal axis of the structure-soil system.

Full-scale measurements of torsional response and of torsional components of soil-structure interaction cannot be performed directly, because, at present, there are no rotational strong motion accelerographs installed in buildings. It is possible to estimate only the average rotations from the differences in translational motions, when there are multiple recorders in the structure arranged accordingly.

The following illustrates thus computed rotations for the Hollywood Storage Building (Figure 1). The locations and orientations of the strong motion accelerographs since 1976 are shown in Figure 1 (bottom). For this instrument configuration, processed strong motion data are available only from four earthquakes: 1987 Whittier-Narrows, 1992 Landers, 1992 Big Bear, and 1994 Northridge. By suitable combination of displacements computed from the recorded accelerograms after double integration, it is possible to estimate the average torsion in the west side of the building. Trifunac et al. (2001d) show that, most of the time, the relative motions of the west side of the roof were about one-half of the motions of the center of the roof (respectively channels 12 and 10 in Figure 3.1 of Trifunac et al., 2001d), and that the two motions were in phase. An exception to this is the response to the 1994 Northridge earthquake, 8 to 12 s after trigger time (see Figure 5.1d in Trifunac et al., 2001d). Thus, most of the time, this building is twisting about a point west of the center of symmetry of the base. A similar behavior was reported by Trifunac et al. (1999) for a seven-story reinforced concrete building in Van Nuys, California, also supported by a pile foundation. For the Hollywood Storage Building, such a behavior may have been caused in part by the non-symmetry of the foundation (the building has a basement only beneath its western half, see Figure 1). Such torsional eccentricity thus causes whipping of the eastern end of the building, particularly for EW arrivals of SH and Love waves (e.g., during Whittier-Narrows, 1987, Landers, 1992, and Big Bear, 1992 earthquakes; see Figure 17 in Todorovska and Trifunac, 1989). Unfortunately, there are no strong motion instruments along the eastern end of Hollywood Storage Building to verify this interpretation.

5. Time and Amplitude-Dependent Response

Trifunac et al. (2001a, 2001b) reported on systematic and significant amplitude-dependent changes of soil-structure system frequency $\tilde{f} = 1/\tilde{T}$ of a seven-story reinforced concrete frame building supported by piles, in Van Nuys, California, damaged by the 1994 Northridge earthquake. They used the conceptual model in Figure 6 to explain the observed changes. This model consists of a building with height H and an embedded foundation. In the initial stages of the response when the amplitudes are small and the soil stiffness is "linear", as the building begins to "push" the soil sideways, its effective depth of "fixity" (indicated by d_{eq} in Figure 6a) changes as a function of the response amplitudes and history. Larger d_{eq} leads to smaller stiffness $K \sim 1/(H + d_{eq})^2$ and smaller $\tilde{f}$. While the building pushes the soil, d_{eq} decreases and K increases ("hardening" behavior). When the direction of motion reverses and the building moves away from the soil, a gap forms between the two, d_{eq} increases and K decreases ("softening" behavior). This results in non-linear system behavior, which can be modeled by a non-linear spring or by a group of springs with gap elements. As the amplitudes of motion increase further, the soil begins to yield and material non-linearity is introduced into the system, reducing or canceling the "hardening" part of the cycle. This behavior repeats as long as the successive amplitudes of vibration increase and the soil can be pushed sideways. At the time of the largest response amplitudes $(\theta_{\max})$, the gap between the building foundation and the soil sidewalls is the largest. By forcing it to yield, the soil can be "compacted" also below the corners of the "rigid" foundation (see Figure 6b), reducing the equivalent length, L_{eq} of the contact between the foundation and the soil, thus resulting in reduction of the system stiffness ($K \sim L_{eq}^3$; Luco et al., 1987) and reduction of $\tilde{f}$. Following the largest amplitudes of response, as the strong motion amplitudes begin to decrease, the depth of "fixity" d_{eq} and the contact length L_{eq} remain constant (many equivalent gap elements remain open). The building responds with smaller amplitudes, and the period of response is longer. Continued shaking, aftershocks and subsequent earthquakes may activate a "healing process". Through dynamic compaction and settlement of the soil material, which was loosened and pushed aside by the preceding strong motion, the soil is packed back

around the piles, grade beams, and sides of the building, thus rebuilding or even increasing the previous system stiffness. It seems that this cycle may be repeated many times, depending on the sequence of aftershocks and earthquakes during the "quiet" intervals between strong motion events.

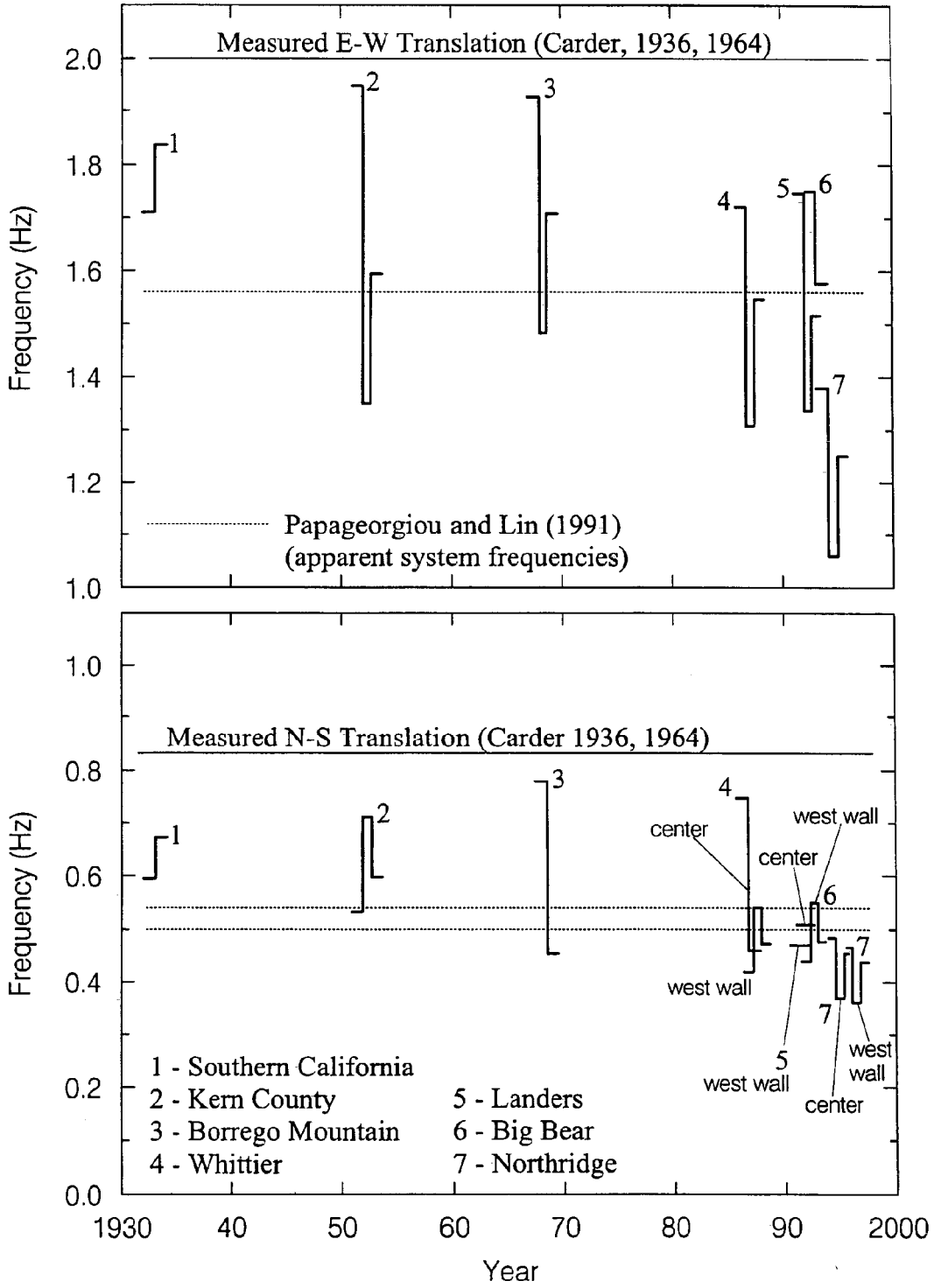

Fig. 7 Hollywood Storage Building: summary of the time-dependent changes of the system frequency during seven earthquakes, between 1933 and 1994 (the horizontal lines show the system frequencies determined from ambient vibration and forced vibration tests (EW and NS translations, light solid lines, Carder, 1936, 1964), and those identified by Papageorgiou and Lin (1991) (dashed lines); for each earthquake, the horizontal ticks represent pre- and post-earthquake estimates of the system frequencies) (from Trifunac et al., 2001d)

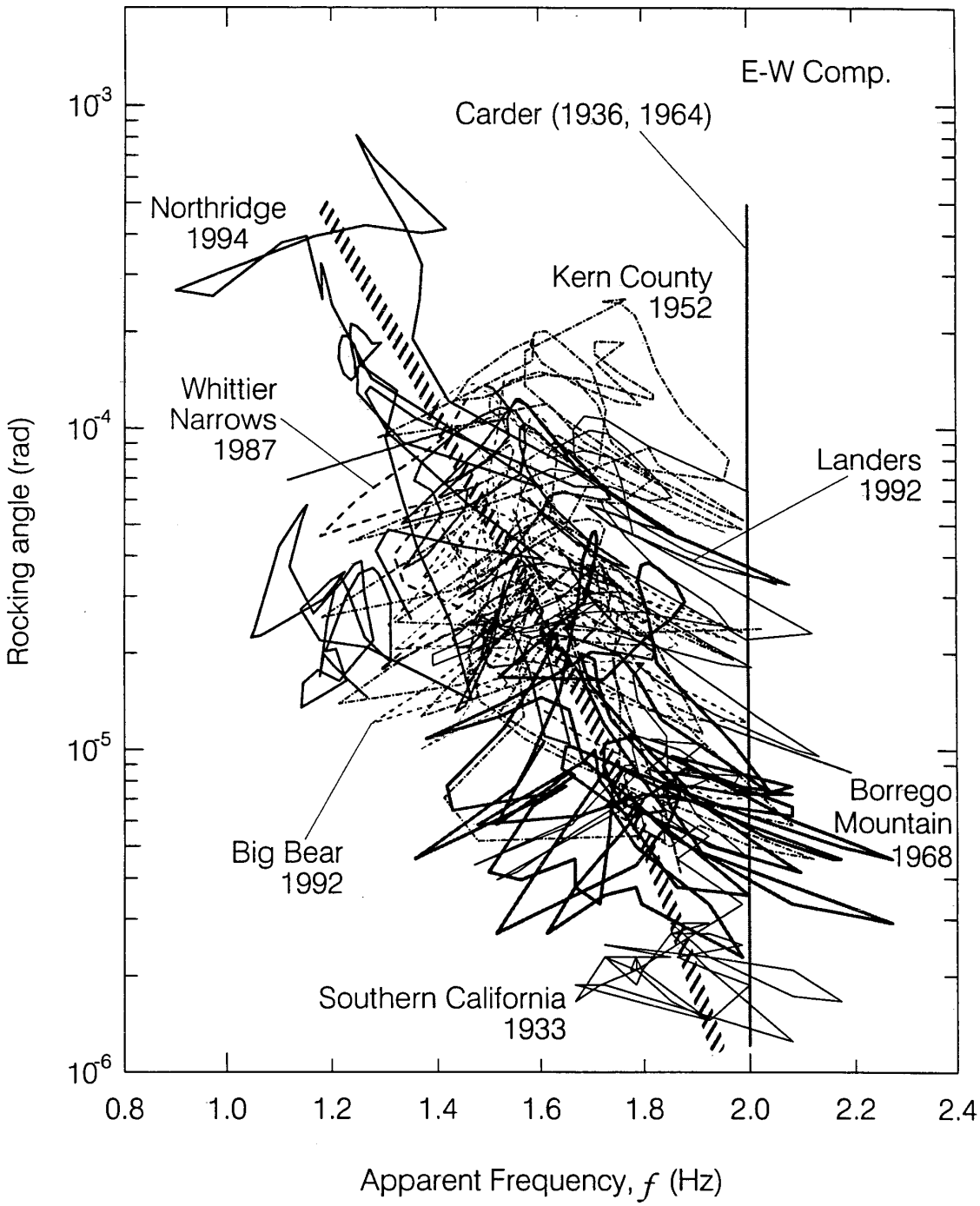

Fig. 8(a) Hollywood Storage Building: dependence of the apparent system frequency on the amplitude of EW response ("rocking angle") (the solid vertical lines show estimates of the system frequencies determined from small amplitude (ambient vibration and forced vibration) tests by Carder (1936, 1964)) (redrawn from Trifunac et al., 2001d)

An interpretation of the data recorded in Hollywood Storage Building, assuming that a similar conceptual model may apply (Trifunac et al., 2001d), is as follows. The system became softer with increasing amplitudes of the ground shaking. For EW motions and for the small shaking during Borrego Mountain Earthquake of 1968, the system frequency was near 1.9 Hz (close to 2.0 Hz as reported by Carder, 1936, 1964). For larger amplitudes of motion, the system frequency decreased, and was near 1.25 Hz for the larger shaking during the 1994 Northridge earthquake. For NS translational response, the system frequency was near 0.6 to 0.7 Hz for small ground shaking (Southern California earthquake of 1933), and fell to ~ 0.45 Hz during the largest recorded motions (Northridge earthquake of 1994). From ambient and forced vibration tests, this frequency was 0.83 Hz (Carder, 1964). The fundamental torsional frequency was reported by Carder (1964) to be in the range of 1.57-1.67 Hz. This frequency was as low as

1.1 Hz during the shaking from the 1992 Landers earthquake (waves arriving from the east). Figure 7 summarizes the above trends. It also shows the EW and NS translational frequencies observed by Carder (1936, 1964). The dashed lines show the apparent system frequencies identified by Papageorgiou and Lin (1991).

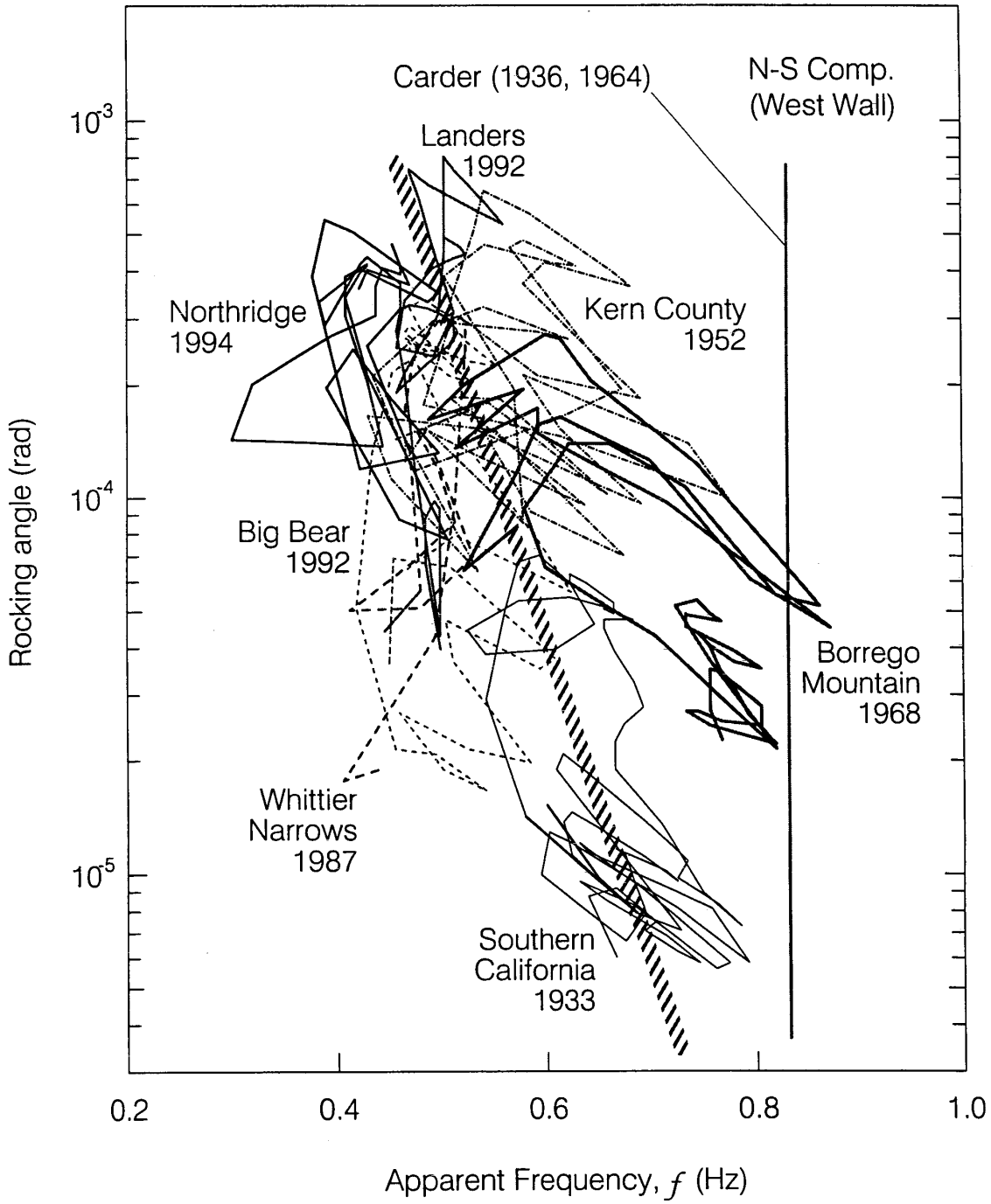

Fig. 8(b) Hollywood Storage Building: dependence of the apparent system frequency on the amplitude of NS response ("rocking angle") (the solid vertical lines show estimates of the system frequencies determined from small amplitude (ambient vibration and forced vibration) tests by Carder (1936, 1964)) (redrawn from Trifunac et al., 2001d)

Figures 8(a) and 8(b) compare the "rocking angles" (displacement at the roof minus displacement at ground level divided by the building height) versus the instantaneous apparent frequency computed for most half-period segments of the response of the Hollywood Storage Building to all seven earthquakes. It can be seen that the apparent system frequency depends on the amplitude of shaking, and for small amplitudes, approaches the frequencies from full-scale ambient and forced vibration tests measured by

Carder (1936, 1964). These trends are consistent with the non-linear soil structure model shown in Figure 6.

It should be noted here that, for the same building analyzed by Trifunac et al. (2001a, 2001b) (a seven-story reinforced concrete building in Van Nuys, California), there have also been more traditional interpretations of the lengthening of the period of the building. For example, De la Llera et al. (2001), Islam (1996), and Li and Jirsa (1998), who analyzed the 1994 Northridge earthquake data, completely ignored the effects of the soil-structure interaction and interpreted the lengthening of the system period to have resulted entirely from structural damage incurred during this earthquake. Both of these conflicting interpretations fit the Northridge response data, which are not adequate to separate uniquely the effects of the soil-structure interaction. In fact, much of the non-uniqueness problem in interpretation of non-linear response of soil-structure systems is due to the fact that most of the current instrumentation in buildings is inadequate to isolate the effects of the soil-structure interaction. For realistic modeling of soil-structure systems, it is very important that the hypotheses that fit earthquake response data are at least narrowed down to a consistent set. This would require much denser instrumentation in structures than currently deployed, deployment of rotational transducers, direct measurement of strain along the contact between the foundation and the soil, and many repeated measurements over a longer period of time and under different levels of excitation.

GENERAL TRENDS IN RESEARCH ON SOIL-STRUCTURE INTERACTION AND FULL-SCALE TESTING

After a brief and productive period, from 1965 to about 1975, when many informative and useful full-scale experiments were conducted (see Luco et al., 1986, for an example of a detailed study of a forced-vibration test, and Ivanović et al., 2000, for a review of ambient vibration tests), the Earthquake Engineering profession seems to have converged toward small-scale laboratory experiments. In 1996, "Earthquake Spectra" (Abrams, 1996) published a theme issue entitled "Experimental Methods". Interestingly, none of the nine papers mentioned or referenced full-scale tests of structures.

Papers dealing with experimental aspects of soil-structure-interaction do not exhibit major fluctuations, and since 1970, appear at an average rate of 3.3/year. Analysis of these papers shows that only about 1.2 papers/year deal with full-scale experiments, about 2/3 of the experimental papers being devoted to laboratory testing. The only year with five papers on full-scale tests involving soil-structure-interaction was 1975. During 1972–1974, 1976, 1979, 1982, 1995, 1997 and 1998 (or 45 percent of the time), there were no contributions in the leading Earthquake Engineering journals. Our search may have missed to identify some papers, but this finding is nevertheless alarming.

It is instructive to consider the trend of the number of papers presented at World Conferences on Earthquake Engineering (WCEE). During the first conference, in 1956 in San Francisco, 40 papers were presented, and during the last two conferences (Acapulco, 1996 and Auckland, 2000) about 1440 papers (each) were presented. The proceedings of the 10th World Conference in Madrid in 1992 were the last to be published in printed form, and the proceedings of the two most recent conferences (11th and 12th) are published on a CD-ROM. Analysis of the percentage of papers dealing with soil-structure interaction, relative to the total number, shows that the largest number of papers was presented in 1988, during the 9th conference, held in Tokyo and Kyoto. The largest percentage of papers devoted to soil-structure interaction was presented in 1973 during the 5th conference. It is seen that the general interest in soil-structure-interaction, at least among researchers and practitioners who publish in World Conference Proceedings, is decreasing.

A more detailed analysis of the above trends for the period 1988 to 1997 in Japan has been presented by Iguchi and Yasui (1999). They find that the number of papers dealing with piles has increased significantly after the 1995 (following Hyogo-Ken Nanbu earthquake).

It is interesting to note that there is a strong correlation between the percentage of papers in WCEE proceedings and the number of papers published in journals, other conferences, and reports, if percentage of papers devoted to soil-structure interaction during world conferences is plotted with a 7 year shift forward relative to the total number of journal papers on the same subject. An explanation may be that the world conferences contribute toward influencing the researchers on what is relevant and useful to work on. The process which begins with recognition that a subject or an idea is worth working on, organization (funding) and actual beginning of work, successful completion of work, submission of the finished papers

to journals, peer review, revisions, and eventual publication, all appear to take, on average, about 7 years. If this is indeed so, it is interesting to contrast this with the typical 5 to 6 years probation period for tenure track assistant professors, or with duration of funding initiatives of the National Science Foundation in United States, for example. All of this is based on an old fashioned assumption that a recognized and true measure of successful completion of a research task is marked by publication in a respectable professional journal.

DISCUSSION AND CONCLUSIONS

1. State of Soil-Structure Interaction Research and Full-Scale Testing

Monitoring earthquake response in and around buildings and comprehensive full-scale tests of structures are the best experimental method for investigating soil-structure interaction, because the scaling and similarity laws problems are eliminated, and because the boundary conditions are satisfied exactly (Trifunac and Todorovska, 1999). Surprisingly, full-scale testing of structures and soil-structure interaction research in the United States (except for piles) has dropped to an alarmingly low level, and the reasons appear to lie in our educational programs. Small-scale laboratory tests and computer simulations are useful for understanding selected phenomena in soil-structure interaction. However, laboratory experiments lack the completeness of the full-scale tests, which is particularly true for investigation of soil-structure interaction phenomena (the semi-infinite soil boundary is practically impossible to model in the laboratory). Laboratory experiments are designed to measure what the researcher has decided to study and may help discover new physics only by accident. On the other hand, the as-built environment contains all the physical properties of reality, and the investigators only need to find ingenious ways to record and interpret them. Obviously, the priorities in earthquake engineering research are not properly balanced and precious time is being lost. If public safety is to be improved and financial losses from future earthquakes are to be reduced, an immediate action is needed to change these trends.

2. Difficulties in Interpreting Earthquake Response Data

The physical completeness and the reality of the full-scale structures are necessary but not sufficient conditions to guarantee correct end results. The discovery and understanding of the true nature of response tend to be born by the difficult labor involving reconciliation between our imperfect theories, modeling and analyses, with often incomplete data from measurements. Experienced experimentalists know that the first test rarely produces results, as we inevitably forget to measure something, or what we measure does not turn out to be useful. Thus, iterations are almost a rule, in both experiments and in the analyses (Trifunac and Todorovska, 1999).

Often, the difficulty in interpreting earthquake response data recorded in buildings lies in the non-uniqueness of the starting models and assumptions. For example, the transfer-functions of horizontal roof displacement of a fixed-base building, and of the same building on flexible soil, have very similar appearance near the first fixed-base frequency, or near the apparent frequency of the soil-structure system. Using a simple identification technique, it is easy to estimate the frequency and the associated fraction of critical damping from full-scale measurements during an earthquake, but it is not easy to identify the factors that control these peaks. The separation of the structure's fixed-base frequency from the rocking and translation frequencies associated with soil-structure interaction is less straightforward and can be performed only if additional instrumentation is available. The list of investigators who overlook this non-uniqueness is so long that it seems that this problem is ignored in most published work. Along the same lines, it is common to find papers presenting analyses of non-linear response of structural components, with discussions of structural ductility and how it relates to the observed changes in the response period, without including in their analyses the fact that, shortly after the earthquake, the apparent period of the soil-structure system was back at or near its pre-earthquake value, suggesting that an important source of non-linearity was not only in the structure, but also in the soil supporting it (Trifunac et al., 2001a, 2001b).

The non-uniqueness in future data can be eliminated in great part by placing additional instruments to measure the rotation of the building foundation (Luco et al., 1986; Moslem and Trifunac, 1986). It is interesting to note that in spite of the fact that transducers that record rotational acceleration and velocity have been constructed and tested (Shibata et al., 1976; Whitcomb, 1969), essentially no buildings are

equipped with such instruments, and so far the earthquake engineers do not seem to request such data.

Rocking of the foundation can be calculated from the difference of recorded vertical motions at two points on a line perpendicular to the axis of rotation. The result represents the average rotations between the two points. To evaluate the actual point rotations, it is necessary to map the pattern of deformations of the building foundation, associated with the apparent frequency of the system prior to and following the earthquake (provided no damage occurred), by using forced vibration or ambient vibration tests, for example. This requires detailed full-scale testing, which has not been done for most buildings (Ivanović et al., 2000).

3. Practical Benefits from Full-Scale Testing

Soil-structure interaction can be used to reduce the structural response, by utilizing and increasing the effects of scattering of the incident waves from the foundation, radiation of the structural vibration energy into the soil, and (under controlled conditions) via non-linear response of the soil (Trifunac and Todorovska, 1999b). Namely, in presence of soil-structure interaction, the system damping depends on the damping in the building and in the soil, and on the scattering of wave energy from and through the foundation (Luco et al., 1986). Design of foundations to scatter efficiently high frequency (short) waves can increase the apparent system damping and can reduce the amplification of the system response near the first mode of vibration (Todorovska and Trifunac, 1992).

Studies of the dissipation of seismic wave energy by scattering of incident waves from the foundation, and by radiation of vibrational energy from the structure into the half-space, are among the oldest topics studied in the subject area of soil-structure interaction (Sezawa and Kanai, 1935, 1936). Modeling the dissipation of energy of a vibrating structure is constrained by the mathematical methods of analysis, and by the lack of comprehensive measurements, which would show the physical nature of this dissipation (Moslem and Trifunac, 1986; Crouse, 1999). Many linear response analyses use normal mode representation and, to maintain the advantages of working with decoupled equations, those approximate the damping matrix by a linear combination $\alpha[m]+\beta[k]$ of the mass and stiffness matrices, $[m]$ and $[k]$, where α and β are constants. For an n degree-of-freedom system, this allows one to choose the damping only for two modal frequencies, ω_i and ω_j, and the remaining $n-2$ modes then have equivalent damping ratios $\zeta = 0.5(\alpha/\omega_k + \beta\omega_k)$, which are not realistic. A common practice is to use constant damping ratios for all mode-shapes in the response analyses. This, of course, ignores the fact that the solution then violates the original differential equations, and can lead to erroneous responses.

Earthquake response records in combination with detailed full-scale testing of structures, before and after significant earthquake shaking, may be used to detect the location and extent of damage in the structure. However, this would require improved models and theory, which can be done through design of more detailed experiments and more detailed earthquake-monitoring instrumentation in building.

It is often assumed that symmetric buildings, supported by symmetric foundations on uniformly layered soil, will experience little or no torsional response. Also, most response analyses ignore torsional excitation caused by the passage of seismic waves across the finite horizontal dimensions of the foundation. Hidden asymmetries in the foundation and structural systems, coupled with the wave passage effects, can result in significant torsional response, which cannot be ignored (Lin et al., 2001). Such asymmetries can be detected only by full-scale tests of structures (using forced vibration, microtremors and recorded earthquake response). Systematic tests on different structures can be carried out to find how widespread these asymmetries are and to estimate them empirically for use in the design process, e.g., via accidental torsion eccentricities.

4. Recommendations

The bulk of processed earthquake response data recorded in buildings is for large amplitude response (e.g., rocking angles greater than 10^{-4} rad). This results in very different system frequency estimates from strong motion response, and from estimates based on microtremor excitation (e.g., see Figures 8(a) and 8(b)). These large differences have led investigators to conclude that the ambient vibration tests are difficult to interpret or are not reliable for inferences on strong motion response. However, as it is seen from Figures 8(a) and 8(b), both strong motion data and ambient vibration tests give mutually consistent

results, and together help determine the expected changes of the system frequencies for a range of response amplitudes. Consequently, to develop sound mathematical models of soil-structure systems, such changes of the system frequencies must be modeled realistically, by incorporating geometric and material non-linearities into the representations of soil and structure. To enable this work, numerous intermediate and small amplitude earthquake recordings in structures must be processed and distributed to researchers. These data will enable researchers to quantify the changes in the system frequencies, and to define empirically how those depend on type of structure, foundation, and on the properties of the underlying soil. Correct estimate of the extent of the variability of the system frequency of structures is important in design as the seismic design coefficient *C(T)* depends on the system period.

The significant changes in the system frequencies shown in Figures 8(a) and 8(b), for the Hollywood Storage Building are not unique to this building and to the soil at this site. Similar changes have been documented for other buildings with and without pile foundations (Luco et al., 1986; Trifunac et al., 2001a, 2001b). The range of system frequency variations, shown in Figures 8(a) and 8(b), is probably similar for many other buildings. This range may become broader for buildings on piles and on very soft soil, and narrower for buildings on stronger soil and on "rock". Thus, the dynamic response analyses of soil-structure systems must be based on models that can incorporate the observed non-linear mechanisms. This, coupled with the fact that most foundation systems of buildings cannot be assumed to be rigid (for purposes of soil-structure interaction analysis), implies that more complex and realistic models must be developed both in research and in design applications. Simple models using equivalent linear single-degree-of-freedom system, supported by rigid foundation on elastic soil, neither have adequate number of degrees-of-freedom, nor have the right physical properties to allow one to model the response of full-scale structures to moderate and strong ground shaking. Ignoring this and fitting simple models to the recorded response of full-scale structures, can only create confusion, erroneous interpretation, and misleading generalizations, all caused by the non-unique nature of the relationships between the hypotheses and the observed data.

The next generation of realistic models of soil-structure systems can be developed and refined only through full-scale studies of buildings and their response to excitations ranging from microtremors, to aftershocks, and all the way to large and destructive motions. To gather key new data and to support future work in full-scale studies of soil-structure interaction, rotational strong motion accelerographs must be added to the existing instrumented structures, or new accelerographs capable of recording three translations and three rotations simultaneously, must be deployed in place of the old instruments which record translation only. Also, the non-linear and time-dependent changes of the system behavior will require defining instantaneous system transfer-functions.

Finally, the above discussion and recommendations are consistent with the discussion and consensus recommendations by the participants of the 1st and 2nd UJNR (U.S.-Japan National Resources) Workshops on Soil-Structure Interaction, which took place in 1998 in Menlo Park, California, and in 2001 in Tsukuba, Japan (Celebi and Okawa, 1999; Building Research Institute, 2001). At both workshops, it was resolved that "research to advance soil-structure interaction methodologies be given high priority and that design provisions related thereto be introduced into the codes, thus enhancing the seismic safety of structures designed accordingly."

ACKNOWLEDGEMENTS

The author is indebted to one of the anonymous reviewers for the many valuable and detailed suggestions, which led to improvement of this paper.

REFERENCES

1. Abdel-Ghaffar, A.M. and Trifunac, M.D. (1977). "Antiplane Dynamic Soil-Bridge Interaction for Incident Plane SH-waves", Earthquake Eng. and Structural Dynamics, Vol. 5, pp. 107-129.
2. Abrams, D.P. (editor) (1996). "Experimental Methods", Earthquake Spectra, Vol. 12, No. 1, pp. 1-80.
3. Biot, M.A. (1932). "Vibrations of Buildings during Earthquake", Chapter II in Ph.D. Thesis No. 259 Entitled "Transient Oscillations in Elastic Systems", Aeronautics Department, Calif. Inst. of Tech., Pasadena, California, U.S.A.

4. Biot, M.A. (1933). "Theory of Elastic Systems Vibrating under Transient Impulse with an Application to Earthquake–Proof Buildings", Proc. National Academy of Sciences, Vol. 19, No. 2, pp. 262-268.
5. Biot, M.A. (1934). "Theory of Vibration of Buildings during Earthquake", Zeitschrift für Angewandte Matematik and Mechanik, Vol. 14, No. 4, pp. 213-223.
6. Biot, M.A. (1941a). "A Mechanical Analyzer for the Prediction of Earthquake Stresses", Bull. Seism. Soc. Amer., Vol. 31, No. 2, pp. 151-171.
7. Biot, M.A. (1941b). "Influence of Foundation on Motion of Blocks", Unpublished Note.
8. Biot, M.A. (1942). "Analytical and Experimental Methods in Engineering Seismology", ASCE Transactions, Vol. 108, pp. 365-408.
9. Blume, J.A. (1936). "The Building and Ground Vibrator", Chapter 7 in "Earthquake Investigations in California 1934-1935", Special Publication No. 201, U.S. Dept. of Commerce, Coast and Geodetic Survey, Washington, D.C., U.S.A.
10. Building Research Institute (2001). "The 2nd UJNR Workshop on SSI", CD ROM Proc., Building Research Institute, Tsukuba, Japan.
11. Carder, D.S. (1936). "Vibration Observation", Chapter 5 in "Earthquake Investigations in California 1934-1935", Special Publication No. 201, U.S. Dept. of Commerce, Coast and Geodetic Survey, pp. 49-106.
12. Carder, D.S. (editor) (1964). "Earthquake Investigations in the Western United States 1931-1964", Publication No. 412, U.S. Dept. of Commerce, Coast and Geodetic Survey.
13. Casirati, M., Castoldi, A., Panzeri, P., Pezzoli, P., Martelli, A. and Masoni, P. (1988). "On-Site Experimental Dynamic Analysis to Assess the Seismic Behavior of the Italian PEC Fast Reactor Building Taking into Account the Soil-Structure Interaction Effect", Proc. Ninth World Conf. on Earthquake Eng., Vol. VI, pp. 741-746.
14. Celebi, M. and Okawa, I. (editors) (1999). "Proc. UJNR Workshop on Soil Structure Interaction, Menlo Park, California, September 22-23, 1998", Open File Report 99-142, U.S. Geological Survey, Menlo Park, California, U.S.A.
15. Chopra, A.K. and Gutierrez, J.A. (1973). "Earthquake Analysis of Multistory Buildings Including Foundation Interaction", Report EERC-73/13, Earthquake Eng. Res. Center, U.C. Berkeley, Berkeley, California, U.S.A.
16. Cloud, W.K. (1978). "Modification of Seismic Waves by a Building", Proc. Sixth European Conf. on Earthquake Eng., Dubrovnik, Yugoslavia, pp. 289-295.
17. Crouse, C.B. and Jennings, P.C. (1975). "Soil-Structure Interaction during the San Fernando Earthquake", Bull. Seism. Soc. Amer., Vol. 65, No. 1, pp. 13-36.
18. Crouse, C.B. (1999). "Energy Dissipation in Soil-Structure Interaction: A Consultant's Perspective", in "Proc. UJNR Workshop on Soil Structure Interaction, Menlo Park, California, September 22-23, 1998", Open File Report 99-142, U.S. Geological Survey, Menlo Park, California, pp. 6/1-17.
19. Crouse, C.B. and Hushmand, B. (1990). "Soil-Structure Interaction and Non-linear Site Response at the Differential Array Accelerograph Station", Proc. 4th U.S. National Conf. on Earthquake Eng., Vol. 3, pp. 815-823.
20. Crouse, C.B., Liang, G.C. and Martin, G.R. (1984). "Experimental Study of Soil-Structure Interaction at an Accelerograph Station", Bull. Seism. Soc. Amer., Vol. 74, No. 15, pp. 1995-2013.
21. Crouse, C.B., Hushmand, B. and Martin, G.R. (1987). "Dynamic Soil-Structure Interaction of a Single-Span Bridge", Earthquake Eng. and Structural Dynamics, Vol. 15, pp. 711-729.
22. de Barros, F.C.P. and Luco, J.E. (1995). "Identification of Foundation Impedance Functions and Soil Properties from Vibration Tests of the Hualien Containment Model", Soil Dynam. and Earthquake Engrg, Vol. 14, No. 4, pp. 229-248.
23. De la Llera, J.C., Chopra, A. and Almazan, J. (2001). "Three-Dimensional Inelastic Response of an RC Building during the Northridge Earthquake", J. of Struct. Engrg, ASCE, Vol. 127, No. 5, pp. 482-489.

24. Douglas, B.M., Maragakis, E.A. and Vrontinos, S. (1990). "Analytical Studies of the Static and Dynamic Response of the Meloland Road Overcrossing", Proc. Fourth U.S. National Conf. on Earthquake Eng., Vol. 1, pp. 987-996.
25. Douglas, B.M., Maragakis, E.A. and Nath, B. (1990). "Static Deformations of Bridges from Quick-Release Dynamic Experiments", J. of Structural Eng., ASCE, Vol. 116, No. 8, pp. 2201-2213.
26. Duke, C.M., Luco, J.E., Carriveau, A.R., Hradilek, P.J., Lastrico, R. and Ostrom, D. (1970). "Strong Earthquake Motion and Site Conditions: Hollywood", Bull. Seism. Soc. Amer., Vol. 60, No. 4, pp. 1271-1289.
27. Ellis, B.R. (1986). "The Significance of Dynamic Soil-Structure Interaction in Tall Buildings", Proc. Instn. Civil Engrs, Vol. 81, Part 2, pp. 221-242.
28. Erdik, M. and Gülkan, P. (1984). "Assessment of Soil-Structure Interaction Effects on Prefabricated Structures", Proc. 8th World Conf. on Earthquake Eng., Vol. III, pp. 913-920.
29. Erdik, M., Yilmaz, C. and Gülkan, P. (1985). "Experimental Assessment of the Soil-Structure Interaction Effects for a Research Reactor", Trans. 8th International Conf. on Structural Mechanics in Reactor Technology, Vol. K(a), Paper K 7/9, pp. 311-316.
30. Ergunay, O. and Erdik, M. (editors) (1981). "State of the Art in Earthquake Engineering: State of the Art Panel Reports Prepared for the Occasion of Seventh World Conference on Earthquake Engineering, September 8-13, 1980, Istanbul, Turkey", Turkish National Committee on Earthquake Eng., Ankara, Turkey, p. 503.
31. Ewing, W.M., Jardetsky, W.S. and Press, F. (1957). "Elastic Waves in Layered Media", McGraw Hill, New York, U.S.A.
32. Foutch, D.A., Luco, J.E., Trifunac, M.D. and Udwadia, F.E. (1975). "Full Scale Three-Dimensional Tests of Structural Deformations during Forced Excitation of a Nine-Story Reinforced Concrete Building", Proc. U.S. National Conf. on Earthquake Eng., pp. 206-215.
33. Fujimori, T., Tsunoda, T., Izumi, M. and Akino, K. (1992). "Partial Embedment Effects on Soil-Structure Interaction", Proc. 10th World Conf. on Earthquake Eng., Vol. 3, pp. 1713-1718.
34. Fukuoka, M. (1977). "Interaction Problems of Well Foundation and Piers", International Symposium on Soil-Structure Interaction, Sarita Prakashan, Vol. I, pp. 537-556.
35. Ganev, T., Nagata, S. and Katayama, T. (1993). "Creation of Database of Earthquake Records from a Reinforced Concrete Tower and Observation of Soil-Structure Interaction Effects", Bull. Earthquake Resistant Structure Research Center, Vol. 26, pp. 57-73.
36. Goel, R. and Chopra, A.K. (1994). "Seismic Response Study of the U.S. 101/Painter Street Overpass Using Strong Motion Records", SMIP 94 Seminar on Seismological and Engineering Implication of Recent Strong Motion Data, California Division of Mines and Geology, pp. 75-88.
37. Gupta, V.K. and Trifunac, M.D. (1990). "A Note on Contributions of Ground Torsion to Seismic Response of Symmetric Multistoried Buildings", Earthquake Eng. and Eng. Vibration, Vol. 10, No. 3, pp. 27-40.
38. Gupta, V.K. and Trifunac, M.D. (1991). "Seismic Response of Multistoried Buildings Including the Effects of Soil Structure Interaction", Soil Dynamics and Earthquake Eng., Vol. 10, No. 8, pp. 414-422.
39. Hadjian, A.H., Tseng, W.S., Tang, Y.K. and Tang, H.T. (1990). "Assessment of Soil-Structure Interaction Practice Based on Synthesized Results from Lotung Experiment - Forced Vibration Tests", Proc. Fourth U.S. National Conf. on Earthquake Engrg, Earthquake Engineering Research Inst., El Cerrito, California, Vol. 3, pp. 845-854.
40. Hayir, A., Todorovska, M.I. and Trifunac, M.D. (2001). "Antiplane Response of a Dyke with Flexible Soil-Structure Interface to Incident SH Waves", Soil Dynamics and Earthquake Eng., Vol. 21, No. 7, pp. 603-613.
41. Housner, G.W. (1957). "Interaction of Building and Ground during an Earthquake", Bull. Seism. Soc. Amer., Vol. 47, pp. 179-186.
42. Housner, G.W. and McCann, G.D. (1949). "The Analysis of Strong-Motion Earthquake Records with the Electric Analog Computer", Bull. Seism. Soc. Amer., Vol. 39, pp. 47-56.

43. Hradilek, P.J., Carriveau, A.R., Saragoni, G.R. and Duke, C.M. (1973). "Evidence of Soil Structure Interaction in Earthquakes", Fifth World Conf. on Earthquake Eng., Rome, Italy, Vol. 2, pp. 2076-2079.
44. Hudson, D.E. (1970). "Dynamic Tests of Full-Scale Structures", Chapter 7 in "Earthquake Engineering (edited by R. Wiegel)", Prentice Hall, New Jersey, U.S.A.
45. Iguchi, M. and Luco, J.E. (1982). "Vibration of Flexible Plate on Viscoelastic Medium", J. of Engng. Mech., ASCE, Vol. 108, No. 6, pp. 1103-1120.
46. Iguchi, M. and Yasui, Y. (1999). "Soil-Structure Interaction Researches Relating to Recent Strong Earthquakes in Japan", in "Proc. UJNR Workshop on Soil Structure Interaction, Menlo Park, California, September 22-23, 1998", Open File Report 99-142, U.S. Geological Survey, Menlo Park, California, U.S.A., pp. 1/1-17.
47. Iguchi, M., Akino, K., Jido, J., Kawamura, S., Ishikawa, Y. and Nakata, M. (1988a). "Large Scale Model Tests on Soil-Reactor Building Interaction, Part I: Forced Vibration Tests", Proc. Ninth World Conf. on Earthquake Eng., Vol. III, pp. 697-702.
48. Iguchi, M., Niwa, M., Tsunoda, T., Nakai, S., Akino, K. and Noguchi, K. (1988b). "Large-Scale Model Tests on Soil-Reactor Building Interaction, Part II: Earthquake Observation", Proc. 9th World Conference on Earthquake Eng., Vol. VIII, pp. 315-320.
49. International Symposium on Soil Structure Interaction (1977). Sarita Prakashan, Meerut.
50. Inukai, T., Imazawa, T., Kusakabe, K. and Yamaoto, M. (1992). "Dynamic Behavior of Embedded Structure on Hard Rock Site", Proc. 10th World Conf. on Earthquake Eng., Vol. 3, pp. 1695-1700.
51. Islam, M.S. (1996). "Analysis of the Response of an Instrumented 7-Story Non-ductile Concrete Frame Building Damaged during the Northridge Earthquake", 1996 Annual Meeting, Los Angeles Tall Buildings Structural Design Council, Professional Paper No. 96-9.
52. Ivanović, S.S., Trifunac, M.D. and Todorovska, M.I. (2000). "Ambient Vibration Tests of Structures – A Review", ISET Journal of Earthquake Technology, Vol. 37, No. 4, pp. 165-197.
53. Kaino, T. and Kikuchi, T. (1988). "Earthquake Response of Pier with Caisson-Type Wall Foundation and its Analysis", Proc. Ninth World Conf. on Earthquake Eng., Vol. III, pp. 751-756.
54. Kanai, K. (1983). "Engineering Seismology", Univ. of Tokyo Press, Tokyo, Japan.
55. Kanai, K. and Suzuki, T. (1953). "Relation between the Property of Building Vibration and the Nature of Ground", Bull. Earthq. Res. Inst., Vol. 31, pp. 301-317.
56. Kanai, K., Suzuki, T., Hisada, T. and Nakagawa, K. (1955a). "Vibration Experiments in the Buildings on Various Kinds of Ground, I", Report Archit. Inst., Japan, Vol. 33, p. 185.
57. Kanai, K., Tanaka, T. and Suzuki, T. (1955b). "Relation between the Property of Building Vibration and the Nature of Ground", Bull. Earthq. Res. Inst., Vol. 34, p. 61.
58. Kanai, K., Kishinouye, F. and Nasu, N. (1958a). "Vibration of Reinforced Concrete Building Moved with Vibration Generators", Bull. Earthq. Res. Inst., Vol. 36, pp. 165-182.
59. Kanai, K., Tanaka, T. and Suzuki, T. (1958b). "Rocking and Elastic Vibrations of Actual Building I (Experiments with Vibration Generator)", Bull. Earthq. Res. Inst., Vol. 36, pp. 183-199.
60. Kanai, K., Tanaka, T. and Suzuki, T. (1958c). "Rocking and Elastic Vibrations of Actual Buildings II (Observation of Earthquake Motion)", Bull. Earthq. Res. Inst., Vol. 36, pp. 201-226.
61. Kashima, T. and Kitagawa, Y. (1988). "Observation and Analysis of Earthquake Motions in and around the SRC Building as Local Earthquake Instrument Array System", Proc. Ninth World Conf. on Earthquake Eng., Vol. III, pp. 721-726.
62. Kimura, T., Kusakabe, O. and Takemura, J. (editors) (1998). "Centrifuge 98", Balkema, Rotterdam, Netherlands.
63. Kitada, Y., Kinoshita, M., Iguchi, M. and Fukuwa, N. (1999). "Soil-Structure Interaction Effect on an NPP Reactor Building - Activities of NPEC, Achievements and the Current Status", in "Proc. UJNR Workshop on Soil Structure Interaction, Menlo Park, California, September 22-23, 1998", Open File Report 99-142, U.S. Geological Survey, Menlo Park, California, pp. 18/1-14.

64. Krishna, J. (1981). "On Earthquake Engineering", in "State of the Art in Earthquake Engineering, 1981 (edited by O. Ergunay and M. Erdik)", Kelaynak Publishing House, Ankara, Turkey.

65. Lee, V.W. (1979). "Investigation of Three-Dimensional Soil-Structure Interaction", Report 79-11, Dept. of Civil Eng., Univ. of Southern California, Los Angeles, California, U.S.A.

66. Lee, V.W., Trifunac, M.D. and Feng, C.C. (1982). "Effects of Foundation Size on Fourier Spectrum Amplitudes of Earthquake Acceleration Recorded in Buildings", Soil Dynamics and Earthquake Eng., Vol. 1, No. 2, pp. 52-58.

67. Li, Y.R. and Jirsa, J.O. (1998). "Non-linear Analyses of an Instrumented Structure Damaged in the 1994 Northridge Earthquake", Earthquake Spectra, Vol. 14, No. 2, pp. 265-283.

68. Liou, G.-S. and Huang, P.H. (1994). "Effect of Flexibility on Impedance Functions for Circular Foundations", J. of Engng. Mech., ASCE, Vol. 120, No. 7, pp. 1429-1446.

69. Lin, W.H., Chopra, A.K. and De la Llera, J.C. (2001). "Accidental Torsion in Buildings: Analysis versus Earthquake Motions", J. Structural Eng., ASCE, Vol. 127, No. 5, pp. 475-481.

70. Luco, J.E. (1969a). "Application of Singular Integral Equations on the Problem of Forced Vibrations of a Rigid Foundation", Ph.D. Thesis, University of California, Los Angeles, California, U.S.A.

71. Luco, J.E. (1969b). "Dynamic Interaction of a Shear Wall with the Soil", J. Eng. Mechanics Division, ASCE, Vol. 95, pp. 333-346.

72. Luco, J.E. (1976). "Torsional Response of Structures to Obliquely Incident Seismic SH Waves", Earthquake Eng. and Structural Dynamics, Vol. 4, No. 3, pp. 207-219.

73. Luco, J.E. (1980). "Linear Soil Structure Interaction", in "Seismic Safety Margins Research Program (Phase I)", U.S. Nuclear Regulatory Commission, Washington, D.C., U.S.A.

74. Luco, J.E., Trifunac, M.D. and Udwadia, F.E. (1975). "An Experimental Study of Ground Deformations Caused by Soil-Structure Interaction", Proc. U.S. National Conf. on Earthquake Eng., pp. 136-145.

75. Luco, J.E., Wong, H.L. and Trifunac, M.D. (1975). "A Note on Dynamic Response of Rigid Embedded Foundations", Earthquake Eng. and Structural Dynamics, Vol. 4, pp. 119-127.

76. Luco, J.E., Wong, H.L., and Trifunac, M.D. (1986). "Soil-Structure Interaction Effects on Forced Vibration Tests", Report 86-05, Dept. of Civil Engrg, University of Southern California, Los Angeles, California, U.S.A.

77. Luco, J.E., Trifunac, M.D. and Wong, H.L. (1987). "On the Apparent Change in Dynamic Behavior of a Nine-Story Reinforced Concrete Building", Bull. Seism. Soc. Amer., Vol. 77, No. 6, pp. 1961-1983.

78. Luco, J.E., Trifunac, M.D. and Wong, H.L. (1988). "Isolation of Soil-Structure Interaction Effects by Full-Scale Forced Vibration Tests", Earthquake Eng. and Structural Dynamics, Vol. 16, pp. 1-21.

79. Luco, J.E. and Wong, H.L. (1990). "Forced Vibration of Lotung Containment Model: Theory and Observations", J. Engrg Mech., Vol. 116, No. 4, pp. 845-861.

80. Maragakis, E., Douglas, B.M., Hagne, S. and Sharma, V. (1996). "Full-Scale Resonance Tests of a Railway Bridge", in "Building an International Community of Structural Eng.", Proc. Structures Congress XIV, Chicago, U.S.A., Vol. 1, pp. 183-190.

81. McLean, F.G. and Ko, H.-Y. (1991). "Centrifuge 91", Balkema, Rotterdam, Netherlands.

82. Merritt, R.G. (1953). "Effect of Foundation Compliance on the Earthquake Stresses in Typical Buildings", Ph.D. Thesis, Calif. Inst. of Tech., Pasadena, California, U.S.A.

83. Merritt, G.H. and Housner, G.W. (1954). "Effects of Foundation Compliance on Earthquake Stresses in Multistory Buildings", Bull. Seism. Soc. Amer., Vol. 44, No. 4, pp. 551-569.

84. Mizuno, H. (1978). "Effect of Dynamic Inputs on Structure-Soil-Structure Interaction", Proc. 5th Japan Earthquake Eng. Symposium, Paper 68, pp. 539-544.

85. Mizuno, H. (1980). "Effects of Structure-Soil-Structure Interaction during Various Excitations", Proc. 7th World Conf. on Earthquake Eng., Vol. 5, pp. 149-156.

86. Mizuno, N. and Tsushima, Y. (1975). "Experimental and Analytical Studies for a BWR Nuclear Reactor Building, Evaluation of Soil-Structure Interaction Behavior", Trans. 3rd International Conf. on Structural Mechanics in Reactor Technology, Vol. 4, Paper K3/2, pp. 1-13.

87. Moslem, K. and Trifunac, M.D. (1986). "Effects of Soil Structure Interaction on the Response of Buildings during Strong Earthquake Ground Motions", Report 86-04, Dept. of Civil Engrg, Univ. of Southern California, Los Angeles, California, U.S.A.

88. Moslem, K. and Trifunac, M.D. (1987). "Spectral Amplitudes of Strong Earthquake Acceleration Recorded in Buildings", Soil Dynamics and Earthquake Eng., Vol. 6, No. 2, pp. 100-107.

89. Muria-Vila, D. and Alcorta, R.G. (1992). "Soil-Structure Interaction Effects in a Building", Proc. Tenth World Conf. on Earthquake Eng., Vol. 3, pp. 1905-1910.

90. Ohtsuka, Y., Fukuoka, A., Yanagisawa, E. and Fukudome, H. (1992). "Embedment Effect on Dynamic Soil-Structure Interaction", Proc. 10th World Conf. on Earthquake Eng., Vol. 3, pp. 1707-1712.

91. Ohtsuka, Y., Fukuoka, A., Akino, K. and Ishida, K. (1996). "Experimental Studies on Embedment Effects on Dynamic Soil-Structure Interaction", Proc. 11th World Conf. on Earthquake Eng., Disc 1, Paper 59.

92. Papageorigiou, A.S. and Lin, B.C. (1991). "Analysis of Recorded Earthquake Response and Identification of a Multi-story Structure Accounting for Foundation Interaction Effects", Soil Dynamics and Earthquake Eng., Vol. 10, No. 1, pp. 5-64.

93. Petrovski, J. (1975). "Evaluation of Soil Structure Interaction Parameters from Dynamic Response of Embedded Footing", Proc. 5th European Conf. on Earthquake Eng., Vol. 1, Paper 43, pp. 1-8.

94. Petrovski, J. (1978). "Influence of Soil-Structure Interaction Effects on Dynamic Response of Large Panel Prefabricated Buildings", Proc. Second International Conf. on Microzonation for Safer Construction - Research and Application, Vol. III, pp. 1269-1277.

95. Ramirez-Centeno, M. and Ruiz-Sandoval, M. (1996). "Experimental Study of the Soil-Structure Interaction Effects on Three Different Kinds of Accelerometric Bases", Proc. 11th World Conf. on Earthquake Eng., Disc 2, Paper 719.

96. Richardson, J.A. and Douglas, B.M. (1993). "Results from Field Testing a Curved Box Girder Bridge Using Simulated Earthquake Loads", Earthquake Eng. and Structural Dynamics, Vol. 22, No. 10, pp. 905-922.

97. Safak, E. (1992). "On Identification of Soil-Structure Interaction from Recorded Motions of Buildings", Proc. Tenth World Conf. on Earthquake Eng., Vol. 3, pp. 1885-1890.

98. Serino, G. and Fenves, G.L. (1990). "Evaluation of Soil-Structure Effects in the Earthquake Response of a Building", Proc. Fourth U.S. Conf. on Earthquake Eng., Vol. 3, pp. 895-904.

99. Sezawa, K. and Kanai, K. (1935). "Decay in the Seismic Vibration of a Simple or Tall Structure by Dissipation of Their Energy into the Ground", Bull. Earth. Res. Inst., Vol. XIII, Part 3, pp. 681-697.

100. Sezawa, K. and Kanai, K. (1936). "Improved Theory of Energy Dissipation in Seismic Vibrations in a Structure", Bull. Earth. Res. Inst., Vol. XIV, Part 2, pp. 164-168.

101. Shibata, H., Shigeta, T. and Sone, A. (1976). "A Note on Some Results of Observation of Torsional Ground Motions and Their Response Analysis", Bull. Earthquake Resistant Struct. Research Center, Vol. 10, pp. 43-47.

102. Shinozaki, Y., Kobori, T., Nagashima, I., Nakamura, M. and Ichikawa, M. (1994). "Soil-Structure Interaction Tests of Five-Story Steel-Frame Building by Servo Hydraulic-Type Vibrator: Part 2" (in Japanese), Jour. of Structural and Construction Eng., Transactions AIJ, Vol. 465, pp. 53-59.

103. Shioya, K. and Yamahara, H. (1980). "Study on Filtering Effect of Foundation Slab Based on Observational Records", Seventh World Conf. on Earthquake Eng., Istanbul, Turkey, Vol. 5, pp. 181-188.

104. Stewart, J.P. and Stewart, A.F. (1997). "Analysis of Soil-Structure Interaction Effects on Building Response from Strong Earthquake Recording at 58 Sites", Report EERC-97/01, Univ. Cal. Berkeley, Berkeley, California, U.S.A.

105. Suyehiro, K. (1932). "Engineering Seismology Notes on American Lectures", Proc. ASCE, Vol. 58, No. 4, pp. 1-110.

106. Tang, H.T., Tang, Y.K., Stepp, J.C., Wall, I.B., Lin, E., Chang, S.C. and Lee, S.K. (1989). "A Large-Scale Soil-Structure Interaction Experiment: Design and Construction", Nuclear Eng. and Design, Vol. III, pp. 371-379.

107. Tobita, J., Fukuwa, N. and Yagi, S. (2000). "Experimental Evaluation of Dynamic Characteristics of Low and Medium-Rise Buildings with Soil-Structure Interaction", Proc. 12th World Conf. on Earthquake Eng., Paper 2244.

108. Todorovska, M.I. and Trifunac, M.D. (1989). "Antiplane Earthquake Waves in Long Structures", J. Engrg. Mech., ASCE, Vol. 115, No. 12, pp. 2687-2708.

109. Todorovska, M.I. and Trifunac, M.D. (1990a). "Analytical Model for Building Foundation Soil Interaction: Incident P, SV and Rayleigh Waves", Report 90-01, Dept. of Civil Eng., Univ. of Southern California, Los Angeles, California, U.S.A.

110. Todorovska, M.I. and Trifunac, M.D. (1990b). "A Note on the Propagation of Earthquake Waves in Buildings with Soft First Floor", J. Engrg Mech., ASCE, Vol. 116, No. 4, pp. 892-900.

111. Todorovska, M.I. and Trifunac, M.D. (1991). "Radiation Damping during Two-Dimensional Building-Soil Interaction", Report CE 91-01, Dept. of Civil Eng., Univ. of Southern California, Los Angeles, California, U.S.A.

112. Todorovska, M.I. and Trifunac, M.D. (1992a). "Effects of the Input Base Rocking on the Response of Long-Buildings on Embedded Foundations", European Earthquake Eng., Vol. VI, No. 1, pp. 36-46.

113. Todorovska, M.I. and Trifunac, M.D. (1992b). "The System Damping, the System Frequency and the System Response Peak Amplitudes during In-plane Building-Soil Interaction", Earthquake Engrg and Struct. Dynam., Vol. 21, No. 2, pp. 127-144.

114. Todorovska, M.I. and Trifunac, M.D. (1993). "The Effects of Wave Passage on the Response of Base Isolated Buildings in Rigid Embedded Foundation", Report CE 93-10, Dept. of Civil Eng., Univ. of Southern California, Los Angeles, California, U.S.A.

115. Todorovska, M.I., Hayir, A. and Trifunac, M.D. (2001a). "Antiplane Response of a Dike on Flexible Embedded Foundation to Incident SH-Waves", Soil Dynamics and Earthquake Eng., Vol. 21, No. 7, pp. 593-601.

116. Todorovska, M.I., Hayir, A. and Trifunac, M.D. (2001b). "Flexible versus Rigid Foundation Models of Soil-Structure Interaction: Incident SH-Waves", Proc. 2nd U.S.-Japan Workshop on Soil Structure Interaction, Tsukuba City, Japan.

117. Tohma, J., Ohmoto, K., Kurimoto, M. and Arii, K. (1985). "Experimental Study on Dynamic Soil-Structure Interaction", Trans. 8th International Conf. on Structural Mechanics in Reactor Technology, Vol. K(a), Paper K 7/3, pp. 287-292.

118. Toki, K. and Kiyono, J. (1992). "Seismic Analysis of Non-linear Soil-Structure Interaction System Using a Hybrid Experiment", Proc. 10th World Conf. on Earthquake Eng., Vol. 3, pp. 1839-1844.

119. Trifunac, M.D. (1970a). "Wind and Microtremor Induced Vibrations of a 22-Story Steel Frame Building", Report EERL 70-01, Earthquake Engrg Res. Lab., Calif. Inst. of Tech., Pasadena, California, U.S.A.

120. Trifunac, M.D. (1970b). "Ambient Vibration Test of a 39-Story Steel Frame Building", Report EERL 70-01, Earthq. Engrg Res. Lab., Calif. Inst. of Tech., Pasadena, California, U.S.A.

121. Trifunac, M.D. (1972a). "Comparison between Ambient and Forced Vibration Experiments", Earthq. Engrg and Struct. Dynam., Vol. 1, pp. 133-150.

122. Trifunac, M.D. (1972b). "Interaction of Shear Wall with the Soil for Incident Plane SH Waves", Bull. Seism. Soc. Amer., Vol. 62, No. 1, pp. 63-83.

123. Trifunac, M.D. (1997). "Differential Earthquake Motion of Building Foundations", J. of Structural Engrg, ASCE, Vol. 123, No. 4, pp. 414-422.

124. Trifunac, M.D. and Todorovska, M.I. (1997). "Response Spectra and Differential Motion of Columns", Earthquake Eng. and Structural Dynamics, Vol. 26, No. 2, pp. 251-268.

125. Trifunac, M.D. and Todorovska, M.I. (1998). "Non-linear Soil Response as a Natural Passive Isolation Mechanism - the 1994 Northridge, California, Earthquake", Soil Dynam. and Earthquake Engrg., Vol. 17, No. 1, pp. 41-51.

126. Trifunac, M.D. and Todorovska, M.I. (1999a). "Recording and Interpreting Earthquake Response of Full Scale Structures", Proc. NATO Advanced Research Workshop on Strong Motion Instrumentation for Civil Eng. Structures, Istanbul, Turkey.

127. Trifunac, M.D. and Todorovska, M.I. (1999b). "Reduction of Structural Damage by Non-linear Soil Response", J. Structural Eng., ASCE, Vol. 125, No. 1, pp. 89-97.

128. Trifunac, M.D. and Todorovska, M.I. (1999c). "Relative Flexibility of a Building Foundation", in "Proc. UJNR Workshop on Soil Structure Interaction, Menlo Park, California, September 22-23, 1998", Open File Report 99-142, U.S. Geological Survey, Menlo Park, California, pp. 17/1-20.

129. Trifunac, M.D., Ivanović, S.S., Todorovska, M.I., Novikova, E.I. and Gladkov, A.P. (1999). "Experimental Evidence for Flexibility of a Building Foundation Supported by Concrete Friction Piles", Soil Dynamics and Earthquake Eng., Vol. 18, No. 3, pp. 169-187.

130. Trifunac, M.D., Hao, T.Y. and Todorovska, M.I. (2001a). "On Energy Flow in Earthquake Response", Report CE 01-03, Dept. of Civil Eng., Univ. of Southern California, Los Angeles, California, U.S.A.

131. Trifunac, M.D., Ivanović, S.S. and Todorovska, M.I. (2001b). "Apparent Periods of a Building, Part I: Fourier Analysis", J. of Structural Engrg, ASCE, Vol. 127, No. 5, pp. 517-526.

132. Trifunac, M.D., Ivanović, S.S. and Todorovska, M.I. (2001c). "Apparent Periods of a Building, Part II: Time-Frequency Analysis", J. of Structural Engrg, ASCE, Vol. 127, No. 5, pp. 527-537.

133. Trifunac, M.D., Hao, T.Y. and Todorovska, M.I. (2001d). "Response of a 14 Story Reinforced Concrete Structure to Excitation by Nine Earthquakes: 61 Years of Observation in the Hollywood Storage Building", Report CE 01-02, Dept. of Civil Eng., Univ. of Southern California, Los Angeles, California, U.S.A.

134. Tuzuki, M., Inada, O., Yamaguchi, M., Yahata, K., Naito, Y. and Kitamura, E. (1992). "Field Testing and Analysis of Dynamic Loaded Pile Group", Proc. 10th World Conf. on Earthquake Eng., Vol. 3, pp. 1787-1790.

135. Uchiyama, S., Suzuki, Y. and Konno, T. (1992). "Dynamic Tests of Concrete Block on Gravel Deposits", Proc. 10th World Conf. on Earthquake Eng., Vol. 3, pp. 1859-1864.

136. Udwadia, F.E. and Trifunac, M.D. (1974). "Time and Amplitude Dependent Response of Structures", Earthquake Engrg and Struct. Dynam., Vol. 2, pp. 359-378.

137. Ucshima, T., Sawada, Y., Yajima, H., Ohtomo, K. and Sawada, M. (1988). "Dynamic Characteristics of Large Structure 'JOYO' Deeply Embedded in Quaternary Ground and Evaluation of Embedment Effect", Proc. 9th World Conf. on Earthquake Eng., Vol. III, pp. 739-744.

138. Urao, K., Masuda, K., Kitamura, E., Sasaki, F., Ueno, K., Miyamoto, Y. and Mori, T. (1988). "Forced Vibration Test and its Analytical Study for Embedded Foundation Supported by Pile Group", Proc. Ninth World Conf. on Earthquake Eng., Vol. III, pp. 673-678.

139. Ventura, C.E., Finn, W.D.L. and Felber, A.J. (1995). "Ambient Vibration Study of the Painter Street Overpass", Seventh Canadian Conf. on Earthquake Eng., pp. 787-794.

140. Watakabe, M., Matsumoto, H., Ariizumi, K., Fukahori, Y., Shikama, Y., Yamanouchi, K. and Kuniyoshi, H. (1992). "Earthquake Observation of Deeply Embedded Building Structure", Proc. Tenth World Conf. on Earthquake Eng., Vol. 3, pp. 1831-1838.

141. Werner, S.D., Lee, L.C., Wong, H.L. and Trifunac, M.D. (1977). "An Evaluation of the Effects of Traveling Seismic Waves on the Three-Dimensional Response of Structures", Report R07730-4514, Agbabian Associates, El Segundo, California, U.S.A.

142. Werner, S.D., Lee, L.C., Wong, H.L. and Trifunac, M.D. (1979). "Structural Response to Traveling Seismic Waves", J. of Structural Div., ASCE, Vol. 105, No. ST12, pp. 2547-2564.

143. Werner, S.D., Crouse, C.B., Katafygiotis, L.S. and Beck, J.L. (1994). "Use of Strong Motion Records for Model Evaluation on Seismic Analysis of a Bridge Structure", Fifth U.S. National Conf. on Earthquake Eng., Vol. I, pp. 511-520.

144. Whitcomb, J. (1969). "Detecting of SH-Type Seismic Shear Waves by Means of Angular Accelerometers", U.S. Geol. Survey, Professional Paper No. 599-D.

145. Whitley, J.R., Morgan, J.R., Hall, W.J. and Newmark, N.M. (1977). "Base Response Arising from Free-Field Motion", Trans. 4th International Conf. on Structural Mechanics in Reactor Technology, Vol. K2/15, pp. 1-10.

146. Wolf, J.P. (1985). "Dynamic Soil-Structure Interaction", Prentice-Hall, Englewood Cliffs, New Jersey, U.S.A.

147. Wolf, J.P. (1994). "Foundation Vibration Analysis Using Simple Physical Models", Prentice-Hall, Englewood Cliffs, New Jersey, U.S.A.

148. Wong, H.L. and Trifunac, M.D. (1974). "Interaction of a Shear Wall with the Soil for Incident Plane SH Waves: Elliptical Rigid Foundation", Bull. Seism. Soc. Amer., Vol. 64, pp. 1825-1842.

149. Wong, H.L. and Trifunac, M.D. (1975). "Two-Dimensional, Antiplane, Building-Soil-Building Interaction for Two or More Buildings and for Incident Plane SH-Waves", Bull. Seism. Soc. Amer., Vol. 65, pp. 1863-1885.

150. Wong, H.L., Trifunac, M.D. and Lo, K.K. (1976). "Influence of Canyon on Soil-Structure Interaction", J. Eng. Mechanics Div., ASCE, Vol. 102, No. EM4, pp. 671-684.

151. Wong, H.L., Luco, J.E. and Trifunac, M.D. (1977). "Contact Stresses and Ground Motion Generated by Soil-Structure Interaction", Earthquake Eng. and Structural Dynamics, Vol. 5, pp. 67-79.

152. Wong, H.L., Trifunac, M.D. and Luco, J.E. (1988). "A Comparison of Soil Structure Interaction Calculations with Results of a Full-Scale Forced Vibration Test", Soil Dynamics and Earthquake Eng., Vol. 7, No. 1, pp. 22-31.

153. Wong, H.L. and Luco, J.E. (1990). "Seismic Response of Lotung Containment Model: Theory and Observations", J. Engrg Mech., Vol. 116, No. 6, pp. 1332-1350.

154. Yahata, K., Naito, Y., Urao, K., Nakayama, T., Inada, O., Mori, F. and Tuzuki, M. (1992). "Full Scale Vibration Test on Pile-Structure and Analysis", Proc. 10th World Conf. on Earthquake Eng., Vol. 3, pp. 1781-1786.

ISET Journal of Earthquake Technology, Paper No. 416, Vol. 39, No. 1-2, March-June 2002, pp. 21-53

ENERGY OF EARTHQUAKE RESPONSE – RECENT DEVELOPMENTS

Tzong-Ying Hao
Department of Civil Engineering, University of Southern California
Los Angeles, CA 90089-2531, U.S.A.

ABSTRACT

This paper reviews research related to energy methods for earthquake-resistant design of structures, with an emphasis on the most recent developments, which for the first time consider all the stages of the seismic energy flow, starting from the earthquake source, and including the effects of the soil-structure interaction. Results are presented for five case studies (four reinforced concrete buildings and one steel structure). For these buildings, the correspondence between the total incident wave energy and the sum of all energies associated with the response of their soil-structure systems is analyzed. Some elementary aspects of design, based on the power of the incident wave pulses, are discussed. It is shown how this power can be compared with the capacity of the structure to absorb the incident wave energy. The advantages of using the computed power of incident strong motion to design a structure for linear or for partially destructive relative response are discussed.

KEYWORDS: Flow of Earthquake Energy, Non-linear Soil Response, Soil-Structure Interaction, Energy Absorption Capacity, Earthquake Resistant Design

INTRODUCTION

1. General

Spatial distributions of earthquake damage are far too complicated and can change over so short distances (Trifunac and Todorovska, 1997a, 1997b, 1998a, 1998b, 1998c, 1998d, 1999) that it is not possible, at present, to associate those with same amplitude characteristics of recorded motions. The most densely instrumented metropolitan areas still have too sparse distributions of strong motion accelerographs (e.g., Trifunac and Todorovska, 2001) to help identify the principal causes of damage. Numerous empirical correlations of the degree of damage versus simple indicators of the severity of strong motion (e.g., peak velocity, site intensity) have been published, but only limited results exist on the use of energy and power of incident strong motion waves. Before such correlations are initiated, it seems appropriate to review the details of energy flow through a soil-foundation-structure system, so that the nature of motion leading to damage, geographically, and within a structure may be understood (Trifunac and Hao, 2001; Trifunac et al., 1999b, 2001d, 2001e).

Traditionally, displacement ductility has been used as a criterion for earthquake-resistant design of structures. Alternative energy-related concepts were discussed by Benioff (1934), Sezawa and Kanai (1936), Tanabashi (1937), and later by Tanabashi (1956), Housner (1956) and Blume (1960). Figure 1 outlines the milestones of the work on earthquake-resistant design, the years of the significant earthquakes (from earthquake engineering point of view), and the years of the World Conferences on Earthquake Engineering.

In 1934, Benioff proposed a measure of seismic destructiveness to be computed via the area under the relative displacement response spectrum. It can be shown that this result can be related to the energy of response to strong motion (Arias, 1970; Trifunac and Brady, 1975). Benioff did not discuss strong motion energy explicitly. However, his definition of destructiveness as "the integral with respect to pendulum frequency of the maximum displacement of an infinite series of undamped pendulums" is directly related to the energy of response.

The current seismic design codes describe the earthquake excitation as an acceleration response spectrum, which prescribes the required horizontal loads representing a design earthquake. An acceleration response spectrum displays the maximum absolute acceleration response, and its shape reflects the frequency content of the excitation (Biot, 1932, 1933, 1934, 1941, 1942). Although the acceleration response spectra provide a convenient tool for quantifying an earthquake input, research

indicates that this is not sufficient for expressing the damage potential of earthquake ground motion. The seismic energy input, and the seismic energy dissipation during strong shaking, can represent the damage potential of an earthquake ground motion more directly than spectral acceleration.

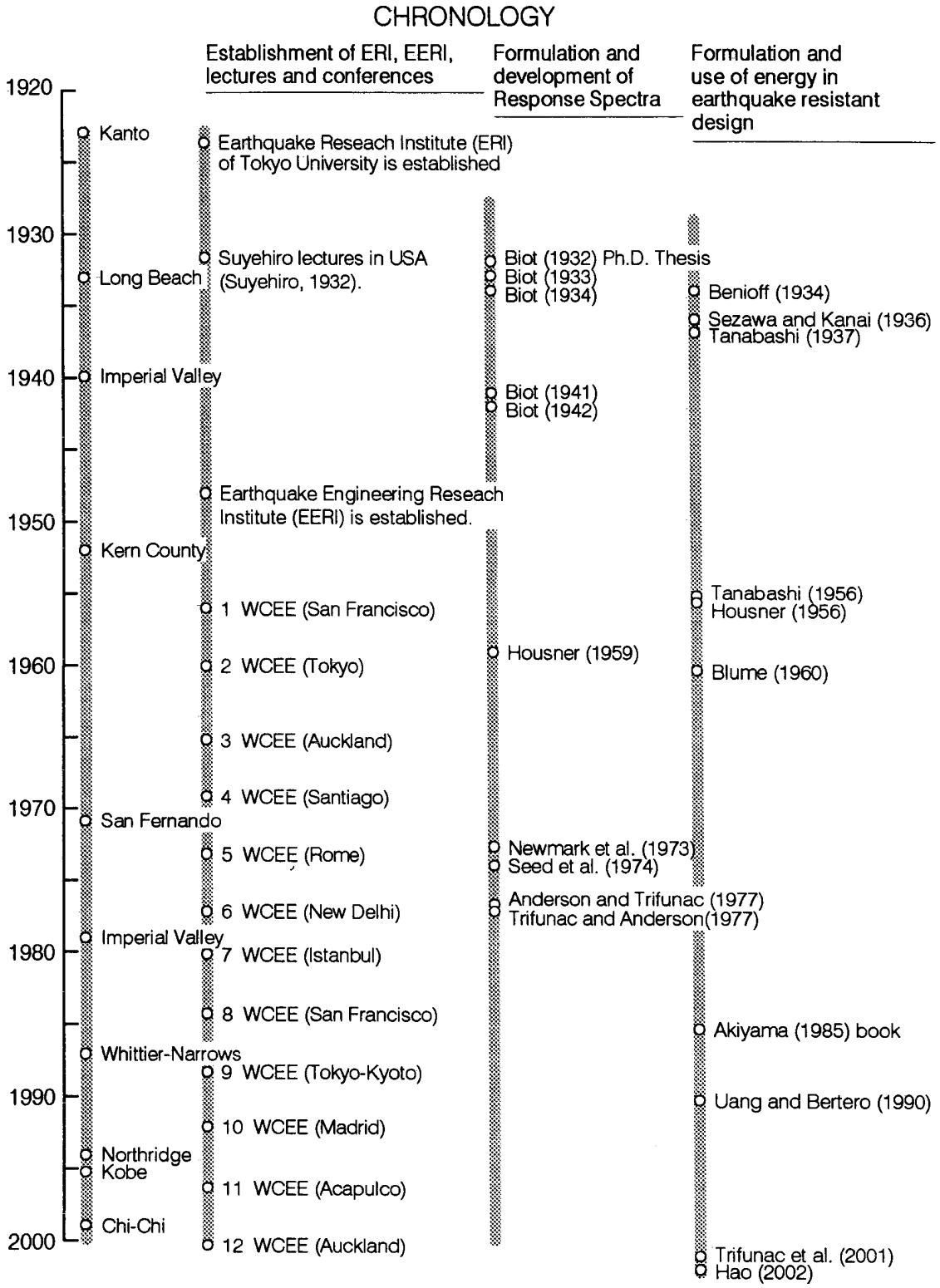

Fig. 1 Historical milestones in Earthquake Engineering, with emphasis on the subject of earthquake-resistant design (the years of selected significant earthquakes (from earthquake engineering point of view) and of the World Conferences on Earthquake Engineering are marked)

In this paper, we review an alternative to the spectral method of earthquake-resistant design by analyzing the flow of energy associated with strong motion, and by focusing on the energy during soil-foundation-structure system response. In Figure 2, the principal stages of the earthquake wave energy flow, from the earthquake source, along the propagation path, and finally to the work leading to relative response of the structure, are outlined. The losses of energy at every stage are also outlined. These losses must be accounted for to accurately quantify the remaining energy that will excite the structure.

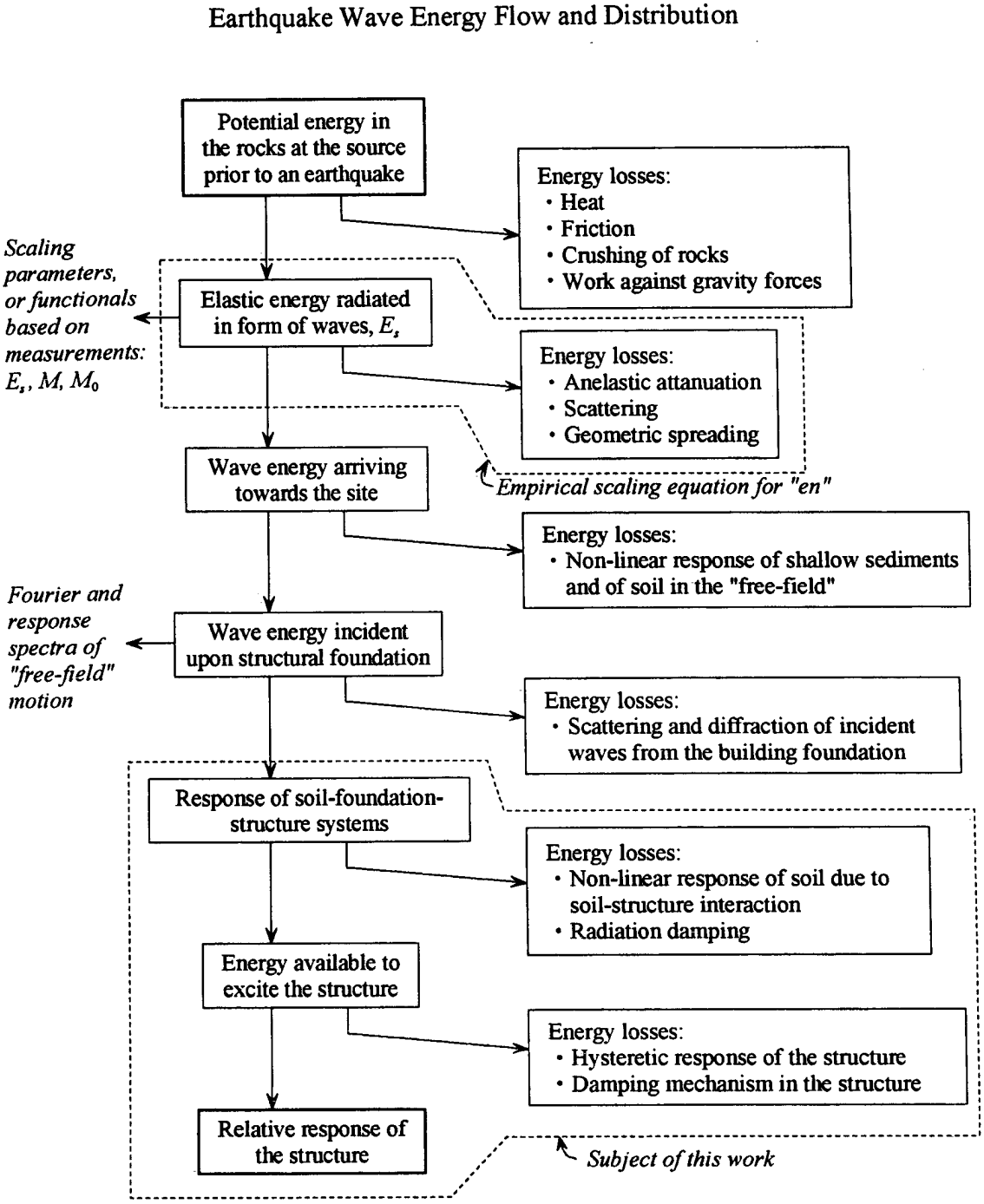

Fig. 2 An outline of the principal stages in the flow of earthquake wave energy from the earthquake source to a structure

2. Literature Review and Key Issues on Energy in Structural Response

The formulation of a rational design approach based on energy concepts requires understanding of the effects of the incident energy and other relevant parameters external to the structure (e.g., earthquake magnitude, distance to the causative fault) on the response of earthquake-resistant structures.

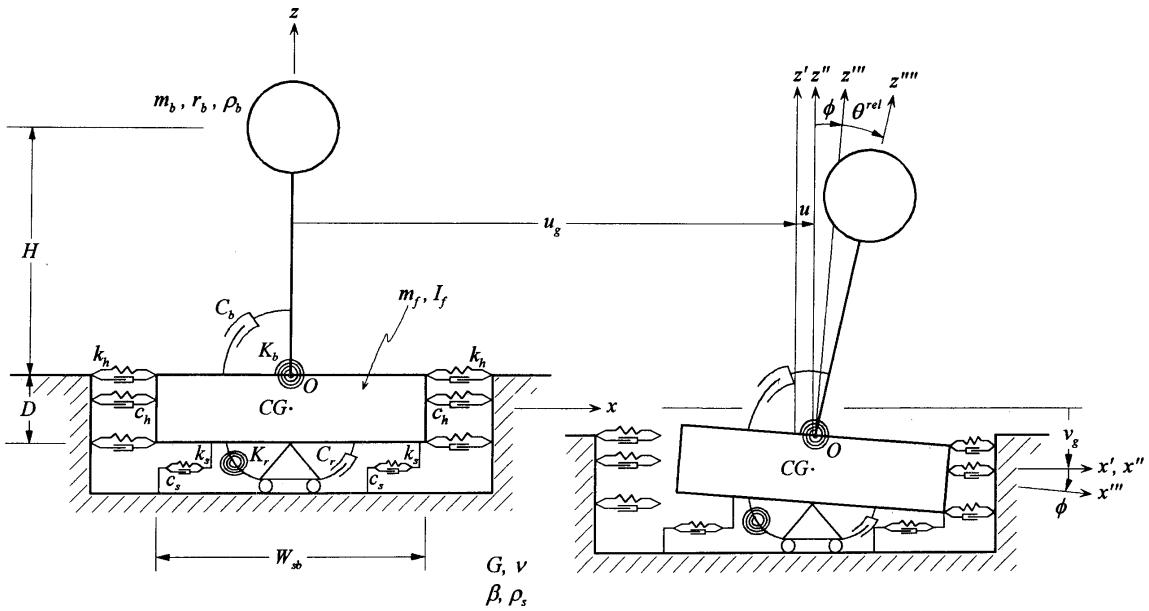

Fig. 3 A model of a soil-foundation-building system in an undeformed (left) and a deformed (right) configuration

The energy associated with the elastic waves radiated from the earthquake source, E_s (Gutenberg and Richter, 1956), is attenuated with increasing epicentral distance, R, through the mechanisms of inelastic attenuation, scattering, and geometric spreading (Trifunac, 1994; Trifunac et al., 2001f). The earthquake wave energy arriving towards the site is next dissipated by non-linear response of the shallow sediments and soil in the free-field (Joyner, 1975; Joyner and Chen, 1975; Trifunac, 1995; Trifunac and Todorovska, 1996, 1998), before it begins to excite the foundation. Once the foundation is excited by the incident earthquake waves, the response of the soil-structure system is initiated. The available incident wave energy is reduced by non-linear deformation of the soil during soil-structure interaction (Trifunac et al., 1999a, 2001a, 2001b) and by radiation damping (Luco et al., 1986; Rodrigues and Montes, 2000; Todorovska and Trifunac, 1991). The earthquake wave energy flow and distribution involving the last three stages in Fig. 2: (1) the response of the soil-foundation-structure system, (2) the energy available to excite the structure, and (3) the relative response of the structure, will be reviewed in this work.

The total energy input into a structure exerted by an earthquake depends mainly on the total mass and on the fundamental natural period of the structure (Akiyama, 1985, 1988, 1997; Uang and Bertero, 1988). Energy dissipation, as a means of reducing the seismic response of structures, has become also an important topic among the designers who develop friction dampers, fluid dampers, and isolators.

A natural form of energy dissipation occurs during interaction between a structure, its foundation, and the supporting soil medium. This dissipated energy can be significant and will contribute towards reduction of the seismic response. Unfortunately, this energy sink is often disregarded by researchers and engineers. Moreover, most modern structures are designed to resist severe loading conditions for which inelastic action exists only in the superstructure response. Hence, there is a need to develop soil-foundation analysis models which can account for inelastic behavior of the soil. The non-linearity can occur either in the superstructure, in the foundation, in the supporting soil medium, or in all of those simultaneously. Consequently, a good and realistic model must have features describing the response of the soil-foundation-structure system as completely and as accurately as possible.

For the majority of structures, inelastic behavior is accepted in the design for severe earthquake shaking. The effects of such inelastic behavior on the intensity and spectral distribution of the energy demands were investigated by Rodrigues and Montes (2000) and Decanini and Mollaioli (2001). Fajfar and Fischinger (1990), Uang and Bertero (1990), and Tembulkar and Nau (1987) evaluated the effect of non-linear behavior on the seismic input energy of SDOF systems. Zahrah and Hall (1984) evaluated the non-linear response of simple structures and the damage potential of an earthquake ground motion, as measured in terms of the amount of energy imparted to a structure, the amount of energy dissipated by inelastic deformation and by damping, as well as by the assessment of the displacement ductility of the

structure and the number of yielding excursions and reversals experienced during the excitation. Uang and Bertero (1988) discussed the derivation of the two "energy equations" (absolute and relative), and showed that the maximum values of the absolute and relative energy input, E_I, for any given constant displacement ductility ratio are very close in the period range of practical interest for earthquake-resistant design of buildings (0.3 to 5.0 seconds).

In most published studies, the derivation of energy equations begins by integrating the differential equation of dynamic equilibrium of a single-degree-of-freedom system with respect to displacement, which results in

$$E_I = E_E + E_D = E_K + E_S + E_{H\xi} + E_{H\mu} \tag{1}$$

where E_I is the energy input, E_E is the stored elastic energy, E_D is the dissipated energy through viscous-damping mechanisms, E_K is the kinetic energy, E_S is the elastic strain energy, $E_{H\xi}$ is the energy dissipated through hysteretic damping, and $E_{H\mu}$ is the energy dissipated by the hysteretic plastic deformation.

An important omission in many of the published studies is that the effects of soil-structure interaction are ignored. Because of that, significant energy loss mechanisms (non-linear response of the soil and radiation damping) are neglected (Figure 2; see also Rodrigues and Montes, 2000). The other extreme is to neglect the stiffness of the foundation system (and the soil-structure interaction), and to assume that the wave energy in the soil drives the building to follow the motions specified by the wave propagation in the free-field. This approximate approach underestimates the scattering of incident wave energy by the foundation and overestimates the energy transmitted into the building. The reality is somewhere between these two extremes, and can be studied further in detail only by numerical methods. Other simplifications and omissions in Equation (1) are that the dynamic instability and the effects of gravity on non-linear response are ignored (Husid, 1967; Lee, 1979; Todorovska and Trifunac, 1991, 1993).

At present, the model most commonly used by engineers for the design of buildings assumes the structure to be fixed to a "rigid" ground. Current design methods thus disregard the influence that the flexibility of the ground has on the response of a structure. Such a procedure simplifies the analysis. The assumption that there is no coupling or interaction between the structure, its foundation and the supporting soil is however contrary to recorded observations (Trifunac et al., 1999a; 2001a, 2001b). The conceptual model proposed by Trifunac et al. (2001f) and Hao (2002) attempts to capture the main characteristics of the non-linear behavior of soil-structure systems, and will be described in the following.

ENERGY DURING SOIL-FOUNDATION-STRUCTURE SYSTEM RESPONSE

1. Model

To describe the energy flow through a soil-foundation-structure system, Hao (2002) and Trifunac et al. (2001f) use the idealized mathematical model shown in Figure 3. In this model, the building is represented by an equivalent single-degree-of-freedom (SDOF) oscillator founded on a rigid embedded rectangular foundation. The soil has shear modulus G, shear wave velocity β, Poisson's ratio ν, and mass density ρ_s. The oscillator has only one degree-of-freedom with respect to the foundation, θ^{rel}. The mass of the oscillator is m_b. It has height H and radius of gyration r_b. The oscillator is connected to the foundation at point O through a rotational spring and a viscous damper. The spring has stiffness K_b, and the viscous damper has damping constant C_b. The stiffness is chosen such that the natural period of the oscillator, T_1, is equal to the corresponding fixed-base period of the fundamental mode of the building. Assuming that the equivalent SDOF oscillator has same mass per unit length as the real building, assumed to deform in shear only, H and r_b are related to H_{sb} and W_{sb}, the height and width of the real building (Todorovska and Trifunac, 1993), as $H = H_{sb}/\sqrt{3}$ and $r_b = W_{sb}/\sqrt{3}$.

The rectangular foundation has width W_{sb}, depth D, mass m_f, and mass moment of inertia I_f. To simplify the analysis, Hao (2002) and Trifunac et al. (2001f) assume that the stiffness of the soil in the vertical direction is infinite. The foundation has two degrees-of-freedom with respect to its center of

gravity (point *CG*): horizontal translation, u, and rotation, ϕ. The foundation is surrounded by springs and dashpots, which model the reactive forces caused by deformation developed in the soil (Richart et al., 1970). In Figure 3, k_h and c_h are the stiffness and damping constants of horizontal springs and dashpots around the foundation representing the horizontal reactive forces on the vertical faces of the foundation; k_s and c_s are the stiffness and damping constants of the horizontal springs and dashpots at the base of the foundation representing the shear forces acting on the interface; and K_r and C_r are the rotational stiffness and damping constant representing the resisting moments in the half-space. The evaluation of the stiffness $(k_h,\ k_s \text{ and } K_r)$ and damping $(c_h,\ c_s \text{ and } C_r)$ constants is discussed in Trifunac et al. (2001f). This soil-foundation-oscillator system is subjected to horizontal and vertical excitations $(u_g \text{ and } v_g)$.

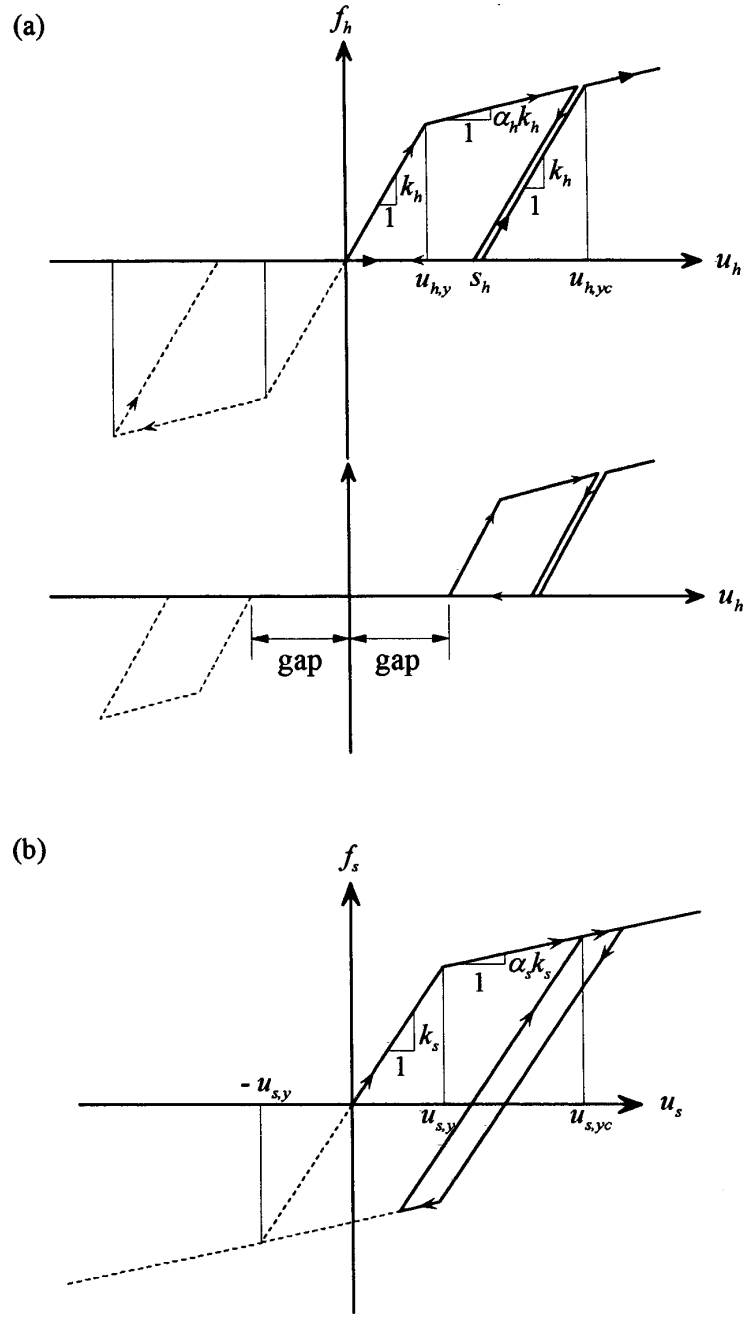

Fig. 4 Force-deformation relations used to represent the nonlinear behavior of soil: (a) slip model for horizontal springs on two sides of the foundation, (b) bilinear model for springs at the base of the foundation

Hao (2002) and Trifunac et al. (2001f) further assume that the foundation is rigid, in order to reduce the number of degrees-of-freedom of the model (Duncan, 1952; Trifunac and Todorovska, 2001). Such models give an approximation of the system response for long wavelengths relative to the foundation dimensions (Lee, 1979). For short wavelengths, this assumption can result in nonconservative estimates of the relative deformations in the structure (Trifunac, 1997; Trifunac and Todorovska, 1997), and, in general, is expected to result in excessive estimates of scattering of the incident wave energy and in excessive radiation damping (Todorovska and Trifunac, 1990a, 1990b, 1990c, 1991, 1992, 1993). The extent to which this simplifying assumption is valid, depends on the stiffness of the foundation system relative to that of the soil, and also on the overall rigidity of the structure (Iguchi and Luco, 1982; Liou and Huang, 1994; Hayir et al., 2001; Todorovska et al., 2001a, 2001b, 2001c; Trifunac et al., 1999a).

Ivanović et al. (2000) and Trifunac et al. (2001a, 2001b, 2001c) suggested that the soil behavior is non-linear during most earthquakes, and that it can recover its stiffness after consolidation with time, and after small amplitude shaking from aftershocks and smaller earthquakes. The observed "softening" and "hardening" behavior of the system can be explained by a model with *gap* elements along the contact between the foundation and the soil. We can assume that the soil on the side of the foundation is represented by a hysteretic slip model (see Figure 4(a)) to simulate the non-linear behavior of the soil. This slip model emphasizes the pinching effects of soil with large stresses and the *gap* generated by soil compression. For the soil at the base of the foundation, the bilinear and softening characteristics are represented in Figure 4(b). A detailed description of these slip and bilinear hysteretic systems is presented in Trifunac et al. (2001f).

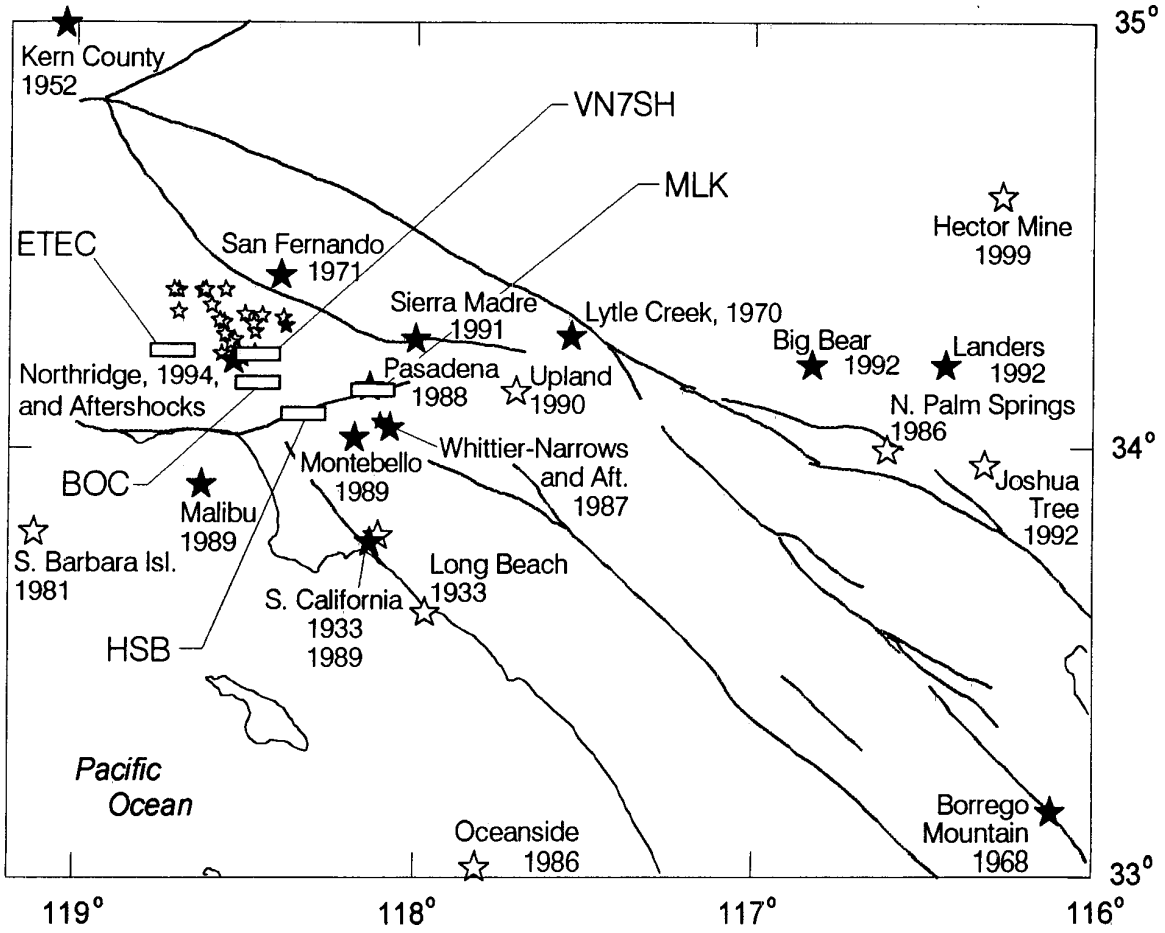

Fig. 5 Earthquakes in Southern California, large enough to trigger the strong motion accelerographs in HSB, VN7SH, BOC, MLK and ETEC (the rectangles indicate the five buildings being studied; the events for which strong motion data was recorded and is available in digitized form can be found in Hao, 2002)

2. Equations of Motion

The equations of motion for the system are derived and solved including the non-linear geometry and soil behavior, coupling of the vertical acceleration with the rocking and horizontal translation, and the effects of the gravity forces $(m_b g \text{ and } m_f g)$. It is not required to assume small deformations assumption, and arbitrary material non-linearity is allowed. The response of the building and of the soil can enter inelastic range during strong ground shaking. In that case, the analysis of soil-structure interaction (SSI) will be quite complicated. Consequently, at first, the building will be assumed to be linear, and the soil will be assumed to exhibit inelastic force-deformation relation. Later on, we will briefly consider the non-linear response of the building also.

The equations of motion for the system then can be derived from the equilibrium of forces and moments. From the equations of dynamic equilibrium of forces in the horizontal and vertical directions and all moments acting on the oscillator about point O, the interactive forces and the moment between the oscillator and foundation are

$$\Sigma F_x = 0 \Rightarrow f_{x,b} = m_b \ddot{u}_b \tag{2}$$

$$\Sigma F_z = 0 \Rightarrow f_{z,b} = -m_b(\ddot{v}_b - g) \tag{3}$$

$$\begin{aligned} \sum M_O = 0 \Rightarrow & I_O(\ddot{\phi} + \ddot{\theta}^{rel}) + m_b \ddot{u}_O H \cos(\phi + \theta^{rel}) + m_b(\ddot{v}_O - g) H \sin(\phi + \theta^{rel}) \\ & + K_b \theta^{rel} + C_b \dot{\theta}^{rel} = 0 \end{aligned} \tag{4}$$

where $I_O = m_b r_b^2 [1 + (\frac{r_b}{H})^2]$.

From the equations of dynamic equilibrium of all forces and moments acting on the foundation about point *CG*, it follows that

$$\Sigma F_x = 0 \Rightarrow \sum_{i=1}^{m} f_{h,i} + \sum_{j=1}^{n} f_{s,j} = -m_f \ddot{u}_{CG} - f_{x,b} \tag{5}$$

$$\Sigma F_z = 0 \Rightarrow f_{z,f} = -m_f(\ddot{v}_{CG} - g) + f_{z,b} \tag{6}$$

$$\begin{aligned} \Sigma M_{CG} = 0 \Rightarrow M_{B,f} = & (f_{z,b} + f_{z,f}) \frac{D}{2} \sin\phi - f_{x,b} \frac{D}{2} \cos\phi + M_{O,b} - I_f \ddot{\phi} \\ & - \sum_{i=1}^{m} (f_{h,i} \cos\phi) d_i + \sum_{i=1}^{m} (f_{h,i} \sin\phi) \frac{W_{sb}}{2} - \sum_{j=1}^{n} (f_{s,j} \sin\phi) l_i + \sum_{j=1}^{n} (f_{s,j} \cos\phi) \frac{D}{2} \end{aligned} \tag{7}$$

and

$$M_{B,f} = K_r \phi + C_r \dot{\phi} \,. \tag{8}$$

3. Derivation of the Energy Equations

When a system is subjected to earthquake shaking, the incident waves propagate into it. During strong ground motion, part of the incident energy is dissipated by scattering from the foundation and by the deformation of the soil, and the rest is transmitted into the building.

Referring to the model in Figure 3, all forces and moments move through the corresponding displacements and thus do work. To evaluate this work, we integrate all six equilibrium equations of the system, Equations (2), (3), (4), (5), (6) and (7), with respect to the corresponding displacements. The total work done in the system is then computed by superposition of integrals of those equations.

To simplify these energy formulae, we keep only the first order terms of the Taylor series expansions of the sine and cosine functions of the angles θ^{rel} and ϕ (and their linear combination), and eliminate the products of small angles and of their derivatives. Then, the above six equations give

$$\int \{m_b[\ddot{u} + \frac{D}{2}\ddot{\phi} + H(\ddot{\phi} + \ddot{\theta}^{rel})] - f_{x,b}\} \dot{u}_b \, dt = -\int m_b \ddot{u}_g \dot{u}_b dt \tag{9}$$

$$\int (-m_b g + f_{z,b}) \dot{v}_b \, dt = -\int m_b \ddot{v}_g \dot{v}_b \, dt \tag{10}$$

$$\int [m_b(\ddot{u}_O + \frac{D}{2}\ddot{\phi})H - m_b g H\phi_b + I_O\ddot{\phi}_b + K_b\theta^{rel} + C_b\dot{\theta}^{rel}]\,\dot{\phi}_b\ dt = -\int (m_b\ddot{u}_g H + m_b\ddot{v}_g H\phi_b)\,\dot{\phi}_b\ dt \tag{11}$$

$$\int (m_f\ddot{u} + f_{x,b})\,\dot{u}_{CG}\ dt + \int (\sum_{i=1}^{m} f_{h,i} + \sum_{j=1}^{n} f_{s,j})\,\dot{u}\ dt = -\int m_f\ddot{u}_g\dot{u}_{CG}\ dt \tag{12}$$

$$\int (-m_f g - f_{z,b} + f_{z,f})\,\dot{v}_{CG}\ dt = -\int m_f\ddot{v}_g\dot{v}_{CG}\ dt \tag{13}$$

and

$$\int (K_r\phi + C_r\dot{\phi} - f_{z,b}\frac{D}{2}\phi - f_{z,f}\frac{D}{2}\phi + f_{x,b}\frac{D}{2} - K_b\theta^{rel} - C_b\dot{\theta}^{rel} + I_f\ddot{\phi} + \sum_{i=1}^{m} f_{h,i}d_i - \sum_{i=1}^{m} f_{h,i}\phi\frac{W_{sb}}{2} + \sum_{j=1}^{n} f_{s,j}\phi\, l_j - \sum_{j=1}^{n} f_{s,j}\frac{D}{2})\,\dot{\phi}_{CG}\ dt = 0 \tag{14}$$

Next, we group the energy terms, according to their physical nature, into the following categories:

$E_K(t)$ = kinetic energy

$E_P(t)$ = potential energy of gravity forces

$E_D^{bldg}(t)$ = damping energy dissipated in the building

$E_S^{bldg}(t)$ = recoverable elastic strain energy in the building

$E_D^{soil}(t)$ = energy dissipated by "dashpots" of the soil

$E_S^{soil}(t)$ = elastic strain energy in the soil

$E_Y^{soil}(t)$ = irrecoverable hysteretic energy in the soil

$E_{S+Y}^{soil}(t) = E_S^{soil}(t) + E_Y^{soil}(t)$

$E_I(t)$ = total earthquake input energy.

First, based on Equations (9) through (14), the earthquake input energy is the sum of all the right hand side terms

$$E_I(t) = -\int [m_b\ddot{u}_g\dot{u}_b + m_b\ddot{v}_g\dot{v}_b + (m_b\ddot{u}_g H + m_b\ddot{v}_g H\phi_b)\dot{\phi}_b + m_f\ddot{u}_g\dot{u}_{CG} + m_f\ddot{v}_g\dot{v}_{CG}]\,dt \tag{15}$$

The kinetic energy associated with the absolute motion of the two masses is

$$E_K(t) = \int \{m_b(\ddot{u} + \frac{D}{2}\ddot{\phi} + H\ddot{\phi}_b)\dot{u}_b + [m_b(\ddot{u} + \frac{D}{2}\ddot{\phi})H + I_O\ddot{\phi}_b]\,\dot{\phi}_b + m_f\ddot{u}\dot{u}_{CG} + I_f\ddot{\phi}\,\dot{\phi}_{CG}\}dt \tag{16}$$

It can be seen that $E_K(t)$ is equal to the integrals of the inertial forces with respect to their absolute velocities. The potential energy associated with the gravity forces is

$$E_P(t) = -\int (m_b g\dot{v}_b + m_b g H\phi_b\dot{\phi}_b + m_f g\dot{v}_{CG})\,dt \tag{17}$$

The energy dissipated by viscous damping in the building can be calculated from

$$E_D^{bldg}(t) = \int C_b(\dot{\theta}^{rel})^2\,dt \tag{18}$$

The recoverable strain energy of the building (for linear response) is

$$E_S^{bldg}(t) = \frac{1}{2}K_b(\theta^{rel})^2 \tag{19}$$

For this illustration, the building is assumed to deform in linear manner only, and the irrecoverable hysteretic energy in the building will be zero. Then, the energy dissipated by the dashpots in the soil is

$$E_D^{soil}(t) = \int (\sum_{i=1}^{m} f_{h,i}^D + \sum_{j=1}^{n} f_{s,j}^D)\, \dot{u}\, dt + \int C_r \dot{\phi}^2\, dt + \int \{\sum_{i=1}^{m} f_{h,i}^D (d_i - \frac{W_{sb}}{2}\phi) + \sum_{j=1}^{n} f_{s,j}^D (l_j \phi - \frac{D}{2})\} \dot{\phi}\, dt \tag{20}$$

The energy dissipated by the yielding and by the recoverable strain energy of the soil can be obtained from

$$E_{S+Y}^{soil}(t) = \int (\sum_{i=1}^{m} f_{h,i}^S + \sum_{j=1}^{n} f_{s,j}^S)\, \dot{u}\, dt + \int K_r \phi\, \dot{\phi}\, dt + \int \{\sum_{i=1}^{m} f_{h,i}^S (d_i - \frac{W_{sb}}{2}\phi) + \sum_{j=1}^{n} f_{s,j}^S (l_j \phi - \frac{D}{2})\} \dot{\phi}\, dt \tag{21}$$

in which

$$E_S^{soil}(t) = \sum_{i=1}^{m} \frac{(f_{h,i}^S)^2}{2k_{h,i}} + \sum_{j=1}^{n} \frac{(f_{s,j}^S)^2}{2k_{s,j}} + \frac{K_r \phi^2}{2} \tag{22}$$

where $k_{h,i}$ and $k_{s,j}$ are the initial stiffness coefficients of the inelastic soil.

Based on these energy "components," the statement of energy balance of the system is then expressed as

$$E_K(t) + E_P(t) + E_D^{bldg}(t) + E_S^{bldg}(t) + E_D^{soil}(t) + E_{S+Y}^{soil}(t) = E_I(t) \tag{23}$$

The foregoing analysis of the non-linear system models the energy components of the simple non-linear SSI system in Figure 3, rather than that of the fixed-base system (e.g., Akiyama, 1985, 1988, 1997; Anderson and Bertero, 1969; Uang and Bertero, 1988, 1990). Comparing Equation (23) with Equation (1), the simplifications and omissions in Equation (1) become clear.

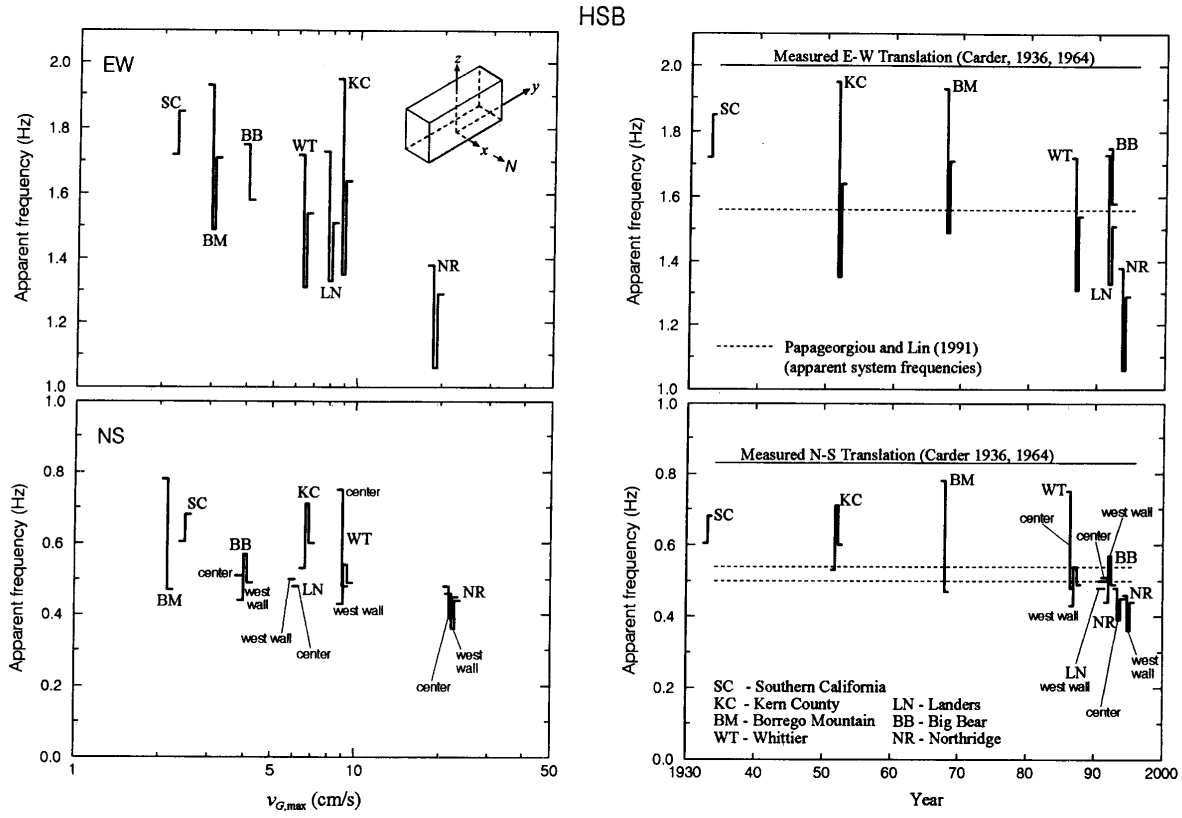

Fig. 6 Schematic diagram of the observed variations of the EW (top) and NS (bottom) system frequencies, f_p, of the Hollywood Storage Building versus peak measured ground velocity, $v_{G,\max}$ (left), and time (right), during seven earthquakes (for each earthquake, the horizontal ticks represent pre- and post-earthquake estimates of the system frequencies)

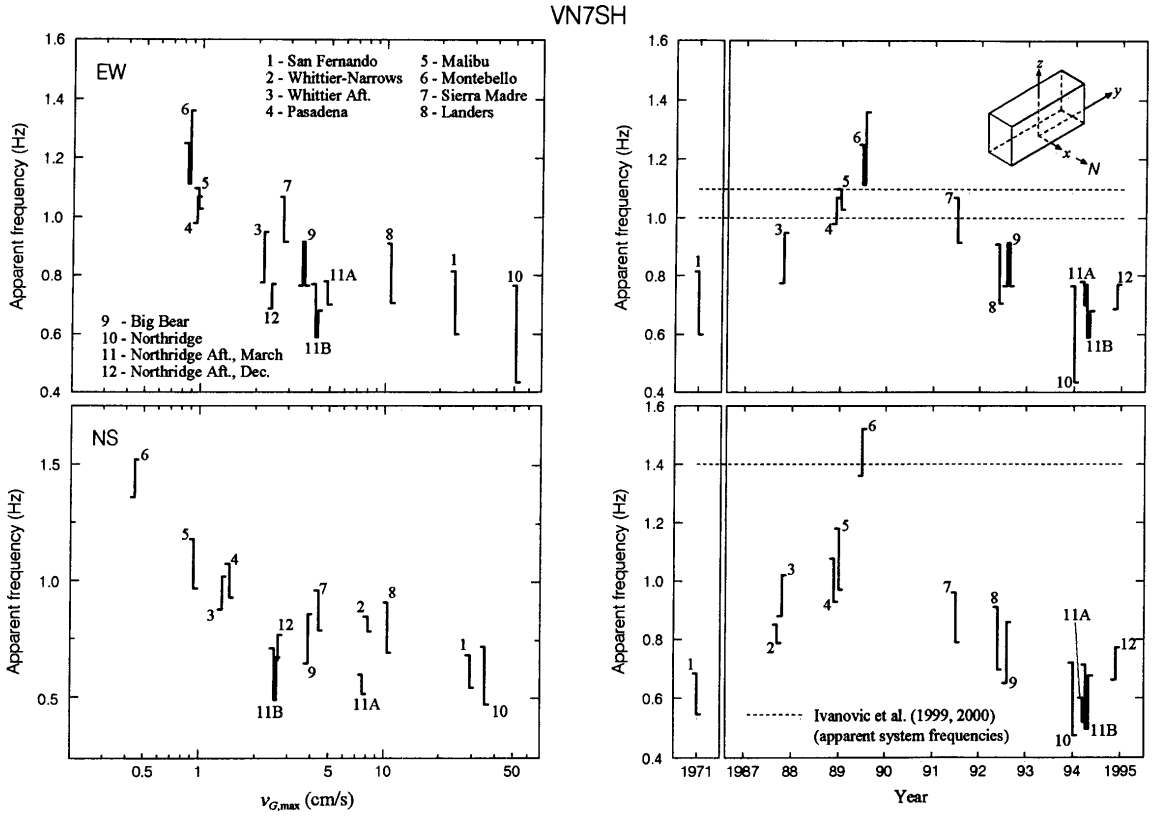

Fig. 7 Same as Figure 6 but for the Van Nuys 7-story hotel

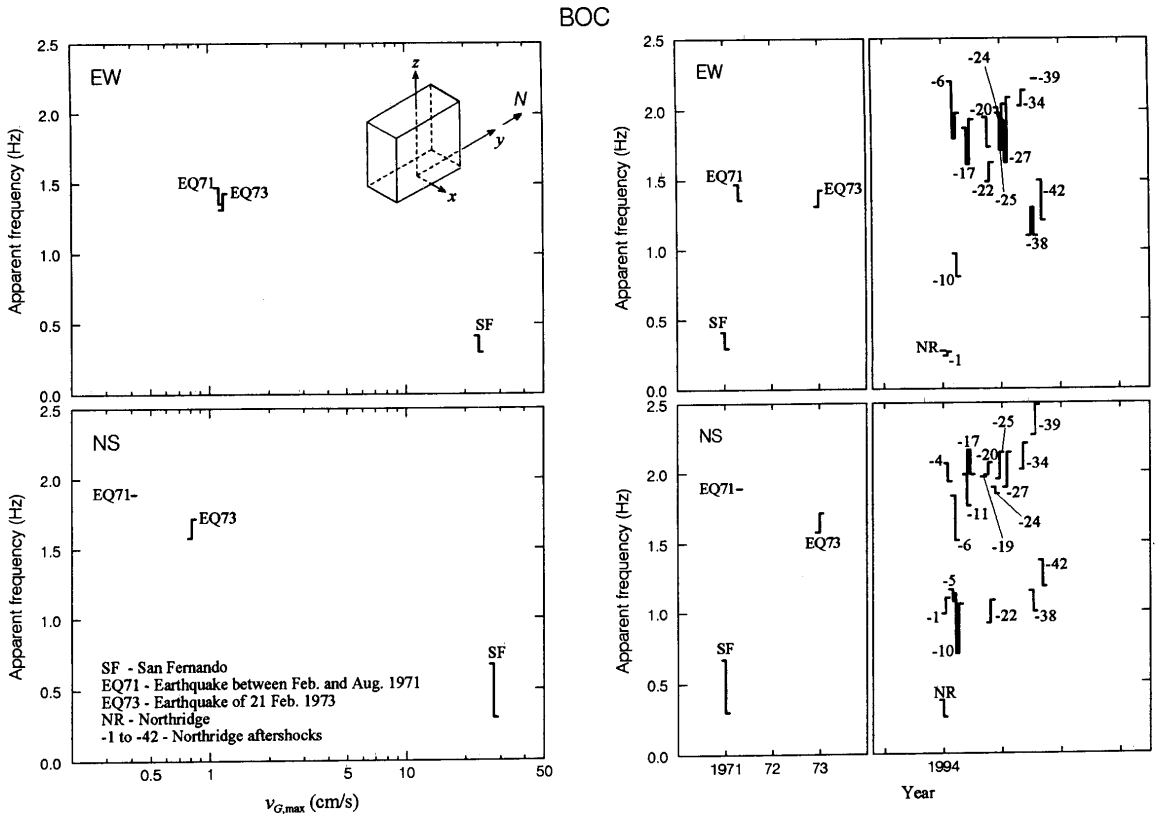

Fig. 8 Same as Figure 6 but for the Bank of California building

EXAMPLE STUDIES OF FIVE BUILDINGS

To illustrate the behavior of the model for energy partitioning in a soil-structure system, shown in Figure 3, Trifunac et al. (2001f) and Hao (2002) analyzed the Hollywood Storage building (HSB), the Van Nuys seven story hotel (VN7SH), the Sherman Oaks Bank of California building (BOC), the Pasadena (Caltech) Millikan Library (MLK), and the Santa Susana ETEC building #462 (ETEC). These five buildings have been studied previously by many investigators (see references in Trifunac et al., 2001f; Trifunac et al., 2001a, 2001b; and Trifunac and Todorovska, 2001). There are multiple recordings in the buildings of weak, intermediate and strong earthquake responses, and three of these buildings were tested using ambient vibration methods. All, except the Santa Susana ETEC building, are reinforced concrete structures and the sites lie on recent alluvium. The ETEC building is a steel structure, and its site lies on sandstone bedrock, which makes the response of this building different from the others.

The building descriptions and the earthquake recordings are described in Hao (2002) and will not be repeated here.

1. Analysis of Recorded Motions: Time and Amplitude-Dependent Response

To evaluate the changes of the system frequency, f_p, during a particular earthquake motion, as a function of the level of response and of the previous response history, the "instantaneous" value of the system predominant frequency, f_p, was approximated by two methods: (1) zero-crossing analysis and (2) moving window Fourier analysis. To isolate the lowest frequency mode, the data was band-pass filtered. The cutoff frequencies for the band-pass filter were chosen to include the system frequency, and were determined after analyzing the instantaneous transfer-functions between the relative horizontal motions recorded on the roof and at the base. The zero-crossing analysis consisted of determining the half periods for all approximately symmetric peaks in the relative response, assuming that the filtered relative displacements can be approximated locally by a sine wave.

Figure 5 shows geographical distribution of the buildings studied here and of the earthquakes which contributed to the recorded data. Figures 6 through 10 show schematically the observed variations of f_p versus $v_{G,\max}$ (the peak measured ground velocity at the base of the building) and time. In these figures, f_p is proportional to the square root of the system stiffness, while $v_{G,\max}$ can be related to the strain levels in the supporting soil. Excluding the EW response of ETEC building, it appears that these soil-building systems behave like non-linear soft spring systems. For $v_{G,\max} \leq 1$ cm/s, the system frequency of the EW response of ETEC building increases with increasing $v_{G,\max}$ ("stiffer" non-linear response). Beyond $v_{G,\max} \approx 1$ cm/s, the system frequency becomes slightly smaller.

The evaluation of the instantaneous system frequency requires complete recordings on the roof and at the base. However, during the 1994 Northridge earthquake and its aftershocks, only the motions on the roof were recorded in the Bank of California building (BOC; Figure 8). The possibility and accuracy of performing the approximate analysis, using motions on the roof only, are discussed in Hao (2002).

Figures 6 through 10 also summarize the time-dependent changes of the instantaneous system frequency, f_p, for the recorded earthquakes ordered in chronological order. Figures 6, 7 and 9 also compare the variations in the system frequencies during strong-motion with the values from low amplitude testing (horizontal lines).

The amplitude-dependent changes of f_p are illustrated in Figures 11 and 12, by plotting f_p versus the corresponding amplitude of the envelope of the analyzed data. Based on the time- and amplitude-frequency analyses, we found that the predominant system frequencies change from one earthquake to another, and also during the response to a particular earthquake. The results also indicate that what is "loosened" by the severe strong motion shaking, appears to be "strengthened" by aftershocks and by intermediate and small earthquakes. The changes of the system frequency of the ETEC building were the smallest (Figure 12). The ETEC building is a steel structure founded on hard bedrock. It experienced no damage during the 1994 Northridge earthquake.

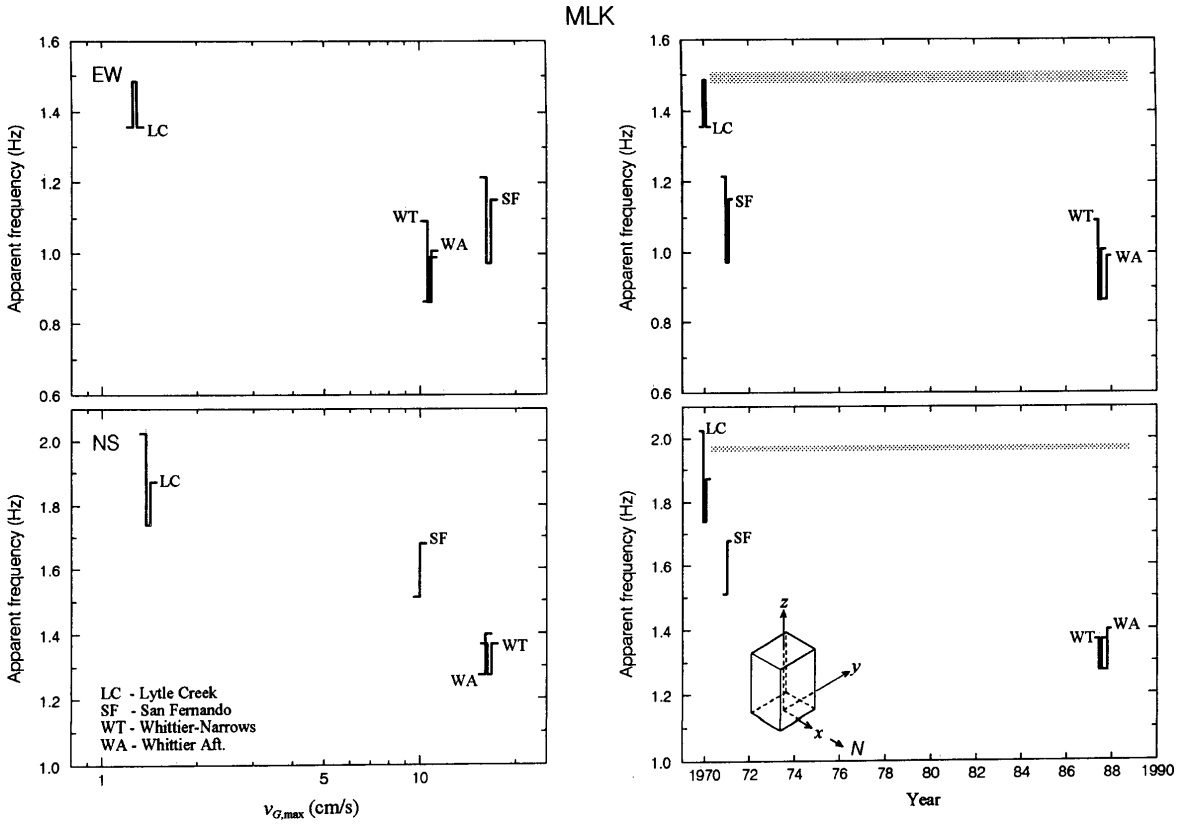

Fig. 9 Same as Figure 6 but for the Millikan Library building

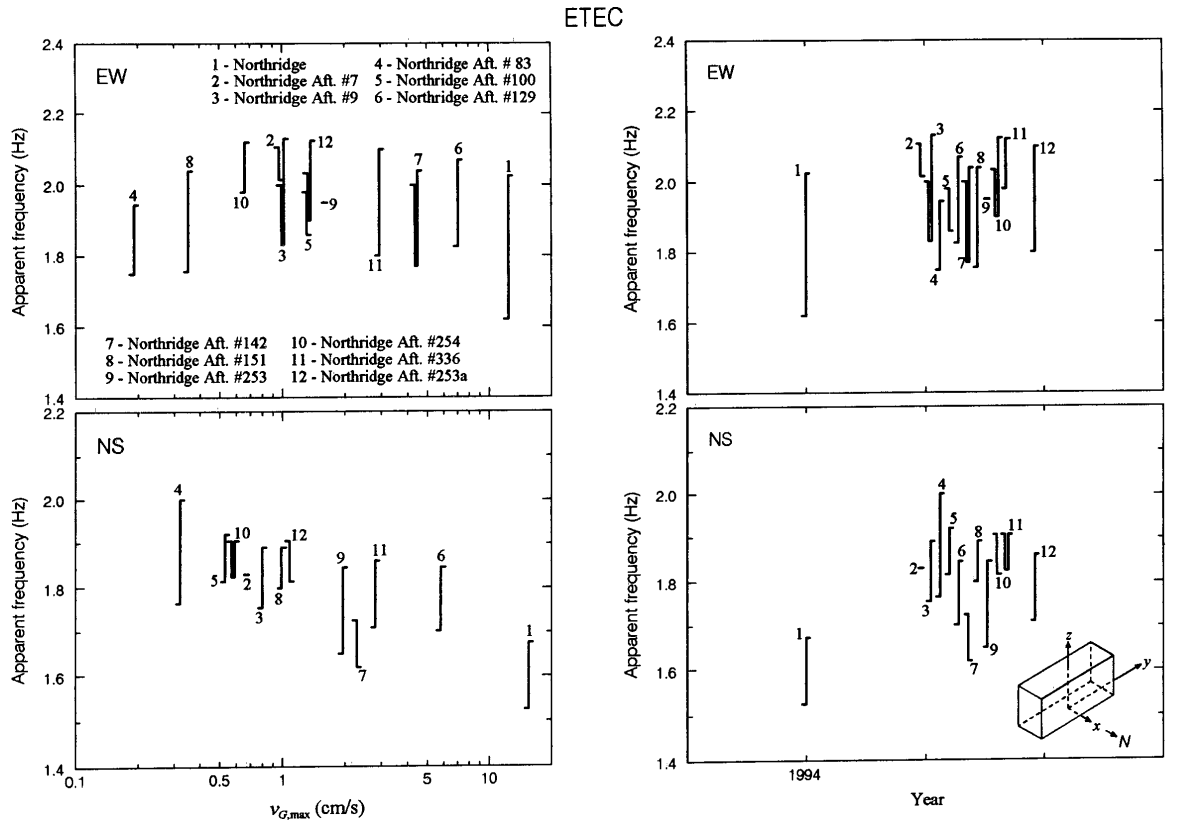

Fig. 10 Same as Figure 6 but for the ETEC building

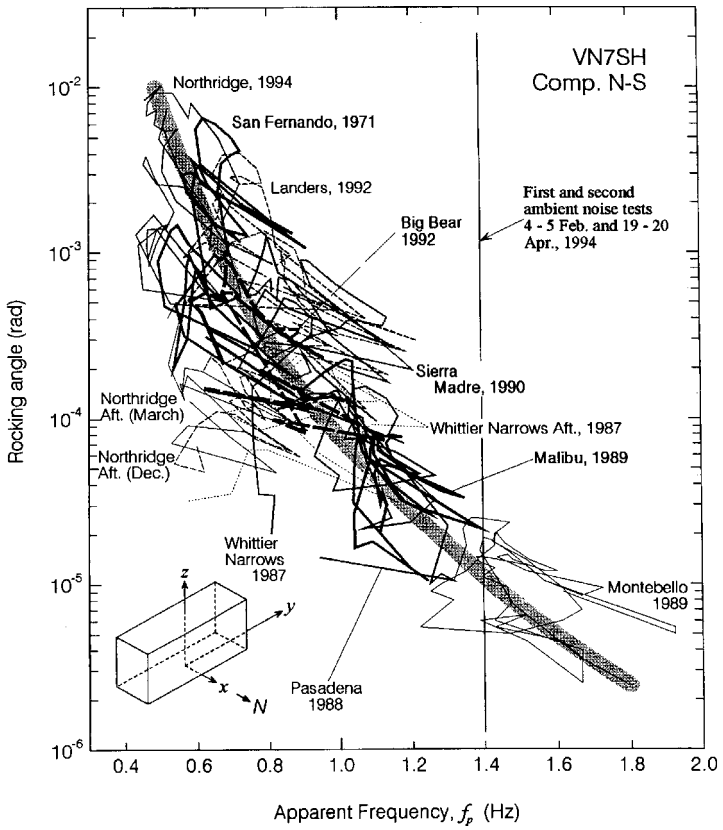

Fig. 11 Dependence of the apparent system frequency of Van Nuys 7-story hotel on the peak amplitude of the NS relative response (rocking angle) (the solid lines show estimates of the system frequencies determined from ambient vibration tests by Ivanović et al., 1999, 2000)

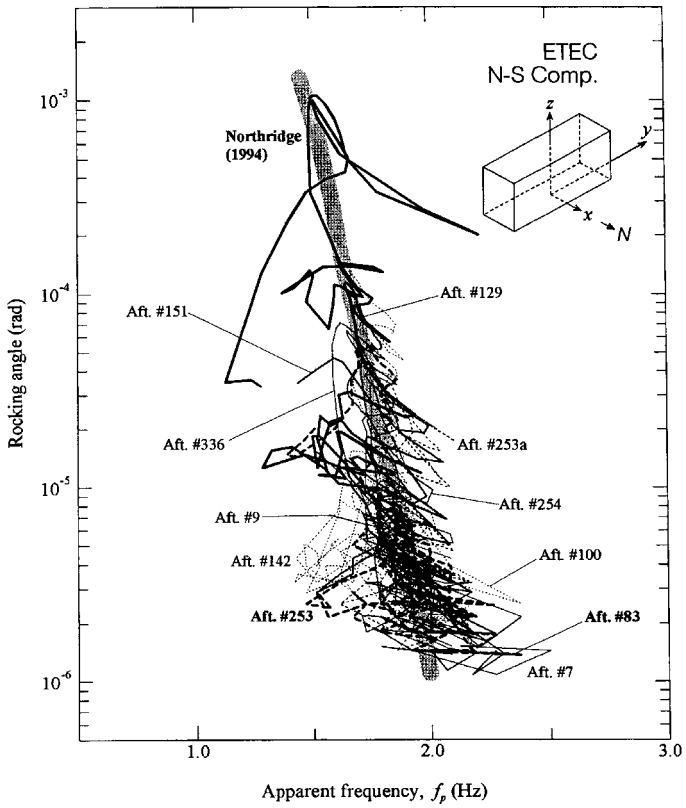

Fig. 12 Dependence of the apparent system frequency of Santa Susana ETEC building on the peak amplitude of the NS relative response

2. Numerical Response Simulation

The accelerations recorded at the base of the buildings were used by Hao (2002) and Trifunac et al. (2001f) as the input excitations for the idealized mathematical model. The values of the model parameters corresponding to the five studied structures are presented and discussed in detail in Hao (2002). From the equations of motion, the unknown displacements were solved numerically in the time domain. Then the associated system energies were determined. In the following, we summarize the results of their simulation, compare the recorded and predicted responses, and discuss the system energies.

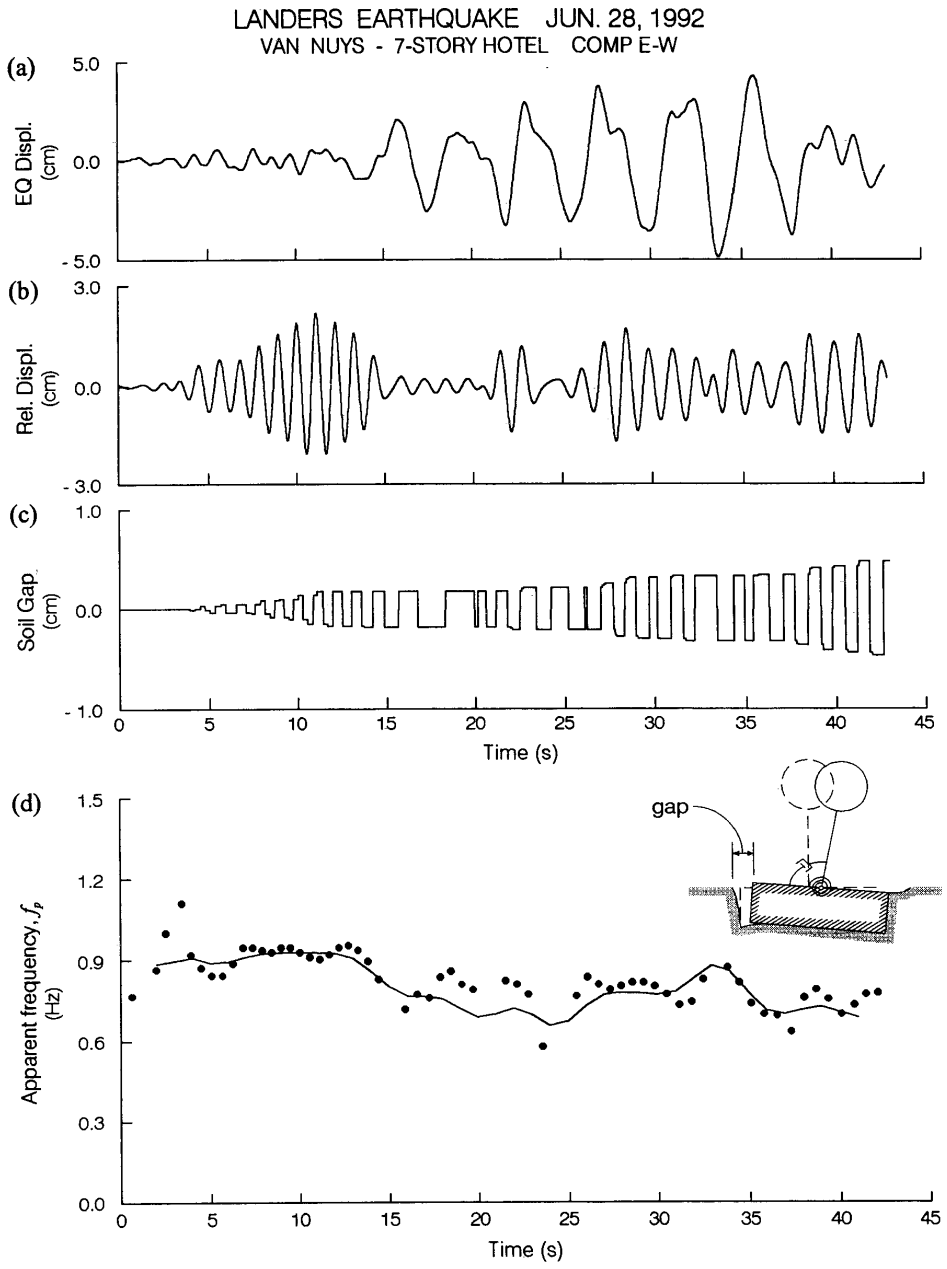

Fig. 13 An example of predicted response for the 1992 Landers earthquake modeling the EW response of VN7SH building

2.1 Predicted Responses

Figure 13 illustrates sample results of the simulated response of the VN7SH building EW response for 1992 Landers earthquake. Part (a) of Figure 13 shows the displacement recorded at the base of the building, which is used as input excitation for the simulation. The predicted displacement of the roof relative to the base is plotted in part (b). During the shaking, the soil on the sides of the foundation is

pushed sideways by the vibration of the foundation. This is shown in part (c) (the gaps shown here represent the separations at the surface level). Part (d) of this figure shows the results of the zero-crossing (solid points) and of the moving window Fourier (solid lines) analyses for the changes of system frequency. In part (c) of Figure 13, it is found that the separation between the foundation and the side-soil occurs at 3.9 s and keeps increasing between 3.9 to 6.0 s. The system is oscillating with partially contacting the soil springs on the sides, and the system stiffness decreases a little. At about 7.35 s, the larger vibration of the foundation pushes the soil on the sides further. This phenomenon increases the system stiffness (i.e. increases f_p). Again, the gap increases between 7.35 to 12.0 s and when the system is oscillating without touching the soil on the sides (between 12 to 22 s), the system stiffness decreases. This phenomenon, referred to as "pinching," can also be seen at about 27.0, 30.9 and 37.7 s.

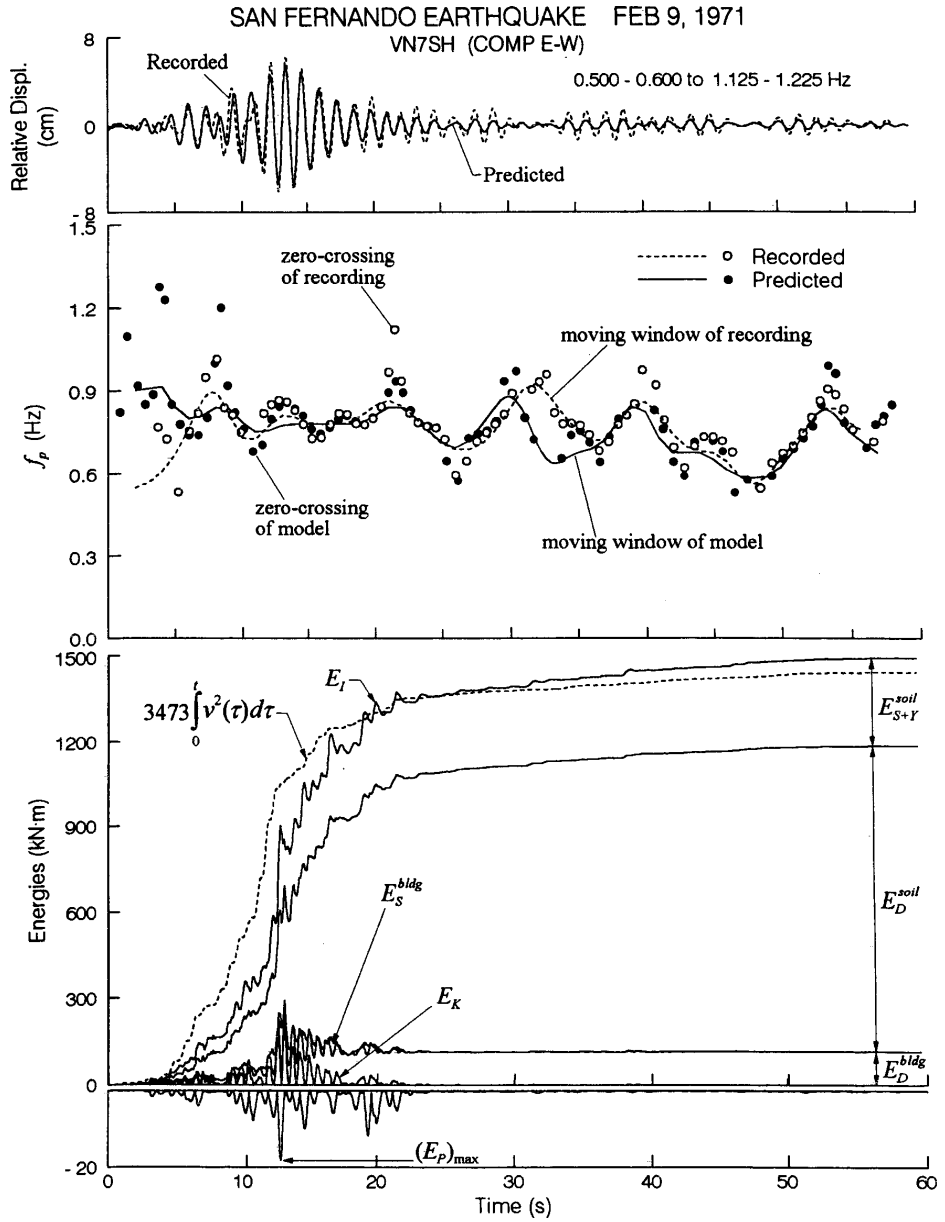

Fig. 14 Top: comparison of recorded (dashed line) and predicted (solid line) EW relative displacement response at the roof of VN7SH during the 1971 San Fernando earthquake; center: time dependent changes of the system frequency f_p computed from recorded (dashed line and open circles) and predicted (continuous line and solid dots) responses; bottom: contributions to the system energy: E_{S+Y}^{soil}, E_D^{soil}, E_S^{bldg}, E_D^{bldg}, E_K and E_P and their sum E_I (input wave energy $a_0\int_0^t v^2(\tau)\,d\tau$ is shown by dashed line)

2.2 Comparison of the Recorded and Predicted Responses

Figure 14 shows an example of the predicted response together with the recorded response of the VN7SH during 1971 San Fernando earthquake. The top part of Figure 14 shows a comparison of the band-pass filtered relative response of recorded motions (dashed line), and the simulated motions (solid line) using the model presented in Figure 3. The central part of Figure 14 shows the time-dependent changes of the system frequency, f_p. The dashed lines show the changes in f_p evaluated by moving window Fourier analysis of the recorded data, and the open circles show the estimates by the zero-crossing analysis also using the recorded data. The solid line and solid points show the corresponding quantities for the predicted response. A complete set of figures showing further details of these results for HSB and VN7SH buildings during all recorded earthquakes can be found in Trifunac et al. (2001f). The results corresponding respectively to the BOC, MLK and ETEC buildings are presented in Hao (2002).

The bottom part of Figure 14 shows a comparison of the predicted total system energy with the input wave energy (detailed discussion on the "input wave energy" can be found in Trifunac et al., 2001f). The distribution of the predicted total system energy, E_I, among E_D^{bldg}, E_S^{bldg}, E_D^{soil}, E_{S+Y}^{soil}, E_k and $(E_P)_{\max}$ is also illustrated in this figure.

2.3 Energies of the System

The bottom part of Figure 14 shows a comparison of the predicted total system energy with the input wave energy versus time. To properly compare these results, we band-pass filtered the model results and the input wave energy (the processed velocity was filtered before integration). In these figures, the top solid line represents the sum of different partitions of energy resulting in the "total" system energy, E_I. The dotted line represents $a_0 \int_0^t v^2(\tau)\, d\tau$, with a_0 determined by least squares fit of the "total" energy in terms of $\int_0^t v^2(\tau)\, d\tau$. As explained in Trifunac et al. (2001f), the integral $a_0 \int_0^t v^2(\tau)\, d\tau$ represents the cumulative energy arriving at the site in the form of seismic waves. The "total" energy represents the sum of all response energies of the soil-structure system (Figure 3).

In fitting the data for the total system energy in terms of the input wave energy for different earthquake excitations, it can be assumed that the relationship is linear; that is

$$y = a_0 x \tag{24}$$

or

$$y = a_1 x + b_1 \tag{25}$$

where x and y represent $\int_0^t v^2(\tau)\, d\tau$ and E_I, respectively; and a_0, a_1 and b_1 are constants.

Figures 15 through 19 show the trends of the computed E_I (total energy of the soil-structure system response) versus $\int_0^t v^2(\tau)\, d\tau$ (input wave energy factor) for the EW (solid circles) and NS (solid triangles) responses of five selected buildings, for all recorded earthquakes. For the 1970 Lytle Creek and 1971 San Fernando earthquakes recorded in the HSB, the system energies are predicted based on assumed model parameters only, since without recorded roof motion, it is not possible to find the best estimates of the system parameters. The least squares fit through the data gives $\bar{a}_0 = 1.71\times10^4$ kg/s for the HSB, $\bar{a}_0 = 0.48\times10^4$ kg/s for the VH7SH, $\bar{a}_0 = 1.55\times10^4$ kg/s for the BOC, $\bar{a}_0 = 4.11\times10^4$ kg/s for the MLK, and $\bar{a}_0 = 0.56\times10^4$ kg/s for the ETEC building. In Figure 17, the earthquake motions at the ground floor in the Bank of California building were recorded only during the 1971 San Fernando earthquake and its aftershocks, between 9 February and 4 August 1971, and during the earthquake of 21 February 1973. Because there are not enough data, $\bar{a}_1$ and $\bar{b}_1$ are not considered in this case.

For vertically incident plane shear waves, and neglecting the wave scattering from the foundation, the coefficient a_0 should be approximately equal to $\rho_s A \beta$, where ρ_s is density, β is the shear wave velocity in the soil surrounding the foundation, and A is the area of the plan of the building foundation (Trifunac, 1995; Trifunac and Brady, 1975; Trifunac et al., 2001f). Tables in Hao (2002) present values

for ρ_s, β, plan dimensions and computed $\rho_s A\beta$ for each building. From those tables, we obtain $a_0' = \rho_s A\beta / 10^4 = 3.6\times10^4$ kg/s for HSB, $a_0' = 3.0\times10^4$ kg/s for VN7SH, $a_0' = 3.2\times10^4$ kg/s for BOC, $a_0' = 4.6\times10^4$ kg/s for MLK and $a_0' = 3.5\times10^4$ kg/s for ETEC building. It is seen that $a_0' \log_{10} \int_0^t v^2(\tau)\, d\tau$ is an upper bound for all points shown in Figures 15, 16 and 19. With increasing amplitudes of shaking, the effective $\rho_s A\beta$ reduces. The effective $\rho_s A\beta$ is reduced, because the strong ground motion does not consist of plane vertically arriving S-waves, and is a complex sequence of body and surface waves whose angles of approach vary vertically and horizontally. Furthermore, coefficients a_0 and a_1 depend on the soil-structure interaction, which involves various types of foundation systems. We conclude that considering the complexities of the energy transfer from the soil into the building (Trifunac et al., 1999a; 2001b; 2001f), the agreement of the predicted E_I versus $\int_0^t v^2(\tau)\, d\tau$ is satisfactory to warrant further and more detailed studies of the energy transfer mechanisms. Therefore, if the input wave energy factor, $\int_0^t v^2(\tau)\, d\tau$, of the strong motion at a given site is known, it is possible to estimate approximately the total system energy, E_I, for an expected future earthquake.

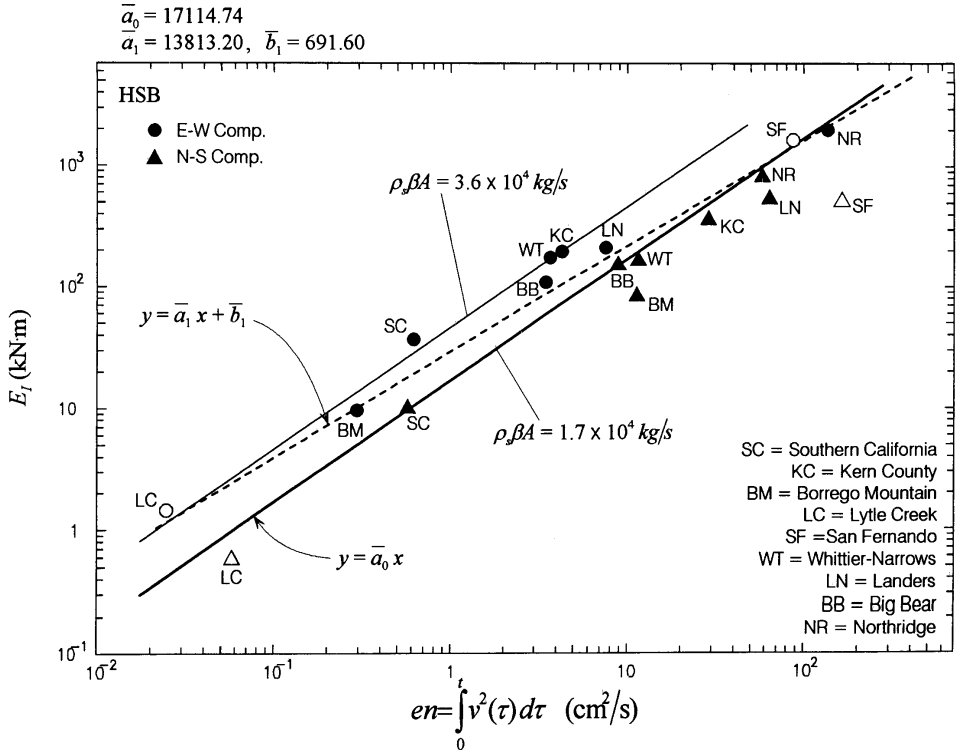

Fig. 15 Total computed response energy E_I (kN·m) versus input energy factor, *en*, for nine earthquakes recorded in the HSB

ENERGY-BASED DESIGN CONSIDERATIONS

For design purposes, it is important to define the meaning of "energy demand". Uang and Bertero (1990) defined the input energies E_i *and* E_i' (absolute and relative) in terms of the relative response of a fixed-base SDOF model subjected to horizontal ground motion only. They used these energies to convert the results to an equivalent spectral velocity and proposed the input energy equivalent velocity spectra for future design. It should be noted that the equivalent spectral velocity depends on the vibration period of the buildings and the predominant periods of the earthquake ground motions. Furthermore, the soil-structure interaction effects were not considered by Uang and Bertero (1990). Consequently, their approach is not fundamentally different from the classical Response Spectrum Method. In the following, we use the model in Figure 3 and the energy of incident ground motion, to develop more realistic

procedures for estimation of the energy demand. Then the designer has to decide how to balance this demand with all available resources, including the energy absorption capacity of the supporting soils.

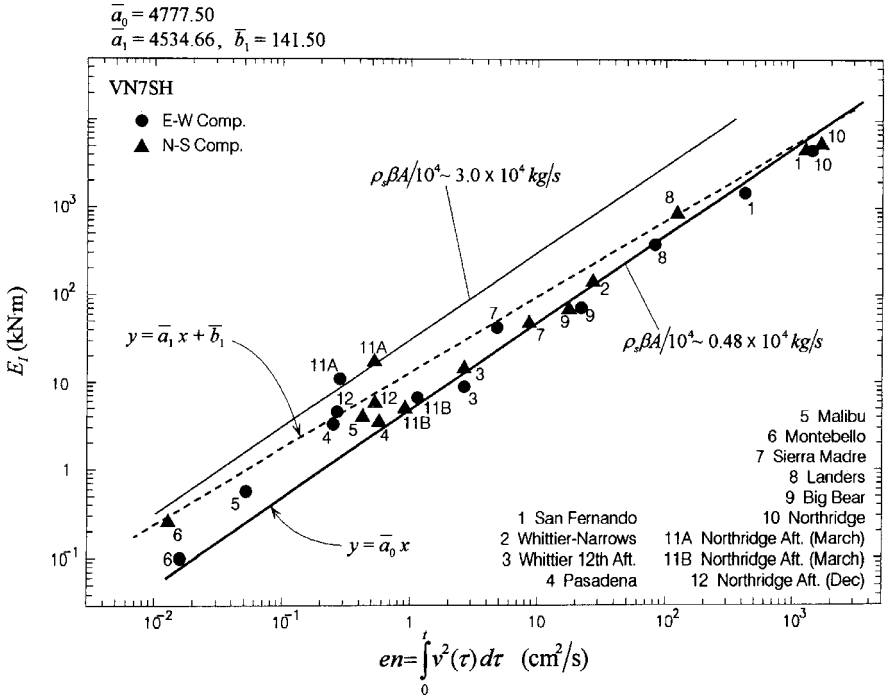

Fig. 16 Total computed response energy E_I (kN·m) versus input energy factor, *en*, for twelve earthquakes recorded in the VN7SH

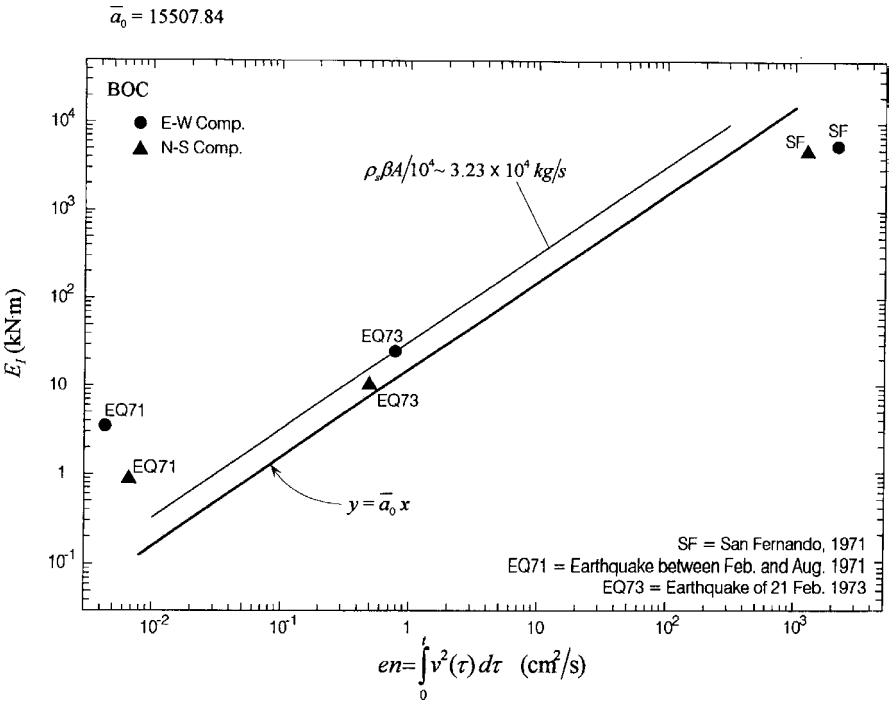

Fig. 17 Total computed response energy E_I (kN·m) versus input energy factor, *en*, for three earthquakes recorded in the BOC

1. Energy Demand

For a building supported by flexible soil, the soil-structure interaction will lead to horizontal and rocking deformations of the soil, and in general, this will reduce the amplitude of the strong-motion

pulses entering the structure. Partitioning of the incident seismic wave energy into horizontal and rocking motions of the soil-foundation-building system and scattering of the incident waves from the foundation will thus reduce the energy available to cause relative deformation of the structure. This implies that the effective energy to be absorbed by structural damping and hysteretic response of structures (for non-linear response) will be less than the traditional estimates, which consider the system as a fixed-base model (the case of "rigid" soil without soil-structure interaction).

Figures 20a and 20b illustrate the maximum kinetic energy, $(E_K + E_P)_{\max}$ versus $E_I^* + E_I$ for VN7SH structure, where $E_I^* =$ the total system response energy computed at the instant when $(E_K + E_P)_{\max}$ occurs, and $E_I =$ the total system response energy at the end of excitation. This implies that the amplitudes of velocity pulses entering the structure and causing the relative response have been reduced by soil-structure interaction, soil damping, and the energy absorbed by hysteretic response of the soil.

In the use of energy concepts for seismic-resistant design, E_I in Equation (23) represents the demand, and the summation of the left hand side terms shows what should be supplied. It is important to note that this demand does not only deform the building, but also affects the soil-foundation interaction effects. The advantages of not ignoring SSI are apparent. The challenge for future research is to quantify all these energies and to show how those can be estimated for use in design.

2. Energy Absorption Capacity of the Structure – A Case Study (VN7SH)

In the study of Trifunac et al. (2001f), a shear beam model of a building with bilinear force-deformation relation was used to examine some elementary aspects of transient waves propagating in a structure. The results are based on dimensional analysis of the problem and represent conceptual relationships between the amplitude of peak velocity of the wave propagating upwards in the structure, and the energy and power of the response. An application to the VN7SH building is illustrated in the following.

For the EW response of VN7SH building, the maximum accumulated energy, equal to 387 to 442 kN·m is estimated assuming that the building is responding in the linear range of response. The largest power of the incident waves which the VN7SH building can take without damage is estimated to be 1932 to 2208 kN·m/s (Appendix A; Trifunac et al., 2001f). A larger and longer lasting incident wave would force the building to deform monotonically, entering far into the non-linear response amplitude range. The work dissipated by the hysteresis during one quarter of the vibration cycle up to ductility of 2, is estimated to be 1240 to 1414 kN·m, and the associated power in the range from 4816 to 5492 kN·m/s. The work dissipated by the closed hysteretic loop (for one complete cycle of response) is estimated to be between 2480 to 2829 kN·m, and the corresponding maximum power is 2407 to 2746 kN·m/s.

Table 1 Description of the Different Cases Used for Comparison of Relative Response of the Building, Defined Based on whether a Fixed-Base or a Flexible-Base System is Assumed, and whether the Building and Soil are Linear or Non-linear

	Classification					
Case	**Case I**	**Case II**	**Case III**	**Case IV**	**Case V**	**Case VI**
Soil-structure interaction	no	no	yes	yes	yes	yes
Building property	linear	non-linear	linear	non-linear	linear	non-linear
Soil property	--	--	linear	linear	non-linear	non-linear

The above estimates of the building capacity to absorb energy and power are shown by the gray bands in Figure 21a. The three examples, in order of increasing amplitudes, are for (1) monotonic load increasing up to ductility of one (this represents maximum elastic strain energy), (2) one complete cycle of non-linear response (assuming ductility of two), and (3) for monotonic response, during one quarter of the system period, up to the ductility of two. All other transient capacities (e.g., for more than one complete cycle) are larger and therefore not shown in Figure 21a.

The VN7SH building was damaged by the Northridge earthquake of 17 January 1994 and its aftershocks. Clearly, inelastic action took place in the building response. To illustrate the contribution of the non-linearity in the building to the dissipation of energy, we present a comparison of the relative responses assuming fixed-base ("w/o SSI") and flexible-base ("w/ SSI") cases, when the building and soil are linear, and non-linear using the model in Figure 3. The considered cases are summarized in Table 1.

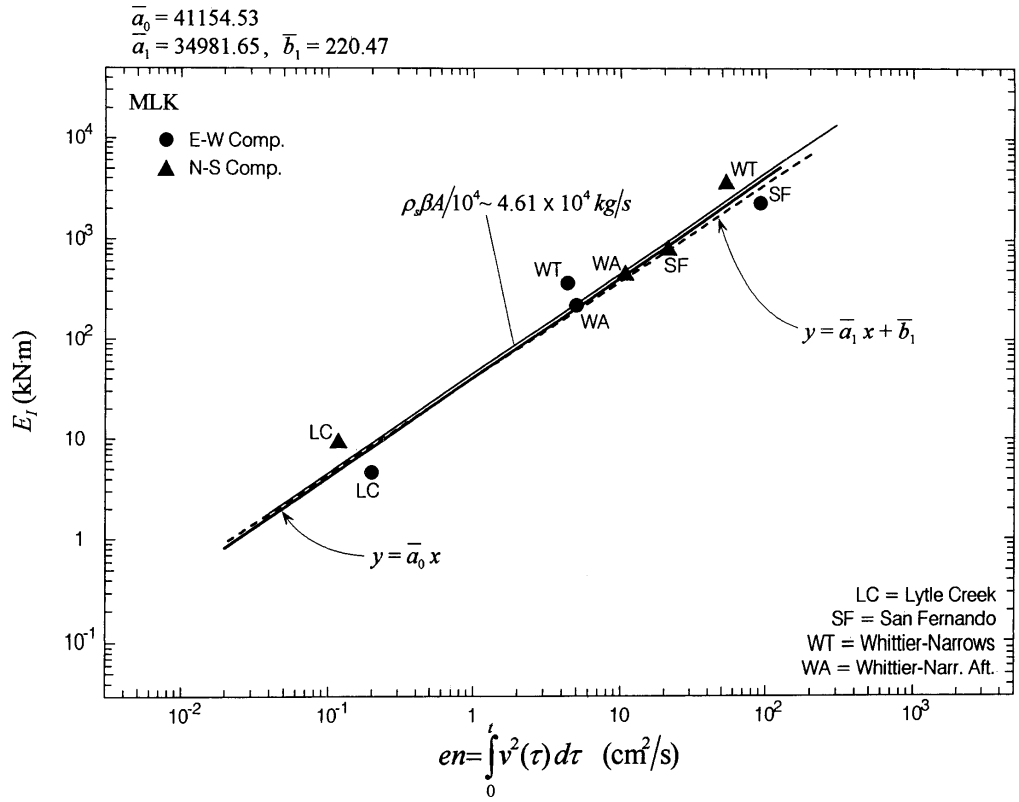

Fig. 18 Total computed response energy E_I (kN·m) versus input energy factor, *en*, for four earthquakes recorded in the MLK

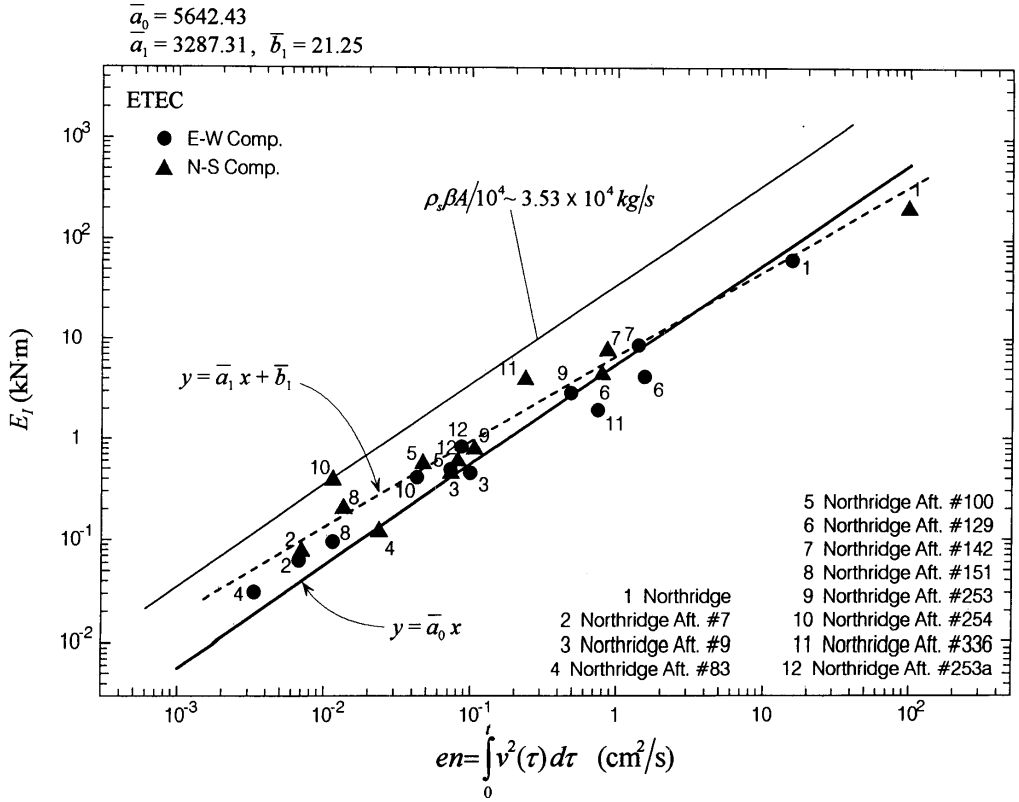

Fig. 19 Total computed response energy E_I (kN·m) versus input energy factor, *en*, for twelve earthquakes recorded in the ETEC

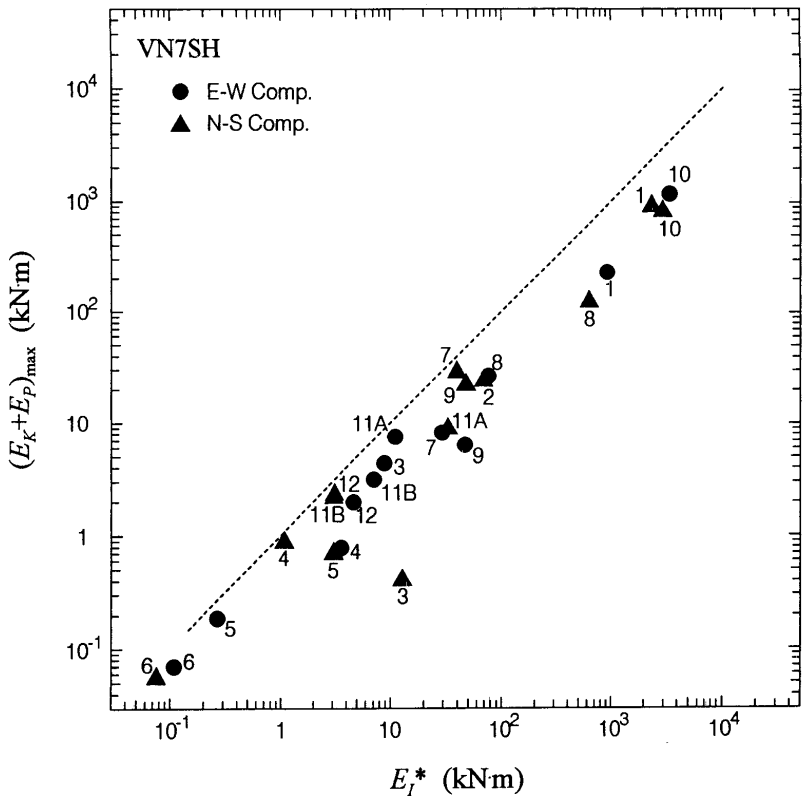

Fig. 20a Total computed kinetic energy $(E_K + E_P)_{\max}$ versus E_I^* (kN·m), total system response energy computed at the instant when $(E_K + E_P)_{\max}$ occurs, for twelve earthquakes recorded in the VN7SH

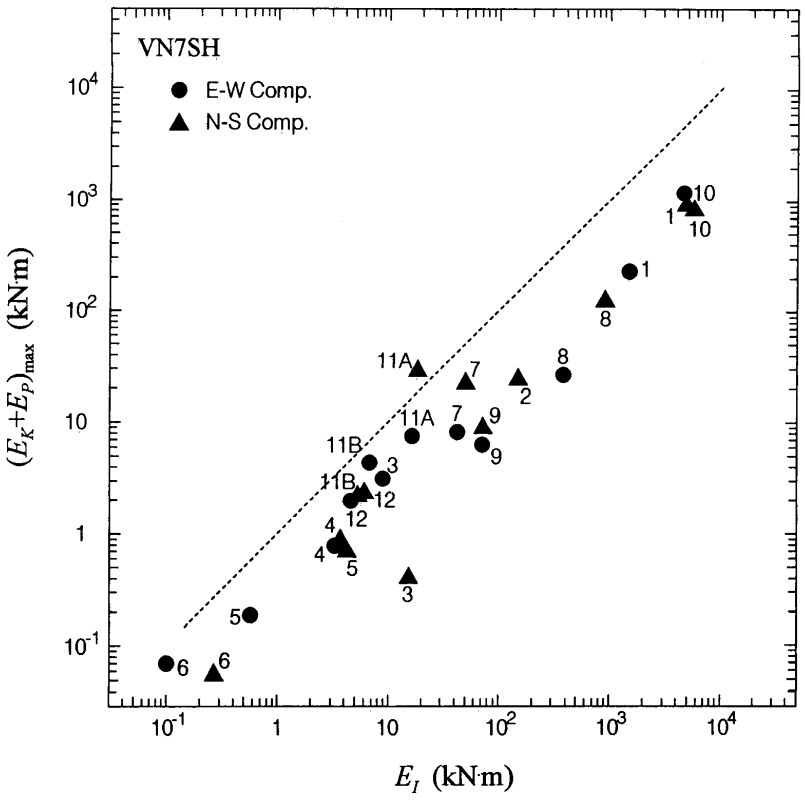

Fig. 20b Total computed kinetic energy $(E_K + E_P)_{\max}$ versus E_I (kN·m), total system response energy at the end of excitation, for twelve earthquakes recorded in the VN7SH

The responses plotted in Figures 21a and b were calculated by using the same starting parameters. The 1994 Northridge earthquake was used as input excitation to compare the predictions with the estimated energy and power demands as summarized above (Trifunac et al., 2001f). Figure 21b shows the relative responses of the model in Figure 3. Part (i) of Figure 21b shows the ground velocity during 1994 Northridge earthquake. The relative responses for Cases I and II are plotted in the Part (ii), Cases III and IV are plotted in the Part (iii); and Cases V and VI are plotted in the Part (iv). The dashed lines show the relative responses for linear building, and solid lines show the corresponding quantities for non-linear building.

Top part of Figure 21a shows the sum of all energies in the relative building response (kinetic, potential and hysteretic, when the building models are linear and non-linear), for all of the above cases. It is seen that for the "w/o SSI" cases (Cases I and II), a large ground motion pulse starting at about 3.4 s (see Part (i) of Figure 21b) would have resulted in energy jump of about 590 kN·m, during about 0.22 s, resulting in input power approaching 3000 kN·m/s (see bottom of Figure 21a). This pulse would have deformed the building beyond its linear response range, between 3.5 to 4 s into the earthquake (see also Islam, 1996). In the presence of soil-structure interaction, assuming the soil is linear (Cases III and IV), the amplitude of the incident wave is slightly reduced, and the response energy in the building is reduced by a factor of about 1.25. When the soil is non-linear (Cases V and VI), the amplitude of the incident wave is reduced considerably, and the building continues to respond in essentially a linear manner until 8.4 s into the earthquake. At about 8.9 s and 9.7 s, the SSI model with non-linear soil (Case VI) experiences a sudden jump in the energy of the relative response during short "stiff" episodes of response, for example, during closure of the gaps between the foundation and the non-linear springs representing the soil. Nevertheless, the benefits of not ignoring SSI should be apparent from Figure 21a (top), which shows that the response energy in the building is reduced by a factor of about 3 due to SSI and non-linear soil response. These results lead to the conclusion that if the VN7SH system behaved like a "fixed-base model", the building would have collapsed during the 1994 Northridge earthquake.

3. Duration of Strong Ground Motion

One of the major shortcomings of the classical Biot's response spectrum method (Biot, 1932; 1933; 1934; 1941; 1942) has been its dependence on the peak response amplitude alone, without explicit consideration of the duration of strong shaking and of the rate of arrival of the incident strong motion energy. We use the following example to show why it is important for a realistic design method to reflect the effects of strong motion duration.

Figure 22 shows the time history of two "earthquakes" that result in the same amount of the input wave energy, $\int_0^T v^2\,dt$, but different durations. The energy absorbing capacity of a hypothetical structure is shown by a wide gray line. The integral of Earthquake 1 increases rapidly and tends asymptotically towards its final value, while the integral of Earthquake 2 increases "slowly". The large average and instantaneous power produced by Earthquake 1 will cause damage and collapse of the structure, with design capacity as shown in the figure. Thus it is important to relate the maximum and average power of incident wave energy with the capacity of the structure to absorb this energy, and to choose sufficiently high energy absorbing capacity for safe earthquake-resistant design. Appendix A shows an elementary example of how to estimate the energy absorbing capacity of a hypothetical structure; but these ideas must be developed further, and calibrated against the observed full-scale responses of many structures to damaging levels of strong earthquake ground motion, before this tool can be used in engineering design.

SUMMARY AND CONCLUSIONS

In this work, an alternative (proposed by Trifunac et al., 2001f and Hao, 2002) to the spectral method in earthquake-resistant design is reviewed, by analyzing the flow of energy associated with strong motion, and by focusing on the energy during soil-foundation-structure system response. Starting with the derivation of energy equations, we reviewed the work of Trifunac et al. (2001f) and Hao (2002) on how to identify and how to quantify the energy dissipation mechanisms. For design considerations, it is necessary first to understand and to quantify all these energies, and then to show how it is possible to incorporate maximum power demands into the design process.

To illustrate the energy flow and dissipation through a soil-structure system, as a basic vehicle, a simple model in which both the soil and structural response can be non-linear has been adopted. This

model, shown in Figure 3, consists of a rigid foundation supported by non-linear soil springs, and a structure represented by a single-degree-of-freedom oscillator. For illustration, we summarized the results of Hao (2002) for a 14-story storage building in Hollywood, a 7-story hotel in Van Nuys, a 12-story commercial building in Sherman Oaks, a 9-story library building in Pasadena, and a 8-story research building in Santa Susana, for which processed strong motion data was available. All of the currently processed strong motion data were analyzed, and the simple model was used to quantify approximately the distribution of the incident wave energy. Hao (2002) and Trifunac et al. (2001f) were able to show that there is good correspondence between the estimates of the incident wave energy and the sum of all response energies in the soil-structure system. This result points to the need to research the transfer of the incident wave energy into soil-structure systems.

The above presented results show that a typical soil-structure system is capable of reflecting large fractions of the incident strong motion energy back into the soil by means of scattering (not present for the model in Figure 3) and non-linear soil response. Clearly, the nature of these powerful energy dissipation mechanisms must be carefully studied to provide reliable and verifiable estimates for use in the future earthquake-resistant design. Towards this end, we first reviewed a definition for the energy demand. Hao (2002) and Trifunac et al. (2001f) showed that this demand does not only result in deformation of the building, but also leads to strong soil-foundation interaction effects. Then, we illustrated some elementary aspects of energy absorption capacity of structures, and pointed out the roles of the duration of strong shaking and of the rate of arrival of the incident strong motion energy. The reviewed analyses are, of course, preliminary, but those indicate that there exist major advantages and rational reasons for adoption of power-based description of seismic demands in the design of earthquake-resistant structures.

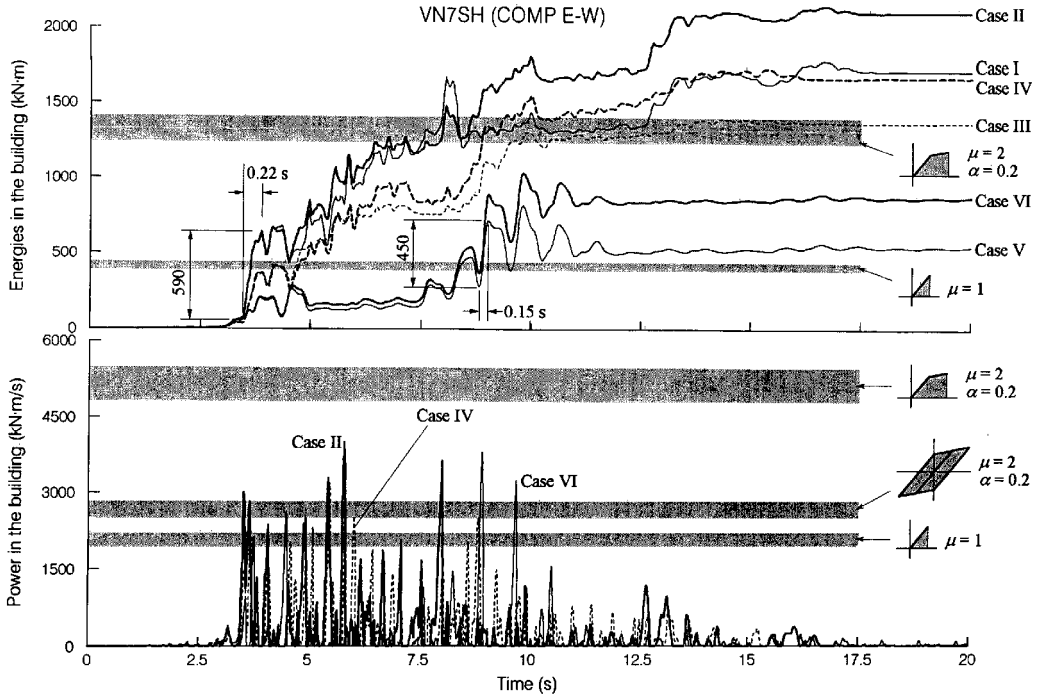

Fig. 21a Comparison of the EW response of VN7SH, during 1994 Northridge earthquake, in the presence and absence of soil-structure interaction, with linear and non-linear soil considerations; top: energies of relative response; bottom: power of relative response

ACKNOWLEDGEMENTS

The material presented in this paper is drawn mostly from the Ph.D. thesis of the author presented to the Graduate School of the University of Southern California in May of 2002. This paper is dedicated to the author's thesis advisor, Professor Mihailo D. Trifunac, on the occasion of his 60th birthday, and in recognition of his leadership and many original contributions to the fields of earthquake engineering and engineering seismology, including work on the topic reviewed in this paper. The author would like to express her most sincere gratitude to Professors M. D. Trifunac and M. I. Todorovska for their guidance throughout her doctoral studies, and for their encouragements and advice.

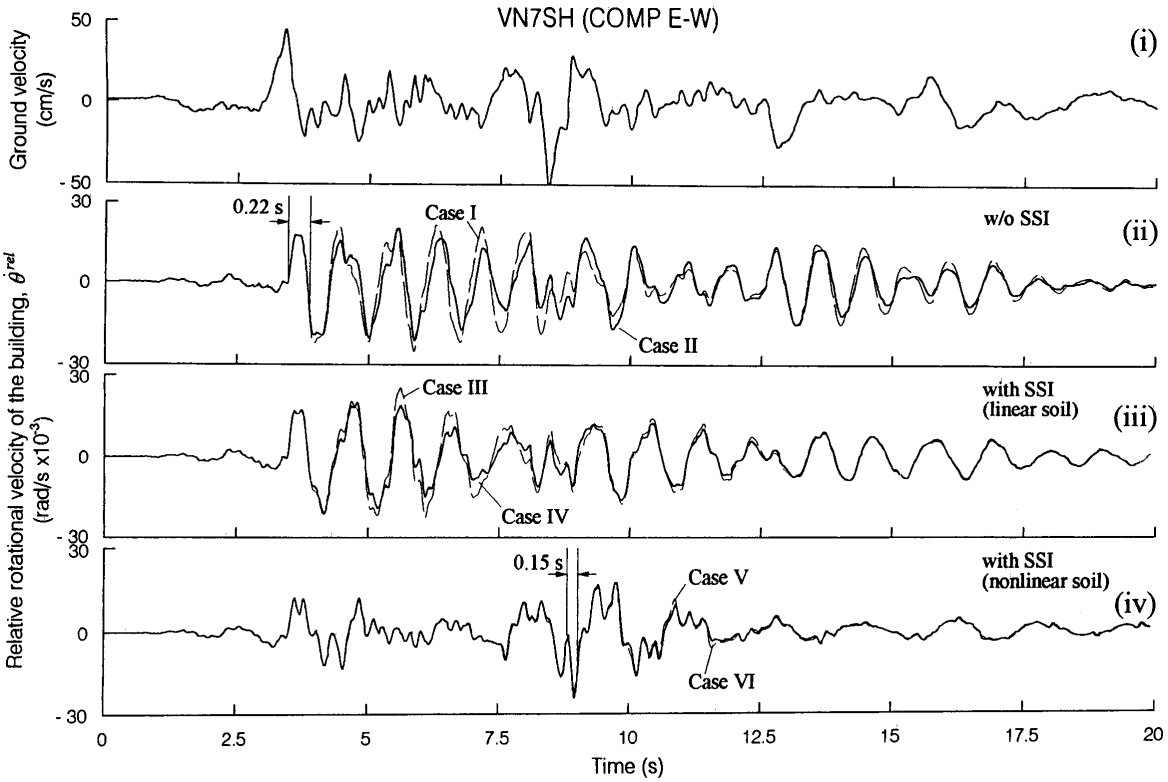

Fig. 21b Comparison of the simulated EW relative velocity response of VN7SH, during 1994 Northridge earthquake, in the presence and absence of soil-structure interaction (dashed lines show the responses for linear building assumption, and solid lines show the corresponding quantities but for non-linear building assumption): (i) ground input velocity, (ii) simulation without soil-structure interaction (SSI) (iii) simulation with SSI assuming soil behaves linearly (iv) simulation with SSI assuming soil behaves non-linearly

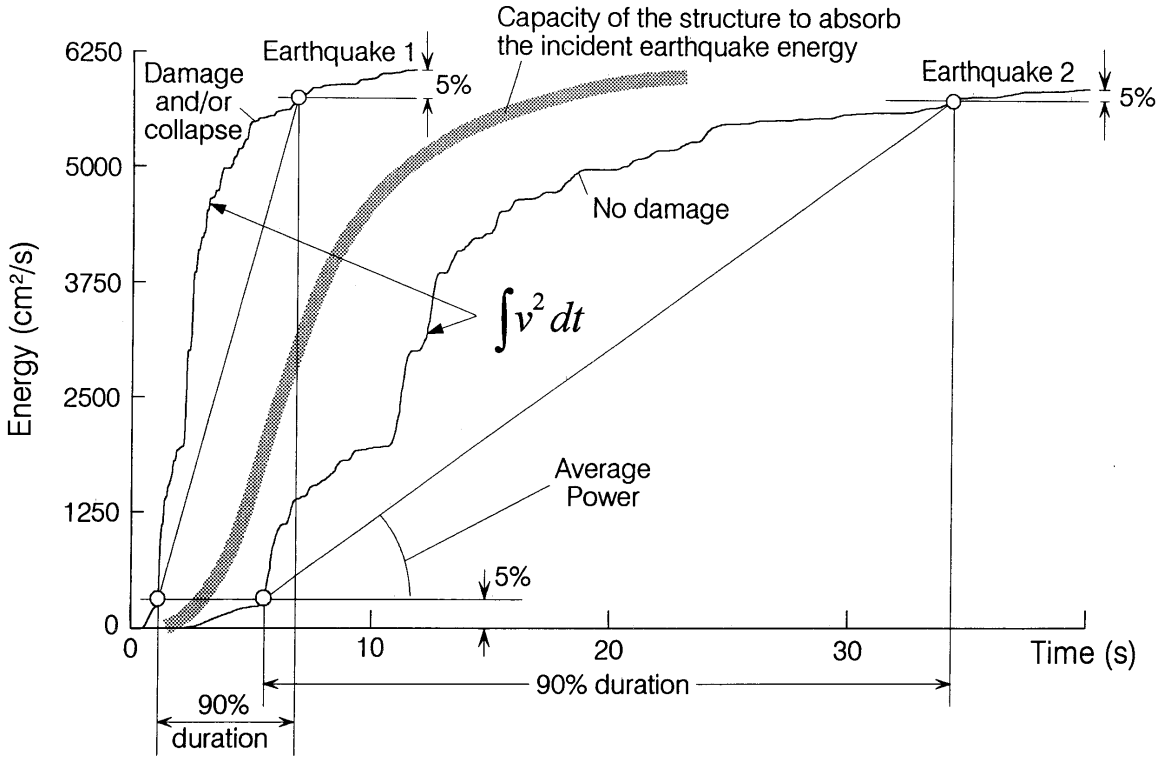

Fig. 22 Comparison of the time histories of two earthquakes that have same input wave energy but different durations, with the energy absorbing capacity of a hypothetical structure

APPENDIX A : POWER DEMAND AND ABSORPTION CAPACITY OF THE STRUCTURE

It is assumed that the velocity pulse entering the structure and deforming it (as shown in Fig. A.1) has amplitude v_b. When the soil-structure interaction can be neglected, $v_b = v_{G,\max}$ ($v_{G,\max}$ is peak velocity of ground motion in the free-field), and when it is present and redistributes the incident wave energy, $v_b = P v_{G,\max}$ where $P \leq 1$. Assuming that the soil foundation system has equivalent density ρ_e and shear wave velocity β_e, the energy carried by the incident waves, per unit time and across unit area normal to the direction of propagation, is $\rho_e \beta_e v_b^2$.

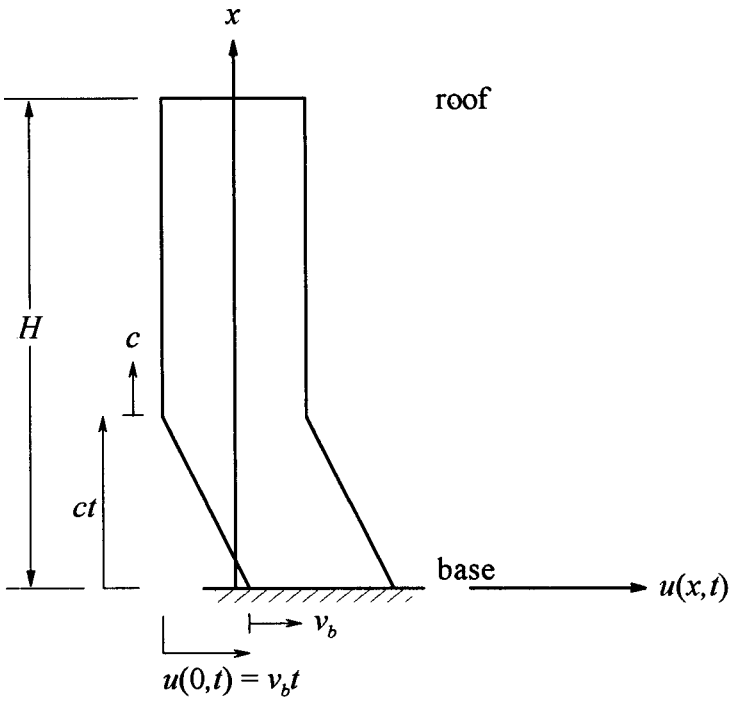

Fig. A.1 Wave caused by sudden movement at the base of the shear building, for constant velocity pulse with amplitude v_b, for time $t < t_0$ (= pulse duration)

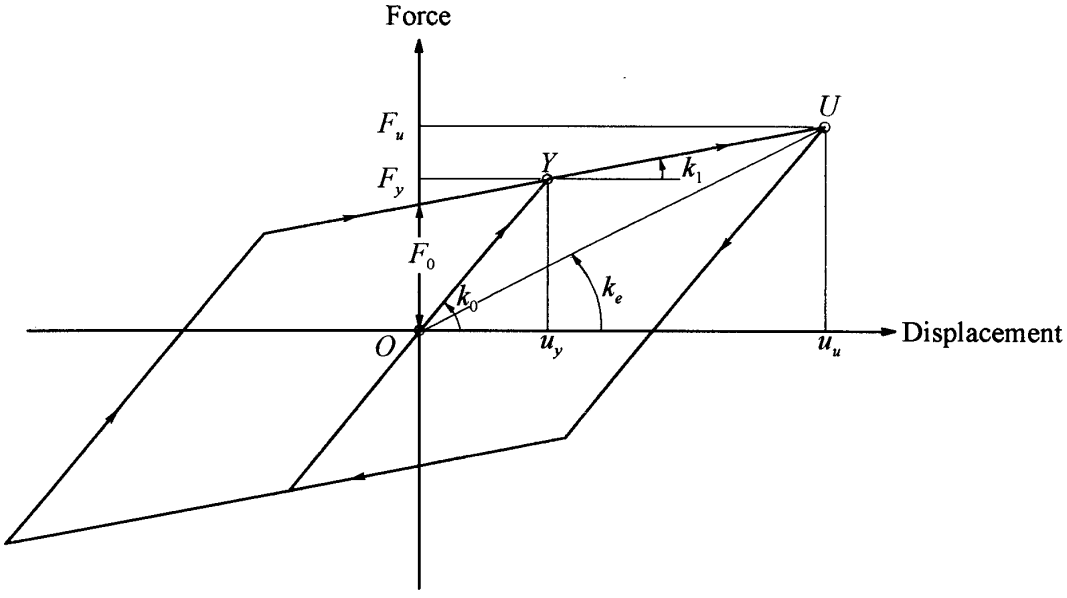

Fig. A.2 Bilinear force-deformation representation of a shear-beam building model experiencing non-linear response

The hysteretic work per one complete cycle of non-linear relative response of the structure is (Figure A.2)

$$W_{\square} = 4F_0\left(u_u - u_y\right) \tag{A.1}$$

Defining $k_0 u_y \equiv F_y = ma_y$, where a_y is the static acceleration which produces deflection u_y, $k_1 = \alpha k_0$, and using the standard definition of ductility, $\mu = u_u / u_y$, one can write

$$W_{\square} = 4(1-\alpha)\, m_b a_y \,(\mu - 1)/u_y \tag{A.2}$$

By approximating the equivalent stiffness of the non-linear system by the secant modulus (see Figure A.2)

$$k_e = k_0\left[\frac{1+\alpha(\mu-1)}{\mu}\right], \tag{A.3}$$

gives the approximate period of non-linear oscillator $T_e = T_n \xi$ where

$$\xi = \left[\frac{\mu}{1+\alpha(\mu-1)}\right]^{1/2}. \tag{A.4}$$

The maximum power, the oscillator can absorb during one cycle of response, is then

$$W_{\square}/T_e = 4(1-\alpha)(\mu-1) m_b a_u \, u_y \,/T_n \, \xi \tag{A.5}$$

and since, for the first mode of vibration $T_n = 4\,H_{sb}/\beta_b$,

$$W_{\square}/T_e = 4(1-\alpha)(\mu-1)\frac{m_b a_y u_y \beta_b}{4H_{sb}\xi}. \tag{A.6}$$

It is not probable that the incident motion will be so regular to allow completion of the complete hysteretic cycle. Instead, the pulse v_b may be one-directional, with low frequency content, and of considerable duration causing monotonic increase in the relative displacement u. Therefore, it is also of interest to examine the relationship of the input power demand relative to the capacity of the structure to absorb this power along the path *OYU* (as shown in Figure A.2). The work accompanying non-linear response in going from *O* to *U* is

$$W_{\rightarrow} = \frac{1}{2}k_0 u_y^2 + \left(u_u - u_y\right)k_0 u_y + \frac{1}{2}k_1\left(u_u - u_y\right)^2 \tag{A.7}$$

or

$$\begin{aligned} W_{\rightarrow} &= k_0\left[\frac{1}{2} + (\mu-1) + \frac{1}{2}\alpha(\mu-1)^2\right]u_y^2 \\ &= \left[\frac{1}{2} + (\mu-1) + \frac{1}{2}\alpha(\mu-1)^2\right]m_b a_y u_y \end{aligned} \tag{A.8}$$

The time required to reach *U* starting at *O* is approximately $T_e/4$, and this gives the associated power absorbing capacity of the structure

$$4W_{\rightarrow}/T_n\xi = \left[\frac{1}{2} + (\mu-1) + \frac{1}{2}\alpha(\mu-1)^2\right]\frac{m_b a_y u_y 4\beta_b}{4H_{sb}\xi} \tag{A.9}$$

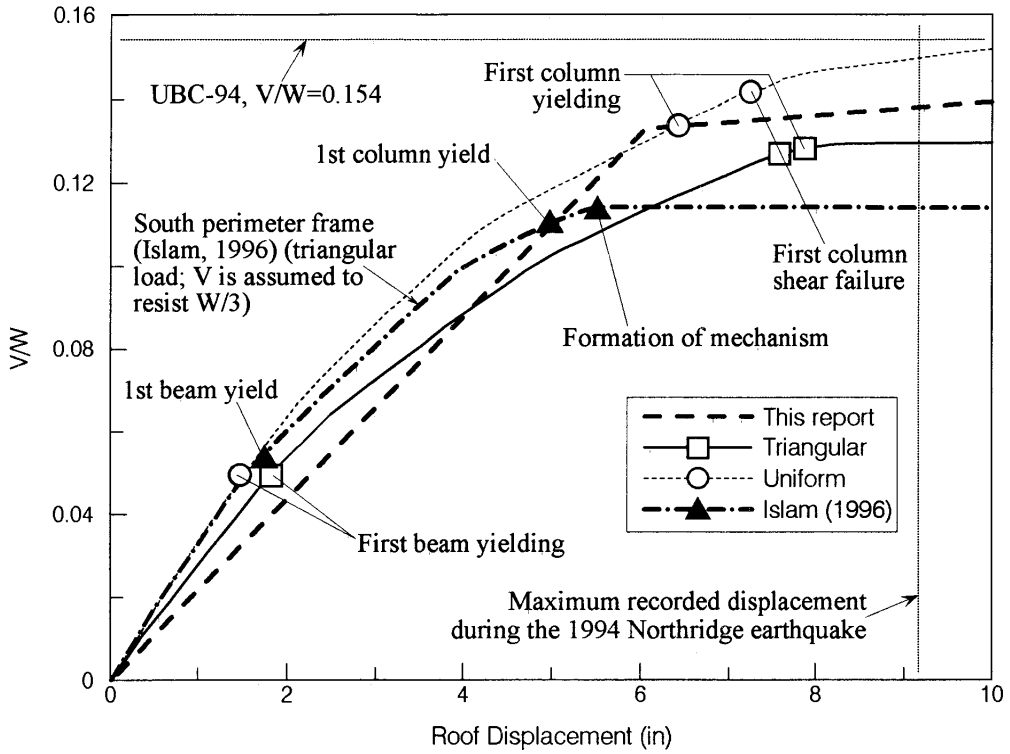

Fig. A.3 Base shear (V) coefficient normalized by 1/3 of the total building weight, W, versus EW roof displacement of VN7SH (after Islam, 1996; and Li and Jirsa, 1998)

For illustration purposes, the values of a_y = 0.13g and u_y = 15.3 cm have been estimated based on non-linear static push-over analysis of the EW response of VN7SH building by Islam (1996) and Li and Jirsa (1998). Their results are summarized in Figure A.3, showing the base shear coefficient, V/W, where V is the computed base shear, and W is total weight of the building $\left(W \sim 10^4 \text{ kips}\right)$, plotted versus roof displacement for triangular and uniform load distribution patterns. Also shown in this figure are the "maximum roof displacement" determined by Islam (1996) and by Li and Jirsa (1998) from the recorded data, and the computed UBC-94 base shear $V = 0.154\ W$.

For fixed-base EW response, the two independent estimates of F_y are F_y = 1300 kips (5780 kN) (Li and Jirsa, 1998) and F_y = 1140 kips (5070 kN) (Islam, 1996). Assuming u_y = 15.3 cm, these two estimates imply $F_y u_y$ = 775 to 884 kN·m. During 1/4 cycle of the response, and linear deformation in the building, the maximum accumulated potential energy is equal to 387 to 442 kN·m (see Figure A.4, left-top). For $T_n \sim$ 0.8 s, we can estimate the largest power of the EW component of the incident waves, which the VN7SH building can take without damage, to be 1932 to 2208 kN·m/s.

The time-dependent evolution of the energy dissipated by non-linear building response will depend on the history of the excitation, but several characteristic milestone values can be estimated *a priori.* This is illustrated in Figure A.4. The shaded area in the top-left of this figure illustrates the largest potential energy in the oscillator, which is still responding in the linear range of response ($u < u_y$), when $\mu = 1$ and when $F = F_y$. For VN7SH building, using static push over analyses of Islam (1996) and Li and Jirsa (1998), for EW response, as indicators of the possible range of F_y, we obtain the estimates of 5070 kN and 5783 kN respectively. A larger and longer lasting incident velocity pulse might force the equivalent oscillator to deform monotonically to, say $u = 2u_y$ ($\mu = 2$), during $T_e/4$. This case is illustrated in the left-bottom part of Figure A.4. Assuming $\alpha = 0.2$ implies the work dissipated by the hysteresis in going from O to Y to U to be 1240 to 1414 kN·m (see Equation (A.8)), and the associated power $4W_{\rightarrow}/T_n\xi$ to be in the range from 4816 to 5492 kN·m/s. The right part of Fig. A.4 shows the closed hysteretic loop, starting at OYU and returning to Y after one complete cycle lasting $T_n\xi$ seconds. The work dissipated by such a loop, assuming F_y as above, with $\mu = 2$ and $\alpha = 0.2$ is 2480 to 2829 kN·m. The corresponding maximum

power this oscillator can dissipate along this path is then 2407 to 2746 kN·m/s. These estimates of the building capacity to absorb energy and power are shown by the gray bands in Figure 21a.

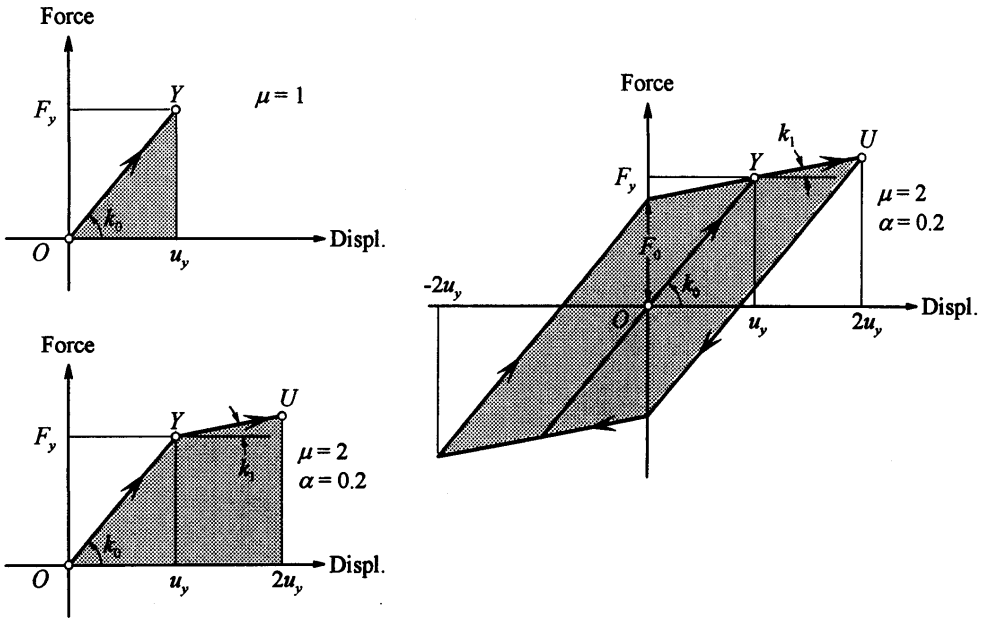

Fig. A.4 The shaded areas represent: (left-top) maximum potential energy associated with linear response; (left-bottom) hysteretic energy associated with monotonic non-linear response; and (right) hysteretic energy associated with oscillatory (periodic, one cycle) excitation

REFERENCES

1. Akiyama, H. (1985). "Earthquake-Resistant Limit-State Design for Buildings", Univ. of Tokyo Press, Tokyo, Japan.
2. Akiyama, H. (1988). "Earthquake Resistant Design Based on the Energy Concept", Proc. of the Ninth World Conference on Earthquake Engg., Tokyo, Japan, pp. 905-910.
3. Akiyama, H. (1997). "Damage-Controlled Earthquake Resistant Design Method Based on the Energy Concept", in Report UCB/EERC-97/05, Earthquake Engineering Research Center, University of California, Berkeley, California, U.S.A., pp. 49-56.
4. Anderson, J.C. and Bertero, V.V. (1969). "Seismic Behavior of Multistory Frames by Different Philosophies", Report UCB/EERC-69/11, Earthquake Engineering Research Center, University of California, Berkeley, California, U.S.A..
5. Arias, A. (1970). "A Measure of Earthquake Intensity", in Seismic Design of Nuclear Power Plants (ed. R.J. Hansen), The Mass. Inst. of Tech. Press, U.S.A.
6. Benioff, H. (1934). "The Physical Evaluation of Seismic Destructiveness", Bull. Seism. Soc. Amer., Vol. 24, pp. 398-403.
7. Biot, M.A. (1932). "Vibrations of Buildings during Earthquake", Chapter II in Ph.D. thesis No. 259 entitled "Transient Oscillations in Elastic Systems", Aeronautic Dept., Calif. Inst. Of Tech., Pasadena, California, U.S.A.
8. Biot, M.A. (1933). "Theory of Elastic Systems Vibrating under Transient Impulse with an Application to Earthquake–Proof Buildings", Proc. National Academy of Science, Vol. 19, No. 2, pp. 262-268.
9. Biot, M.A. (1934). "Theory of Vibration of Buildings during Earthquake", Zeitschrift für Angewandte Matematik and Mechanik, Vol. 14, No. 5, pp. 213-223.
10. Biot, M.A. (1941). "A Mechanical Analyzer for the Prediction of Earthquake Stresses", Bull. Seism. Soc. Amer., Vol. 31, No. 2, pp. 151-171.

11. Biot, M.A. (1942). "Analytical and Experimental Methods in Engineering Seismology", ASCE Transactions, Vol. 108, pp. 365-408.
12. Blume, J.A. (1960). "A Reserve Energy Technique for the Earthquake Design and Rating of Structures in the Inelastic Range", Proc. of the Second World Conference on Earthquake Engg., Tokyo, Japan, pp. 1061-1083.
13. Decanini, L.D. and Mollaioli, F. (2001). "An Energy-Based Methodology for the Assessment of Seismic Demand", Soil Dyn. and Earthquake Engg., Vol. 21, No. 2, pp. 113-137.
14. Duncan, W.J. (1952). "A Critical Examination of the Representation of Massive and Elastic Bodies by Systems of Rigid Masses Elastically Connected", Quart. J. Mech. Appl. Math., Vol. 5, No. 1, pp. 97-108.
15. Fajfar, P. and Fischinger, M.A. (1990). "A Seismic Design Procedure including Energy Concept", Proc. of the Ninth European Conference on Earthquake Engg., Moscow, USSR.
16. Gutenberg, B. and Richter, C.F. (1956). "Earthquake Magnitude, Intensity, Energy, and Acceleration", Bull. Seism. Soc. Amer., Vol. 46, No. 2, pp. 105-145.
17. Hao, T.-Y. (2002). "Investigation of Energy Flow in Earthquake Response of Structures", Ph.D. Thesis, Dept. of Civil Engrg., Univ. of Southern California, Los Angeles, California, U.S.A..
18. Hayir, A., Todorovska, M.I. and Trifunac, M.D. (2001). "Antiplane Response of a Dike with Flexible Soil-Structure Interaction to Incident SH-Waves", Soil Dyn. and Earthquake Engg., Vol. 21, No. 7, pp. 603-613.
19. Housner, G.W. (1956). "Limit Design of Structures to Resist Earthquakes", Proc. of the First World Conference on Earthquake Engg., Berkeley, California, pp. 5.1-5.13.
20. Husid, R. (1967). "Gravity Effects on the Earthquake Response of Yielding Structures", Ph.D. Thesis, Calif. Inst. of Tech., Pasadena, California, U.S.A.
21. Iguchi, M. and Luco, J.E. (1982). "Vibration of Flexible Plate on Viscoelastic Medium", J. of Engg. Mech., ASCE, Vol. 108, No. 6, pp. 1103-1120.
22. Islam, M.S. (1996). "Analysis of the Response of an Instrumented 7-story Nonductile Concrete Frame Building Damaged during the Northridge Earthquake", Professional Paper 96-9, Los Angeles Tall Buildings Structural Design Council.
23. Ivanović, S.S., Trifunac, M.D., Novikova, E.I., Gladkov, A.A. and Todorovska, M.I. (1999). "Instrumented 7-story Reinforced Concrete Building in Van Nuys, California: Ambient Vibration Surveys Following the Damage from the 1994 Northridge Earthquake", Report CE 99-03, Dept. of Civil Eng., Univ. of Southern California, Los Angeles, California, U.S.A.
24. Ivanović, S.S., Trifunac, M.D., Novikova, E.I., Gladkov, A.A. and Todorovska, M.I. (2000). "Ambient Vibration Tests of a Seven-Story Reinforced Concrete Building in Van Nuys, California, Damaged by the 1994 Northridge Earthquake", Soil Dyn. and Earthquake Engg., Vol. 19, No. 6, pp. 391-411.
25. Joyner, W.B. (1975). "A Method for Calculating Nonlinear Seismic Response in Two Dimensions", Bull. Seism. Soc. Amer., Vol. 65, No. 5, pp. 1337-1357.
26. Joyner, W.B. and Chen, A.T.F. (1975). "Calculating of Nonlinear Ground Response in Earthquakes", Bull. Seism. Soc. Amer., Vol. 65, No. 5, pp. 1315-1336.
27. Lee, V.W. (1979). "Investigation of Three-Dimensional Soil-Structure Interaction", Report CE 79-11, Dept. of Civil Eng., University of Southern California, Los Angeles, California, U.S.A..
28. Li, R.Y. and Jirsa, J.D. (1998). "Nonlinear Analysis of an Instrumented Structure Damaged in the 1994 Northridge Earthquake", Earthquake Spectra, Vol. 14, No. 2, pp. 265-283.
29. Liou, G.-S. and Huang, P.R. (1994). "Effects of Flexibility on Impedance Functions for Circular Foundations", J. of Engg. Mech., ASCE, Vol. 120, No. 7, pp. 1429-1446.
30. Luco, J.E., Trifunac, M.D. and Wong, H.L. (1986). "Soil Structure Interaction Effects on Forced Vibration Tests", Report 86-05, Dept. of Civil Eng., Univ. of Southern California, Los Angeles, California, U.S.A.
31. Papageorgiou, A.S. and Lin, B.C. (1991). "Analysis of Recorded Earthquake Response and Identification of a Multi-story Structure Accounting for Foundation Interaction Effects", Soil Dyn. and Earthquake Engg., Vol. 10, No. 1, pp. 55-64.

32. Richart, F.E., Jr., Hall, J.R., Jr. and Woods, R.D. (1970). "Vibrations of Soils and Foundations", Prentice-Hall, Englewood Cliffs, New Jersey, U.S.A.
33. Rodrigues, M.E. and Montes, R. (2000). "Seismic Response and Damage Analysis of Buildings Supported on Flexible Soils", Earthquake Engg. and Structural Dynamics, Vol. 29, No. 5, pp. 647-665.
34. Sezawa, K. and Kanai, K. (1936). "Improved Theory of Energy Dissipation in Seismic Vibrations on a Structure", Bull. Earth. Res. Inst., Vol. XIV, Part 2, pp. 164-168.
35. Tanabashi, R. (1937). "On the Resistance of Structures to Earthquake Shocks", Memoirs of the College of Engineering, Kyoto Imperial University, Japan.
36. Tanabashi, R. (1956). "Studies of the Nonlinear Vibrations of Structures Subjected to Destructive Earthquakes", Proc. of the First World Conference on Earthquake Engg., Berkeley, California, U.S.A.
37. Tembulkar, J.M. and Nau, J.M. (1987). "Inelastic Modeling and Seismic Energy Dissipation", J. of Struct. Engg., ASCE, Vol. 113, No. 6, pp. 1373-1377.
38. Todorovska, M.I. and Trifunac, M.D. (1990a). "A Note on the Propagation of Earthquake Waves in Buildings with Soft First Floor", J. of Engg. Mech., ASCE, Vol. 116, No. 4, pp. 892-900.
39. Todorovska, M.I. and Trifunac, M.D. (1990b). "A Note on Excitation of Long Structures by Ground Waves", J. of Engg Mech., ASCE, Vol. 116, No. 4, pp. 952-964.
40. Todorovska, M.I. and Trifunac, M.D. (1990c). "Analytical Model for In-plane Building-Foundation-Soil Interaction: Incident P-, SV- and Rayleigh Waves", Report 90-01, Dept. of Civil Engg., Univ. of Southern California, Los Angeles, California, U.S.A..
41. Todorovska, M.I. and Trifunac, M.D. (1991). "Radiation Damping during Two-Dimensional Building-Soil Interaction", Report 91-01, Dept. of Civil Eng., Univ. of Southern California, Los Angeles, California, U.S.A.
42. Todorovska, M.I. and Trifunac, M.D. (1992). "The System Damping, the System Frequency and the System Response Peak Amplitudes during In-plane Building-Soil Interaction", Earthquake Eng. and Struct. Dyn., Vol. 21, No. 2, pp. 127-144.
43. Todorovska, M.I. and Trifunac, M.D. (1993). "The Effects of Wave Passage on the Response of Base-Isolated Buildings on Rigid Embedded Foundations", Report CE 93-10, Dept of Civil Eng., Univ. of Southern California, Los Angeles, California, U.S.A.
44. Todorovska, M.I., Ivanović, S.S. and Trifunac, M.D. (2001a). "Wave Propagation in a Seven-Story Reinforced Concrete Building, I: Theoretical Models", Soil Dyn. and Earthquake Engg., Vol. 21, No. 3, pp. 211-223.
45. Todorovska, M.I., Ivanović, S.S. and Trifunac, M.D. (2001b). "Wave Propagation in a Seven-Story Reinforced Concrete Building, II: Observed Wave Numbers", Soil Dyn. and Earthquake Engg., Vol. 21, No. 3, pp. 225-236.
46. Todorovska, M.I., Hayir, A. and Trifunac, M.D. (2001c). "Antiplane Response of a Dike on Flexible Embedded Foundation to Incident SH-Waves", Soil Dyn. and Earthquake Engg., Vol. 21, No. 7, pp. 593-601.
47. Trifunac, M.D. (1994). "Q and High Frequency Strong Motion Spectra", Soil Dyn. and Earthquake Engg., Vol. 13, No. 3, pp. 149-161.
48. Trifunac, M.D. (1995). "Empirical Criteria for Liquefaction of Sands via Standard Penetration Tests and Seismic Wave Energy", Soil Dyn. and Earthquake Engg., Vol. 14, No. 4, pp. 419-426.
49. Trifunac, M.D. (1997). "Differential Earthquake Motion of Building Foundation", J. of Struct. Engg., ASCE, Vol. 123, No. 4, pp. 414-422.
50. Trifunac, M.D. and Brady, A.G. (1975). "A Study of the Duration of Strong Earthquake Ground Motion", Bull. Seism. Soc. Amer., Vol. 65, pp. 581-626.
51. Trifunac, M.D. and Hao, T.-Y. (2001). "7-Story Reinforced Concrete Building in Van Nuys, California: Photographs of the Damage from the 1994 Northridge Earthquake", Report CE 01-05, Dept. of Civil Engrg., Univ. of Southern California, Los Angeles, California, U.S.A.
52. Trifunac, M.D. and Todorovska, M.I. (1996). "Nonlinear Soil Response – 1994 Northridge California Earthquake", J. Geotechnical Engg., ASCE, Vol. 122, No. 9, pp. 725-735.

53. Trifunac, M.D. and Todorovska, M.I. (1997a). "Northridge, California, Earthquake of January 17, 1994: Density of Red-Tagged Buildings versus Peak Horizontal Velocity and Site Intensity of Strong Motion", Soil Dyn. and Earthquake Engg., Vol. 16, No. 3, pp. 209-222.
54. Trifunac, M.D. and Todorovska, M.I. (1997b). "Northridge, California, Earthquake of January 17, 1994: Density of Pipe Breaks and Surface Strains", Soil Dyn. and Earthquake Engg., Vol. 16, No. 3, pp. 193-207.
55. Trifunac, M.D. and Todorovska, M.I. (1997c). "Response Spectra for Differential Motion of Columns", Earthquake Engg. and Struct. Dyn., Vol. 26, No. 2, pp. 251-268.
56. Trifunac, M.D. and Todorovska, M.I. (1998a). "Nonlinear Soil Response as a Natural Passive Isolation Mechanism – The 1994 Northridge, California Earthquake", Soil Dynamics and Earthquake Eng., Vol. 17, No. 1, pp. 41-51.
57. Trifunac, M.D. and Todorovska, M.I. (1998b). "The Northridge, California, Earthquake of 1994: Fire Ignition by Strong Shaking", Soil Dyn. and Earthquake Engg., Vol. 17, No. 3, pp. 165-175.
58. Trifunac, M.D. and Todorovska, M.I. (1998c). "Damage Distribution during the 1994 Northridge, California, Earthquake Relative to Generalized Categories of Surficial Geology", Soil Dyn. and Earthquake Engg., Vol. 17, No. 7, pp. 239-253.
59. Trifunac, M.D. and Todorovska, M.I. (1998d). "Amplification of Strong Ground Motion and Damage Patterns during the 1994 Northridge, California, Earthquake", Proc. ASCE Specialty Conf. on Geotechnical Earthquake Engg. and Soil Dyn., Seattle, Washington, Geotechnical Special Publ. No. 75, ASCE, Vol. I, pp. 714-725.
60. Trifunac, M.D. and Todorovska, M.I. (1999). "Reduction of Structural Damage by Nonlinear Soil Response", J. Structural Engrg., ASCE, Vol. 125, No. 1, pp. 89-97.
61. Trifunac, M.D. and Todorovska, M.I. (2001a). "Evolution of Accelerographs, Data Processing, Strong Motion Arrays and Amplitude and Spatial Resolution in Recording Strong Earthquake Motion", Soil Dyn. and Earthquake Engg., Vol. 21, No. 6, pp. 537-555.
62. Trifunac, M.D. and Todorovska, M.I. (2001b). "Recording and Interpreting Earthquake Response of Full-Scale Structures", in Proc. NATO Workshop on Strong Motion Instrumentation for Civil Engineering Structures (eds. M. Erdik et al.), Kluwer Academic Publishers, pp. 131-155.
63. Trifunac, M.D., Ivanović, S.S., Todorovska, M.I., Novikova, E.I. and Gladkov, A.A. (1999a). "Experimental Evidence for Flexibility of a Building Foundation Supported by Concrete Friction Piles", Soil Dyn. and Earthquake Engg., Vol. 18, No. 3, pp. 169-187.
64. Trifunac, M.D., Ivanović, S.S. and Todorovska, M.I. (1999b). "Seven Story Reinforced Concrete Building in Van Nuys, California: Strong Motion Data Recorded between 7 February 1971 and 9 December 1994, and Description of Damage Following Northridge, 17 January 1994 Earthquake", Report 99-02, Dept. of Civil Eng., Univ. of Southern California, Los Angeles, California, U.S.A.
65. Trifunac, M.D., Ivanović, S.S. and Todorovska, M.I. (2001a). "Apparent Periods of a Building, Part I: Fourier Analysis", J. of Struct. Engg., ASCE, Vol. 127, No. 5, pp. 517-526.
66. Trifunac, M.D., Ivanović, S.S. and Todorovska, M.I. (2001b). "Apparent Periods of a Building, Part II: Time-Frequency Analysis", J. of Struct. Engg., ASCE, Vol. 127, No. 5, pp. 527-537.
67. Trifunac, M.D., Todorovska, M.I. and Hao, T.-Y. (2001c). "Full-Scale Experimental Studies of Soil-Structure Interaction – A Review", Proc. 2nd U.S.-Japan Workshop on Soil-Structure Interaction, Tsukuba City, Japan.
68. Trifunac, M.D., Ivanović, S.S. and Todorovska, M.I. (2001d). "Wave Propagation in a Seven-Story Reinforced Concrete Building, III: Damage Detection via Changes in Wave Numbers", Soil Dyn. and Earthquake Engrg. (in press).
69. Trifunac, M.D., Hao, T.-Y. and Todorovska, M.I. (2001e). "Response of a 14-Story Reinforced Concrete Structure to Nine Earthquakes: 61 Years of Observation in the Hollywood Storage Building", Report 01-02, Dept. of Civil Eng., Univ. of Southern California, Los Angeles, California, U.S.A.
70. Trifunac, M.D., Hao, T-Y. and Todorovska, M.I. (2001f). "On Energy Flow in Earthquake Response", Report 01-03, Dept. of Civil Eng., Univ. of Southern California, Los Angeles, California, U.S.A.

71. Uang, C.M. and Bertero, V.V. (1988). "Use of Energy as a Design Criterion in Earthquake-Resistant Design", Report UCB/EERC-88/18, Earthquake Engineering Research Center, Univ. of California, Berkeley, California, U.S.A.
72. Uang, C.M. and Bertero, V.V. (1990). "Evaluation of Seismic Energy in Structures", Earthquake Engg. and Struct. Dyn., Vol. 19, No. 1, pp. 77-90.
73. Zahrah, T.F. and Hall, W.J. (1984). "Earthquake Energy Absorption in SDOF Structures", J. of Struct. Engg., Vol. 110, No. 8, pp. 1757-1772.

LIST OF DATA REPORTS[1]
BY
PROFESSOR MIHAILO D. TRIFUNAC

1. "Strong-Motion Earthquake Accelerograms, Digitized and Plotted Data, Volume I, Part A", *Report EERL 70-20*, California Institute of Technology, Pasadena, 1970.
2. "Strong-Motion Earthquake Accelerograms, Digitized and Plotted Data, Volume I, Part B", *Report EERL 70-21*, California Institute of Technology, Pasadena, 1970.
3. "Strong-Motion Earthquake Accelerograms, Digitized and Plotted Data, Volume I, Part C", *Report EERL 71-20*, California Institute of Technology, Pasadena, 1971.
4. "Strong-Motion Earthquake Accelerograms, Digitized and Plotted Data, Volume I, Part D", *Report EERL 71-21*, California Institute of Technology, Pasadena, 1971.
5. "Strong-Motion Earthquake Accelerograms, Digitized and Plotted Data, Volume I, Part E", *Report EERL 71-22*, California Institute of Technology, Pasadena, 1971.
6. "Strong-Motion Earthquake Accelerograms, Digitized and Plotted Data, Volume I, Part F", *Report EERL 71-23*, California Institute of Technology, Pasadena, 1971.
7. "Strong Motion Earthquake Accelerograms, Corrected Accelerograms and Integrated Velocity and Displacement Curves, Volume II, Part A", *Report EERL 71-51*, California Institute of Technology, Pasadena, 1971.
8. "Strong-Motion Earthquake Accelerograms, Digitized and Plotted Data, Volume I, Part G", *Report EERL 72-20*, California Institute of Technology, Pasadena, 1972.
9. "Strong-Motion Earthquake Accelerograms, Digitized and Plotted Data, Volume I, Part H", *Report EERL 72-21*, California Institute of Technology, Pasadena, 1972.
10. "Strong-Motion Earthquake Accelerograms, Digitized and Plotted Data, Volume I, Part I", *Report EERL 72-22*, California Institute of Technology, Pasadena, 1972.
11. "Strong-Motion Earthquake Accelerograms, Digitized and Plotted Data, Volume I, Part J", *Report EERL 72-23*, California Institute of Technology, Pasadena, 1972.
12. "Strong-Motion Earthquake Accelerograms, Digitized and Plotted Data, Volume I, Part K", *Report EERL 72-24*, California Institute of Technology, Pasadena, 1972.
13. "Strong-Motion Earthquake Accelerograms, Digitized and Plotted Data, Volume I, Part L", *Report EERL 72-25*, California Institute of Technology, Pasadena, 1972.
14. "Strong-Motion Earthquake Accelerograms, Digitized and Plotted Data, Volume I, Part M", *Report EERL 72-26*, California Institute of Technology, Pasadena, 1972.
15. "Strong-Motion Earthquake Accelerograms, Digitized and Plotted Data, Volume I, Part N", *Report EERL 72-27*, California Institute of Technology, Pasadena, 1972.

[1] Edited by D.E. Hudson, M.D. Trifunac and A.G. Brady

16. "Strong Motion Earthquake Accelerograms, Corrected Accelerograms and Integrated Velocity and Displacement Curves, Volume II, Part B", *Report EERL 72-50*, California Institute of Technology, Pasadena, 1972.

17. "Strong Motion Earthquake Accelerograms, Corrected Accelerograms and Integrated Velocity and Displacement Curves, Volume II, Part C", *Report EERL 72-51*, California Institute of Technology, Pasadena, 1972.

18. "Strong Motion Earthquake Accelerograms, Corrected Accelerograms and Integrated Velocity and Displacement Curves, Volume II, Part D", *Report EERL 72-52*, California Institute of Technology, Pasadena, 1972.

19. "Strong-Motion Earthquake Accelerograms, Response Spectra, Volume III, Part A", *Report EERL 72-80*, California Institute of Technology, Pasadena, 1972.

20. "Strong Motion Earthquake Accelerograms, Fourier Spectra, Volume IV, Part A", *Report EERL 72-100*, California Institute of Technology, Pasadena, 1972.

21. "Strong-Motion Earthquake Accelerograms, Digitized and Plotted Data, Volume I, Part O", *Report EERL 73-20*, California Institute of Technology, Pasadena, 1973.

22. "Strong-Motion Earthquake Accelerograms, Digitized and Plotted Data, Volume I, Part P", *Report EERL 73-21*, California Institute of Technology, Pasadena, 1973.

23. "Strong-Motion Earthquake Accelerograms, Digitized and Plotted Data, Volume I, Part Q", *Report EERL 73-22*, California Institute of Technology, Pasadena, 1973.

24. "Strong-Motion Earthquake Accelerograms, Digitized and Plotted Data, Volume I, Part R", *Report EERL 73-23*, California Institute of Technology, Pasadena, 1973.

25. "Strong-Motion Earthquake Accelerograms, Digitized and Plotted Data, Volume I, Part S", *Report EERL 73-24*, California Institute of Technology, Pasadena, 1973.

26. "Strong-Motion Earthquake Accelerograms, Digitized and Plotted Data, Volume I, Part T", *Report EERL 73-25*, California Institute of Technology, Pasadena, 1973.

27. "Strong-Motion Earthquake Accelerograms, Digitized and Plotted Data, Volume I, Part U", *Report EERL 73-26*, California Institute of Technology, Pasadena, 1973.

28. "Strong-Motion Earthquake Accelerograms, Digitized and Plotted Data, Volume I, Part V", *Report EERL 73-27*, California Institute of Technology, Pasadena, 1973.

29. "Strong-Motion Earthquake Accelerograms, Digitized and Plotted Data, Volume I, Part W", *Report EERL 73-28*, California Institute of Technology, Pasadena, 1973.

30. "Strong-Motion Earthquake Accelerograms, Digitized and Plotted Data, Volume I, Part X", *Report EERL 73-29*, California Institute of Technology, Pasadena, 1973.

31. "Strong-Motion Earthquake Accelerograms, Digitized and Plotted Data, Volume I, Part Y", *Report EERL 73-30*, California Institute of Technology, Pasadena, 1973.

32. "Strong Motion Earthquake Accelerograms, Corrected Accelerograms and Integrated Velocity and Displacement Curves, Volume II, Part E", *Report EERL 73-50*, California Institute of Technology, Pasadena, 1973.

33. "Strong Motion Earthquake Accelerograms, Corrected Accelerograms and Integrated Velocity and Displacement Curves, Volume II, Part F", *Report EERL 73-51*, California Institute of Technology, Pasadena, 1973.

34. "Strong Motion Earthquake Accelerograms, Corrected Accelerograms and Integrated Velocity and Displacement Curves, Volume II, Part G", *Report EERL 73-52*, California Institute of Technology, Pasadena, 1973.

35. "Strong-Motion Earthquake Accelerograms, Response Spectra, Volume III, Part B", *Report EERL 73-80*, California Institute of Technology, Pasadena, 1973.

36. "Strong-Motion Earthquake Accelerograms, Response Spectra, Volume III, Part C", *Report EERL 73-81*, California Institute of Technology, Pasadena, 1973.

37. "Strong-Motion Earthquake Accelerograms, Response Spectra, Volume III, Part D", *Report EERL 73-82*, California Institute of Technology, Pasadena, 1973.

38. "Strong-Motion Earthquake Accelerograms, Response Spectra, Volume III, Part E", *Report EERL 73-83*, California Institute of Technology, Pasadena, 1973.

39. "Strong-Motion Earthquake Accelerograms, Response Spectra, Volume III, Part F", *Report EERL 73-84*, California Institute of Technology, Pasadena, 1973.

40. "Strong-Motion Earthquake Accelerograms, Response Spectra, Volume III, Part G", *Report EERL 73-85*, California Institute of Technology, Pasadena, 1973.

41. "Strong Motion Earthquake Accelerograms, Fourier Spectra, Volume IV, Part B", *Report EERL 73-100*, California Institute of Technology, Pasadena, 1973.

42. "Strong Motion Earthquake Accelerograms, Fourier Spectra, Volume IV, Part C", *Report EERL 73-101*, California Institute of Technology, Pasadena, 1973.

43. "Strong Motion Earthquake Accelerograms, Fourier Spectra, Volume IV, Part D", *Report EERL 73-102*, California Institute of Technology, Pasadena, 1973.

44. "Strong Motion Earthquake Accelerograms, Fourier Spectra, Volume IV, Part E", *Report EERL 73-103*, California Institute of Technology, Pasadena, 1973.

45. "Strong Motion Earthquake Accelerograms, Fourier Spectra, Volume IV, Part F", *Report EERL 73-104*, California Institute of Technology, Pasadena, 1973.

46. "Strong Motion Earthquake Accelerograms, Fourier Spectra, Volume IV, Part G", *Report EERL 73-105*, California Institute of Technology, Pasadena, 1973.

47. "Strong Motion Earthquake Accelerograms, Corrected Accelerograms and Integrated Velocity and Displacement Curves, Volume II, Part H", *Report EERL 74-50*, California Institute of Technology, Pasadena, 1974.

48. "Strong Motion Earthquake Accelerograms, Corrected Accelerograms and Integrated Velocity and Displacement Curves, Volume II, Part I", *Report EERL 74-51*, California Institute of Technology, Pasadena, 1974.

49. "Strong Motion Earthquake Accelerograms, Corrected Accelerograms and Integrated Velocity and Displacement Curves, Volume II, Parts J and K", *Report EERL 74-52*, California Institute of Technology, Pasadena, 1974.

50. "Strong Motion Earthquake Accelerograms, Corrected Accelerograms and Integrated Velocity and Displacement Curves, Volume II, Parts L and M", *Report EERL 74-53*, California Institute of Technology, Pasadena, 1974.

51. "Strong Motion Earthquake Accelerograms, Corrected Accelerograms and Integrated Velocity and Displacement Curves, Volume II, Part N", *Report EERL 74-54*, California Institute of Technology, Pasadena, 1974.

52. "Strong Motion Earthquake Accelerograms, Corrected Accelerograms and Integrated Velocity and Displacement Curves, Volume II, Parts O and P", *Report EERL 74-55*, California Institute of Technology, Pasadena, 1974.

53. "Strong Motion Earthquake Accelerograms, Corrected Accelerograms and Integrated Velocity and Displacement Curves, Volume II, Parts Q and R", *Report EERL 74-56*, California Institute of Technology, Pasadena, 1974.

54. "Strong Motion Earthquake Accelerograms, Corrected Accelerograms and Integrated Velocity and Displacement Curves, Volume II, Part S", *Report EERL 74-57*, California Institute of Technology, Pasadena, 1974.

55. "Strong-Motion Earthquake Accelerograms, Response Spectra, Volume III, Part H", *Report EERL 74-80*, California Institute of Technology, Pasadena, 1974.

56. "Strong-Motion Earthquake Accelerograms, Response Spectra, Volume III, Part I", *Report EERL 74-81*, California Institute of Technology, Pasadena, 1974.

57. "Strong-Motion Earthquake Accelerograms, Response Spectra, Volume III, Parts J, K and L", *Report EERL 74-82*, California Institute of Technology, Pasadena, 1974.

58. "Strong-Motion Earthquake Accelerograms, Response Spectra, Volume III, Parts M and N", *Report EERL 74-83*, California Institute of Technology, Pasadena, 1974.

59. "Strong-Motion Earthquake Accelerograms, Response Spectra, Volume III, Parts O and P", *Report EERL 74-84*, California Institute of Technology, Pasadena, 1974.

60. "Strong-Motion Earthquake Accelerograms, Response Spectra, Volume III, Parts Q and R", *Report EERL 74-85*, California Institute of Technology, Pasadena, 1974.

61. "Strong-Motion Earthquake Accelerograms, Response Spectra, Volume III, Part S", *Report EERL 74-86*, California Institute of Technology, Pasadena, 1974.

62. "Strong Motion Earthquake Accelerograms, Fourier Spectra, Volume IV, Part H", *Report EERL 74-100*, California Institute of Technology, Pasadena, 1974.

63. "Strong Motion Earthquake Accelerograms, Fourier Spectra, Volume IV, Part I", *Report EERL 74-101*, California Institute of Technology, Pasadena, 1974.

64. "Strong Motion Earthquake Accelerograms, Fourier Spectra, Volume IV, Parts J, K, L and M", *Report EERL 74-102*, California Institute of Technology, Pasadena, 1974.

65. "Strong Motion Earthquake Accelerograms, Fourier Spectra, Volume IV, Parts N, O and P", *Report EERL 74-103*, California Institute of Technology, Pasadena, 1974.

66. "Strong Motion Earthquake Accelerograms, Fourier Spectra, Volume IV, Parts Q, R and S", *Report EERL 74-103*, California Institute of Technology, Pasadena, 1974.

67. "Strong Motion Earthquake Accelerograms, Corrected Accelerograms and Integrated Velocity and Displacement Curves, Volume II, Part T", *Report EERL 75-50*, California Institute of Technology, Pasadena, 1975.

68. "Strong Motion Earthquake Accelerograms, Corrected Accelerograms and Integrated Velocity and Displacement Curves, Volume II, Part U", *Report EERL 75-51*, California Institute of Technology, Pasadena, 1975.

69. "Strong Motion Earthquake Accelerograms, Corrected Accelerograms and Integrated Velocity and Displacement Curves, Volume II, Part V", *Report EERL 75-52*, California Institute of Technology, Pasadena, 1975.

70. "Strong Motion Earthquake Accelerograms, Corrected Accelerograms and Integrated Velocity and Displacement Curves, Volume II, Parts W and Y", *Report EERL 75-53*, California Institute of Technology, Pasadena, 1975.

71. "Strong-Motion Earthquake Accelerograms, Response Spectra, Volume III, Part T", *Report EERL 75-80*, California Institute of Technology, Pasadena, 1975.

72. "Strong-Motion Earthquake Accelerograms, Response Spectra, Volume III, Part U", *Report EERL 75-81*, California Institute of Technology, Pasadena, 1975.

73. "Strong-Motion Earthquake Accelerograms, Response Spectra, Volume III, Part V", *Report EERL 75-82*, California Institute of Technology, Pasadena, 1975.

74. "Strong-Motion Earthquake Accelerograms, Response Spectra, Volume III, Parts W and Y", *Report EERL 75-83*, California Institute of Technology, Pasadena, 1975.

75. "Strong Motion Earthquake Accelerograms, Fourier Spectra, Volume IV, Parts T and U", *Report EERL 75-100*, California Institute of Technology, Pasadena, 1975.

76. "Strong Motion Earthquake Accelerograms, Fourier Spectra, Volume IV, Parts V, W and Y", *Report EERL 75-101*, California Institute of Technology, Pasadena, 1975.

LIST OF PUBLICATIONS[1]
OF
PROFESSOR MIHAILO D. TRIFUNAC

1. "Analysis of Accelerograms – Parkfield Earthquake", with G.W. Housner, *Bulletin of the Seismological Society of America*, **57**(6), 1193-1220, 1967.
2. "Analysis of Strong Motion Accelerograph Records", with D.E. Hudson and N.C. Nigam, *Proceedings of the Fourth World Conference on Earthquake Engineering, Santiago, Chile, 1969,* **I**, 1-17 (also Appendix I in "Strong Motion Earthquake Accelerograms, Volume I – Uncorrected Accelerograms", *Report EERL 70-20*, California Institute of Technology, Pasadena, 1969).
3. "Strong-Motion Earthquake Accelerograms, Digitized and Plotted Data, Vol. I", with D.E. Hudson and A.G. Brady, *Report EERL 70-20*, California Institute of Technology, Pasadena, 1969.
4. "Investigation of Strong Earthquake Ground Motion", *Report EERL.1969.003,* California Institute of Technology, Pasadena, 1969.
5. "Complexity of Energy Release during the Imperial Valley, California Earthquake of 1940", with J.N. Brune, *Bulletin of the Seismological Society of America*, **60**(1), 137-160, 1970.
6. "Analysis of the Station No. 2, Seismoscope Record – 1966 Parkfield, California Earthquake", with D.E. Hudson, *Bulletin of the Seismological Society of America*, **60**(3), 785-794, 1970.
7. "Wind and Microtremor Induced Vibrations of a 22-Story Steel Frame Building", *Report EERL 70-01*, California Institute of Technology, Pasadena, 1970.
8. "Ambient Vibration Test of a 39-Strory Steel Frame Building", *Report EERL 70-02,* California Institute of Technology, Pasadena, 1970.
9. "On the Statistics and Possible Triggering Mechanism of Earthquakes in Southern California", *Report EERL 70-03*, California Institute of Technology, Pasadena, 1970.
10. "Laboratory Evaluation and Instrument Corrections of Strong Motion Accelerographs", with D.E. Hudson, *Report EERL 70-04*, California Institute of Technology, Pasadena, 1970.
11. "Response Envelope Spectrum and Interpretation of Strong Earthquake Ground Motion", *Report EERL 70-06*, California Institute of Technology, Pasadena, 1970.
12. "Low Frequency Digitization Errors and a New Method for Zero Baseline Correction of Strong Motion Accelerograms", *Report EERL 70-07*, California Institute of Technology, Pasadena, 1970.
13. "Response Envelope Spectrum and Interpretation of Strong Earthquake Ground Motion", *Bulletin of the Seismological Society of America*, **61**(2), 343-356, 1971.

[1] in different sequence than that given on the web-site, http://www.usc.edu/dept/civil_eng/Earthquake_eng/

14. "Zero Baseline Correction of Strong-Motion Accelerograms", *Bulletin of the Seismological Society of America*, **61**(5), 1201-1211, 1971.
15. "Analysis of the Pacoima Dam Accelerogram, San Fernando, California Earthquake of 1971", with D.E. Hudson, *Bulletin of the Seismological Society of America*, **61**(5), 1393-1411, 1971.
16. "A Method for Synthesizing Realistic Strong Ground Motion", *Bulletin of the Seismological Society of America*, **61**(6), 1739-1753, 1971.
17. "Surface Motion of a Semi-cylindrical Alluvial Valley for Incident Plane SH Waves", *Bulletin of the Seismological Society of America*, **61**(6), 1755-1770, 1971.
18. "Engineering Features of the San Fernando Earthquake, February 9, 1971", with G.W. Housner, D.E. Hudson, G.A. Frazier, J.H. Wood, W.D. Iwan, P.C. Jennings and A.G. Brady, *Report EERL 71-02*, California Institute of Technology, Pasadena, 1971.
19. "High Frequency Errors and Instrument Corrections of Strong-Motion Accelerograms", with F.E. Udwadia and A.G. Brady, *Report EERL 71-05*, California Institute of Technology, Pasadena, 1971.
20. "Strong-Motion Earthquake Accelerograms, II: Corrected Accelerograms and Integrated Velocity and Displacement Curves", with D.E. Hudson, A.G. Brady and A. Vijayaraghavan, *Report EERL 71-51*, California Institute of Technology, Pasadena, 1971.
21. "Interaction of a Shear Wall with the Soil for Incident Plane SH Waves", *Bulletin of the Seismological Society of America*, **62**(1), 63-83, 1972.
22. "A Note on Correction of Strong-Motion Accelerograms for Instrument Response", *Bulletin of the Seismological Society of America*, **62**(1), 401-409, 1972.
23. "Stress Estimates for San Fernando, California Earthquake of February 9, 1971: Main Event and Thirteen Aftershocks", *Bulletin of the Seismological Society of America*, **62**(3), 721-750, 1972.
24. "Tectonic Stress and Source Mechanism of the Imperial Valley, California Earthquake of 1940", *Bulletin of the Seismological Society of America,* **62**(5), 1283-1302, 1972.
25. "Comparison between Ambient and Forced Vibration Experiments", *Earthquake Engineering and Structural Dynamics,* **1**(2), 133-150, 1972.
26. "Studies of Strong Earthquake Motions and Microtremor Processes", with F.E. Udwadia, *Proceedings of the International Conference of Microzonation, Seattle, 1972*, **I**, 319-334.
27. "Strong-Motion Accelerograms, III: Response Spectra", with D.E. Hudson and A.G. Brady, *Report EERL 72-80*, California Institute of Technology, Pasadena, 1972.
28. "Strong-Motion Earthquake Accelerograms, IV: Fourier Spectra", with D.E. Hudson, F.E. Udwadia, A. Vijayaraghavan and A.G. Brady, *Report EERL 72-100*, California Institute of Technology, Pasadena, 1972.
29. "Analysis of Errors in Digitized Strong-Motion Accelerograms", with F.E. Udwadia and A.G. Brady, *Bulletin of the Seismological Society of America*, **63**(1), 157-187, 1973.

30. "Comparison of Earthquake and Microtremor Ground Motions in El Centro, California", with F.E. Udwadia, *Bulletin of the Seismological Society of America,* **63**(4), 1227-1253, 1973.
31. "Damped Fourier Spectrum and Response Spectra", with F.E. Udwadia, *Bulletin of the Seismological Society of America*, **63**(5), 1775-1783, 1973.
32. "A Note on Scattering of Plane SH Waves by a Semi-cylindrical Canyon", *Earthquake Engineering and Structural Dynamics,* **1**(3), 267-281, 1973.
33. "Analysis of Strong Earthquake Ground Motion for Prediction of Response Spectra", *Earthquake Engineering and Structural Dynamics,* **2**(1), 59-69, 1973.
34. "Characterization of Response Spectra by Parameters Governing the Gross Nature of Earthquake Source Mechanism", *Proceedings of the Fifth World Conference on Earthquake Engineering, Rome, Italy, 1973*, **1**, 701-704.
35. "Recent Developments in Data Processing and Accuracy Evaluations of Strong-Motion Acceleration Measurements", with F.E. Udwadia and A.G. Brady, *Proceedings of the Fifth World Conference on Earthquake Engineering*, *Rome, Italy, 1973*, **I**, 1214-1223.
36. "Ambient Vibration Tests of Full-Scale Structures", with F.E. Udwadia, *Proceedings of the Fifth World Conference on Earthquake Engineering*, *Rome, Italy, 1973*, **II**, 1430-1439.
37. "The Fourier Transform, Response Spectra and Their Relationship through the Statistics of Oscillator Response", with F.E. Udwadia, *Report EERL 73-01*, California Institute of Technology, Pasadena, 1973.
38. "Routine Computer Processing of Strong-Motion Accelerograms", with V.W. Lee, *Report EERL 73-03*, California Institute of Technology, Pasadena, 1973.
39. "A Three-Dimensional Dislocation Model for the San Fernando, California, Earthquake of February 9, 1971", *Bulletin of the Seismological Society of America*, **64**(1), 149-172, 1974.
40. "Characterization of Response Spectra through the Statistics of Oscillator Response", with F.E. Udwadia, *Bulletin of the Seismological Society of America*, **64**(1), 205-219, 1974.
41. "Parkfield, California, Earthquake of June 27, 1966: A Three-Dimensional Moving Dislocation", with F.E. Udwadia, *Bulletin of the Seismological Society of America*, **64**(3), 511-533, 1974.
42. "A Note on the Accuracy of Computed Ground Displacements from Strong-Motion Accelerograms", with V.W. Lee, *Bulletin of the Seismological Society of America*, **64**(4), 1209-1219, 1974.
43. "Surface Motion of a Semi-elliptical Alluvial Valley for Incident Plane SH-Waves", with H.L. Wong, *Bulletin of the Seismological Society of America*, **64**(5), 1389-1408, 1974.
44. "Variations of Strong Earthquake Ground Shaking in the Los Angeles Area", with F.E. Udwadia, *Bulletin of the Seismological Society of America*, **64**(5), 1429-1454, 1974.
45. "Interaction of a Shear Wall with the Soil for Incident Plane SH-Waves: Elliptical Rigid Foundation", with H.L. Wong, *Bulletin of the Seismological Society of America*, **64**(6), 1825-1842, 1974.

46. "Time and Amplitude Dependent Response of Structures", with F.E. Udwadia, *Earthquake Engineering and Structural Dynamics,* **2**(4), 359-378, 1974.

47. "Scattering of Plane SH-Waves by a Semi-elliptical Canyon", with H.L. Wong, *Earthquake Engineering and Structural Dynamics*, **3**(2), 157-169, 1974.

48. "An Array of Strong Motion Accelerographs in Bear Valley, California", with R.J. Dielman and T.C. Hanks, *Bulletin of the Seismological Society of America*, **65**(1), 1-12, 1975.

49. "On the Correlation of Seismic Intensity Scales with the Peaks of Recorded Strong Ground Motion", with A.G. Brady, *Bulletin of the Seismological Society of America*, **65**(1), 139-162, 1975.

50. "On the Correlation of Seismoscope Response with Earthquake Magnitude and Modified Mercalli Intensity", with A.G. Brady, *Bulletin of the Seismological Society of America*, **65**(2), 307-321, 1975.

51. "A Study on the Duration of Strong Earthquake Ground Motion", with A.G. Brady, *Bulletin of the Seismological Society of America*, **65**(3), 581-626, 1975.

52. "Two-Dimensional, Antiplane, Building-Soil-Building Interaction for Two or More Buildings and for Incident Plane SH-Waves", with H.L. Wong, *Bulletin of the Seismological Society of America*, **65**(6), 1863-1885, 1975.

53. "A Note on the Dynamic Response of Rigid Embedded Foundations", with J.E. Luco and H.L. Wong, *Earthquake Engineering and Structural Dynamics,* **4**(2), 119-127, 1975.

54. "On the Correlation of Peak Accelerations of Strong-Motion with Earthquake Magnitude, Epicentral Distance and Site Conditions", with A.G. Brady, *Proceedings of U.S. National Conference on Earthquake Engineering, Ann Arbor, 1975*, 43-52.

55. "An Experimental Study of Ground Deformations Caused by Soil-Structure Interaction", with J.E. Luco and F.E. Udwadia, *Proceedings of U.S. National Conference on Earthquake Engineering, Ann Arbor, Michigan, 1975*, 136-145.

56. "Full Scale Three-Dimensional Tests of Structural Deformations during Forced Excitation of a Nine-Story Reinforced Concrete Building", with D.A. Foutch, J.E. Luco and F.E. Udwadia, *Proceedings of U.S. National Conference on Earthquake Engineering, Ann Arbor, 1975*, 206-215.

57. "Preliminary Analysis of the Peaks of Strong Earthquake Ground Motion – Dependence of Peaks on Earthquake Magnitude, Epicentral Distance and the Recording Site Conditions", *Bulletin of the Seismological Society of America*, **66**(1), 189-219, 1976.

58. "Preliminary Empirical Model for Scaling Fourier Amplitude Spectra of Strong Ground Acceleration in Terms of Earthquake Magnitude, Source to Station Distance and Recording Site Conditions", *Bulletin of the Seismological Society of America*, **66**(4), 1343-1373, 1976.

59. "Correlations of Peak Acceleration, Velocity and Displacement with Earthquake Magnitude, Epicentral Distance and Site Conditions", with A.G. Brady, *Earthquake Engineering and Structural Dynamics,* **4**(5), 455-471, 1976.

60. "A Note on the Range of Peak Amplitudes of Recorded Accelerations, Velocities and Displacements with Respect to the Modified Mercalli Intensity", *Earthquake Notes,* **47**(2), 9-24, 1976.

61. "Influence of a Canyon on Soil-Structure Interaction", with H.L. Wong and K.K. Lo, *Journal of the Engineering Mechanics Division*, ASCE, **102**(EM4), 671-684, 1976.

62. "Dependence of Duration of Strong Earthquake Ground Motion on Magnitude, Epicentral Distance, Geologic Conditions at the Recording Station and Frequency of Motion", with B.D. Westermo, *Report CE 76-02*, University of Southern California, Los Angeles, 1976.

63. "Correlations of Frequency Dependent Duration of Strong Earthquake Ground Motion with the Modified Mercalli Intensity and the Geologic Conditions at the Recording Stations", with B.D. Westermo, *Report CE 76-03*, University of Southern California, Los Angeles, 1976.

64. "Effects of Surface and Subsurface Irregularities on the Amplitudes of Monochromatic Waves", with H.L. Wong and B.D. Westermo*, Bulletin of the Seismological Society of America*, **67**(2), 353-368, 1977.

65. "A Note on the Correlation of Frequency Dependent Duration of Strong Ground Motion with the Modified Mercalli Intensity and the Geologic Conditions at the Recording Stations", with B.D. Westermo, *Bulletin of the Seismological Society of America*, **67**(3), 917-927, 1977.

66. "Effects of Cross-Axis Sensitivity and Misalignment on Response of Mechanical-Optical Accelerographs", with H.L. Wong, *Bulletin of the Seismological Society of America*, **67**(3), 929-956, 1977.

67. "Contact Stresses and Ground Motion Generated by Soil-Structure Interaction", with H.L. Wong and J.E. Luco, *Earthquake Engineering and Structural Dynamics*, **5**(1), 67-79, 1977.

68. "Antiplane Dynamic Soil-Bridge-Soil Interaction for Incident Plane SH Waves", with A.M. Abdel-Ghaffar, *Earthquake Engineering and Structural Dynamics*, **5**(2), 107-129, 1977.

69. "Uniform Risk Absolute Acceleration Spectra", with J.G. Anderson, *Proceedings of the Second Annual ASCE EMD Specialty Conference, Raleigh, 1977*, 332-335.

70. "Forecasting the Spectral Amplitudes of Strong Earthquake Ground Motion", *Proceedings of the Sixth World Conference on Earthquake Engineering, New Delhi, India, 1977*, **I**, 139-152.

71. "Recent Developments in the Analysis of the Duration of Strong Earthquake Ground Motion", with B.D. Westermo, *Proceedings of the Sixth World Conference on Earthquake Engineering, New Delhi, India, 1977*, **I**, 365-371.

72. "A Note on the Effects of Recording Site Conditions on Amplitudes of Strong Earthquake Ground Motions", with H.L. Wong, *Proceedings of the Sixth World Conference on Earthquake Engineering, New Delhi, India, 1977*, **I**, 452-457.

73. "An Instrumental Comparison of the Modified Mercalli (M.M.I.) and Medvedev-Karnik-Sponheuer (M.K.S.) Intensity Scales", *Proceedings of the Sixth World Conference on Earthquake Engineering, New Delhi, India, 1977*, **I**, 715-721.

74. "Problems in the Construction of Microzoning Maps", with F.E. Udwadia, *Proceedings of the Sixth World Conference on Earthquake Engineering, New Delhi, India, 1977*, **I**, 735-741.

75. "Antiplane Dynamic Soil-Bridge-Soil Interaction for Incident Plane SH-Waves", with A.M. Abdel-Ghaffar, *Proceedings of the Sixth World Conference on Earthquake Engineering, New Delhi, India, 1977*, **II**, 1609-1614.

76. "Statistical Analysis of the Computed Response of Structural Response Recorders (S.R.R.) for Accelerograms Recorded in the United States of America", *Proceedings of the Sixth World Conference on Earthquake Engineering, New Delhi, India, 1977*, **III**, 2956-2961.

77. "Current Computational Methods in Studies of Earthquake Source Mechanisms and Strong Ground Motion", with J.G. Anderson, *Proceedings of Symposium on Applications of Computer Methods in Engineering, Los Angeles, 1977*, **II**, 929-937.

78. "A Note on the Estimation of the Fourier Amplitude Transforms", with F.E. Udwadia, *Report CE 77-01*, University of Southern California, Los Angeles, 1977.

79. "Uniform Risk Functionals for Characterization of Strong Earthquake Ground Motion", with J.G. Anderson, *Report CE 77-02*, University of Southern California, Los Angeles, 1977.

80. "Preliminary Empirical Models for Scaling Absolute Acceleration Spectra", with J.G. Anderson, *Report CE 77-03*, University of Southern California, Los Angeles, 1977.

81. "Uniformly Processed Strong Earthquake Ground Accelerations in the Western United States of America for the Period from 1933 to 1971: Pseudo Relative Velocity Spectra and Processing Noise", *Report CE 77-04*, University of Southern California, Los Angeles, 1977.

82. "An Evaluation of the Effects of Traveling Seismic Waves on the Three-Dimensional Response of Structures", with S.D. Werner, L.C. Lee and H.L. Wong, *Report R07720-4514*, Agbabian Associates, El Segundo, 1977.

83. "Uniform Risk Functionals for Characterization of Strong Earthquake Ground Motion", with J.G. Anderson, *Bulletin of the Seismological Society of America*, **68**(1), 205-218, 1978.

84. "Response Spectra of Earthquake Ground Motion", *Journal of the Engineering Mechanics Division*, ASCE, **104**(EM5), 1081-1097, 1978.

85. "Application of Seismic Risk Procedures to Problems in Microzonation", with J.G. Anderson, *Proceedings of the Second International Conference on Microzonation for Safer Construction, Research and Applications, San Francisco, 1978*, **I**, 559-569.

86. "Estimation of Relative Velocity Spectra", with J.G. Anderson, *Proceedings of the Sixth Symposium on Earthquake Engineering, Roorkee, India, 1978*, **I**, 9-18.

87. "A Note on the Dependence of the Duration of Strong Earthquake Ground Motion on Magnitude, Epicentral Distance, Geologic Conditions at the Recording Station and Frequency of Motion" in "Bulletin of the Institute of Earthquake Engineering and Seismology", with B.D. Westermo, *Publication No. 59*, University Kiril i Metodij Skopje, Skopje, Yugoslavia, 1-26, 1978.

88. "Uniformly Processed Strong Earthquake Ground Accelerations in the Western United States of America for the Period from 1933 to 1971: Corrected Acceleration, Velocity and

Displacement Curves", with V.W. Lee, *Report CE 78-01*, University of Southern California, Los Angeles, 1978.

89. "Preliminary Empirical Models for Scaling Pseudo Relative Velocity Spectra", with J.G. Anderson, *Report CE 78-04*, University of Southern California, Los Angeles, 1978.
90. "Preliminary Models for Scaling Relative Velocity Spectra", with J.G. Anderson, *Report CE 78-05*, University of Southern California, Los Angeles, 1978.
91. "Synthesizing Realistic Strong Motion Accelerograms", with H.L. Wong, *Report CE 78-07*, University of Southern California, Los Angeles, 1978.
92. "Correlations of the Frequency Dependent Duration of Strong Earthquake Ground Motion with the Magnitude, Epicentral Distance and the Depth of Sediments at the Recording Site", with B.D. Westermo, *Report CE 78-12*, University of Southern California, Los Angeles, 1978.
93. "Dependence of the Fourier Amplitude Spectra of Strong Motion Acceleration on the Depth of Sedimentary Deposits", with V.W. Lee, *Report CE 78-14*, University of Southern California, Los Angeles, 1978.
94. "A Comparison of the Modified Mercalli (MMI) and the Japanese Meteorological Agency (JMA) Intensity Scales", with H.L. Wong, *Earthquake Engineering and Structural Dynamics*, **7**(1), 75-83, 1979.
95. "Preliminary Empirical Model for Scaling Fourier Amplitude Spectra of Strong Motion Acceleration in Terms of Modified Mercalli Intensity and Geologic Site Conditions", *Earthquake Engineering and Structural Dynamics*, **7**(1), 63-74, 1979.
96. "Generation of Artificial Strong Motion Accelerograms", with H.L. Wong, *Earthquake Engineering and Structural Dynamics*, **7**(6), 509-527, 1979.
97. "Discussion on the Paper: Effect of Initial Base Motion on Response Spectra (by D.A. Pecknold and R. Riddell)", with F.E. Udwadia, *Journal of the Engineering Mechanics Division*, ASCE, **105**(EM1), 204-206, 1979.
98. "Response of Tunnels to Incident SH-Waves", with V.W. Lee, *Journal of the Engineering Mechanics Division*, ASCE, **105**(EM4), 643-659, 1979.
99. "Structural Response to Travelling Seismic Waves", with S.D. Werner, L.C. Lee and H.L. Wong, *Journal of the Structural Division*, ASCE, **105**(ST12), 2547-2564, 1979.
100. "A Note on Probabilistic Computation of Earthquake Response Spectrum Amplitudes", with J.G. Anderson, *Nuclear Engineering and Design*, **51**(2), 285-294, 1979.
101. "A Note on Surface Strains Associated with Incident Body Waves", *The Bulletin of the European Association for Earthquake Engineering,* **5**, 85-95, 1979.
102. "Correlations of the Frequency Dependent Duration of Strong Ground Motion with the Modified Mercalli Intensity and the Depth of Sediments at the Recording Site", with B.D. Westermo, *Report CE 79-01*, University of Southern California, Los Angeles, 1979.
103. "Dependence of the Pseudo Relative Velocity Spectra of Strong Motion Acceleration on the Depth of Sedimentary Deposits", with V.W. Lee, *Report CE 79-02*, University of Southern California, Los Angeles, 1979.

104. "Static, Dynamic and Rotational Components of Strong Shaking near Faults", with M. Dravinski, *Report CE 79-06*, University of Southern California, Los Angeles, 1979.

105. "Time of Maximum Response of Single-Degree-of-Freedom Oscillator for Earthquake Excitation", with V.W. Lee, *Report CE 79-14*, University of Southern California, Los Angeles, 1979.

106. "Automatic Digitization and Processing of Strong-Motion Accelerograms, Part I and Part II", with V.W. Lee, *Report CE 79-15*, University of Southern California, Los Angeles, 1979.

107. "Response of Layer to Strike-Slip Vertical Fault", with M. Dravinski, *Journal of the Engineering Mechanics Division*, ASCE, **106**(EM4), 609-621, 1980.

108. "Fourier Amplitude Spectra of Strong Motion Acceleration", with V.W. Lee, *The Bulletin of the European Association for Earthquake Engineering*, **6**, 2-18, 1980.

109. "Effects of Site Geology on Amplitude of Strong Motion", *Proceedings of the Seventh World Conference on Earthquake Engineering, Istanbul, Turkey, 1980*, **2**, 145-152.

110. "Recent Developments in Automatic Digitization of Analog Film Records", *Proceedings of the Seventh World Conference on Earthquake Engineering, Istanbul, Turkey, 1980*, **2**, 545-552.

111. "Seismic Risk Tables for Pseudo Relative Velocity Spectra in Regions with Shallow Seismicity", with B.D. Westermo, J.G. Anderson and M. Dravinski, Department of Civil Engineering, *Report CE 80-01*, University of Southern California, Los Angeles, 1980.

112. "Ratios of Uniform Risk Spectra for Different Probabilities of Exceedance and for Shallow, Random Seismicity Surrounding the Site", with M. Dravinski and B.D. Westermo, *Report CE 80-02*, University of Southern California, Los Angeles, 1980.

113. "A Note on the Vibrations of a Semi-circular Canal Excited by Plane SH-Wave", with N. Moeen-Vaziri, *Bulletin of Indian Society of Earthquake Technology,* **18**(2), 88-100, 1981.

114. "Distribution of Peaks in Linear Earthquake Response", with A. Amini, *Journal of the Engineering Mechanics Division*, ASCE, **107**(EM1), 207-227, 1981.

115. "Los Angeles Vicinity Strong Motion Accelerograph Network", with J.G. Anderson, T.L. Teng, A. Amini and K. Moslem, *Report CE 81-04*, University of Southern California, Los Angeles, 1981.

116. "A Note on Rotational Components of Earthquake-Motions for Incident Body Waves", *International Journal of Soil Dynamics and Earthquake Engineering*, **1**(1), 11-19, 1982.

117. "Effects of Foundation Size on Fourier Spectrum Amplitudes of Earthquake Accelerations Recorded in Building", with V.W. Lee and C.C. Feng, *Soil Dynamics and Earthquake Engineering*, **1**(2), 52-58, 1982.

118. "Duration of Strong Earthquake Shaking", with B.D. Westermo, *International Journal of Soil Dynamics and Earthquake Engineering*, **1**(3), 117-121, 1982.

119. "Optimum Frequency and Damping for Optically Recording Strong Motion Accelerograms", with A. Amini, *International Journal of Soil Dynamics and Earthquake Engineering*, **1**(4), 189-194, 1982.

120. "Body Wave Excitation of Embedded Hemisphere", with V.W. Lee, *Journal of the Engineering Mechanics Division*, ASCE, **108**(EM3), 546-563, 1982.

121. "Noise in Earthquake Accelerograms", with V.W. Lee and A. Amini, *Journal of the Engineering Mechanics Division*, ASCE, **108**(EM12), 1121-1129, 1982.

122. "EQINFOS (The Strong-Motion Earthquake Data Information System)", with V.W. Lee, *Report CE 82-01*, University of Southern California, Los Angeles, 1982.

123. "Analysis of a Feedback Transducer", with A. Amini, *Report CE 83-03*, University of Southern California, Los Angeles, 1983.

124. "A Statistical Basis for Spectrum Superposition in Response to Earthquake Excitation", with A. Amini, *Proceedings of the Eighth World Conference on Earthquake Engineering, San Francisco, 1984*, **IV**, 179-186.

125. "A Design Analysis of the Imperial County Services Building", with S. Kojic and J.C. Anderson, *Proceedings of the Eighth World Conference on Earthquake Engineering, San Francisco, 1984*, **V**, 355-362.

126. "Current Developments in Data Processing of Strong Motion Accelerograms", with V.W. Lee, *Report CE 84-01*, University of Southern California, Los Angeles, 1984.

127. "A Postearthquake Response Analysis of the Imperial County Services Building in El Centro", with S. Kojic and J.C. Anderson, *Report CE 84-02*, University of Southern California, Los Angeles, 1984.

128. "Scattering of Plane SH-Waves by Cylindrical Canals of Arbitrary Shape", with N. Moeen-Vaziri, *International Journal of Soil Dynamics and Earthquake Engineering*, **4**(1), 18-23, 1985.

129. "A Note on Controlling the Optical Density of Analog Film Records in Strong Motion Accelerographs", with D.K. Markus and K. Moslem, *International Journal of Soil Dynamics and Earthquake Engineering*, **4**(1), 31-34, 1985.

130. "Statistical Extension of Response Spectrum Superposition", with A. Amini, *International Journal of Soil Dynamics and Earthquake Engineering*, **4**(2), 54-63, 1985.

131. "Analysis of a Force Balance Accelerometer", with A. Amini, *International Journal of Soil Dynamics and Earthquake Engineering*, **4**(2), 82-90, 1985.

132. "Torsional Accelerograms", with V.W. Lee, *International Journal of Soil Dynamics and Earthquake Engineering*, **4**(3), 132-139, 1985.

133. "Attenuation of Modified Mercalli Intensity for Small Epicentral Distance in California", *Report CE 85-01*, University of Southern California, Los Angeles, 1985.

134. "Frequency Dependent Attenuation of Strong Earthquake Ground Motion", with V.W. Lee, *Report CE 85-02*, University of Southern California, Los Angeles, 1985.

135. "Preliminary Empirical Model for Scaling Fourier Amplitude Spectra of Strong Ground Acceleration in Terms of Earthquake Magnitude, Source to Station Distance, Site Intensity and Recording Site Conditions", with V.W. Lee, *Report CE 85-03*, University of Southern California, Los Angeles, 1985.

136. "Preliminary Empirical Model for Scaling Pseudo Relative Velocity Spectra of Strong Earthquake Acceleration, in Terms of Magnitude, Distance, Site Intensity and Recording Site Conditions", with V.W. Lee, *Report CE 85-04*, University of Southern California, Los Angeles, 1985.

137. "Uniform Risk Spectra of Strong Earthquake Ground Motion", with V.W. Lee, *Report CE 85-05*, University of Southern California, Los Angeles, 1985.

138. "A Note on Time of Maximum Response of Single Degree of Freedom Oscillator to Earthquake Excitation", with V.W. Lee, *Soil Dynamics and Earthquake Engineering*, **5**(2), 119-129, 1986.

139. "Investigation of Numerical Methods in Inversion of Earthquake Source Mechanism", with L.R. Jordanovski and V.W. Lee, *Report CE 86-01*, University of Southern California, Los Angeles, 1986.

140. "Investigation of Earthquake Response of Simple Bridge Structures", with I. Kashefi, *Report CE 86-02*, University of Southern California, Los Angeles, 1986.

141. "Investigation of Scattering and Diffraction of Plane Seismic Waves through Two-Dimensional Inhomogeneities", with N. Moeen-Vaziri, *Report CE 86-03*, University of Southern California, Los Angeles, 1986.

142. "Effects of Soil Structure Interaction on the Response of Buildings during Strong Earthquake Ground Motions", with K. Moslem, *Report CE 86-04*, University of Southern California, Los Angeles, 1986.

143. "Soil Structure Interaction Effects on Forced Vibration Tests", with J.E. Luco and H.L. Wong, *Report CE 86-05*, University of Southern California, Los Angeles, 1986.

144. "Order Statistics of Peaks of Response to Multi-component Seismic Excitation", with I.D. Gupta, *Bulletin of Indian Society of Earthquake Technology*, **24**(3-4), 135-159, 1987.

145. "On the Apparent Changes in Dynamic Behavior of a Nine-Story Reinforced Concrete Building", with J.E. Luco and H.L.Wong, *Bulletin of the Seismological Society of America*, **77**(6), 1961-1983, 1987.

146. "Order Statistics of Peaks in Earthquake Response of Multi-Degree-of-Freedom Systems", with I.D. Gupta, *Earthquake Engineering and Engineering Vibration*, **7**(4), 15-50, 1987.

147. "A Note on Contribution of Torsional Excitation to Earthquake Response of Simple Symmetric Buildings", with I.D. Gupta, *Earthquake Engineering and Engineering Vibration*, **7**(3), 27-46, 1987.

148. "Rocking Strong Earthquake Accelerations", with V.W. Lee, *Soil Dynamics and Earthquake Engineering*, **6**(2), 75-89, 1987.

149. "Spectral Amplitudes of Strong Earthquake Accelerations Recorded in Buildings", with K. Moslem, *Soil Dynamics and Earthquake Engineering*, **6**(2), 100-107, 1987.

150. "A Note on the Noise Amplitudes in Some Strong Motion Accelerographs", with A. Amini and R.L. Nigbor, *Soil Dynamics and Earthquake Engineering*, **6**(3), 180-185, 1987.

151. "Strong Earthquake Ground Motion Data in EQINFOS: Part I", with V.W. Lee, *Report CE 87-01*, University of Southern California, Los Angeles, 1987.

152. "Microzonation of a Metropolitan Area", with V.W. Lee, *Report CE 87-02*, University of Southern California, Los Angeles, 1987.

153. "Statistical Analysis of Response Spectra Method in Earthquake Engineering", with I.D. Gupta, *Report CE 87-03*, University of Southern California, Los Angeles, 1987.

154. "Influence of Local Soil and Geologic Site Conditions on Fourier Spectrum Amplitudes of Recorded Strong Motion Accelerations", *Report CE 87-04*, University of Southern California, Los Angeles, 1987.

155. "Strong Earthquake Ground Motion Data in EQINFOS: Yugoslavia, Part I", with L.R. Jordanovski, V.W. Lee, M.I. Manic, T. Olumceva, C. Sinadinovski and M.I. Todorovska, *Report CE 87-05*, University of Southern California, Los Angeles, 1987.

156. "Direct Empirical Scaling of Response Spectral Amplitudes from Various Site and Earthquake Parameters", with V.W. Lee, *Report NUREG/CR-4903: Volume 1, U.S. Nuclear Regulatory Commission*, Washington, D.C., 1987.

157. "Methods for Introduction of Geological Data into Characterization of Active Faults and Seismicity and Upgrading of the Uniform Risk Spectrum Technique", with J.G. Anderson and V.W. Lee, *Report NUREG/CR-4903: Volume 2, U.S. Nuclear Regulatory Commission*, Washington, D.C., 1987.

158. "A Note on Contribution of Rocking Excitation to Earthquake Response of Simple Buildings", with I.D. Gupta, *Bulletin of Indian Society of Earthquake Technology*, **25**(2), 73-89, 1988.

159. "Isolation of Soil-Structure Interaction Effects by Full-Scale Forced Vibration Tests", with J.E. Luco and H.L. Wong, *Earthquake Engineering and Structural Dynamics*, **16**(1), 1-21, 1988.

160. "Transient Pressures in Hydrotechnical Tunnels during Earthquakes", with S. Kojic, *Earthquake Engineering and Structural Dynamics*, **16**(3), 523-539, 1988.

161. "A Note on Peak Accelerations during 1 and 4 October, 1987 Earthquakes in Los Angeles, California", *Earthquake Spectra*, **4**(1), 101-113, 1988.

162. "Order Statistics of Peaks in Earthquake Response", with I.D. Gupta, *Journal of Engineering Mechanics*, ASCE, **114**(10), 1605-1627, 1988.

163. "A Comparison of Soil-Structure Interaction Calculations with Results of a Full-Scale Forced Vibration Test", with J.E. Luco and H.L. Wong, *Soil Dynamics and Earthquake Engineering*, **7**(1), 22-31, 1988.

164. "Attenuation of Intensity with Epicentral Distance in India", with I.D. Gupta, *Soil Dynamics and Earthquake Engineering*, **7**(3), 162-169, 1988.

165. "Scattering and Diffraction of Plane SH-waves by Two-Dimensional Inhomogeneities", with N. Moeen-Vaziri, *Soil Dynamics and Earthquake Engineering*, **7**(4), 179-188, 1988.

166. "Scattering and Diffraction of Plane P- and SV-waves by Two-Dimensional Inhomogeneities", with N. Moeen-Vaziri, *Soil Dynamics and Earthquake Engineering*, **7**(4), 189-200, 1988.

167. "Seismic Microzonation Mapping via Uniform Risk Spectra", *Proceedings of the Ninth World Conference on Earthquake Engineering, Tokyo-Kyoto, Japan, 1988*, **VII**, 75-80.

168. "Attenuation of Seismic Intensity in Balkan Countries", with V.W. Lee, H. Cao and M.I. Todorovska, *Report CE 88-01*, University of Southern California, Los Angeles, 1988.

169. "Investigation of Earthquake Response of Long Buildings", with M.I. Todorovska and V.W. Lee, *Report CE 88-02*, University of Southern California, Los Angeles, 1988.

170. "Earthquake Response of Arch Dams to Nonuniform Canyon Motion", with S. Kojic and V.W. Lee, *Report CE 88-03*, University of Southern California, Los Angeles, 1988.

171. "Empirical Scaling of Fourier Spectrum Amplitudes of Recorded Strong Earthquake Accelerations in Terms of Magnitude and Local Soil and Geologic Conditions", *Earthquake Engineering and Engineering Vibration*, **9**(2), 23-44, 1989.

172. "Attenuation of Seismic Intensity in Albania and Yugoslavia", with M.I. Todorovska, *Earthquake Engineering and Structural Dynamics*, **18**(5), 617-631, 1989.

173. "Dependence of Fourier Spectrum Amplitudes of Recorded Strong Earthquake Accelerations on Magnitude, Local Soil Conditions and on Depth of Sediments", *Earthquake Engineering and Structural Dynamics*, **18**(7), 999-1016, 1989.

174. "A Note on Filtering Strong Motion Accelerograms to Produce Response Spectra of Specified Shape and Amplitude", with V.W. Lee, *European Earthquake Engineering*, **III**(2), 38-45, 1989.

175. "Threshold Magnitudes Which Cause Ground Motion Exceeding the Values Expected during the Next 50 Years in a Metropolitan Area", *Geofizika*, **6**, 1-12, 1989.

176. "Antiplane Earthquake Waves in Long Structures", with M.I. Todorovska, *Journal of Engineering Mechanics*, ASCE, **115**(2), 2687-2708, 1989.

177. "Empirical Models for Scaling Fourier Amplitude Spectra of Strong Ground Acceleration in Terms of Earthquake Magnitude, Source to Station Distance, Site Intensity and Recording Site Conditions", with V.W. Lee, *Soil Dynamics and Earthquake Engineering*, **8**(3), 110-125, 1989.

178. "Empirical Models for Scaling Pseudo Relative Velocity Spectra of Strong Earthquake Accelerations in Terms of Magnitude, Distance, Site Intensity and Recording Site Conditions", with V.W. Lee, *Soil Dynamics and Earthquake Engineering*, **8**(3), 126-144, 1989.

179. "Scaling Strong Motion Fourier Spectra by Modified Mercalli Intensity, Local Soil and Geologic Site Conditions", *Structural Engineering/Earthquake Engineering,* JSCE, **6**(2), 217-224, 1989.

180. "Inversion of Earthquake Source Mechanism Using Near Field Strong Motion Data", *Proceedings of Conference on Computational Methods in Experimental Measurements (edited by G.M. Carlomagno and C.A. Brebbia)*, *Capri, Italy, 1989*, 65-75.

181. "Seismic Microzonation", *Proceedings of UNDRO Seminar on Lessons Learned from Earthquakes, Moscow, U.S.S.R., 1989*, 21-27.

182. "Selection of Earthquake Design Motions for Important Engineering Structures", *Proceedings of UNDRO Seminar on Lessons Learned from Earthquakes, Moscow, U.S.S.R., 1989*, 28-38.

183. "Methodology for Selection of Earthquake Design Motions for Important Engineering Structures", *Report CE 89-01*, University of Southern California, Los Angeles, 1989.

184. "Investigation of Building Response to Translational and Rotational Earthquake Excitations", with V.K. Gupta, *Report CE 89-02*, University of Southern California, Los Angeles, 1989.

185. "A Note on Contributions of Ground Torsion to Seismic Response of Symmetric Multistoried Buildings", with V.K. Gupta, *Earthquake Engineering and Engineering Vibration*, **10**(3), 27-40, 1990.

186. "How to Model Amplification of Strong Earthquake Motions by Local Soil and Geologic Site Conditions", *Earthquake Engineering and Structural Dynamics*, **19**(6), 833-846, 1990.

187. "M_L^{SM} in Yugoslavia", with D. Herak, M. Herak, V.W. Lee and M. Zivcic, *Earthquake Engineering and Structural Dynamics*, **19**(8), 1167-1179, 1990.

188. "Response of Multistoried Buildings to Ground Translation and Torsion during Earthquakes", with V.K. Gupta, *European Earthquake Engineering*, **IV**(1), 34-42, 1990.

189. "Propagation of Earthquake Waves in Buildings with Soft First Floor", with M.I. Todorovska, *Journal of Engineering Mechanics*, ASCE, **116**(4), 892-900, 1990.

190. "Note on Excitation of Long Structures by Ground Waves", with M.I. Todorovska, *Journal of Engineering Mechanics*, ASCE, **116**(4), 952-964, 1990.

191. "Curvograms of Strong Ground Motion", *Journal of Engineering Mechanics*, ASCE, **116**(6), 1426-1432, 1990.

192. "Probabilistic Spectrum Superposition for Response Analysis Including the Effects of Soil-Structure Interaction", with I.D. Gupta, *Journal of Probabilistic Engineering Mech*anics, **5**(1), 9-18, 1990.

193. "Response of Multistoried Buildings to Ground Translation and Rocking during Earthquakes", with V.K. Gupta, *Journal of Probabilistic Engineering Mechanics*, **5**(3), 138-145, 1990.

194. "Frequency Dependent Attenuation of Strong Earthquake Ground Motion", with V.W. Lee, *Soil Dynamics and Earthquake Engineering*, **9**(1), 3-15, 1990.

195. "A Microzonation Method Based on Uniform Risk Spectra", *Soil Dynamics and Earthquake Engineering*, **9**(1), 34-43, 1990.

196. "Least Square Inversion with Time Shift Optimization and an Application to Earthquake Source Mechanism", with L.R. Jordanovski, *Soil Dynamics and Earthquake Engineering*, **9**(5), 243-254, 1990.

197. "Least Square Model with Spatial Expansion: Application to the Inversion of Earthquake Source Mechanism", with L.R. Jordanovski, *Soil Dynamics and Earthquake Engineering*, **9**(6), 279-283, 1990.

198. "Analytical Model for Building-Foundation-Soil Interaction: Incident P, SV and Rayleigh Waves", with M.I. Todorovska, *Report CE 90-01*, University of Southern California, Los Angeles, 1990.

199. "Automatic Digitization and Processing of Accelerograms Using PC", with V.W. Lee, *Report CE 90-03*, University of Southern California, Los Angeles, 1990.

200. "Strong Earthquake Ground Motion Data in EQINFOS: Accelerograms Recorded in Bulgaria between 1981 and 1987", with G. Georgiev, V.W. Lee, D. Nenov and I. Paskaleva, *Technical Report*, Bulgarian Academy of Sciences, Sofia, 1990 (also *CE 90-02 Report*, University of Southern California, Los Angeles, 1990).

201. "Experimental Analysis of RJL-1, Chinese Force Balance Accelerometer", with A. Amini and O. Hata, *Earthquake Engineering and Engineering Vibration*, **11**(1), 77-88, 1991.

202. "Discussion on the Paper: A Note on the Fast Computation of Earthquake Response Spectra Estimates (by E. Reinoso, M. Ordaz and F.J. Sanchez-Sesma)", *Earthquake Engineering and Structural Dynamics*, **20**(8), 803-804, 1991.

203. "A Note on Instrumental Comparison of the Modified Mercalli Intensity (MMI) in the Western United States and the Mercalli-Cancani-Sieberg (MCS) Intensity in Yugoslavia", with M. Zivcic, *European Earthquake Engineering*, **V**(1), 22-26, 1991.

204. "On the Correlation of Mercalli-Cancani-Sieberg Intensity Scale in Yugoslavia with the Peaks of Recorded Strong Earthquake Ground Motion", with V.W. Lee, M. Zivcic and M. Manic, *European Earthquake Engineering*, **V**(1), 27-33, 1991.

205. "Earthquake Stresses in Arch Dams: I – Theory and Antiplane Excitation", with S. Kojic, *Journal of Engineering Mechanics*, ASCE, **117**(3), 532-552, 1991.

206. "Earthquake Stresses in Arch Dams: II – Excitation by SV, P and Rayleigh Waves", with S. Kojic, *Journal of Engineering Mechanics*, ASCE, **117**(3), 553-574, 1991.

207. "Pseudo Relative Acceleration Spectrum", with V.K. Gupta, *Journal of Engineering Mechanics*, ASCE, **117**(4), 924-927, 1991.

208. "M_L^{SM}", *Soil Dynamics and Earthquake Engineering*, **10**(1), 17-25, 1991.

209. "Empirical Scaling of Fourier Spectrum Amplitudes of Recorded Strong Earthquake Accelerations in Terms of Modified Mercalli Intensity, Local Soil Conditions and Depth of Sediments", *Soil Dynamics and Earthquake Engineering*, **10**(1), 65-72, 1991.

210. "Seismic Response of Multistoried Buildings Including the Effects of Soil Structure Interaction", with V.K. Gupta, *Soil Dynamics and Earthquake Engineering*, **10**(8), 414-422, 1991.

211. "A Note on the Differences in Magnitudes Estimated from Strong Motion Data and from Wood-Anderson Seismometer", *Soil Dynamics and Earthquake Engineering*, **10**(8), 423-428, 1991.

212. "Effects of Ground Rocking on Dynamic Response of Multistoried Buildings during Earthquakes", with V.K. Gupta, *Structural Engineering/Earthquake Engineering,* JSCE, **8**(2), 43-50, 1991.

213. "Recording and Interpreting Strong Earthquake Accelerograms", *Proceedings of the First International Conference on Seismology and Earthquake Engineering*, *Tehran, Islamic Republic of Iran, 1991*, **III**, 55-73.

214. "Remote Testing and Interrogation of Strong Motion Accelerographs", with A. Amini, *Proceedings of the First International Conference on Seismology and Earthquake Engineering*, *Tehran, Islamic Republic of Iran, 1991*, **III**, 75-83.

215. "Radiation Damping during Two-Dimensional Building-Soil Interaction", with M.I. Todorovska, *Report CE 91-01*, University of Southern California, Los Angeles, 1991.

216. "Instrument Correction for the Coupled Transducer-Galvanometer Systems", with E.I. Novikova, *Report CE 91-02*, University of Southern California, Los Angeles, 1991.

217. "A Model for Assessment of the Total Loss in a Building Exposed to Earthquake Hazard", with L.R. Jordanovski and M.I. Todorovska, *Report CE 91-05*, University of Southern California, Los Angeles, 1991.

218. "The System Damping, the System Frequency and the System Response Peak Amplitudes during In-Plane Building-Soil Interaction", with M.I. Todorovska, *Earthquake Engineering and Structural Dynamics*, **21**(2), 127-144, 1992.

219. "Digital Instrument Response Correction for the Force Balance Accelerometer", with E.I. Novikova, *Earthquake Spectra*, **8**(3), 429-442, 1992.

220. "Frequency Dependent Attenuation of Strong Earthquake Ground Motion in Yugoslavia", with V.W. Lee, *European Earthquake Engineering*, **VI**(1), 3-13, 1992.

221. "Effects of the Input Base Rocking on the Relative Response of Long-Buildings on Embedded Foundations", with M.I. Todorovska, *European Earthquake Engineering*, **VI**(1), 36-46, 1992.

222. "Total Loss in a Building Exposed to Earthquake Hazard, Part I: Theory", with L.R. Jordanovski and M.I. Todorovska, *European Earthquake Engineering*, **VI**(3), 14-25, 1992.

223. "Total Loss in a Building Exposed to Earthquake Hazard, Part II: A Hypothetical Example", with L.R. Jordanovski and M.I. Todorovska, *European Earthquake Engineering*, **VI**(3), 26-32, 1992.

224. "A Note on Scaling Peak Acceleration, Velocity and Displacement of Strong Earthquake Shaking by Modified Mercalli Intensity (MMI) and Site Soil and Geologic Conditions", with V.W. Lee, *Soil Dynamics and Earthquake Engineering*, **11**(2), 101-110, 1992.

225. "Relationship of M_L^{SM} and Magnitudes Determined by Regional Seismological Stations in Southeastern and Central Europe", with D. Herak, *Soil Dynamics and Earthquake Engineering*, **11**(4), 229-241, 1992.

226. "Higher Order Peaks in Response of Multistoried Buildings", with V.K. Gupta, *Proceedings of the Tenth World Conference on Earthquake Engineering, Madrid, Spain, 1992*, **7**, 3819-3824.

227. "Should Peak Accelerations be Used to Scale Design Spectrum Amplitudes?" *Proceedings of the Tenth World Conference on Earthquake Engineering, Madrid, Spain, 1992,* **10**, 5817-5822.

228. "An Example of Computing M_L^{SM} for Dharamshala Earthquake in India", *Bulletin of Indian Society of Earthquake Technology*, **30**(1), 19-25, 1993.

229. "A Note on the Effects of Ground Rocking in Response of Buildings during 1989 Loma Prieta Earthquake", with V.K. Gupta, *Earthquake Engineering and Engineering Vibration*, **13**(2), 12-28, 1993.

230. "Earthquake Response of the Imperial County Services Building in El Centro", with S. Kojic and J.C. Anderson, *Earthquake Engineering and Engineering Vibration*, **13**(4), 47-72, 1993.

231. "Empirical Scaling of Fourier Amplitude Spectra in Former Yugoslavia", with V.W. Lee, *European Earthquake Engineering*, **VII**(2), 47-61, 1993.

232. "Modified Mercalli Intensity and the Geometry of the Sedimentary Basin as the Scaling Parameters of the Frequency Dependent Duration of Strong Ground Motion", with E.I. Novikova, *Soil Dynamics and Earthquake Engineering*, **12**(4), 209-225, 1993.

233. "Modified Mercalli Intensity Scaling of the Frequency Dependent Duration of Strong Ground Motion", with E.I. Novikova, *Soil Dynamics and Earthquake Engineering*, **12**(5), 309-322, 1993.

234. "Long Period Fourier Amplitude Spectra of Strong Motion Acceleration", *Soil Dynamics and Earthquake Engineering*, **12**(6), 363-382, 1993.

235. "Broad Band Extension of Fourier Amplitude Spectra of Strong Motion Acceleration", *Report CE 93-01*, University of Southern California, Los Angeles, 1993.

236. "Duration of Strong Earthquake Ground Motion: Physical Basis and Empirical Equations", with E.I. Novikova, *Report CE 93-02*, University of Southern California, Los Angeles, 1993.

237. "Strong Earthquake Ground Motion Data in EQINFOS for India: Part 1A (by I.D. Gupta, V. Rambabu and R.G. Joshi)", (edited) with M.I. Todorovska and V.W. Lee, *Report CE 93-03*, University of Southern California, Los Angeles, 1993.

238. "Strong Earthquake Ground Motion Data in EQINFOS for India: Part 1B (by A.R. Chandrasekaran and J.D. Das)", (edited) with M.I. Todorovska and V.W. Lee, *Report CE 93-04*, University of Southern California, Los Angeles, 1993.

239. "A Preliminary Study of the Duration of Strong Earthquake Ground Motion on the Territory of Former Yugoslavia", with E.I. Novikova and M.I. Todorovska, *Report CE 93-09*, University of Southern California, Los Angeles, 1993.

240. "The Effects of Wave Passage on the Response of Base-Isolated Buildings on Rigid Embedded Foundations", with M.I. Todorovska, *Report CE 93-10*, University of Southern California, Los Angeles, 1993.

241. "Influence of Geometry of Sedimentary Basins on the Frequency Dependent Duration of Strong Ground Motion", with E.I. Novikova, *Earthquake Engineering and Engineering Vibration*, **14**(2), 7-44, 1994.

242. "Fourier Amplitude Spectra of Strong Motion Acceleration: Extension to High and Low Frequencies", *Earthquake Engineering and Structural Dynamics*, **23**(4), 389-411, 1994.

243. "Duration of Strong Ground Motion in Terms of Earthquake Magnitude, Epicentral Distance, Site Conditions and Site Geometry", with E.I. Novikova, *Earthquake Engineering and Structural Dynamics*, **23**(6), 1023-1043, 1994.

244. "Similarity of Strong Motion Earthquakes in California", *European Earthquake Engineering*, **VIII**(1), 38-48, 1994.

245. "Frequency Dependent Duration of Strong Earthquake Ground Motion on the Territory of Former Yugoslavia, Part I: Magnitude Models", with E.I. Novikova and M.I. Todorovska, *European Earthquake Engineering*, **VIII**(3), 11-25, 1994.

246. "Frequency Dependent Duration of Strong Earthquake Ground Motion on the Territory of Former Yugoslavia, Part II: Local Intensity Models", with E.I. Novikova and M.I. Todorovska, *European Earthquake Engineering*, **VIII**(3), 26-37, 1994.

247. "The Magnitude 6.7, Northridge, California Earthquake of January 17, 1994", with L. Jones, K. Aki, D. Boore, M. Celebi, A. Donnellan, J. Hall, R. Harris, E. Hauksson, T. Heaton, S. Hough, K. Hudnut, K. Hutton, M. Johnston, W. Joyner, H. Kanamori, G. Marshall, A. Michael, J. Mori, M. Murray, D. Ponti, P. Reasenberg, D. Schwartz, L. Seeber, A. Shakal, R. Simpson, H. Thio, J. Tinsley, M.I. Todorovska, D. Wald and M.L. Zoback, *Science*, **266**(5184), 389-397, 1994.

248. "*Q* and High Frequency Strong Motion Spectra", *Soil Dynamics and Earthquake Engineering*, **13**(3), 149-161, 1994.

249. "A Note on Distribution of Uncorrected Peak Ground Accelerations during the Northridge, California, Earthquake of 17 January 1994", with M.I. Todorovska and S.S. Ivanovic, *Soil Dynamics and Earthquake Engineering*, **13**(3), 187-196, 1994.

250. "M_L^{SM} of the 1989 Loma Prieta Earthquake", *Soil Dynamics and Earthquake Engineering*, **13**(5), 313-316, 1994.

251. "State of the Art Review on Strong Motion Duration", with E.I. Novikova, *Proceedings of the Tenth European Conference on Earthquake Engineering, Vienna, Austria, 1994*, **1**, 131-140.

252. "Response Spectra of Strong Motion Acceleration: Extension to High and Low Frequencies", *Proceedings of the Tenth European Conference on Earthquake Engineering, Vienna, Austria, 1994*, **1**, 203-208.

253. "Earthquake Source Variables for Scaling Spectral and Temporal Characteristics of Strong Ground Motion", *Proceedings of the Tenth European Conference on Earthquake Engineering, Vienna, Austria, 1994*, **4**, 2585-2590.

254. "Empirical Models of the Duration of Strong Earthquake Ground Motion Based on the Modified Mercalli Intensity", with E.I. Novikova, *Report CE 94-01*, University of Southern California, Los Angeles, 1994.

255. "Broad Band Extension of Pseudo Relative Velocity Spectra of Strong Motion", *Report CE 94-02*, University of Southern California, Los Angeles, 1994.

256. "Duration of Earthquake Fault Motion in California", with E.I. Novikova, *Earthquake Engineering and Structural Dynamics*, **24**(6), 781-799, 1995.

257. "Pseudo Relative Velocity Spectra of Earthquake Ground Motion at High Frequencies", *Earthquake Engineering and Structural Dynamics*, **24**(8), 1113-1130, 1995.

258. "Discussion on the Paper: Efficient Modal Analysis for Structures with Soil-Structure Interaction (by W.-H. Wu and H.A. Smith)", with V.K. Gupta, *Earthquake Engineering and Structural Dynamics*, **24**(11), 1541-1542, 1995.

259. "Pseudo Relative Velocity Spectra of Earthquake Ground Motion at Long Periods", *Soil Dynamics and Earthquake Engineering*, **14**(5), 331-346, 1995.

260. "Empirical Criteria for Liquefaction in Sands via Standard Penetration Tests and Seismic Wave Energy", *Soil Dynamics and Earthquake Engineering*, **14**(6), 419-426, 1995.

261. "Scaling Earthquake Motion in Geotechnical Design", *Proceedings of the Third International Conference on Recent Advances in Geotechnical Earthquake Engineering and Soil Dynamics, St. Louis, 1995*, **II**, 607-612.

262. "Frequency Dependent Duration of Strong Earthquake Ground Motion: Updated Empirical Equations", with E.I. Novikova, *Report CE 95-01*, University of Southern California, Los Angeles, 1995.

263. "Empirical Equations Describing Attenuation of the Peaks of Strong Ground Motion, in terms of Magnitude, Distance, Path Effects and Site Conditions", with V.W. Lee, M.I. Todorovska and E.I. Novikova, *Report CE 95-02*, University of Southern California, Los Angeles, 1995.

264. "Frequency Dependent Attenuation Function and Fourier Amplitude Spectra of Strong Earthquake Ground Motion in California", with V.W. Lee, *Report CE 95-03*, University of Southern California, Los Angeles, 1995.

265. "Pseudo Relative Velocity Spectra of Strong Earthquake Ground Motion in California", with V.W. Lee, *Report CE 95-04*, University of Southern California, Los Angeles, 1995.

266. "Ambient Vibration Survey of Full Scale Structures Using Personal Computers (with Examples in Kaprielian Hall)", with S.S. Ivanovic, *Report CE 95-05*, University of Southern California, Los Angeles, 1995.

267. "Correction for Misalignment and Cross Axis Sensitivity of Strong Earthquake Motion Recorded by SMA-1 Accelerographs", with M.I. Todorovska, E.I. Novikova and S.S. Ivanovic, *Report CE 95-06*, University of Southern California, Los Angeles, 1995.

268. "Selected Topics in Probabilistic Seismic Hazard Analysis", with M.I. Todorovska, I.D. Gupta, V.K. Gupta and V.W. Lee, *Report CE 95-08*, University of Southern California, Los Angeles, 1995.

269. "A Seismic Hazard Model for Peak Strains in Soils during Strong Earthquake Shaking", with M.I. Todorovska, *Earthquake Engineering and Engineering Vibration*, **16**(Supplement), 1-12, 1996.

270. "Nonlinear Soil Response – 1994 Northridge California, Earthquake", with M.I. Todorovska, *Journal of Geotechnical Engineering*, ASCE, **122**(9), 725-735, 1996.

271. "Peak Velocities and Peak Surface Strains during Northridge, California, Earthquake of 17 January 1994", with M.I. Todorovska and S.S. Ivanovic, *Soil Dynamics and Earthquake Engineering*, **15**(5), 301-310, 1996.

272. "Peak Surface Strains during Strong Earthquake Motion", with V.W. Lee, *Soil Dynamics and Earthquake Engineering*, **15**(5), 311-319, 1996.

273. "Hazard Mapping of Normalized Peak Strain in Soil during Earthquakes – Microzonation of a Metropolitan Area", with M.I. Todorovska, *Soil Dynamics and Earthquake Engineering*, **15**(5), 321-329, 1996.

274. "Investigation of Nonstationarity in Stochastic Seismic Response of Structures", with I.D. Gupta, *Report CE 96-01*, University of Southern California, Los Angeles, 1996.

275. "Response Spectra and Differential Motion of Columns", with M.I. Todorovska, *Earthquake Engineering and Structural Dynamics*, **26**(2), 251-268, 1997.

276. "Nonlinear Soil Response – 1994 Northridge, California Earthquake: Closure to Discussion by R. Richards Jr.", with M.I. Todorovska, *Journal of Geotechnical and Geoenvironmental Engineering,* ASCE, **123**(10), 988-989, 1997.

277. "Differential Earthquake Motion of Building Foundations", *Journal of Structural Engineering,* ASCE, **123**(4), 414-422, 1997.

278. "Distribution of Pseudo Spectral Velocity during the Northridge, California Earthquake of 17 January 1994", with M.I. Todorovska, *Soil Dynamics and Earthquake Engineering*, **16**(3), 173-192, 1997.

279. "Northridge, California, Earthquake of 1994: Density of Pipe Breaks and Surface Strains", with M.I. Todorovska, *Soil Dynamics and Earthquake Engineering*, **16**(3), 193-207, 1997.

280. "Northridge, California, Earthquake of 1994: Density of Red-Tagged Buildings versus Peak Horizontal Velocity and Intensity of Shaking", with M.I. Todorovska, *Soil Dynamics and Earthquake Engineering*, **16**(3), 209-222, 1997.

281. "Amplitudes, Polarity and Time of Peaks of Strong Ground Motion during the 1994 Northridge, California, Earthquake", with M.I. Todorovska, *Soil Dynamics and Earthquake Engineering*, **16**(4), 235-258, 1997.

282. "Advanced Accelerograph Calibration of the Los Angeles Strong Motion Array", with M.I. Todorovska, E.I. Novikova and S.S. Ivanovic, *Earthquake Engineering and Structural Dynamics*, **27**(10), 1053-1068, 1998.

283. "The Rinaldi Strong Motion Accelerogram of the Northridge, California, Earthquake of 17 January, 1994", with M.I. Todorovska and V.W. Lee, *Earthquake Spectra*, **14**(1), 225-239, 1998.

284. "Discussion on the Paper – The Role of Earthquake Hazard Maps in Loss Estimation: A Study of the Northridge Earthquake (by R.B. Olshansky)", with M.I. Todorovska, *Earthquake Spectra*, **14**(3), 557-563, 1998.

285. "A Note on Statistics of Level Crossings and Peak Amplitude in Stationary Stochastic Processes", with I.D. Gupta, *European Earthquake Engineering*, **XII**(3), 52-58, 1998.

286. "Stresses and Intermediate Frequencies of Strong Motion Acceleration", *Geofizika*, **14**, 1-27, 1998.

287. "Comments on the Paper: Microseismic Field of the Balkan Area (by C. Papazachos and Ch. Papaionnou)", *Journal of Seismology*, **2**(4), 359-362, 1998 (*Erratum*, **3**(4), 437, 1999).

288. "An Improved Probabilistic Spectrum Superposition", with I.D. Gupta, *Soil Dynamics and Earthquake Engineering*, **17**(1), 1-11, 1998.

289. "Nonlinear Soil Response as a Natural Passive Isolation Mechanism – The 1994 Northridge, California Earthquake", with M.I. Todorovska, *Soil Dynamics and Earthquake Engineering*, **17**(1), 41-51, 1998.

290. "Defining Equivalent Stationary PSDF to Account for Nonstationarity of Earthquake Ground Motion", with I.D. Gupta, *Soil Dynamics and Earthquake Engineering*, **17**(2), 89-99, 1998.

291. "The Northridge, California, Earthquake of 1994: Fire Ignition by Strong Shaking", with M.I. Todorovska, *Soil Dynamics and Earthquake Engineering*, **17**(3), 165-175, 1998.

292. "Damage Distribution during the 1994 Northridge, California, Earthquake in Relation to Generalized Categories of Surficial Geology", with M.I. Todorovska, *Soil Dynamics and Earthquake Engineering*, **17**(4), 239-253, 1998.

293. "A Note on the Statistics of Ordered Peaks in Stationary Stochastic Processes", with I.D. Gupta, *Soil Dynamics and Earthquake Engineering,* **17**(5), 317-328, 1998.

294. "Amplification of Strong Ground Motion and Damage Patterns during the 1994 Northridge, California, Earthquake" in "Geotechnical Earthquake Engineering and Soil Dynamics III (edited by P. Dakoulas, M. Yegian, and R. Holtz)", with M.I. Todorovska, *Geotechnical Special Publication No. 75*, ASCE, Reston (also *Proceedings of the Third ASCE Specialty Conference on Geotechnical Earthquake Engineering and Soil Dynamics, Seattle, 1998*), **1**, 714-725, 1998.

295. "Relative Flexibility of a Building Foundation", with M.I. Todorovska, *Proceedings of US-Japan Workshop on Soil-Structure Interaction, Menlo Park, 1998* (also *Open File Report 99-142*, U.S. Geological Survey, Reston, 1999), 17.1-17.20.

296. "Comments on the Paper: Assessment of Liquefaction Potential during Earthquakes by Arias Intensity (by R.E. Kayen and J.K. Mitchell)", *Journal of Geotechnical and Geoenvironmental Engineering*, ASCE, **125**(7), 627, 1999.

297. "Liquefaction Opportunity Mapping via Seismic Wave Energy", with M.I. Todorovska, *Journal of Geotechnical and Geoenvironmental Engineering*, ASCE, **125**(12), 1032-1042, 1999.

298. "Reduction of Structural Damage by Nonlinear Soil Response", with M.I. Todorovska, *Journal of Structural Engineering*, ASCE, **125**(1), 89-97, 1999.

299. "Comments on the Paper: Period Formulas for Concrete Shear Wall Buildings (by R.K. Goel and A.K. Chopra)", *Journal of Structural Engineering*, ASCE, **125**(7), 797-798, 1999.

300. "Statistics of Ordered Peaks in the Response of Nonclassically Damped Structures", with I.D. Gupta, *Probabilistic Engineering Mechanics*, **14**(4), 329-337, 1999.

301. "Experimental Evidence for Flexibility of a Building Foundation Supported by Concrete Friction Piles", with S.S. Ivanovic, M.I. Todorovska, E.I. Novikova and A.A Gladkov, *Soil Dynamics and Earthquake Engineering*, **18**(3), 169-187, 1999.

302. "Simulation of Strong Earthquake Ground Motion by Explosions – Experiments at the Lyaur Testing Range in Tajikistan", with S.Kh. Negmatullaev and M.I. Todorovska, *Soil Dynamics and Earthquake Engineering*, **18**(3), 189-207, 1999.

303. "Common Problems in Automatic Digitization of Strong Motion Accelerograms", with V.W. Lee and M.I. Todorovska, *Soil Dynamics and Earthquake Engineering*, **18**(7), 519-530, 1999.

304. "On Reoccurrence of Site Specific Response", with T.-Y. Hao and M.I. Todorovska, *Soil Dynamics and Earthquake Engineering*, **18**(8), 569-592, 1999.

305. "Recording and Interpreting Earthquake Response of Full-Scale Structures", with M.I. Todorovska, *Proceedings of NATO Advanced Research Workshop on Strong-Motion Instrumentation for Civil Engineering Structures, Istanbul, Turkey*, *1999* (Kluwer Academic Publishers, Dordrecht, The Netherlands, 2001), 131-155.

306. "On Identification of Damage in Structures via Wave Travel Times", with S.S. Ivanovic and M.I. Todorovska, *Proceedings of NATO Advanced Research Workshop on Strong-Motion Instrumentation for Civil Engineering Structures, Istanbul, Turkey, 1999* (Kluwer Academic Publishers, Dordrecht, The Netherlands, 2001), 447-468.

307. "The M_L = 6.4 Northridge, California, Earthquake and Five M > 5 Aftershocks between 17 January and 20 March 1994 – Summary of Processed Strong Motion Data", with M.I. Todorovska, V.W. Lee, C.D. Stephens, K.A. Fogleman, C. Davis and R. Tognazzini, *Report CE 99-01*, University of Southern California, Los Angeles, 1999.

308. "Instrumented 7-Storey Reinforced Concrete Building in Van Nuys, California: Description of Damage from the 1994 Northridge Earthquake and Strong Motion Data", with S.S. Ivanovic and M.I. Todorovska, *Report CE 99-02*, University of Southern California, Los Angeles, 1999.

309. "Instrumented 7-Storey Reinforced Concrete Building in Van Nuys, California: Ambient Vibration Surveys Following the Damage from the 1994 Northridge Earthquake", with S.S. Ivanovic, E.I. Novikova, A.A. Gladkov and M.I. Todorovska, *Report CE 99-03*, University of Southern California, Los Angeles, 1999.

310. "A Note on Nonstationarity of Seismic Response of Structures", with I.D. Gupta, *Engineering Structures*, **22**(11), 1567-1577, 2000.

311. "Ambient Vibration Tests of Structures – A Review", with S.S. Ivanovic and M.I. Todorovska, *ISET Journal of Earthquake Technology,* **37**(4), 165-197, 2000.

312. "Comments on the Papers: Seismic Soil-Structure Interaction in Buildings, I: Analytical Methods, and II: Empirical Findings (by J.P. Stewart)", *Journal of Geotechnical and Geoenvironmental Engineering*, ASCE, **126**(7), 668-670, 2000.

313. "Can Aftershock Studies Predict Site Amplification? Northridge, CA, Earthquake of 17 January, 1996", with M.I. Todorovska, *Soil Dynamics and Earthquake Engineering*, **19**(4), 233-251, 2000.

314. "Long Period Microtremors, Microseisms and Earthquake Damage: Northridge, CA, Earthquake of 17 January, 1994", with M.I. Todorovska, *Soil Dynamics and Earthquake Engineering*, **19**(4), 253-267, 2000.

315. "Ambient Vibration Tests of a Seven-Story Reinforced Concrete Building in Van Nuys, California, Damaged by the 1994 Northridge Earthquake", with S.S. Ivanovic, E.I. Novikova, A.A. Gladkov and M.I. Todorovska, *Soil Dynamics and Earthquake Engineering*, **19**(6), 391-411, 2000.

316. "Apparent Periods of a Building, I: Fourier Analysis", with S.S. Ivanovic and M.I. Todorovska, *Journal of Structural Engineering*, ASCE, **127**(5), 517-526, 2001.

317. "Apparent Periods of a Building, II: Time-Frequency Analysis", with S.S. Ivanovic and M.I. Todorovska, *Journal of Structural Engineering*, ASCE, **127**(5), 527-537, 2001.

318. "Generation of Tsunamis by Slowly Spreading Uplift of the Sea Floor", with M.I. Todorovska, *Soil Dynamics and Earthquake Engineering*, **21**(2), 151-167, 2001.

319. "Wave Propagation in a Seven-Story Reinforced Concrete Building, Part I: Theoretical Models", with M.I. Todorovska and S.S. Ivanovic, *Soil Dynamics and Earthquake Engineering*, **21**(3), 211-223, 2001.

320. "Wave Propagation in a Seven-Story Reinforced Concrete Building, Part II: Observed Wavenumbers", with M.I. Todorovska and S.S. Ivanovic, *Soil Dynamics and Earthquake Engineering*, **21**(3), 225-236, 2001.

321. "A Note on the Useable Dynamic Range of Accelerographs Recording Translation", with M.I. Todorovska, *Soil Dynamics and Earthquake Engineering*, **21**(4), 275-286, 2001.

322. "Evolution of Accelerographs, Data Processing, Strong Motion Arrays and Amplitude and Spatial Resolution in Recording Strong Earthquake Motion", with M.I. Todorovska, *Soil Dynamics and Earthquake Engineering*, **21**(6), 537-555, 2001.

323. "Anti-plane Response of a Dike on a Flexible Embedded Foundation to Incident SH-Waves", with M.I. Todorovska and A. Hayir, *Soil Dynamics and Earthquake Engineering*, **21**(7), 593-601, 2001.

324. "Anti-plane Response of a Dike with Flexible Structure-Soil Interface to Incident SH-Waves", with A. Hayir and M.I. Todorovska, *Soil Dynamics and Earthquake Engineering*, **21**(7), 603-613, 2001.

325. "Energy of Earthquake Response as a Design Tool", with T.-Y. Hao and M.I. Todorovska, *Proceedings of the Thirteenth Mexican National Conference on Earthquake Engineering, Guadalajara, Mexico, 2001 (on CD).*

326. "Response Spectra for Differential Motion of Columns", with M.I. Todorovska, *Proceedings of the Twelfth World Conference on Earthquake Engineering, Auckland, New Zealand, 2001 (on CD)*, Paper 2638.

327. "Near-Field Amplitudes of Tsunami from Submarine Slumps and Slides", with M.I. Todorovska and A. Hayir, *Proceedings of NATO Advanced Research Workshop on Underwater Ground Failures, Tsunami Generation, Modeling, Risk and Mitigation, Istanbul, Turkey, 2001* (also in *Submarine Landslides and Tsunamis (edited by A.C.*

Yalciner, E.N. Pelinovsky, E. Okal, and C.E. Synolakis), Kluwer Academic Publishers, Dordrecht, The Netherlands, 59-68, 2003).

328. "Full-Scale Experimental Studies of Soil-Structure Interaction – A Review", with M.I. Todorovska and T.-Y. Hao, *Proceedings of the Second US-Japan Workshop on Soil-Structure Interaction, Tsukuba City, Japan, 2001 (on CD).*

329. "Flexible versus Rigid Foundation Models of Soil-Structure Interaction: Incident SH-Waves", with M.I. Todorovska and A. Hayir, *Proceedings of the Second US-Japan Workshop on Soil-Structure Interaction, Tsukuba City, Japan, 2001 (on CD).*

330. "Near-Field Tsunami Waveforms from Submarine Slumps and Slides", with A. Hayir and M.I. Todorovska, *Report CE 01-01*, University of Southern California, Los Angeles, 2001.

331. "Response of a 14-Story Reinforced Concrete Structure to Nine Earthquakes: 61 Years of Observation in the Hollywood Storage Building", with T.-Y. Hao and M.I. Todorovska, *Report CE 01-02*, University of Southern California, Los Angeles, 2001.

332. "On Energy Flow in Earthquake Response", with T.-Y. Hao and M.I. Todorovska, *Report CE 01-03*, University of Southern California, Los Angeles, 2001.

333. "Effects of Boundary Drainage on the Reflection of Elastic Waves in a Poroelastic Half-Space Saturated with Non-viscous Fluid", with C.H. Lin and V.W. Lee, *Report CE 01-04*, University of Southern California, Los Angeles, 2001.

334. "7-Storey Reinforced Concrete Building in Van Nuys, California: Photographs of the Damage from the 1994 Northridge Earthquake", with T.-Y. Hao, *Report CE 01-05*, University of Southern California, Los Angeles, 2001.

335. "Tsunami Waveforms from Submarine Slides and Slumps Spreading in Two Dimensions", with A. Hayir and M.I. Todorovska, *Report CE 01-06*, University of Southern California, Los Angeles, 2001.

336. "A Note on Tsunami Amplitudes above Submarine Slides and Slumps", with M.I. Todorovska and A. Hayir, *Soil Dynamics and Earthquake Engineering*, **22**(2), 129-141, 2002.

337. "A Note on the Differences in Tsunami Source Parameters for Submarine Slides and Earthquakes", with M.I. Todorovska, *Soil Dynamics and Earthquake Engineering*, **22**(2), 143-155, 2002.

338. "A Note on the Effects of Nonuniform Spreading Velocity of Submarine Slides and Slumps on the Near-Field Tsunami Amplitudes", with A. Hayir and M.I. Todorovska, *Soil Dynamics and Earthquake Engineering*, **22**(3), 167-180, 2002.

339. "Was the Great Banks Event of 1929 a Slump Spreading in Two Directions?", with A. Hayir and M.I. Todorovska, *Soil Dynamics and Earthquake Engineering*, **22**(5), 349-360, 2002.

340. "23rd ISET Annual Lecture: 70th Anniversary of Biot Spectrum", *ISET Journal of Earthquake Technology*, **40**(1), 19-50, 2003.

341. "Wave Propagation in a Seven-Story Reinforced Concrete Building, Part III: Damage Detection via Changes in Wavenumbers", with S.S. Ivanovic and M.I. Todorovska, *Soil Dynamics and Earthquake Engineering*, **23**(1), 65-75, 2003.

342. "A Note on Tsunami Caused by Submarine Slides and Slumps Spreading in One Dimension with Nonuniform Displacement Amplitudes", with A. Hayir and M.I. Todorovska, *Soil Dynamics and Earthquake Engineering*, **23**(3), 223-234, 2003.

343. "Nonlinear Soil Response as a Natural Passive Isolation Mechanism, Paper II – The 1933, Long Beach, California Earthquake", *Soil Dynamics and Earthquake Engineering*, **23**(7), 549-562, 2003.

344. "Reocurrence of Site Specific Response in Former Yugoslavia – Part I: Montenegro", with S.S. Ivanovic, *Soil Dynamics and Earthquake Engineering*, **23**(8), 637-661, 2003.

345. "Reoccurrence of Site Specific Response in Former Yugoslavia – Part II: Friuli, Banja Luka and Kopaonik", with S.S. Ivanovic, *Soil Dynamics and Earthquake Engineering*, **23**(8), 663-681, 2003.

346. "Tsunami Source Parameters of Submarine Earthquakes and Slides", with M.I. Todorovska, *Proceedings of the First International Symposium on Submarine Mass Movements and Their Consequences (edited by J. Locat and J. Mienert), Nice, France*, 2003 (Kluwer Academic Publishers, Dordrecht, The Netherlands, 2003), 121-128.

347. "Analysis of Drifts in a Seven-Story Reinforced Concrete Structure", with S.S. Ivanovic, *Report CE 03-01*, University of Southern California, Los Angeles, 2003.

348. "Maximum Distance to a Site and Minimum Energy to Initiate Liquefaction in Water Saturated Sands", with M.I. Todorovska, *Soil Dynamics and Earthquake Engineering*, **24**(2), 89-101, 2004.

349. "1971 San Fernando and 1994 Northridge, California, Earthquakes: Did the Zones with Severely Damaged Buildings Reoccur?", with M.I. Todorovska, *Soil Dynamics and Earthquake Engineering*, **24**(3), 225-239, 2004.

350. "Time and Amplitude Variations of Building-Soil System Frequencies during Strong Earthquake Shaking for Selected Buildings in the Los Angeles", with M.I. Todorovska and T.-Y. Hao, *Proceedings of the Third UJNR Workshop on Soil-Structure Interaction, Menlo Park, 2004 (on CD).*

351. "Instrumented Buildings of University of Southern California – Strong Motion Data, Metadata and Soil-Structure System Frequencies", with T.-Y. Hao and M.I. Todorovska, *Report CE 04-01*, University of Southern California, Los Angeles, 2004.

352. "Building Periods for Use in Earthquake Resistant Design Codes – Earthquake Response, Data Compilation and Analysis of Time and Amplitude Variations", with M.I. Todorovska and T.-Y. Hao, *Report CE 04-02*, University of Southern California, Los Angeles, 2004.

353. "A Study of the Relative Ranking of Twelve Faculty of the USC Civil Engineering Department – Experiments with Science Citation Index", with V.W. Lee, *Report CE 04-03*, University of Southern California, Los Angeles, 2004.

354. "The Role of Brune Spectrum in Earthquake Engineering", *Journal of Seismology and Earthquake Engineering* (in press).

355. "The Reflection of Plane Waves in a Poroelastic Half-Space Saturated with Inviscid Fluid", with C.-H. Lin and V.W. Lee, *Soil Dynamics and Earthquake Engineering* (in press).

356. "On Publication Rates in Earthquake Engineering", *Soil Dynamics and Earthquake Engineering* (in press).

357. "On Citation Rates in Earthquake Engineering", *Soil Dynamics and Earthquake Engineering* (in press).

358. "A Note on Publication and Citation Rates of Female Academics in Earthquake Engineering", *Soil Dynamics and Earthquake Engineering* (in press).

359. "Shaking Hazard Compatible Methodology for Probabilistic Assessment of Permanent Ground Displacement across Earthquake Faults", with M.I. Todorovska and V.W. Lee, *Soil Dynamics and Earthquake Engineering* (in press).

360. "Response Spectra for Differential Motion of Columns, Paper II: Out-of-Plane Response", with V. Gicev, *Soil Dynamics and Earthquake Engineering* (in press).

361. "Historical Notes on Response Spectrum and the Role of the Brune Spectrum in Earthquake Engineering", *Proceedings of Brune Symposium, Reno, 2004* (in press).

362. "A Note on Publication and Citation Rates of J.N. Brune", *Proceedings of Brune Symposium, Reno, 2004* (in press).